

Dissertation zur Erlangung des Doktorgrades
der Fakultät für Chemie und Pharmazie
der Ludwig-Maximilians-Universität München

A Marcus-Theory-Based Approach to Ambident Reactivity



Robert Martin Breugst

aus München

2010

Erklärung

Diese Dissertation wurde im Sinne von § 13 Abs. 3 bzw. 4 der Promotionsordnung vom 29. Januar 1998 (in der Fassung der vierten Änderungssatzung vom 26. November 2004) von Herrn Professor Dr. Herbert Mayr betreut.

Ehrenwörtliche Versicherung

Diese Dissertation wurde selbständig, ohne unerlaubte Hilfe erarbeitet.

München, 28.10.2010

Dissertation eingereicht am: 28.10.2010
1. Gutachter: Prof. Dr. Herbert Mayr
2. Gutachter: Prof. Dr. Hendrik Zipse
Mündliche Prüfung am: 21.12.2010

Acknowledgements

First of all, I would like to express my cordial gratitude to Professor Dr. Herbert Mayr for the opportunity to compose this thesis in his group. I have cherished all the valuable discussions with him, his endless support, and his inspiring confidence very much and I have always appreciated working under these excellent conditions. From the very first day in his group Professor Mayr made me feel welcome, has always been willing to discuss my ideas, and encouraged me to pursue a scientific career.

Furthermore, I would like to thank Professor Dr. Hendrik Zipse for numerous discussions and helpful comments on quantum chemical calculations, and of course also for reviewing my thesis.

Additionally, I am very indebted to Professor J. Peter Guthrie, Ph.D., for giving me the opportunity to spend almost 4 months in his group at the University of Western Ontario. During this time, I have learned so many new things and I am grateful for the reams of discussions in his office.

The financial support by the Fonds der Chemischen Industrie (scholarship for Ph.D. students) is gratefully acknowledged which did not only fund two years of my time during my Ph.D. but also funded my stay at the University of Western Ontario and my visits to several international conferences.

Sincere thanks for the great working atmosphere and many fruitful discussions are given to all my colleagues, especially those from the “Olah” lab: Roland Appel, Dr. Frank Brotzel, Dr. Tanja Kanzian, Dr. Sami Lakhdar, and Christoph Nolte. I would also like to thank Francisco Corral for his collaboration during his undergraduate research course, Nathalie Hampel not only for the synthesis of our reference electrophiles but also for her helping hand for several product studies, and Brigitte Janker for quickly solving any emerging problems.

I cannot overemphasize my deepest gratitude to our kind soul Hildegard Lipfert for all her help and support.

Acknowledgements

For the fast and efficient proof reading of this thesis, I am very thankful to Johannes Ammer, Roland Appel, Nicola Breugst, Francisco Corral, Waltraud Härtel, Dr. Tanja Kanzian, Hans Laub, Christoph Nolte, and Dr. Nicolas Streidl. I am also grateful to Dr. Armin Ofial for very valuable suggestions and critical comments.

Besides the support from my colleagues I am very happy that I had a couple of private “motivational coaches” around who helped me to focus on my work when it was necessary and who also distracted me from it when it was necessary. Therefore, I am grateful to all my friends, especially to Thorsten Allscher who accompanied me for the past nine years of our chemistry studies.

My deepest and most sincere gratitude belongs to my whole family, Wolfgang, Irmgard, Nicki, and Waltraud, for their unconditional support. You have always helped me wherever you could to make my life easier and more enjoyable. Thank you very much!

Parts of this thesis have already been published as follows:

Marcus-Analysis of Ambident Reactivity [Marcus-Analyse ambidenter Reaktivität]

M. Breugst, H. Zipse, J. P. Guthrie, H. Mayr, *Angew. Chem.* **2010**, *122*, 5291-5295; *Angew. Chem. Int. Ed.* **2010**, *49*, 5165-5169.

Nucleophilic Reactivities of Imide and Amide Anion

M. Breugst, T. Tokuyasu, H. Mayr, *J. Org. Chem.* **2010**, *75*, 5250-5258.

Ambident Reactivities of Pyridone Anions

M. Breugst, H. Mayr, *J. Am. Chem. Soc.* **2010**, *132*, 15380-15389.

A Farewell to the HSAB Principle of Ambident Reactivity

H. Mayr, M. Breugst, A. R. Ofial, *Angew. Chem.* accepted, DOI: 10.1002/anie.201007100.

Table of Contents

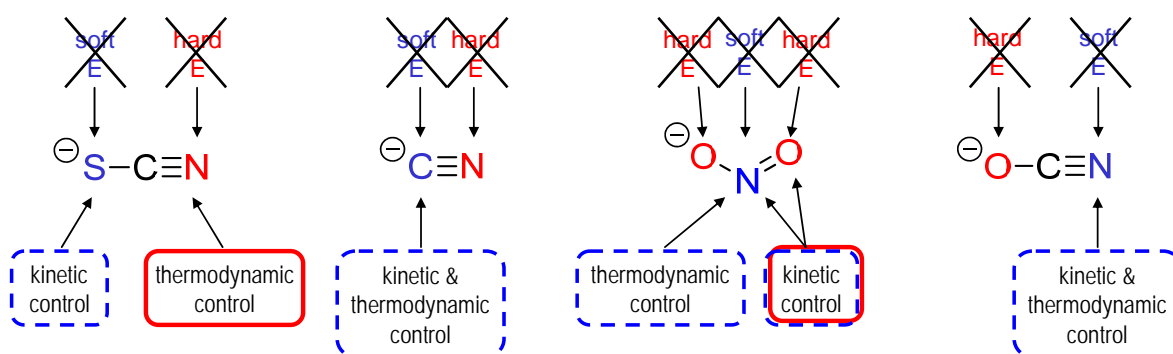
Chapter 1: Summary	1
Chapter 2: Introduction	13
Chapter 3: Marcus Analysis of Ambident Reactivity	23
Chapter 4: Nucleophilic Reactivities of Imide and Amide Anions	87
Chapter 5: Ambident Reactivities of Pyridone Anions	145
Chapter 6: Ambident Reactivities of the Anions of Nucleobases and Their Subunits	217
Chapter 7: A Farewell to the HSAB Principle of Ambident Reactivity	317

Chapter 1: Summary

1 General

Pearson's principle of hard and soft acids and bases (HSAB) and the related Klopman–Salem concept of charge- and orbital-controlled reactions have been considered to provide a consistent rationalization for ambident reactivity. However, in a series of experimental investigations, it has previously been shown that the reactivities of typical ambident nucleophiles cannot be properly described by these concepts (Scheme 1).

This thesis was designed to examine the reactivities of other ambident nucleophiles and to provide a consistent rationalization of ambident reactivity.



Scheme 1: Failure of the HSAB principle to correctly predict the regioselectivities of the reactions of hard and soft electrophiles E with some prototypes of ambident nucleophiles.

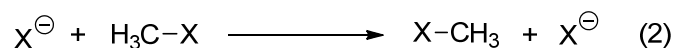
2 Marcus Analysis of Ambident Reactivity

According to the Marcus equation (1), the Gibbs energy of activation can be calculated from the Gibbs energy of reaction ΔG^0 and the intrinsic barrier ΔG_0^\ddagger , which corresponds to the Gibbs energy of activation (ΔG^\ddagger) of an identity reaction (with $\Delta G^0 = 0$).

$$\Delta G^\ddagger = \Delta G_0^\ddagger + 0.5 \Delta G^0 + (\Delta G^0)^2 / 16 \Delta G_0^\ddagger \quad (1)$$

We have extended earlier work by Hoz and co-workers and calculated the intrinsic barriers for the identity methyl transfer reaction [Eq. (2)] at G3(+) and MP2/6-311+G(2d,p) level of theory for different nucleophiles X (e.g., X = F, OMe, NMe₂, CH₃). Consistent with previous results, we have found that the intrinsic barriers are smaller, when the attacking atom is further right in the periodic table, i.e., ΔG_0^\ddagger (F) < ΔG_0^\ddagger (OMe) < ΔG_0^\ddagger (NMe₂) < ΔG_0^\ddagger (CH₃).

The same trend also controls ambident reactivity and it was shown that *N*-attack of CN^- , *S*-attack of SCN^- , and *O*-attack of enolates are intrinsically favored, in accordance with their relative positions in the periodic table.



Substitution of the calculated intrinsic barriers (ΔG_0^\ddagger) and the calculated reaction free energies (ΔG^0) for the reactions with methyl chloride into the Marcus equation (1) gave the Gibbs energy profiles depicted in Figure 1.

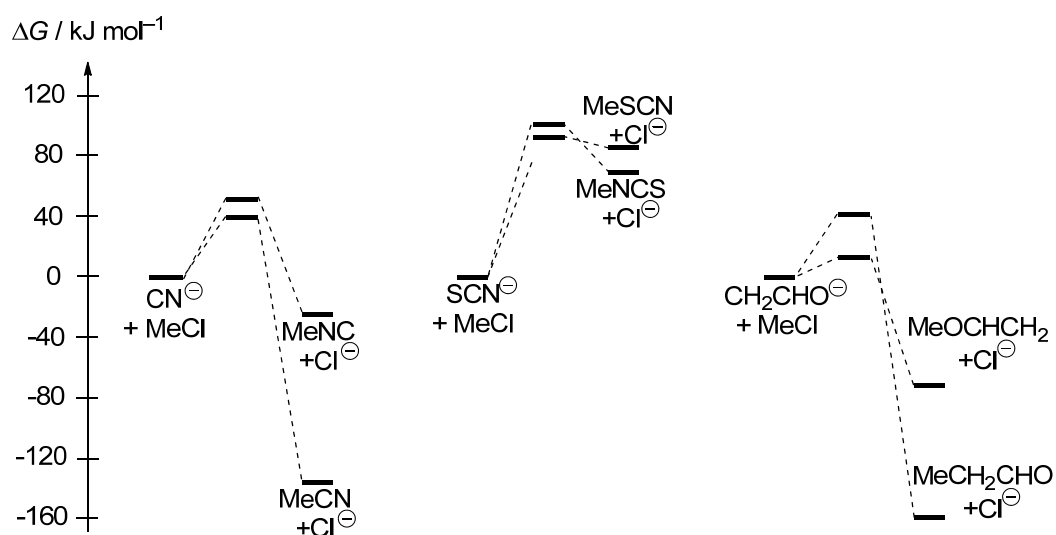


Figure 1: Gibbs energy profiles for the methylation of ambident nucleophiles with methyl chloride in the gas phase [G3(+)].

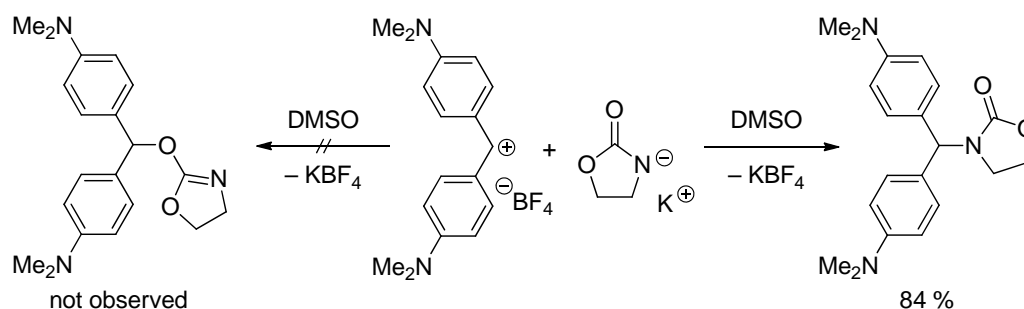
It is shown that the ΔG^0 term in the Marcus equation favors *C*-attack at cyanide, while *N*-attack is preferred by the intrinsic barrier (ΔG_0^\ddagger). As the difference of the intrinsic terms is much smaller than the difference in the reaction free energies ($\Delta\Delta G^0$), free cyanide ions preferentially react with the carbon atom.

In reactions of SCN^- , *N*-attack is preferred by the thermodynamic term $\Delta\Delta G^0$, while the attack at the sulfur terminus is preferred intrinsically. As the $\Delta\Delta G^0$ -term for *S*- and *N*-attack of thiocyanate is rather small, kinetically controlled alkylations of SCN^- occur preferentially at the intrinsically preferred sulfur atom.

For enolates, the product stability term ($\Delta\Delta G^0$) highly favors *C*-attack over *O*-attack. However, the significantly higher intrinsic barrier for *C*-attack compensates this effect and as a result, enolates are either attacked at oxygen or carbon in kinetically controlled reactions, depending on the “freeness” of the enolate anion.

3 Nucleophilic Reactivities of Imide and Amide Anions

The reactions of several amide and imide anions with benzhydrylium ions and structurally related quinone methides have been studied kinetically by UV-Vis spectroscopy in DMSO and in acetonitrile solution. ^1H - and ^{13}C -NMR spectroscopy revealed that in all cases examined in this work, amides are formed exclusively (*N*-attack) and no traces of imidates (*O*-attack) were observed (Scheme 2). Therefore, Kornblum’s interpretation of the ambident reactivity of amide anions – greater $\text{S}_{\text{N}}1$ character leads to more *O*-attack – needs to be revised.



Scheme 2: Exemplary reaction of an amide anions with the bis-(4,4'-dimethylamino) benzhydrylium ion in DMSO yielding only the product of *N*-attack.

The second-order rate constants ($\log k_2$) for these reactions correlate linearly with the electrophilicity parameters E of the electrophiles according to the correlation equation [Eq. (3)], allowing us to determine the nucleophilicity parameters N and s for these nucleophiles (Figure 2).

$$\log k_2 = s(N + E) \quad (3)$$

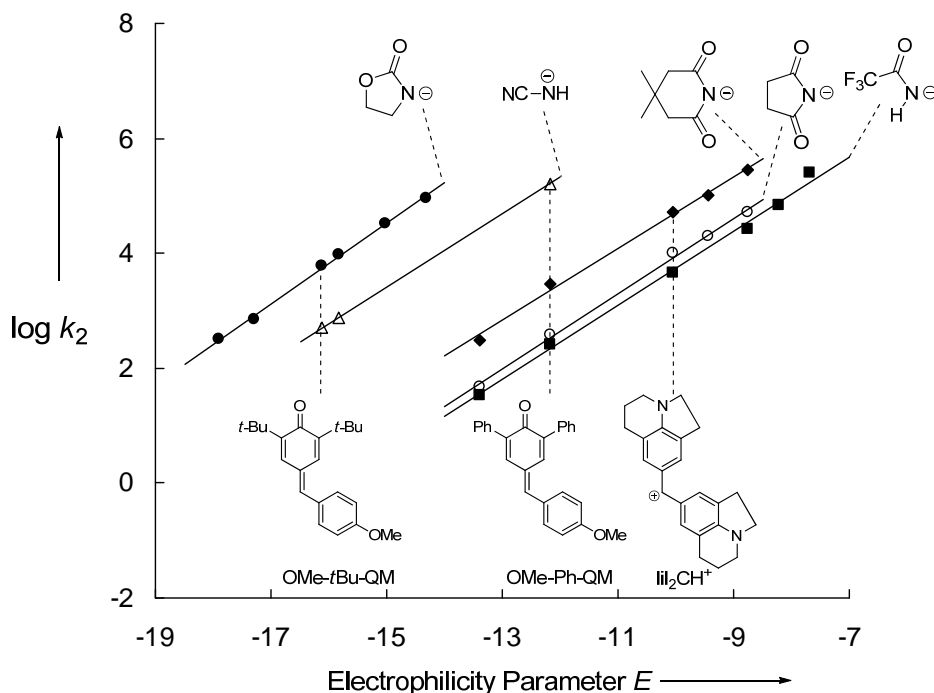


Figure 2: Plots of the rate constants $\log k_2$ of the reactions of imide and amide anions with reference electrophiles in DMSO versus their electrophilicity parameters E .

The comparison of imide anions with the structurally related carbanions in Figure 3 shows that similar stabilizing effects of imide anions are found for acetyl and ethoxycarbonyl substituents, whereas acetyl groups stabilize carbanions better than ethoxycarbonyl groups.

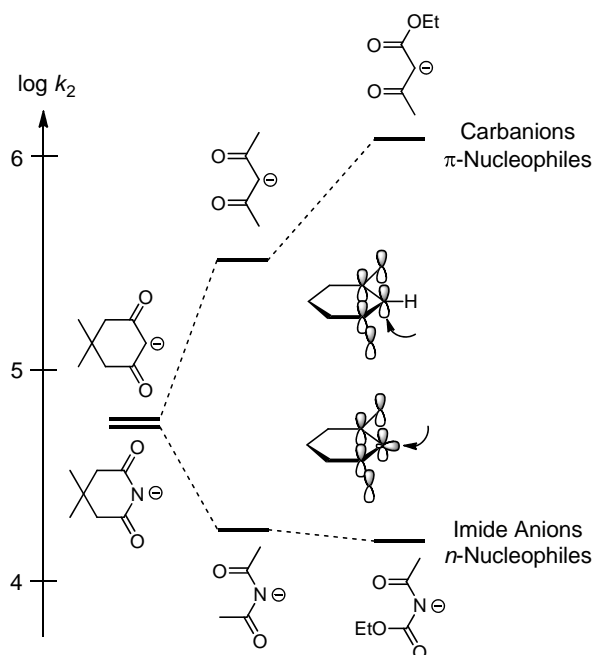
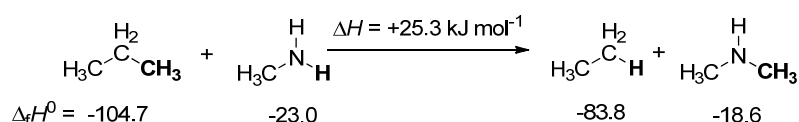


Figure 3: Comparison of the nucleophilic reactivities of structurally related imide anions and carbanions towards the benzhydrylium ion lil_2CH^+ (20 °C; DMSO; for structure of lil_2CH^+ see Figure 2).

Furthermore, it was found that amide and imide anions are less reactive than carbanions of the same pK_{aH} . These effects can be explained by the reaction shown in Scheme 3, which illustrates that the proton prefers nitrogen while the CH_3 group prefers carbon. Therefore, carbanions that have a similar affinity towards protons as amide anions (comparable pK_{aH}) have a higher affinity towards carbon that is also reflected by the kinetics, i.e., by higher k_2 values.



Scheme 3: Reaction enthalpy (gas phase, in kJ mol^{-1}) for the methyl-hydrogen-exchange between carbon and nitrogen.

Figure 4 shows that the investigated sulfonamide and diacylimide anions cover a similar reactivity range in DMSO ($15 < N < 22$) as acceptor-stabilized carbanions. Phthalimide and maleimide anions have similar nucleophilicities in DMSO as primary alkylamines and are weaker nucleophiles than secondary alkylamines, although the amide anions are significantly stronger bases.

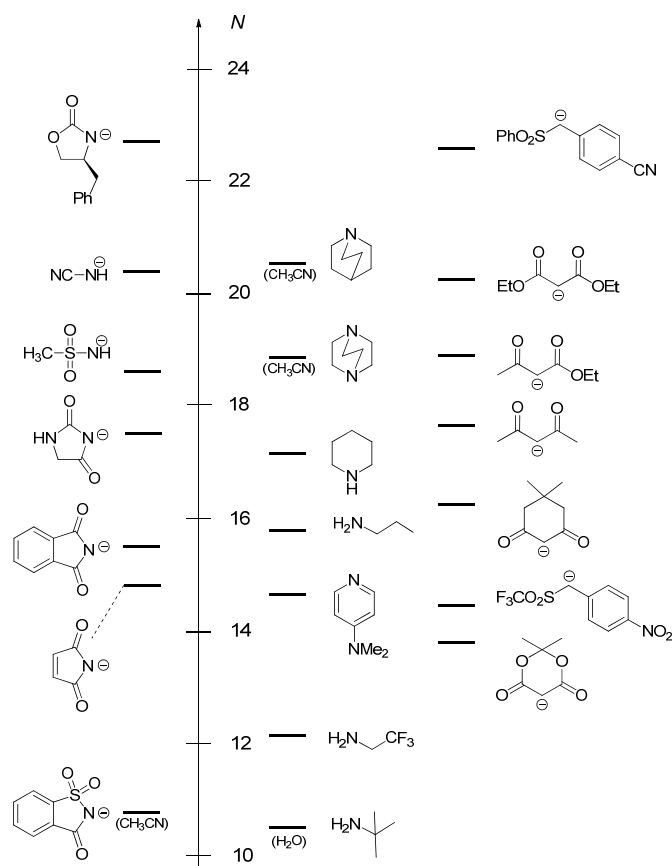
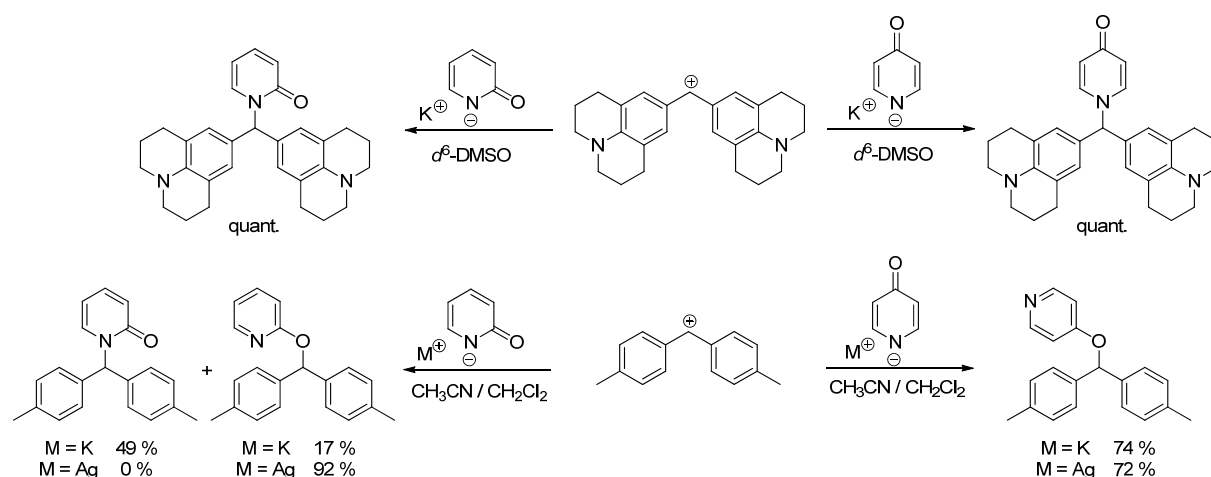


Figure 4: Comparison of the nucleophilicity parameters N of imide and amide anions with those of other C- and N-nucleophiles in DMSO (unless stated otherwise).

4 Ambident Reactivities of Pyridone Anions

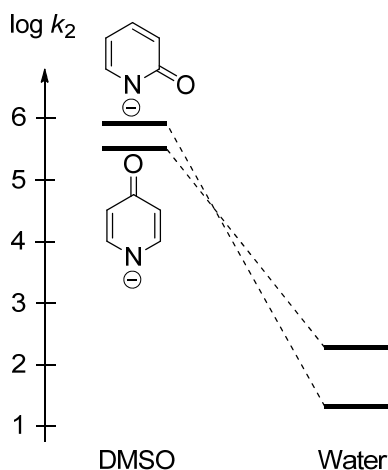
The kinetics of the reactions of the ambident 2- and 4-pyridone anions with benzhydrylium ions and structurally related Michael acceptors have been studied in DMSO, in CH₃CN, and in water. The reactions with stabilized amino-substituted benzhydrylium ions and Michael acceptors are reversible and yield the thermodynamically more stable *N*-substituted pyridones exclusively. In contrast, highly reactive benzhydrylium ions (e.g., the 4,4'-dimethylbenzhydrylium ion), which react with these nucleophiles diffusionally limited, give mixtures arising from *N*- and *O*-attack with the 2-pyridone anion and only *O*-substituted products with the 4-pyridone anion (Scheme 4). Complete suppression of the *N*-attack in the 2-pyridone series can be obtained when the silver salt of the 2-pyridone was employed.



Scheme 4: Reactions of the pyridone anions with benzhydrylium ions of different reactivity.

No significant changes of the rate constants were found when the counterion was varied (Li⁺, K⁺, Bu₄N⁺) or the solvent was changed from DMSO to CH₃CN, whereas a large decrease of nucleophilicity was observed in aqueous solution (Scheme 5).

Linear correlations of the second-order rate constants ($\log k_2$) with the electrophilicity parameters E of the electrophiles allowed us to determine the nucleophilicity parameters N and s for the pyridone anions according to the correlation equation [Eq. (3)]. Rate and equilibrium constants showed that the 2-pyridone anion is a just 2 – 4 times stronger nucleophile, but a 100 times stronger Lewis base than the 4-pyridone anion.



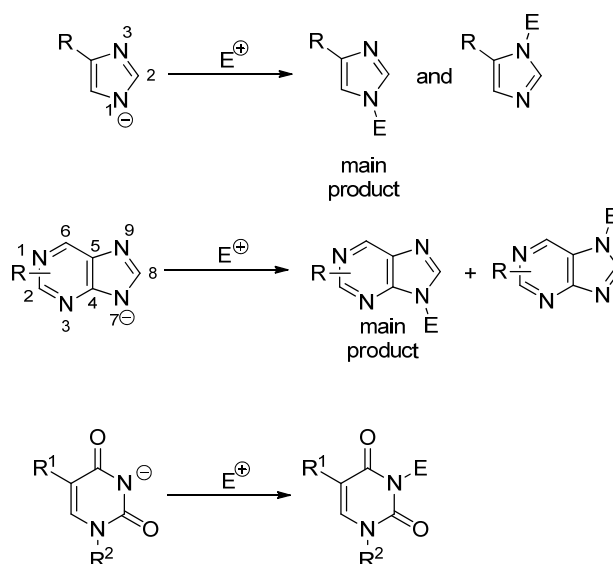
Scheme 5: Solvent dependence of the rate constant of the reactions of pyridone anions with LiCH_2^+ (see Figure 2 for structure) at 20 °C.

Consistent with Hoz' rule, quantum chemical calculations at MP2/6-311+G(2d,p) level of theory showed that the attack at oxygen is intrinsically favored, while the attack at nitrogen gives rise to the thermodynamically more stable products.

Marcus theory was employed to develop a consistent scheme which rationalizes the manifold of regioselectivities previously reported for the reactions of these anions with electrophiles. In particular, Kornblum's rationalization of the silver ion effect, one of the main pillars of the hard and soft acid base concept of ambident reactivity, has been revised.

5 Ambident Reactivities of the Anions of Nucleobases and their Subunits

The reactions of the anions of imidazoles, purines, and pyrimidines with benzhydrylium ions and quinone methides have been studied kinetically in DMSO and in aqueous solutions. Product analyses revealed that the anions of pyrimidines are selectively attacked at nitrogen by the studied electrophiles, and typically *N1*- or *N7*-alkylation dominated for the anions of imidazoles and purines (Scheme 6). The linear correlations of the second-order rate constants ($\log k_2$) for the reactions of the heterocyclic anions with the reference electrophile against the electrophilicity parameters E enabled us to determine the nucleophilicity parameters N and s for these nucleophiles (Figure 6).



Scheme 6: Products of the reactions of the heterocyclic anions (for detailed structures see Figure 6) with the reference electrophiles in DMSO.

A change of solvent from DMSO to water results in approximately 10000 times slower reactions of the anions of pyrimidines, whereas only a factor of 500 – 5000 is found for the anions of imidazoles and purines (Figure 6). Furthermore, the anionic heterocycles are approximately 20000 times more reactive than their neutral analogues in DMSO or in acetonitrile solution (Figure 5).

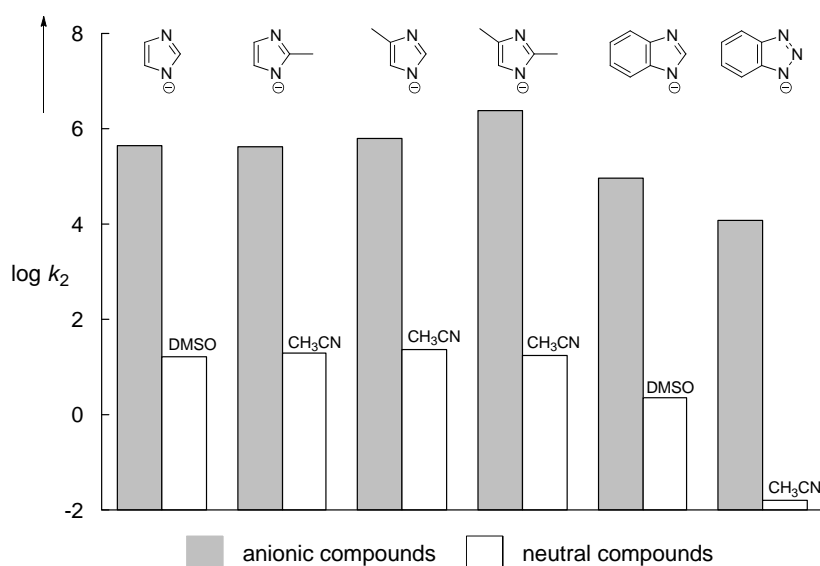
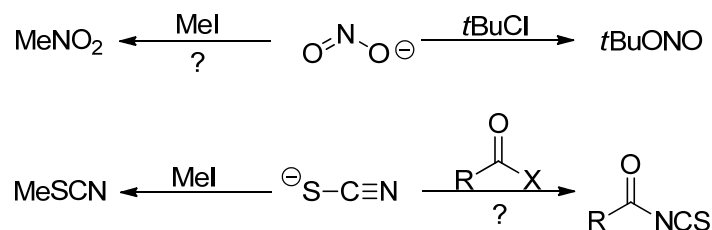


Figure 5: Comparison of the second-order rate constants of the reaction of IiI_2CH^+ (see Figure 2 for structure) with either the heterocyclic anions or with their neutral analogues in DMSO or CH_3CN .

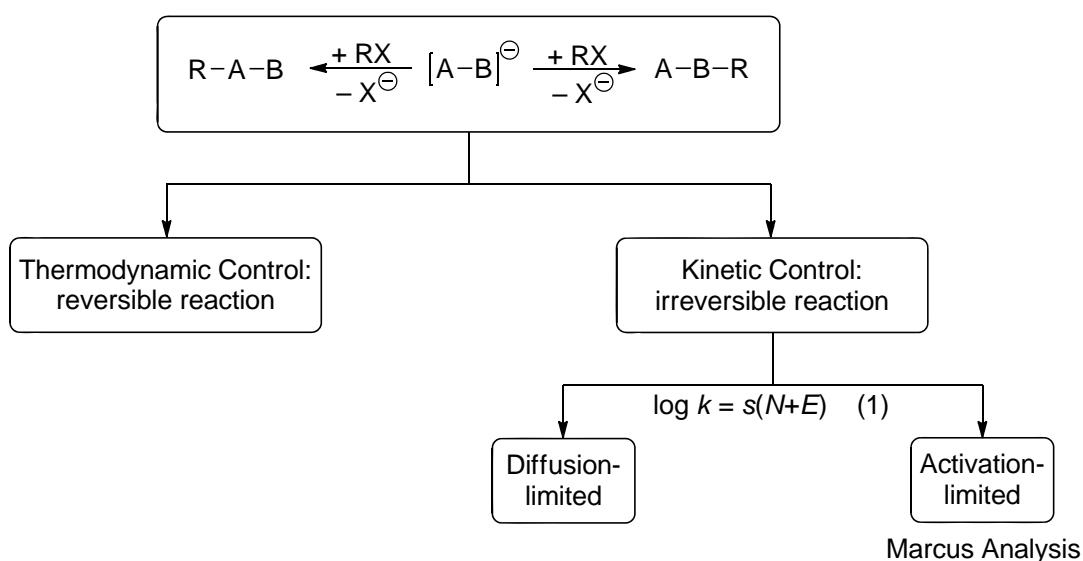
Klopman justified the need for a general treatment of chemical reactivity, which led to the concept of charge- and frontier-orbital-controlled reactions with the need to explain “*why a given reagent attacks a particular position and another reagent a different one, e.g.,:*”



Scheme 7: Reactions used by Klopman to develop his concept of charge- and orbital-controlled reactions.

Ironically, the two examples which Klopman selected as a motivation for developing his concept do not proceed as postulated in Scheme 7. Methyl iodide gives a mixture of nitromethane and methyl nitrite, and seven years before Klopman’s work, Ruske provided evidence that SCN^- is attacked by acyl chlorides at sulfur to give acyl thiocyanates which may rearrange to the corresponding isothiocyanates under certain conditions.

We now suggest abandoning the HSAB principle and the related Klopman-Salem concept of charge- and orbital-controlled reactions as guides for predicting ambident reactivity and to replace them by the approach depicted in Scheme 8.



Scheme 8: A systematic approach to ambident reactivity.

A systematic approach to ambident reactivity has been based on Scheme 8. In the first step, it should always be analyzed whether the isolated products are the result of kinetic or thermodynamic control. In the case of kinetic product control, one has to examine whether the reactions proceed with or without activation energy. As most ambident anions analyzed in this thesis undergo diffusion controlled reactions with carbocations, which are less stabilized than the tritylium ion, transition state models are inappropriate to rationalize the resulting regioselectivities. Eventually, Marcus theory which calculates the Gibbs energy of activation ΔG^\ddagger from the Gibbs energy of reaction ΔG^0 and the intrinsic barrier ΔG_0^\ddagger has been shown suitable for rationalizing the regioselectivities of kinetically controlled reactions proceeding over activation barriers. It has been shown that relative magnitudes of intrinsic barriers can be derived from Hoz' rule which states that the further right the center of nucleophilicity is located in the periodic table, the lower is the intrinsic barrier.

Chapter 2: Introduction

1 General

Most synthetically used reactions in organic chemistry can be rationalized by combinations of electron-deficient compounds with reagents having a surplus of electrons. Much of our contemporary understanding of these reactions is based on Lewis' work on valence electron theory^[1] and the acid-base-theories of Brønsted^[2] and Lowry.^[3] In the 1930s, Ingold replaced Lapworth's^[4] older notation of "cationoid" and "anionoid" systems and called electron-deficient compounds "electrophiles" and electron-rich species "nucleophiles".^[5]

A very important class of nucleophiles are molecules that can react via different atoms and the control of their reactivities is of crucial importance for organic chemistry.^[6] The development of nucleophilicity scales (among others by Swain and Scott^[7] or Ritchie^[8]) contributed much to our understanding of the regioselectivities of nucleophiles with independent reactive sites, so-called ambifunctional nucleophiles (e.g., ethanolamine or mercaptophenol). In contrast, the regioselectivities of connected nucleophilic sites (e.g., two termini of a mesomeric structure) cannot be explained as easily.

The first approach to rationalize the reactivities of these compounds was reported by Kornblum in 1955.^[9] He concluded on the basis of studies of the reactions of metal nitrites with alkyl halides that the attack at the nitrogen atom will be preferred, if the transition state of the reaction is S_N2-like. In contrast, the attack at oxygen predominately occurs in S_N1-type reactions. He also suggested calling this class of anions "ambident nucleophiles" and this definition still holds today. According to the IUPAC, ambident nucleophiles consist of two (or more) alternative and strongly interacting distinguishable reactive centers which all can undergo the reaction. However, when the reaction occurs at either site, it generally stops or greatly retards a subsequent attack at the other sites.^[10]

In the following years, Kornblum's rationalization was implemented in different concepts trying to explain ambident reactivity, such as Pearson's principle of hard and soft acids and bases of the related Klopman-Salem concept of charge- and orbital-controlled reactions.

2 The Principle of Hard and Soft Acids and Bases (HSAB)

A more general approach for explaining ambident reactivity can be derived from Pearson's concept of hard and soft acids and bases (HSAB).^[11] This principle employs Lewis' concept of acids and bases that considers acids as electron-acceptors and bases as electron-donors.

Later, Ahrland, Chatt, and Davies^[12] as well as Schwarzenbach^[13] divided Lewis acids in two categories: Class *a* (later to be the hard acids) forms the most stable complexes with electron-donors of the first row of the periodic table (N, O, and F), while class *b* (later the soft acids) gives the most stable adducts with elements of the other rows (P, S, Cl, Br, and I). This approach also includes the earlier observations of Berzelius that certain metal ions tend to occur in nature as sulfides, while others occur predominantly as oxides, carbonates, sulfates, or silicates.^[14]

Pearson generalized these quantitative aspects from further studies of Lewis-acid-base reactions in the 1960s, where a Lewis acid A (an electron acceptor) reacted with a Lewis base B (an electron donor) to give the acid-base complex A-B [Eq. (1)].^[11a] As the reaction product can either be an organic or inorganic molecule or a complex ion, the scope of this investigation included most chemical fields.

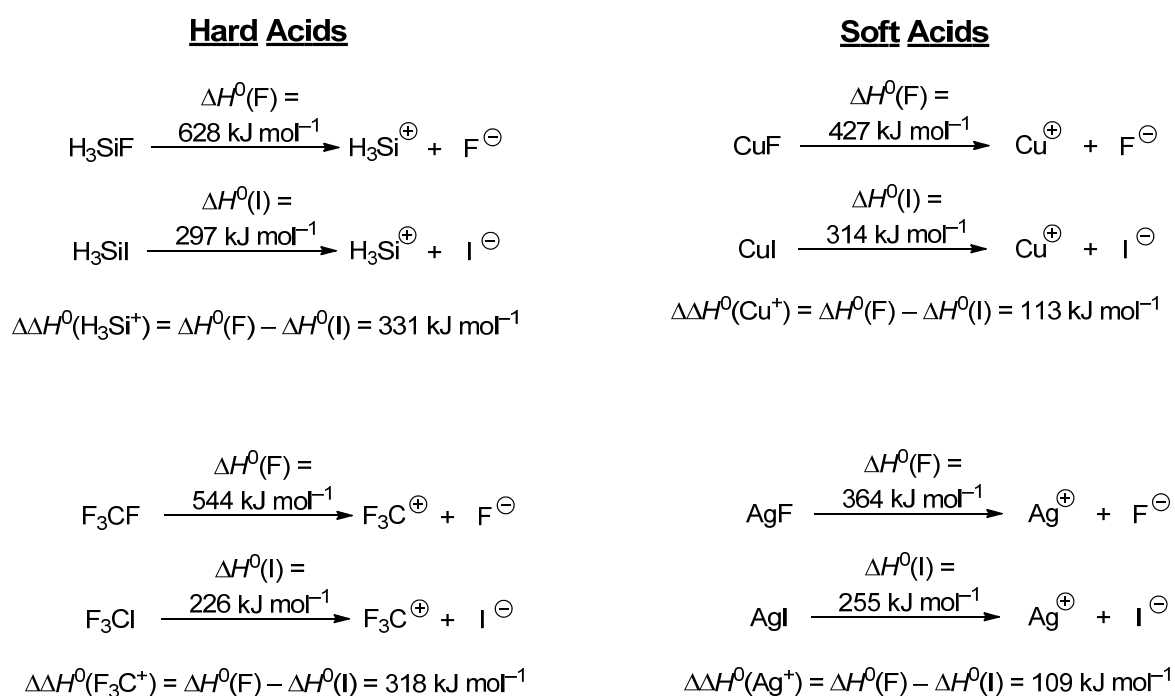


As hard-hard and soft-soft interactions gave rise to very negative ΔH^0 values and hard-soft combinations resulted in less exothermic reactions, the reaction partners were classified as hard or soft acids and bases according to the magnitude of ΔH^0 (Table 1). The tenet of the HSAB principle that hard acids prefer to react with hard bases, while soft acids prefer to react with soft bases was first introduced into inorganic chemistry,^[11b] and later into organic chemistry as well.^[11d]

Table 1: Classification of Acids and Bases According to Pearson.^[7g]

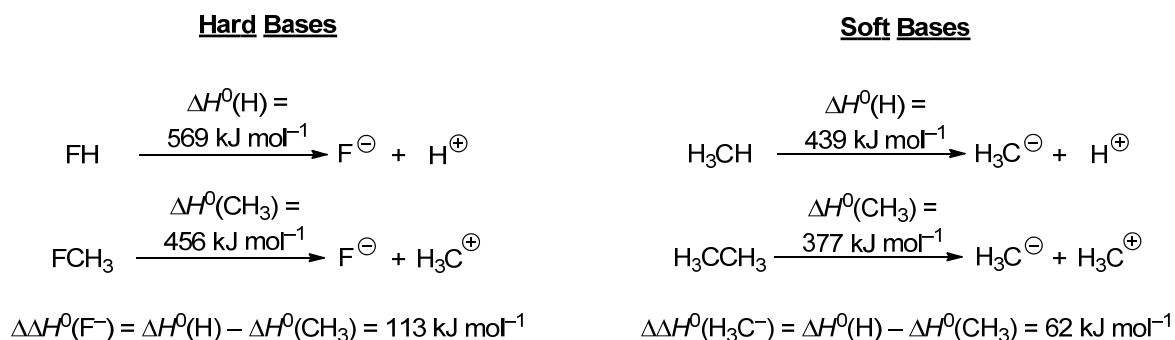
	Acids	Bases
hard	H ⁺ , Li ⁺ , Na ⁺ , K ⁺ , Be ²⁺ , Mg ²⁺ , Ca ²⁺ , Sn ²⁺ , Al ³⁺ , Se ³⁺ , Ga ³⁺ , Fe ³⁺ , Ti ⁴⁺ , R ₃ C ⁺ , CO ₂	H ₂ O, OH ⁻ , F ⁻ , CH ₃ CO ₂ ⁻ , NH ₃ , SO ₄ ²⁻ , Cl ⁻ , CO ₃ ²⁻ , ROH, RO ⁻
soft	Cu ⁺ , Ag ⁺ , Au ⁺ , Cs ⁺ , Cd ²⁺ , Pd ²⁺ , Pt ²⁺ , Hg ²⁺ , I ₂ , quinones	RS ⁻ , RSH, I ⁻ , SCN ⁻ , CO, H ⁻ , R ⁻

Later, these classifications were substantiated by an empirical hardness scale. Lewis acids were ranked according to the differences of the gas phase dissociation enthalpies $\Delta\Delta H^0$ of their adducts with the hard fluoride anion (MF) or with the soft iodide anion (MI). The differences of the gas phase dissociation enthalpies of $\text{H}_3\text{Si-F}$ and $\text{H}_3\text{Si-I}$ ($\Delta\Delta H^0 = 331 \text{ kJ mol}^{-1}$) as well as between $\text{F}_3\text{C-F}$ and $\text{F}_3\text{C-I}$ ($\Delta\Delta H^0 = 318 \text{ kJ mol}^{-1}$) were found to be rather large, which was rationalized by the hardness of H_3Si^+ and F_3C^+ . On the other hand, relatively small enthalpy differences were found for the dissociation of CuF and CuI ($\Delta\Delta H^0 = 113 \text{ kJ mol}^{-1}$) as well as for the dissociation of AgF and AgI ($\Delta\Delta H^0 = 109 \text{ kJ mol}^{-1}$), which was attributed to the softness of Cu^+ and Ag^+ (Scheme 1).^[11h]



Scheme 1: Gas phase dissociation energies of fluorides and iodides of singly charged cations as a measure for hardness and softness.

A similar analysis can also be employed to characterize Lewis bases. In this case, H^+ and CH_3^+ were chosen to be the reference acids, with H^+ being the harder one. Again, large differences in dissociation enthalpies (Scheme 2) were correlated with hardness (e.g., enthalpy difference between F-H and F-CH_3 : $\Delta\Delta H^0 = 113 \text{ kJ mol}^{-1}$), while small enthalpy differences were associated with soft bases (e.g., CH_3^- enthalpy difference between $\text{H}_3\text{C-H}$ and $\text{H}_3\text{C-CH}_3$: $\Delta\Delta H^0 = 62 \text{ kJ mol}^{-1}$).^[11h]



Scheme 2: Gas phase dissociation energies as a measure for hardness and softness of Lewis bases.

As a rule of thumb, hard acids are small, highly positively charged, and not polarizable, while hard bases are also small, electronegative, and highly oxidized.^[15] However, the hardness of bases is in general independent of the charge, i.e., H_2O and HO^- are comparable in hardness.

On the basis of these experimental observations, an empirical parameter η called the absolute or chemical hardness was introduced. According to Eq. (2), the absolute hardness η can be calculated from the ionization energy IE and the electron affinity EA . Similarly, the absolute softness σ can be considered as the reciprocal of η .

$$\eta = 0.5 (IE - EA) \quad (2)$$

As the proton does not possess an ionization potential, it can be considered as the hardest acid with $\eta = \infty$ and Table 2 summarizes the absolute hardness η for selected compounds. As ionization energies and electron affinities can easily be obtained from DFT calculations, Eq. (2) is presently the most commonly used scale to define chemical hardness.

Table 2: Absolute Hardness (in eV) for Selected Compounds.^[16]

Compound	η	Compound	η
H^+	∞	F^-	7.0
Al^{3+}	45.8	Cu^+	6.3
Li^+	35.1	OH^-	5.7
K^+	13.6	CN^-	5.1
Zn^{2+}	10.9	Cl^-	4.7
H_2O	9.5	I^-	3.7

3 The Klopman-Salem-Equation

Employing perturbation theory, Klopman and Salem derived a three-terms-expression for the energy difference for the overlapping of the orbitals of two reactants.^[17] The first term of the Klopman-Salem-equation (3) considers the interactions of filled orbitals of one molecule with filled orbitals of the other and is called closed-shell repulsion term. This is a repulsive interaction and usually accounts for the largest contribution to the energy. The second term represents the Coulombic attraction or repulsion between the different atoms which is attributed to the charge distribution in both molecules. The third term includes the interactions of filled orbitals with unfilled ones of correct symmetry (HOMO-LUMO interactions) and will be of special importance if the Coulombic interaction is small.

$$\Delta E = \underbrace{-\sum_{ab} (q_a + q_b) \beta_{ab} S_{ab}}_{\text{closed-shell repulsion}} + \underbrace{\sum_{k < l} \frac{Q_k Q_l}{\epsilon R_{kl}}}_{\text{Coulomb interaction}} + \underbrace{\sum_r^{\text{occ}} \sum_s^{\text{unocc}} - \sum_s^{\text{occ}} \sum_r^{\text{unocc}} \frac{2(\sum_{ab} c_{ra} c_{sb} \beta_{ab})^2}{E_r - E_s}}_{\text{HOMO-LUMO interaction}} \quad (3)$$

q_a and q_b :	electron population in atomic orbitals a and b	R_{kl} :	distance between atoms k and l
β and S :	resonance and overlap integrals	c_{ra} and c_{sb} :	coefficient of atomic orbitals a and b in molecular orbitals r and s
Q_k and Q_l :	total charges on atoms k and l	E_r and E_s :	Energy of molecular orbitals r and s
ϵ :	local dielectric constant		

According to this concept, hard nucleophiles possess a low-energy HOMO (highest occupied molecular orbital) and a negative charge, while soft nucleophiles usually have a high-energy HOMO and do not necessarily bear a negative charge. In contrast, hard electrophiles have a high-energy LUMO (lowest unoccupied molecular orbital) and a positive charge, while soft electrophiles are typically neutral compounds with a low-energy LUMO.^[18]

Hard-hard reactions proceed fast due to the large Coulombic attraction and should be charge-controlled. Soft-soft reactions are also fast because of the larger interaction between the HOMO of the nucleophiles and the LUMO of the electrophile and should therefore occur orbital-controlled.

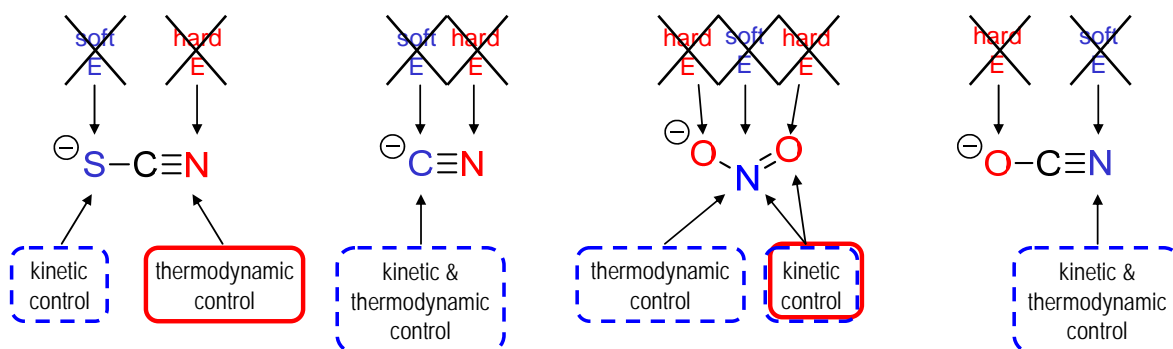
4 HSAB-Treatment of Ambident Nucleophiles

Ambident reactivity has commonly been rationalized on the basis of Pearson's principle of hard and soft acids and bases (HSAB) or, more quantitatively, on the basis of the Klopman-Salem concept of charge and frontier orbital controlled reactions. These concepts predict that hard electrophiles will preferentially be attacked by the harder part of the ambident nucleophiles, i.e., by *N*-attack of CN^- and SCN^- or by *O*-attack of OCN^- , NO_2^- , and enolates. In contrast, the softer part of these nucleophiles should attack soft electrophiles. Most canonical organic textbooks adapted this interpretation as illustrated by a quotation from the latest edition of March's Advanced Organic Chemistry:^[16]

“The principle of hard and soft acids and bases states that hard acids prefer hard bases and soft acids prefer soft bases. In an S_N1 mechanism, the nucleophile attacks a carbocation, which is a hard acid. In an S_N2 mechanism, the nucleophile attacks the carbon atom of a molecule, which is a softer acid. The more electronegative atom of an ambident nucleophile is a harder base than the less electronegative atom. We may thus make the statement: As the character of a given reaction changes from S_N1 - to S_N2 -like, an ambident nucleophile becomes more likely to attack with its less electronegative atom. Therefore, changing from S_N1 to S_N2 conditions should favor C attack by CN^- , N attack by NO_2^- , C attack by enolate or phenoxide ions, etc.”

Already in 1976, Gompper and Wagner pointed out that the HSAB-concept does not differentiate between thermodynamic and kinetic control, although it has long been known that often different products are formed under these conditions.^[19]

During the last years, Mayr and co-workers showed that the reactivities of the prototype ambident nucleophiles like thiocyanate,^[20] cyanide,^[21] nitrite,^[22] or cyanate^[23] are not correctly described by the HSAB principle or the related Klopman-Salem model (Scheme 3). Thiocyanate and cyanide anions are preferentially attacked at the softer *S*- or *C*-terminus by hard and soft electrophiles. It was concluded that absolute rate constants and not the absolute hardness are needed to predict regioselectivities. Nitrite ions undergo diffusion-controlled reactions with all carbocations that are less stabilized than the tritylium ion with the result that attempts to describe reactivity with classical transition state models must be obsolete.



Scheme 3: Failure of the HSAB principle to correctly predict the regioselectivities of the reactions of hard and soft electrophiles E with some prototypes of ambident nucleophiles.

5 Problem Statement

As it was not even possible to explain the reactivities of the prototypes of ambident nucleophiles in terms of the HSAB principle, this thesis set out to search for a new model explaining ambident reactivity. Detailed studies of the reactions of several classes of ambident nucleophiles, like amide and imide anions, pyridone anions, or the biologically important anions of nucleobases and their subunits, with benzhydrylium ions and structurally related quinone methides should give insights into their ambident behavior. For that purpose, the kinetics of these reactions should be analyzed applying the linear free-energy relation [Eq. (4)], which was shown to hold for the reactions of n -nucleophiles (alcohols, amines, etc.), π -nucleophiles (alkenes, arenes, etc.), and σ -nucleophiles (hydrides) with benzhydrylium ions and structurally related Michael acceptors.^[24] According to Eq. (4), the nucleophilicity parameters N and s of these compounds can be calculated from the second-order rate constants k_2 of these reactions and the electrophilicity parameter E .

$$\log k_2 = s(N + E) \quad (4)$$

As benzhydrylium ions and structurally related quinone methides can be used as electrophiles with tunable reactivity,^[24c] it should be possible to study the change of regioselectivity in activation and diffusion-controlled reactions.

A theoretical investigation of the role of the intrinsic barriers in ambident reactions should additionally give a deeper understanding of the regioselectivities of these systems. Finally, using these results, a consistent rationalization of ambident reactivity should be developed in

terms of Marcus theory,^[25] which is also applicable to older experimental data from the literature.

As most parts of this thesis have already been published or submitted for publication, individual introductions will be given at the beginning of each chapter. In order to identify my contributions to the multi-author publications, the Experimental Sections exclusively report of the experiments performed by me.

6 References

- [1] G. N. Lewis, *Valence and the structure of atoms and molecules*, The Chemical Catalog Co., **1923**.
- [2] J. N. Brønsted, *Recl. Trav. Chim. Pays-Bas* **1923**, *42*, 718-728.
- [3] T. M. Lowry, *Chem. Ind.* **1923**, *42*, 43-47.
- [4] a) A. Lapworth, *Mem. Manchester. Lit. Phil. Soc.* **1920**, *64*, 1-16; b) A. Lapworth, *Nature* **1925**, *115*, 625.
- [5] a) C. K. Ingold, *J. Chem. Soc.* **1933**, 1120-1128; b) C. K. Ingold, *Chem. Rev.* **1934**, *15*, 225-274.
- [6] a) S. Hünig, *Angew. Chem.* **1964**, *76*, 400-412; *Angew. Chem. Int. Ed. Engl.* **1964**, *3*, 548-560; b) R. Gompper, *Angew. Chem.* **1964**, *76*, 412-423; *Angew. Chem. Int. Ed. Engl.* **1964**, *3*, 560-570; c) A. R. Katritzky, M. Piffl, H. Lang, E. Anders, *Chem. Rev.* **1999**, *99*, 665-722.
- [7] C. G. Swain, C. B. Scott, *J. Am. Chem. Soc.* **1953**, *75*, 141-147.
- [8] C. D. Ritchie, *Acc. Chem. Res.* **1972**, *5*, 348-354.
- [9] N. Kornblum, R. A. Smiley, R. K. Blackwood, D. C. Iffland, *J. Am. Chem. Soc.* **1955**, *77*, 6269-6280.
- [10] P. Müller, *Pure Appl. Chem.* **1994**, *66*, 1077-1184.
- [11] a) J. O. Edwards, R. G. Pearson, *J. Am. Chem. Soc.* **1962**, *84*, 16-24; b) R. G. Pearson, *J. Am. Chem. Soc.* **1963**, *85*, 3533-3539; c) R. G. Pearson, *Science* **1966**, *151*, 172-177; d) R. G. Pearson, J. Songstad, *J. Am. Chem. Soc.* **1967**, *89*, 1827-1836; e) R. G. Pearson, *J. Chem. Educ.* **1968**, *45*, 581-587; f) R. G. Pearson, *J. Chem. Educ.* **1968**, *45*, 643-648; g) R. G. Pearson, *J. Am. Chem. Soc.* **1988**, *110*, 7684-7690; h) R. G. Pearson, *Chemical Hardness*, Wiley-VCH, Weinheim, **1997**.
- [12] S. Ahrland, J. Chatt, N. R. Davies, *Quart. Revs.* **1958**, *12*, 265-276.

- [13] a) G. Schwarzenbach, in *Adv. Inorg. Chem. Radiochem., Vol. Volume 3* (Eds.: H. J. Emeleus, A. G. Sharpe), Academic Press, **1961**, pp. 257-285; b) G. Schwarzenbach, M. Schellenberg, *Helv. Chim. Acta* **1965**, *48*, 28-46.
- [14] G. Wulfsberg, *Inorganic Chemistry*, University Science Books, Sausalito, CA, **2000**.
- [15] A. F. Holleman, E. Wiberg, *Lehrbuch der anorganischen Chemie*, de Gruyter, Berlin, **1995**.
- [16] M. B. Smith, J. March, *March's Advanced Organic Chemistry: Reactions, Mechanisms, and Structure*, 6th ed., Wiley, Hoboken, **2007**.
- [17] a) G. Klopman, *J. Am. Chem. Soc.* **1968**, *90*, 223-234; b) L. Salem, *J. Am. Chem. Soc.* **1968**, *90*, 543-552.
- [18] I. Fleming, *Molecular Orbitals and Organic Chemical Reactions; Student Edition*, John Wiley & Sons, Chichester, **2009**.
- [19] R. Gompper, H. U. Wagner, *Angew. Chem.* **1976**, *88*, 389-401; *Angew. Chem. Int. Ed. Engl.* **1976**, *15*, 321-333.
- [20] R. Loos, S. Kobayashi, H. Mayr, *J. Am. Chem. Soc.* **2003**, *125*, 14126-14132.
- [21] A. A. Tishkov, H. Mayr, *Angew. Chem.* **2005**, *117*, 145-148; *Angew. Chem. Int. Ed.* **2005**, *44*, 142-145.
- [22] A. A. Tishkov, U. Schmidhammer, S. Roth, E. Riedle, H. Mayr, *Angew. Chem.* **2005**, *117*, 4699-4703; *Angew. Chem. Int. Ed.* **2005**, *44*, 4623-4626.
- [23] H. F. Schaller, U. Schmidhammer, E. Riedle, H. Mayr, *Chem. Eur. J.* **2008**, *14*, 3866-3868.
- [24] a) H. Mayr, M. Patz, *Angew. Chem.* **1994**, *106*, 990-1010; *Angew. Chem. Int. Ed. Engl.* **1994**, *33*, 938-957; b) H. Mayr, T. Bug, M. F. Gotta, N. Hering, B. Irrgang, B. Janker, B. Kempf, R. Loos, A. R. Ofial, G. Remennikov, H. Schimmel, *J. Am. Chem. Soc.* **2001**, *123*, 9500-9512; c) H. Mayr, B. Kempf, A. R. Ofial, *Acc. Chem. Res.* **2003**, *36*, 66-77; d) H. Mayr, A. R. Ofial, *Pure Appl. Chem.* **2005**, *77*, 1807-1821.
- [25] R. A. Marcus, *Pure Appl. Chem.* **1997**, *69*, 13-29.

Chapter 3: Marcus-Analysis of Ambident Reactivity

Martin Breugst, Hendrik Zipse, J. Peter Guthrie, and Herbert Mayr

Angew. Chem. **2010**, *122*, 5291–5295; *Angew. Chem. Int. Ed.* **2010**, *49*, 5165–5169.

1 Introduction

Pearson's principle of hard and soft acids and bases (HSAB)^[1] and the related Klopman-Salem concept of charge and frontier controlled reactions^[2] has been considered to provide a consistent rationalization of ambident reactivity. In a series of experimental investigations we have shown, however, that the reactivities of SCN⁻,^[3] CN⁻,^[4] NO₂⁻,^[5] OCN⁻,^[6] R₂C=NO₂⁻,^[7] and PhSO₂⁻,^[8] that is, the typical ambident nucleophiles, cannot be described by these concepts. In the cited articles,^[3–8] we quoted older experimental studies that had already indicated the inconsistency of applying the HSAB principle. In the new edition of his groundbreaking monograph,^[9] Fleming has accepted our analysis, and referred to “*other factors which are at work*” which are responsible for the failure of HSAB predictions. As a model which fails in more than 50 % of cases, it eventually has to be abandoned; therefore we have searched for a more consistent rationalization of ambident reactivity and now suggest Marcus theory as the better alternative.

Marcus theory^[10] and related concepts consider reactant and product nestling in a parabolic bowl, and the transition state is approximated as the point of intersection of the two bowls. For electron-transfer reactions, that is, the types of reactions that led to the formulation of the Marcus equation, the parabolic displacements refer to the movement of solvent molecules around the reactants and products. In the case of group-transfer reactions [Eq. (1)], which are depicted in Figure 1, a major contribution to the parabolic term comes from the A-X and B-X vibrations.^[10e]



The point of intersection of the two parabolas in Figure 1 can be expressed by the Marcus equation [Eq. (2)].

$$\Delta G^\ddagger = \Delta G_0^\ddagger + 0.5 \Delta G^0 + (\Delta G^0)^2 / 16 \Delta G_0^\ddagger \quad (2)$$

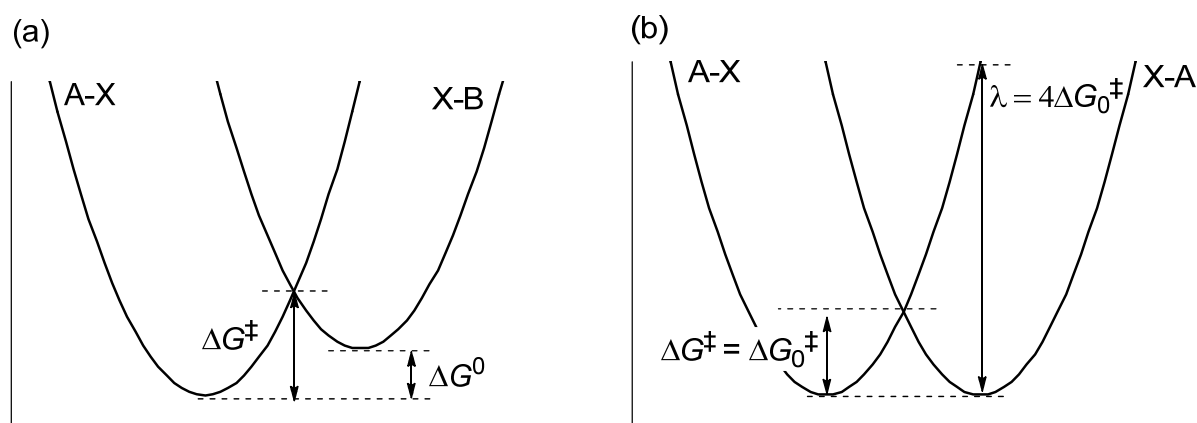
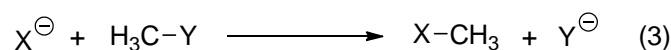


Figure 1: Definition of the intrinsic barrier ΔG_0^\ddagger for a) a non-identity reaction, and b) an identity reaction.

The Gibbs energy of activation, ΔG^\ddagger , is therefore expressed by a combination of the Gibbs energy of reaction, ΔG^0 , and the intrinsic barrier ΔG_0^\ddagger , which corresponds to ΔG^\ddagger of an identity reaction, where $\Delta G^0 = 0$ (Figure 1). In other words: ΔG_0^\ddagger reflects the kinetic contribution to ΔG^\ddagger from which the thermodynamic component has been eliminated. Marcus suggested calculating the intrinsic barrier of a non-identity reaction as the average of the two corresponding identity reactions.^[10c, 10d, 11]

2 Results and Discussion

Application of this so-called additivity principle to methyl transfer reactions yields equation (6), wherein the intrinsic barrier ΔG_0^\ddagger for the S_N2 reaction in equation (3) is calculated as the average of the activation energies of the identity reactions in equations (4) and (5).



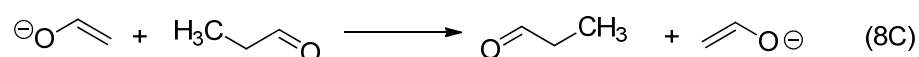
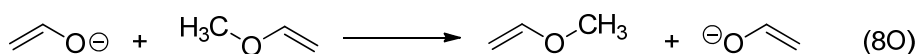
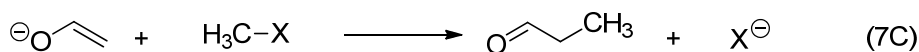
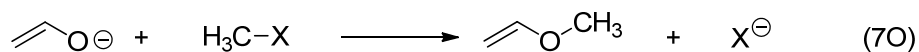
$$\Delta G_0^\ddagger [\text{Eq. (3)}] = 0.5(\Delta G_0^\ddagger [\text{Eq. (4)}] + \Delta G_0^\ddagger [\text{Eq. (5)}]) \quad (6)$$

The validity of this approach has been confirmed computationally and experimentally. Already in 1981, Wolfe, Mitchell, and Schlegel^[12] reported RHF/4-31G calculations showing that the S_N2 barriers for equation (3), estimated by the Marcus approach [Eqs (2) and (6)],

agreed well with the explicitly computed barriers for these reactions. Using various high-level theoretical methods, Gonzales, Allen, and Schaefer III, et al. confirmed these results and reported that the explicitly calculated barriers differed from those derived by the Marcus approach by less than 12 kJ mol^{-1} .^[13]

This agreement implies that there are no variable hard-hard or soft-soft interactions between the different groups in equations (3)–(5), which is in perfect agreement with Brauman's seminal investigations on the kinetics of methyl- and benzyl transfer reactions in the gas phase.^[10d, 14] Directly measured rate constants for gas phase S_N2 reactions [Eq. (3)] deviated only slightly from those calculated by using equation (2) from ΔG^0 and the rate constants for the corresponding identity reactions [Eqs (4) and (5)].^[14c]

As an example for the use of Marcus theory to analyze ambident reactivity, first consider the *O*- and *C*-methylation of the enolate [Eqs (7O) and (7C)]. In analogy to equation (6), the intrinsic barrier for *O*-methylation [Eq. (7O)] is obtained by the average of the Gibbs energies of activation for the identity reactions [Eqs (4) and (8O)] as expressed by equation (9O). According to equation (9C), the intrinsic barrier for *C*-methylation [Eq. (7C)] is obtained as the average of the identity reactions [Eqs (4) and (8C)].



$$\Delta G_0^\ddagger [\text{Eq. (7O)}] = 0.5(\Delta G_0^\ddagger [\text{Eq. (8O)}] + \Delta G_0^\ddagger [\text{Eq. (4)}]) \quad (9\text{O})$$

$$\Delta G_0^\ddagger [\text{Eq. (7C)}] = 0.5(\Delta G_0^\ddagger [\text{Eq. (8C)}] + \Delta G_0^\ddagger [\text{Eq. (4)}]) \quad (9\text{C})$$

As illustrated for the identity reaction [Eq. (4)] in Figure 2, ΔG_0^\ddagger can either be defined with respect to the free reactants (ΔG_0^\ddagger) or with respect to the reactant complexes [$\Delta G_0^\ddagger(\text{RC}) = \Delta G_0^\ddagger - \Delta G^0(\text{RC})$]. According to theory, intrinsic barriers should be considered with respect to reactant complexes [$\Delta G_0^\ddagger(\text{RC})$]. However, previous theoretical^[12b, 13c] and experimental gas phase^[14b, 15] investigations demonstrated the advantages of using ΔG_0^\ddagger , that is, the intrinsic barrier with respect to the free reactants. Furthermore, ΔG^0 for the formation of the reactant complex is rather small in solution, which makes the interpretation of reactions in solution

simpler if it is based on ΔG_0^\ddagger and not on $\Delta G_0^\ddagger(\text{RC})$. Since calculations at the G3(+) and MP2/6-311+G(2d,p) level of theory showed the same trends, the following discussion will be restricted to the G3(+) results. The results at the MP2 level can be found in the Supporting Information.

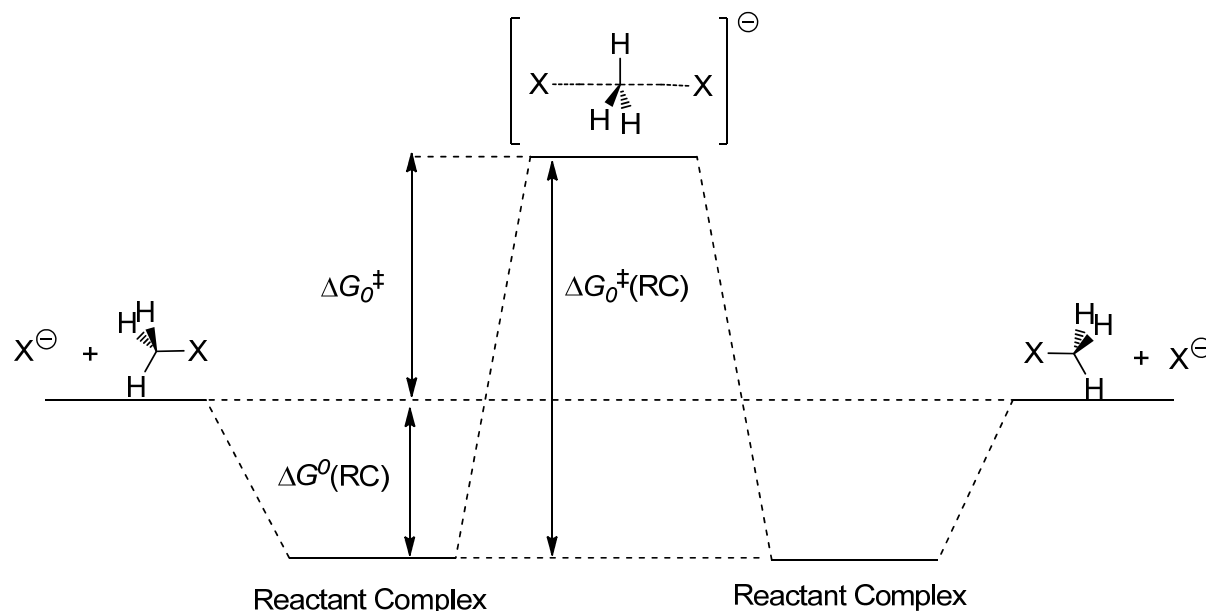


Figure 2: Definition of the intrinsic barrier in identity reactions with respect to the free reactants (ΔG_0^\ddagger) or the reactant complex [$\Delta G_0^\ddagger(\text{RC})$].

As previously recognized by Hoz and co-workers,^[16] our calculations also show that the intrinsic barriers of the identity reactions [Eq. (4)] increase dramatically when one moves from right to left in the periodic table (Table 1, $\Delta G_0^\ddagger = 15 \text{ kJ mol}^{-1}$ for F^- , 78 for MeO^- , 124 for Me_2N^- , and 206 for H_3C^-). Uggerud correlated this trend with the ionization energy of the nucleophile X^- .^[17] Those nucleophiles that form bonds to carbon atoms with stronger electrostatic character give rise to lower barriers due to decreased electron repulsion in the transition state.

Furthermore, Hoz and co-workers noticed that the intrinsic barriers ΔG_0^\ddagger change only slightly as one moves from top to bottom within one group in the periodic table. This trend, which is also revealed by our calculations (Table 1; F, Cl, Br 15–31 kJ mol^{-1} and HO^- , MeO^- , HS^- , MeS^- 78–92 kJ mol^{-1}) has been rationalized by Arnaut, Formosinho.^[18] When moving from top to bottom within the periodic table the C-X bond length increases, thereby leading to increasing the separation of the parabolas and a rise of the energy of the transition state. At the same time, in moving from the top to the bottom of the column the force constants

decrease, which causes a flattening of the parabolas and a lowering of the transition-state energy. Both effects obviously compensate each other and result in almost constant values of ΔG_0^\ddagger within one group.

The last two entries of Table 1, which reflect ΔG^\ddagger for equations (8O) and (8C), that is, special cases of equation (4), show the same trend: The intrinsic barrier for *O*-attack (77 kJ mol⁻¹) is much lower than that for *C*-attack (181 kJ mol⁻¹).

Table 1: Intrinsic Barriers ΔG_0^\ddagger ($=\Delta G^\ddagger$) for the Identity Reactions [Eq. (4)] and Gibbs Energies $\Delta G^0(\text{RC})$ of the Formation of the Reactant Complexes [G3(+); kJ mol⁻¹].^[a]

X	ΔG_0^\ddagger	$\Delta G^0(\text{RC})$	$\Delta G_0^\ddagger(\text{RC})$
F	+14.7	-38.5	+53.2
Cl	+31.2	-26.8	+58.0
Br	+24.7	-22.3	+47.0
OH	+81.4	-98.6	+180
OMe	+77.6	-20.4	+97.9
SH	+85.8	-24.6	+110
SMe	+92.1	-21.1	+113
NH₂	+146	-36.3	+183
NMe₂	+124	-18.3	+142
CH₃	+206	-11.1	+218
OCHCH₂	+77.0	-19.7	+96.7
CH₂CHO	+181	-28.8	+210

[a] $\Delta G_0^\ddagger(\text{RC}) = \Delta G_0^\ddagger - \Delta G^0(\text{RC})$.

Let us now examine the suitability of the Marcus approach for deriving the activation free energies ΔG^\ddagger for equations (7O) and (7C). For that purpose, we have directly calculated ΔG^\ddagger for equations (7O) and (7C) and listed them in the last column in Table 2. Comparison of the two right columns of Table 2 shows that the directly calculated ΔG^\ddagger values agree within a mean unsigned error of 5.1 kJ mol⁻¹ with those derived from the Marcus equation using ΔG^0 and ΔG_0^\ddagger . In accord with the results of theoretical and experimental investigations of ordinary S_N2 reactions, which are discussed above,^[12b, 13c, 14c] Marcus theory can therefore be used to elucidate the trends underlying ambident reactivity.

Table 2: Gibbs Reaction Energies (ΔG^0) and Gibbs Activation Energies (ΔG^\ddagger) for the *O*- and *C*-Methylation of the Enolate of Acetaldehyde [Eqs (7O) and (7C); G3(+); kJ mol⁻¹].^[a]

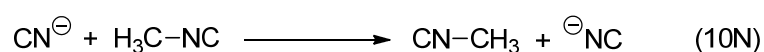
<i>O</i> -attack of enolate [Eq. (7O)]				
X in MeX	ΔG_0^\ddagger ([Eq. (9O)])	ΔG^0	ΔG^\ddagger ([Eq. (2)])	ΔG^\ddagger (direct)
F	+45.9	+57.0	+78.8	+71.7
Cl	+54.1	-78.4	+22.0	+16.0
Br	+50.9	-110	+10.8	+6.9
OH	+79.2	+130	+158	+146
OMe	+77.3	+116	+146	+136
SH	+81.4	+3.4	+83.1	+85.7
SMe	+84.6	+41.2	+106	+108
<i>C</i> -attack of enolate [Eq. (7C)]				
X in MeX	ΔG_0^\ddagger ([Eq. (9O)])	ΔG^0	ΔG^\ddagger ([Eq. (2)])	ΔG^\ddagger (direct)
F	+97.9	-25.1	+85.8	+89.3
Cl	+106	-160	+41.1	+34.4
Br	+103	-192	+29.4	+18.2
OH	+131	+48.4	+156	+155
OMe	+129	+34.0	+147	+150
SH	+133	-78.6	+96.6	+95.9
SMe	+137	-40.8	+117	+115

[a] For clarity, only Gibbs energies referring to the free reactants are given. The corresponding data referring to the reactant complexes are given in the Supporting Information.

Table 2 shows that the difference (ΔG_0^\ddagger [Eq. (7O)] - ΔG_0^\ddagger [Eq. (7C)]) between the intrinsic barriers for *O*- and *C*-attack is independent of the nature of the electrophile, because the electrophile-specific terms ΔG_0^\ddagger [Eq. (4)] cancel when subtracting equation (9C) from equation (9O). The fair agreement between directly calculated ΔG^\ddagger (last column of Table 2) and ΔG^\ddagger derived from the Marcus equation (Table 2, column 2 from right) therefore implies that the “hardness” of the electrophile has little influence upon the *C*/*O* alkylation ratio. In line with our analysis, Houk and Paddon-Row concluded from quantum-chemical calculations (HF/6-31G*) already in 1986 that “*O*-alkylation of enolates is favored with all electrophiles. Changes in *C*/*O* alkylation ratios with the nature of the alkyl halide are probably not related to ‘hardness’ or ‘softness’ of the alkyl halide, but to the ability of the halide to influence the structure of metal enolate aggregates.”^[19]

The middle column of Table 2 shows, that for all electrophiles the product stability term (ΔG^0) highly favors *C*-attack over *O*-attack. However, the much higher intrinsic barrier ΔG_0^\ddagger for *C*-attack compensates for this effect; as a result, ΔG^\ddagger is similar for *O*- and *C*-attack

independent of the methylating agent (Table 2, right columns). It depends upon the reaction conditions whether the site of attack is controlled by the thermodynamic or the intrinsic term. For an analogous Marcus analysis of the ambident reactivities of CN^- , OCN^- , SCN^- , and NO_2^- we have calculated the activation energies of the corresponding identity reactions [e.g., Eqs (10C) and (10N)] with respect to the free reactants and to the reactant complexes, which are listed in Table 3 as ΔG_0^\ddagger and $\Delta G_0^\ddagger(\text{RC})$, respectively.



The relationship between intrinsic barrier and location of the attacking atom of the nucleophile in the periodic table noted by Hoz and co-workers^[16] and confirmed by Table 1 also controls ambident reactivity. According to Table 3, ΔG_0^\ddagger and $\Delta G_0^\ddagger(\text{RC})$ are generally smaller when the attacking site of the nucleophile (corresponds to the departing site of the leaving group) is located further to the right in the periodic table. Therefore, intrinsically favored are thus *N*-attack by CN^- , *O*-attack by NCO^- , and *S*-attack by NCS^- .

Table 3: Intrinsic Barriers ΔG_0^\ddagger ($= \Delta G^\ddagger$) for the Identity Reactions, e.g. in equations (10C) and (10N), and Gibbs Energies $\Delta G^0(\text{RC})$ of the Formation of the Reactant Complexes

[G3(+); kJ mol⁻¹].^[a]

X	ΔG_0^\ddagger	$\Delta G^0(\text{RC})$	$\Delta G_0^\ddagger(\text{RC})$
CN	+156	-29.3	+185
NC	+93.8	-32.9	+127
OCN	+21.6	-40.7	+62.2
NCO	+78.4	-23.6	+102
SCN	+52.2	-36.5	+88.7
NCS	+93.7	-25.3	+119
NO₂	+61.4	-35.5	+96.8
ONO	+61.1	-19.2	+80.2

[a] $\Delta G_0^\ddagger(\text{RC}) = \Delta G_0^\ddagger - \Delta G^0(\text{RC})$.

An exception is NO_2^- , where ΔG_0^\ddagger (with respect to the free reactants) is almost the same for *N*- and *O*-attack. The higher stability of the reactant complex of NO_2^- with $\text{H}_3\text{C}-\text{NO}_2$ than with $\text{H}_3\text{C}-\text{ONO}$ accounts for the fact that $\Delta G_0^\ddagger(\text{RC})$ is again smaller for *O*-attack than for *N*-attack.

Use of the additivity principle [Eqs (6), (9O), and (9C)] yields the intrinsic barriers ΔG_0^\ddagger for the reactions of CN^- , OCN^- , SCN^- , and NO_2^- with CH_3Cl (Table 4) using the ΔG_0^\ddagger values of the identity reactions in Table 3 and ΔG_0^\ddagger for the chloride exchange (Table 1, entry 2). Table 4 shows that cyanide prefers *C*-attack thermodynamically (ΔG^0) and *N*-attack intrinsically (ΔG_0^\ddagger). As the differences of the intrinsic terms are much smaller than the differences in the reaction free energies ($\Delta\Delta G^0$), free cyanide ions always preferentially attack *C*-electrophiles with the carbon atom (for a rationalization of the reaction with AgCN , see Ref.^[4]).

Table 4: Gibbs Energies of Reactions (ΔG^0), Intrinsic Barriers (ΔG_0^\ddagger) and Gibbs Energies of Activation (ΔG^\ddagger) for the Methylation of Ambident Nucleophiles with MeCl

[Eqs (6), (10C), and (10N); G3(+); kJ mol^{-1}].^[a]

X	ΔG_0^\ddagger	ΔG^0	ΔG^\ddagger
CN	+93.6	-131	+39.6
NC	+62.5	-29.8	+48.5
OCN	+26.4	+119	+119
NCO	+54.8	+3.2	+56.4
SCN	+41.7	+87.1	+96.6
NCS	+62.5	+71.7	+103
NO₂	+46.3	-18.1	+37.7
ONO	+46.2	-9.2	+41.7

[a] For clarity, only Gibbs energies referring to the free reactants are given. The corresponding data referring to the reactant complexes are given in the Supporting Information.

N-attack is preferred by the ΔG^0 term in the reactions of NCO^- and NCS^- , and in both cases attack at the chalcogen terminus is preferred intrinsically (Table 4 and Figure 3). The large thermodynamic preference for *N*-attack at NCO^- is not overcompensated by the intrinsic term, and NCO^- generally reacts faster at the nitrogen atom. In contrast, $\Delta\Delta G^0$ for *S*- and *N*-attack for thiocyanate is rather small, such that kinetically controlled alkylations of NCS^- occur

preferentially at the intrinsically preferred site (*S*) to give thiocyanates, which may rearrange to isothiocyanates under thermodynamically controlled conditions (Figure 3). Finally, nitroalkanes are more stable than alkyl nitrites; however, under conditions of kinetic control methyl halides and NO_2^- usually give mixtures resulting from *O*- and *N*-attack.

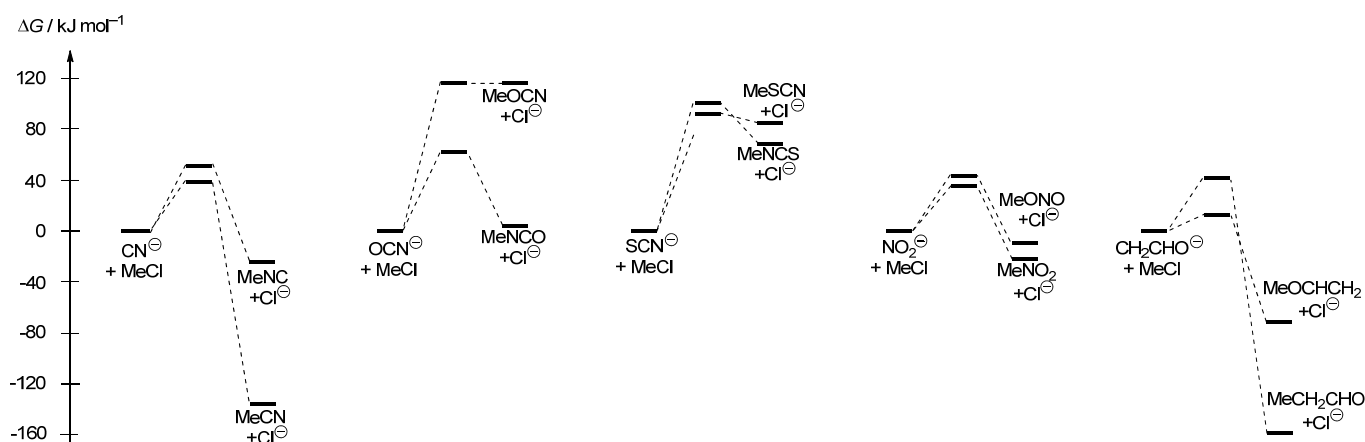


Figure 3: Gibbs energy profiles for the methylation of ambident nucleophiles with methyl chloride in the gas phase [G3(+)].

Unfortunately, this analysis cannot be used to predict how variation of the electrophile affects the product ratio. The reason is that the gas-phase calculations do not provide correct absolute values of ΔG^0 and ΔG_0^\ddagger for reactions in solution. Instead of introducing quantitative solvation models into this treatment, we suggest using the results of this investigation qualitatively to interpret ambident reactivity through the combination of Gibbs reaction energy ΔG^0 and intrinsic barrier ΔG_0^\ddagger . Whenever a product obtained under kinetic control is thermodynamically less stable, it must be favored intrinsically.

3 Conclusion

We have demonstrated that attack at the atom further right in the periodic table is usually preferred intrinsically. An alternative approach to relative intrinsic barriers comes from the principle of least nuclear motion because according to Figure 1, the reorganization energy λ is the four-fold value of the intrinsic barrier, as explicitly discussed by Hine.^[20] The coincident conclusions from both approaches will be reported in a subsequent review (see Chapter 7).

More than three decades ago, Gompper and Wagner^[21] emphasized that the HSAB concept does not differentiate between kinetic and thermodynamic product control though it has long

been known that in many cases ambident systems give different products under kinetic and thermodynamic control. The clear differentiation between kinetic and thermodynamic product control,^[22a] which used to be common in the past,^[22b] has been neglected in more recent treatments of ambident reactivity and thus led to considerable confusion. By taking into account intrinsic (ΔG_0^\ddagger) as well as the thermodynamic (ΔG^0) contributions to the Gibbs energies of activation ΔG^\ddagger , that is, by considering the role of thermodynamics also in kinetically controlled reactions, Marcus theory provides a consistent approach to ambident reactivity.

4 Theoretical Methods

Gibbs energies G were calculated at two different theoretical levels. The first level, termed MP2/6-311+G(2d,p), involves geometry optimizations and frequency calculations at MP2(FC)/6-311+G(2d,p) level of theory. Thermal corrections to 298.15 K have been calculated using unscaled harmonic vibrational frequencies in this case. The second level, termed G3(+), is identical to the standard G3 compound model,^[23] but adds additional sets of diffuse basis functions on all non-hydrogen atoms in geometry optimizations. Thermal corrections have therefore been calculated at RHF/6-31+G(d) level (instead of RHF/6-31G(d)), keeping the scaling factor for vibrational frequencies constant at 0.8929. All subsequent single point calculations of the G3 scheme were performed on geometries optimized at MP2(FULL)/6-31+G(d) level (instead of MP2(FULL)/6-31G(d)). All calculations were performed with Gaussian 03.^[24]

5 Supporting Information

5.1 Further Tables

As calculations at the G3(+) and MP2/6-311+G(2d,p) level of theory manifested the same trends, the discussion in the in Section 2 was restricted to the G3(+) results. The results at MP2 level are shown below.

Table 1a: Intrinsic Barriers ΔG_0^\ddagger ($=\Delta G^\ddagger$) for the Identity Reactions [Eq. (4)] and Gibbs Energies $\Delta G^0(\text{RC})$ of the Formation of the Reactant Complexes

[MP2/6-311+G(2d,p); kJ mol⁻¹].^[a]

X	ΔG_0^\ddagger	$\Delta G^0(\text{RC})$	$\Delta G_0^\ddagger(\text{RC})$
F	+24.7	-32.0	+56.7
Cl	+38.2	-23.5	+61.7
Br	+38.0	-17.3	+55.2
OH	+86.6	-110	+196
OMe	+85.5	-19.4	+105
SH	+90.7	-27.3	+118
SMe	+97.1	-10.1	+107
NH₂	+148	-36.6	+185
NMe₂	+121	-6.57	+128
CH₃	+210	-6.92	+203
OCHCH₂	+87.3	-2.08	+89.4
CH₂CHO	+178	-19.9	+197

[a] $\Delta G_0^\ddagger(\text{RC}) = \Delta G_0^\ddagger - \Delta G^0(\text{RC})$.

Table 2a: Gibbs Reaction Energies (ΔG^0) and Gibbs Activation Energies (ΔG^\ddagger) for the *O*- and *C*-Methylation of the Enolate of Acetaldehyde [Eqs (7O) and (7C); MP2/6-311+G(2d,p); kJ mol⁻¹].

<i>O</i> -attack of enolate [Eq. (7O)]				
X in MeX	ΔG_0^\ddagger ([Eq. (9O)])	ΔG^0	ΔG^\ddagger ([Eq. (2)])	ΔG^\ddagger (direct)
F	+56.4	+56.0	+87.8	+82.9
Cl	-72.8	+62.8	+31.7	+30.8
Br	-106	+62.7	+20.9	+19.0
OH	+134	+87.0	+167	+157
OMe	+118	+86.4	+155	+148
SH	+19.3	+89.0	+98.9	+103
SMe	+52.4	+92.2	+120	+123
<i>C</i> -attack of enolate [Eq. (7C)]				
X in MeX	ΔG_0^\ddagger ([Eq. (9O)])	ΔG^0	ΔG^\ddagger ([Eq. (2)])	ΔG^\ddagger (direct)
F	-37.5	+101	+83.1	+90.1
Cl	-167	+108	+40.6	+34.1
Br	-200	+108	+31.1	+20.1
OH	+40.6	+132	+153	+155
OMe	+23.9	+132	+144	+149
SH	-74.5	+134	+99.3	+98.1
SMe	-41.5	+138	+118	+117

Table 3a: Intrinsic Barriers ΔG_0^\ddagger ($= \Delta G^\ddagger$) for the Identity Reactions, e.g. in Equations (10C) and (10N), and Gibbs Energies $\Delta G^0(\text{RC})$ of the Formation of the Reactant Complexes

[MP2/6-311+G(2d,p); kJ mol⁻¹].^[a]

X	ΔG_0^\ddagger	$\Delta G^0(\text{RC})$	$\Delta G_0^\ddagger(\text{RC})$
CN	+161	-25.9	+187
NC	+90.4	-32.1	+123
OCN	+29.5	-34.4	+63.9
NCO	+90.8	-22.5	+113
SCN	+56.8	-29.5	+86.3
NCS	+94.2	-27.5	+122
NO₂	+73.3	-25.2	+98.5
ONO	+70.2	-12.1	+82.3

[a] $\Delta G_0^\ddagger(\text{RC}) = \Delta G_0^\ddagger - \Delta G^0(\text{RC})$.

Table 4a: Gibbs Energies of Reactions (ΔG^0), Intrinsic Barriers (ΔG_0^\ddagger) and Gibbs Energies of Activation (ΔG^\ddagger) for the Methylation of Ambident Nucleophiles with MeCl
 [Eqs (6), (10C), and (10N); MP2/6-311+G(2d,p); kJ mol⁻¹].

X	ΔG_0^\ddagger	ΔG^0	ΔG^\ddagger
CN	-135	+99.6	+43.5
NC	-19.7	+64.3	+54.8
OCN	+89.3	+33.9	+93.3
NCO	-28.1	+64.5	+51.2
SCN	+49.0	+47.5	+75.2
NCS	+31.9	+66.2	+83.1
NO₂	-37.5	+55.8	+38.6
ONO	-9.2	+54.2	+49.7

5.2 G3(+) and MP2 Energies for the Identity Reactions

<u>F⁻ + MeF</u>				
Method	F ⁻	MeF	Reactant Complex	Transition State
QCISD(T,FC) / 6-31G(d)	-99.5307040	-139.3604050	-238.9291251	-238.9131864
MP4(FC)/6-31G(d)	-99.5307477	-139.3605150	-238.9297356	-238.9146174
MP4(FC)/6-31+G(d)	-99.6297500	-139.3791769	-239.0316128	-239.0145270
MP4(FC)/6-31G(2df,p)	-99.5927206	-139.4703150	-239.1020031	-239.0890922
MP2(FC)/6-31G(d)	-99.5266066	-139.3356508	-238.9005693	-238.8835481
MP2(FC)/6-31+G(d)	-99.6238467	-139.3534935	-238.9994353	-238.9790109
MP2(FC)/6-31G(2df,p)	-99.5837754	-139.4379754	-239.0605246	-239.0449961
MP2(FULL)/GTLarge	-99.7736485	-139.6096162	-239.4056823	-239.3834550
Thermal Corrections (HF/6-31+G(d))				
Zero-point correction=	0.000000	0.037806	0.038294	0.037714
Thermal correction to Energy=	0.001416	0.040727	0.043347	0.041842
Thermal correction to Enthalpy=	0.002360	0.041671	0.044291	0.042786
Thermal correction to Gibbs Free Energy=	-0.014159	0.016410	0.010844	0.012107
$G_{298} =$	<u>-99.8233472</u>	<u>-139.6709570</u>	<u>-239.5089635</u>	<u>-239.4887059</u>
MP2(FC)/6-311+G(2d,p)	-99.703831	139.4785434	-239.2044553	-239.1837645
Thermal Corrections (MP2/6-311+G(2d,p))				
Zero-point correction=	0.000000	0.039995	0.040396	0.039620
Thermal correction to Energy=	0.001416	0.042901	0.045340	0.043601
Thermal correction to Enthalpy=	0.002360	0.043845	0.046284	0.044546
Thermal correction to Gibbs Free Energy=	-0.014159	0.017531	0.013254	0.014154

<u>Cl⁻ + MeCl</u>				
Method	Cl ⁻	MeCl	Reactant Complex	Transition State
QCISD(T,FC) / 6-31G(d)	-459.6665483	-499.3898601	-959.0735725	-959.0520119
MP4(FC)/6-31G(d)	-459.6662592	-499.3886962	-959.0720975	-959.0498606
MP4(FC)/6-31+G(d)	-459.6858399	-499.3919796	-959.0931919	-959.0681518
MP4(FC)/6-31G(2df,p)	-459.7314657	-499.4962489	-959.2459446	-959.2264180
MP2(FC)/6-31G(d)	-459.6521044	-499.3545596	-959.0238452	-958.9994238
MP2(FC)/6-31+G(d)	-459.6711454	-499.3574655	-959.0438910	-959.0164121
MP2(FC)/6-31G(2df,p)	-459.7082425	-499.4506060	-959.1772752	-959.1556945
MP2(FULL)/GTLarge	-460.0746719	-499.8574752	-959.9491228	-959.9256803
Thermal Corrections (HF/6-31+G(d))				
Zero-point correction=	0.000000	0.036297	0.036605	0.035875
Thermal correction to Energy=	0.001416	0.039333	0.042110	0.040638
Thermal correction to Enthalpy=	0.002360	0.040278	0.043054	0.041582
Thermal correction to Gibbs Free Energy=	-0.015023	0.013682	0.006039	0.007685
$G_{298} =$	<u>-460.1386229</u>	<u>-499.9356795</u>	<u>-960.0845228</u>	<u>-960.0624190</u>
MP2(FC)/6-311+G(2d,p)	-459.7315876	-499.4562803	-959.2046817	-959.1827309
Thermal Corrections (MP2/6-311+G(2d,p))				
Zero-point correction=	0.000000	0.038448	0.038712	0.038001
Thermal correction to Energy=	0.001416	0.041450	0.044090	0.042536
Thermal correction to Enthalpy=	0.002360	0.042394	0.045034	0.043480
Thermal correction to Gibbs Free Energy=	-0.015023	0.015829	0.008665	0.010229

<u>Br⁻ + MeBr</u>				
Method	Br ⁻	MeBr	Reactant Complex	Transition State
QCISD(T,FC) / 6-31G(d)	-2570.0634975	-2609.7769953	-5179.8609931	-5179.8456094
MP4(FC)/6-31G(d)	-2570.0634342	-2609.7761579	-5179.8601483	-5179.8444867
MP4(FC)/6-31+G(d)	-2570.1006685	-2609.7918466	-5179.9129738	-5179.8936796
MP4(FC)/6-31G(2df,p)	-2570.2904175	-2610.0524398	-5180.3629539	-5180.3444299
MP2(FC)/6-31G(d)	-2570.0528126	-2609.7448159	-5179.8184182	-5179.8013865
MP2(FC)/6-31+G(d)	-2570.0895335	-2609.7601359	-5179.8701460	-5179.8492247
MP2(FC)/6-31G(2df,p)	-2570.2692129	-2610.0094252	-5180.2989767	-5180.2782226
MP2(FULL)/GTLarge	-2573.6061702	-2613.3768207	-5186.9998265	-5186.9797890
Thermal Corrections (HF/6-31+G(d))				
Zero-point correction=	0.000000	0.035709	0.036262	0.035529
Thermal correction to Energy=	0.001416	0.038828	0.041696	0.040394
Thermal correction to Enthalpy=	0.002360	0.039773	0.042640	0.041339
Thermal correction to Gibbs Free Energy=	-0.016176	0.011852	0.004587	0.005234
$G_{298} =$	<u>-2573.6690035</u>	<u>-2613.4538914</u>	<u>-5187.1314052</u>	<u>-5187.1134857</u>
MP2(FC)/6-311+G(2d,p)	-2572.5770495	-2612.2872185	-5184.8797681	-5184.8601436
Thermal Corrections (MP2/6-311+G(2d,p))				
Zero-point correction=	0.000000	0.037779	0.037985	0.037199
Thermal correction to Energy=	0.001416	0.040853	0.043520	0.042006
Thermal correction to Enthalpy=	0.002360	0.041797	0.044464	0.042950
Thermal correction to Gibbs Free Energy=	-0.016176	0.012899	0.005646	0.007056

OH⁻ + MeOH

Method	HO ⁻	MeOH	Reactant Complex	Transition State
QCISD(T,FC) / 6-31G(d)	-75.5217844	-115.3747656	-190.9701054	-190.8911583
MP4(FC)/6-31G(d)	-75.5213372	-115.3737564	-190.9692820	-190.8906233
MP4(FC)/6-31+G(d)	-75.5966594	-115.3861425	-191.0293840	-190.9638961
MP4(FC)/6-31G(2df,p)	-75.5874369	-115.4834891	-191.1470909	-191.0684691
MP2(FC)/6-31G(d)	-75.5131337	-115.3460225	-190.9353001	-190.8530085
MP2(FC)/6-31+G(d)	-75.5883642	-115.3578372	-190.9938686	-190.9240582
MP2(FC)/6-31G(2df,p)	-75.5744750	-115.4487310	-191.1009359	-191.0187344
MP2(FULL)/GTLarge	-75.7288728	-115.5975128	-191.3768230	-191.3049707
Thermal Corrections (HF/6-31+G(d))				
Zero-point correction=	0.008071	0.049287	0.058961	0.057630
Thermal correction to Energy=	0.010432	0.052651	0.064968	0.063343
Thermal correction to Enthalpy=	0.011376	0.053595	0.065912	0.064287
Thermal correction to Gibbs Free Energy=	-0.008157	0.026542	0.029927	0.030617
G_{298}^{\ddagger} =	<u>-75.7760746</u>	<u>-115.6520115</u>	<u>-191.4656539</u>	<u>-191.3970925</u>
MP2(FC)/6-311+G(2d,p)	-75.6595631	-115.4691855	-191.1810400	-191.1076980
Thermal Corrections (MP2/6-311+G(2d,p))				
Zero-point correction=	0.008658	0.052031	0.060484	0.060466
Thermal correction to Energy=	0.011019	0.055377	0.066098	0.066002
Thermal correction to Enthalpy=	0.011963	0.056321	0.067042	0.066946
Thermal correction to Gibbs Free Energy=	-0.007600	0.029253	0.032151	0.033580

OMe⁻ + MeOMe

Method	MeO ⁻	MeOMe	Reactant Complex	Transition State
QCISD(T,FC) / 6-31G(d)	-114.7266946	-154.5493898	-269.3039938	-269.2628225
MP4(FC)/6-31G(d)	-114.7265927	-154.5482046	-269.3030679	-269.2627630
MP4(FC)/6-31+G(d)	-114.7709898	-154.5603406	-269.3530486	-269.3158158
MP4(FC)/6-31G(2df,p)	-114.8288905	-154.6939294	-269.5531310	-269.5139060
MP2(FC)/6-31G(d)	-114.7006724	-154.5034038	-269.2325328	-269.1903600
MP2(FC)/6-31+G(d)	-114.7445329	-154.5146249	-269.2803849	-269.2403733
MP2(FC)/6-31G(2df,p)	-114.7955339	-154.6394841	-269.4656806	-269.4242550
MP2(FULL)/GTLarge	-114.9761385	-154.8423668	-269.8397439	-269.8002841
Thermal Corrections (HF/6-31+G(d))				
Zero-point correction=	0.034454	0.076742	0.112485	0.111250
Thermal correction to Energy=	0.037371	0.081160	0.120813	0.119608
Thermal correction to Enthalpy=	0.038316	0.082104	0.121757	0.120552
Thermal correction to Gibbs Free Energy=	0.013271	0.051259	0.077982	0.078073
G_{298}^{\ddagger} =	<u>-115.0415646</u>	<u>-154.9115132</u>	<u>-269.9608288</u>	<u>-269.9235231</u>
MP2(FC)/6-311+G(2d,p)	-114.8492252	-154.6561942	-269.5259646	-269.4880584
Thermal Corrections (MP2/6-311+G(2d,p))				
Zero-point correction=	0.036287	0.080992	0.118882	0.117662
Thermal correction to Energy=	0.039192	0.085277	0.127657	0.125371
Thermal correction to Enthalpy=	0.040136	0.086221	0.128601	0.126315
Thermal correction to Gibbs Free Energy=	0.015073	0.055632	0.083876	0.085897

$\text{SH}^- + \text{MeSH}$

Method	HS ⁻	MeSH	Reactant Complex	Transition State
QCISD(T,FC) / 6-31G(d)	-398.2308385	-437.9933162	-836.2458171	-836.2011705
MP4(FC)/6-31G(d)	-398.2299660	-437.9915145	-836.2433193	-836.1981253
MP4(FC)/6-31+G(d)	-398.2495496	-437.9949488	-836.2633954	-836.2168915
MP4(FC)/6-31G(2df,p)	-398.3013416	-438.1017940	-836.4257537	-836.3843973
MP2(FC)/6-31G(d)	-398.2104510	-437.9526667	-836.1859763	-836.1372528
MP2(FC)/6-31+G(d)	-398.2296047	-437.9557494	-836.2050216	-836.1547298
MP2(FC)/6-31G(2df,p)	-398.2739990	-438.0532767	-836.3513013	-836.3067950
MP2(FULL)/GTLarge	-398.6320383	-438.4505598	-837.1033706	-837.0581779
Thermal Corrections (HF/6-31+G(d))				
Zero-point correction=	0.005664	0.044239	0.051093	0.049522
Thermal correction to Energy=	0.008025	0.047877	0.058299	0.056405
Thermal correction to Enthalpy=	0.008969	0.048821	0.059244	0.057349
Thermal correction to Gibbs Free Energy=	-0.012174	0.020003	0.017883	0.018726
$G_{298} =$	<u>-398.6984013</u>	<u>-438.5259294</u>	<u>-837.2337146</u>	<u>-837.1916346</u>
MP2(FC)/6-311+G(2d,p)	-398.2972868	-438.060487	-836.378964	-836.3346758
Thermal Corrections (MP2/6-311+G(2d,p))				
Zero-point correction=	0.006209	0.046877	0.053646	0.052540
Thermal correction to Energy=	0.008570	0.050467	0.060277	0.059096
Thermal correction to Enthalpy=	0.009514	0.051412	0.061221	0.060041
Thermal correction to Gibbs Free Energy=	-0.011628	0.022656	0.021835	0.022464

 $\text{SMe}^- + \text{MeSMe}$

Method	MeS ⁻	MeSMe	Reactant Complex	Transition State
QCISD(T,FC) / 6-31G(d)	-437.4021376	-477.1771062	-914.5986455	-914.5526217
MP4(FC)/6-31G(d)	-437.4009078	-477.1750053	-914.5954110	-914.5492308
MP4(FC)/6-31+G(d)	-437.4203270	-477.1803112	-914.6181851	-914.5722113
MP4(FC)/6-31G(2df,p)	-437.5095697	-477.3227271	-914.8521379	-914.8102447
MP2(FC)/6-31G(d)	-437.3658978	-477.1211005	-914.5066742	-914.4581573
MP2(FC)/6-31+G(d)	-437.3846392	-477.1258810	-914.5280521	-914.4794778
MP2(FC)/6-31G(2df,p)	-437.4642787	-477.2568901	-914.7416268	-914.6977637
MP2(FULL)/GTLarge	-437.8764008	-477.7109290	-915.6058095	-915.5615359
Thermal Corrections (HF/6-31+G(d))				
Zero-point correction=	0.034642	0.072668	0.108088	0.106887
Thermal correction to Energy=	0.037721	0.077607	0.118322	0.116719
Thermal correction to Enthalpy=	0.038666	0.078551	0.119266	0.117663
Thermal correction to Gibbs Free Energy=	0.012078	0.045592	0.067592	0.068826
$G_{298} =$	<u>-437.9562234</u>	<u>-477.7976603</u>	<u>-915.7619213</u>	<u>-915.7188038</u>
MP2(FC)/6-311+G(2d,p)	-437.4840725	-477.261417	-914.7632881	-914.7215024
Thermal Corrections (MP2/6-311+G(2d,p))				
Zero-point correction=	0.036641	0.076860	0.114626	0.112999
Thermal correction to Energy=	0.039692	0.081678	0.124163	0.122203
Thermal correction to Enthalpy=	0.040636	0.082622	0.125108	0.123147
Thermal correction to Gibbs Free Energy=	0.014073	0.049917	0.077958	0.076976

<u>NH₂⁻ + MeNH₂</u>				
Method	H ₂ N ⁻	MeNH ₂	Reactant Complex	Transition State
QCISD(T,FC) / 6-31G(d)	-55.6619064	-95.5411895	-151.2415656	-151.1721305
MP4(FC)/6-31G(d)	-55.6613426	-95.5396818	-151.2396665	-151.1703625
MP4(FC)/6-31+G(d)	-55.7230884	-95.5493228	-151.2999160	-151.2275057
MP4(FC)/6-31G(2df,p)	-55.7240138	-95.6409211	-151.4032903	-151.3365352
MP2(FC)/6-31G(d)	-55.6459928	-95.5064012	-151.1919048	-151.1197006
MP2(FC)/6-31+G(d)	-55.7084528	-95.5156998	-151.2518370	-151.1765041
MP2(FC)/6-31G(2df,p)	-55.7048941	-95.6014890	-151.3457256	-151.2763729
MP2(FULL)/GTLarge	-55.8366088	-95.7356720	-151.5992732	-151.5271899
Thermal Corrections (HF/6-31+G(d))				
Zero-point correction=	0.017689	0.061441	0.081320	0.079081
Thermal correction to Energy=	0.020527	0.064904	0.088583	0.085464
Thermal correction to Enthalpy=	0.021471	0.065848	0.089527	0.086409
Thermal correction to Gibbs Free Energy=	0.000058	0.038518	0.051255	0.051293
G_{298} =	<u>-55.8810641</u>	<u>-95.7831382</u>	<u>-151.6780453</u>	<u>-151.6084129</u>
MP2(FC)/6-311+G(2d,p)	-55.770518	-95.6121979	-151.4096877	-151.3392321
Thermal Corrections (MP2/6-311+G(2d,p))				
Zero-point correction=	0.018829	0.064892	0.085324	0.083206
Thermal correction to Energy=	0.021667	0.068307	0.092110	0.089170
Thermal correction to Enthalpy=	0.022612	0.069251	0.093054	0.090114
Thermal correction to Gibbs Free Energy=	0.001162	0.041972	0.056169	0.056037

<u>NMe₂⁻ + MeNMe₂</u>				
Method	Me ₂ N ⁻	MeNMe ₂	Reactant Complex	Transition State
QCISD(T,FC) / 6-31G(d)	-134.0457477	-173.8959192	-307.9638587	-307.9079742
MP4(FC)/6-31G(d)	-134.0443874	-173.8936446	-307.9604910	-307.9058487
MP4(FC)/6-31+G(d)	-134.0817339	-173.9055021	-308.0042692	-307.9543203
MP4(FC)/6-31G(2df,p)	-134.1802831	-174.0708149	-308.2752501	-308.2228788
MP2(FC)/6-31G(d)	-133.9970167	-173.8285670	-307.8478949	-307.7926001
MP2(FC)/6-31+G(d)	-134.0334858	-173.8394949	-307.8893962	-307.8384434
MP2(FC)/6-31G(2df,p)	-134.1244401	-173.9949107	-308.1437600	-308.0909573
MP2(FULL)/GTLarge	-134.3431453	-174.2410856	-308.6007541	-308.5521157
Thermal Corrections (HF/6-31+G(d))				
Zero-point correction=	0.071766	0.115365	0.188175	0.186863
Thermal correction to Energy=	0.075985	0.120959	0.200218	0.197742
Thermal correction to Enthalpy=	0.076929	0.121903	0.201162	0.198686
Thermal correction to Gibbs Free Energy=	0.047300	0.088963	0.145776	0.150819
G_{298} =	<u>-134.4177860</u>	<u>-174.3142490</u>	<u>-308.7389908</u>	<u>-308.6848500</u>
MP2(FC)/6-311+G(2d,p)	-134.1614608	-174.0019534	-308.1807409	-308.1329537
Thermal Corrections (MP2/6-311+G(2d,p))				
Zero-point correction=	0.075740	0.121878	0.198715	0.197368
Thermal correction to Energy=	0.079827	0.127235	0.209637	0.207378
Thermal correction to Enthalpy=	0.080771	0.128179	0.210581	0.208322
Thermal correction to Gibbs Free Energy=	0.051373	0.095705	0.161900	0.162888

$\text{CH}_3^- + \text{MeCH}_3$				
Method	H_3C^-	MeCH ₃	Reactant Complex	Transition State
QCISD(T,FC) / 6-31G(d)	-39.6193124	-79.5345861	-119.1665974	-119.095437
MP4(FC)/6-31G(d)	-39.6184831	-79.5328106	-119.1639345	-119.0929531
MP4(FC)/6-31+G(d)	-39.6750728	-79.5360411	-119.2169693	-119.1322381
MP4(FC)/6-31G(2df,p)	-39.6791697	-79.6281673	-119.3201699	-119.2516913
MP2(FC)/6-31G(d)	-39.5977577	-79.4947419	-119.1049794	-119.0313813
MP2(FC)/6-31+G(d)	-39.6544291	-79.4975995	-119.1575576	-119.0708176
MP2(FC)/6-31G(2df,p)	-39.6543537	-79.5838719	-119.2511918	-119.1807901
MP2(FULL)/GTLarge	-39.7690698	-79.7034456	-119.4800341	-119.4006634
Thermal Corrections (HF/6-31+G(d))				
Zero-point correction=	0.027049	0.071023	0.098616	0.095525
Thermal correction to Energy=	0.029979	0.074571	0.107207	0.102982
Thermal correction to Enthalpy=	0.030923	0.075515	0.108152	0.103927
Thermal correction to Gibbs Free Energy=	0.008962	0.049572	0.061902	0.066556
$G_{298} =$	<u>-39.811215</u>	<u>-79.745019</u>	<u>-119.560476</u>	<u>-119.477587</u>
MP2(FC)/6-311+G(2d,p)	-39.7100517	-79.5863122	-119.3031792	-119.2233922
Thermal Corrections (MP2/6-311+G(2d,p))				
Zero-point correction=	0.029185	0.075716	0.106256	0.101811
Thermal correction to Energy=	0.032101	0.079180	0.114003	0.108887
Thermal correction to Enthalpy=	0.033045	0.080125	0.114948	0.109831
Thermal correction to Gibbs Free Energy=	0.011089	0.054311	0.074850	0.072566

$\text{CN}^- + \text{MeCN}$				
Method	NC^-	MeCN	Reactant Complex	Transition State
QCISD(T,FC) / 6-31G(d)	-92.5817435	-132.3736427	-224.9786971	-224.9169423
MP4(FC)/6-31G(d)	-92.5844354	-132.3758111	-224.9837602	-224.9217591
MP4(FC)/6-31+G(d)	-92.6247183	-132.3832024	-225.0263212	-224.9587206
MP4(FC)/6-31G(2df,p)	-92.6409703	-132.4732763	-225.1377743	-225.0768606
MP2(FC)/6-31G(d)	-92.5630595	-132.3382430	-224.9249291	-224.8590854
MP2(FC)/6-31+G(d)	-92.6034004	-132.3453543	-224.9670925	-224.8954053
MP2(FC)/6-31G(2df,p)	-92.6157752	-132.4298593	-225.0693234	-225.0039807
MP2(FULL)/GTLarge	-92.7681910	-132.6106073	-225.3987328	-225.3278101
Thermal Corrections (HF/6-31+G(d))				
Zero-point correction=	0.004740	0.043567	0.048693	0.048467
Thermal correction to Energy=	0.007101	0.047208	0.056533	0.055333
Thermal correction to Enthalpy=	0.008045	0.048152	0.057477	0.056277
Thermal correction to Gibbs Free Energy=	-0.014277	0.019547	0.013855	0.018242
$G_{298} =$	<u>-92.8368432</u>	<u>-132.6836769</u>	<u>-225.5316812</u>	<u>-225.4612908</u>
MP2(FC)/6-311+G(2d,p)	-92.6557428	-132.4368784	-225.111986	-225.0436424
Thermal Corrections (MP2/6-311+G(2d,p))				
Zero-point correction=	0.004504	0.045366	0.050289	0.049508
Thermal correction to Energy=	0.006865	0.049016	0.058018	0.056374
Thermal correction to Enthalpy=	0.007810	0.049960	0.058962	0.057319
Thermal correction to Gibbs Free Energy=	-0.014558	0.021301	0.016238	0.018940

$\text{CN}^- + \text{MeNC}$

Method	NC^-	MeNC	Reactant Complex	Transition State
QCISD(T,FC) / 6-31G(d)	-92.5817435	-132.3333772	-224.9399908	-224.8958505
MP4(FC)/6-31G(d)	-92.5844354	-132.3346739	-224.9443439	-224.9002389
MP4(FC)/6-31+G(d)	-92.6247183	-132.3454933	-224.9915401	-224.9456495
MP4(FC)/6-31G(2df,p)	-92.6409703	-132.4337246	-225.1007416	-225.0579062
MP2(FC)/6-31G(d)	-92.5630595	-132.2928687	-224.8817239	-224.8356027
MP2(FC)/6-31+G(d)	-92.6034004	-132.3034784	-224.9285848	-224.8805197
MP2(FC)/6-31G(2df,p)	-92.6157752	-132.3863276	-225.0288369	-224.9836015
MP2(FULL)/GTLarge	-92.7681910	-132.5671612	-225.3583390	-225.3102520
Thermal Corrections (HF/6-31+G(d))				
Zero-point correction=	0.004740	0.043490	0.048833	0.048010
Thermal correction to Energy=	0.007101	0.047341	0.056763	0.055154
Thermal correction to Enthalpy=	0.008045	0.048285	0.057707	0.056098
Thermal correction to Gibbs Free Energy=	-0.014277	0.019320	0.014629	0.017341
$G_{298} =$	<u>-92.8368432</u>	<u>-132.6452392</u>	<u>-225.4946149</u>	<u>-225.4463389</u>
MP2(FC)/6-311+G(2d,p)	-92.6557428	-132.393841	-225.0733005	-225.0264106
Thermal Corrections (MP2/6-311+G(2d,p))				
Zero-point correction=	0.004504	0.045457	0.050581	0.049736
Thermal correction to Energy=	0.006865	0.049354	0.057434	0.056738
Thermal correction to Enthalpy=	0.007810	0.050298	0.058378	0.057682
Thermal correction to Gibbs Free Energy=	-0.014558	0.022216	0.019145	0.018922

 $\text{OCN}^- + \text{MeOCN}$

Method	NCO^-	MeOCN	Reactant Complex	Transition State
QCISD(T,FC) / 6-31G(d)	-167.6779097	-207.3780207	-375.0850240	-375.0607471
MP4(FC)/6-31G(d)	-167.6843869	-207.3814773	-375.0954625	-375.0718617
MP4(FC)/6-31+G(d)	-167.7193546	-207.3945833	-375.1399835	-375.1174533
MP4(FC)/6-31G(2df,p)	-167.7921084	-207.5322128	-375.3544836	-375.3326913
MP2(FC)/6-31G(d)	-167.6590735	-207.3370899	-375.0256994	-375.0003434
MP2(FC)/6-31+G(d)	-167.6937188	-207.3493608	-375.0687343	-375.0440026
MP2(FC)/6-31G(2df,p)	-167.7597984	-207.4785260	-375.2685140	-375.2445387
MP2(FULL)/GTLarge	-167.9853496	-207.7389729	-375.7510339	-375.7253185
Thermal Corrections (HF/6-31+G(d))				
Zero-point correction=	0.010432	0.048884	0.059888	0.058524
Thermal correction to Energy=	0.013103	0.053396	0.068803	0.066819
Thermal correction to Enthalpy=	0.014048	0.054341	0.069747	0.067764
Thermal correction to Gibbs Free Energy=	-0.010858	0.022348	0.022505	0.022450
$G_{298} =$	<u>-168.0734508</u>	<u>-207.8251642</u>	<u>-375.9141081</u>	<u>-375.8904009</u>
MP2(FC)/6-311+G(2d,p)	-167.7997406	-207.4946389	-375.3204728	-375.2958346
Thermal Corrections (MP2/6-311+G(2d,p))				
Zero-point correction=	0.010342	0.050621	0.061802	0.060524
Thermal correction to Energy=	0.013030	0.055127	0.070474	0.068483
Thermal correction to Enthalpy=	0.013975	0.056071	0.071418	0.069427
Thermal correction to Gibbs Free Energy=	-0.010998	0.024062	0.026072	0.025758

OCN⁻ + MeNCO

Method	NCO ⁻	MeNCO	Reactant Complex	Transition State
QCISD(T,FC) / 6-31G(d)	-167.6779097	-207.4181748	-375.1165235	-375.0747405
MP4(FC)/6-31G(d)	-167.6843869	-207.4248562	-375.1296625	-375.0887695
MP4(FC)/6-31+G(d)	-167.7193546	-207.4372805	-375.1751955	-375.1334697
MP4(FC)/6-31G(2df,p)	-167.7921084	-207.5772786	-375.3894550	-375.3504548
MP2(FC)/6-31G(d)	-167.6590735	-207.3798789	-375.0596936	-375.0170028
MP2(FC)/6-31+G(d)	-167.6937188	-207.3916097	-375.1041092	-375.0603054
MP2(FC)/6-31G(2df,p)	-167.7597984	-207.5232715	-375.3035546	-375.2626175
MP2(FULL)/GTLarge	-167.9853496	-207.7844366	-375.7889032	-375.7455641
Thermal Corrections (HF/6-31+G(d))				
Zero-point correction=	0.010432	0.048585	0.059525	0.058625
Thermal correction to Energy=	0.013103	0.053459	0.069003	0.067390
Thermal correction to Enthalpy=	0.014048	0.054403	0.069947	0.068334
Thermal correction to Gibbs Free Energy=	-0.010858	0.020630	0.019604	0.016439
$G_{298} =$	<u>-168.0734508</u>	<u>-207.8692998</u>	<u>-375.9517400</u>	<u>-375.9128930</u>
MP2(FC)/6-311+G(2d,p)	-167.7997406	-207.5390434	-375.357335	-375.3154434
Thermal Corrections (MP2/6-311+G(2d,p))				
Zero-point correction=	0.010342	0.051115	0.061828	0.060819
Thermal correction to Energy=	0.013030	0.055804	0.071038	0.069018
Thermal correction to Enthalpy=	0.013975	0.056749	0.071983	0.069962
Thermal correction to Gibbs Free Energy=	-0.010998	0.023755	0.022722	0.024000

SCN⁻ + MeSCN

Method	NCS ⁻	MeSCN	Reactant Complex	Transition State
QCISD(T,FC) / 6-31G(d)	-490.3065146	-530.0097314	-1020.3394720	-1020.3026675
MP4(FC)/6-31G(d)	-490.3105848	-530.0120502	-1020.3466489	-1020.3094729
MP4(FC)/6-31+G(d)	-490.3312200	-530.0219030	-1020.3755854	-1020.3399608
MP4(FC)/6-31G(2df,p)	-490.4210470	-530.1622788	-1020.6087142	-1020.5745338
MP2(FC)/6-31G(d)	-490.2764943	-529.9584695	-1020.2590490	-1020.2204697
MP2(FC)/6-31+G(d)	-490.2966554	-529.9677834	-1020.2867488	-1020.2495425
MP2(FC)/6-31G(2df,p)	-490.3769473	-530.0970774	-1020.4998863	-1020.4642227
MP2(FULL)/GTLarge	-490.8466466	-530.6126456	-1021.4838761	-1021.4490974
Thermal Corrections (HF/6-31+G(d))				
Zero-point correction=	0.008397	0.045191	0.054219	0.053050
Thermal correction to Energy=	0.011430	0.050204	0.064101	0.062578
Thermal correction to Enthalpy=	0.012374	0.051149	0.065046	0.063522
Thermal correction to Gibbs Free Energy=	-0.014181	0.017243	0.012713	0.013737
$G_{298} =$	<u>-490.9524192</u>	<u>-530.7162981</u>	<u>-1021.6826128</u>	<u>-1021.6488432</u>
MP2(FC)/6-311+G(2d,p)	-490.397231	-530.1057275	-1020.5254768	-1020.4934642
Thermal Corrections (MP2/6-311+G(2d,p))				
Zero-point correction=	0.008227	0.046901	0.055705	0.054513
Thermal correction to Energy=	0.011216	0.051865	0.065419	0.063661
Thermal correction to Enthalpy=	0.012160	0.052809	0.066363	0.064606
Thermal correction to Gibbs Free Energy=	-0.014340	0.018985	0.015921	0.016772

SCN⁻ + MeNCS

Method	NCS ⁻	MeNCS	Reactant Complex	Transition State
QCISD(T,FC) / 6-31G(d)	-490.3065146	-530.0148271	-1020.3424286	-1020.2978572
MP4(FC)/6-31G(d)	-490.3105848	-530.0199312	-1020.3511091	-1020.3074716
MP4(FC)/6-31+G(d)	-490.3312200	-530.0285739	-1020.3780902	-1020.3350395
MP4(FC)/6-31G(2df,p)	-490.4210470	-530.1727452	-1020.6153805	-1020.5733128
MP2(FC)/6-31G(d)	-490.2764943	-529.9658894	-1020.2639440	-1020.2182275
MP2(FC)/6-31+G(d)	-490.2966554	-529.9738648	-1020.2896330	-1020.2442865
MP2(FC)/6-31G(2df,p)	-490.3769473	-530.1071110	-1020.5065952	-1020.4622689
MP2(FULL)/GTLarge	-490.8466466	-530.6218214	-1021.4893056	-1021.4434257
Thermal Corrections (HF/6-31+G(d))				
Zero-point correction=	0.008397	0.046287	0.055306	0.054323
Thermal correction to Energy=	0.011430	0.051417	0.065243	0.063591
Thermal correction to Enthalpy=	0.012374	0.052361	0.066187	0.064535
Thermal correction to Gibbs Free Energy=	-0.014181	0.018320	0.015054	0.016027
$G_{298} =$	<u>-490.9524192</u>	<u>-530.7221728</u>	<u>-1021.6842105</u>	<u>-1021.6388991</u>
MP2(FC)/6-311+G(2d,p)	-490.397231	-530.1129173	-1020.5330978	-1020.4862617
Thermal Corrections (MP2/6-311+G(2d,p))				
Zero-point correction=	0.008227	0.048541	0.057297	0.056372
Thermal correction to Energy=	0.011216	0.053629	0.067034	0.065240
Thermal correction to Enthalpy=	0.012160	0.054574	0.067978	0.066184
Thermal correction to Gibbs Free Energy=	-0.014340	0.019664	0.017805	0.017324

NO₂⁻ + MeNO₂

Method	NO ₂ ⁻	MeNO ₂	Reactant Complex	Transition State
QCISD(T,FC) / 6-31G(d)	-204.6181533	-244.3669176	-449.0168545	-448.9779525
MP4(FC)/6-31G(d)	-204.6246901	-244.3743463	-449.0313705	-448.9937167
MP4(FC)/6-31+G(d)	-204.6772547	-244.3956839	-449.0986874	-449.0626057
MP4(FC)/6-31G(2df,p)	-204.7570501	-244.5537877	-449.3434045	-449.3082411
MP2(FC)/6-31G(d)	-204.5976597	-244.3319471	-448.9616003	-448.9203341
MP2(FC)/6-31+G(d)	-204.6482695	-244.3517581	-449.0254056	-448.9852911
MP2(FC)/6-31G(2df,p)	-204.7204902	-244.4994315	-449.2522305	-449.2132015
MP2(FULL)/GTLarge	-204.9825010	-244.7890184	-449.7979558	-449.7575299
Thermal Corrections (HF/6-31+G(d))				
Zero-point correction=	0.008137	0.048519	0.057762	0.056606
Thermal correction to Energy=	0.011066	0.052003	0.066792	0.065052
Thermal correction to Enthalpy=	0.012010	0.052947	0.067736	0.065996
Thermal correction to Gibbs Free Energy=	-0.015449	0.022767	0.019984	0.019481
$G_{298} =$	<u>-205.0874019</u>	<u>-244.8913375</u>	<u>-449.9922474</u>	<u>-449.9553623</u>
MP2(FC)/6-311+G(2d,p)	-204.7851469	-244.5321677	-449.3428809	-449.3034532
Thermal Corrections (MP2/6-311+G(2d,p))				
Zero-point correction=	0.007827	0.050545	0.059627	0.058293
Thermal correction to Energy=	0.010762	0.054872	0.068318	0.066484
Thermal correction to Enthalpy=	0.011706	0.055816	0.069263	0.067428
Thermal correction to Gibbs Free Energy=	-0.015865	0.023020	0.023110	0.021209

<u>NO₂⁻ + MeONO</u>				
Method	NO ₂ ⁻	MeONO	Reactant Complex	Transition State
QCISD(T,FC) / 6-31G(d)	-204.6181533	-244.3650740	-449.0081025	-448.9803951
MP4(FC)/6-31G(d)	-204.6246901	-244.3691473	-449.0193683	-448.9942578
MP4(FC)/6-31+G(d)	-204.6772547	-244.3892275	-449.0866333	-449.0614598
MP4(FC)/6-31G(2df,p)	-204.7570501	-244.5458579	-449.3289930	-449.3047423
MP2(FC)/6-31G(d)	-204.5976597	-244.3212565	-448.9443425	-448.9166797
MP2(FC)/6-31+G(d)	-204.6482695	-244.3397612	-449.0079512	-448.9796812
MP2(FC)/6-31G(2df,p)	-204.7204902	-244.4864688	-449.2329630	-449.2057025
MP2(FULL)/GTLarge	-204.9825010	-244.7746922	-449.7776703	-449.7485663
Thermal Corrections (HF/6-31+G(d))				
Zero-point correction=	0.008137	0.047209	0.056251	0.055543
Thermal correction to Energy=	0.011066	0.051970	0.065965	0.064302
Thermal correction to Enthalpy=	0.012010	0.052915	0.066909	0.065246
Thermal correction to Gibbs Free Energy=	-0.015449	0.020239	0.017520	0.019938
$G_{298} =$	<u>-205.0874019</u>	<u>-244.8879765</u>	<u>-449.9826768</u>	<u>-449.9521119</u>
MP2(FC)/6-311+G(2d,p)	-204.7851469	-244.5189629	-449.3237405	-449.2951434
Thermal Corrections (MP2/6-311+G(2d,p))				
Zero-point correction=	0.007827	0.047895	0.057445	0.057104
Thermal correction to Energy=	0.010762	0.051967	0.066885	0.065422
Thermal correction to Enthalpy=	0.011706	0.052911	0.067829	0.066367
Thermal correction to Gibbs Free Energy=	-0.015865	0.021757	0.019760	0.022518
<u>CH₂CHO⁻ + CH₂CHOCH₃</u>				
Method	CH ₂ CHO ⁻	CH ₂ CHOCH ₃	Reactant Complex	Transition State
QCISD(T,FC) / 6-31G(d)	-152.7579014	-192.5335287	-345.3156527	-345.2763182
MP4(FC)/6-31G(d)	-152.7593624	-192.5325622	-345.3160111	-345.2784329
MP4(FC)/6-31+G(d)	-152.8023030	-192.5470377	-345.3697859	-345.3323451
MP4(FC)/6-31G(2df,p)	-152.8845279	-192.7005817	-345.6096636	-345.5739272
MP2(FC)/6-31G(d)	-152.7221989	-192.4759470	-345.2220563	-345.1820130
MP2(FC)/6-31+G(d)	-152.7647355	-192.4897437	-345.2742988	-345.2338309
MP2(FC)/6-31G(2df,p)	-152.8393957	-192.6339300	-345.4978682	-345.4592908
MP2(FULL)/GTLarge	-153.0699020	-192.8924102	-345.9815046	-345.9424643
Thermal Corrections (HF/6-31+G(d))				
Zero-point correction=	0.040373	0.082000	0.122944	0.121287
Thermal correction to Energy=	0.043865	0.086875	0.133580	0.131387
Thermal correction to Enthalpy=	0.044809	0.087819	0.134524	0.132331
Thermal correction to Gibbs Free Energy=	0.016181	0.055166	0.083640	0.083070
$G_{298} =$	<u>-153.1552702</u>	<u>-192.9821732</u>	<u>-346.1449399</u>	<u>-346.1081163</u>
MP2(FC)/6-311+G(2d,p)	-152.8861988	-192.6493293	-345.547962	-345.5165721
Thermal Corrections (MP2/6-311+G(2d,p))				
Zero-point correction=	0.041975	0.085948	0.127894	0.127213
Thermal correction to Energy=	0.045493	0.090654	0.138489	0.136736
Thermal correction to Enthalpy=	0.046437	0.091599	0.139433	0.137680
Thermal correction to Gibbs Free Energy=	0.017730	0.059304	0.088674	0.091339



Method	CH_2CHO^-	$\text{H}_3\text{CCH}_2\text{CHO}$	Reactant Complex	Transition State
QCISD(T,FC) / 6-31G(d)	-152.7579014	-192.5691554	-345.3541635	-345.2718325
MP4(FC)/6-31G(d)	-152.7593624	-192.5698029	-345.3562792	-345.2761775
MP4(FC)/6-31+G(d)	-152.8023030	-192.5824122	-345.4082457	-345.3284558
MP4(FC)/6-31G(2df,p)	-152.8845279	-192.7347172	-345.6476001	-345.5700402
MP2(FC)/6-31G(d)	-152.7221989	-192.5139520	-345.2632279	-345.1831352
MP2(FC)/6-31+G(d)	-152.7647355	-192.5257451	-345.3136410	-345.2337066
MP2(FC)/6-31G(2df,p)	-152.8393957	-192.6686670	-345.5365628	-345.4594690
MP2(FULL)/GTLarge	-153.0699020	-192.9241536	-346.0172944	-345.9420296
Thermal Corrections (HF/6-31+G(d))				
Zero-point correction=	0.040373	0.080979	0.122699	0.120521
Thermal correction to Energy=	0.043865	0.086071	0.133376	0.130222
Thermal correction to Enthalpy=	0.044809	0.087016	0.134321	0.131166
Thermal correction to Gibbs Free Energy=	0.016181	0.053583	0.082197	0.084418
$G_{298} =$	<u>-153.1552702</u>	<u>-193.0134215</u>	<u>-346.1796784</u>	<u>-346.0996507</u>
MP2(FC)/6-311+G(2d,p)	-152.8861988	-192.6836966	-345.5942324	-345.5181933
Thermal Corrections (MP2/6-311+G(2d,p))				
Zero-point correction=	0.041975	0.085150	0.128930	0.126611
Thermal correction to Energy=	0.045493	0.090106	0.138949	0.135772
Thermal correction to Enthalpy=	0.046437	0.091050	0.139893	0.136716
Thermal correction to Gibbs Free Energy=	0.017730	0.057922	0.092410	0.091557

5.3 G3(+) and MP2 Energies for the Methylation of the Enolate of Acetaldehyde

Method	CH ₂ CHO	MeF	Reactant Complex	Transition State	Product Complex	CH ₂ CHOCH ₃	F ⁻
QCISD(T,FC) / 6-31G(d)	-152.7579014	-139.360405	-292.1397262	-292.0953092	-292.1250744	-192.535287	-99.5297119
MP4(FC)/6-31G(d)	-152.7593624	-139.360515	-292.1413754	-292.0971538	-292.1250449	-192.5325622	-99.5307477
MP4(FC)/6-31+G(d)	-152.802303	-139.3791769	-292.2008375	-292.1737262	-292.2050717	-192.5470377	-99.6297500
MP4(FC)/6-31G(2df,p)	-152.8845279	-139.470315	-292.3759884	-292.3322476	-292.3583094	-192.7005817	-99.5927206
MP2(FC)/6-31G(d)	-152.7221989	-139.3356508	-292.0792705	-292.0333533	-292.0639747	-192.475947	-99.5266066
MP2(FC)/6-31+G(d)	-152.7647355	-139.3534935	-292.1370931	-292.1066754	-292.1410317	-192.4897437	-99.6238467
MP2(FC)/6-31G(2df,p)	-152.8393957	-139.4379754	-292.2986184	-292.252814	-292.2822245	-192.633930	-99.5837754
MP2(FULL)/GTLarge	-153.0699020	-139.6096162	-292.6974501	-292.6637676	-292.6971929	-192.8924102	-99.7736485
Thermal Corrections (HF/6-31+G(d))							
Zero-point correction=	0.040373	0.037806	0.079006	0.079601	0.081269	0.082000	0.000000
Thermal correction to Energy=	0.043865	0.040727	0.087502	0.086653	0.08901	0.086875	0.001416
Thermal correction to Enthalpy=	0.044809	0.041671	0.088446	0.087597	0.089954	0.087819	0.00236
Thermal correction to Gibbs Free Energy=	0.016181	0.01641	0.041496	0.047857	0.047551	0.055166	-0.014159
$G_{298} =$	<u>-153.1552702</u>	<u>-139.670957</u>	<u>-292.8354904</u>	<u>-292.7989259</u>	<u>-292.8309021</u>	<u>-192.9821732</u>	<u>-99.8223551</u>
MP2(FC)/6-31+G(2d,p)	-152.8861988	139.4785434	-292.3827186	-292.3508514	-292.3825809	-192.6493293	-99.703831
Thermal Corrections (MP2/6-31+G(2d,p))							
Zero-point correction=	0.041975	0.039995	0.083471	0.083534	0.085429	0.085948	0.000000
Thermal correction to Energy=	0.045493	0.042901	0.091347	0.090218	0.09244	0.090654	0.001416
Thermal correction to Enthalpy=	0.046437	0.043845	0.092292	0.091162	0.093384	0.091599	0.00236
Thermal correction to Gibbs Free Energy=	0.017730	0.017531	0.050322	0.052941	0.053193	0.059304	-0.014159

O-Attack by MeF

C-Attack by MeF

Method	CH ₂ CHO ⁻	MeF	Reactant Complex	Transition State	Product Complex	H ₃ CCH ₂ CHO	F ⁻
QCISD(T,FC) / 6-31G(d)	-152.7579014	-139.360405	-292.1397262	-292.0912932	-292.1594539	-192.5691554	-99.5297119
MP4(FC)/6-31G(d)	-152.7593624	-139.360515	-292.1413754	-292.0943852	-292.1610403	-192.5698029	-99.5307477
MP4(FC)/6-31+G(d)	-152.802303	-139.3791769	-292.2008375	-292.168379	-292.2423944	-192.5824122	-99.6297500
MP4(FC)/6-31G(2df,p)	-152.8845279	-139.470315	-292.3759884	-292.3288735	-292.3914035	-192.7347172	-99.5927206
MP2(FC)/6-31G(d)	-152.7221989	-139.3356508	-292.0792705	-292.0316515	-292.1008214	-192.513952	-99.5266066
MP2(FC)/6-31+G(d)	-152.7647355	-139.3534935	-292.1370931	-292.102453	-292.1791651	-192.5257451	-99.6238467
MP2(FC)/6-31G(2df,p)	-152.8393957	-139.4379754	-292.2986184	-292.250706	-292.3160248	-192.6686670	-99.5837754
MP2(FULL)/GTLarge	-153.0699020	-139.6096162	-292.6974501	-292.6598606	-292.7311899	-192.9241536	-99.7736485
Thermal Corrections (HF/6-31+G(d))							
Zero-point correction=	0.040373	0.037806	0.079006	0.079065	0.081873	0.080979	0.000000
Thermal correction to Energy=	0.043865	0.040727	0.087502	0.085933	0.089025	0.086071	0.001416
Thermal correction to Enthalpy=	0.044809	0.041671	0.088446	0.086877	0.089970	0.087016	0.00236
Thermal correction to Gibbs Free Energy=	0.016181	0.016410	0.041496	0.048092	0.050173	0.053583	-0.014159
$G_{298} =$	<u>-153.1552702</u>	<u>-139.670957</u>	<u>-292.8354904</u>	<u>-292.7922124</u>	<u>-292.8599956</u>	<u>-193.0134215</u>	<u>-99.8223551</u>
MP2(FC)/6-31+G(2d,p)	-152.8861988	139.4785434	-292.3827186	-292.3479248	-292.4190725	-192.6836966	-99.703831
Thermal Corrections (MP2/6-31+G(2d,p))							
Zero-point correction=	0.041975	0.039995	0.083471	0.083121	0.085889	0.085150	0.000000
Thermal correction to Energy=	0.045493	0.042901	0.091347	0.089623	0.092769	0.090106	0.001416
Thermal correction to Enthalpy=	0.046437	0.043845	0.092292	0.090567	0.093713	0.091050	0.00236
Thermal correction to Gibbs Free Energy=	0.017730	0.017531	0.050322	0.052751	0.054783	0.057922	-0.014159

O-Attack by MeCl

Method	CH ₂ CHO ⁻	MeCl	Reactant Complex	Transition State	Product Complex	CH ₂ CHOCH ₃	Cl ⁻
QCISD(T,FC) / 6-31G(d)	-152.7579014	-499.3898601	-652.1714442	-652.160035	-652.2169036	-192.5335287	-459.6665483
MP4(FC)/6-31G(d)	-152.7593624	-499.3886962	-652.171889	-652.1603726	-652.2153333	-192.5325622	-459.6662592
MP4(FC)/6-31+G(d)	-152.802303	-499.3919796	-652.2140342	-652.1981536	-652.2485374	-192.5470377	-459.6858399
MP4(FC)/6-31G(2df,p)	-152.8845279	-499.4962489	-652.4061278	-652.3969658	-652.4480987	-192.7005817	-459.7314657
MP2(FC)/6-31G(d)	-152.7221989	-499.3545596	-652.1006495	-652.0866541	-652.1443837	-192.475947	-459.6521044
MP2(FC)/6-31+G(d)	-152.7647355	-499.3574655	-652.1416259	-652.1228156	-652.1761756	-192.4897437	-459.6711454
MP2(FC)/6-31G(2df,p)	-152.8393957	-499.450606	-652.3156411	-652.3039081	-652.3581835	-192.633930	-459.7082425
MP2(FULL)/GTLarge	-153.0699020	-499.8574752	-652.9476395	-652.9310374	-652.981966	-192.8924102	-460.0746719
Thermal Corrections (HF/6-31+G(d))							
Zero-point correction=	0.040373	0.036297	0.077414	0.077911	0.081788	0.082000	0.000000
Thermal correction to Energy=	0.043865	0.039333	0.086158	0.085563	0.089385	0.086875	0.001416
Thermal correction to Enthalpy=	0.044809	0.040278	0.087102	0.086507	0.090329	0.087819	0.00236
Thermal correction to Gibbs Free Energy=	0.016181	0.013682	0.038845	0.042692	0.047900	0.055166	-0.015023
$G_{298} =$	<u>-153.1552702</u>	<u>-499.9356795</u>	<u>-653.1021812</u>	<u>-653.084861</u>	<u>-653.1291397</u>	<u>-192.9821732</u>	<u>-460.1386229</u>
MP2(FC)/6-31+G(2d,p)	-152.8861988	-499.4562803	-652.362523	-652.3471711	-652.3956365	-192.6493293	-459.7315876
Thermal Corrections (MP2/6-31+G(2d,p))							
Zero-point correction=	0.041975	0.038448	0.081939	0.082177	0.085611	0.085948	0.000000
Thermal correction to Energy=	0.045493	0.041450	0.089951	0.089293	0.092967	0.090654	0.001416
Thermal correction to Enthalpy=	0.046437	0.042394	0.090895	0.090237	0.093911	0.091599	0.00236
Thermal correction to Gibbs Free Energy=	0.017730	0.015829	0.048033	0.049999	0.052673	0.059304	-0.015023

C-Attack by MeCl

Method	CH ₂ CHO ⁻	MeCl	Reactant Complex	Transition State	Product Complex	H ₃ CCH ₂ CHO	Cl ⁻
QCISD(T,FC) / 6-31G(d)	-152.7579014	-499.3898601	-652.1714442	-652.1566916	-652.2554127	-192.5691554	-459.6665483
MP4(FC)/6-31G(d)	-152.7593624	-499.3886962	-652.171889	-652.1576332	-652.255663	-192.5698029	-459.6662592
MP4(FC)/6-31+G(d)	-152.802303	-499.3919796	-652.2140342	-652.1941554	-652.2874548	-192.5824122	-459.6858399
MP4(FC)/6-31G(2df,p)	-152.8845279	-499.4962489	-652.4061278	-652.3931606	-652.4864709	-192.7347172	-459.7314657
MP2(FC)/6-31G(d)	-152.7221989	-499.3545596	-652.1006495	-652.0855076	-652.1856684	-192.513952	-459.6521044
MP2(FC)/6-31+G(d)	-152.7647355	-499.3574655	-652.1416259	-652.1205757	-652.2160278	-192.5257451	-459.6711454
MP2(FC)/6-31G(2df,p)	-152.8393957	-499.450606	-652.3156411	-652.302082	-652.3973511	-192.6686670	-459.7082425
MP2(FULL)/GTLarge	-153.0699020	-499.8574752	-652.9476395	-652.9291758	-653.0190045	-192.9241536	-460.0746719
Thermal Corrections (HF/6-31+G(d))							
Zero-point correction=	0.040373	0.036297	0.077414	0.077751	0.081740	0.080979	0.000000
Thermal correction to Energy=	0.043865	0.039333	0.086158	0.085110	0.089226	0.086071	0.001416
Thermal correction to Enthalpy=	0.044809	0.040278	0.087102	0.086055	0.090170	0.087016	0.002360
Thermal correction to Gibbs Free Energy=	0.016181	0.013682	0.038845	0.045102	0.048012	0.053583	-0.015023
G_{298}^{\ddagger} =	<u>-153.1552702</u>	<u>-499.9356795</u>	<u>-653.1021812</u>	<u>-653.0778409</u>	<u>-653.1634704</u>	<u>-193.0134215</u>	<u>-460.1386229</u>
MP2(FC)/6-31+G(2d,p)	-152.8861988	-499.4562803	-652.362523	-652.3459791	-652.4353177	-192.6836966	-459.7315876
Thermal Corrections (MP2/6-31+G(2d,p))							
Zero-point correction=	0.041975	0.038448	0.081939	0.081834	0.085964	0.085150	0.000000
Thermal correction to Energy=	0.045493	0.041450	0.089951	0.088774	0.093183	0.090106	0.001416
Thermal correction to Enthalpy=	0.046437	0.042394	0.090895	0.089718	0.094128	0.091050	0.00236
Thermal correction to Gibbs Free Energy=	0.017730	0.015829	0.048033	0.050036	0.053156	0.057922	-0.015023

O-Attack by MeBr

Method	CH ₂ CHO ⁻	MeBr	Reactant Complex	Transition State	Product Complex	CH ₂ CHOCH ₃	Br ⁻
QCISD(T,FC) / 6-31G(d)	-152.7579014	-2609.776995	-2762.560178	-2762.554937	-2762.610586	-192.5335287	-2570.063498
MP4(FC)/6-31G(d)	-152.7593624	-2609.776158	-2762.560978	-2762.555758	-2762.609382	-192.5325622	-2570.063434
MP4(FC)/6-31+G(d)	-152.802303	-2609.791847	-2762.620178	-2762.611028	-2762.659751	-192.5470377	-2570.100669
MP4(FC)/6-31G(2df,p)	-152.8845279	-2610.05244	-2762.962892	-2762.954411	-2763.003939	-192.7005817	-2570.290418
MP2(FC)/6-31G(d)	-152.7221989	-2609.744816	-2762.49258	-2762.485509	-2762.541988	-192.475947	-2570.052813
MP2(FC)/6-31+G(d)	-152.7647355	-2609.760136	-2762.550572	-2762.539065	-2762.590926	-192.4897437	-2570.089534
MP2(FC)/6-31G(2df,p)	-152.8393957	-2610.009425	-2762.874908	-2762.86361	-2762.916031	-192.633930	-2570.269213
MP2(FULL)/GTLarge	-153.0699020	-2613.376821	-2766.467722	-2766.455878	-2766.508743	-192.8924102	-2573.60617
Thermal Corrections (HF/6-31+G(d))							
Zero-point correction=	0.040373	0.035709	0.077381	0.077787	0.081403	0.082000	0.000000
Thermal correction to Energy=	0.043865	0.038828	0.085813	0.085413	0.089264	0.086875	0.001416
Thermal correction to Enthalpy=	0.044809	0.039773	0.086757	0.086357	0.090208	0.087819	0.002360
Thermal correction to Gibbs Free Energy=	0.016181	0.011852	0.040969	0.043216	0.044955	0.055166	-0.016176
$G_{298} =$	<u>-153.1552702</u>	<u>-2613.453891</u>	<u>-2766.61732</u>	<u>-2766.606533</u>	<u>-2766.656508</u>	<u>-192.9821732</u>	<u>-2573.669004</u>
MP2(FC)/6-31+G(2d,p)	-152.8861988	-2612.287219	-2765.194288	-2765.18349	-2765.238111	-192.6493293	-2572.57705
Thermal Corrections (MP2/6-31+G(2d,p))							
Zero-point correction=	0.041975	0.037779	0.08126	0.081506	0.085512	0.085948	0.000000
Thermal correction to Energy=	0.045493	0.040853	0.089389	0.088833	0.092989	0.090654	0.001416
Thermal correction to Enthalpy=	0.046437	0.041797	0.090333	0.089777	0.093933	0.091599	0.00236
Thermal correction to Gibbs Free Energy=	0.017730	0.012899	0.046239	0.04793	0.051056	0.059304	-0.016176

C-Attack by MeBr

Method	CH ₂ CHO ⁻	MeBr	Reactant Complex	Transition State	Product Complex	H ₃ CCH ₂ CHO	Br ⁻
QCISD(T,FC) / 6-31G(d)	-152.7579014	-2609.776995	-2762.560178	-2762.55223	-2762.65595	-192.5691554	-2570.063498
MP4(FC)/6-31G(d)	-152.7593624	-2609.776158	-2762.560978	-2762.553596	-2762.656518	-192.5698029	-2570.063434
MP4(FC)/6-31+G(d)	-152.802303	-2609.791847	-2762.620178	-2762.608228	-2762.703562	-192.5824122	-2570.100669
MP4(FC)/6-31G(2df,p)	-152.8845279	-2610.05244	-2762.962892	-2762.951575	-2763.047743	-192.7347172	-2570.290418
MP2(FC)/6-31G(d)	-152.7221989	-2609.744816	-2762.49258	-2762.485105	-2762.590218	-192.513952	-2570.052813
MP2(FC)/6-31+G(d)	-152.7647355	-2609.760136	-2762.550572	-2762.538234	-2762.635759	-192.5257451	-2570.089534
MP2(FC)/6-31G(2df,p)	-152.8393957	-2610.009425	-2762.874908	-2762.862947	-2762.960798	-192.6686670	-2570.269213
MP2(FULL)/GTLarge	-153.0699020	-2613.376821	-2766.467722	-2766.455273	-2766.548847	-192.9241536	-2573.606170
Thermal Corrections (HF/6-31+G(d))							
Zero-point correction=	0.040373	0.035709	0.077381	0.077634	0.081739	0.080979	0.000000
Thermal correction to Energy=	0.043865	0.038828	0.085813	0.084998	0.089255	0.086071	0.001416
Thermal correction to Enthalpy=	0.044809	0.039773	0.086757	0.085942	0.090199	0.087016	0.00236
Thermal correction to Gibbs Free Energy=	0.016181	0.011852	0.040969	0.043995	0.046829	0.053583	-0.016176
$G_{298} =$	<u>-153.1552702</u>	<u>-2613.453891</u>	<u>-2766.61732</u>	<u>-2766.602219</u>	<u>-2766.692075</u>	<u>-193.0134215</u>	<u>-2573.669004</u>
MP2(FC)/6-31+G(2d,p)	-152.8861988	-2612.287219	-2765.194288	-2765.183229	-2765.277913	-192.6836966	-2572.57705
Thermal Corrections (MP2/6-31+G(2d,p))							
Zero-point correction=	0.041975	0.037779	0.08126	0.081191	0.085858	0.085150	0.000000
Thermal correction to Energy=	0.045493	0.040853	0.089389	0.088332	0.093171	0.090106	0.001416
Thermal correction to Enthalpy=	0.046437	0.041797	0.090333	0.089277	0.094115	0.091050	0.002360
Thermal correction to Gibbs Free Energy=	0.017730	0.012899	0.046239	0.048089	0.051659	0.057922	-0.016176

O-Attack by MeOH

Method	CH ₂ CHO	MeOH	Reactant Complex	Transition State	Product Complex	CH ₂ CHOCH ₃	HO
QCISD(T,FC) / 6-31G(d)	-152.7579014	-115.3747656	-268.1726431	-268.0803997	-268.1022836	-192.5335287	-75.5217844
MP4(FC)/6-31G(d)	-152.7593624	-115.3737564	-268.1731734	-268.0807813	-268.1010921	-192.5325622	-75.5213372
MP4(FC)/6-31+G(d)	-152.802303	-115.3861425	-268.2212259	-268.1470223	-268.1749721	-192.5470377	-75.5966594
MP4(FC)/6-31G(2df,p)	-152.8845279	-115.4834891	-268.4085953	-268.3177237	-268.3378586	-192.7005817	-75.5874369
MP2(FC)/6-31G(d)	-152.7221989	-115.3460225	-268.1089379	-268.0137298	-268.0365161	-192.475947	-75.5131337
MP2(FC)/6-31+G(d)	-152.7647355	-115.3578372	-268.1555493	-268.0779167	-268.1087492	-192.4897437	-75.5883642
MP2(FC)/6-31G(2df,p)	-152.8393957	-115.448731	-268.3293186	-268.2355316	-268.2586139	-192.633930	-75.574475
MP2(FULL)/GTLarge	-153.0699020	-115.5975128	-268.7003334	-268.622649	-268.6520067	-192.8924102	-75.7288728
Thermal Corrections (HF/6-31+G(d))							
Zero-point correction=	0.040373	0.049287	0.091972	0.089391	0.091151	0.082000	0.008071
Thermal correction to Energy=	0.043865	0.052651	0.100079	0.0973	0.099442	0.086875	0.010432
Thermal correction to Enthalpy=	0.044809	0.053595	0.101023	0.098244	0.100386	0.087819	0.011376
Thermal correction to Gibbs Free Energy=	0.016181	0.026542	0.057401	0.057057	0.058745	0.055166	-0.008157
$G_{298} =$	<u>-153.1552702</u>	<u>-115.6520115</u>	<u>-268.8252959</u>	<u>-268.7516326</u>	<u>-268.7775208</u>	<u>-192.9821732</u>	<u>-75.7754066</u>
MP2(FC)/6-31+G(2d,p)	-152.8861988	-115.4691855	-268.3880418	-268.311012	-268.3393858	-192.6493293	-75.6595631
Thermal Corrections (MP2/6-31+G(2d,p))							
Zero-point correction=	0.041975	0.052031	0.096274	0.093761	0.095641	0.085948	0.008658
Thermal correction to Energy=	0.045493	0.055377	0.10393	0.101317	0.103416	0.090654	0.011019
Thermal correction to Enthalpy=	0.046437	0.056321	0.104874	0.102261	0.10436	0.091599	0.011963
Thermal correction to Gibbs Free Energy=	0.017730	0.029253	0.06379	0.062412	0.064256	0.059304	-0.0076

C-Attack by MeOH

Method	CH ₂ CHO ⁻	MeOH	Reactant Complex	Transition State	Product Complex	H ₃ CCH ₂ CHO	HO ⁻
QCISD(T,FC)/6-31G(d)	-152.7579014	-115.3747656	-268.1726431	-268.0799942	-268.139248	-192.5691554	-75.5217844
MP4(FC)/6-31G(d)	-152.7593624	-115.3737564	-268.1731734	-268.0819347	-268.1397492	-192.5698029	-75.5213372
MP4(FC)/6-31+G(d)	-152.802303	-115.3861425	-268.2212259	-268.1455884	-268.2130749	-192.5824122	-75.5966594
MP4(FC)/6-31G(2df,p)	-152.8845279	-115.4834891	-268.4085953	-268.3180237	-268.373897	-192.7347172	-75.5874369
MP2(FC)/6-31G(d)	-152.7221989	-115.3460225	-268.1089379	-268.016025	-268.0759779	-192.513952	-75.5131337
MP2(FC)/6-31+G(d)	-152.7647355	-115.3578372	-268.1555493	-268.0775821	-268.147616	-192.5257451	-75.5883642
MP2(FC)/6-31G(2df,p)	-152.8393957	-115.448731	-268.3293186	-268.2372186	-268.2953054	-192.6686670	-75.574475
MP2(FULL)/GTLarge	-153.0699020	-115.5975128	-268.7003334	-268.6223344	-268.687361	-192.9241536	-75.7288728
Thermal Corrections (HF/6-31+G(d))							
Zero-point correction=	0.040373	0.049287	0.091972	0.088968	0.091143	0.080979	0.008071
Thermal correction to Energy=	0.043865	0.052651	0.100079	0.096643	0.09933	0.086071	0.010432
Thermal correction to Enthalpy=	0.044809	0.053595	0.101023	0.097587	0.100274	0.087016	0.011376
Thermal correction to Gibbs Free Energy=	0.016181	0.026542	0.057401	0.057375	0.05877	0.053583	-0.008157
$G_{298} =$	<u>-153.1552702</u>	<u>-115.6520115</u>	<u>-268.8252959</u>	<u>-268.7480966</u>	<u>-268.810545</u>	<u>-193.0134215</u>	<u>-75.7754066</u>
MP2(FC)/6-31+G(2d,p)	-152.8861988	-115.4691855	-268.3880418	-268.3118658	-268.3767802	-192.6836966	-75.6595631
Thermal Corrections (MP2/6-31+G(2d,p))							
Zero-point correction=	0.041975	0.052031	0.096274	0.093544	0.095757	0.085150	0.008658
Thermal correction to Energy=	0.045493	0.055377	0.10393	0.100824	0.103649	0.090106	0.011019
Thermal correction to Enthalpy=	0.046437	0.056321	0.104874	0.101768	0.104593	0.091050	0.011963
Thermal correction to Gibbs Free Energy=	0.017730	0.029253	0.06379	0.062556	0.063899	0.057922	-0.0076

O-Attack by MeOMe

Method	CH ₂ CHO ⁻	MeOMe	Reactant Complex	Transition State	Product Complex	CH ₂ CHOCH ₃	MeO ⁻
QCISD(T,FC)/6-31G(d)	-152.7579014	-154.5493898	-307.3266276	-307.267739	-307.2947209	-192.5335287	-114.7266946
MP4(FC)/6-31G(d)	-152.7593624	-154.5482046	-307.3270717	-307.2683838	-307.2938105	-192.5325622	-114.7265927
MP4(FC)/6-31+G(d)	-152.802303	-154.5603406	-307.3790722	-307.3224122	-307.3459498	-192.5470377	-114.7709898
MP4(FC)/6-31G(2df,p)	-152.8845279	-154.6939294	-307.5987365	-307.5417426	-307.5659142	-192.7005817	-114.8288905
MP2(FC)/6-31G(d)	-152.7221989	-154.5034038	-307.2450134	-307.1839674	-307.2114489	-192.475947	-114.7006724
MP2(FC)/6-31+G(d)	-152.7647355	-154.5146249	-307.2953119	-307.2354384	-307.2616106	-192.4897437	-114.7445329
MP2(FC)/6-31G(2df,p)	-152.8393957	-154.6394841	-307.4992513	-307.4396052	-307.4661736	-192.633930	-114.7955339
MP2(FULL)/GTLarge	-153.0699020	-154.8423668	-307.9282668	-307.8698697	-307.8948792	-192.8924102	-114.9761385
Thermal Corrections (HF/6-31+G(d))							
Zero-point correction=	0.040373	0.076742	0.118083	0.116157	0.117361	0.082000	0.034454
Thermal correction to Energy=	0.043865	0.08116	0.128122	0.125435	0.127282	0.086875	0.037371
Thermal correction to Enthalpy=	0.044809	0.082104	0.129066	0.126379	0.128226	0.087819	0.038316
Thermal correction to Gibbs Free Energy=	0.016181	0.051259	0.078725	0.080388	0.079129	0.055166	0.013271
$G_{298} =$	<u>-153.1552702</u>	<u>-154.9115132</u>	<u>-308.0716189</u>	<u>-308.0148657</u>	<u>-308.0397128</u>	<u>-192.9821732</u>	<u>-115.0403956</u>
MP2(FC)/6-31+G(2d,p)	-152.8861988	-154.6561942	-307.557828	-307.5008102	-307.5245466	-192.6493293	-114.8492252
Thermal Corrections (MP2/6-31+G(2d,p))							
Zero-point correction=	0.041975	0.080992	0.124242	0.122247	0.123153	0.085948	0.036287
Thermal correction to Energy=	0.045493	0.085277	0.133794	0.130945	0.132724	0.090654	0.039192
Thermal correction to Enthalpy=	0.046437	0.086221	0.134738	0.13189	0.133669	0.091599	0.040136
Thermal correction to Gibbs Free Energy=	0.017730	0.055632	0.087689	0.088249	0.086639	0.059304	0.015073

C-Attack by MeOMe

Method	CH ₂ CHO	MeOMe	Reactant Complex	Transition State	Product Complex	H ₃ CCH ₂ CHO	MeO
QCISD(T,FC) / 6-31G(d)	-152.7579014	-154.5493898	-307.3266276	-307.2647432	-307.3322297	-192.5691554	-114.7266946
MP4(FC)/6-31G(d)	-152.7593624	-154.5482046	-307.3270717	-307.2670177	-307.3330344	-192.5698029	-114.7265927
MP4(FC)/6-31+G(d)	-152.802303	-154.5603406	-307.3790722	-307.3201478	-307.3840698	-192.5824122	-114.7709898
MP4(FC)/6-31G(2df,p)	-152.8845279	-154.6939294	-307.5987365	-307.5396118	-307.6024191	-192.7347172	-114.8288905
MP2(FC)/6-31G(d)	-152.7221989	-154.5034038	-307.2450134	-307.1838114	-307.251526	-192.513952	-114.7006724
MP2(FC)/6-31+G(d)	-152.7647355	-154.5146249	-307.2953119	-307.2344039	-307.3004845	-192.5257451	-114.7445329
MP2(FC)/6-31G(2df,p)	-152.8393957	-154.6394841	-307.4992513	-307.4389145	-307.5033626	-192.6686670	-114.7955339
MP2(FULL)/GTLarge	-153.0699020	-154.8423668	-307.9282668	-307.8683273	-307.9302619	-192.9241536	-114.9761385
Thermal Corrections (HF/6-31+G(d))							
Zero-point correction=	0.040373	0.076742	0.118083	0.115726	0.11716	0.080979	0.034454
Thermal correction to Energy=	0.043865	0.08116	0.128122	0.124804	0.127077	0.086071	0.037371
Thermal correction to Enthalpy=	0.044809	0.082104	0.129066	0.125748	0.128021	0.087016	0.038316
Thermal correction to Gibbs Free Energy=	0.016181	0.051259	0.078725	0.080845	0.078155	0.053583	0.013271
$G_{298} =$	<u>-153.1552702</u>	<u>-154.9115132</u>	<u>-308.0716189</u>	<u>-308.0097767</u>	<u>-308.0737696</u>	<u>-193.0134215</u>	<u>-115.0403956</u>
MP2(FC)/6-31+G(2d,p)	-152.8861988	-154.6561942	-307.557828	-307.5006388	-307.5623104	-192.6836966	-114.8492252
Thermal Corrections (MP2/6-31+G(2d,p))							
Zero-point correction=	0.041975	0.080992	0.124242	0.122062	0.123366	0.085150	0.036287
Thermal correction to Energy=	0.045493	0.085277	0.133794	0.130529	0.132928	0.090106	0.039192
Thermal correction to Enthalpy=	0.046437	0.086221	0.134738	0.131473	0.133872	0.091050	0.040136
Thermal correction to Gibbs Free Energy=	0.017730	0.055632	0.087689	0.088486	0.086563	0.057922	0.015073

O-Attack by MeSH

Method	CH ₂ CHO ⁻	MeSH	Reactant Complex	Transition State	Product Complex	CH ₂ CHOCH ₃	HS ⁻
QCISD(T,FC) / 6-31G(d)	-152.7579014	-437.9933162	-590.802058	-590.7365288	-590.7802615	-192.5335287	-398.2308385
MP4(FC)/6-31G(d)	-152.7593624	-437.9915145	-590.8003715	-590.7362925	-590.778167	-192.5325622	-398.229966
MP4(FC)/6-31+G(d)	-152.802303	-437.9949488	-590.8330879	-590.7737571	-590.812479	-192.5470377	-398.2495496
MP4(FC)/6-31G(2df,p)	-152.8845279	-438.101794	-591.0404041	-590.977366	-591.0162363	-192.7005817	-398.3013416
MP2(FC)/6-31G(d)	-152.7221989	-437.9526667	-590.7268433	-590.6574707	-590.7019607	-192.475947	-398.210451
MP2(FC)/6-31+G(d)	-152.7647355	-437.9557494	-590.7582884	-590.6931951	-590.7348848	-192.4897437	-398.2296047
MP2(FC)/6-31G(2df,p)	-152.8393957	-438.0532767	-590.9493931	-590.8809132	-590.9222997	-192.633930	-398.273999
MP2(FULL)/GTLarge	-153.0699020	-438.4505598	-591.5631712	-591.4981279	-591.5378031	-192.8924102	-398.6320383
Thermal Corrections (HF/6-31+G(d))							
Zero-point correction=	0.040373	0.044239	0.086033	0.085183	0.087996	0.082000	0.005664
Thermal correction to Energy=	0.043865	0.047877	0.094709	0.093725	0.097047	0.086875	0.008025
Thermal correction to Enthalpy=	0.044809	0.048821	0.095653	0.094669	0.097991	0.087819	0.008969
Thermal correction to Gibbs Free Energy=	0.016181	0.020003	0.049131	0.050168	0.052182	0.055166	-0.012174
$G_{298} =$	<u>-153.1552702</u>	<u>-438.5259294</u>	<u>-591.710185</u>	<u>-591.6485652</u>	<u>-591.6852161</u>	<u>-192.9821732</u>	<u>-398.6977333</u>
MP2(FC)/6-31+G(2d,p)	-152.8861988	-438.060487	-590.9861128	-590.9238086	-590.9609635	-192.6493293	-398.2972868
Thermal Corrections (MP2/6-31+G(2d,p))							
Zero-point correction=	0.041975	0.046877	0.093678	0.089797	0.092326	0.085948	0.006209
Thermal correction to Energy=	0.045493	0.050467	0.101658	0.097826	0.101086	0.090654	0.00857
Thermal correction to Enthalpy=	0.046437	0.051412	0.102602	0.098771	0.10203	0.091599	0.009514
Thermal correction to Gibbs Free Energy=	0.017730	0.022656	0.058937	0.056815	0.057541	0.059304	-0.011628

C-Attack by MeSH

Method	CH ₂ CHO ⁻	MeSH	Reactant Complex	Transition State	Product Complex	H ₃ CCH ₂ CHO	HS ⁻
QCISD(T,FC) / 6-31G(d)	-152.7579014	-437.9933162	-590.802058	-590.7354104	-590.8180522	-192.5691554	-398.2308385
MP4(FC)/6-31G(d)	-152.7593624	-437.9915145	-590.8003715	-590.7360813	-590.8177832	-192.5698029	-398.229966
MP4(FC)/6-31+G(d)	-152.802303	-437.9949488	-590.8330879	-590.7725213	-590.8510947	-192.5824122	-398.2495496
MP4(FC)/6-31G(2df,p)	-152.8845279	-438.101794	-591.0404041	-590.9760913	-591.0544349	-192.7347172	-398.3013416
MP2(FC)/6-31G(d)	-152.7221989	-437.9526667	-590.7268433	-590.6590582	-590.7425588	-192.513952	-398.210451
MP2(FC)/6-31+G(d)	-152.7647355	-437.9557494	-590.7582884	-590.6939896	-590.7745027	-192.5257451	-398.2296047
MP2(FC)/6-31G(2df,p)	-152.8393957	-438.0532767	-590.9493931	-590.8819777	-590.9613404	-192.6686670	-398.273999
MP2(FULL)/GTLarge	-153.0699020	-438.4505598	-591.5631712	-591.4990963	-591.5755393	-192.9241536	-398.6320383
Thermal Corrections (HF/6-31+G(d))							
Zero-point correction=	0.040373	0.044239	0.086033	0.084976	0.087873	0.080979	0.005664
Thermal correction to Energy=	0.043865	0.047877	0.094709	0.093224	0.096872	0.086071	0.008025
Thermal correction to Enthalpy=	0.044809	0.048821	0.095653	0.094169	0.097816	0.087016	0.008969
Thermal correction to Gibbs Free Energy=	0.016181	0.020003	0.049131	0.051535	0.052091	0.053583	-0.012174
$G_{298} =$	<u>-153.1552702</u>	<u>-438.5259294</u>	<u>-591.710185</u>	<u>-591.6446886</u>	<u>-591.7203554</u>	<u>-193.0134215</u>	<u>-398.6977333</u>
MP2(FC)/6-31+G(2d,p)	-152.8861988	-438.060487	-590.9861128	-590.9258231	-591.0002663	-192.6836966	-398.2972868
Thermal Corrections (MP2/6-31+G(2d,p))							
Zero-point correction=	0.041975	0.046877	0.093678	0.089506	0.092546	0.085150	0.006209
Thermal correction to Energy=	0.045493	0.050467	0.101658	0.097328	0.101333	0.090106	0.00857
Thermal correction to Enthalpy=	0.046437	0.051412	0.102602	0.098273	0.102277	0.091050	0.009514
Thermal correction to Gibbs Free Energy=	0.017730	0.022656	0.058937	0.056879	0.057289	0.057922	-0.011628

O-Attack by MeSMe

Method	CH ₂ CHO ⁻	MeSMe	Reactant Complex	Transition State	Product Complex	CH ₂ CHOCH ₃	MeS ⁻
QCISD(T,FC) / 6-31G(d)	-152.7579014	-477.1771062	-629.95938	-629.912763	-629.9532548	-192.5335287	-437.4021376
MP4(FC)/6-31G(d)	-152.7593624	-477.1750053	-629.9589414	-629.9121911	-629.9508649	-192.5325622	-437.4009078
MP4(FC)/6-31+G(d)	-152.802303	-477.1803112	-630.0021839	-629.9510082	-629.9851332	-192.5470377	-437.420327
MP4(FC)/6-31G(2df,p)	-152.8845279	-477.3227271	-630.2336829	-630.1905279	-630.2267989	-192.7005817	-437.5095697
MP2(FC)/6-31G(d)	-152.7221989	-477.1211005	-629.8681638	-629.8183298	-629.8591366	-192.475947	-437.3658978
MP2(FC)/6-31+G(d)	-152.7647355	-477.125881	-629.9100045	-629.8552113	-629.8917666	-192.4897437	-437.3846392
MP2(FC)/6-31G(2df,p)	-152.8393957	-477.2568901	-630.1232035	-630.0766639	-630.1151252	-192.633930	-437.4642787
MP2(FULL)/GTLarge	-153.0699020	-477.710929	-630.8002599	-630.7499159	-630.7848709	-192.8924102	-437.8764008
Thermal Corrections (HF/6-31+G(d))							
Zero-point correction=	0.040373	0.072668	0.114216	0.111395	0.116651	0.082000	0.034642
Thermal correction to Energy=	0.043865	0.077607	0.124734	0.123943	0.127232	0.086875	0.037721
Thermal correction to Enthalpy=	0.044809	0.078551	0.125678	0.124887	0.128177	0.087819	0.038666
Thermal correction to Gibbs Free Energy=	0.016181	0.045592	0.073227	0.075654	0.074426	0.055166	0.012078
$G_{298} =$	<u>-153.1552702</u>	<u>-477.7976603</u>	<u>-630.9606867</u>	<u>-630.9119674</u>	<u>-630.9474808</u>	<u>-192.9821732</u>	<u>-437.9550544</u>
MP2(FC)/6-31+G(2d,p)	-152.8861988	-477.261417	-630.1660499	-630.1169916	-630.1498522	-192.6493293	-437.4840725
Thermal Corrections (MP2/6-31+G(2d,p))							
Zero-point correction=	0.041975	0.07686	0.120044	0.12005	0.122935	0.085948	0.036641
Thermal correction to Energy=	0.045493	0.081678	0.12936	0.129436	0.132685	0.090654	0.039692
Thermal correction to Enthalpy=	0.046437	0.082622	0.130304	0.130381	0.133629	0.091599	0.040636
Thermal correction to Gibbs Free Energy=	0.017730	0.049917	0.082466	0.084005	0.086005	0.059304	0.014073

C-Attack by MeSMe

Method	CH ₂ CHO	MeSMe	Reactant Complex	Transition State	Product Complex	H ₃ CCH ₂ CHO	MeS
QCISD(T,FC) / 6-31G(d)	-152.7579014	-477.1771062	-629.95938	-629.91194	-629.9898859	-192.5691554	-437.4021376
MP4(FC)/6-31G(d)	-152.7593624	-477.1750053	-629.9589414	-629.912443	-629.989349	-192.5698029	-437.4009078
MP4(FC)/6-31+G(d)	-152.802303	-477.1803112	-630.0021839	-629.9503448	-630.0231193	-192.5824122	-437.420327
MP4(FC)/6-31G(2df,p)	-152.8845279	-477.3227271	-630.2336829	-630.189846	-630.2635899	-192.7347172	-437.5095697
MP2(FC)/6-31G(d)	-152.7221989	-477.1211005	-629.8681638	-629.820393	-629.8986534	-192.513952	-437.3658978
MP2(FC)/6-31+G(d)	-152.7647355	-477.125881	-629.9100045	-629.8565462	-629.9307004	-192.5257451	-437.3846392
MP2(FC)/6-31G(2df,p)	-152.8393957	-477.2568901	-630.1232035	-630.078351	-630.1527738	-192.6686670	-437.4642787
MP2(FULL)/GTLarge	-153.0699020	-477.710929	-630.8002599	-630.7515998	-630.8210786	-192.9241536	-437.8764008
Thermal Corrections (HF/6-31+G(d))							
Zero-point correction=	0.040373	0.072668	0.114216	0.113663	0.116625	0.080979	0.034642
Thermal correction to Energy=	0.043865	0.077607	0.124734	0.123425	0.127086	0.086071	0.037721
Thermal correction to Enthalpy=	0.044809	0.078551	0.125678	0.124369	0.12803	0.087016	0.038666
Thermal correction to Gibbs Free Energy=	0.016181	0.045592	0.073227	0.076665	0.074925	0.053583	0.012078
$G_{298} =$	<u>-153.1552702</u>	<u>-477.7976603</u>	<u>-630.9606867</u>	<u>-630.9090094</u>	<u>-630.9805639</u>	<u>-193.0134215</u>	<u>-437.9550544</u>
MP2(FC)/6-31+G(2d,p)	-152.8861988	-477.261417	-630.1660499	-630.1197245	-630.1884418	-192.6836966	-437.4840725
Thermal Corrections (MP2/6-31+G(2d,p))							
Zero-point correction=	0.041975	0.07686	0.120044	0.119789	0.123032	0.085150	0.036641
Thermal correction to Energy=	0.045493	0.081678	0.12936	0.12898	0.132786	0.090106	0.039692
Thermal correction to Enthalpy=	0.046437	0.082622	0.130304	0.129924	0.133731	0.091050	0.040636
Thermal correction to Gibbs Free Energy=	0.017730	0.049917	0.082466	0.084216	0.085954	0.057922	0.014073

5.4 Archive Entries for Geometry Optimization

F⁻ + MeF

Fluoride:

```
1|1|UNPC-UNK|FOpt|RMP2-FC|6-311+G(2d,p)|F1(1-)|PCUSER|05-Sep-2009|0||#
P MP2/6-311+G(2D,P) POPT FREQ NOSYMM||Fluorid||-1,1|F,0.,0.,0.||Versi
on=x86-Wi n32-G03RevB.03|HF=-99.4456557|MP2=-99.703831|RMSD=9.404e-010|R
MSF=1.822e-030|Di pol e=0.,0.,0.|PG=OH [O(F1)]||@
```

Methyl Fluoride:

```
1|1|UNPC-UNK|POpt|RMP2-FC|6-311+G(2d,p)|C1H3F1|PCUSER|05-Sep-2009|1||#
P MP2/6-311+G(2D,P) POPT FREQ NOSYMM||Methyl fluori d||0,1|F|C,1,R2|H,2,
R3,1,A3|H,2,R4,1,A4,3,D4,0|H,2,R5,1,A5,3,D5,0||R2=1.39234653|R3=1.0890
8683|A3=108.66287918|R4=1.08908683|A4=108.66287938|D4=119.9999991|R5=1
.08908683|A5=108.66287938|D5=-120.00000035||Versi on=x86-Wi n32-G03RevB.
03|HF=-139.0856945|MP2=-139.4785434|RMSD=5.565e-009|RMSF=1.293e-004|Di
pol e=0.,0.,0.7775211|PG=C01 [X(C1H3F1)]||@
```

Reactant Complex:

```
1|1|UNPC-UNK|FOpt|RMP2-FC|6-311+G(2d,p)|C1H3F2(1-)|PCUSER|09-Nov-2009|
0||#P MP2/6-311+G(2D,P) OPT FREQ||Reactant Compl ex F---Me-F||-1,1|C,0.
4166310272,0.0001011741,-0.0000851138|H,0.0767730016,0.9553736627,-0.3
774753942|H,0.0765428704,-0.8042576251,-0.6386871662|H,0.0764347739,-0
.1506693825,1.0157879112|F,-2.1613783801,-0.0000280424,0.0000249857|F,
1.8580965124,-0.0000890353,0.0000733846||Versi on=x86-Wi n32-G03RevB.03|
State=1-A|HF=-238.5510592|MP2=-239.2044553|RMSD=6.234e-009|RMSF=6.057e
-005|Di pol e=2.6720856,0.0001331,-0.0001136|PG=C01 [X(C1H3F2)]||@
```

Transition State:

```
1\1\GINC-NODE25\FTS\RMP2-FC\6-311+G(2d,p)\C1H3F2(1-)\MAY04\17-Oct-2009
\0\#p opt=(cal cfc,ts,noieigentest) freq mp2/6-311+g(2d,p)\F---Me---F\
-1,1\C,-0.0031556415,-0.0273643619,0.0044137209\H,-0.0032780128,-0.56
50405155,-0.9227572483\H,-0.0033175965,-0.5616431088,0.9335505389\H,-0
.0030809679,1.0443129572,0.0026457382\F,-1.8335778266,-0.0270505903,0.
0043341421\F,1.8272268853,-0.0269965807,0.0043676382\\Versi on=AM64L-G0
3RevD.01\State=1-A\HF=-238.521582\MP2=-239.1837645\RMSD=8.800e-09\RMSF
=4.064e-05\Thermal =0.\Di pol e=0.0001565,-0.0004319,0.0001109\PG=C01 [X(
C1H3F2)]\@
```

Cl⁻ + MeCl

Chloride:

```
1|1|UNPC-UNK|FOpt|RMP2-FC|6-311+G(2d,p)|Cl1(1-)|PCUSER|05-Sep-2009|0||#
P MP2/6-311+G(2D,P) POPT FREQ NOSYMM||Chl ori d||-1,1|Cl,0.,0.,0.||Versi
on=x86-Wi n32-G03RevB.03|HF=-459.5654251|MP2=-459.7315876|RMSD=7.676e-
009|RMSF=0.000e+000|Di pol e=0.,0.,0.|PG=OH [O(Cl1)]||@
```

Methyl Chloride:

```
1|1|UNPC-UNK|POpt|RMP2-FC|6-311+G(2d,p)|C1H3Cl1|PCUSER|05-Sep-2009|1||#
P MP2/6-311+G(2D,P) POPT FREQ NOSYMM||Methyl chl ori d||0,1|Cl|C,1,R2|H,
2,R3,1,A3|H,2,R4,1,A4,3,D4,0|H,2,R5,1,A5,3,D5,0||R2=1.7934343|R3=1.085
88928|A3=108.43976523|R4=1.08588928|A4=108.43976525|D4=120.00000016|R5
=1.08588928|A5=108.43976528|D5=-119.99999988||Versi on=x86-Wi n32-G03Rev
B.03|HF=-499.1351046|MP2=-499.4562803|RMSD=1.610e-009|RMSF=9.458e-006|
Di pol e=0.,0.,0.7728089|PG=C03V [C3(C1Cl1),3SGV(H1)]||@
```

Reactant Complex:

```
1|1|UNPC-UNK|FOpt|RMP2-FC|6-311+G(2d,p)|C1H3Cl2(1-)|PCUSER|02-Dec-2009|0|
|#P MP2/6-311+G(2D,P) OPT FREQ||Reactant Complex Cl---Me-Cl||-1,1|C
,0.5526011731,0.0000549945,-0.0000274195|H,0.2137040965,1.0174060319,-
0.1440032257|H,0.2136100985,-0.6332634976,-0.8090856198|H,0.2135653893
,-0.3839087647,0.9529723369|Cl,-2.6156918069,0.0000354464,-0.000017685
5|Cl,2.3829572997,-0.0000686074,0.0000342164||Version=x86-Win32-G03Rev
B.03|State=1-A|HF=-958.7145553|MP2=-959.2046817|RMSD=6.214e-009|RMSF=9
.158e-006|Dipole=3.4573239,-0.0000033,0.0000017|PG=C01 [X(C1H3Cl2)]|@
```

Transition State:

```
1\1\GINC-NODE25\FTS\RMP2-FC\6-311+G(2d,p)\C1H3Cl2(1-)\MAY04\17-Oct-200
9\0\#p opt=(calcf,ts,noigentest) freq mp2/6-311+g(2d,p)\Cl---Me---
Cl\|-1,1\C,-0.003211983,-0.0272879447,0.004478998\H,-0.0031469759,-0.5
645152455,-0.9227621162\H,-0.0032092584,-0.561616899,0.9331394681\H,-0
.0032145565,1.0441321408,0.0028496962\Cl,-2.3039419437,-0.0273450916,0
.0042867788\Cl,2.2975415575,-0.02714916,0.0045617051\Version=AM64L-G0
3RevD.01\State=1-A|HF=-958.6894913\MP2=-959.1827309\RMSD=8.304e-09\RMS
F=5.906e-05\Thermal=0.\Dipole=-0.0001165,-0.0000597,0.000011\PG=C01 [X
(C1H3Cl2)]\@
```

Br⁻ + MeBrBromide:

```
1|1|UNPC-UNK|FOpt|RMP2-FC|6-311+G(2d,p)|Br1(1-)|PCUSER|05-Sep-2009|0|
|#P MP2/6-311+G(2D,P) POPT FREQ NOSYMM||Bromid||-1,1|Br,0.,0.,0.||Versi
on=x86-Win32-G03RevB.03|HF=-2572.4370609|MP2=-2572.5770495|RMSD=8.671e
-010|RMSF=2.332e-028|Dipole=0.,0.,0.|PG=OH [O(Br1)]|@
```

Methyl Bromide:

```
1|1|UNPC-UNK|POpt|RMP2-FC|6-311+G(2d,p)|C1H3Br1|PCUSER|05-Sep-2009|1|
|#P MP2/6-311+G(2D,P) POPT FREQ NOSYMM||Methyl chlorid||0,1|Br|C,1,R2|H,
2,R3,1,A3|H,2,R4,1,A4,3,D4,0|H,2,R5,1,A5,3,D5,0||R2=1.94276926|R3=1.08
498525|A3=108.03965831|R4=1.08498525|A4=108.03965806|D4=119.9999784|R
5=1.08498525|A5=108.03965845|D5=-120.0000012||Version=x86-Win32-G03Rev
B.03|HF=-2611.9898206|MP2=-2612.2872185|RMSD=5.554e-009|RMSF=9.134e-00
5|Dipole=0.,0.,0.7546475|PG=C01 [X(C1H3Br1)]|@
```

Reactant Complex:

```
1|1|UNPC-UNK|FOpt|RMP2-FC|6-311+G(2d,p)|C1H3Br2(1-)|PCUSER|02-Dec-2009
|0||#P MP2/6-311+G(2D,P) OPT FREQ||Reactant Complex Br---Me-Br||-1,1|C
,-0.6096351771,0.0423003379,-0.001554953|H,-0.2100029546,1.0371979497,
0.1436954855|H,-0.3261046092,-0.6139726493,0.8105671822|H,-0.304229433
6,-0.3647957256,-0.9563462028|Br,2.7112827779,-0.1878839803,0.00703527
01|Br,-2.5827637198,0.1789626791,-0.0067098567||Version=x86-Win32-G03R
evB.03|State=1-A|HF=-5184.4399962|MP2=-5184.8797681|RMSD=8.665e-009|RM
SF=6.361e-007|Dipole=0.0006052,-0.0487265,-3.5802901|PG=C01 [X(C1H3Br2
)]|@
```

Transition State:

```
1\1\GINC-NODE15\FTS\RMP2-FC\6-311+G(2d,p)\C1H3Br2(1-)\MAY04\17-Oct-200
9\0\#p opt=(calcf,ts,noigentest) freq mp2/6-311+g(2d,p)\Br---Me---
Br\|-1,1\C,-0.0035200387,-0.0273270239,0.0043939397\H,-0.0029017262,-0
.5649079558,-0.9234689819\H,-0.0030667666,-0.5620645989,0.9338561486\H
,-0.0030150598,1.0449809066,0.0028196978\Br,-2.4611492546,-0.027405166
,0.0042609445\Br,2.4544696859,-0.027058362,0.0046927812\Version=AM64L
-G03RevD.01\State=1-A|HF=-5184.4191294\MP2=-5184.8601436\RMSD=2.532e-0
9\RMSF=2.149e-05\Thermal=0.\Dipole=-0.0022561,-0.0000664,-0.0000545\PG
=C01 [X(C1H3Br2)]\@
```

OH⁻ + MeOH

Hydroxide:

1|1|UNPC-UNK|FOpt|RMP2-FC|6-311+G(2d,p)|H101(1-)|PCUSER|05-Sep-2009|0|
|#P MP2/6-311+G(2D,P) POPT FREQ NOSYMM||Hydroxid||-1,1|0,-1.7280480537
, -1.5946909, -0.02087565|H, -0.7602276663, -1.5946909, -0.02087565||Versi
on=x86-Wi n32-G03RevB.03|HF=-75.4055813|MP2=-75.6595631|RMSD=1.249e-009|
RMSF=1.917e-004|Di pol e=0.6936267,0.,0.|PG=C*V [C*(H101)]||@

Methanol:

1|1|UNPC-UNK|FOpt|RMP2-FC|6-311+G(2d,p)|C1H401|PCUSER|05-Sep-2009|0|
P MP2/6-311+G(2D,P) POPT FREQ NOSYMM||Methanol||0,1|C,-0.0182878701,-0
.0000109666,1.7760087696|H,1.0164543206,0.0000113813,2.1116660591|H,-0
.5138268815,0.8912016012,2.1711353466|H,-0.5137973369,-0.8912247512,2.
1711713358|0,0.0165172163,-0.0000352226,0.3501554044|H,-0.8919952584,-
0.0001173516,0.0304374945||Versi on=x86-Wi n32-G03RevB.03|HF=-115.081928
8|MP2=-115.4691855|RMSD=2.368e-009|RMSF=6.863e-005|Di pol e=-0.5919366,-
0.0000442,0.4148373|PG=C01 [X(C1H401)]||@

Reactant Complex:

1\1\GINC-NODE25\FOpt\RMP2-FC\6-311+G(2d,p)\C1H502(1-)\MAY04\08-Dec-200
9\0\#P MP2/6-311+G(2d,p) opt=cal cfc freq\Reactant Complex HO---Me-OH
\-1,1\C,1.3553231438,-0.4259054125,-0.0111046096\H,0.8714702743,-1.21
17194229,0.6101615287\H,1.8700709847,-0.976902682,-0.8321041732\H,2.17
79565971,-0.0150424652,0.6183037866\0,0.4755233149,0.532859544,-0.4558
047465\0,-1.8476975957,-0.119529882,0.1226793096\H,-0.8373739004,0.155
2415106,-0.1609831208\H,-2.0141526549,0.4532985749,0.8775116749\Versi
on=AM64L-G03RevD.01\State=1-A\HF=-190.5311698\MP2=-191.18104\RMSD=3.15
8e-09\RMSF=1.622e-05\Thermal=0.\Di pol e=0.4539835,-0.2260521,0.7507513\
PG=C01 [X(C1H502)]\@

Transition State:

1\1\GINC-NODE27\FTS\RMP2-FC\6-311+G(2d,p)\C1H502(1-)\MAY04\17-Oct-2009
\0\#P MP2/6-311+g(2d,p) Opt=(ts,noi gentest,cal cfc) freq\H0---Me---0
H\ -1,1\C,0.0045076692,0.0273101542,-0.0677078009\H,0.0555503513,1.080
0649187,-0.2738117747\H,-0.0663853295,-0.3252585754,0.9439282716\H,0.0
253385101,-0.6685010167,-0.8854652612\0,-1.8985004155,0.0029367226,-0.
2419389078\H,-2.1893649843,0.6721381358,0.3931961115\0,1.9115483247,0.
0715574824,0.0501644895\H,2.149380954,-0.8589184415,0.166182822\Versi
on=AM64L-G03RevD.01\State=1-A\HF=-190.4464863\MP2=-191.107698\RMSD=4.4
30e-09\RMSF=2.145e-05\Thermal=0.\Di pol e=-0.0342854,-0.1681697,0.483179
2\PG=C01 [X(C1H502)]\@

MeO⁻ + MeOMe

Methanolate:

1|1|UNPC-UNK|FOpt|RMP2-FC|6-311+G(2d,p)|C1H301(1-)|PCUSER|09-Dec-2009|
0||#P MP2/6-311+G(2D,P) OPT FREQ||Methoxi de||-1,1|C,-0.1837673195,-0.2
5987935,-0.4501285172|H,0.1382702158,-1.3382147522,-0.5467962349|H,0.1
382898393,0.1955658619,-1.4323244786|H,-1.3077789257,-0.315676184,-0.5
467964213|0,0.2667278485,0.3772001468,0.6533360297||Versi on=x86-Wi n32-
G03RevB.03|State=1-A1|HF=-114.4460748|MP2=-114.8492252|RMSD=8.219e-009
|RMSF=1.342e-004|Di pol e=-0.3570028,-0.5048648,-0.8744598|PG=C03V [C3(C
101),3SGV(H1)]||@

Dimethylether:

1|1|UNPC-UNK|FOpt|RMP2-FC|6-311+G(2d,p)|C2H601|PCUSER|09-Dec-2009|0|
P MP2/6-311+G(2D,P) OPT FREQ||Dimethyl ether||0,1|C,-0.1158959247,-0.9
281170169,-0.7250846534|H,0.2726806895,-1.944123025,-0.6771055099|H,0.

Chapter 3: Marcus-Analysis of Ambident Reactivity

2433817642, -0.4451895713, -1.6425218686|H, -1.2123942639, -0.9598602123, -0.7510498299|O, 0.3474774611, -0.2458419968, 0.42550086|C, -0.1155292121, 1.0918514292, 0.4416947773|H, -1.2120147726, 1.1305021383, 0.4563900936|H, 0.273315929, 1.5578280426, 1.345700997|H, 0.2437617679, 1.6451721192, -0.4350814966||Versi on=x86-Wi n32-G03RevB.03|State=1-A|HF=-154.114872|MP2=-154.6561942|RMSD=5.966e-009|RMSF=9.145e-005|Di pol e=-0.3256971, 0.2304323, -0.3988299|PG=C01 [X(C2H6O1)]||@

Reactant Complex:

1\1\GINC-NODE18\F0pt\RMP2-FC\6-311+G(2d,p)\C3H9O2(1-)\MAY04\10-Dec-2009\O\#P MP2/6-311+G(2d,p) Opt Freq\Reactant Complex MeO---Me-OMe\ -1, 1\0, -1.9265083948, 0.0390626221, -0.6698608801\0, 1.4844847788, 0.0696115623, 0.3408766698\C, -1.5306425752, 0.8250198238, 0.4554644894\H, -1.9046371413, 0.3707823654, 1.3858858012\H, -0.4358867937, 0.9019496776, 0.5104204436\H, -1.9960857009, 1.8058873293, 0.3334602695\C, 2.8273688832, 0.2972351989, 0.3598586559\H, 3.1156223625, 1.3817568805, 0.3520881045\H, 3.3575996332, -0.1184010195, 1.2570246674\H, 3.3853735194, -0.1376692324, -0.5112486976\C, -1.1753736018, -1.1760169884, -0.6830111373\H, -1.5122846169, -1.8391031918, 0.1285891197\H, -1.380355489, -1.6622082291, -1.6396844949\H, -0.103195008, -0.9719199052, -0.5557096619\|Versi on=AM64L-G03RevD.01\State=1-A\HF=-268.5749203\MP2=-269.5259646\RMSD=5.634e-09\RMSF=1.199e-05\Thermal=0.\Di pol e=-1.7925815, -0.2223434, -0.1685956\PG=C01 [X(C3H9O2)]\@

Transition State:

1\1\GINC-NODE24\FTS\RMP2-FC\6-311+G(2d,p)\C3H9O2(1-)\MAY04\10-Dec-2009\O\#p MP2/6-311+G(2d,p) opt=(cal cfc, ts, noei gentest) freq\Transi sti on State MeO---Me---OMe\ -1, 1\C, -0.0447793808, -0.0644179749, -0.0811245191\H, -0.0828828124, 0.78570893, -0.7455214819\H, 0.0614218548, 0.0885160265, 0.9848903364\H, -0.1124298399, -1.0667300804, -0.4767116623\0, -1.900355503, -0.0669554799, 0.0861312308\0, 1.8072211644, -0.0668856972, -0.2834429795\C, -2.2483993316, 1.1546572229, 0.6202912638\H, -1.7928358677, 1.3415402037, 1.6191467908\H, -1.9365202766, 2.0148011675, -0.0142866405\H, -3.3405309096, 1.2475303797, 0.7548119089\C, 2.2857167365, -1.1007644419, 0.4917649385\H, 3.3854924603, -1.1820683725, 0.4339884327\H, 2.0361913822, -0.9901263983, 1.5714341491\H, 1.8818665734, -2.0947484051, 0.1936654325\|Versi on=A M64L-G03RevD.01\State=1-A\HF=-268.5175344\MP2=-269.4880584\RMSD=4.012e-09\RMSF=1.666e-05\Thermal=0.\Di pol e=0.0543448, 0.0777637, 0.5423465\PG=C01 [X(C3H9O2)]\@

HS⁻ + MeSH

Hydrogensulfide:

1|1|UNPC-UNK|F0pt|RMP2-FC|6-311+G(2d,p)|H1S1(1-)|PCUSER|05-Sep-2009|0| |#P MP2/6-311+G(2D,P) POPT FREQ NOSYMM|Hydrogensul fi d| -1, 1|S, -1.7385585355, -1.5946909, -0.02087565|H, -0.3997171845, -1.5946909, -0.02087565| |Versi on=x86-Wi n32-G03RevB.03|HF=-398.1367984|MP2=-398.2972868|RMSD=1.971e-009|RMSF=2.089e-004|Di pol e=0.3568005, 0., 0.|PG=C*V [C*(H1S1)]||@

Methanethiole:

1|1|UNPC-UNK|F0pt|RMP2-FC|6-311+G(2d,p)|C1H4S1|PCUSER|05-Sep-2009|0| |# P MP2/6-311+G(2D,P) POPT FREQ NOSYMM| |Methanthi ol| |0, 1|C, -0.026535625, -0.000015602, 1.7603655285|H, 0.9988068553, 0.0000344722, 2.1274433185|H, -0.5279262403, 0.8931141374, 2.1269334182|H, -0.5278553205, -0.8931642015, 2.126985214|S, 0.0810225402, -0.0000656761, -0.0605080331|H, -1.232372537, -0.0001423604, -0.2874774356| |Versi on=x86-Wi n32-G03RevB.03|HF=-437.7449965|MP2=-438.060487|RMSD=9.922e-009|RMSF=6.896e-005|Di pol e=-0.354788, -0.0000035, 0.5229464|PG=C01 [X(C1H4S1)]||@

Reactant Complex:

1\1\G\NC-NODE12\FOpt\RMP2-FC\6-311+G(2d,p)\C1H5S2(1-)\MAY04\03-Dec-2009\O\#\#P MP2/6-311+G(2d,p) opt freq\Reactant Complex HS---Me-SH\ -1, 1\C, -1. 5758485874, 1. 0693482141, 0. 1378970987\H, -1. 7181852403, 1. 5084643183, 1. 1260231537\H, -0. 6639117961, 1. 4723687262, -0. 305448015\H, -2. 4325286752, 1. 3177281047, -0. 4896866826\S, -1. 3723320649, -0. 7449439775, 0. 2412123928\S, 1. 9872025585, -0. 0249293681, -0. 4137320962\H, 0. 0070534169, -0. 6667910759, 0. 0114605082\H, 2. 2775883885, 0. 1658790581, 0. 8773186403\Version=AM64L-G03RevD. 01\State=1-A\HF=-835. 8890003\MP2=-836. 378964\RMSD=5. 314e-09\RMSF=1. 177e-05\Thermal =0. \Di pol e=-2. 2268435, 0. 5903686, 0. 6152497\PG=C01 [X(C1H5S2)]\@\

Transition State:

1\1\G\NC-NODE10\FTS\RMP2-FC\6-311+G(2d,p)\C1H5S2(1-)\MAY04\17-Oct-2009\O\#\#P MP2/6-311+G(2d,p) Opt=(ts,noigentest,calcfc) freq\HS---Me---SH\ -1, 1\C, 0. 0080646335, 0. 0488446777, -0. 1683321825\H, -0. 0040943689, 1. 0833667837, -0. 4519739038\H, -0. 0450675849, -0. 2294301566, 0. 8651099669\H, 0. 0751856619, -0. 7043956758, -0. 9292325776\S, -2. 3720872693, -0. 0599679474, -0. 3210720923\H, -2. 5415031765, 0. 8061676703, 0. 6812012273\S, 2. 3894129472, 0. 1570022872, -0. 0163418139\H, 2. 482164237, -1. 1002582592, 0. 4251893259\Version=AM64L-G03RevD. 01\State=1-A\HF=-835. 8434301\MP2=-836. 3346758\RMSD=3. 881e-09\RMSF=5. 725e-05\Thermal =0. \Di pol e=-0. 0216044, -0. 0832505, 0. 309416\PG=C01 [X(C1H5S2)]\@\

MeS⁻ + MeSMe

Methanethiolate:

1|1|UNPC-UNK|FOpt|RMP2-FC|6-311+G(2d,p)|C1H3S1(1-)|PCUSER|09-Dec-2009|O|P MP2/6-311+G(2D,P) OPT FREQ||MeS- Anion||-1, 1\C, -0. 3763758665, -0. 5322617611, -0. 9219131318|H, -0. 0315717827, -1. 5722503838, -0. 9592643005|H, -0. 0315522715, -0. 0446207778, -1. 8412412892|H, -1. 4718217761, -0. 553812571, -0. 9592644789|S, 0. 2370750643, 0. 3352658937, 0. 5807030537||Version=x86-Win32-G03RevB. 03|State=1-A|HF=-437. 1635301|MP2=-437. 4840725|RMSD=6. 901e-009|RMSF=2. 634e-005|Di pol e=-0. 4580659, -0. 6477858, -1. 1220086|PG=C03V [C3(C1S1), 3SGV(H1)]||@\

Dimethylthioether:

1|1|UNPC-UNK|FOpt|RMP2-FC|6-311+G(2d,p)|C2H6S1|PCUSER|09-Dec-2009|O|P MP2/6-311+G(2D,P) OPT FREQ||Dimethyl thioether||0, 1\C, -0. 2999476388, -0. 9735409122, -1. 0518663952|H, 0. 0292681707, -2. 0106356235, -1. 1130002875|H, 0. 0674580116, -0. 4342176456, -1. 9256196|H, -1. 3900717103, -0. 9495095731, -1. 0330740331|S, 0. 3863695548, -0. 2733587031, 0. 4731264843|C, -0. 2995168768, 1. 3976655256, 0. 3177958021|H, -1. 3896503792, 1. 3696766432, 0. 3065386381|H, 0. 0299896692, 1. 9687118587, 1. 1855615326|H, 0. 0678805447, 1. 8849659418, -0. 5860064945||Version=x86-Win32-G03RevB. 03|State=1-A|HF=-476. 7868915|MP2=-477. 261417|RMSD=2. 849e-009|RMSF=2. 450e-005|Di pol e=-0. 3694767, 0. 2614069, -0. 4524405|PG=C01 [X(C2H6S1)]||@\

Reactant Complex:

1\1\G\NC-NODE18\FOpt\RMP2-FC\6-311+G(2d,p)\C3H9S2(1-)\MAY04\10-Dec-2009\O\#\#p MP2/6-311+G(2d,p) opt=calcfc freq\Reactant Complex MeS---Me-SMe\ -1, 1\S, 2. 0533297721, -0. 0265290431, 0. 3876814739\S, -2. 2633809036, 0. 02037413, -0. 5904522239\C, 1. 2043421299, -1. 3378221405, -0. 5448158444\H, 0. 1246499209, -1. 1506074346, -0. 5418859426\H, 1. 5634536011, -1. 372302656, -1. 5751552037\H, 1. 4262621877, -2. 2871310038, -0. 0549984992\C, -1. 9288766552, -0. 108731986, 1. 2154076346\H, -2. 3627398302, 0. 73331469, 1. 7653594421\H, -2. 3526092392, -1. 0262838758, 1. 6376299195\H, -0. 8536360491, -0. 1183701039, 1. 4342043629\C, 1. 1887999956, 1. 396852838, -0. 3447568565\H, 0. 111326698, 1. 1989500553, -0. 3699269456\H, 1. 4003273215, 2. 2672884532, 0. 2780548611\H, 1. 5464610505, 1. 5849740772, -1. 3588851782\Version=AM64L-G03RevD. 01\State=1-

Chapter 3: Marcus-Analysis of Ambident Reactivity

A\HF=-913.957297\MP2=-914.7632881\RMSD=3.287e-09\RMSF=2.054e-05\Thermal=0.\Di pol e=2.9323306,-0.0264793,0.5955494\PG=C01 [X(C3H9S2)]\@

Transition State:

1\1\GINC-NODE20\FTS\RMP2-FC\6-311+G(2d,p)\C3H9S2(1-)\MAY04\11-Dec-2009\0\#p MP2/6-311+G(2d,p) opt=(cal cfc,ts,noeigentest) freq\Transition State MeS---Me---SMe\ -1,1\C,-0.0503478935,-0.0629606201,-0.3387004087\H,-0.2051268643,0.8080565633,-0.9496631173\H,0.0251814831,0.0325189515,0.7297538296\H,0.0284202467,-1.0299773787,-0.8019491515\S,-2.3801356881,-0.2978250801,-0.0978989499\S,2.2870278027,0.1822013811,-0.4708347545\C,-2.474430676,1.2957173899,0.7882453256\H,-1.8780526781,1.274068272,1.7060889464\H,-2.1040071266,2.1164292748,0.1656706085\H,-3.5074258454,1.5215111461,1.0633993247\C,2.52488136,-1.2325079653,0.6586950903\H,3.5890146428,-1.4175946725,0.8233918106\H,2.0607922641,-1.0440122678,1.6321750983\H,2.0833852225,-2.1455679142,0.246663548\Version=AM64L-G03RevD.01\State=1-A\HF=-913.9037725\MP2=-914.7215024\RMSD=4.210e-09\RMSF=6.611e-06\Thermal=0.\Di pol e=0.0541721,0.0669091,0.7566009\PG=C01 [X(C3H9S2)]\@

NH₂⁻ + MeNH₂

Amide Anion:

1|1|UNPC-UNK|FOpt|RMP2-FC|6-311+G(2d,p)|H2N1(1-)|PCUSER|17-Oct-2009|0|P MP2/6-311+G(2D,P) OPT FREQ||NH2||-1,1|N,0.1388361144,0.0117059177,0.031298955|H,-0.3024016343,-0.1407885287,-0.8862945204|H,-0.6694511664,0.0588471051,0.6672018354|Version=x86-Win32-G03RevB.03|State=1-A|HF=-55.5423536|MP2=-55.770518|RMSD=2.838e-009|RMSF=1.493e-005|Di pol e=-0.8625426,-0.072725,-0.19445|PG=C02V [C2(N1),SGV(H2)]||@

Methylamine:

1|1|UNPC-UNK|FOpt|RMP2-FC|6-311+G(2d,p)|C1H5N1|PCUSER|17-Oct-2009|0|P MP2/6-311+G(2D,P) OPT FREQ||MeNH2||0,1|N,0.4763924911,0.2361371765,-0.544932743|H,0.1830414412,-0.177908173,-1.4238268121|H,1.3982734628,-0.1376276477,-0.3439887091|C,-0.4613826126,-0.1255946075,0.5239173726|H,-0.1294421484,0.331366069,1.4567979207|H,-1.4429422555,0.2878283138,0.2896401773|H,-0.5753822619,-1.2030511524,0.6924023885|Version=x86-Win32-G03RevB.03|State=1-A'|HF=-95.2475477|MP2=-95.6121979|RMSD=2.372e-009|RMSF=6.053e-005|Di pol e=-0.0162543,-0.568885,0.0395131|PG=CS [SG(C1H1N1),X(H4)]||

Reactant Complex:

1\1\GINC-NODE25\FOpt\RMP2-FC\6-311+G(2d,p)\C1H7N2(1-)\MAY04\08-Dec-2009\0\#p MP2/6-311+g(2d,p) Opt Freq\Reactant Complex H2N---Me-NH2\ -1,1\N,0.6966388819,0.7438630054,-0.0810722063\H,-0.3368018041,0.4790739005,-0.0877868677\H,0.8322481324,1.2205156508,0.8079303562\N,-2.0291290636,-0.0323692776,0.1156966276\H,-2.2805367444,-0.9802513797,0.4191911686\H,-2.6865211099,0.1561357013,-0.6498427562\C,1.4525968868,-0.5047834978,-0.0521381684\H,1.256571593,-1.0542312024,-0.9764548024\H,2.5328322504,-0.3167437597,-0.0046367293\H,1.1930566524,-1.1807114785,0.7791285375\Version=AM64L-G03RevD.01\State=1-A\HF=-150.8079399\MP2=-151.4096877\RMSD=3.530e-09\RMSF=2.312e-05\Thermal=0.\Di pol e=2.3366274,-0.612299,0.0996771\PG=C01 [X(C1H7N2)]\@

Transition State:

1\1\GINC-NODE12\FTS\RMP2-FC\6-311+G(2d,p)\C1H7N2(1-)\MAY04\17-Oct-2009\0\#p MP2/6-311+g(2d,p) Opt=(ts,noeigentest,cal cfc) freq\H2N---Me---NH2\ -1,1\C,-0.0241936997,0.0210610129,0.0527437202\H,0.0466635771,0.8760070603,-0.5969251508\H,-0.0909037454,0.1646060164,1.1171219976\H,-0.0288620803,-0.9760996501,-0.3518421191\N,-2.009533594,0.2072186465,-0

Chapter 3: Marcus-Analysis of Ambident Reactivity

. 0557053148\H, -2. 230942338, -0. 010902984, -1. 0348765461\H, -2. 3641420854, -0. 6078558541, 0. 4590687054\N, 1. 9562050123, -0. 1538867552, 0. 2418809856\H, 2. 2996650792, -0. 1982707262, -0. 7253141554\H, 2. 2576065742, 0. 7741854934, 0. 5626167473\Versi on=AM64L-G03RevD. 01\State=1-A\HF=-150. 7210751\MP2=-151. 3392321\RMSD=5. 870e-09\RMSF=1. 283e-05\Thermal =0. \Di pol e=0. 0399257, -0. 0874571, -0. 6472868\PG=C01 [X(C1H7N2)]\@

NMe₂⁻ + MeNMe₂

Dimethylamide Anion:

1 | 1 | UNPC-UNK | FOpt | RMP2-FC | 6-311+G(2d, p) | C2H6N1(1-) | PCUSER | 10-Dec-2009 | 0 | #P MP2/6-311+G(2D, P) OPT FREQ | NMe2-Ani on | -1, 1 | N, -0. 3452050679, 0. 3049502966, -0. 4876139108 | C, 0. 199542041, 0. 9221234794, 0. 6706121618 | H, -0. 0119615698, 2. 0009615383, 0. 6883768211 | H, -0. 1908954899, 0. 5019116475, 1. 6440495708 | H, 1. 3198738035, 0. 8125370813, 0. 7685924764 | C, -0. 0235655092, -1. 0775791797, -0. 4220393196 | H, -0. 4258500442, -1. 6023076725, 0. 4942465203 | H, -0. 41564034, -1. 623222793, -1. 2923790763 | H, 1. 085049925, -1. 2917976762, -0. 3810259901 | Versi on=x86-Wi n32-G03RevB. 03 | State=1-A | HF=-133. 620174 | MP2=-134. 1614608 | RMSD=5. 829e-009 | RMSF=8. 228e-005 | Di pol e=0. 3777536, -0. 3337033, 0. 5335898 | PG=C02 [C2(N1), X(C2H6)] | @

Trimethylamine:

1\1\GI NC-NODE20\FOpt\RMP2-FC\6-311+G(2d, p)\C3H9N1\MAY04\27-Jan-2010\0\ \#p MP2/6-311+g(2d, p) opt freq\Trimethyl ami ne\0, 1\N, 0. 2766020389, 0. 1127902754, -0. 2709867863\C, 0. 3383562564, 1. 0181245713, 0. 8663973043\H, 0. 1437828238, 2. 0398587197, 0. 5347831503\H, -0. 3998492257, 0. 759202317, 1. 6469097737\H, 1. 33485114, 0. 9835824649, 1. 3108882803\C, 0. 56585044, -1. 2479440872, 0. 1554211136\H, -0. 1614743081, -1. 6152492897, 0. 9019285693\H, 0. 5410343027, -1. 9171616817, -0. 7067270224\H, 1. 5632286284, -1. 2912847891, 0. 5971515413\C, -1. 03866612, 0. 1749908694, -0. 890088633\H, -1. 0697122064, -0. 4887018134, -1. 7562962301\H, -1. 842732689, -0. 1242573106, -0. 1935864709\H, -1. 2385861968, 1. 193451334, -1. 2285227963\Versi on=AM64L-G03RevD. 01\State=1-A1\HF=-173. 3211456\MP2=-174. 0019534\RMSD=4. 529e-09\RMSF=1. 885e-05\Thermal =0. \Di pol e=-0. 1965345, -0. 0801411, 0. 1925447\PG=C03V [C3(N1), 3SGV(C1H1), X(H6)]\@

Reactant Complex:

1\1\GI NC-NODE24\FOpt\RMP2-FC\6-311+G(2d, p)\C5H15N2(1-)\MAY04\12-Dec-2009\0\ \#p MP2/6-311+g(2d, p) opt=cal cfc freq\Reactant Complex Me2N--Me-NMe2\ -1, 1\C, -0. 5699637409, -1. 0048593038, -1. 2663605983\H, 0. 4662539975, -1. 0366457654, -0. 9027470099\H, -0. 8671871243, -1. 9741291358, -1. 6798776203\H, -0. 6400080825, -0. 2486982177, -2. 0737881033\N, -1. 4435739978, -0. 6630317284, -0. 1475317696\N, 2. 233320076, -0. 1853505703, 0. 2073573288\C, -0. 944294904, 0. 5485844609, 0. 4973971783\H, -1. 5111231805, 0. 7375224365, 1. 4141768175\H, 0. 1226315485, 0. 4035530265, 0. 7139825925\H, -1. 0513981961, 1. 4292378487, -0. 16542333\C, -2. 8063583564, -0. 479716997, -0. 5968853128\H, -2. 8955664999, 0. 3405357783, -1. 3386129785\H, -3. 1745554115, -1. 3987081315, -1. 0632536163\H, -3. 4522385276, -0. 2382800121, 0. 2528432633\C, 2. 4002468281, 1. 0618262135, -0. 4602651326\H, 3. 4579252449, 1. 4404628156, -0. 4730786763\H, 2. 0747641434, 1. 0010612349, -1. 5095384404\H, 1. 8195074156, 1. 9100897144, 0. 0081529545\C, 2. 649627893, -0. 0039179538, 1. 5575976286\H, 2. 0610325496, 0. 786935249, 2. 1098135515\H, 2. 5483846193, -0. 9332899238, 2. 1348549136\H, 3. 7158656457, 0. 3339911911, 1. 6706032799\Versi on=AM64L-G03RevD. 01\State=1-A\HF=-306. 9468213\MP2=-308. 1807409\RMSD=8. 947e-09\RMSF=3. 550e-06\Thermal =0. \Di pol e=-2. 8880852, 0. 0261661, -0. 6185306\PG=C01 [X(C5H15N2)]\@

Transition State:

1\1\GI NC-NODE24\FTS\RMP2-FC\6-311+G(2d, p)\C5H15N2(1-)\MAY04\10-Dec-2009\0\ \#p MP2/6-311+g(2d, p) opt=(cal cfc, ts, noei gentest) freq\Transi ti on State Me2N--Me--NMe2\ -1, 1\C, -0. 0002065568, -0. 0447659733, -0. 0000182065\H, -0. 0020167974, 0. 4962306944, 0. 947958835\H, -0. 0003489089, -1. 129669

59, 0. 0002651448\H, 0. 0018288671, 0. 4957136142, -0. 9483001731\N, -1. 9176872
 408, -0. 0276807903, 0. 0044768977\N, 1. 9173397625, -0. 0279793136, -0. 0042344
 337\C, -2. 2564497891, 1. 3662648867, -0. 0487975892\H, -3. 3421792703, 1. 54008
 70728, -0. 158986763\H, -1. 9290376909, 1. 8725300674, 0. 8676512916\H, -1. 7670
 782201, 1. 8908778008, -0. 9081658424\C, -2. 2784719549, -0. 6327446935, -1. 247
 006467\H, -1. 7908610764, -0. 1295239931, -2. 1195097936\H, -1. 9679965703, -1.
 6847586491, -1. 264516352\H, -3. 3661096518, -0. 6012693867, -1. 4412128416\C,
 2. 2560708075, 1. 3659796009, 0. 0488049322\H, 3. 3417857592, 1. 5398514234, 0. 1
 590568449\H, 1. 9287213374, 1. 8720540327, -0. 8677731219\H, 1. 7666110843, 1. 8
 907561116, 0. 9080240881\C, 2. 2778886543, -0. 6328519342, 1. 2473961586\H, 1. 7
 899610418, -0. 1296218443, 2. 1196919237\H, 1. 9675721315, -1. 6849127678, 1. 26
 49361826\H, 3. 3654712519, -0. 601175179, 1. 4418767148\Version=AM64L-G03Re
 vD. 01\State=1-A\HF=-306. 8714532\MP2=-308. 1329537\RMSD=3. 654e-09\RMSF=8
 . 944e-06\Thermal=0. \Di pol e=-0. 0002732, 0. 344914, -0. 0001032\PG=C01 [X(C5
 H15N2)]\@

CH₃⁻ + MeCH₃

Methyl Anion:

1\1\GINC-NODE18\FOpt\RMP2-FC\6-311+G(2d,p)\C1H3(1-)\MAY04\17-Oct-2009\
 O\#P MP2/6-311+G(2d,p) Opt Freq\Methyl Anion\ -1, 1\C, -2. 6896653265, 1
 . 3638396243, 0. 0105326924\H, -2. 3254162039, 0. 3233267205, 0. 0046321952\H, -
 2. 3253972562, 1. 8789790758, -0. 8935245297\H, -3. 792086758, 1. 3604464046, 0.
 0046322093\Version=AM64L-G03RevD. 01\State=1-A1\HF=-39. 5195182\MP2=-39
 . 7100517\RMSD=2. 119e-09\RMSF=1. 364e-05\Thermal=0. \Di pol e=-0. 2286507, -0
 . 3233525, -0. 5600676\PG=C03V [C3(C1), 3SGV(H1)]\@

Ethane:

1\1\GINC-NODE18\FOpt\RMP2-FC\6-311+G(2d,p)\C2H6\MAY04\17-Oct-2009\O\#\#
 P MP2/6-311+G(2d,p) Opt Freq\Ethane\ 0, 1\C, -2. 6918544438, 1. 3607438143,
 0. 0051705345\H, -2. 344160173, 0. 3263156614, -0. 0227252353\H, -2. 3428950603
 , 1. 8529124098, -0. 9046143332\H, -3. 7830211569, 1. 3450924284, -0. 0234881753
 \C, -2. 1827341429, 2. 0807295813, 1. 2522343977\H, -1. 0915678434, 2. 095993663
 , 1. 2811168845\H, -2. 5300629856, 3. 1152864938, 1. 2799066409\H, -2. 532058540
 8, 1. 5888195303, 2. 1620190151\Version=AM64L-G03RevD. 01\State=1-A1\HF=-7
 9. 2541437\MP2=-79. 5863122\RMSD=2. 209e-09\RMSF=3. 192e-05\Thermal=0. \Di p
 ol e=0. , 0. , 0. \PG=D03 [C3(C1. C1), X(H6)]\@

Reactant Complex:

1\1\GINC-NODE25\FOpt\RMP2-FC\6-311+G(2d,p)\C3H9(1-)\MAY04\08-Dec-2009\
 O\#P MP2/6-311+G(2d,p) opt, freq\Reactant Complex H3C---Me-CH3\ -1, 1
 \C, 1. 4378438003, -0. 6496379767, 0. 0278094217\H, 0. 8250017557, -1. 204602872
 3, 0. 7400396552\H, 1. 3177895305, -1. 1338495624, -0. 9437202413\H, 2. 48730867
 51, -0. 7416945819, 0. 327637211\C, -2. 3865400553, -0. 0980365152, -0. 11274857
 35\H, -3. 4382246493, -0. 4265061272, -0. 0878604434\H, -2. 2567816812, 0. 73055
 02295, 0. 6038228678\H, -1. 7459924953, -0. 9410434107, 0. 1962440453\C, 0. 9813
 012365, 0. 8059499495, -0. 0391763738\H, 1. 580397097, 1. 3727353234, -0. 758841
 226\H, -0. 0699604818, 0. 8477446479, -0. 3425096443\H, 1. 0813742679, 1. 292088
 8961, 0. 9352693014\Version=AM64L-G03RevD. 01\State=1-A\HF=-118. 775546\M
 P2=-119. 3031792\RMSD=5. 520e-09\RMSF=2. 140e-06\Thermal=0. \Di pol e=3. 8611
 055, 0. 0562364, 0. 5037682\PG=C01 [X(C3H9)]\@

Transition State:

1\1\GINC-NODE20\FTS\RMP2-FC\6-311+G(2d,p)\C3H9(1-)\MAY04\17-Oct-2009\
 O\#P MP2/6-311+G(2d,p) Opt=(ts, noigentest, cal cfc) freq\H3C---Me---CH
 3\ -1, 1\C, -0. 0012611816, -0. 0000019303, -0. 0000016641\H, 0. 0033827046, -0.
 6588569843, 0. 8514401348\H, 0. 0033799635, 1. 0667958138, 0. 144862653\H, 0. 00
 33834895, -0. 4079446188, -0. 996307774\C, 2. 1076482064, 0. 0000019927, -0. 000
 0002081\H, 2. 4574575336, 0. 5082034771, 0. 9084349065\H, 2. 4574610755, -1. 040
 8254447, -0. 0141025489\H, 2. 4574588003, 0. 5326298867, -0. 8943322213\C, -2. 1
 067708828, -0. 0000058317, -0. 0000031401\H, -2. 4599909657, 0. 9434208614, -0.

Chapter 3: Marcus-Analysis of Ambident Reactivity

4371880347\H, -2. 4599901273, -0. 0931070743, 1. 0356209773\H, -2. 459987616, -0. 8503331475, -0. 5984430803\Versi on=AM64L-G03RevD. 01\State=1-A\HF=-118. 6716709\MP2=-119. 2233922\RMSD=4. 394e-09\RMSF=1. 244e-04\Thermal =0. \Di pol e=-0. 0319822, 0. , 0. \PG=C01 [X(C3H9)]\@

CN⁻ + MeCN (C-Attack)

Cyanide:

1\1\GI NC-NODE19\F0pt\RMP2-FC\6-311+G(2d,p)\C1N1(1-)\MAY04\15-Oct-2009\0\#p MP2/6-311+G(2d,p) Opt Freq\Cyani d\ -1,1\C,0.,0., -0. 6399699026\N,0.,0.,0. 5498469026\Versi on=AM64L-G03RevD. 01\State=1-SG\HF=-92. 3354609\MP2=-92. 6557428\RMSD=6. 782e-09\RMSF=1. 288e-06\Thermal =0. \Di pol e=0. ,0.,0. 3018409\PG=C*V [C*(C1N1)]\@

Methyl Cyanide:

1\1\GI NC-NODE15\F0pt\RMP2-FC\6-311+G(2d,p)\C2H3N1\MAY04\15-Oct-2009\0\#p MP2/6-311+G(2d,p) Opt Freq nosymm\Acetoni tri l\0,1\C,0. 0000000002,0. 0000000777,0. 2790390944\N, -0. 0000000002, -0. 0000000289, 1. 4480860428\C,0.,0. 0000002196, -1. 1822899425\H,0.,1. 0245804692, -1. 5539679732\H,0. 8873125021, -0. 5122898688, -1. 5539681109\H, -0. 8873125021, -0. 5122898688, -1. 5539681106\Versi on=AM64L-G03RevD. 01\HF=-131. 9626222\MP2=-132. 4368784\RMSD=2. 211e-09\RMSF=1. 707e-05\Thermal =0. \Di pol e=0. ,0. 0000001, -1. 5473884\PG=C01 [X(C2H3N1)]\@

Reactant Complex:

1\1\GI NC-NODE27\F0pt\RMP2-FC\6-311+G(2d,p)\C3H3N2(1-)\MAY04\08-Dec-2009\0\#p MP2/6-311+G(2d,p) opt=cal cfc freq\Reactant Complex NC---Me-CN\ -1,1\C, -2. 496507461, -0. 0031989428,0. 0014708346\N, -3. 6853003425, -0. 0030378329,0. 0013860943\C, 2. 1650030251, -0. 0019507578,0. 0013839214\N, 3. 3356854684, -0. 0016720056,0. 0013724553\C,0. 7014819069, -0. 0023000879,0. 0013986078\H,0. 3056648793, -0. 5345186036, -0. 8610218903\H,0. 3056682376, -0. 4832146079,0. 8934463691\H,0. 3053112862, 1. 0105518384, -0. 0282173922\Versi on=AM64L-G03RevD. 01\State=1-A\HF=-224. 3156539\MP2=-225. 111986\RMSD=9. 480e-09\RMSF=1. 680e-06\Thermal =0. \Di pol e=3. 5040441,0. 0008175, -0. 0000423\PG=C01 [X(C3H3N2)]\@

Transition State:

1\1\GI NC-NODE11\FTS\RMP2-FC\6-311+G(2d,p)\C3H3N2(1-)\MAY04\15-Oct-2009\0\#p MP2/6-311+G(2d,p) Opt=(ts,noei gentest,cal cfc) Freq\NC---Me---C\N\ -1,1\C,0. 000761404, -0. 000209581, -0. 0420748276\N, -0. 0010470087, -0. 0005398114, 1. 1401086188\C,0. 0046412953,0. 000384826, -2. 1081744191\H, -0. 9062301625,0. 5652923046, -2. 1097581989\H,0. 9493011839,0. 5067708884, -2. 106214526\H, -0. 0291446986, -1. 0709073088, -2. 1085504313\C,0. 0085877053,0. 0010375711, -4. 1742734714\N,0. 0107212813,0. 0016699611, -5. 3564562744\Versi on=AM64L-G03RevD. 01\State=1-A\HF=-224. 2402366\MP2=-225. 0436424\RMSD=6. 116e-09\RMSF=4. 175e-05\Thermal =0. \Di pol e=-0. 000145, -0. 0001331, -0. 0000018\PG=C01 [X(C3H3N2)]\@

CN⁻ + MeNC (N-Attack)

Methyl Isocyanide:

1\1\GI NC-NODE19\F0pt\RMP2-FC\6-311+G(2d,p)\C2H3N1\MAY04\15-Oct-2009\0\#p MP2/6-311+G(2d,p) Opt Freq\Isoni tri l\0,1\N,0.,0.,0. 3114251623\C,0.,0.,1. 4899574892\C,0.,0., -1. 1149885372\H,0.,1. 0270831834, -1. 4762063714\H,0. 8894801286, -0. 5135415917, -1. 4762063714\H, -0. 8894801286, -0. 5135415917, -1. 4762063714\Versi on=AM64L-G03RevD. 01\State=1-A1\HF=-131. 931465\MP2=-132. 393841\RMSD=8. 043e-09\RMSF=1. 062e-04\Thermal =0. \Di pol e=0. ,0., -1. 6330263\PG=C03V [C3(C1N1C1), 3SGV(H1)]\@

Reactant Complex:

1\1\GI NC-NODE10\F0pt\RMP2-FC\6-311+G(2d,p)\C3H3N2(1-)\MAY04\09-Dec-2009\0\#p MP2/6-311+G(2d,p) opt=cal cfc freq\Reactant Complex CN---Me-NC \-1, 1\N, -1. 8935699059, -0. 0067206347, -0. 0120264372\C, -3. 0709387787, 0. 007207145, -0. 0305334713\N, 2. 4727304882, 0. 7349213098, 0. 0427622266\C, 2. 7435991711, -0. 4195855739, -0. 0571416982\C, -0. 4516333455, -0. 0138325533, 0. 0104689006\H, -0. 0641003542, 0. 9997671366, -0. 0405257905\H, -0. 1016388198, -0. 4769318211, 0. 92843128\H, -0. 0715914552, -0. 5772195779, -0. 8368290099\Version=AM64L-G03RevD. 01\State=1-A\HF=-224. 2841918\MP2=-225. 0733005\RM SD=3. 307e-09\RMSF=9. 034e-06\Thermal =0. \Di pol e=-2. 6871393, 0. 0497577, 0. 0460179\PG=C01 [X(C3H3N2)]\@

Transition State:

1\1\GI NC-NODE11\FTS\RMP2-FC\6-311+G(2d,p)\C3H3N2(1-)\MAY04\15-Oct-2009\0\#p MP2/6-311+G(2d,p) Opt=(ts, noigentest, cal cfc) Freq\CN---Me---NC \-1, 1\N, 0. 0001764663, -0. 0000082876, -0. 0419834135\C, -0. 0003504343, -0. 0000654944, 1. 1441287329\C, 0. 0012027665, 0. 0000848479, -2. 0048915159\H, -0. 9751629022, -0. 4420507849, -2. 0054272121\H, 0. 1064849289, 1. 0667104944, -2. 0047856931\H, 0. 8722866667, -0. 6244048739, -2. 0044622378\N, 0. 002234935, 0. 000183614, -3. 9677998246\C, 0. 002856573, 0. 0002955944, -5. 1539119059\Version=AM64L-G03RevD. 01\State=1-A\HF=-224. 2335731\MP2=-225. 0264106\RM SD=1. 640e-09\RMSF=4. 289e-05\Thermal =0. \Di pol e=-0. 0000551, -0. 0000333, 0. 0000009\PG=C01 [X(C3H3N2)]\@

OCN⁻ + MeOCN (*O*-Attack)Cyanate:

1\1\GI NC-NODE19\F0pt\RMP2-FC\6-311+G(2d,p)\C1N101(1-)\MAY04\16-Oct-2009\0\#p MP2/6-311+G(2d,p) Opt Freq\Cyanate\ -1, 1\N, 0. , 0. , 0. 014055842\C, 0. , 0. , 1. 2173623105\O, 0. , 0. , 2. 4515158475\Version=AM64L-G03RevD. 01\State=1-SG\HF=-167. 2593703\MP2=-167. 7997406\RM SD=9. 309e-09\RMSF=1. 072e-04\Thermal =0. \Di pol e=0. , 0. , 0. 622632\PG=C*V [C*(N1C101)]\@

Methyl Cyanate:

1\1\GI NC-NODE19\F0pt\RMP2-FC\6-311+G(2d,p)\C2H3N101\MAY04\16-Oct-2009\0\#p opt freq mp2/6-311+g(2d,p)\Methyl cyanate\0, 1\N, -0. 8451655074, -1. 5412561695, -3. 0332445805\C, -0. 8179899168, -1. 5003799943, -1. 8594209585\O, -0. 8057435095, -1. 4881819849, -0. 5641332851\C, -0. 1655341724, -0. 3052035356, -0. 0054310097\H, -0. 2286845198, -0. 431073737, 1. 0706457628\H, 0. 8727523958, -0. 2657270869, -0. 3311321577\H, -0. 7053915447, 0. 5850783867, -0. 3242267723\Version=AM64L-G03RevD. 01\State=1-A\HF=-206. 810456\MP2=-207. 4946389\RM SD=6. 113e-09\RMSF=7. 174e-05\Thermal =0. \Di pol e=0. 4179872, 0. 7627431, 1. 548704\PG=C01 [X(C2H3N101)]\@

Reactant Complex:

1\1\GI NC-NODE27\F0pt\RMP2-FC\6-311+G(2d,p)\C3H3N202(1-)\MAY04\09-Dec-2009\0\#p MP2/6-311+g(2d,p) opt=cal cfc freq\Reactant Complex NCO---Me-OCN\ -1, 1\C, -2. 4508321257, -0. 020110126, -0. 1697535638\C, 2. 8732011075, 0. 189102767, -0. 0220813966\N, -3. 4572692744, 0. 5909876693, -0. 1613387223\N, 3. 2678004927, -0. 9453667044, -0. 0772781667\O, -1. 3895242087, -0. 742477093, -0. 1828902195\O, 2. 4166519943, 1. 3352553327, 0. 0321637179\C, -0. 1212534099, 0. 0307863509, -0. 109807083\H, -0. 1077979666, 0. 5946905128, 0. 8179598771\H, 0. 6674410903, -0. 7139263053, -0. 1311091723\H, -0. 0640822294, 0. 6918570961, -0. 9691409408\Version=AM64L-G03RevD. 01\State=1-A\HF=-374. 09115\MP2=-375. 3204728\RM SD=7. 260e-09\RMSF=4. 939e-05\Thermal =0. \Di pol e=-2. 5909917, 0. 0538609, -0. 0644054\PG=C01 [X(C3H3N202)]\@

Transition State:

1\1\GI NC-NODE10\FTS\RMP2-FC\6-311+G(2d,p)\C3H3N2O2(1-)\MAY04\16-Oct-2009\0\#p MP2/6-311+G(2d,p) Opt=(ts,noigentest,calcfc) Freq\NCO---Me--OCN\ -1,1\C,0.000024212,0.0000258509,-0.2052882394\H,-0.4172955467,0.8341736601,-0.7399666175\H,0.4172610932,-0.8339376429,-0.7402810293\H,0.00004503,-0.0001545963,0.8694752572\C,-2.6279422388,-0.1435863749,0.0799810728\C,2.6279374674,0.1435363375,0.0799923319\N,-3.5128793381,0.5941815977,0.3756610534\N,3.5128524115,-0.5943196581,0.3755195016\O,-1.687594874,-0.9156763508,-0.2364312478\O,1.6876125743,0.9157201768,-0.236257083\Versi on=AM64L-G03RevD.01\State=1-A\HF=-374.0600532\MP2=-375.2958346\RMSD=2.289e-09\RMSF=2.573e-06\Thermal=0.\Di pol e=0.0000053,0.0000884,-0.5418664\PG=C01 [X(C3H3N2O2)]\@

OCN⁻ + MeNCO (N-Attack)

Methyl Isocyanate:

1\1\GI NC-NODE19\FOpt\RMP2-FC\6-311+G(2d,p)\C2H3N1O1\MAY04\16-Oct-2009\0\#p MP2/6-311+G(2d,p) Opt Freq\Methyl isothi cyanate\0,1\C,0.0034832026,-0.0000003063,0.0327751704\N,-0.1121712881,-0.0000006936,1.4731082567\C,0.6379928533,-0.000000557,2.4210503085\H,-0.9960655302,-0.0000501781,-0.3969812229\H,0.5331252354,0.8893139279,-0.3116244144\H,0.5332128658,-0.889264217,-0.3116196461\O,1.2477034111,-0.0000097396,3.4330748378\Versi on=AM64L-G03RevD.01\State=1-A\HF=-206.8523208\MP2=-207.5390434\RMSD=9.677e-09\RMSF=2.338e-04\Thermal=0.\Di pol e=-0.1255704,0.0000044,-1.1681064\PG=C01 [X(C2H3N1O1)]\@

Reactant Complex:

1\1\GI NC-NODE10\FOpt\RMP2-FC\6-311+G(2d,p)\C3H3N2O2(1-)\MAY04\10-Dec-2009\0\#p MP2/6-311+g(2d,p) opt=calcfc freq\Reactant Complex OCN--Me-NCO\ -1,1\N,2.1170033409,0.512355203,-0.003053176\C,3.1639034647,-0.0692841285,0.0015854585\O,4.266770592,-0.5255409152,0.0052559761\N,-2.2050921096,0.0527526744,-0.0001592107\C,-3.4002241789,-0.0949424913,0.0011909531\O,-4.6201168356,-0.2456075045,0.002550546\C,0.6650846621,0.3537112894,-0.0019668995\H,0.3380102601,-0.1798894694,0.8859148029\H,0.1926790471,1.3295667136,-0.0097634132\H,0.3382117573,-0.1939063717,-0.8813500372\Versi on=AM64L-G03RevD.01\State=1-A\HF=-374.1272657\MP2=-375.357335\RMSD=7.135e-09\RMSF=4.316e-06\Thermal=0.\Di pol e=3.7608834,0.2483288,-0.0014888\PG=C01 [X(C3H3N2O2)]\@

Transition State:

1\1\GI NC-NODE20\FTS\RMP2-FC\6-311+G(2d,p)\C3H3N2O2(1-)\MAY04\18-Oct-2009\0\#p opt=(calcfc,ts,noigentest) freq MP2/6-311+g(2d,p)\NCO---Me--NCO\ -1,1\C,-0.0011379983,-0.1712554115,0.2217542238\H,0.2744751598,0.8202915217,0.5194201451\H,0.0070733224,-0.4435052989,-0.8154035562\H,-0.2849816041,-0.8898551175,0.9638957877\N,-1.8760601154,0.4350949197,0.0590653221\C,-2.8509098427,-0.2368725843,-0.1847269253\O,-3.8526520677,-0.8738942189,-0.4256333895\N,1.8735962984,-0.7721095276,0.4056281447\C,2.8545914855,-0.3026306536,-0.1221474157\O,3.8622953621,0.137926371,-0.6298503366\Versi on=AM64L-G03RevD.01\State=1-A\HF=-374.0769304\MP2=-375.3154434\RMSD=9.322e-09\RMSF=2.920e-06\Thermal=0.\Di pol e=-0.0010425,0.0349916,0.1332097\PG=C01 [X(C3H3N2O2)]\@

SCN⁻ + MeSCN (S-Attack)

Thiocyanate:

1\1\GI NC-NODE14\FOpt\RMP2-FC\6-311+G(2d,p)\C1N1S1(1-)\MAY04\16-Oct-2009\0\#p MP2/6-311+G(2d,p) Opt Freq\Thi cyanate\ -1,1\N,0.,0.,-0.0123223712\C,0.,0.,1.1784945489\S,0.,0.,2.8475228223\Versi on=AM64L-G03RevD.01\State=1-SG\HF=-489.9288519\MP2=-490.397231\RMSD=4.229e-09\RMSF=1.982e-04\Thermal=0.\Di pol e=0.,0.,0.6199334\PG=C*V [C*(N1C1S1)]\@

Methyl Thiocyanate:

1\1\GI NC-NODE14\FOpt\RMP2-FC\6-311+G(2d,p)\C2H3N1S1\MAY04\16-Oct-2009\0\#\p MP2/6-311+G(2d,p) Opt, Freq\Methyl thiocyanate\0,1\C, -1.4907680053, 0.7971971572, -0.0000819076\H, -2.5259362774, 0.4571427491, 0.0005481964\H, -1.293939095, 1.3802711159, 0.8961930895\H, -1.2950583132, 1.380087008, -0.8967192159\S, -0.4782881449, -0.7239056972, -0.0006796929\C, 1.0561309628, 0.0089999073, 0.0001057743\N, 2.1311158731, 0.4862737596, 0.0006249666\Version=AM64L-G03RevD.01\State=1-A\HF=-529.4839458\MP2=-530.1057275\RMSD=3.862e-09\RMSF=3.496e-05\Thermal=0.\Di pol e=-1.6442875, 0.0599118, -0.0003608\PG=C01 [X(C2H3N1S1)]\@\

Reactant Complex:

1\1\GI NC-NODE18\FOpt\RMP2-FC\6-311+G(2d,p)\C3H3N2S2(1-)\MAY04\09-Dec-2009\0\#\p MP2/6-311+g(2d,p) opt=calcfrc freq\Reactant Complex NCS---Me-SCN\ -1,1\S, 3.6073029915, 1.2513437727, -0.0081962355\S, -1.4219981071, -0.7391477663, -0.04655504\C, -2.6136625641, 0.4710809858, -0.1094855582\C, 3.2825639462, -0.3779056991, 0.0296130204\N, -3.4802992853, 1.2672991754, -0.1521128411\N, 2.9930809787, -1.5347359533, 0.0549565302\C, 0.0886646585, 0.2942434271, -0.0710385141\H, 0.1184648175, 0.9388960065, 0.8024405335\H, 0.9135095766, -0.4198696676, -0.0349396923\H, 0.1357213775, 0.8700530087, -0.9907079028\Version=AM64L-G03RevD.01\State=1-A\HF=-1019.4291571\MP2=-1020.5254768\RMSD=8.307e-09\RMSF=6.722e-06\Thermal=0.\Di pol e=-2.7042803, -0.090209, -0.0585141\PG=C01 [X(C3H3N2S2)]\@\

Transition State:

1\1\GI NC-NODE9\FTS\RMP2-FC\6-311+G(2d,p)\C3H3N2S2(1-)\MAY04\16-Oct-2009\0\#\p MP2/6-311+G(2d,p) Opt=(ts,noeigentest,calcfrc) Freq\NCS---Me---SCN\ -1,1\C, -0.0000215011, 0.0000661655, -0.1629680147\H, -0.4462539914, 0.8176102201, -0.7021772495\H, 0.4461593176, -0.8161333194, -0.7042319225\H, 0.0000794772, -0.001206161, 0.9114103795\S, 2.0735013284, 1.1202834389, -0.1892783787\S, -2.073516372, -1.1200066089, -0.1916611403\C, -2.9782046756, 0.2468779786, 0.1586976002\C, 2.9782274103, -0.247070166, 0.1591330724\N, -3.6062223569, 1.2217250643, 0.4017823178\N, 3.6062903636, -1.222224612, 0.4008683357\Version=AM64L-G03RevD.01\State=1-A\HF=-1019.3876397\MP2=-1020.4934642\RMSD=5.555e-09\RMSF=1.933e-06\Thermal=0.\Di pol e=-0.0003229, 0.0001893, -0.4598512\PG=C01 [X(C3H3N2S2)]\@\

SCN⁻ + MeNCS (N-Attack)

Methyl Isothiocyanate:

1\1\GI NC-NODE14\FOpt\RMP2-FC\6-311+G(2d,p)\C2H3N1S1\MAY04\16-Oct-2009\0\#\p MP2/6-311+G(2d,p) opt=(calcfrc,maxstep=10) freq\Methyl isothiocyanate\0,1\C, 0.0110623853, -0.0263906708, -0.0024776155\N, 0.1584507024, -0.3284152195, 1.3904151717\C, 0.6460825902, -0.0367086465, 2.4455222683\S, 1.2282406071, 0.2427886091, 3.8943420978\H, -0.6427558163, -0.7630947592, -0.4662232041\H, -0.4269667026, 0.9659760884, -0.1230190638\H, 0.9853199234, -0.0541063923, -0.4936446994\Version=AM64L-G03RevD.01\State=1-A\HF=-529.4894218\MP2=-530.1129173\RMSD=1.800e-09\RMSF=6.690e-07\Thermal=0.\Di pol e=-0.2977498, 0.0682053, -1.3222256\PG=C01 [X(C2H3N1S1)]\@\

Reactant Complex:

1\1\GI NC-NODE26\FOpt\RMP2-FC\6-311+G(2d,p)\C3H3N2S2(1-)\MAY04\09-Dec-2009\0\#\p MP2/6-311+g(2d,p) opt=calcfrc freq\Reactant Complex SCN-Me-NCs\ -1,1\C, 3.0300251929, -0.3396011783, 0.1655764478\C, -2.5945218173, 0.3519544388, 0.1362526094\S, 3.3655482819, 1.2838471558, 0.0251479812\S, -4.1844452383, 0.6110300047, 0.1213927594\N, 2.7407252202, -1.4916026235, 0.2656967307\N, -1.4232672383, 0.1971641035, 0.1446177504\C, -0.058282719, -0.2493198173, 0.1764902477\H, 0.1236363166, -0.9277281577, -0.6550474178\H, 0.6178712997, 0.6022651188, 0.0993410548\H, 0.1322945416, -0.7747309249, 1.1105591564\Version=AM64L-G03RevD.01\State=1-A\HF=-1019.437114\MP2=-1020.

Chapter 3: Marcus-Analysis of Ambident Reactivity

5330978\RMSD=7.057e-09\RMSF=1.177e-05\Thermal =0.\Di pol e=-3.0256902, 0.1627882, 0.0038084\PG=C01 [X(C3H3N2S2)]\@

Transition State:

1\1\GINC-NODE26\FTS\RMP2-FC\6-311+G(2d,p)\C3H3N2S2(1-)\MAY04\16-Oct-2009\0\#P MP2/6-311+G(2d,p) Opt=(ts,noigentest,calcfc) Freq\NCS---Me--SCN\ -1,1\C, -0.0007401957, 0.0309092466, -0.1432955722\H, 0.0133667051, -0.1873881613, 0.907838556\H, -0.3485350847, 0.9852863338, -0.4881083464\H, 0.3329635392, -0.7054520783, -0.8483480106\C, -2.9371390067, -0.3246243835, 0.0213782596\C, 2.9405520398, 0.3070618282, 0.0761809321\S, -4.4696824742, 0.1027045993, 0.3847787246\S, 4.4793257322, -0.2215405151, 0.2030919442\N, -1.8250996068, -0.6658208019, -0.2581961269\N, 1.8237593517, 0.7254869322, -0.0181883603\Version=AM64L-G03RevD.01\State=1-A\HF=-1019.3851344\MP2=-1020.4862617\RMSD=6.207e-09\RMSF=1.124e-06\Thermal =0.\Di pol e=-0.0016316, 0.0276724, -0.1339774\PG=C01 [X(C3H3N2S2)]\@

$\text{NO}_2^- + \text{MeNO}_2$ (N-Attack)

Nitrite:

1|1|UNPC-UNK|FOpt|RMP2-FC|6-311+G(2d,p)|N102(1-)|PCUSER|16-Oct-2009|0| |#P MP2/6-311+G(2D,P) OPT FREQ| |Nitrite| | -1,1|N, -0.2216100025, -0.4099777473, 0. |0, 1.0455548391, -0.3333918107, 0. |0, -0.8516460869, 0.6921223396, 0. | |Version=x86-Wi n32-G03RevB.03|State=1-A'|HF=-204.1463156|MP2=-204.7851469|RMSD=6.127e-009|RMSF=5.277e-005|Di pol e=-0.0395435, -0.0731503, 0. |PG=CS [SG(N102)]| |@

Nitromethane:

1|1|UNPC-UNK|FOpt|RMP2-FC|6-311+G(2d,p)|C1H3N102|PCUSER|16-Oct-2009|0| |#P MP2/6-311+G(2D,P) OPT FREQ| |Nitromethane| |0,1|N, 0.0791774922, 0.1475559036, 0.009094574|0, 1.2992501083, 0.1209140294, -0.1696206056|0, -0.6043596082, 1.1644333862, 0.1546436929|C, -0.6280146729, -1.1598080705, 0.0106948457|H, -0.7748976659, -1.4428975282, -1.0302782358|H, 0.0105372254, -1.8839668276, 0.5083485095|H, -1.5809179676, -1.0299578714, 0.5139139361| |Version=x86-Wi n32-G03RevB.03|State=1-A|HF=-243.7380432|MP2=-244.5321677|RM SD=5.858e-009|RMSF=1.517e-004|Di pol e=-0.6659531, -1.229605, 0.0099081|PG =C01 [X(C1H3N102)]| |@

Reactant Complex:

1\1\GINC-NODE23\FOpt\RMP2-FC\6-311+G(2d,p)\C1H3N204(1-)\MAY04\09-Dec-2009\0\#p MP2/6-311+g(2d,p) opt=calcfc freq\REactant Complex 02N---Me-N02\ -1,1\N, 2.6864959751, -0.133623565, 0.0877810366\0, 2.3588958754, 0.6865490272, -0.8346294618\0, 3.9207108923, -0.3184371819, 0.262955377\N, -1.6770533051, 0.1822390813, -0.1490602527\0, -2.1879945163, 1.16670897, 0.4004877812\0, -2.2283003795, -0.4731878001, -1.0428083389\C, -0.3111719512, -0.2133039029, 0.2622173003\H, 0.4264070102, 0.3152068476, -0.3586796708\H, -0.1795497871, 0.0716393561, 1.30077839\H, -0.2127658639, -1.2827844922, 0.1084567492\Version=AM64L-G03RevD.01\State=1-A\HF=-447.9071135\MP2=-449.3428809\RMSD=7.746e-09\RMSF=1.766e-06\Thermal =0.\Di pol e=-2.8349172, -0.3672663, 0.4966304\PG=C01 [X(C1H3N204)]\@

Transition State:

1\1\GINC-NODE14\FTS\RMP2-FC\6-311+G(2d,p)\C1H3N204(1-)\MAY04\18-Oct-2009\0\#p mp2/6-311+g(2d,p) opt=(calcfc,ts,noigentest) freq\02N---Me--N02\ -1,1\C, 0.00006568, -0.0064220049, 0.0090019723\H, 0.0080892743, 0.9717623101, -0.4454304594\H, 0.0006950876, -0.0877697671, 1.0841340425\H, -0.0087371828, -0.9051681795, -0.5873149242\N, 1.9318849192, -0.0053920717, -0.0022092667\0, 2.547110604, 0.9651966841, -0.4951837387\0, 2.5488550076, -0.9774908012, 0.4844053579\N, -1.9318806451, -0.0059140104, 0.0001396346\0, -2.5481353418, 0.8835483192, 0.6258453469\0, -2.5478162909, -0.893122478

Chapter 3: Marcus-Analysis of Ambident Reactivity

6, -0.6299829653\\Version=AM64L-G03RevD.01\\State=1-A\\HF=-447.8594462\\MP2=-449.3034532\\RMSD=5.959e-09\\RMSF=1.327e-06\\Thermal=0.\\Di pol e=-0.0000286, -0.0009084, 0.0121944\\PG=C01 [X(C1H3N2O4)]\\@

NO₂⁻ + MeONO (O-Attack)

Methyl Nitrite:

1|1|UNPC-UNK|FOpt|RMP2-FC|6-311+G(2d,p)|C1H3N102|PCUSER|16-Oct-2009|0|
|#P MP2/6-311+G(2D,P) OPT FREQ|Methyl nitrite||0,1|C,-0.2903498219,-1
.2385587639,-1.0341380978|H,0.0829253858,-2.2584196226,-0.988634814|H,
0.0588298596,-0.7546908771,-1.946030085|H,-1.3796468211,-1.2387305854,
-0.9989559207|0,0.2544882198,-0.5834240311,0.1280501112|N,-0.159471618
9,0.7767457358,0.1061963982|0,0.2575482601,1.3641707209,1.0463342162|
Version=x86-Win32-G03RevB.03|State=1-A|HF=-243.738061|MP2=-244.5189629
|RMSD=7.239e-009|RMSF=1.252e-004|Di pol e=-0.2826355,-0.5567673,-0.70716
73|PG=C01 [X(C1H3N102)]||@

Reactant Complex:

1\\1\\GINC-NODE23\\FOpt\\RMP2-FC\\6-311+G(2d,p)\\C1H3N2O4(1-)\\MAY04\\10-Dec-2
009\\0\\#p MP2/6-311+g(2d,p) opt=cal cfc freq\\Reactant Complex ONO--Me--
-ONO\\-1,1\\0,2.5886918439,0.8853048469,0.0469445161\\0,-1.485623531,-0.
3917507964,0.364446312\\N,2.9463057552,-0.3373213019,0.0217583189\\N,-2.
3630054236,0.2608884997,-0.4533686813\\0,4.1884428827,-0.5626950572,0.0
051254047\\0,-3.4872982732,-0.153917488,-0.3260130629\\C,-0.1318298183,0
.1564924221,0.2124822829\\H,0.0923402569,0.7564309629,1.089037958\\H,0.5
581316588,-0.6778404024,0.1431388055\\H,-0.0887622615,0.7624077644,-0.6
874574937\\Version=AM64L-G03RevD.01\\State=1-A\\HF=-447.9012321\\MP2=-449
.3237405\\RMSD=8.574e-09\\RMSF=1.684e-05\\Thermal=0.\\Di pol e=-3.5734373,0.
1156234,0.0312501\\PG=C01 [X(C1H3N2O4)]\\@

Transition State:

1\\1\\GINC-NODE9\\FTS\\RMP2-FC\\6-311+G(2d,p)\\C1H3N2O4(1-)\\MAY04\\17-Oct-200
9\\0\\#p opt=(cal cfc,ts,noeigentest) freq mp2/6-311+g(2d,p)\\ONO--Me--
-ONO\\-1,1\\C,-0.1879631064,-0.1328918305,0.2011519792\\H,0.2137586538,-
1.1182173858,0.0356878235\\H,-0.2399663095,0.2619299195,1.2001433528\\H,
-0.5379628341,0.4597006715,-0.6270721997\\0,-1.9217966764,-0.8748564192
,0.4332162373\\0,1.5432408812,0.6289229525,0.0192224591\\N,-2.7179986175
, -0.3233647724,-0.4349097586\\N,2.3941333337,-0.3377486041,-0.163220946
2\\0,-3.8933544254,-0.7113717049,-0.3809031128\\0,3.5729026206,0.0242493
134,-0.2831673946\\Version=AM64L-G03RevD.01\\State=1-A\\HF=-447.8607159\\
MP2=-449.2951434\\RMSD=8.684e-09\\RMSF=2.546e-06\\Thermal=0.\\Di pol e=-0.01
21614,0.0928271,0.2349708\\PG=C01 [X(C1H3N2O4)]\\@

CH₂CHO⁻ + CH₂CHOCH₃ (O-Attack)

Enolate:

1|1|UNPC-UNK|POpt|RMP2-FC|6-311+G(2d,p)|C2H3O1(1-)|PCUSER|05-Sep-2009|
1|1|#P MP2/6-311+G(2D,P) POPT FREQ NOSYMM|Acetaldehyd-Enolat||-1,1|C|C
,1,R2|0,2,R3,1,A3|H,1,R4,2,A4,3,D4,0|H,1,R5,2,A5,3,D5,0|H,2,R6,1,A6,4,
D6,0||R2=1.38564943|R3=1.2740079|A3=130.06107042|R4=1.08734841|A4=121.
24524429|D4=-0.00000358|R5=1.0860646|A5=119.57236535|D5=180.00000209|R
6=1.12211816|A6=112.94180684|D6=179.99999716||Version=x86-Win32-G03Rev
B.03|HF=-152.3540351|MP2=-152.8861988|RMSD=8.373e-009|RMSF=4.643e-005|
Di pol e=-0.5530588,0.,-0.3271597|PG=C01 [X(C2H3O1)]||@

Methylvinylether:

1|1|UNPC-UNK|FOpt|RMP2-FC|6-311+G(2d,p)|C3H6O1|PCUSER|05-Sep-2009|1|1|
P MP2/6-311+G(2D,P) POPT FREQ NOSYMM|Methyl-vinyl-ether (O-Angriff)||#

```

0, 1 | C | C, 1, R2 | 0, 1, R3, 2, A3 | C, 3, R4, 1, A4, 2, D4, 0 | H, 1, R5, 2, A5, 3, D5, 0 | H, 2, R6,
1, A6, 3, D6, 0 | H, 2, R7, 1, A7, 3, D7, 0 | H, 4, R8, 3, A8, 1, D8, 0 | H, 4, R9, 3, A9, 1, D9, 0 | H
, 4, R10, 3, A10, 1, D10, 0 | | R2=1. 33936507 | R3=1. 35709357 | A3=127. 89537075 | R4=1
. 42281393 | A4=115. 28594083 | D4=-0. 05833682 | R5=1. 08442484 | A5=121. 87086747
| D5=179. 99100032 | R6=1. 08105898 | A6=118. 06034489 | D6=180. 00209585 | R7=1. 08
048089 | A7=123. 71681175 | D7=0. 00155471 | R8=1. 08704948 | A8=106. 15368721 | D8=
180. 08920103 | R9=1. 09378644 | A9=110. 72516963 | D9=-60. 65224846 | R10=1. 09378
804 | A10=110. 72505089 | D10=60. 82922011 | | Versi on=x86-Wi n32-G03RevB. 03 | HF=
-191. 9764911 | MP2=-192. 6493293 | RMSD=3. 381e-009 | RMSF=8. 006e-005 | Di pol e=0
. 320984, 0. 0005697, 0. 2541183 | PG=C01 [X(C3H601)] | | @

```

Reactant Complex:

```

1\1\G\I NC-NODE15\FOpt\RMP2-FC\6-311+G(2d, p)\C5H9O2(1-)\MAY04\12-Dec-200
9\0\#\#p MP2/6-311+g(2d, p) opt=cal cfc Freq\Reactant Complex CH2CHO--M
e-OCHCH2\ -1, 1\0, -1. 6521445172, -0. 0394492484, -0. 8664283811\0, 2. 5829037
997, -0. 2843747871, -1. 0348618349\C, -1. 9677248735, 0. 2877402801, 0. 4012569
972\H, -1. 1222416996, 0. 4138248898, 1. 0778666189\C, -3. 2300896587, 0. 451767
3334, 0. 8220853776\H, -3. 4114788403, 0. 7146568906, 1. 8547782815\H, -4. 06845
63221, 0. 3259632309, 0. 147929794\C, 2. 8229132561, 0. 0044154594, 0. 185226262
6\H, 1. 9331190019, 0. 2095462314, 0. 843348837\C, 4. 0226382239, 0. 1121969522,
0. 8590633991\H, 4. 0224670219, 0. 3716427733, 1. 9129974271\H, 4. 9695745699, -
0. 0580796292, 0. 3539649916\C, -0. 2203344201, -0. 1634139294, -1. 091951846\H
, 0. 2058086517, -0. 9440018122, -0. 4659020969\H, -0. 099113438, -0. 426587868,
-2. 1376636752\H, 0. 2879981346, 0. 7764919833, -0. 8893584325\Versi on=AM64L
-G03RevD. 01\State=1-A\HF=-344. 3392988\MP2=-345. 547962\RMSD=3. 679e-09\R
MSF=3. 486e-06\Thermal =0. \Di pol e=-3. 6285656, 0. 2622067, 0. 3556932\PG=C01
[X(C5H9O2)]\ | | @

```

Transition State:

```

1\1\G\I NC-NODE19\FTS\RMP2-FC\6-311+G(2d, p)\C5H9O2(1-)\MAY04\16-Oct-2009
\0\#\# MP2/6-311+G(2d, p) Opt=(ts, noei gentest, cal cfc) Freq\CH2CHO--Me-
--OCHCH2\ -1, 1\C, -0. 7986860498, -2. 6845789051, -0. 1565342882\H, -0. 452510
1981, -3. 6147183252, -0. 573213644\H, -0. 2086716393, -2. 1765675935, 0. 586719
6701\H, -1. 7345213545, -2. 2625749801, -0. 4830118202\0, -1. 674085574, -3. 594
9259149, 1. 2362927348\0, 0. 108469341, -1. 7884099121, -1. 5382315148\C, -2. 60
29455619, -4. 3865907034, 0. 771653662\H, -2. 7377219207, -4. 3809654947, -0. 32
61397674\C, -3. 4197762178, -5. 213973842, 1. 4783501384\H, -4. 1515307203, -5.
8151891708, 0. 9521697479\H, -3. 3551993266, -5. 2819060524, 2. 5589184455\C, -
0. 0695064277, -0. 4970949892, -1. 4591449253\H, -0. 7194473297, -0. 1486614999
, -0. 6348102495\C, 0. 4500662952, 0. 4646788771, -2. 2692265455\H, 0. 210332462
6, 1. 5044167583, -2. 0814411941\H, 1. 0977150016, 0. 2113229579, -3. 1015582197
\Versi on=AM64L-G03RevD. 01\State=1-A\HF=-344. 2914745\MP2=-345. 5165721\
RMSD=6. 983e-09\RMSF=2. 311e-06\Thermal =0. \Di pol e=-0. 2091268, 0. 0942359, -
0. 0728222\PG=C01 [X(C5H9O2)]\ | | @

```

CH₂CHO⁻ + CH₃CH₂CHO (C-Attack)

Propanal:

```

1 | 1 | UNPC-UNK | FOpt | RMP2-FC | 6-311+G(2d, p) | C3H601 | PCUSER | 05-Sep-2009 | 1 | | #
P MP2/6-311+G(2D, P) POPT FREQ NOSYMM | | Propanal (C-Angri ff) | | 0, 1 | C | C, 1,
R2 | C, 2, R3, 1, A3 | 0, 3, R4, 2, A4, 1, D4, 0 | H, 1, R5, 2, A5, 3, D5, 0 | H, 1, R6, 2, A6, 3, D6,
0 | H, 1, R7, 2, A7, 3, D7, 0 | H, 2, R8, 1, A8, 5, D8, 0 | H, 2, R9, 1, A9, 5, D9, 0 | H, 3, R10, 2, A
10, 1, D10, 0 | | R2=1. 52071 | R3=1. 50494037 | A3=113. 70723913 | R4=1. 21580275 | A4=
124. 42445135 | D4=-0. 01781158 | R5=1. 09083963 | A5=110. 66684212 | D5=179. 95389
464 | R6=1. 09047312 | A6=110. 7389735 | D6=59. 49682761 | R7=1. 09048441 | A7=110. 7
4589428 | D7=-59. 58466865 | R8=1. 09708418 | A8=111. 80362486 | D8=58. 79316166 | R
9=1. 09704698 | A9=111. 81097894 | D9=-58. 86690786 | R10=1. 10932551 | A10=115. 48
57751 | D10=-179. 99594246 | | Versi on=x86-Wi n32-G03RevB. 03 | HF=-192. 0108258 |
MP2=-192. 6836966 | RMSD=6. 643e-009 | RMSF=9. 671e-006 | Di pol e=-0. 9943227, 0. 0
00136, 0. 3508566 | PG=C01 [X(C3H601)] | | @

```

Reactant Complex:

1\1\GI NC-NODE18\FOpt\RMP2-FC\6-311+G(2d,p)\C5H9O2(1-)\MAY04\11-Dec-2009\0\#\#P MP2/6-311+G(2d,p) opt freq\Reactant Complex OHCH2--Me-CH2CH0\ -1, 1\C, -0.6390284978, 1.5288968053, -0.4703313465\H, -0.3425456959, 2.4785426646, -0.01947811\H, -1.2587126502, 1.7468579073, -1.3458161453\H, 0.2696754395, 1.0083861802, -0.7774621257\C, -1.4022275792, 0.6704113525, 0.5450504686\H, -2.2928115285, 1.176095224, 0.9296158062\H, -0.7134484393, 0.4232751134, 1.3580029358\C, 2.9693375141, 0.5658574444, 0.2028719824\H, 2.5364199244, 1.3283905022, 0.8455089251\H, 3.9524897883, 0.7349232863, -0.2252172485\C, -1.8172910593, -0.6264020857, -0.0842773548\O, -2.9844158452, -0.975015699, -0.2301490883\H, -0.9783269921, -1.2558259326, -0.4248358947\C, 2.3126743698, -0.6235761713, -0.0410588452\O, 1.1604303676, -1.0090750452, 0.3657282754\H, 2.8795996164, -1.3244960153, -0.7003601461\Version=AM64L-G03RevD.01\State=1-A\HF=-344.3823628\MP2=-345.5926272\RMSD=6.376e-09\RMSF=4.273e-05\Thermal=0.\Di pol e=-1.6273233, 1.0565204, -0.2407923\PG=C01 [X(C5H9O2)]\@\

Transition State:

1\1\GI NC-NODE15\FTS\RMP2-FC\6-311+G(2d,p)\C5H9O2(1-)\MAY04\15-Oct-2009\0\#\#P MP2/6-311+G(2d,p) Opt=(ts,noeigentest,calcfc) Freq\OCHHCH--Me--CHCHCHO\ -1, 1\C, -0.0462460271, -3.045748323, 0.0389327371\H, 0.4381306674, -3.9777736066, -0.2042675549\H, 0.3737917988, -2.3747697238, 0.770125951\H, -0.9653209984, -2.7712233671, -0.4503796257\C, -1.0685277737, -4.0306434608, 1.6255044429\H, -0.1987603385, -4.3071941677, 2.2152839907\H, -1.576073137, -4.836477474, 1.1011396886\C, 1.0154057801, -2.1591131716, -1.5821909754\H, 0.5176896608, -2.6709905098, -2.4021032442\H, 0.7744562965, -1.1077810569, -1.447201575\C, -1.8747651416, -2.9675915652, 2.0977059513\O, -1.5539799573, -2.0697657711, 2.9074287705\H, -2.866168467, -2.8855630438, 1.5880011969\C, 2.334821937, -2.5646612373, -1.2694120284\O, 2.8827567487, -3.6502370993, -1.5658657337\H, 2.8824231414, -1.866411602, -0.5925786816\Version=AM64L-G03RevD.01\State=1-A\HF=-344.279385\MP2=-345.5181933\RMSD=2.480e-09\RMSF=7.617e-06\Thermal=0.\Di pol e=-0.7361605, 0.0039501, -0.5314406\PG=C01 [X(C5H9O2)]\@\

O-Attack by MeF

Reactant Complex:

1\1\GI NC-NODE22\FOpt\RMP2-FC\6-311+G(2d,p)\C3H6F101(1-)\MAY04\11-Jan-2010\0\#\#p MP2/6-311+G(2d,p) Opt Freq\Reactant Complex Enolat-O--Me-F\ -1, 1\C, 1.9593266283, 1.0831585703, 0.1387201179\C, 1.8157651372, -0.2342385495, -0.2568018205\O, 1.0996240977, -1.1602758314, 0.2557552475\H, 1.4602560578, 1.4644944398, 1.0260339491\H, 2.6172878902, 1.7422949491, -0.4192721465\H, 2.40811048, -0.4934067246, -1.1695401189\C, -1.4938163696, -0.1702427938, 0.0307129831\H, -1.3599764409, -0.4591738669, 1.0680774367\H, -1.4149888681, -1.0380775693, -0.6160406879\H, -0.7643520692, 0.5844773092, -0.2476390172\F, -2.8026085435, 0.375166067, -0.1167179432\Version=AM64L-G03RevD.01\State=1-A\HF=-291.4526507\MP2=-292.3827186\RMSD=8.170e-09\RMSF=3.975e-05\Thermal=0.\Di pol e=-1.4505527, 0.2051428, -0.2495936\PG=C01 [X(C3H6F101)]\@\

Transition State:

1\1\GI NC-NODE11\FTS\RMP2-FC\6-311+G(2d,p)\C3H6F101(1-)\MAY04\26-Jul-2009\1\#\#P MP2/6-311+G(2d,p) Opt=(Z-Matrix,ts,noeigentest,calcfc) Freq\O-Angri ff von MeOH an Enolat - TS mit MP2/6-311+g(2d,p) (Lee)\ -1, 1\C\C, 1, R2\O, 1, R3, 2, A3\H, 1, R4, 2, A4, 3, D4, O\H, 2, R5, 1, A5, 3, D5, O\H, 2, R6, 1, A6, 3, D6, O\C, 3, R7, 1, A7, 2, D7, O\H, 7, R8, 3, A8, 1, D8, O\H, 7, R9, 3, A9, 1, D9, O\H, 7, R10, 3, A10, 1, D10, O\F, 7, R11, 8, A11, 3, D11, O\R2=1.36115071\R3=1.30475653\A3=127.54710677\R4=1.10506067\A4=116.601199\A5=119.37813955\A6=121.34583543\A7=111.36834531\A8=90.13291347\A9=92.33484612\A10=92.3347555\A11=88.72679691\A12=179.99998228\Version=AM64L-G03RevD.01\State=1-A\HF=-2

Chapter 3: Marcus-Analysis of Ambident Reactivity

91. 4074392\MP2=-292. 3508514\RMSD=5. 508e-09\RMSF=5. 945e-05\Thermal =0. \Di pol e=-0. 1047826, -0. 0000404, 1. 4020384\PG=C01 [X(C3H6F101)]\@

Product Complex:

1\1\GINC-NODE27\FOpt\RMP2-FC\6-311+G(2d,p)\C3H6F101(1-)\MAY04\11-Jan-2010\0\#p MP2/6-311+G(2d,p) Opt Freq\Product Complex Enolat-0-Me---F\ -1, 1\C, -0. 7782045874, -0. 3409861802, 0. 0235514155\C, -2. 0155426314, -0. 8625287142, 0. 0121404622\O, -0. 6089850744, 1. 0131562258, 0. 0513221914\C, 0. 7691965409, 1. 4400713028, 0. 0907783746\H, 0. 1595112618, -0. 9225117653, 0. 0084530411\H, -2. 9015353214, -0. 2362887528, 0. 0271179824\H, -2. 1273873772, -1. 9379899374, -0. 0147780731\H, 0. 9329079718, 2. 1096721867, -0. 7584221086\H, 0. 9201363475, 2. 0026201071, 1. 0170565995\H, 1. 4435155716, 0. 5677655439, 0. 0456066269\F, 2. 0087672982, -1. 2057250163, -0. 0139745119\Version=AM64L-G03RevD. 01\State=1-A\HF=-291. 4484706\MP2=-292. 3825809\RMSD=3. 784e-09\RMSF=2. 841e-05\Thermal =0. \Di pol e=-1. 9225977, 1. 7085942, 0. 0749482\PG=C01 [X(C3H6F101)]\@

C-Attack by MeF

Transition State:

1\1\GINC-NODE11\FTS\RMP2-FC\6-311+G(2d,p)\C3H6F101(1-)\MAY04\26-Jul -2009\1\#p MP2/6-311+G(2d,p) Opt=(Z-Matrix, ts, noeigentest, calcfc) Freq\C-Angriff von MeF an Enolat - TS mit MP2/6-311+G(2d,p)\ -1, 1\C\C, 1, R2\O, 1, R3, 2, A3\H, 1, R4, 2, A4, 3, D4, O\H, 2, R5, 1, A5, 3, D5, O\H, 2, R6, 1, A6, 3, D6, O\C, 2, R7, 1, A7, 3, D7, O\H, 7, R8, 2, A8, 1, D8, O\H, 7, R9, 2, A9, 1, D9, O\H, 7, R10, 2, A10, 1, D10, O\F, 7, R11, 10, A11, 2, D11, O\R2=1. 41280127\R3=1. 25057454\A3=127. 88166978\R4=1. 11810062\A4=113. 93750479\D4=-173. 26804656\R5=1. 08755566\A5=117. 3474584\D5=-19. 36537788\R6=1. 08767782\A6=116. 55942442\D6=-164. 27979389\R7=2. 13128132\A7=99. 90538645\D7=87. 57286957\R8=1. 07502272\A8=86. 23798787\D8=-178. 66683803\R9=1. 07614287\A9=88. 10305176\D9=-57. 62095905\R10=1. 07514072\A10=91. 77389726\D10=61. 90560922\R11=1. 82049511\A11=91. 43828374\D11=-177. 8582872\Version=AM64L-G03RevD. 01\State=1-A\HF=-291. 3985126\MP2=-292. 3479248\RMSD=6. 031e-09\RMSF=9. 228e-05\Thermal =0. \Di pol e=-0. 7335215, -1. 2041798, 0. 320965\PG=C01 [X(C3H6F101)]\@

Product Complex:

1\1\GINC-NODE9\FOpt\RMP2-FC\6-311+G(2d,p)\C3H6F101(1-)\MAY04\16-Dec-2009\0\#p MP2/6-311+G(2d,p) Opt Freq\Product Complex Enolat-C-Me---F\ -1, 1\C, 0. 7993655825, -0. 5254214568, 0. 0128633168\C, 0. 4553985671, 0. 843223215, 0. 5427147368\O, 1. 9529767936, -0. 8773484274, -0. 2291405143\H, -0. 0934351734, -1. 1646323529, -0. 1412968917\H, 1. 3742067989, 1. 4260423688, 0. 6649376374\H, -0. 0103458484, 0. 6879042586, 1. 5221242964\F, -2. 0220688764, -1. 0568056155, 0. 0540010188\C, -0. 577128977, 1. 5122706172, -0. 3720611774\H, -0. 9011912822, 2. 4717230782, 0. 0418086676\H, -0. 1518138973, 1. 6984126949, -1. 3637292941\H, -1. 4289776875, 0. 8235006199, -0. 4511787963\Version=AM64L-G03RevD. 01\State=1-A\HF=-291. 4853958\MP2=-292. 4190725\RMSD=6. 788e-09\RMSF=1. 180e-05\Thermal =0. \Di pol e=1. 8325021, 1. 9309155, 0. 1735042\PG=C01 [X(C3H6F101)]\@

O-Attack by MeCl

Reactant Complex:

1\1\GINC-NODE10\FOpt\RMP2-FC\6-311+G(2d,p)\C3H6Cl101(1-)\MAY04\11-Jan-2010\0\#p MP2/6-311+G(2d,p) Opt Freq\Reactant Complex Enolat-0---Me-Cl\ -1, 1\C, -2. 3780152535, 1. 168281502, 0. 1556069816\C, -2. 3819845641, -0. 1447787293, -0. 2792634852\O, -1. 7935085774, -1. 1638156388, 0. 2203926633\H, -1. 8751839381, 1. 4579020044, 1. 0750542568\H, -2. 9449308571, 1. 9157209536, -0. 3908862157\H, -2. 9721274251, -0. 3041550552, -1. 2156698757\C, 0. 8438053211, -0. 35773222, 0. 0849736629\H, 0. 182190279, 0. 4583638082, -0. 1855945243\H, 0. 7333560217, -1. 1941524098, -0. 5931013149\H, 0. 6720536154, -0. 6676480018, 1

Chapter 3: Marcus-Analysis of Ambident Reactivity

. 107666787\CI, 2. 5717023781, 0. 2339147865, -0. 0397149357\\Version=AM64L-G03RevD. 01\State=1-A\HF=-651. 5042555\MP2=-652. 362523\RMSD=9. 505e-09\RMSF=5. 853e-05\Thermal=0. \Di pol e=2. 241982, 0. 1883958, -0. 2203991\PG=C01 [X(C3H6Cl 101)]\@

Transition State:

1\1\GINC-NODE17\FTS\RMP2-FC\6-311+G(2d,p)\C3H6Cl 101(1-)\MAY04\26-Jul -2009\1\#\P MP2/6-311+G(2d,p) Opt=(Z-Matrix, ts, noigentest, cal cfc) Freq\ \C-Angri ff von MeCl an Enolat - TS mit MP2/6-311+G(2d,p) (Lee)\-1, 1\C\, 1, R2\0, 1, R3, 2, A3\H, 1, R4, 2, A4, 3, D4, 0\H, 2, R5, 1, A5, 3, D5, 0\H, 2, R6, 1, A6, 3, D6, 0\C, 3, R7, 1, A7, 2, D7, 0\H, 7, R8, 3, A8, 1, D8, 0\H, 7, R9, 3, A9, 1, D9, 0\H, 7, R10, 3, A10, 1, D10, 0\CI, 7, R11, 8, A11, 3, D11, 0\\R2=1. 36506221\R3=1. 29941408\A3=128. 30403811\R4=1. 10995096\A4=115. 49939913\D4=180. 0005857\R5=1. 08396815\A5=119. 41484599\D5=179. 99668114\R6=1. 08508132\A6=121. 29601045\D6=-0. 00091135\R7=2. 02208558\A7=110. 62027748\D7=-180. 03601181\R8=1. 07323529\A8=85. 345329\D8=-180. 0415075\R9=1. 07355784\A9=86. 95670366\D9=-60. 03504857\R10=1. 07356043\A10=86. 95644771\D10=59. 95195138\R11=2. 17221611\A11=93. 72370036\D11=-180. 00008474\\Version=AM64L-G03RevD. 01\State=1-A\HF=-651. 4868436\MP2=-652. 3471711\RMSD=5. 943e-09\RMSF=2. 355e-06\Thermal=0. \Di pol e=-0. 1946041, 0. 0000585, -0. 0005833\PG=C01 [X(C3H6Cl 101)]\@

Product Complex:

1\1\GINC-NODE16\F0pt\RMP2-FC\6-311+G(2d,p)\C3H6Cl 101(1-)\MAY04\16-Dec-2009\0\#\p MP2/6-311+G(2d,p) Opt Freq\\Product Complex Enolat0-Me---C I\\-1, 1\C, -1. 2147918271, -0. 5216851654, 0. 0226310852\C, -2. 1379599449, -1. 490771249, 0. 0559690841\0, -1. 5699298041, 0. 7793867441, -0. 1817557722\H, -0. 1428190919, -0. 7067600196, 0. 1214993203\H, -1. 8148859157, -2. 5155782923, 0. 1745487362\H, -3. 1941307506, -1. 2715723474, -0. 0513229764\CI, 2. 4475185616, -0. 3345291264, 0. 0194971935\C, -0. 518415795, 1. 7140690203, 0. 1124298902\H, -0. 7530743804, 2. 6239736788, -0. 4399238522\H, -0. 5060693351, 1. 9312897413, 1. 1846409132\H, 0. 4568882834, 1. 3170750155, -0. 1791196218\\Version=AM64L-G03RevD. 01\State=1-A\HF=-651. 5529473\MP2=-652. 3956365\RMSD=6. 141e-09\RMSF=2. 707e-05\Thermal=0. \Di pol e=-3. 0940546, 0. 8649864, 0. 1233502\PG=C01 [X(C3H6Cl 101)]\@

C-Attack by MeCl

Transition State:

1\1\GINC-NODE11\FTS\RMP2-FC\6-311+G(2d,p)\C3H6Cl 101(1-)\MAY04\26-Jul -2009\1\#\P MP2/6-311+G(2d,p) Opt=(Z-Matrix, ts, noigentest, cal cfc) Freq\ \C-Angri ff von MeCl an Enolat - TS mit MP2/6-311+G(2d,p)\-1, 1\C\, 1, R2\0, 1, R3, 2, A3\H, 1, R4, 2, A4, 3, D4, 0\H, 2, R5, 1, A5, 3, D5, 0\H, 2, R6, 1, A6, 3, D6, 0\C, 2, R7, 1, A7, 3, D7, 0\H, 7, R8, 2, A8, 1, D8, 0\H, 7, R9, 2, A9, 1, D9, 0\H, 7, R10, 2, A10, 1, D10, 0\CI, 7, R11, 8, A11, 2, D11, 0\\R2=1. 40581861\R3=1. 25577689\A3=128. 1100309\R4=1. 1186209\A4=113. 79841052\D4=185. 44995992\R5=1. 08690049\A5=118. 74935907\D5=-16. 50612092\R6=1. 08684767\A6=117. 84321351\D6=-169. 04968785\R7=2. 3252883\A7=95. 81788081\D7=84. 28570812\R8=1. 07431697\A8=81. 90482283\D8=183. 03955685\R9=1. 07633803\A9=82. 3566202\D9=-55. 25677688\R10=1. 07491245\A10=87. 84556074\D10=63. 85730347\R11=2. 15488521\A11=95. 00864946\D11=182. 7780071\\Version=AM64L-G03RevD. 01\State=1-A\HF=-651. 4799778\MP2=-652. 3459791\RMSD=6. 335e-09\RMSF=7. 674e-06\Thermal=0. \Di pol e=-0. 7573146, -0. 0531852, 0. 8840007\PG=C01 [X(C3H6Cl 101)]\@

Product Complex:

1\1\GINC-NODE17\F0pt\RMP2-FC\6-311+G(2d,p)\C3H6Cl 101(1-)\MAY04\16-Dec-2009\0\#\p MP2/6-311+G(2d,p) Opt Freq\\Product Complex Enolat-C-Me---C I\\-1, 1\C, 1. 2160804394, -0. 7040773016, -0. 0722063077\C, 1. 0868666906, 0. 6268354013, 0. 6061908602\0, 2. 2674179792, -1. 3266200295, -0. 1719095027\H, 0. 2762795284, -1. 0922914983, -0. 5005298435\H, 2. 0365673405, 0. 8713239435, 1. 0896934584\H, 0. 2862279046, 0. 5333629813, 1. 3459688702\CI, -2. 2879766153, -0. 2286455753, 0. 3242173048\C, 0. 6628645033, 1. 6917117812, -0. 4123196458\H, 0.

5482244456, 2. 6612231458, 0. 0773992222\H, 1. 4059894941, 1. 7947829072, -1. 2090273314\H, -0. 3036387103, 1. 4134062443, -0. 8361010847\Version=AM64L-G03RevD. 01\State=1-A\HF=-651. 5914057\MP2=-652. 4353177\RMSD=5. 497e-09\RMSF=3. 022e-05\Thermal=0. \Di pol e=2. 6935192, 1. 1226747, -0. 2178916\PG=C01 [X(C3H6Cl 101)]\@

O-Attack by MeBr

Reactant Complex:

1\1\GINC-NODE21\F0pt\RMP2-FC\6-311+G(2d,p)\C3H6Br101(1-)\MAY04\11-Jan-2010\0\#P MP2/6-311+G(2d,p) Opt Freq\Reactant Complex Enolat-0---Me-Br\ -1, 1\C, 0. 0315451567, -0. 0263527703, -0. 0003658033\C, -0. 0241721976, -0. 0168725222, 1. 381348141\O, 0. 9338138444, 0. 0057166435, 2. 2281267032\H, 0. 9791568382, 0. 0507022065, -0. 5277804902\H, -0. 8893823246, -0. 0438460483, -0. 5748731001\H, -1. 0642442754, -0. 0608301719, 1. 7887457644\C, 2. 252013964, -2. 3011680223, 1. 5593505053\H, 1. 4697339042, -2. 1026550197, 0. 8345796026\H, 1. 8500840744, -2. 4563021187, 2. 5516494429\H, 2. 9970376508, -1. 5169307777, 1. 5566209497\Br, 3. 1593939976, -3. 9809957977, 1. 0285745176\Version=AM64L-G03RevD. 01\State=1-A\HF=-2764. 3600897\MP2=-2765. 194288\RMSD=9. 643e-09\RMSF=3. 971e-05\Thermal=0. \Di pol e=1. 8892168, -3. 0024525, -0. 1572139\PG=C01 [X(C3H6Br101)]\@

Transition State:

1\1\GINC-NODE26\FTS\RMP2-FC\6-311+G(2d,p)\C3H6Br101(1-)\MAY04\26-Jul -2009\1\#P MP2/6-311+G(2d,p) Opt=(Z-Matrix, ts, noeigentest, cal cfc) Freq\ \O-Angri ff von MeBr an Enolat - TS mit MP2/6-311+G(2d,p) (Lee)\ -1, 1\C\C, 1, R2\O, 1, R3, 2, A3\H, 1, R4, 2, A4, 3, D4, O\H, 2, R5, 1, A5, 3, D5, O\H, 2, R6, 1, A6, 3, D6, O\C, 3, R7, 1, A7, 2, D7, O\H, 7, R8, 3, A8, 1, D8, O\H, 7, R9, 3, A9, 1, D9, O\H, 7, R10, 3, A10, 1, D10, O\Br, 7, R11, 8, A11, 3, D11, O\R2=1. 36630162\R3=1. 29776177\A3=128. 49204245\R4=1. 11131749\A4=115. 21056993\D4=179. 99897589\R5=1. 08414221\A5=119. 42352578\D5=180. 00733827\R6=1. 08520094\A6=121. 28454895\D6=0. 00239651\R7=2. 07786712\A7=110. 45980281\D7=-179. 92585808\R8=1. 07367662\A8=83. 89961533\D8=-179. 86022758\R9=1. 07392464\A9=85. 38627164\D9=-59. 83464262\R10=1. 07389905\A10=85. 38599597\D10=60. 12174934\R11=2. 2818044\A11=95. 2166205\D11=-179. 99891147\Version=AM64L-G03RevD. 01\State=1-A\HF=-2764. 3488809\MP2=-2765. 1834902\RMSD=9. 792e-09\RMSF=6. 043e-05\Thermal=0. \Di pol e=-0. 423291, 0. 0015938, -1. 6198124\PG=C01 [X(C3H6Br101)]\@

Product Complex:

1\1\GINC-NODE13\F0pt\RMP2-FC\6-311+G(2d,p)\C3H6Br101(1-)\MAY04\12-Jan-2010\0\#p opt freq mp2/6-311+g(2d,p)\Product Complex Enolat-0-Me---Br Anordnung II\ -1, 1\C, -1. 2401100753, -0. 5165816725, 0. 0243046841\C, -2. 1615817273, -1. 4866909061, 0. 0575150568\O, -1. 591265776, 0. 7839695963, -0. 1867857461\H, -0. 170334977, -0. 7045349419, 0. 1321611435\H, -1. 8371162613, -2. 5100576336, 0. 1840275332\H, -3. 2171983685, -1. 2691002448, -0. 0567310391\C, -0. 535875909, 1. 7146112874, 0. 1003871498\H, -0. 8059702855, 2. 6456037367, -0. 3972668345\H, -0. 4671171586, 1. 8815992594, 1. 1791019302\H, 0. 4270346882, 1. 3451713667, -0. 2582170489\Br, 2. 6518658502, -0. 3590918475, 0. 0605971709\Version=AM64L-G03RevD. 01\State=1-A\HF=-2764. 422532\MP2=-2765. 2381113\RMSD=8. 362e-09\RMSF=5. 675e-05\Thermal=0. \Di pol e=-2. 1395586, 0. 719774, 0. 0937303\PG=C01 [X(C3H6Br101)]\@

C-Attack by MeBr

Transition State:

1\1\GINC-NODE19\FTS\RMP2-FC\6-311+G(2d,p)\C3H6Br101(1-)\MAY04\26-Jul -2009\1\#P MP2/6-311+G(2d,p) Opt=(Z-Matrix, ts, noeigentest, cal cfc) Freq\ \C-Angri ff von MeBr an Enolat - TS mit MP2/6-311+G(2d,p)\ -1, 1\C\C, 1, R2\O, 1, R3, 2, A3\H, 1, R4, 2, A4, 3, D4, O\H, 2, R5, 1, A5, 3, D5, O\H, 2, R6, 1, A6, 3, D6, O\C, 2, R7, 1, A7, 3, D7, O\H, 7, R8, 2, A8, 1, D8, O\H, 7, R9, 2, A9, 1, D9, O\H, 7, R10, 2, A10, 1, D10, O\Br, 7, R11, 8, A11, 2, D11, O\R2=1. 40391041\R3=1. 25737274\A3=128. 1

7687643\R4=1. 11868233\A4=113. 77424877\D4=184. 9845929\R5=1. 08676435\A5=119. 1146679\D5=-15. 69335039\R6=1. 08666999\A6=118. 18513269\D6=-170. 59799234\R7=2. 39625754\A7=94. 27441132\D7=82. 39131508\R8=1. 07505648\A8=80. 7091009\D8=183. 97049934\R9=1. 07733698\A9=80. 33887084\D9=-54. 06674775\R10=1. 07566954\A10=86. 4689583\D10=64. 96035349\R11=2. 26325599\A11=96. 53048555\D11=183. 03457571\\Version=AM64L-G03RevD. 01\State=1-A\HF=-2764. 3430468\MP2=-2765. 1832291\RMSD=6. 145e-09\RMSF=2. 924e-05\Thermal =0. \Di pol e=-0. 5925444, 1. 4270656, 1. 3415297\PG=C01 [X(C3H6Br101)]\@

Product Complex:

1\1\GINC-NODE16\F0pt\RMP2-FC\6-311+G(2d,p)\C3H6Br101(1-)\MAY04\11-Jan-2010\0\#p MP2/6-311+(2d,p) Opt Freq\\Product Complex Enolat-C-Me---Br\\-1,1\C, 1. 2462024466, -0. 7003642051, -0. 0765545785\C, 1. 0909934625, 0. 6250378694, 0. 6069454622\O, 2. 3069851838, -1. 3051717428, -0. 1752763069\H, 0. 3168614328, -1. 1040978664, -0. 5150729904\H, 2. 0286812384, 0. 8748961521, 1. 1102990543\H, 0. 278747753, 0. 5232305092, 1. 3331794968\C, 0. 6827707914, 1. 692993174, -0. 414898509\H, 0. 5457747742, 2. 6573705465, 0. 078667565\H, 1. 4457417554, 1. 8079784232, -1. 1906507397\H, -0. 2691687003, 1. 414167633, -0. 8702704546\Br, -2. 4786871376, -0. 2450284932, 0. 3550080008\\Version=AM64L-G03RevD. 01\State=1-A\HF=-2764. 4606853\MP2=-2765. 2779131\RMSD=7. 616e-09\RMSF=8. 867e-06\Thermal =0. \Di pol e=1. 7588089, 1. 0101157, -0. 1360042\PG=C01 [X(C3H6Br101)]\@

O-Attack by MeOH

Reactant Complex:

1\1\GINC-NODE21\F0pt\RMP2-FC\6-311+G(2d,p)\C3H7O2(1-)\MAY04\11-Jan-2010\0\#p MP2/6-311+G(2d,p) Opt Freq\\Reactant Complex Enolat-O---Me-OH\\-1,1\C, -1. 6359543287, -0. 2721813034, 0. 2351065056\C, -1. 703424228, 1. 0138129102, -0. 243073407\O, -0. 7051456721, -1. 1543678985, 0. 0854829734\H, -2. 5124226261, -0. 5889575797, 0. 8407184208\H, -2. 5725408532, 1. 6214932133, -0. 0134273566\H, -0. 9145731152, 1. 4312379056, -0. 8615651942\O, 1. 6222520452, -0. 2680761569, -0. 6550430937\H, 0. 6995615088, -0. 639142764, -0. 4588910541\C, 1. 9561395067, 0. 4927752136, 0. 4829121733\H, 2. 8370384674, 1. 1015093291, 0. 2521337717\H, 1. 1388335172, 1. 1615913957, 0. 7794644233\H, 2. 200818778, -0. 1397142651, 1. 3491538374\\Version=AM64L-G03RevD. 01\State=1-A\HF=-267. 4591099\MP2=-268. 3880418\RMSD=5. 764e-09\RMSF=2. 888e-05\Thermal =0. \Di pol e=0. 6696194, 0. 6769788, 0. 6119361\PG=C01 [X(C3H7O2)]\@

Transition State:

1\1\GINC-NODE28\FTS\RMP2-FC\6-311+G(2d,p)\C3H7O2(1-)\MAY04\25-Jul -2009\1\#p MP2/6-311+G(2d,p) Opt=(Z-Matrix,ts,noeigentest,calcfc) Freq\\O-Angri ff von MeOH an Enolat - TS mit MP2/6-311+g(2d,p) (Lee)\-1,1\C\C, 1, R2\O, 1, R3, 2, A3\H, 1, R4, 2, A4, 3, D4, O\H, 2, R5, 1, A5, 3, D5, O\H, 2, R6, 1, A6, 3, D6, O\C, 3, R7, 1, A7, 2, D7, O\H, 7, R8, 3, A8, 1, D8, O\H, 7, R9, 3, A9, 1, D9, O\H, 7, R10, 3, A10, 1, D10, O\O, 7, R11, 8, A11, 2, D11, O\H, 11, R12, 7, A12, 1, D12, O\\R2=1. 35829475\R3=1. 31047276\A3=126. 96471377\R4=1. 10200576\A4=117. 30856156\D4=-180. 06884566\R5=1. 08317369\A5=119. 34303867\D5=-179. 78667304\R6=1. 08448225\A6=121. 38346678\D6=-0. 02752167\R7=1. 77793395\A7=111. 50334299\D7=-179. 08908561\R8=1. 07425422\A8=92. 85792971\D8=181. 01263874\R9=1. 07577755\A9=96. 43282344\D9=-59. 5027538\R10=1. 07539456\A10=95. 43277494\D10=60. 50941457\R11=2. 03018123\A11=87. 46844985\D11=-177. 44320438\R12=0. 96763865\A12=106. 45202842\D12=126. 54524566\\Version=AM64L-G03RevD. 01\State=1-A\HF=-267. 3691198\MP2=-268. 311012\RMSD=6. 421e-09\RMSF=3. 235e-06\Thermal =0. \Di pol e=0. 2062412, 0. 4922742, 1. 6957554\PG=C01 [X(C3H7O2)]\@

Product Complex:

1\1\GINC-NODE23\F0pt\RMP2-FC\6-311+G(2d,p)\C3H7O2(1-)\MAY04\11-Jan-2010\0\#p MP2/6-311+G(2d,p) Opt Freq\\Product Complex Enolat-O---Me-OH\\-1,1\C, 0. 7672674283, -0. 3917794704, 0. 0125215071\C, 1. 9571472798, -1. 0132246015, 0. 0406984943\O, 0. 7088666838, 0. 9663053895, -0. 1104264795\H, -0. 2112

588095, -0.900561325, 0.0509161221\H, 1.9797771298, -2.0927082818, 0.1065087038\H, 2.8915940765, -0.4641302588, -0.0124619866\O, -2.149267368, -1.0284672449, 0.0216263974\H, -2.8052056012, -1.6553341595, -0.3114371575\C, -0.6089631405, 1.5157024068, 0.0922146443\H, -0.7104199089, 2.351238487, -0.6043962053\H, -1.3838653999, 0.7523376887, -0.0764228433\H, -0.6786113703, 1.8969733698, 1.1164618034\\Version=AM64L-G03RevD.01\State=1-A\HF=-267.407922\MP2=-268.3393858\RMSD=5.673e-09\RMSF=6.836e-05\Thermal=0.\Di pol e=1.8431453, 1.239719, -0.1345339\PG=C01 [X(C3H7O2)]\@

C-Attack by MeOH

Transition State:

1\1\GINC-NODE21\FTS\RMP2-FC\6-311+G(2d,p)\C3H7O2(1-)\MAY04\25-Jul-2009
1\1\#p MP2/6-311+G(2d,p) Opt=(Z-Matrix,ts,noeigentest,calcfc) Freq\C-
Angriff von MeOH an Enolat - TS mit MP2/6-311+G(2d,p)\-1,1\C\C,1,R2\O
,1,R3,2,A3\H,1,R4,2,A4,3,D4,O\H,2,R5,1,A5,3,D5,O\H,2,R6,1,A6,3,D6,O\C,
2,R7,1,A7,3,D7,O\H,7,R8,2,A8,1,D8,O\H,7,R9,2,A9,1,D9,O\H,7,R10,2,A10,1
,D10,O\O,7,R11,8,A11,2,D11,O\H,11,R12,7,A12,1,D12,O\O\R2=1.41777993\R3=
1.24882745\A3=127.53100814\R4=1.1173028\A4=114.1336771\D4=-172.5406827
6\R5=1.0874924\A5=116.77015649\D5=-21.13504265\R6=1.08780777\A6=116.04
511267\D6=-163.43751253\R7=2.04210976\A7=101.37384862\D7=87.07101892\R
8=1.07564318\A8=90.55110123\D8=-180.32316717\R9=1.07706297\A9=90.40663
041\D9=-59.97217748\R10=1.07522201\A10=94.78550159\D10=60.27751655\R11
=1.98377888\A11=84.01272808\D11=-178.2829871\R12=0.96835422\A12=103.04
208707\D12=-14.25909265\\Version=AM64L-G03RevD.01\State=1-A\HF=-267.36
17698\MP2=-268.3118658\RMSD=9.162e-09\RMSF=1.620e-05\Thermal=0.\Di pol e
=-0.5711239, -1.3532489, -0.399006\PG=C01 [X(C3H7O2)]\@

Product Complex:

1\1\GINC-NODE13\FOpt\RMP2-FC\6-311+G(2d,p)\C3H7O2(1-)\MAY04\12-Jan-201
0\O\#p MP2/6-311+G(2d,p) Opt Freq\Product Complex EnolatC-Me---OH\-\
1,1\C,0.7897885336, -0.5740539916, -0.0103865896\C,0.499680782, 0.7902361
168, 0.5581828256\O, 1.9320022868, -0.9769606346, -0.2287721049\H, -0.12192
1567, -1.1697746134, -0.2132573653\H, 1.4454788546, 1.3067959586, 0.7531061
637\H, -0.03671486, 0.6272211211, 1.4986664619\C, -0.4306835145, 1.56440373
48, -0.3834813912\H, -0.6886106494, 2.5384973426, 0.0430330323\H, 0.0520464
682, 1.7362883938, -1.3514759193\H, -1.3393612689, 0.9625366542, -0.5134521
692\O, -2.0897935772, -0.9126120036, 0.0592262183\H, -2.9193354883, -1.4026
740787, 0.1384148378\\Version=AM64L-G03RevD.01\State=1-A\HF=-267.445298
1\MP2=-268.3767802\RMSD=5.364e-09\RMSF=2.729e-05\Thermal=0.\Di pol e=1.5
115191, 1.5169497, 0.1889268\PG=C01 [X(C3H7O2)]\@

O-Attack by MeOMe

Reactant Complex:

1\1\GINC-NODE27\FOpt\RMP2-FC\6-311+G(2d,p)\C4H9O2(1-)\MAY04\12-Jan-201
0\O\#p MP2/6-311+G(2d,p) Opt Freq\Reactant Complex EnolatO---Me-OMe
\-1,1\C,2.0573576778, -0.436346208, 0.1439573429\C,2.5977561425, 0.82502
85724, -0.0167642674\O, 1.1750249495, -1.0350812275, -0.5639330937\H, 2.453
1106232, -0.9836633937, 1.0350482937\H, 3.3452530145, 1.1827973527, 0.68478
96272\H, 2.318113751, 1.4555231336, -0.8570054421\O, -2.2898952296, 0.37578
26483, -0.2238571164\C, -2.0256270397, -0.9564050727, 0.2022045312\H, -2.83
84024783, -1.5798961381, -0.1751071856\H, -1.0567449454, -1.3031051227, -0.
1728417688\H, -2.0134475969, -1.0136188726, 1.3006490465\C, -1.1644363015,
1.2034241945, 0.0771318086\H, -0.245286613, 0.785257377, -0.3419837326\H, -
1.3743960988, 2.1870557066, -0.3451300933\H, -1.0359708552, 1.2990330502, 1
.1637620498\\Version=AM64L-G03RevD.01\State=1-A\HF=-306.4775086\MP2=-3
07.5578279\RMSD=5.373e-09\RMSF=1.870e-05\Thermal=0.\Di pol e=-2.0469896,
0.322222, 0.7133175\PG=C01 [X(C4H9O2)]\@

Transition State:

1\1\GI NC-NODE27\FOpt\RMP2-FC\6-311+G(2d, p)\C4H9O2(1-)\MAY04\12-Jan-2010\0\#p MP2/6-311+G(2d, p) Opt Freq\Reactant Complex Enolat-O--Me-OMe\ -1, 1\C, 2. 0573576778, -0. 436346208, 0. 1439573429\C, 2. 5977561425, 0. 8250285724, -0. 0167642674\O, 1. 1750249495, -1. 0350812275, -0. 5639330937\H, 2. 4531106232, -0. 9836633937, 1. 0350482937\H, 3. 3452530145, 1. 1827973527, 0. 6847896272\H, 2. 318113751, 1. 4555231336, -0. 8570054421\O, -2. 2898952296, 0. 3757826483, -0. 2238571164\C, -2. 0256270397, -0. 9564050727, 0. 2022045312\H, -2. 8384024783, -1. 5798961381, -0. 1751071856\H, -1. 0567449454, -1. 3031051227, -0. 1728417688\H, -2. 0134475969, -1. 0136188726, 1. 3006490465\C, -1. 1644363015, 1. 2034241945, 0. 0771318086\H, -0. 245286613, 0. 785257377, -0. 3419837326\H, -1. 3743960988, 2. 1870557066, -0. 3451300933\H, -1. 0359708552, 1. 2990330502, 1. 1637620498\Versi on=AM64L-G03RevD. 01\State=1-A\HF=-306. 4775086\MP2=-307. 5578279\RMSD=5. 373e-09\RMSF=1. 870e-05\Thermal =0. \Di pol e=-2. 0469896, 0. 322222, 0. 7133175\PG=C01 [X(C4H9O2)]\@

Product Complex:

1\1\GI NC-NODE16\FOpt\RMP2-FC\6-311+G(2d, p)\C4H9O2(1-)\MAY04\12-Jan-2010\0\#p MP2/6-311+G(2d, p) Opt Freq\Product Complex Enolat-O-Me--OMe\ -1, 1\C, 1. 1748639599, -0. 575669724, 0. 0174881503\C, 1. 9924642147, -1. 6395158195, 0. 0388232111\O, 1. 6862812741, 0. 6789657975, -0. 1515026295\H, 0. 0772994777, -0. 6253408332, 0. 0978655067\H, 1. 5617272479, -2. 6268874126, 0. 1364711996\H, 3. 0683817298, -1. 5356976592, -0. 0539598336\O, -1. 7648327831, 0. 0706233065, 0. 0745429952\C, 0. 7355276347, 1. 732855277, 0. 0971117354\H, 0. 9974659438, 2. 5524103687, -0. 5752088597\H, -0. 2921367616, 1. 3849526067, -0. 0710621423\H, 0. 8424971012, 2. 0730673735, 1. 1324297049\C, -3. 0165244245, -0. 425727033, -0. 155580823\H, -3. 6596511298, -0. 4915813895, 0. 7580274495\H, -3. 6234623575, 0. 1755609521, -0. 8788678536\H, -3. 0289671272, -1. 4621948111, -0. 5788478109\Versi on=AM64L-G03RevD. 01\State=1-A\HF=-306. 443959\MP2=-307. 5245466\RMSD=8. 116e-09\RMSF=2. 465e-06\Thermal =0. \Di pol e=1. 7469121, 0. 3716765, -0. 0205039\PG=C01 [X(C4H9O2)]\@

C-Attack by MeOMe

Transition State:

1\1\GI NC-NODE24\FOpt\RMP2-FC\6-311+G(2d, p)\C4H9O2(1-)\MAY04\12-Jan-2010\0\#p MP2/6-311+G(2d, p) Opt=(ts, noeigentest, cal cfc) Freq\C-Angri ff des Enolats an MeOMe\ -1, 1\C, 2. 0805258072, -0. 2188824455, 0. 3815624055\C, 1. 5769776029, 1. 0457701265, -0. 0169943853\O, 2. 3725135345, -1. 1855589665, -0. 3520355038\H, 2. 0948881515, -0. 3773619309, 1. 4874269909\H, 1. 7491751285, 1. 3364859033, -1. 0508160629\H, 1. 6527919435, 1. 8433644055, 0. 719114581\C, -0. 4360453219, 0. 6997815085, -0. 0535484986\H, -0. 5994251109, 1. 7190594623, -0. 3619778215\H, -0. 298041904, -0. 0857097856, -0. 7819939932\H, -0. 4942490955, 0. 447901148, 0. 9942117467\O, -2. 3584402134, 0. 4957890342, -0. 1951186353\C, -2. 6276044149, -0. 8159998884, 0. 1396502133\H, -2. 3346831968, -1. 0726233429, 1. 1831714837\H, -3. 7046438623, -1. 0501320951, 0. 0568280296\H, -2. 0990140483, -1. 5511871334, -0. 5065125501\Versi on=AM64L-G03RevD. 01\State=1-A\HF=-306. 3959009\MP2=-307. 5006388\RMSD=3. 426e-09\RMSF=4. 437e-07\Thermal =0. \Di pol e=0. 3065708, 0. 397524, 0. 6100003\PG=C01 [X(C4H9O2)]\@

Product Complex:

1\1\GI NC-NODE24\FOpt\RMP2-FC\6-311+G(2d, p)\C4H9O2(1-)\MAY04\13-Jan-2010\0\#p MP2/6-311+G(2d, p) Opt Freq\Reactant Complex Enolat-C--Me-OMe\ -1, 1\C, -2. 1584694468, -0. 3367355841, -0. 3574210071\C, -2. 5424111937, 0. 7510010158, 0. 4034092814\O, -1. 1899516426, -1. 1524167229, -0. 1716954403\H, -2. 7889095345, -0. 4932973241, -1. 2670614666\H, -2. 0253378281, 1. 0055834349, 1. 3251566739\H, -3. 3981627548, 1. 3451312369, 0. 0974029318\O, 2. 2708361968, 0. 3060804474, -0. 3475338371\C, 2. 032904637, -0. 900113878, 0. 3717330916\H, 2. 8070264065, -1. 6080822371, 0. 0701768891\H, 2. 1138178867, -0. 7239933801, 1. 4543956697\H, 1. 0341039585, -1. 2928310449, 0. 1555788442\C, 1. 1936897664, 1. 2154699822, -0. 1226354923\H, 1. 1931375503, 1. 5591876025, 0. 9212520365\H, 1. 35896683, 2. 071276006, -0. 7782740371\H, 0. 2286631684, 0. 7475204455, -0. 3329551377\Versi on=AM64L-G03RevD. 01\State=1-A\HF=-306. 477796\MP2=-307. 557

Chapter 3: Marcus-Analysis of Ambident Reactivity

7248\RMSD=6.605e-09\RMSF=8.609e-06\Thermal=0.\Di pol e=2.0511647, 0.5361232, 0.1780326\PG=C01 [X(C4H9O2)]\@

O-Attack by MeSH

Reactant Complex:

1\1\GINC-NODE16\F0pt\RMP2-FC\6-311+G(2d,p)\C3H7O1S1(1-)\MAY04\12-Jan-2010\0\#p MP2/6-311+G(2d,p) Opt Freq\Reactant Complex Enolat-0---MeSH\ -1, 1\C, -1.6434787444, 0.0110384965, -0.2532814552\C, -2.9492021621, 0.376229558, -0.2077831949\O, -0.9903981318, -0.631554484, 0.7183435364\H, -1.0338292575, 0.2640852303, -1.1227443252\H, -3.3945335586, 0.8596705779, -1.0443955941\H, -3.564226456, 0.0888424179, 0.64951347\C, 1.9362112969, 1.164937709, 0.153265054\H, 2.7594101644, 1.3260011601, 0.8554929471\H, 2.1164717767, 1.7978818021, -0.720901475\H, 1.0180607642, 1.5158651876, 0.6347343842\S, 1.8008329179, -0.6070268669, -0.3200378636\H, -0.0052646396, -0.7273883162, 0.4129225662\Version=AM64L-G03RevD.01\State=1-A\HF=-590.1334839\MP2=-590.9861128\RMSD=5.967e-09\RMSF=1.508e-06\Thermal=0.\Di pol e=-1.1537188, 1.0603641, 0.015187\PG=C01 [X(C3H7O1S1)]\@

Transition State:

1\1\GINC-NODE26\FTS\RMP2-FC\6-311+G(2d,p)\C3H7O1S1(1-)\MAY04\06-Aug-2009\1\#P MP2/6-311+G(2d,p) Opt=(Z-Matrix, ts, noeigentest, calcf) Freq\O-Angri ff von MeSH an Enolat - TS mit MP2/6-311+G(2d,p) (Lee)\ -1, 1\C\C, 1, R2\O, 1, R3, 2, A3\H, 1, R4, 2, A4, 3, D4, O\H, 2, R5, 1, A5, 3, D5, O\H, 2, R6, 1, A6, 3, D6, O\C, 3, R7, 1, A7, 2, D7, O\H, 7, R8, 3, A8, 1, D8, O\H, 7, R9, 3, A9, 1, D9, O\H, 7, R10, 3, A10, 1, D10, O\S, 7, R11, 8, A11, 2, D11, O\H, 11, R12, 7, A12, 1, D12, O\ R2=1.36116611\R3=1.30642116\A3=127.58612468\R4=1.10566294\A4=116.37761428\D4=-180.01638391\R5=1.08362682\A5=119.35829644\D5=-180.03820262\R6=1.08470013\A6=121.35674551\D6=-0.03059622\R7=1.90914503\A7=110.63055644\D7=-180.79756227\R8=1.07322741\A8=89.35041615\D8=179.14564611\R9=1.07557884\A9=91.95420676\D9=-61.34196945\R10=1.07407174\A10=91.63148963\D10=58.34684216\R11=2.36513904\A11=89.82838526\D11=-179.54218489\R12=1.33551786\A12=94.24992645\D12=119.2014136\Version=AM64L-G03RevD.01\State=1-A\HF=-590.0654669\MP2=-590.9238086\RMSD=3.799e-09\RMSF=1.499e-06\Thermal=0.\Di pol e=0.007437, 0.2781101, 0.6572682\PG=C01 [X(C3H7O1S1)]\@

Product Complex:

1\1\GINC-NODE21\F0pt\RMP2-FC\6-311+G(2d,p)\C3H7O1S1(1-)\MAY04\11-Jan-2010\0\#p MP2/6-311+G(2d,p) Opt Freq\Product Complex Enolat-0-Me---SH\ -1, 1\C, 1.1962308365, -0.5292295722, 0.0257540377\C, 2.0927471239, -1.5235310856, 0.0353596148\O, 1.5734954971, 0.7563270659, -0.2316292484\H, 0.1254995856, -0.6819908582, 0.1855861715\H, 1.7474298348, -2.5350884385, 0.198085727\H, 3.1474359869, -1.3386172566, -0.133894582\S, -2.6071563518, -0.264674476, 0.1581197001\H, -2.7398979114, -0.8614075468, -1.0315382423\C, 0.5695675143, 1.7254301575, 0.1128817871\H, 0.6383809472, 1.9657006595, 1.1786251947\H, 0.7874301468, 2.6175643697, -0.4742192128\H, -0.4341322099, 1.3489679814, -0.1057919474\Version=AM64L-G03RevD.01\State=1-A\HF=-590.1226458\MP2=-590.9609635\RMSD=3.767e-09\RMSF=8.808e-06\Thermal=0.\Di pol e=3.3261985, 0.6990867, -0.2174993\PG=C01 [X(C3H7O1S1)]\@

C-Attack by MeSH

Transition State:

1\1\GINC-NODE11\FTS\RMP2-FC\6-311+G(2d,p)\C3H7O1S1(1-)\MAY04\06-Aug-2009\1\#P MP2/6-311+G(2d,p) Opt=(Z-Matrix, ts, noeigentest, calcf) Freq\C-Angri ff von MeSH an Enolat - TS mit MP2/6-311+G(2d,p)\ -1, 1\C\C, 1, R2\O, 1, R3, 2, A3\H, 1, R4, 2, A4, 3, D4, O\H, 2, R5, 1, A5, 3, D5, O\H, 2, R6, 1, A6, 3, D6, O\C, 2, R7, 1, A7, 3, D7, O\H, 7, R8, 2, A8, 1, D8, O\H, 7, R9, 2, A9, 1, D9, O\H, 7, R10, 2, A10, 1, D10, O\S, 7, R11, 8, A11, 2, D11, O\H, 11, R12, 7, A12, 1, D12, O\ R2=1.41228243\R3=1.25215335\A3=127.7176053\R4=1.11777407\A4=114.00249909\D4=-173.73582729\R5=1.08696212\A5=117.93914667\D5=-18.77389118\R6=1.08705876\A6=11

7. 1457534\D6=-166. 78787541\R7=2. 19041213\A7=99. 07907134\D7=85. 50620539\R8=1. 07523986\A8=86. 72773554\D8=-179. 55731875\R9=1. 07553881\A9=86. 54369824\D9=-58. 95599456\R10=1. 07387961\A10=91. 30582522\D10=61. 32171326\R11=2. 33741792\A11=90. 08392009\D11=-177. 50634318\R12=1. 33496392\A12=92. 3651983\D12=-3. 04600361\\Versi on=AM64L-G03RevD. 01\State=1-A\HF=-590. 0603155\MP2=-590. 9258231\RMSD=5. 920e-09\RMSF=2. 872e-06\Thermal =0. \Di pol e=-0. 7311386, -0. 581841, 0. 3785036\PG=C01 [X(C3H7O1S1)]\@

Product Complex:

1\1\GINC-NODE11\FOpt\RMP2-FC\6-311+G(2d,p)\C3H7O1S1(1-)\MAY04\12-Jan-2010\0\#p MP2/6-311+G(2d,p) Opt Freq\\Product Complex Enol at-C-Me---SH\\-1, 1\C, 1. 324037305, -0. 7246682696, -0. 1208167468\C, 1. 0893486311, 0. 5527233492, 0. 6288048711\O, 2. 3888077095, -1. 3311903872, -0. 1356657901\H, 0. 4488878706, -1. 0891279494, -0. 6866521011\H, 1. 9793633931, 0. 7853666005, 1. 2197781986\H, 0. 2271127994, 0. 3878482315, 1. 2825943066\C, 0. 7381742649, 1. 6772613153, -0. 3531865323\H, 0. 5159798338, 2. 5994658795, 0. 187261702\H, 1. 5675449968, 1. 8719999335, -1. 0401190527\H, -0. 1505683556, 1. 4041426935, -0. 9254712807\S, -2. 294127149, -0. 1369593284, 0. 0318464814\H, -3. 2830032995, -1. 0361710683, 0. 0426629439\\Versi on=AM64L-G03RevD. 01\State=1-A\HF=-590. 1608115\MP2=-591. 0002663\RMSD=5. 379e-09\RMSF=2. 168e-05\Thermal =0. \Di pol e=2. 6511628, 0. 7781769, 0. 0430663\PG=C01 [X(C3H7O1S1)]\@

O-Attack by MeSMe

Reactant Complex:

1\1\GINC-NODE24\FOpt\RMP2-FC\6-311+G(2d,p)\C4H9O1S1(1-)\MAY04\14-Jan-2010\0\#p MP2/6-311+G(2d,p) Opt Freq\\Reactant Complex Enol at-O---Me-SMe\\-1, 1\C, 2. 6940623879, -0. 002036567, -0. 4886175445\C, 3. 6877373866, 0. 0023582686, 0. 4659091766\O, 1. 4196158863, -0. 0024105632, -0. 3365705169\H, 3. 0755951146, -0. 005738568, -1. 5378896081\H, 4. 728362764, 0. 0019938905, 0. 1569569307\H, 3. 4496162134, 0. 0062021866, 1. 5262472737\C, -1. 3358888362, 1. 3713121526, 0. 3244890789\H, -1. 7353869228, 2. 2872939989, -0. 1139203487\H, -1. 3447277349, 1. 4623037821, 1. 4120614174\H, -0. 3157979767, 1. 1849852547, -0. 0237620415\S, -2. 4067016431, 0. 0006452136, -0. 2094761391\C, -1. 3379620955, -1. 3706723221, 0. 3269632447\H, -1. 3467300228, -1. 4595173239, 1. 4147137364\H, -1. 7390172041, -2. 2868727839, -0. 1095666292\H, -0. 3176523167, -1. 1866686195, -0. 0218540304\\Versi on=AM64L-G03RevD. 01\State=1-A\HF=-629. 1539496\MP2=-630. 1660499\RMSD=1. 858e-09\RMSF=1. 873e-05\Thermal =0. \Di pol e=-2. 6534139, 0. 0005491, 0. 2753593\PG=C01 [X(C4H9O1S1)]\@

Transition State:

1\1\GINC-NODE11\FTS\RMP2-FC\6-311+G(2d,p)\C4H9O1S1(1-)\MAY04\12-Jan-2010\0\#p MP2/6-311+G(2d,p) opt=(cal cfc, ts, noei gentest) freq\\0-Angri ff des Enolats an MeSMe\\-1, 1\C, -2. 5135926738, -0. 068321825, -0. 2723821039\C, -3. 8633630725, 0. 0843584959, -0. 3299467875\O, -1. 7168973176, 0. 2777553197, 0. 7070471969\H, -2. 0287165348, -0. 5359131872, -1. 1473354451\H, -4. 3980314086, -0. 2470595123, -1. 2121151684\H, -4. 4161115817, 0. 5336622256, 0. 4878755792\C, 0. 0448068845, -0. 1986160846, 0. 3270369752\H, 0. 3795108569, 0. 2659722398, 1. 2372222745\H, -0. 1723172512, -1. 252883467, 0. 3172183469\H, 0. 0542609439, 0. 3511839481, -0. 5983491211\S, 2. 3267243685, -0. 690924071, -0. 122036886\C, 2. 728298805, 1. 0885489426, -0. 2016110103\H, 2. 1809132559, 1. 5838349814, -1. 0106199972\H, 2. 4713679456, 1. 5945038514, 0. 7352265339\H, 3. 7958697798, 1. 2379811425, -0. 3801253871\\Versi on=AM64L-G03RevD. 01\State=1-A\HF=-629. 0963107\MP2=-630. 1169916\RMSD=2. 100e-09\RMSF=9. 753e-07\Thermal =0. \Di pol e=0. 004323, 0. 6039174, -0. 2237916\PG=C01 [X(C4H9O1S1)]\@

Product Complex:

1\1\GINC-NODE22\FOpt\RMP2-FC\6-311+G(2d,p)\C4H9O1S1(1-)\MAY04\14-Jan-2010\0\#p MP2/6-311+G(2d,p) Opt Freq\\Product Complex Enol at-O-Me---SM e\\-1, 1\C, 1. 4790955558, -0. 5050179888, -0. 1441015947\C, 2. 3503329923, -1. 520325484, -0. 0883793513\O, 1. 8198708108, 0. 7405649442, 0. 2948452105\H, 0. 45

18135205, -0.6111031954, -0.5077798439\H, 2.0245539192, -2.5036917034, -0.3982645295\H, 3.3603722628, -1.3824803023, 0.280728675\S, -2.1578108373, -0.1364297768, -0.6579142954\C, 0.9189885477, 1.7726564105, -0.1403366137\H, 0.9427970797, 2.5529161711, 0.6208580093\H, 1.2695480097, 2.1844162124, -1.09242637\H, -0.0980550985, 1.3853332478, -0.2708968823\C, -1.8634795608, -0.35075693, 1.1446418179\H, -2.6294403651, 0.1581712551, 1.7390452977\H, -1.8739347476, -1.407391763, 1.4316834987\H, -0.8915710894, 0.0547019026, 1.4584879717\Versi on=AM64L-G03RevD.01\State=1-A\HF=-629.1476746\MP2=-630.1498522\RMSD=7.632e-09\RMSF=3.915e-05\Thermal=0.\Di pol e=2.5706194, 0.5620384, 0.8701651\PG=C01 [X(C4H9O1S1)]\@

C-Attack by MeSMe

Transition State:

1\1\GINC-NODE10\FTS\RMP2-FC\6-311+G(2d,p)\C4H9O1S1(1-)\MAY04\12-Jan-2010\0\#p MP2/6-311+G(2d,p) opt=(cal cfc, ts, noeigentest) freq\C-Angri ff des Enol ats an MeSMe\ -1, 1\C, -2.5147459867, 0.2505255009, 0.3544128874\C, -2.1148695964, -1.0647031835, 0.0213835815\O, -2.6740455697, 1.2170429142, -0.4235061225\H, -2.5812225301, 0.4434533363, 1.4529481183\H, -2.2391986897, -1.3839692765, -1.0101485261\H, -2.2430802064, -1.8268342449, 0.7861828633\C, 0.0053562725, -0.7964024475, 0.0096274085\H, 0.108159056, -1.8405351713, -0.2288780503\H, -0.1364537055, -0.0644737839, -0.7678607503\H, 0.0270801382, -0.4898223456, 1.0406232363\S, 2.326389255, -0.4873280194, -0.1354860478\C, 2.1318668681, 1.2992364051, 0.1875825409\H, 1.7704327234, 1.4822279015, 1.2040225503\H, 3.0878270223, 1.8144961614, 0.0698496713\H, 1.4162579489, 1.746413253, -0.5094033607\Versi on=AM64L-G03RevD.01\State=1-A\HF=-629.0910929\MP2=-630.1197245\RMSD=5.951e-09\RMSF=1.417e-06\Thermal=0.\Di pol e=0.0177335, -0.2905803, 0.6337227\PG=C01 [X(C4H9O1S1)]\@

Product Complex:

1\1\GINC-NODE16\FOpt\RMP2-FC\6-311+G(2d,p)\C4H9O1S1(1-)\MAY04\14-Jan-2010\0\#p MP2/6-311+G(2d,p) Opt Freq\Product Complex Enol at-C-Me---SM e\ -1, 1\C, 1.3907000842, -0.7199399804, -0.2785279334\C, 1.3110413664, 0.4153321844, 0.694843289\O, 2.2561068571, -1.5876694272, -0.2658241194\H, 0.6033174082, -0.7089791654, -1.0543423291\H, 2.0214239454, 0.2410815705, 1.5074352617\H, 0.2796614689, 0.4609955914, 1.064270968\C, 1.5843082614, 1.7350711666, -0.0357589603\H, 1.496010292, 2.5757660085, 0.6557080311\H, 2.5866210891, 1.7503573477, -0.4747621202\H, 0.8363884429, 1.8693611279, -0.8196699256\S, -2.0111827379, 0.5829836765, -0.3805236727\C, -2.0175492153, -1.1324632473, 0.2776299943\H, -2.8046727775, -1.2721567608, 1.0259498348\H, -2.1848437023, -1.8703727643, -0.5143375313\H, -1.0682977826, -1.397829328, 0.7655902129\Versi on=AM64L-G03RevD.01\State=1-A\HF=-629.1855792\MP2=-630.1884418\RMSD=7.066e-09\RMSF=2.236e-05\Thermal=0.\Di pol e=2.3232317, -0.08877, 0.6440527\PG=C01 [X(C4H9O1S1)]\@

6 References

- [1] a) R. G. Pearson, *J. Am. Chem. Soc.* **1963**, *85*, 3533–3539; b) R. G. Pearson, *Science* **1966**, *151*, 172–177; c) R. G. Pearson, J. Songstad, *J. Am. Chem. Soc.* **1967**, *89*, 1827–1836; d) R. G. Pearson, *J. Chem. Educ.* **1968**, *45*, 581–587; e) R. G. Pearson, *J. Chem. Educ.* **1968**, *45*, 643–648; f) R. G. Pearson, *Chemical Hardness*, Wiley-VCH, Weinheim, **1997**.
- [2] a) G. Klopman, *J. Am. Chem. Soc.* **1968**, *90*, 223–234; b) L. Salem, *J. Am. Chem. Soc.* **1968**, *90*, 543–552.
- [3] R. Loos, S. Kobayashi, H. Mayr, *J. Am. Chem. Soc.* **2003**, *125*, 14126–14132.
- [4] A. A. Tishkov, H. Mayr, *Angew. Chem.* **2005**, *117*, 145–148; *Angew. Chem. Int. Ed.* **2005**, *44*, 142–145.
- [5] A. A. Tishkov, U. Schmidhammer, S. Roth, E. Riedle, H. Mayr, *Angew. Chem.* **2005**, *117*, 4699–4703; *Angew. Chem. Int. Ed.* **2005**, *44*, 4623–4626.
- [6] H. F. Schaller, U. Schmidhammer, E. Riedle, H. Mayr, *Chem. Eur. J.* **2008**, *14*, 3866–3868.
- [7] T. Bug, T. Lemek, H. Mayr, *J. Org. Chem.* **2004**, *69*, 7565–7576.
- [8] M. Baidya, S. Kobayashi, H. Mayr, *J. Am. Chem. Soc.* **2010**, *132*, 4796–4805.
- [9] I. Fleming, *Molecular Orbitals and Organic Chemical Reactions; Student Edition*, John Wiley & Sons, Chichester, **2009**.
- [10] a) R. A. Marcus, *Annu. Rev. Phys. Chem.* **1964**, *15*, 155–196; b) R. A. Marcus, *J. Phys. Chem.* **1968**, *72*, 891–899; c) R. A. Marcus, *J. Am. Chem. Soc.* **1969**, *91*, 7224–7225; d) W. J. Albery, M. M. Kreevoy, *Adv. Phys. Org. Chem.* **1978**, *16*, 87–157; e) W. J. Albery, *Annu. Rev. Phys. Chem.* **1980**, *31*, 227–263; f) R. A. Marcus, *Pure Appl. Chem.* **1997**, *69*, 13–29; g) R. A. Marcus, *Angew. Chem.* **1993**, *105*, 1161–1172; *Angew. Chem. Int. Ed. Engl.* **1993**, *32*, 1111–1121.
- [11] S. S. Shaik, H. B. Schlegel, P. Wolfe, *Theoretical Aspects of Physical Organic Chemistry: The S_N2 Mechanism*, Wiley, New York, **1992**.
- [12] a) S. Wolfe, D. J. Mitchell, H. B. Schlegel, *J. Am. Chem. Soc.* **1981**, *103*, 7692–7694; b) S. Wolfe, D. J. Mitchell, H. B. Schlegel, *J. Am. Chem. Soc.* **1981**, *103*, 7694–7696.
- [13] a) J. M. Gonzales, R. S. Cox, III, S. T. Brown, W. D. Allen, H. F. Schaefer, III, *J. Phys. Chem. A* **2001**, *105*, 11327–11346; b) J. M. Gonzales, C. Pak, R. S. Cox, W. D. Allen, H. F. Schaefer, III, A. G. Csaszar, G. Tarczay, *Chem. Eur. J.* **2003**, *9*, 2173–2192; c) J. M. Gonzales, W. D. Allen, H. F. Schaefer, III, *J. Phys. Chem. A* **2005**, *109*, 10613–10628.

- [14] a) M. J. Pellerite, J. I. Brauman, *J. Am. Chem. Soc.* **1983**, *105*, 2672–2680; b) J. A. Dodd, J. I. Brauman, *J. Phys. Chem.* **1986**, *90*, 3559–3562; c) B. D. Wladkowski, J. I. Brauman, *J. Phys. Chem.* **1993**, *97*, 13158–13164.
- [15] L. Sun, K. Song, W. L. Hase, *Science* **2002**, *296*, 875–878.
- [16] S. Hoz, H. Basch, J. L. Wolk, T. Hoz, E. Rozenal, *J. Am. Chem. Soc.* **1999**, *121*, 7724–7725.
- [17] E. Uggerud, *J. Phys. Org. Chem.* **2006**, *19*, 461–466.
- [18] a) L. G. Arnaut, A. A. C. C. Pais, S. J. Formosinho, *J. Mol. Struct.* **2001**, *563–564*, 1–17; b) L. G. Arnaut, S. J. Formosinho, *Chem. Eur. J.* **2007**, *13*, 8018–8028.
- [19] K. N. Houk, M. N. Paddon-Row, *J. Am. Chem. Soc.* **1986**, *108*, 2659–2662.
- [20] a) J. Hine, *J. Org. Chem.* **1966**, *31*, 1236–1244; b) J. Hine, *J. Am. Chem. Soc.* **1966**, *88*, 5525–5528; c) J. Hine, *Adv. Phys. Org. Chem.* **1977**, *15*, 1–61.
- [21] R. Gompper, H. U. Wagner, *Angew. Chem.* **1976**, *88*, 389–401; *Angew. Chem. Int. Ed. Engl.* **1976**, *15*, 321–333.
- [22] a) J. A. Berson, *Angew. Chem.* **2006**, *118*, 4842–4847; *Angew. Chem. Int. Ed.* **2006**, *45*, 4724–4729; b) S. Hünig, *Angew. Chem.* **1964**, *76*, 400–412; *Angew. Chem. Int. Ed. Engl.* **1964**, *3*, 548–560.
- [23] L. A. Curtiss, K. Raghavachari, P. C. Redfern, V. Rassolov, J. A. Pople, *J. Chem. Phys.* **1998**, *109*, 7764–7776.
- [24] Gaussian 03, Revision D.01, M. J. Frisch, G. W. Trucks, H. B. Schlegel, G. E. Scuseria, M. A. Robb, J. R. Cheeseman, J. A. Montgomery, Jr., T. Vreven, K. N. Kudin, J. C. Burant, J. M. Millam, S. S. Iyengar, J. Tomasi, V. Barone, B. Mennucci, M. Cossi, G. Scalmani, N. Rega, G. A. Petersson, H. Nakatsuji, M. Hada, M. Ehara, K. Toyota, R. Fukuda, J. Hasegawa, M. Ishida, T. Nakajima, Y. Honda, O. Kitao, H. Nakai, M. Klene, X. Li, J. E. Knox, H. P. Hratchian, J. B. Cross, V. Bakken, C. Adamo, J. Jaramillo, R. Gomperts, R. E. Stratmann, O. Yazyev, A. J. Austin, R. Cammi, C. Pomelli, J. W. Ochterski, P. Y. Ayala, K. Morokuma, G. A. Voth, P. Salvador, J. J. Dannenberg, V. G. Zakrzewski, S. Dapprich, A. D. Daniels, M. C. Strain, O. Farkas, D. K. Malick, A. D. Rabuck, K. Raghavachari, J. B. Foresman, J. V. Ortiz, Q. Cui, A. G. Baboul, S. Clifford, J. Cioslowski, B. B. Stefanov, G. Liu, A. Liashenko, P. Piskorz, I. Komaromi, R. L. Martin, D. J. Fox, T. Keith, M. A. Al-Laham, C. Y. Peng, A. Nanayakkara, M. Challacombe, P. M. W. Gill, B. Johnson, W. Chen, M. W. Wong, C. Gonzalez, J. A. Pople, Gaussian, Inc., Wallingford CT, **2004**.

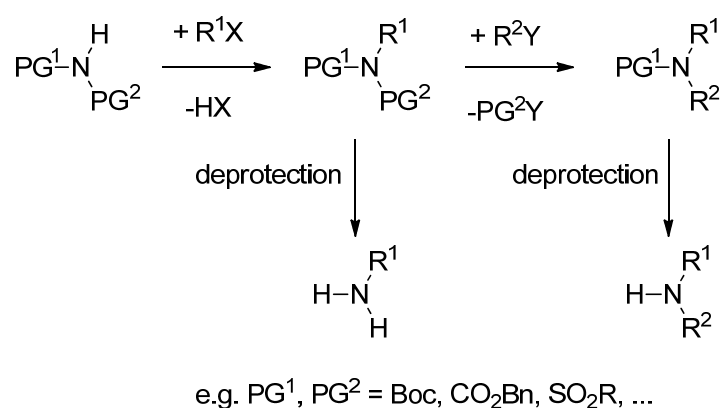
Chapter 4: Nucleophilic Reactivities of Imide and Amide Anions

Martin Breugst, Takahiro Tokuyasu, and Herbert Mayr

J. Org. Chem. **2010**, *75*, 5250–5258.

1 Introduction

Gabriel's phthalimide method, which has been reported more than 120 years ago,^[1] has repeatedly been optimized^[2] and is still an important synthesis for primary amines. Hendrickson modified Gabriel's procedure by replacing the divalent protecting group in phthalimide by two monovalent ones which can subsequently be removed (Scheme 1).^[3] Over the years, Hendrickson's procedure was further optimized for the synthesis of a wide range of primary and secondary amines,^[4] alkylated hydrazines,^[5] and amino acids.^[6]



Scheme 1: Modified Gabriel-synthesis using monovalent protective groups PG¹ and PG².

Amide anions, like lithium benzamide or phthalimide, have furthermore been reported to be effective Lewis base catalysts in Mannich-type reactions between silyl enol ethers and *N*-tosylaldimines.^[7]

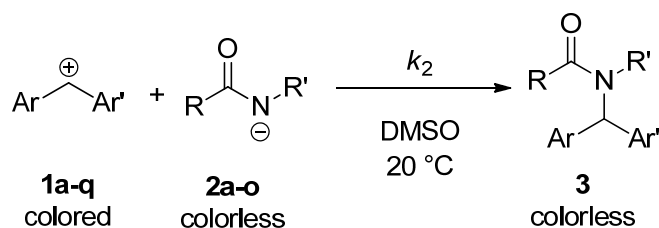
Despite the importance of amide anions in organic synthesis and materials, there is only little quantitative data on their nucleophilic reactivity.^[8, 9] In 1971, Bunnett and Beale studied the kinetics of the reactions of several imide and sulfonamide anions with methyl iodide^[8a] and methyl methanesulfonate^[8b] in methanol and reported that the nucleophilic reactivities of these anions correlate with their basicities. Bordwell and Hughes investigated the reactivities of several amide anions towards benzyl chloride in DMSO and concluded that the anion of 1,2,3,4-tetrahydroquinolin-2-one is 9 times more reactive than the anion of acetanilide and

280 times more reactive than the anion of benzanilide.^[8c] Later, Kondo and co-workers examined the S_N2 reactions of several imide anions with ethyl iodide in acetonitrile and acetonitrile-methanol mixtures.^[9] Although the pK_{aH} values of succinimide and phthalimide anions differ by more than one order of magnitude (9.66 vs. 8.30 in water), the second-order rate constants in acetonitrile vary by less than a factor of 3 (1.65×10^{-1} vs. 6.43×10^{-2} L mol⁻¹ s⁻¹).^[9a]

In earlier work we have reported that benzhydrylium ions (Table 1) can be used as reference electrophiles with tunable reactivity^[10] for characterizing a large variety of π -nucleophiles (e.g., alkenes,^[11] arenes,^[11] enol ethers,^[11] ketene acetals,^[11] enamines,^[11] delocalized carbanions^[12]), n -nucleophiles (e.g., amines,^[13] alcohols^[14]), and σ -nucleophiles like hydrides.^[10, 15] The rate constants at 20 °C of the reactions of these nucleophiles with benzhydrylium ions have been described by equation (1),^[16] where s and N are nucleophile specific parameters and E is an electrophile specific parameter.

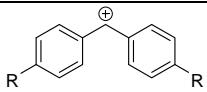
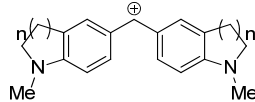
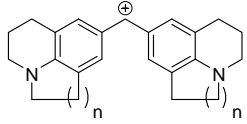
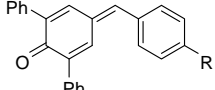
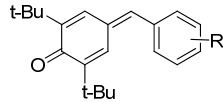
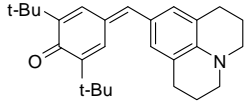
$$\log k_{20\text{ }^\circ\text{C}} = s(N + E) \quad (1)$$

We now report on the kinetics of the reactions of imide and amide anions with the reference electrophiles listed in Table 1 in order to determine the nucleophile specific parameters N and s of these N -centered nucleophiles (Scheme 2) and to include them into our comprehensive nucleophilicity scale.^[17]



Scheme 2: Reaction of amide anions with benzhydrylium ions.

Table 1: Reference Electrophiles Employed in this Work and Wavelengths Monitored in the Kinetic Experiments.

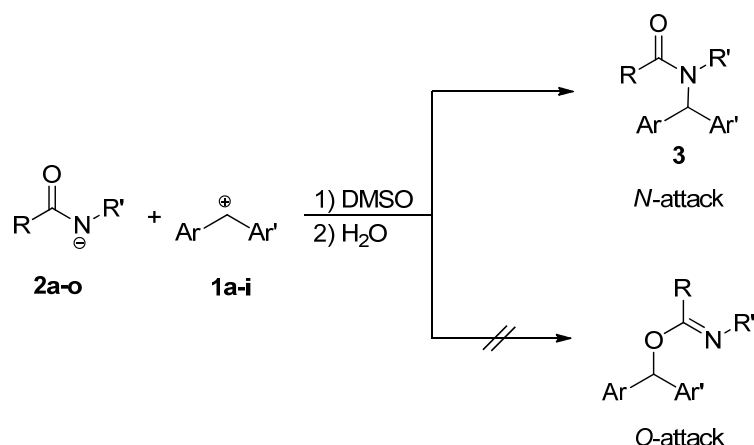
Electrophile		E^a	λ^b / nm	
	R = NPh ₂	1a	-4.72	672
	R = N(CH ₂ CH ₂) ₂ O	1b	-5.53	620
	R = NMePh	1c	-5.89	622
	R = NMe ₂	1d	-7.02	613
	R = N(CH ₂) ₄	1e	-7.69	620
	n = 2	1f	-8.22	618
	n = 1	1g	-8.76	627
	n = 2	1h	-9.45	635
	n = 1	1i	-10.04	630
	R = OMe	1j	-12.18	422
	R = NMe ₂	1k	-13.39	533
	R = 4-NO ₂	1l	-14.32	374
	R = 3-F	1m	-15.03	354
	R = 4-Me	1n	-15.83	371
	R = 4-OMe	1o	-16.11	393
	R = 4-NMe ₂	1p	-17.29	486
		1q	-17.90	521

^a Electrophilicity parameters from ref. ^[10] and ^[18]. ^b Wavelength λ used to follow the kinetics of the reactions.

2 Results

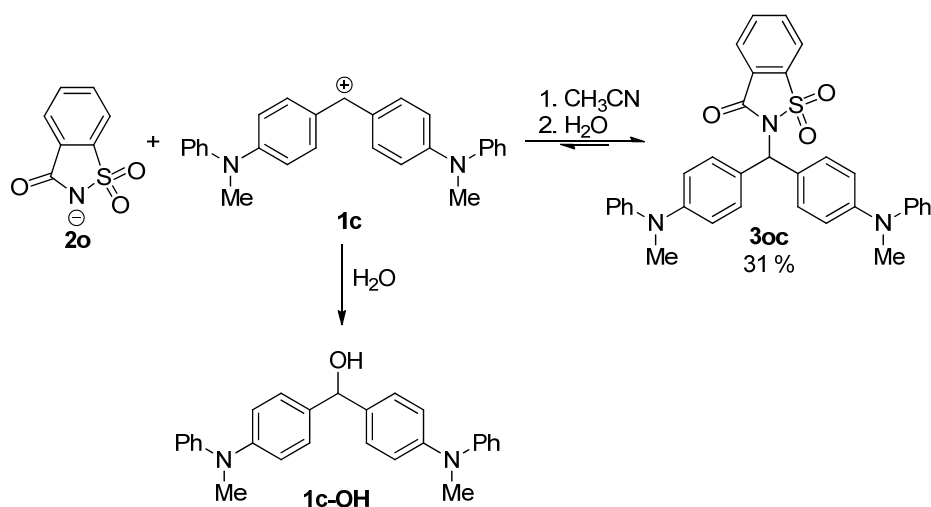
Reaction Products

As ambident nucleophiles, imide and amide anions may react with benzhydrylium ions either at the nitrogen or the oxygen atom (Scheme 3). NMR spectroscopy shows that in all cases examined in this work, amides are formed exclusively (*N*-attack), but we cannot exclude a preceding reversible attack at oxygen. This result is in accordance with the findings of Bordwell and Hughes who observed selective *N*-benzylation in the reactions of several amide anions with benzyl chloride in DMSO.^[8c]



Scheme 3: Reactions of the imide and amide anions **2a–o** with the electrophiles **1a–i** in DMSO.

When equimolar amounts of the potassium or tetraalkylammonium salts of **2a–o** and representative benzhydrylium salts (**1a–i**)- BF_4^- were combined in dry DMSO [saccharin (**2o**) in dry CH_3CN], complete decolorization of the solutions was observed, indicating quantitative consumption of the electrophiles. The fact that some of the reaction products were obtained in only moderate yields (Table 2) is due to non-optimized work-up procedures. As shown by the low $\text{p}K_{\text{aH}}$ values in water (Table 2), many of the investigated amide and imide anions are weak bases, with the consequence that their adducts with stabilized benzhydrylium ions undergo heterolytic cleavage during aqueous workup, as illustrated for **3oc** in Scheme 4. In such cases, the products could not be isolated and identified by mass spectrometry or elemental analysis and the product studies were performed by NMR spectroscopy in d_6 -DMSO solution.



Scheme 4: Reversible reaction of the saccharin anion (**2o**) with **1c**.

Kinetic Investigations

The reactions of the imide and amide anions **2a–n** with the benzhydrylium ions **1a–i** and structurally related quinone methides **1j–q** were studied in DMSO at 20 °C. The reactions were monitored by UV-Vis spectroscopy at or close to the absorption maxima of the electrophiles ($354 < \lambda < 635$ nm, Table 1). Due to the low reactivity of the saccharin anion (**2o**), more electrophilic carbocations (**1a–d**) had to be employed for determining its nucleophilicity. Since these benzhydrylium ions react with DMSO, the corresponding kinetic investigations were performed in acetonitrile.

To simplify the evaluation of the kinetic experiments, the nucleophiles were generally used in large excess over the electrophiles. Therefore, the concentrations of **2a–o** remained almost constant throughout the reactions, and pseudo-first-order kinetics were obtained in all runs. The first-order rate constants k_{obs} were then derived by least-squares fitting of the time-dependent absorbances A_t of the electrophiles to the exponential $A_t = A_0 \exp(-k_{\text{obs}}t) + C$. Second-order rate constants were obtained as the slopes of the plots of k_{obs} versus the concentrations of the nucleophiles (Figure 1).

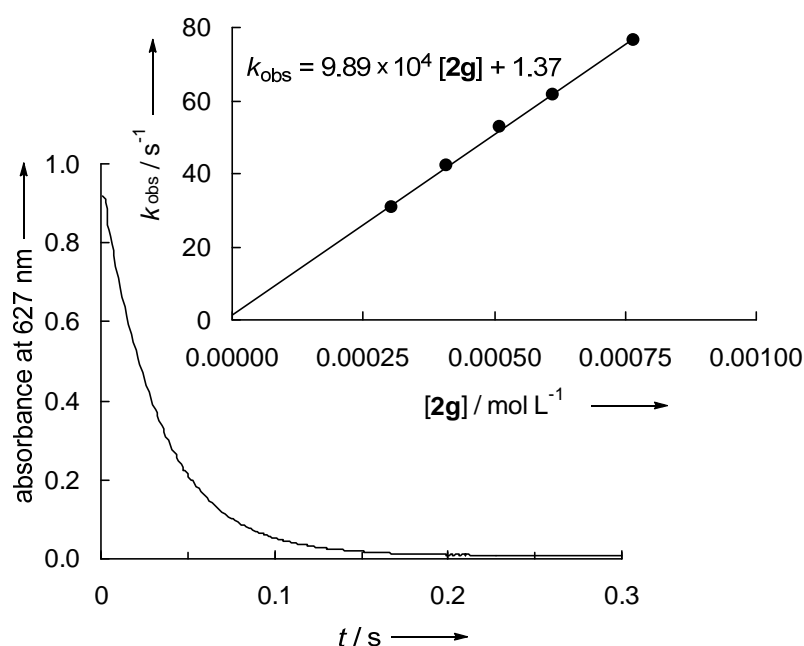


Figure 1: Plot of the absorbance (627 nm) vs. time for the reaction of **1g** with the potassium salt of diacetamide (**2g-K**) in DMSO at 20 °C, and correlation of the first-order rate constants k_{obs} with the concentration of **2g** (insert).

Table 2: Second-Order Rate Constants for the Reactions of Reference Electrophiles **1e–o** with Imide and Amide Potassium Salts **2a–n** in DMSO at 20 °C.

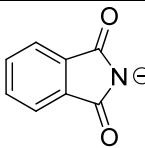
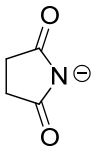
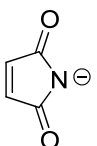
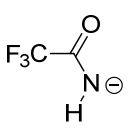
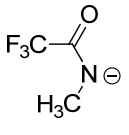
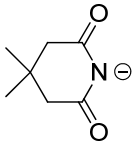
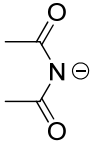
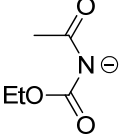
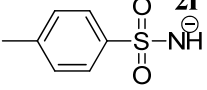
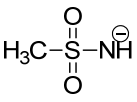
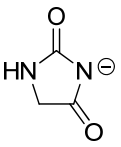
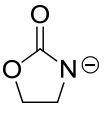
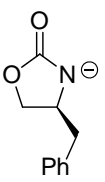
Nucleophile	<i>N</i> / <i>s</i>	p <i>K</i> _{aH} (DMSO)	p <i>K</i> _{aH} (H ₂ O)	Electro phile	Products	<i>k</i> ₂ / L mol ⁻¹ s ⁻¹	
	2a	15.52/ 0.67	13.4 ^a	8.30 ^b	1e		2.51 × 10 ⁵
					1e		2.49 × 10 ^{5,c}
					1f	3af , 51%	6.42 × 10 ⁴
					1g		2.85 × 10 ⁴
					1h		8.86 × 10 ³
					1i		4.05 × 10 ³
					1i		4.21 × 10 ^{3,c}
					1j		1.93 × 10 ²
					1k		2.74 × 10 ¹
					1k		2.60 × 10 ^{1,a}
	2b	16.03/ 0.66	14.7 ^d	9.66 ^b	1g	3bg , 85%	5.25 × 10 ^{4,e}
					1h		2.01 × 10 ^{4,e}
					1i		1.01 × 10 ^{4,e}
					1j		3.91 × 10 ^{2,e}
					1k		4.66 × 10 ^{1,e}
	2c	14.87/ 0.76	10.8 ^f	~ 10 ^g	1d	3cd , NMR	-
					1e		3.79 × 10 ⁵
					1g		3.29 × 10 ⁴
					1h		1.20 × 10 ⁴
					1i		6.32 × 10 ³
	2d	15.81/ 0.64	17.2 ^d	-	1e		2.52 × 10 ⁵
					1f	3df , 85%	6.80 × 10 ⁴
					1g		2.59 × 10 ⁴
					1i		4.66 × 10 ³
					1j		2.65 × 10 ²
	2e	15.70/ 0.71	17.2 ^h	13.2 ⁱ	1d	3ed , NMR	-
					1f		2.29 × 10 ⁵
					1g		6.22 × 10 ⁴
					1h		2.67 × 10 ⁴
					1i		1.06 × 10 ⁴
	2f	17.52/ 0.63	17.3 ^j	-	1d	3fd , 86%	-
					1f	3ff , 51%	-
					1g		2.86 × 10 ⁵
					1h		1.05 × 10 ⁵
					1i		5.15 × 10 ⁴
	2g	16.05/ 0.70	17.9 ^j	12.4 ^k	1d	3gd , NMR	-
					1f		3.45 × 10 ⁵
					1g		9.89 × 10 ⁴
					1h		3.62 × 10 ⁴
					1i		1.77 × 10 ⁴

Table 2: Continued.

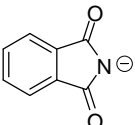
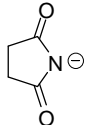
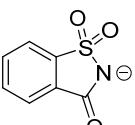
Nucleophile	<i>N</i> / <i>s</i>	p <i>K</i> _{aH} (DMSO)	p <i>K</i> _{aH} (H ₂ O)	Electro- phile	Products	<i>k</i> ₂ / L mol ⁻¹ s ⁻¹	
	2h	15.99/ 0.70	-	-	1d	3hd , 54%	-
					1f		2.97×10^5
					1g		1.03×10^5
					1h		3.45×10^4
					1i		1.57×10^4
	2i	17.14/ 0.60	16.3 ^l	10.2 ^m	1d	3id , 73%	-
					1f		2.72×10^5
					1g		7.33×10^4
					1h		4.40×10^4
					1i		1.86×10^4
	2j	18.61/ 0.53	17.5 ^d	10.8 ⁿ	1d	3jd , NMR	-
					1g		$1.76 \times 10^{5,o}$
					1h		$7.14 \times 10^{4,o}$
					1i		$2.81 \times 10^{4,o}$
					1j		2.74×10^4
	2k	17.52/ 0.55	15.1 ^p	9.2 ^q	1d	3kd , 84%	-
					1g		$6.90 \times 10^{4,o}$
					1h		$2.25 \times 10^{4,o}$
					1i		$1.38 \times 10^{4,o}$
	2l	22.40/ 0.59	20.9 ^r	-	1d	3ld , 84%	-
					1k		7.67×10^4
					1l		9.21×10^4
					1m		3.32×10^4
					1n		9.30×10^3
					1o		5.94×10^3
					1p		7.12×10^2
					1q		3.28×10^2
	2m	22.67/ 0.54	20.6 ^r	-	1d	3md , 94%	-
					1j		3.29×10^5
					1k		5.24×10^4
					1l		9.38×10^4
					1m		2.71×10^4
					1n		6.14×10^3
					1o		4.01×10^3
					1p		5.81×10^2
					1q		2.59×10^2
	2n	20.33/ 0.64	17.0 ^s	-	1d	3nd , 95%	-
					1j		1.63×10^5
					1n		7.38×10^2
					1o		5.10×10^2

^a Ref. [19]. ^b Ref. [9a]. ^c NMe₄⁺ salt, not included in correlation. ^d Ref. [20]. ^e NBu₄⁺ salt. ^f Ref. [21]. ^g Ref. [22]. ^h Ref. [23]. ⁱ Ref. [24]. ^j Ref. [25]. ^k Ref. [26]. ^l Ref. [27]. ^m Ref. [28]. ⁿ Ref. [29]. ^o In situ deprotonation with P₂-*t*Bu base (1-*tert*-butyl-2,2,4,4,4-pentakis(dimethylamino)-2Λ⁵,4Λ⁵-catenadi(phosphazene)), ref. [30]. ^p Ref. [31]. ^q Ref. [32]. ^r Ref. [33]. ^s Ref. [34].

In DMSO solution, where most investigations have been performed, the potassium salts (**2a–n**)-**K** are dissociated into free ions in the concentration range under investigation ($c < 3.4 \times 10^{-3} \text{ mol L}^{-1}$).^[12a, 18a] Consequently, there is no significant change in k_2 when changing the counterion from potassium to tetraalkylammonium as demonstrated for the reactions of **2a** with **1e,i,k** and of **2j** with **1i** (Table 2). Furthermore, for several examples it has been shown that k_{obs} values, which were obtained for potassium salts **2-K** in the presence and in the absence of crown ether, are on the same k_{obs} vs. [**2**] plots (see Experimental Section).

Some kinetic measurements were also performed in acetonitrile. From the linear dependence of the pseudo-first-order rate constants k_{obs} on the concentrations of the amide anions, it is concluded that ion-pairing also is not significant in acetonitrile under these conditions. Table 3 shows that the reactivities towards benzhydrylium ions and quinone methides are differently affected by the change of the solvent. Whereas the reactions with the positively charged reference electrophiles are 4–6 times faster in acetonitrile than in DMSO, the reactions with neutral electrophiles proceed with almost equal rates in both solvents.

Table 3: Second-Order Rate Constants for the Reactions of Reference Electrophiles with Imide Anions **2a**, **2b**, and **2o** in Acetonitrile at 20 °C and Relative Reactivities r in Acetonitrile and DMSO.

Nucleophile		Electrophile	$k_2 / \text{L mol}^{-1} \text{s}^{-1}$	r^a
	2a^b	1e	1.50×10^6	6.00
		1i	2.42×10^4	5.86
	2b^c	1h	7.77×10^4	3.87
		1i	4.76×10^4	4.71
		1j	3.54×10^2	0.91
	2o^{b,d,e}	1k	5.22×10^1	1.12
		1a	2.33×10^5	-
		1b	2.91×10^4	-
		1c	2.04×10^{3f}	-

^a $r = k_2$ (in AN) / k_2 (in DMSO). ^b Employed as NMe_4^+ salt. ^c Employed as NBu_4^+ salt. ^d $\text{p}K_{\text{aH}}(\mathbf{2o}, \text{CH}_3\text{CN}) = 14.6$, Ref. ^[35]. ^e Nucleophile specific parameters for **2o**: $N = 10.78$, $s = 0.89$. ^f Product **3oc** was isolated in 31 % yield.

Correlation Analysis

According to equation (1), linear correlations were obtained, when $\log k_2$ for the reactions of the imide and amide anions **2a–o** with the reference electrophiles **1a–q** were plotted against their electrophilicity parameters E , as shown for some representative examples in Figure 2.

All reactions investigated in this work followed analogous linear correlations as depicted in the Experimental Section, indicating that equation (1) is applicable. The linearity over a wide range of reactivity furthermore supports the assumption that there is no change in the regioselectivity (*N*- vs. *O*-attack) when varying the electrophile. The slopes of these correlations correspond to the nucleophile-specific parameter s , whereas the negative intercepts on the abscissa ($\log k_2 = 0$) yield the nucleophilicity parameter N .

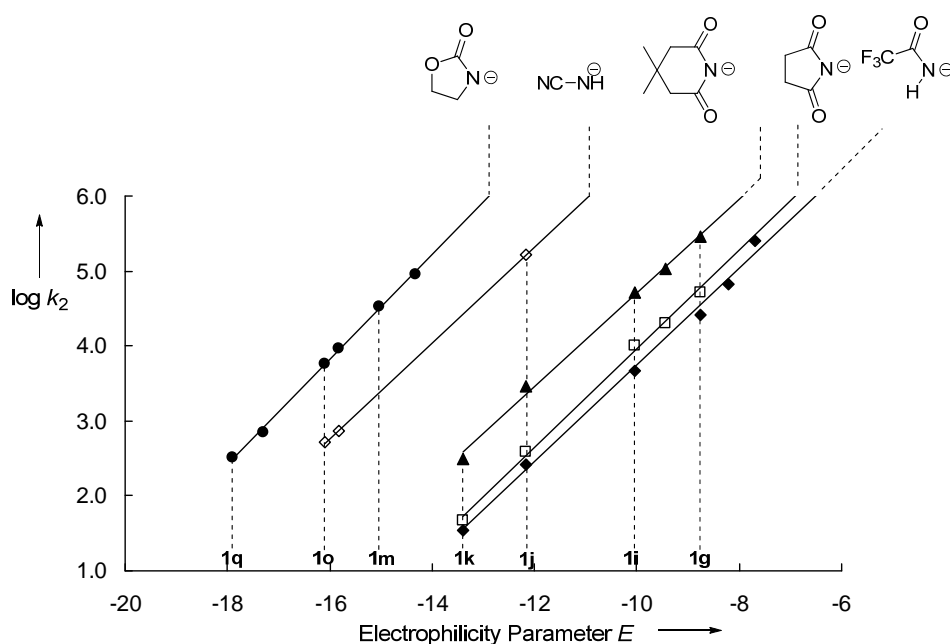
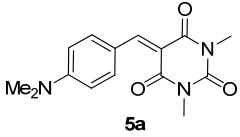
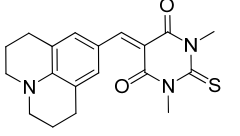


Figure 2: Plots of the rate constants $\log k_2$ for the reactions of imide and amide anions with reference electrophiles in DMSO versus their electrophilicity parameters E .

To examine the suitability of the nucleophilicity parameters N and s given in Table 2 for the prediction of rate constants of reactions with other types of electrophiles, we studied the kinetics of the reactions of the amide anions **2l** and **2n** with the Michael acceptors **5a** and **5b**. As shown in Table 4, the agreement between calculated and experimental data is better than a factor of 2 in the case of **2n** and better than a factor of 21 for the reactions of **2l**, i.e., the three-parameter equation (1), which presently covers a reactivity range of more than 40 orders of magnitude, can also be employed for the semiquantitative prediction of the rates of ordinary Michael additions of amide anions.

Table 4: Rate Constants k_2 ($\text{L mol}^{-1} \text{s}^{-1}$) for the Reactions of **2l,n** with the Michael Acceptors **5a,b** in DMSO at 20 °C.

Electrophile	E^a	Nucleophile	$k_{2,\text{exp}}$	$k_{2,\text{calc}}$
 5a	-12.76	2l	6.70×10^4	4.9×10^5
		2n	1.17×10^5	7.0×10^4
 5b	-11.89	2l	7.55×10^4	1.6×10^6
		2n	2.05×10^5	2.5×10^5

^a Electrophilicity parameters E from ref.^[36].

In previous work, we have shown that the relative reactivities of nucleophiles in $\text{S}_{\text{N}}2$ reactions also correlate with the N and s parameters which were derived from their reactions with benzhydrylium ions.^[37] The linear correlation of $(\log k_2)/s$ for the reactions of the imide anions **2a,b,f** with ethyl iodide,^[9c] shown in Figure 3, is in line with this observation, though the paucity of data inhibits a more detailed analysis.

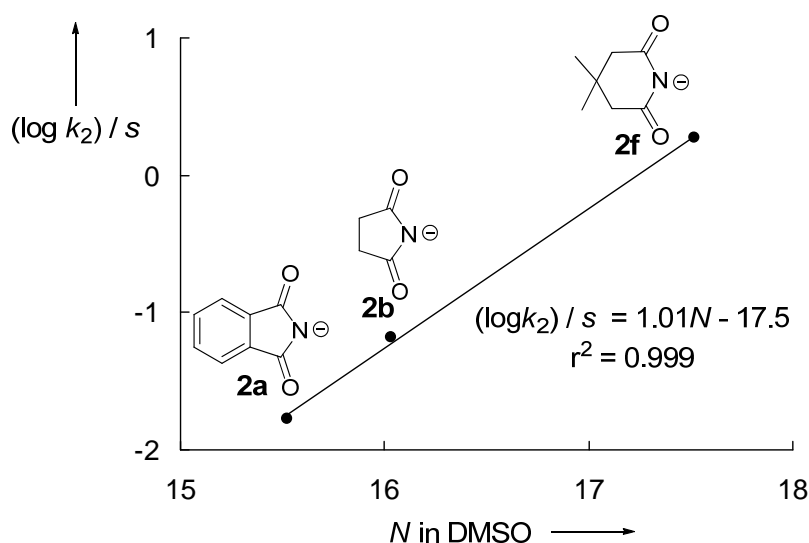


Figure 3: Correlation of the rate constants $(\log k_2 / s)$ for the reactions of the imide anions **2a,b,f** with EtI in CH_3CN (from ref. ^[9c]) with their nucleophilicity parameters N in DMSO.

As the nucleophilic reactivities of the amide anions **2** can be expected to be strongly reduced by hydrogen-bond donor solvents, a comparison of our data with the $\text{S}_{\text{N}}2$ reactivities of these anions in alcoholic solvents^[8a, 8b, 9a] is not possible.

3 Discussion

Ambident Reactivity of Amide and Imide Anions

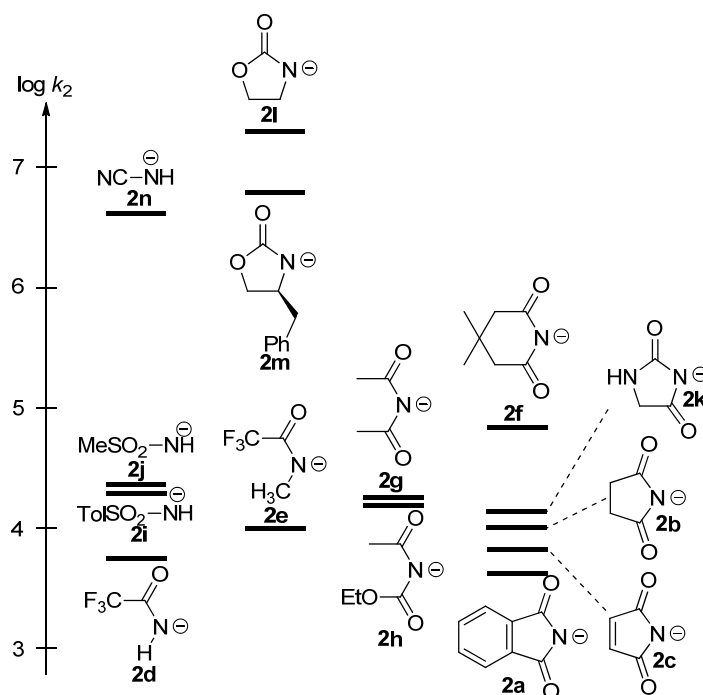
Although all reactions discussed above proceed via nitrogen attack, amide and imide anions are ambident nucleophiles, and oxygen attack is also conceivable. While alkylation reactions of neutral amides often give product mixtures arising from *O*- and *N*-attack,^[38] amide anions typically react at nitrogen.^[39] However, oxygen-alkylation has only been observed when silver salts were employed,^[40] and Kornblum rationalized this change of regioselectivity by the fact that silver ions enhance the carbocationic character of the electrophile and thus promote the alkylation at the more electronegative oxygen atom.^[41] Our observation that only *N*-substituted amides are isolated when amide anions are combined with benzhydrylium ions and that the linear correlations in Figure 2 do not give any clue that the more electrophilic benzhydrylium ions initially give *O*-alkylated products, which subsequently rearrange to the isolated *N*-alkylated products, disagrees with this interpretation. It appears more likely that the selective *O*-attack in the presence of silver salts is due to the coordination of the silver ion to the nitrogen atom of the imide anion, which is well documented by numerous X-ray studies.^[42] In this way, attack at the nitrogen is blocked. The selective formation of isonitriles from alkylation agents and $[\text{Ag}(\text{CN}_2)]^-$ has analogously been explained by the blocking of carbon attack by Ag^+ .^[43]

Structure Reactivity Relationships

The narrow range of *s* for all nucleophiles listed in Table 2 ($0.53 < s < 0.76$), which is illustrated by the almost parallel correlation lines in Figure 2 [exception: saccharin-anion (**20**), $s = 0.89$ in CH_3CN] implies that the relative reactivities of these compounds depend only slightly on the electrophilicity of the reaction partner. The reactivities towards the benzhydrylium ion **1i**, for which most rate constants have directly been measured, can therefore be assumed to reflect general structure reactivity trends (Scheme 5).

The decreasing nucleophilicity of the amide anions RNH^- in the series $\text{R} = \text{CN} > \text{SO}_2\text{CH}_3 \approx \text{SO}_2\text{Tol} > \text{COCF}_3$ (left column of Scheme 5) correlates neither with Hammett's σ_p nor σ_p^- constants of these substituents (see the Experimental Section for correlations) indicating that the mode of interaction of the substituents with N^- differs from the type of interaction with neutral or negatively charged C_{sp^2} -centers.

From the comparison of **2d** and **2e** one can derive that replacement of N-H by N-CH₃ has little effect on nucleophilic reactivity, and the similar reactivities of the cyanamide anion **2n** and Evans' auxiliary **2m** reveal the comparable effects of cyano and ester groups.

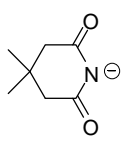
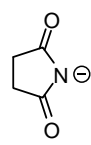
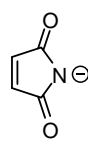
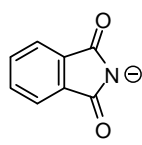


Scheme 5: Comparison of the reactivities of imide and amide anions with the benzhydrylium ion **1i** in DMSO (20 °C) [entries for **2l–n** were calculated by using Eq. (1), *N* and *s* parameters from Table 2 and *E*(**1i**) from Table 1].

A second acceptor group reduces the nucleophilic reactivity only slightly, and the comparison of **2i** (left column) and **2g** (middle column) shows that the effect of one sulfonyl group is comparable to that of two acetyl groups. The anion of saccharin (**2o**), which is simultaneously stabilized by a sulfonyl and an acyl group, is approximately 10⁴ times less nucleophilic than ordinary sulfonamide or diacylimide anions (Table 3, not included in Scheme 5).

Reduction of the ring size (**2f** → **2b**) is associated with a five-fold reduction of nucleophilicity (possibly because of a reduced p-character of the nonconjugated lone pair at N in the smaller ring **2b**), and the replacement of the ethano-bridge in **2b** by a benzo- or etheno-bridge causes a further two-fold reduction of nucleophilic reactivity (Scheme 6). The slight reduction of reactivity from succinimide **2b** to phthalimide **2a** and maleimide **2c** towards **1i** can be explained by the higher electronegativity of sp²- compared to sp³-hybridized carbon atoms. It shall be noted, that due to slightly different values of the slope parameter *s*, relative

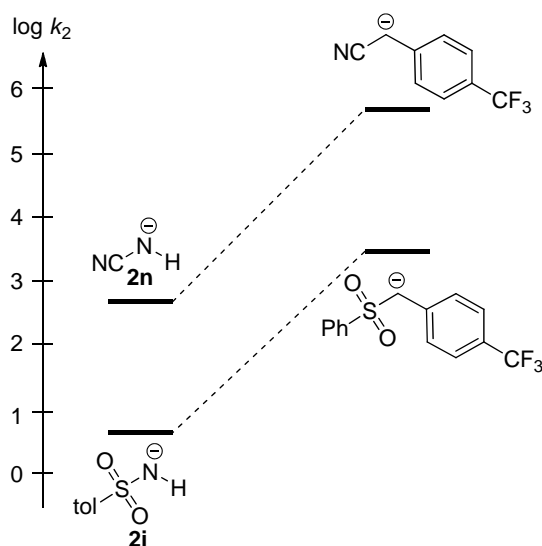
reactivities of compounds with similar reactivities may be inverted when the electrophile is changed, as indicated by the different order of k_2 and the N parameters in Scheme 6.

				
	2f	2b	2c	2a
k_2 [L mol ⁻¹ s ⁻¹]	5.15×10^4	1.01×10^4	6.32×10^3	4.13×10^3
N	17.52	16.03	14.87	15.52

Scheme 6: Reactivities towards benzhydrylium ion **1i** and N -values of imide anions (20 °C).

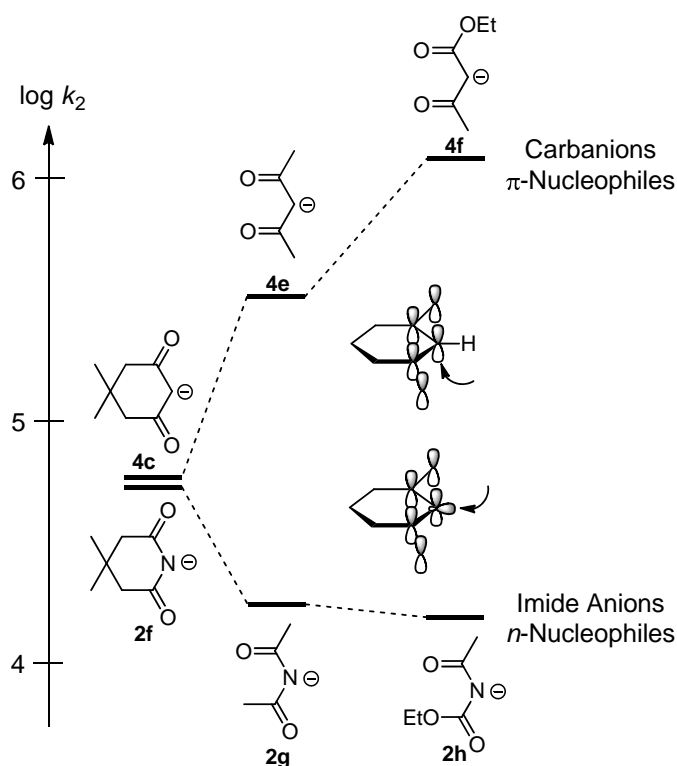
Comparison of Amide Anions and Carbanions

A direct comparison of the nucleophilic reactivities of amide anions and carbanions, which carry only one acceptor group, is not possible, because the high reactivities of mono-acceptor substituted carbanions have so far prevented the characterization of their nucleophilicities. On the other hand, the larger electronegativity of nitrogen enabled us to investigate amide anions carrying only one acceptor substituent. The observation that carbanions, which are stabilized by a trifluoromethyl substituted phenyl group in addition to a sulfonyl or cyano group^[44] are 10^3 times more nucleophilic than amide anions that carry a hydrogen atom instead of the acceptor-substituted phenyl group, reflects the tremendous difference in reactivity of amide anions and carbanions with a single acceptor substituent (Scheme 7).



Scheme 7: Comparison of the reactivity of amide anions and carbanions towards the quinone methide **1o** in DMSO (20 °C) [rate constants for **2i** and for the sulfonyl stabilized carbanion were calculated by Eq. (1) using N and s from Table 2 (this work) and ref^[44]].

A completely different situation is found for imide anions and carbanions bearing two acceptor groups. Coincidentally, the reactivities of the structurally analogous cyclic compounds, glutarimide anion **2f**, an *n*-nucleophile, and dimedone anion **4c**, a π -nucleophile, are almost identical (Scheme 8). Even when the ring is opened, dicarbonyl substituted imide anions and analogously substituted carbanions differ by less than 10^2 in reactivity, as shown in Scheme 8. While ring-opening leads to a slight decrease of the reactivities of the imide anions (\rightarrow **2g,h**), the reactivities of the acyclic carbanions (\rightarrow **4e,f**) are somewhat higher than that of the cyclic analogue **4c**. Whereas acetyl groups stabilize carbanions better than ethoxycarbonyl groups, similar stabilizing effects on imide anions are found for acetyl and ethoxycarbonyl substituents (Scheme 8).



Scheme 8: Comparison of the nucleophilic reactivities of structurally related imide anions and carbanions towards the benzhydrylium ion **1i** (20 °C).

Calculated Structures of the Diacetamide Anion

In order to rationalize why a second carbonyl acceptor group causes only a weak reduction of nucleophilicity in the imide anion series (see Scheme 5), we have investigated the structures of the *N,N*-diacetamide anion by quantum chemical calculations on the B3LYP/6-31+G(d,p) level of theory using Gaussian 03.^[45] For that purpose, we have systematically varied the dihedral angles ϕ and φ in the anion **2g** by relaxed potential energy surface scans. When ϕ is

varied (Figure 4a), ϕ remains at approximately 0° , and when ϕ is varied (Figure 4b), ϕ remains at about 180° . For the sake of clarity, the small deviations of the nonrotating groups from planarity are neglected in the drawings of Figure 4. Figure 4a shows that a slight change of ϕ from -180 to -160° leads to the global minimum **2g-I**, an almost planar conformation, where both carbonyl groups are in conjugation with the same lone pair on nitrogen. When the acetyl group is further turned out of plane ($\phi \rightarrow -90^\circ$), one observes only a small increase of energy, because now the rotating carbonyl group gets into conjugation with the second lone pair on nitrogen. The transition state **2g-II** with almost perpendicular arrangement of the two carbonyl groups is only 17 kJ mol^{-1} above the global minimum. Further rotation leads to a shallow minimum (**2g-III**), which corresponds to a slightly distorted conformation of the planar U-shaped conformer **2g-IV**, the energy maximum of this rotation.

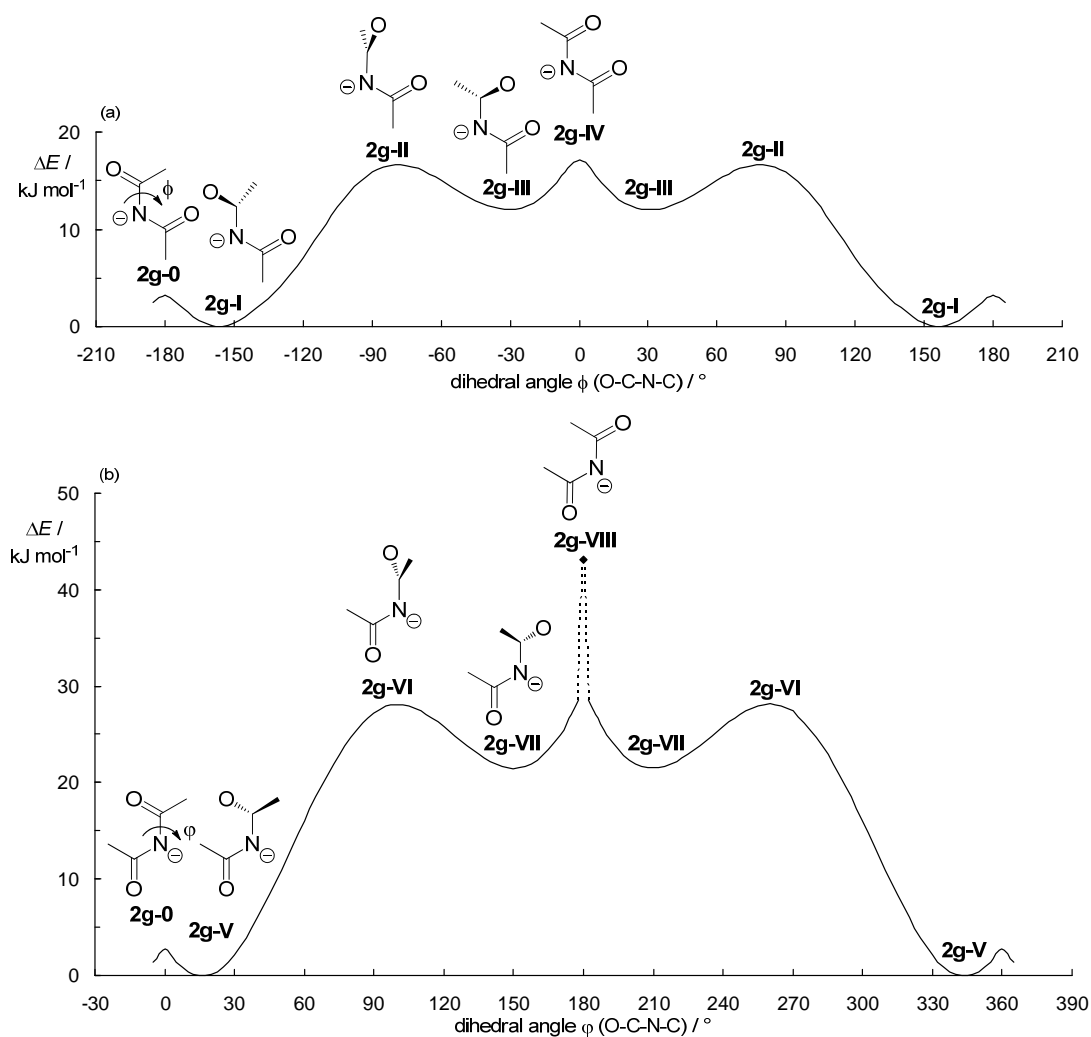


Figure 4: Relaxed potential energy surface scan [at B3LYP/6-31+G(d,p) level of theory] of the anion of diacetamide **2g**.

Figure 4b describes the rotation of the second acetyl group around the C-N-bond (variation of φ). When φ is increased from 0 to 15°, a decrease of energy is found and one arrives at the minimum structure **2g-V**. Though structures **2g-I** and **2g-V** look different in the drawings of Figure 4a and 4b, they are identical in reality because also the non-rotating amide bonds deviate slightly from the planarity. A further increase of φ yields the transition state **2g-VI** with almost perpendicular arrangement of the two carbonyl groups. The 11 kJ mol⁻¹ energy difference between **2g-II** and **2g-VI** can be explained by the more favorable orientation of the dipole moment of the in-plane carbonyl group with the nitrogen lone pair in **2g-II** than in **2g-VI**. A shallow minimum is reached for $\varphi = 150^\circ$, but further increase of φ did not lead to **2g-VIII** as the transition state of the φ -rotation, because the structure converged to **2g-O**, when φ was fixed at 180°. The W-shaped arrangement **2g-VIII** was, therefore, calculated with fixed dihedral angles and found 43 kJ mol⁻¹ above the global minimum **2g-V**. Steric hindrance of the two methyl groups in the W-conformer and unfavorable interactions of the dipole moments of the carbonyl groups with the lone pair on nitrogen account for its low stability. In line with previous studies by Würthwein,^[46] the C-N-C angle remains almost constant (122–124°) during both rotations, and not even the 90°-transition states, where the two carbonyl groups interact with different lone pairs at nitrogen, adopt allenic structures with a quasi-linear C=N=C fragment. Since in the global minimum, one of the two lone pairs at nitrogen is almost unaffected by the substituents, it is not surprising that the second electron acceptor substituent affects the nucleophilicity of imide anions only slightly, contrasting the situation in carbanions.

Correlation with Brønsted Basicities

Figure 5 shows that the correlation between nucleophilicity and Brønsted basicity is even worse for the amide and imide anions **2** than for the carbanions **4**. Thus, the cyanamide anion **2n** and the trifluoroacetamide anions **2d** and **2e**, anions of similar basicity, differ by 10³ in nucleophilic reactivity. Despite the low quality of the correlations for both classes of compounds, it is evident from the two Brønsted plots in Figure 5 that nitrogen centered anions **2** are generally less nucleophilic than carbanions of similar p*K*_{aH}. Bordwell has analogously reported that the anions of substituted anilines (ArNH⁻) react more slowly with *n*-butyl chloride in DMSO than carbanions (ArCHCN⁻) of the same p*K*_{aH}.^[47]

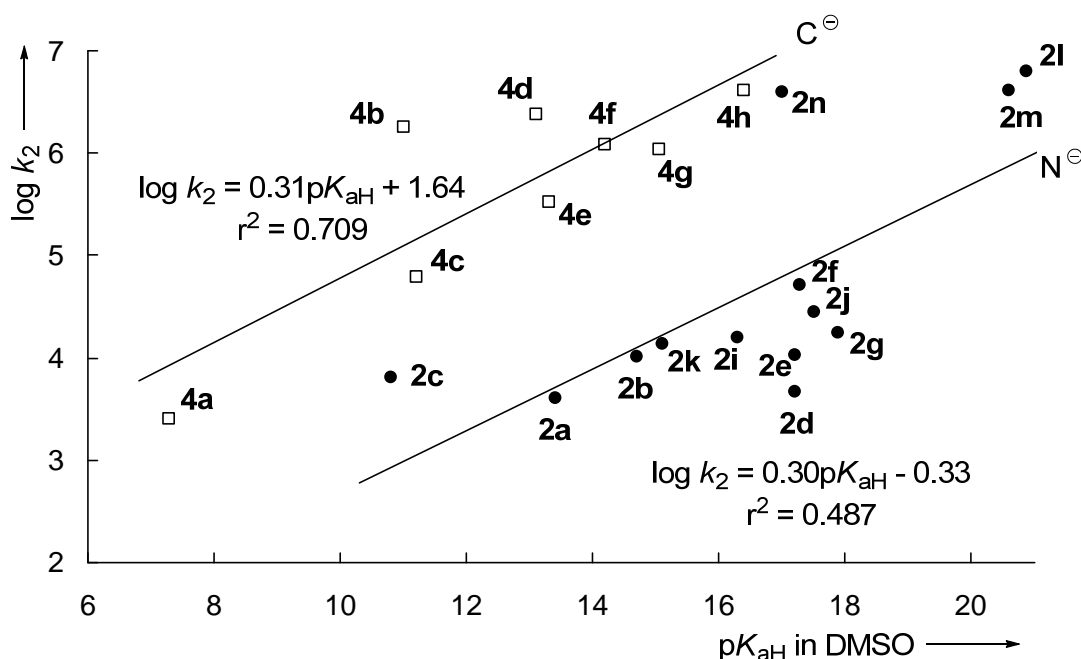
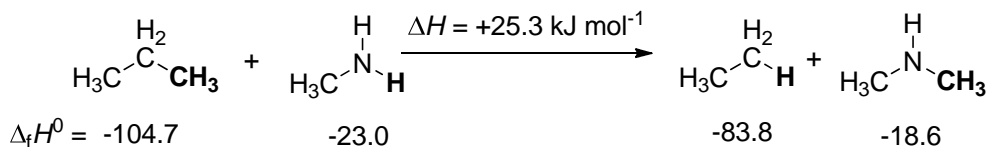


Figure 5: Relationship between Brønsted basicity and $\log k_2$ for the reaction of **1i** with several amide and imide anions (●) as well as with some acceptor-stabilized carbanions (□) in DMSO [pK_{aH} in DMSO from ref. ^[20]: **4a**: Meldrum's acid 7.3, **4b**: malodinitrile 11.1, **4c**: dimedone 11.0, **4e**: acetylacetone 13.3, **4f**: ethyl acetylacetate 14.2, **4g**: 3-methylacetylacetone 15.05, **4h**: diethyl malonate 16.4; pK_{aH} in DMSO from ref. ^[48]: **4d**: ethyl cyanoacetate 13.1].

Two effects have to be considered when explaining the separation of these Brønsted plots. While the Brønsted basicities refer to reactions with the proton (H^+), the nucleophilic reactivities refer to the formation of a bond to carbon. The reaction in Scheme 9 shows that the transfer of a methyl group from carbon to nitrogen is endothermic by 25 kJ mol^{-1} , i.e., hydrogen prefers to sit at nitrogen and CH_3 prefers carbon. As a consequence, carbanions that have a similar affinity towards protons as amide anions (comparable pK_{aH}) have a higher affinity towards carbon, a trend which is also reflected by the kinetics, i.e., the higher k_2 -values of carbanions towards carbon-centered electrophiles shown in Figure 5.



Scheme 9: Reaction enthalpy (gas phase, in kJ mol^{-1}) for the methyl-hydrogen-exchange between carbon and nitrogen.^[50]

Despite the poor correlation between pK_{aH} and nucleophilic reactivity, carbanions are generally stronger nucleophiles than amide anions of similar basicity. Figure 6 furthermore shows that phthalimide and maleimide anions have similar nucleophilicities in DMSO as primary alkylamines and are weaker nucleophiles than secondary alkylamines though the amide anions are significantly stronger bases. The latter comparison again illustrates that Brønsted basicities are a poor guide for estimating nucleophilic reactivities, even when reagents with the same central atom are compared. The knowledge of carbon basicities^[51] is needed to elucidate the reason for the breakdown of the Brønsted correlations.

5 Experimental Section

5.1 General

In order to identify my contribution to this multiauthor publication, this Experimental Section consists exclusively of the experiments, which were performed by me.

Materials

Commercially available DMSO and acetonitrile (both: H₂O content < 50 ppm) were used without further purification. The reference electrophiles used in this work were synthesized according to literature procedures.^[10] Ethyl acetylcarbamate was synthesized according to Ref^[52]. Potassium salts of 2,2,2-trifluoroacetamide and of other amides were prepared by treatment of the corresponding amide with KOtBu in dimethoxyethane.^[53]

NMR spectroscopy

In the ¹H- and ¹³C-NMR spectra chemical shifts are given in ppm and refer to tetramethylsilane ($\delta_{\text{H}} = 0.00$, $\delta_{\text{C}} = 0.0$), *d*₆-DMSO ($\delta_{\text{H}} = 2.50$, $\delta_{\text{C}} = 39.4$), CD₃CN ($\delta_{\text{H}} = 1.94$, $\delta_{\text{C}} = 1.3$ and 118.3), or to CDCl₃ ($\delta_{\text{H}} = 7.26$, $\delta_{\text{C}} = 77.0$) as internal standards. The coupling constants are given in Hz.

Kinetics

As the reactions of colored benzhydrylium ions or quinone methides with colorless imide or amide anions result in colorless products, the reactions were followed by UV-Vis spectroscopy. Slow reactions ($\tau_{1/2} > 10$ s) were determined by using conventional UV-Vis-spectrophotometers. Stopped-flow techniques were used for the investigation of rapid reactions ($\tau_{1/2} < 10$ s). The temperature of solutions was kept constant at 20.0 ± 0.1 °C during all kinetic studies by using a circulating bath thermostat. The nucleophile concentration was always at least 10 times higher than the concentration of the electrophile, resulting in pseudo-first-order kinetics with an exponential decay of the electrophile concentration. First-order rate constants k_{obs} (s⁻¹) were obtained by least-squares fitting of the absorbance data to a single-exponential $A_t = A_0 \exp(-k_{\text{obs}}t) + C$. The second-order rate constants k_2 (L mol⁻¹ s⁻¹) were obtained from the slopes of the linear plots of k_{obs} against the nucleophile concentration.

5.2 Hammett Correlations

As mentioned above, the decreasing nucleophilicity of the amide anions RNH^- in the series $\text{R} = \text{CN} > \text{SO}_2\text{CH}_3 \approx \text{SO}_2\text{Tol} > \text{COCF}_3$ (left column of Scheme 5) correlates neither with Hammett's σ_p nor σ_p^- constants of these substituents. The individual data are summarized in Figure 7 and Table 5.

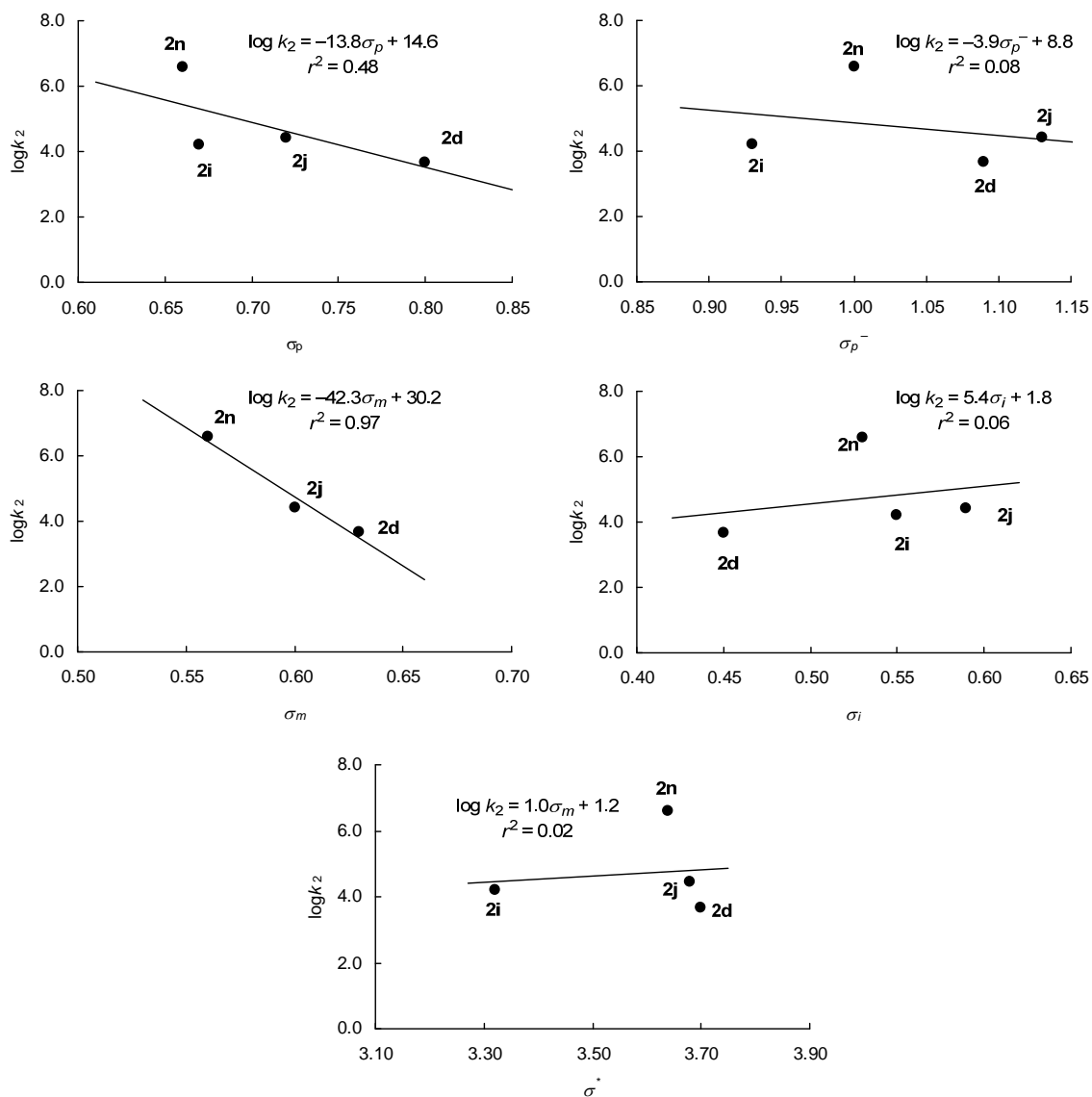
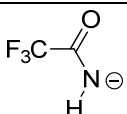
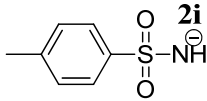
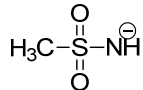


Figure 7: Correlation of the second-order rate constant ($\log k_2$) of **1i** and the amide anions with different σ -parameters (σ_p : top left; σ_p^- : top right; σ_m : middle left; σ_i : middle right and σ^* : bottom).

Table 5: Hammett Substituent Constants for the Amide Anions **2d,i,j,n**.

Nucleophile	k_2 (1i)	$\log k_2$	σ_p	σ_p^-	σ_m	σ^*	σ_i
 2d	4.66×10^3	3.67	0.80 ^a	1.09 ^b	0.63 ^a	3.70 ^a	0.45 ^c
 2i	1.57×10^4	4.20	0.67 ^d	0.93 ^e	—	3.32 ^d	0.55 ^f
 2j	2.73×10^4	4.44	0.72 ^g	1.13 ^h	0.60 ^g	3.68 ^f	0.59 ^c
 2n	3.85×10^6	6.59	0.66 ⁱ	1.00 ^a	0.56 ^g	3.64 ^a	0.53 ^a

^a Ref. [54]. ^b Ref. [55]. ^c Ref. [56]. ^d Ref. [57]. ^e Ref. [58]. ^f Ref. [59]. ^g Ref. [60]. ^h Ref. [61]. ⁱ Ref. [62].

5.3 Synthesis of Potassium Salts of Imides and Amides

General Procedure:

The potassium salts (**2c-n**)-**K** were generated by deprotonation of the corresponding compound (**2c-n**)-**H** with KO^tBu in dry dimethoxyethane or dry ethanol under nitrogen atmosphere. After removal of volatiles, the remaining solid was crushed and washed several times with dry ether.^[53]

Maleimide-Potassium (**2c-K**)

3.0 g (22 mmol, 96 %) of maleimide-potassium (**2c-K**) was obtained from maleimide (2.2 g, 23 mmol) and KO^tBu (2.6 g, 23 mmol).

¹H-NMR (400 MHz, d₆-DMSO): δ = 6.28 (s). ¹³C-NMR (100 MHz, d₆-DMSO): δ = 126.6 (d), 180.1 (s).

N-Methyl-2,2,2-trifluoroacetamide-Potassium (**2e-K**)

2.46 g (14.9 mmol, 95 %) of N-methyl-2,2,2-trifluoroacetamide-potassium (**2e-K**) (mp 249-250 °C, decomp.) was obtained from N-methyl-2,2,2-trifluoroacetamide (2.05 g, 16.1 mmol) and KO^tBu (1.76 g, 15.7 mmol).

¹H-NMR (400 MHz, d₆-DMSO): δ = 2.52 (q, J_{CF} = 2.5 Hz). ¹³C-NMR (100 MHz, d₆-DMSO): δ = 32.3, 119.7 (q, J_{CF} = 287 Hz), 158.9 (q, J_{CF} = 28.9 Hz).

3,3-Dimethylglutarimide-Potassium (2f-K)

2.0 g (11 mmol, 79 %) of 3,3-dimethylglutarimide-potassium (**2f-K**) (mp 247–249 °C) was obtained from 3,3-dimethylglutarimide (2.0 g, 14 mmol) and KO*t*Bu (1.7 g, 15 mmol).

¹H-NMR (400 MHz, d₆-DMSO): δ = 0.86 (s, 6 H), 1.89 (s, 4 H). ¹³C-NMR (100 MHz, d₆-DMSO): δ = 28.4 (q), 30.4 (s), 47.0 (t), 183.4 (s).

Diacetamide-Potassium (2g-K)

2.5 g (18 mmol, 90 %) of diacetamide-potassium (**2g-K**) (mp 140–142 °C) was obtained from diacetamide (2.0 g, 20 mmol) and KO*t*Bu (2.3 g, 20 mmol).

¹H-NMR (400 MHz, d₆-DMSO): δ = 1.75 (s, 6 H). ¹³C-NMR (100 MHz, d₆-DMSO): δ = 27.1 (q), 179.0 (s).

Ethyl acetylcarbamate-Potassium (2h-K)

2.1 g (12 mmol, 80 %) of ethyl acetylcarbamate-potassium (**2h-K**) (mp 260–261 °C, decomp.) was obtained from ethyl acetylcarbamate (2.0 g, 15 mmol) and KO*t*Bu (1.8 g, 16 mmol).

¹H-NMR (400 MHz, d₆-DMSO, 18-crown-6): δ = 1.07 (t, ³*J* = 7.1 Hz), 1.78 (s), 3.78 (q, ³*J* = 7.1 Hz). ¹³C-NMR (100 MHz, d₆-DMSO, 18-crown-6): δ = 15.0 (q), 26.5 (q), 57.9 (t), 162.0 (s), 178.0 (s).

p-Toluenesulfonamide-Potassium (2i-K)

2.10 g (10.0 mmol, 88 %) of *p*-toluenesulfonamide-potassium (**2i-K**) (mp 224–225 °C) was obtained from *p*-toluenesulfonamide (2.00 g, 11.7 mmol) and KO*t*Bu (1.28 g, 11.3 mmol).

¹H-NMR (400 MHz, d₆-DMSO): δ = 2.29 (s, 3 H), 2.88 (br s, 1 H), 7.11 (d, 2 H, ³*J* = 8.0 Hz), 7.61 (d, 2 H, ³*J* = 8.0 Hz). ¹³C-NMR (100 MHz, d₆-DMSO): δ = 20.8 (q), 125.1 (d), 128.0 (d), 137.4 (s), 149.1 (s).

Methanesulfonamide-Potassium (2j-K)

2.61 g (19.6 mmol, 96 %) of methanesulfonamide-potassium (**2j-K**) was obtained from methane sulfonamide (2.00 g, 21.0 mmol) and KO*t*Bu (2.29 g, 20.4 mmol).

¹H-NMR (400 MHz, d₆-DMSO): δ = 2.04 (br s, 1 H), 2.48 (s, 3 H). ¹³C-NMR (100 MHz, d₆-DMSO): δ = 45.4 (q).

2-Oxazolidinon-Potassium (2l-K)

2.45 g (19.6 mmol, 88 %) of 2-Oxazolidinon-potassium (**2l-K**) (mp 180-182 °C) was obtained from 2-Oxazolidinon (2.00 g, 23.0 mmol) and KO*t*Bu (2.50 g, 22.3 mmol).

¹H-NMR (400 MHz, d₆-DMSO, 18-crown-6): δ = 3.27 (t, 2 H, ³J = 8.0 Hz), 3.71 (t, 2 H, ³J = 8.0 Hz). ¹³C-NMR (100 MHz, d₆-DMSO, 18-crown-6): δ = 50.9 (t), 62.2 (t), 165.4 (s).

(S)-4-Benzyloxazolidin-2-one-Potassium (2m-K)

3.31 g (15.4 mmol, 93 %) of (S)-4-benzyloxazolidin-2-one-potassium (**2m-K**) was obtained from (S)-4-benzyloxazolidin-2-one (3.00 g, 16.9 mmol) and KO*t*Bu (1.86 g, 16.6 mmol).

¹H-NMR (400 MHz, d₆-DMSO): δ = 2.36 (dd, 1 H, ³J = 8.0 and 13.2 Hz), 2.72 (dd, 1 H, ³J = 5.3 and 13.2 Hz), 3.64-3.77 (m, 2 H), 7.11-7.25 (m, 5 H). ¹³C-NMR (100 MHz, d₆-DMSO): δ = 44.6 (t), 63.5 (d), 67.0 (t), 125.4 (d), 127.9 (d), 129.0 (d), 140.4 (s), 164.9 (s).

Cyanamide-Potassium (2n-K)

2.21 g (27.6 mmol, 97 %) of cyanamide-potassium (**2n-K**) (mp 200 °C, decomp.) was obtained from cyanamide (1.20 g, 28.5 mmol) and KO*t*Bu (3.40 g, 30.3 mmol).

¹³C-NMR (100 MHz, d₆-DMSO): δ = 134.7 (s).

5.4 Isolated Reaction Products

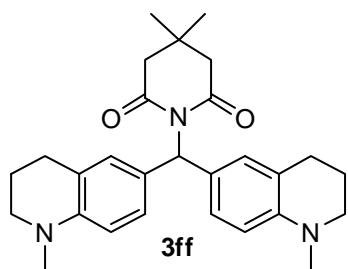
General Procedure:

In a carefully dried, nitrogen-flushed Schlenk-flask a solution of the amide- or imide-salt in approx. 5 mL DMSO was added dropwise to a solution of the benzhydrylium tetrafluoroborate in 5 mL DMSO. After stirring at ambient temperature for several minutes, approx. 50 mL cold water was added and then, the precipitated material was collected by filtration. After washing with water, the solid was dried under reduced pressure.

The differentiation between nitrogen and oxygen attack is based on two-dimensional NMR spectroscopy (HSQC and HMBC).

Reaction of (thq)₂CH⁺ with 3,3'-Dimethylglutarimide potassium salt 2f-K:

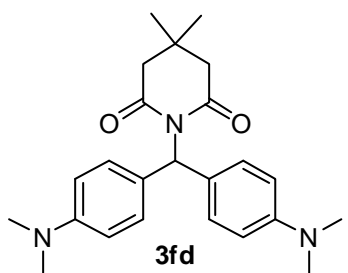
40 mg (0.090 mmol, 51 %) of 1-(Bis(1-methylindolin-5-yl)methyl)-4,4-dimethylpiperidine-2,6-dione (**3ff**) were obtained from 32.2 mg (0.180 mmol) of **2f-K** and 69.4 mg (0.177 mmol) of benzhydrylium tetrafluoroborate **1f**.



$^1\text{H-NMR}$ (400 MHz, d_6 -DMSO): δ = 0.98 (s, 6 H), 1.86 (m, 4 H), 2.51-2.61 (m, 8 H), 2.80 (s, 6 H), 3.15 (m, 4 H), 6.47 (d, 2 H, 3J = 8.3 Hz), 6.73-6.76 (m, 3 H), 6.84 (d, 2 H, 3J = 8.3 Hz). $^{13}\text{C-NMR}$ (100 MHz, d_6 -DMSO): δ = 22.0 (t), 27.0 (q), 27.3 (t), 28.8 (s), 38.7 (q), 46.0 (t), 50.5 (t), 56.7 (d), 110.2 (d), 121.3 (s), 126.6 (s), 127.0 (d), 128.6 (d), 145.2 (s), 171.9 (s).

Reaction of $(\text{dma})_2\text{CH}^+$ with 3,3'-Dimethylglutarimide potassium salt **2f-K**:

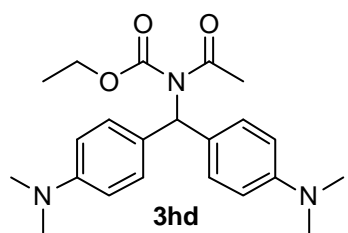
34 mg (0.086 mmol, 86 %) of 1-(Bis(4-(dimethylamino)phenyl)methyl)-4,4-dimethylpiperidine-2,6-dione (**3fd**) were obtained from 18 mg (0.10 mmol) of **2f-K** and 34 mg (0.10 mmol) of benzhydrylium tetrafluoroborate **1d**.



$^1\text{H-NMR}$ (300 MHz, CDCl_3): δ = 1.07 (s, 6 H), 2.51 (s, 4 H), 2.92 (s, 12 H), 6.65 (d, 4 H, 3J = 8.7 Hz), 7.04 (s, 1H), 7.18 (d, 4 H, 3J = 8.7 Hz). $^{13}\text{C-NMR}$ (75 MHz, CDCl_3): δ = 27.8 (q), 29.1 (s), 40.6 (q), 47.2 (t), 57.8 (d), 112.1 (d), 127.3 (s), 129.5 (d), 149.5 (s), 171.9 (s).

Reaction of $(\text{dma})_2\text{CH}^+$ with ethyl acetyl carbamate potassium salt **2h-K**:

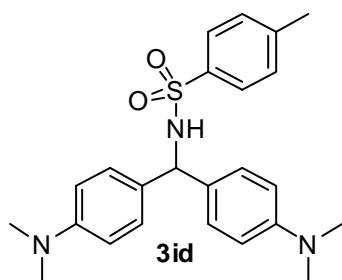
25 mg (0.065 mmol, 54 %) of ethyl acetyl(bis(4-(dimethylamino)phenyl)methyl)carbamate (**3hd**) were obtained from 21 mg (0.12 mmol) of **2h-K** and 41 mg (0.12 mmol) of benzhydrylium tetrafluoroborate **1d**.



$^1\text{H-NMR}$ (300 MHz, CDCl_3): δ = 1.02 (t, 3 H, 3J = 7.1 Hz), 2.49 (s, 3 H), 2.93 (s, 12 H), 3.97 (q, 2 H, 3J = 7.1 Hz), 6.66 (d, 4 H, 3J = 8.8 Hz), 6.98 (s, 1 H), 7.14 (d, 4 H, 3J = 8.7 Hz). $^{13}\text{C-NMR}$ (75 MHz, CDCl_3): δ = 13.7 (q), 26.5 (q), 40.6 (q), 60.2 (d), 62.6 (t), 112.1 (d), 127.6 (s), 129.3 (d), 149.6 (s), 155.3 (s), 172.6 (s).

Reaction of $(\text{dma})_2\text{CH}^+$ with *p*-toluenesulfonamide potassium salt **2i-K**:

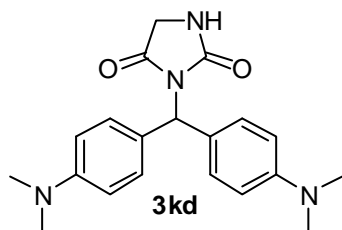
68 mg (0.16 mmol, 73 %) of *N*-(bis(4-(dimethylamino)phenyl)methyl)-4-methylbenzenesulfonamide (**3id**) were obtained from 46 mg (0.22 mmol) of **2i-K** and 75 mg (0.22 mmol) of benzhydrylium tetrafluoroborate **1d**.



$^1\text{H-NMR}$ (400 MHz, CD_3CN): δ = 2.40 (s, 3H), 2.88 (s, 12 H), 6.12 (s, 1H), 6.62 (d, 4 H, 3J = 8.7 Hz), 6.86 (d, 4 H, 3J = 8.7 Hz), 7.30 (d, 2 H, 3J = 8.2 Hz), 7.64 (d, 2 H, 3J = 8.2 Hz). $^{13}\text{C-NMR}$ (100 MHz, CD_3CN): δ = 21.6 (q), 40.8 (q), 64.6 (d), 113.0 (d), 127.7 (d), 128.1 (s), 130.4 (d), 130.6 (d), 138.3 (s), 144.4 (s), 151.1 (s).

Reaction of $(\text{dma})_2\text{CH}^+$ with hydantoin postassium salt **2k-K**:

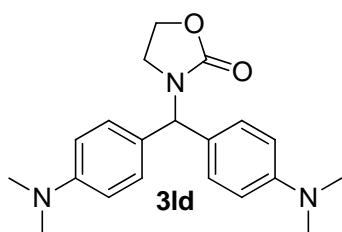
118 mg (0.335 mmol, 84 %) of 3-(bis(4-(dimethylamino)phenyl)methyl)imidazolidine-2,4-dione (**3kd**) were obtained from 43 mg (0.43 mmol) of **2k-H**, 52 mg (0.46 mmol) of $\text{KO}t\text{Bu}$ and 135 mg (0.397 mmol) of benzhydrylium tetrafluoroborate **1d**.



$^1\text{H-NMR}$ (400 MHz, CD_3CN): δ = 2.90 (s, 12 H), 3.84 (d, 2 H, 3J = 1.3 Hz), 6.05 (br s, 1H), 6.22 (s, 1 H), 6.69 (d, 4 H, 3J = 8.7 Hz), 7.13 (d, 4 H, 3J = 8.7 Hz). $^{13}\text{C-NMR}$ (100 MHz, CD_3CN): δ = 40.9 (q), 46.9 (t), 58.2 (d), 113.1 (d), 127.7 (s), 130.3 (d), 151.2 (s), 158.9 (s), 172.8 (s).

Reaction of $(\text{dma})_2\text{CH}^+$ with 2-oxazolidinone potassium salt **2l-K**:

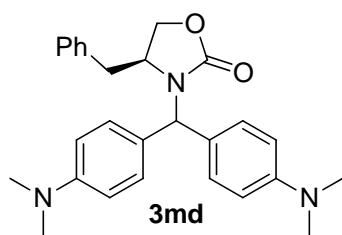
70 mg (0.21 mmol, 84 %) of 3-(bis(4-(dimethylamino)phenyl)methyl)oxazolidin-2-one (**3ld**) were obtained from 32 mg (0.26 mmol) of **2l-K** and 86 mg (0.25 mmol) of benzhydrylium tetrafluoroborate **1d**.



$^1\text{H-NMR}$ (300 MHz, CDCl_3): δ = 2.95 (s, 12 H), 3.37 (t, 2 H, 3J = 8.0 Hz), 4.29 (t, 2 H, 3J = 8.0 Hz), 6.19 (s, 1H), 6.69 (d, 4 H, 3J = 8.5 Hz), 7.09 (d, 4 H, 3J = 8.5 Hz). $^{13}\text{C-NMR}$ (75 MHz, CDCl_3): δ = 40.5 (q), 41.5 (t), 59.7 (d), 62.0 (t), 112.3 (d), 126.2 (s), 129.2 (d), 149.9 (s), 158.3 (s).

Reaction of $(\text{dma})_2\text{CH}^+$ with (*S*)-4-benzyloxazolidin-2-one-potassium salt **2m-K**:

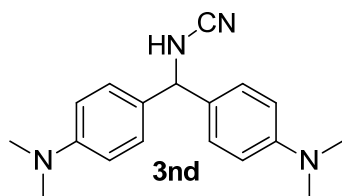
190 mg (0.442 mmol, 94 %) of (*S*)-4-benzyl-3-(bis(4-(dimethylamino)phenyl)methyl)oxazolidin-2-one (**3md**) were obtained from 106 mg (0.492 mmol) of **2m-K** and 160 mg (0.470 mmol) of benzhydrylium tetrafluoroborate **1d**.



$^1\text{H-NMR}$ (400 MHz, d_6 -DMSO): δ = 2.51 (m, 1 H), 2.57-2.60 (m, 1 H), 2.85 (s, 6 H), 2.86 (s, 6 H), 3.80-3.83 (m, 1H), 4.00-4.03 (m, 1 H), 4.11-4.15 (m, 1 H), 5.90 (s, 1 H), 6.69-6.72 (m, 4 H), 6.94-6.95 (m, 2 H), 7.07-7.09 (m, 2 H), 7.14-7.21 (m, 5 H). $^{13}\text{C-NMR}$ (100 MHz, d_6 -DMSO): δ = 40.1 (t), 40.2 (q), 56.0 (d), 60.2 (d), 66.2 (t), 112.0 (d), 112.2 (d), 126.6 (s), 126.9 (d), 128.4 (d), 128.8 (d), 129.0 (d), 129.1 (d), 136.4 (s), 149.7 (s), 157.1 (s).

Reaction of $(\text{dma})_2\text{CH}^+$ with cyanamide potassium salt **2n-K**:

179 mg (0.608 mmol, 95 %) of *N*-(bis(4-(dimethylamino)phenyl)methyl)cyanamide (**3nd**) were obtained from 51.4 mg (0.641 mmol) of **2n-K** and 217 mg (0.638 mmol) of benzhydrylium tetrafluoroborate **1d**.



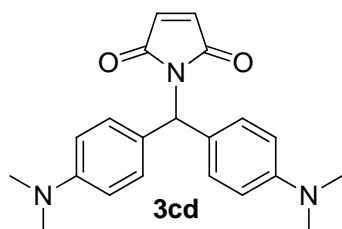
$^1\text{H-NMR}$ (300 MHz, CDCl_3): δ = 2.93 (s, 12 H), 5.05 (s, 1 H), 6.69 (d, 4 H, $^3J = 6.7$ Hz), 6.94 (br s 1H), 7.20 (d, 4 H, $^3J = 6.7$ Hz). $^{13}\text{C-NMR}$ (75 MHz, CDCl_3): δ = 40.6 (q), 66.3 (d), 112.5 (d), 127.0 (s), 128.2 (s), 129.4 (d), 150.2 (s).

5.5 NMR-Characterized Products

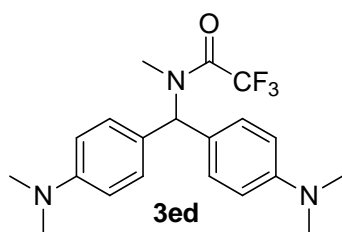
General Procedure:

In an NMR-tube equimolar amounts (approx. 5-20 mg) of the amide- or imide-salt and the benzhydrylium tetrafluoroborate were mixed in 1 mL d_6 -DMSO. NMR spectra were recorded shortly after the mixing.

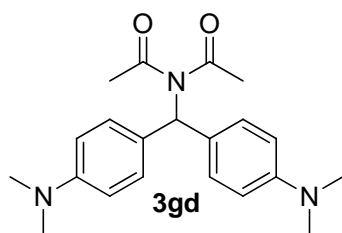
Reaction of $(\text{dma})_2\text{CH}^+$ with maleimide potassium salt **2c-K**:



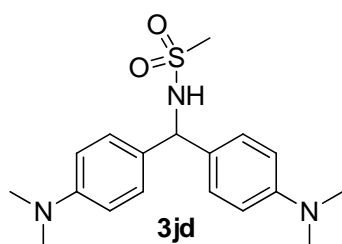
$^1\text{H-NMR}$ (400 MHz, d_6 -DMSO): δ = 2.86 (s, 12 H), 6.19 (s, 1 H), 6.66 (d, 4 H, $^3J = 8.9$ Hz), 7.01-7.03 (m, 6 H). $^{13}\text{C-NMR}$ (100 MHz, d_6 -DMSO): δ = 40.1 (q), 56.1 (d), 112.0 (d), 126.2 (s), 128.9 (d), 134.6 (d), 149.6 (s), 170.9 (s).

Reaction of $(\text{dma})_2\text{CH}^+$ with *N*-methyl-trifluoroacetamide potassium salt **2e-K**:

$^1\text{H-NMR}$ (400 MHz, $\text{d}_6\text{-DMSO}$): δ = 2.83 (s, 3 H), 2.89 (s, 12 H), 6.59 (s, 1 H), 6.72 (d, 4 H, $^3J = 8.8$ Hz), 6.97 (d, 4 H, $^3J = 8.7$ Hz). $^{13}\text{C-NMR}$ (100 MHz, $\text{d}_6\text{-DMSO}$): δ = 40.0 (q), 61.6 (d), 112.3 (d), 116.5 (q, $J_{\text{CF}} = 286$ Hz), 124.5 (s), 129.0 (d), 149.8 (s), 155.9 (q, $J_{\text{CF}} = 35$ Hz).

Reaction of $(\text{dma})_2\text{CH}^+$ with diacetamide potassium salt **2g-K**:

$^1\text{H-NMR}$ (400 MHz, $\text{d}_6\text{-DMSO}$): δ = 2.19 (s, 6 H), 2.88 (s, 12 H), 6.57 (s, 1 H), 6.67 (d, 4 H, $^3J = 8.8$ Hz), 7.03 (d, 4 H, $^3J = 8.8$ Hz). $^{13}\text{C-NMR}$ (100 MHz, $\text{d}_6\text{-DMSO}$): δ = 26.7 (q), 40.1 (q), 61.2 (d), 111.9 (d), 126.4 (s), 128.8 (d), 149.3 (s), 174.1 (s).

Reaction of $(\text{dma})_2\text{CH}^+$ with methanesulfonamide potassium salt **2j-K**:

$^1\text{H-NMR}$ (400 MHz, $\text{d}_6\text{-DMSO}$): δ = 2.52 (s, 3 H), 2.85 (s, 12 H), 5.35 (s, 1 H), 6.67 (d, 4 H, $^3J = 8.9$ Hz), 7.15 (d, 4 H, $^3J = 8.8$ Hz), 7.58 (br s, 1H). $^{13}\text{C-NMR}$ (100 MHz, $\text{d}_6\text{-DMSO}$): δ = 40.2 (q), 41.3 (q), 59.8 (d), 112.1 (d), 127.8 (d), 130.2 (s), 149.4 (s)

5.6 Kinetic StudiesPotassium Salt of Maleimide (**2c-K**)Table 6: Kinetics of the reaction of **2c-K** with **1e** (20 °C, in DMSO, stopped-flow, at 620 nm).

[E] [mol L ⁻¹]	[Nu] [mol L ⁻¹]	[Nu]/[E]	k_{obs} [s ⁻¹]
2.20×10^{-5}	3.70×10^{-4}	16.8	127
2.20×10^{-5}	5.55×10^{-4}	25.2	216
2.20×10^{-5}	7.40×10^{-4}	33.6	274
2.20×10^{-5}	9.25×10^{-4}	42.0	341

$$k_2 = 3.79 \times 10^5 \text{ L mol}^{-1} \text{ s}^{-1}$$

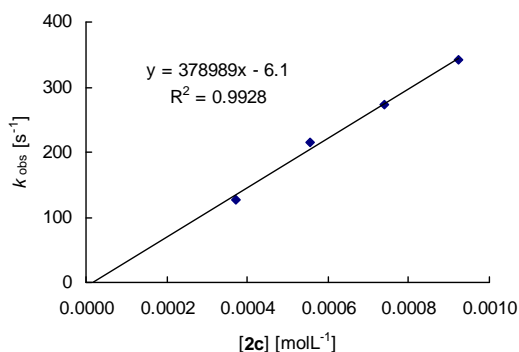
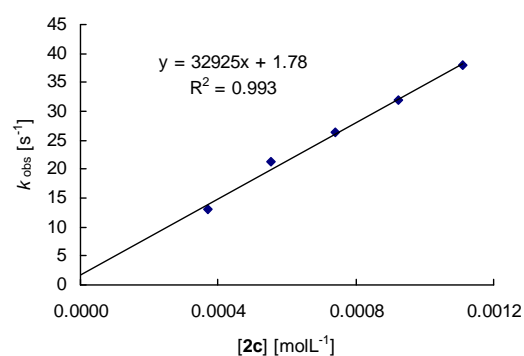


Table 7: Kinetics of the reaction of **2c-K** with **1g** (20 °C, in DMSO, stopped-flow, at 627 nm).

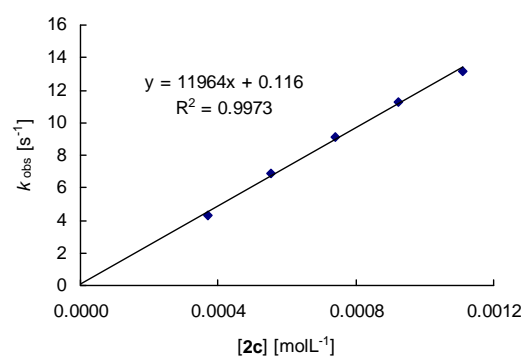
[E] [mol L ⁻¹]	[Nu] [mol L ⁻¹]	[Nu]/[E]	<i>k</i> _{obs} [s ⁻¹]
2.06 × 10 ⁻⁵	3.70 × 10 ⁻⁴	18.0	13.0
2.06 × 10 ⁻⁵	5.55 × 10 ⁻⁴	26.9	21.3
2.06 × 10 ⁻⁵	7.40 × 10 ⁻⁴	35.9	26.3
2.06 × 10 ⁻⁵	9.25 × 10 ⁻⁴	44.9	32.0
2.06 × 10 ⁻⁵	1.11 × 10 ⁻³	53.9	38.1

$$k_2 = 3.29 \times 10^4 \text{ L mol}^{-1} \text{ s}^{-1}$$

Table 8: Kinetics of the reaction of **2c-K** with **1h** (20 °C, in DMSO, stopped-flow, at 635 nm).

[E] [mol L ⁻¹]	[Nu] [mol L ⁻¹]	[Nu]/[E]	<i>k</i> _{obs} [s ⁻¹]
2.34 × 10 ⁻⁵	3.70 × 10 ⁻⁴	15.8	4.34
2.34 × 10 ⁻⁵	5.55 × 10 ⁻⁴	23.7	6.89
2.34 × 10 ⁻⁵	7.40 × 10 ⁻⁴	31.6	9.11
2.34 × 10 ⁻⁵	9.25 × 10 ⁻⁴	39.5	11.3
2.34 × 10 ⁻⁵	1.11 × 10 ⁻³	47.4	13.2

$$k_2 = 1.20 \times 10^4 \text{ L mol}^{-1} \text{ s}^{-1}$$

Table 9: Kinetics of the reaction of **2c-K** with **1i** (20 °C, in DMSO, stopped-flow, at 630 nm).

[E] [mol L ⁻¹]	[Nu] [mol L ⁻¹]	[Nu]/[E]	<i>k</i> _{obs} [s ⁻¹]
2.50 × 10 ⁻⁵	3.70 × 10 ⁻⁴	14.8	2.01
2.50 × 10 ⁻⁵	5.55 × 10 ⁻⁴	22.2	3.06
2.50 × 10 ⁻⁵	7.40 × 10 ⁻⁴	29.6	4.35
2.50 × 10 ⁻⁵	9.25 × 10 ⁻⁴	37.0	5.51
2.50 × 10 ⁻⁵	1.11 × 10 ⁻³	44.4	6.63

$$k_2 = 6.32 \times 10^3 \text{ L mol}^{-1} \text{ s}^{-1}$$

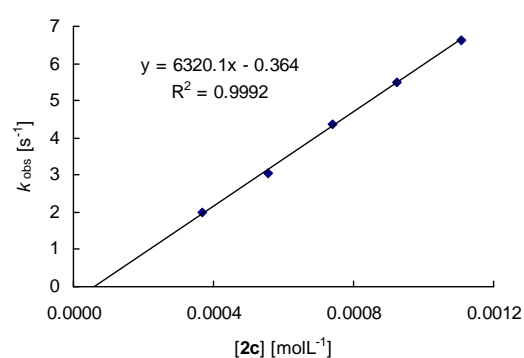
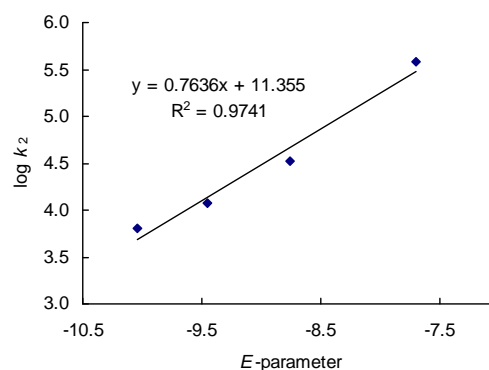


Table 10: Determination of *N*- and *s*-parameters for **2c** at 20 °C in DMSO.

Electrophile	<i>E</i> -parameter	k_2 [L mol ⁻¹ s ⁻¹]	log k_2
1e	-7.69	3.79×10^5	5.58
1g	-8.76	3.29×10^4	4.52
1h	-9.45	1.20×10^4	4.08
1i	-10.04	6.32×10^3	4.80

$$N = 14.87; s = 0.76$$

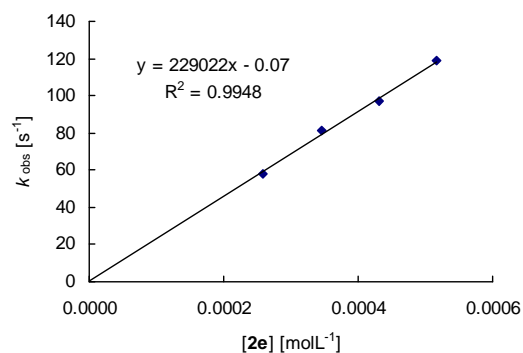


Potassium Salt of *N*-Methyl-2,2,2-Trifluoroacetamide (**2e-K**)

Table 11: Kinetics of the reaction of **2e-K** with **1f** (20 °C, in DMSO, stopped-flow, at 618 nm).

[E] [mol L ⁻¹]	[Nu] [mol L ⁻¹]	[Nu]/[E]	k_{obs} [s ⁻¹]
2.35×10^{-5}	2.59×10^{-4}	11.0	58.3
2.35×10^{-5}	3.45×10^{-4}	14.7	81.3
2.35×10^{-5}	4.31×10^{-4}	18.4	96.8
2.35×10^{-5}	5.18×10^{-4}	22.1	119

$$k_2 = 2.29 \times 10^5 \text{ L mol}^{-1} \text{ s}^{-1}$$

Table 12: Kinetics of the reaction of **2e-K** with **1g** (20 °C, in DMSO, stopped-flow, at 627 nm).

[E] [mol L ⁻¹]	[Nu] [mol L ⁻¹]	[Nu]/[E]	k_{obs} [s ⁻¹]
2.23×10^{-5}	2.59×10^{-4}	11.6	15.2
2.23×10^{-5}	3.88×10^{-4}	17.4	22.8
2.23×10^{-5}	4.31×10^{-4}	19.3	24.7
2.23×10^{-5}	5.18×10^{-4}	23.2	31.6

$$k_2 = 6.22 \times 10^4 \text{ L mol}^{-1} \text{ s}^{-1}$$

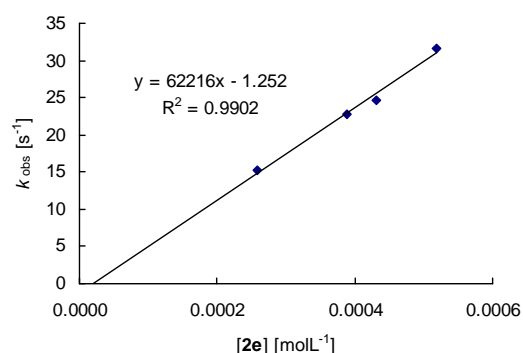
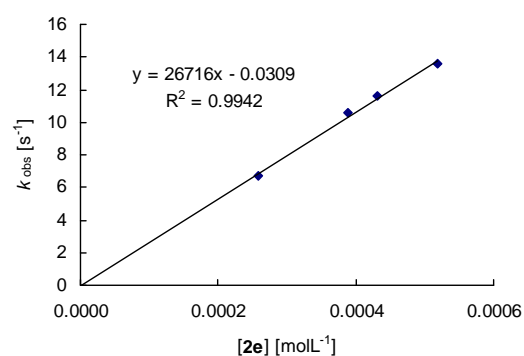


Table 13: Kinetics of the reaction of **2e-K** with **1h** (20 °C, in DMSO, stopped-flow, at 635 nm).

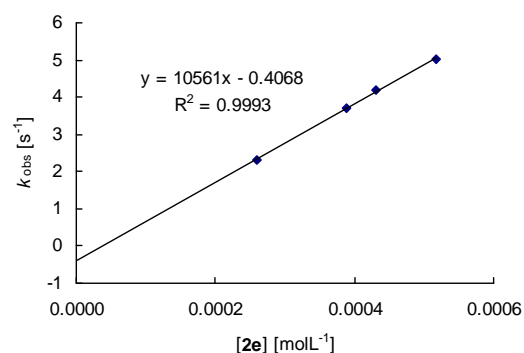
[E] [mol L ⁻¹]	[Nu] [mol L ⁻¹]	[Nu]/[E]	<i>k</i> _{obs} [s ⁻¹]
2.49 × 10 ⁻⁵	2.59 × 10 ⁻⁴	10.4	6.72
2.49 × 10 ⁻⁵	3.88 × 10 ⁻⁴	15.6	10.6
2.49 × 10 ⁻⁵	4.31 × 10 ⁻⁴	17.3	11.6
2.49 × 10 ⁻⁵	5.18 × 10 ⁻⁴	20.8	13.6

$$k_2 = 2.67 \times 10^4 \text{ L mol}^{-1} \text{ s}^{-1}$$

Table 14: Kinetics of the reaction of **2e-K** with **1i** (20 °C, in DMSO, stopped-flow, at 630 nm).

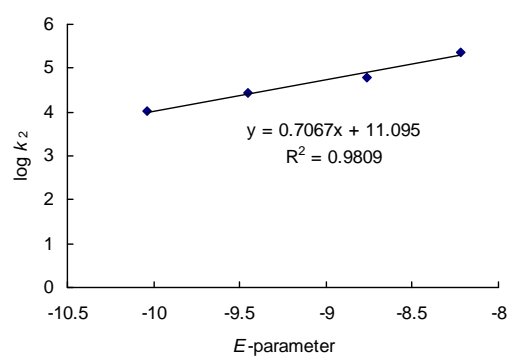
[E] [mol L ⁻¹]	[Nu] [mol L ⁻¹]	[Nu]/[E]	<i>k</i> _{obs} [s ⁻¹]
2.32 × 10 ⁻⁵	2.59 × 10 ⁻⁴	11.2	2.31
2.32 × 10 ⁻⁵	3.88 × 10 ⁻⁴	16.7	3.70
2.32 × 10 ⁻⁵	4.31 × 10 ⁻⁴	18.6	4.19
2.32 × 10 ⁻⁵	5.18 × 10 ⁻⁴	22.3	5.03

$$k_2 = 1.06 \times 10^4 \text{ L mol}^{-1} \text{ s}^{-1}$$

Table 15: Determination of *N*- and *s*-parameters for **2e** at 20 °C in DMSO.

Electrophile	<i>E</i> -parameter	<i>k</i> ₂ [L mol ⁻¹ s ⁻¹]	log <i>k</i> ₂
1f	-8.22	2.29 × 10 ⁵	5.36
1g	-8.76	6.22 × 10 ⁴	4.79
1h	-9.45	2.67 × 10 ⁴	4.42
1i	-10.04	1.06 × 10 ⁴	4.03

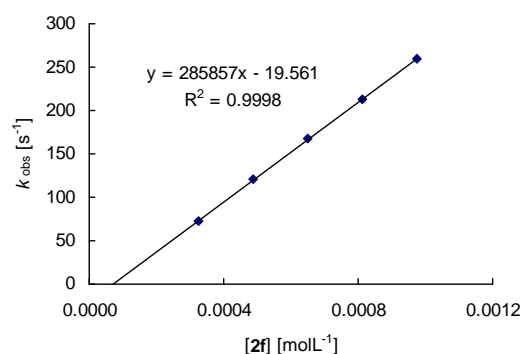
$$N = 15.70; s = 0.71$$



Potassium Salt of 3,3-Dimethylglutarimide (2f-K)Table 16: Kinetics of the reaction of **2f-K** with **1g** (20 °C, in DMSO, stopped-flow, at 627 nm).

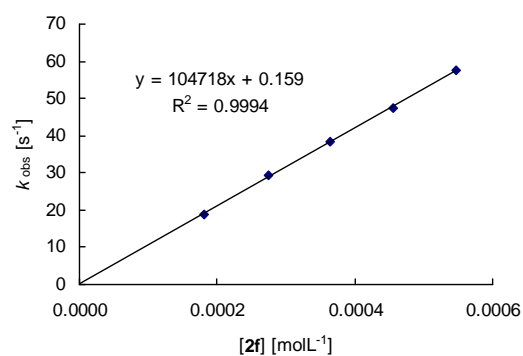
[E] [mol L ⁻¹]	[Nu] [mol L ⁻¹]	[Nu]/[E]	<i>k</i> _{obs} [s ⁻¹]
2.91 × 10 ⁻⁵	3.26 × 10 ⁻⁴	11.2	72.4
2.91 × 10 ⁻⁵	4.89 × 10 ⁻⁴	16.8	121
2.91 × 10 ⁻⁵	6.52 × 10 ⁻⁴	22.4	168
2.91 × 10 ⁻⁵	8.14 × 10 ⁻⁴	28.0	213
2.91 × 10 ⁻⁵	9.77 × 10 ⁻⁴	33.6	259

$$k_2 = 2.86 \times 10^5 \text{ L mol}^{-1} \text{ s}^{-1}$$

Table 17: Kinetics of the reaction of **2f-K** with **1h** (20 °C, in DMSO, stopped-flow, at 635 nm).

[E] [mol L ⁻¹]	[Nu] [mol L ⁻¹]	[Nu]/[E]	<i>k</i> _{obs} [s ⁻¹]
2.95 × 10 ⁻⁵	1.82 × 10 ⁻⁴	8.9	19.0
2.95 × 10 ⁻⁵	2.74 × 10 ⁻⁴	13.4	29.3
2.95 × 10 ⁻⁵	3.65 × 10 ⁻⁴	17.8	38.4
2.95 × 10 ⁻⁵	4.56 × 10 ⁻⁴	22.2	47.4
2.95 × 10 ⁻⁵	5.47 × 10 ⁻⁴	26.7	57.7

$$k_2 = 1.05 \times 10^5 \text{ L mol}^{-1} \text{ s}^{-1}$$

Table 18: Kinetics of the reaction of **2f-K** with **1i** (20 °C, in DMSO, stopped-flow, at 630 nm).

[E] [mol L ⁻¹]	[Nu] [mol L ⁻¹]	[Nu]/[E]	<i>k</i> _{obs} [s ⁻¹]
2.54 × 10 ⁻⁵	1.82 × 10 ⁻⁴	7.2	9.00
2.54 × 10 ⁻⁵	2.74 × 10 ⁻⁴	10.8	13.7
2.54 × 10 ⁻⁵	3.65 × 10 ⁻⁴	14.4	18.3
2.54 × 10 ⁻⁵	4.56 × 10 ⁻⁴	18.0	23.1
2.54 × 10 ⁻⁵	5.47 × 10 ⁻⁴	21.5	27.8

$$k_2 = 5.15 \times 10^4 \text{ L mol}^{-1} \text{ s}^{-1}$$

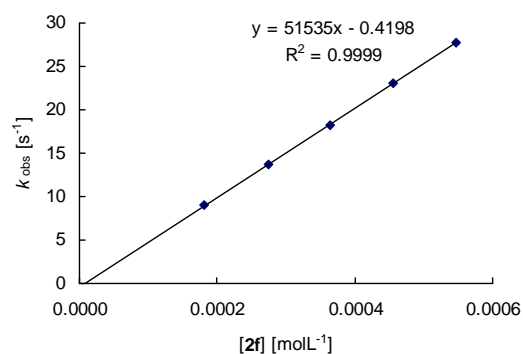
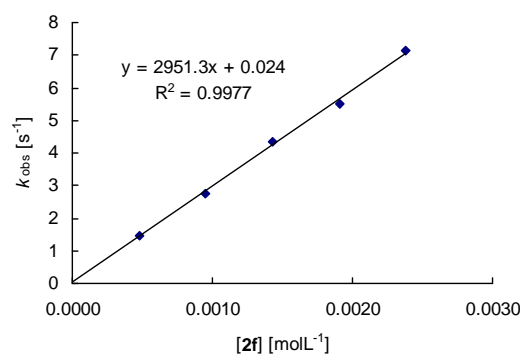


Table 19: Kinetics of the reaction of **2f-K** with **1j** (20 °C, additive: 18-crown-6, in DMSO, stopped-flow, at 422 nm).

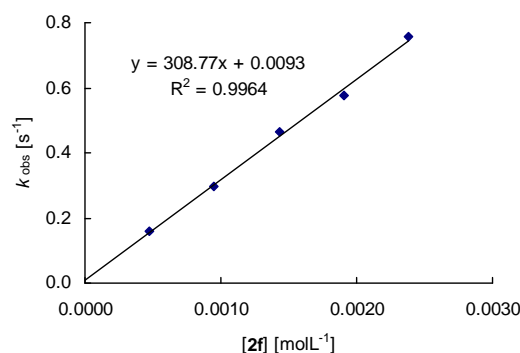
[E] [mol L ⁻¹]	[Nu] [mol L ⁻¹]	[18-crown-6] [mol L ⁻¹]	[Nu]/[E]	<i>k</i> _{obs} [s ⁻¹]
2.74 × 10 ⁻⁵	4.76 × 10 ⁻⁴	–	17.4	1.47
2.74 × 10 ⁻⁵	9.53 × 10 ⁻⁴	1.18 × 10 ⁻³	34.8	2.75
2.74 × 10 ⁻⁵	1.43 × 10 ⁻³	–	52.2	4.36
2.74 × 10 ⁻⁵	1.91 × 10 ⁻³	2.53 × 10 ⁻³	69.5	5.51
2.74 × 10 ⁻⁵	2.38 × 10 ⁻³	–	86.9	7.12

$$k_2 = 2.95 \times 10^3 \text{ L mol}^{-1} \text{ s}^{-1}$$

Table 20: Kinetics of the reaction of **2f-K** with **1k** (20 °C, additive: 18-crown-6, in DMSO, stopped-flow, at 533 nm).

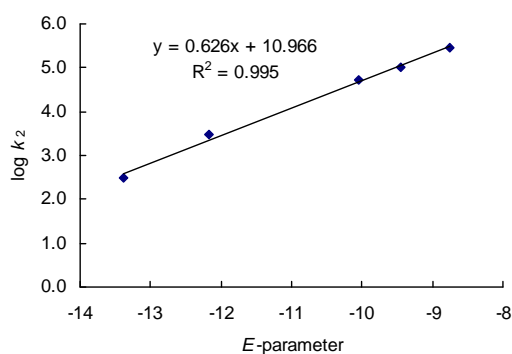
[E] [mol L ⁻¹]	[Nu] [mol L ⁻¹]	[18-crown-6] [mol L ⁻¹]	[Nu]/[E]	<i>k</i> _{obs} [s ⁻¹]
2.07 × 10 ⁻⁵	4.76 × 10 ⁻⁴	–	23.1	0.161
2.07 × 10 ⁻⁵	9.53 × 10 ⁻⁴	1.18 × 10 ⁻³	46.1	0.296
2.07 × 10 ⁻⁵	1.43 × 10 ⁻³	–	69.2	0.463
2.07 × 10 ⁻⁵	1.91 × 10 ⁻³	2.53 × 10 ⁻³	92.2	0.577
2.07 × 10 ⁻⁵	2.38 × 10 ⁻³	–	115	0.756

$$k_2 = 3.09 \times 10^2 \text{ L mol}^{-1} \text{ s}^{-1}$$

Table 21: Determination of *N*- and *s*-parameters for **2f** at 20 °C in DMSO.

Electrophile	<i>E</i> -parameter	<i>k</i> ₂ [L mol ⁻¹ s ⁻¹]	log <i>k</i> ₂
1g	-8.76	2.86 × 10 ⁵	5.46
1h	-9.45	1.05 × 10 ⁵	5.02
1i	-10.04	5.15 × 10 ⁴	4.71
1j	-12.18	2.95 × 10 ³	3.47
1k	-13.39	3.09 × 10 ²	2.49

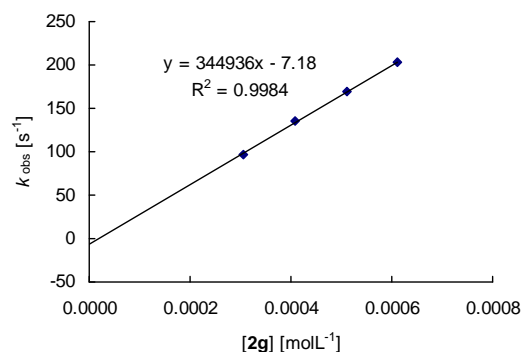
$$N = 17.52; s = 0.63$$



Potassium Salt of Diacetamide (2g-K)Table 22: Kinetics of the reaction of **2g-K** with **1f** (20 °C, in DMSO, stopped-flow, at 618 nm).

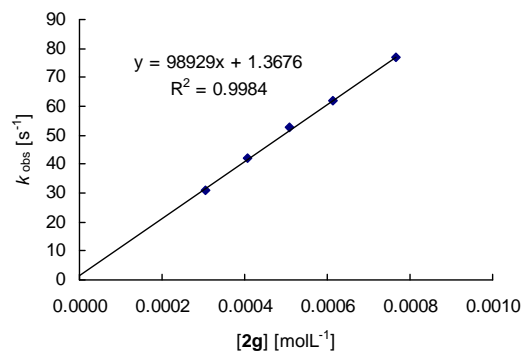
[E] [mol L ⁻¹]	[Nu] [mol L ⁻¹]	[Nu]/[E]	k_{obs} [s ⁻¹]
3.31×10^{-5}	3.06×10^{-4}	9.2	96.7
3.31×10^{-5}	4.08×10^{-4}	12.3	136
3.31×10^{-5}	5.10×10^{-4}	15.4	169
3.31×10^{-5}	6.12×10^{-4}	23.1	203

$$k_2 = 3.45 \times 10^5 \text{ L mol}^{-1} \text{ s}^{-1}$$

Table 23: Kinetics of the reaction of **2g-K** with **1g** (20 °C, in DMSO, stopped-flow, at 627 nm).

[E] [mol L ⁻¹]	[Nu] [mol L ⁻¹]	[Nu]/[E]	k_{obs} [s ⁻¹]
2.80×10^{-5}	3.06×10^{-4}	10.9	30.8
2.80×10^{-5}	4.08×10^{-4}	14.6	42.3
2.80×10^{-5}	5.10×10^{-4}	18.2	52.7
2.80×10^{-5}	6.12×10^{-4}	21.9	61.7
2.80×10^{-5}	7.65×10^{-4}	27.3	76.7

$$k_2 = 9.89 \times 10^4 \text{ L mol}^{-1} \text{ s}^{-1}$$

Table 24: Kinetics of the reaction of **2g-K** with **1h** (20 °C, in DMSO, stopped-flow, at 635 nm).

[E] [mol L ⁻¹]	[Nu] [mol L ⁻¹]	[Nu]/[E]	k_{obs} [s ⁻¹]
2.93×10^{-5}	3.06×10^{-4}	10.5	11.0
2.93×10^{-5}	4.08×10^{-4}	13.9	15.3
2.93×10^{-5}	5.10×10^{-4}	17.4	19.6
2.93×10^{-5}	6.12×10^{-4}	20.9	22.5
2.93×10^{-5}	7.65×10^{-4}	26.2	27.8

$$k_2 = 3.62 \times 10^4 \text{ L mol}^{-1} \text{ s}^{-1}$$

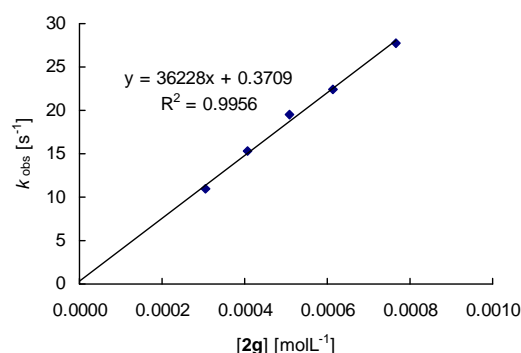
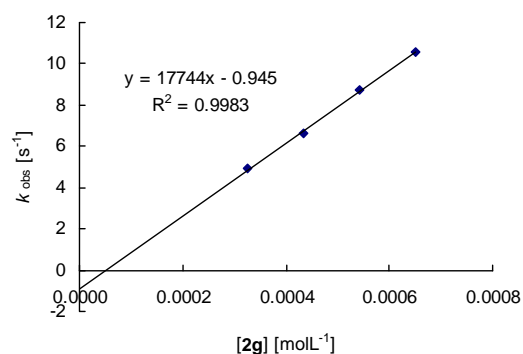


Table 25: Kinetics of the reaction of **2g-K** with **1i** (20 °C, in DMSO, stopped-flow, at 630 nm).

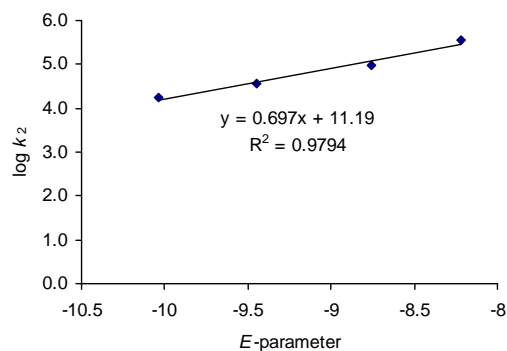
[E] [mol L ⁻¹]	[Nu] [mol L ⁻¹]	[Nu]/[E]	<i>k</i> _{obs} [s ⁻¹]
3.17 × 10 ⁻⁵	3.25 × 10 ⁻⁴	10.3	4.91
3.17 × 10 ⁻⁵	4.34 × 10 ⁻⁴	13.7	6.61
3.17 × 10 ⁻⁵	5.42 × 10 ⁻⁴	17.1	8.76
3.17 × 10 ⁻⁵	6.51 × 10 ⁻⁴	20.5	10.6

$$k_2 = 1.77 \times 10^4 \text{ L mol}^{-1} \text{ s}^{-1}$$

Table 26: Determination of *N*- and *s*-parameters for **2g** at 20 °C in DMSO.

Electrophile	<i>E</i> -parameter	<i>k</i> ₂ [L mol ⁻¹ s ⁻¹]	log <i>k</i> ₂
1f	-8.22	3.45 × 10 ⁵	5.54
1g	-8.76	9.85 × 10 ⁴	4.99
1h	-9.45	3.62 × 10 ⁴	4.56
1i	-10.04	1.77 × 10 ⁴	4.25

$$N = 16.05; s = 0.70$$



Potassium Salt of Ethyl Acetylcarbamate (**2h-K**)

Table 27: Kinetics of the reaction of **2h-K** with **1f** (20 °C, in DMSO, stopped-flow, at 618 nm).

[E] [mol L ⁻¹]	[Nu] [mol L ⁻¹]	[Nu]/[E]	<i>k</i> _{obs} [s ⁻¹]
2.24 × 10 ⁻⁵	2.59 × 10 ⁻⁴	11.5	75.8
2.24 × 10 ⁻⁵	3.88 × 10 ⁻⁴	17.3	118
2.24 × 10 ⁻⁵	5.18 × 10 ⁻⁴	23.1	151
2.24 × 10 ⁻⁵	6.47 × 10 ⁻⁴	28.8	193

$$k_2 = 2.97 \times 10^5 \text{ L mol}^{-1} \text{ s}^{-1}$$

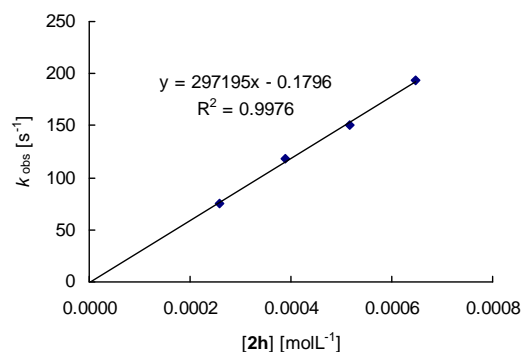
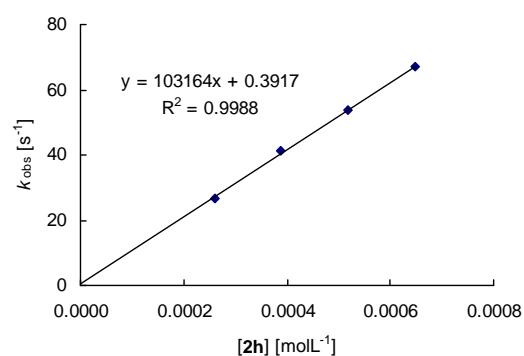


Table 28: Kinetics of the reaction of **2h-K** with **1g** (20 °C, in DMSO, stopped-flow, at 627 nm).

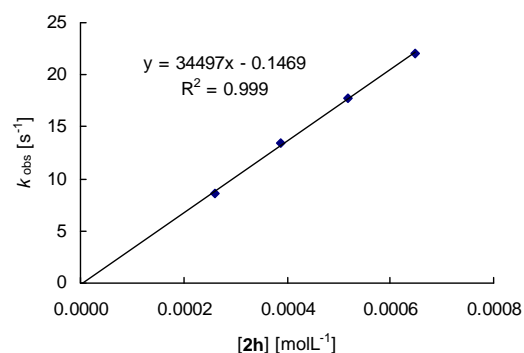
[E] [mol L ⁻¹]	[Nu] [mol L ⁻¹]	[Nu]/[E]	<i>k</i> _{obs} [s ⁻¹]
2.46 × 10 ⁻⁵	2.59 × 10 ⁻⁴	10.5	26.6
2.46 × 10 ⁻⁵	3.88 × 10 ⁻⁴	15.8	41.3
2.46 × 10 ⁻⁵	5.18 × 10 ⁻⁴	21.0	53.6
2.46 × 10 ⁻⁵	6.47 × 10 ⁻⁴	26.3	67.0

$$k_2 = 1.03 \times 10^5 \text{ L mol}^{-1} \text{ s}^{-1}$$

Table 29: Kinetics of the reaction of **2h-K** with **1h** (20 °C, in DMSO, stopped-flow, at 635 nm).

[E] [mol L ⁻¹]	[Nu] [mol L ⁻¹]	[Nu]/[E]	<i>k</i> _{obs} [s ⁻¹]
2.70 × 10 ⁻⁵	2.59 × 10 ⁻⁴	9.6	8.62
2.70 × 10 ⁻⁵	3.88 × 10 ⁻⁴	14.4	13.5
2.70 × 10 ⁻⁵	5.18 × 10 ⁻⁴	19.2	17.7
2.70 × 10 ⁻⁵	6.47 × 10 ⁻⁴	24.0	22.1

$$k_2 = 3.45 \times 10^4 \text{ L mol}^{-1} \text{ s}^{-1}$$

Table 30: Kinetics of the reaction of **2h-K** with **1i** (20 °C, in DMSO, stopped-flow, at 630 nm).

[E] [mol L ⁻¹]	[Nu] [mol L ⁻¹]	[Nu]/[E]	<i>k</i> _{obs} [s ⁻¹]
2.31 × 10 ⁻⁵	2.59 × 10 ⁻⁴	11.2	4.00
2.31 × 10 ⁻⁵	3.88 × 10 ⁻⁴	16.8	6.07
2.31 × 10 ⁻⁵	5.18 × 10 ⁻⁴	22.4	8.08
2.31 × 10 ⁻⁵	6.47 × 10 ⁻⁴	28.1	10.1

$$k_2 = 1.57 \times 10^4 \text{ L mol}^{-1} \text{ s}^{-1}$$

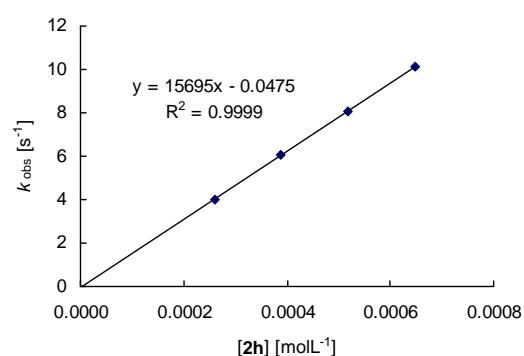
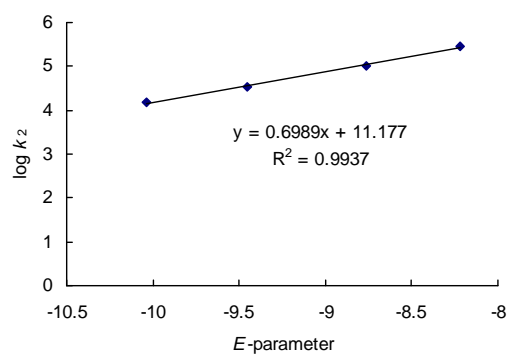


Table 31: Determination of *N*- and *s*-parameters for **2h** at 20 °C in DMSO.

Electrophile	<i>E</i> -parameter	k_2 [L mol ⁻¹ s ⁻¹]	log k_2
1f	-8.22	2.97×10^5	5.47
1g	-8.76	1.03×10^5	5.01
1h	-9.45	3.45×10^4	4.54
1i	-10.04	1.57×10^4	4.20

$$N = 15.99; s = 0.70$$

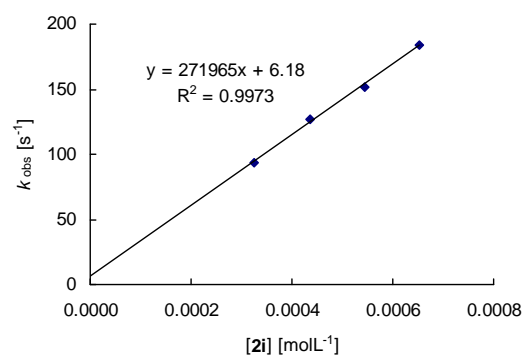


Potassium Salt of *p*-Toluenesulfonamide (**2i-K**)

Table 32: Kinetics of the reaction of **2i-K** with **1f** (20 °C, in DMSO, stopped-flow, at 618 nm).

[E] [mol L ⁻¹]	[Nu] [mol L ⁻¹]	[Nu]/[E]	k_{obs} [s ⁻¹]
2.35×10^{-5}	3.26×10^{-4}	13.9	93.8
2.35×10^{-5}	4.35×10^{-4}	18.5	127
2.35×10^{-5}	5.43×10^{-4}	23.2	152
2.35×10^{-5}	6.52×10^{-4}	27.8	184

$$k_2 = 2.72 \times 10^5 \text{ L mol}^{-1} \text{ s}^{-1}$$

Table 33: Kinetics of the reaction of **2i-K** with **1g** (20 °C, in DMSO, stopped-flow, at 627 nm).

[E] [mol L ⁻¹]	[Nu] [mol L ⁻¹]	[Nu]/[E]	k_{obs} [s ⁻¹]
2.23×10^{-5}	3.26×10^{-4}	14.6	26.9
2.23×10^{-5}	4.35×10^{-4}	19.5	36.0
2.23×10^{-5}	5.43×10^{-4}	24.4	42.7
2.23×10^{-5}	6.52×10^{-4}	29.2	51.2

$$k_2 = 7.33 \times 10^4 \text{ L mol}^{-1} \text{ s}^{-1}$$

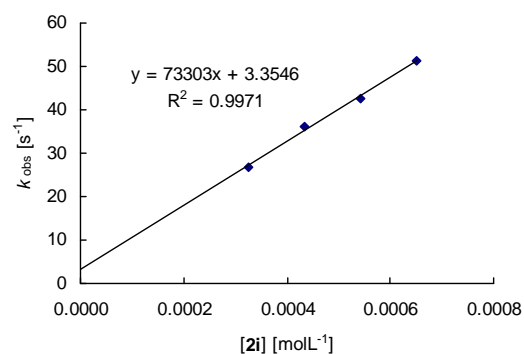
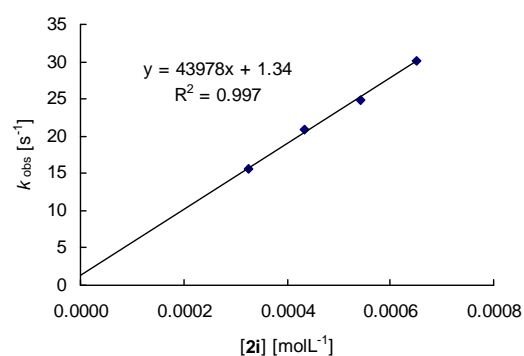


Table 34: Kinetics of the reaction of **2i-K** with **1h** (20 °C, in DMSO, stopped-flow, at 635 nm).

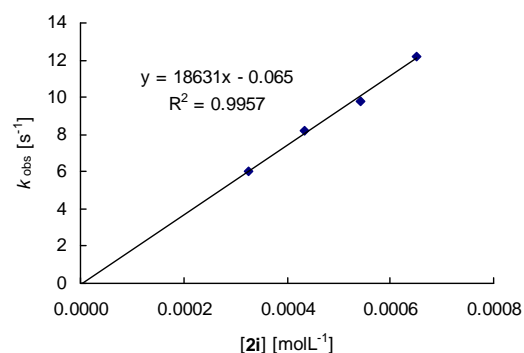
[E] [mol L ⁻¹]	[Nu] [mol L ⁻¹]	[Nu]/[E]	<i>k</i> _{obs} [s ⁻¹]
2.49 × 10 ⁻⁵	3.26 × 10 ⁻⁴	13.1	15.6
2.49 × 10 ⁻⁵	4.35 × 10 ⁻⁴	17.5	20.8
2.49 × 10 ⁻⁵	5.43 × 10 ⁻⁴	21.8	24.8
2.49 × 10 ⁻⁵	6.52 × 10 ⁻⁴	26.2	30.2

$$k_2 = 4.40 \times 10^4 \text{ L mol}^{-1} \text{ s}^{-1}$$

Table 35: Kinetics of the reaction of **2i-K** with **1i** (20 °C, in DMSO, stopped-flow, at 630 nm).

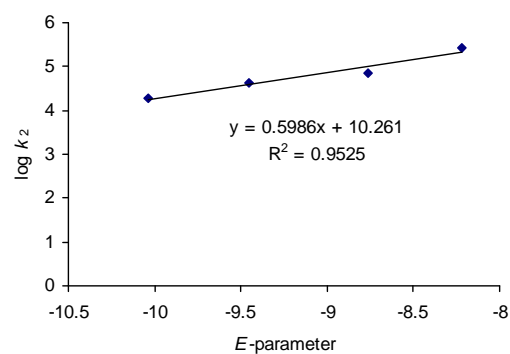
[E] [mol L ⁻¹]	[Nu] [mol L ⁻¹]	[Nu]/[E]	<i>k</i> _{obs} [s ⁻¹]
2.32 × 10 ⁻⁵	3.26 × 10 ⁻⁴	14.1	6.00
2.32 × 10 ⁻⁵	4.35 × 10 ⁻⁴	18.7	8.17
2.32 × 10 ⁻⁵	5.43 × 10 ⁻⁴	23.4	9.82
2.32 × 10 ⁻⁵	6.52 × 10 ⁻⁴	28.1	12.2

$$k_2 = 1.86 \times 10^4 \text{ L mol}^{-1} \text{ s}^{-1}$$

Table 36: Determination of *N*- and *s*-parameters for **2i** at 20 °C in DMSO.

Electrophile	<i>E</i> -parameter	<i>k</i> ₂ [L mol ⁻¹ s ⁻¹]	log <i>k</i> ₂
1f	-8.22	2.72 × 10 ⁵	5.44
1g	-8.76	7.33 × 10 ⁴	4.87
1h	-9.45	4.40 × 10 ⁴	4.64
1i	-10.04	1.86 × 10 ⁴	4.27

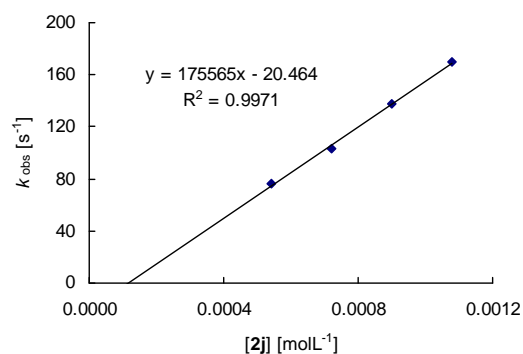
$$N = 17.14; s = 0.60$$



Anion of Methanesulfonamide (2j)Table 37: Kinetics of the reaction of **2j** (generated in situ by addition of 1.11 equivalents P₂-*t*Bu-base) with **1g** (20 °C, in DMSO, stopped-flow, at 627 nm).

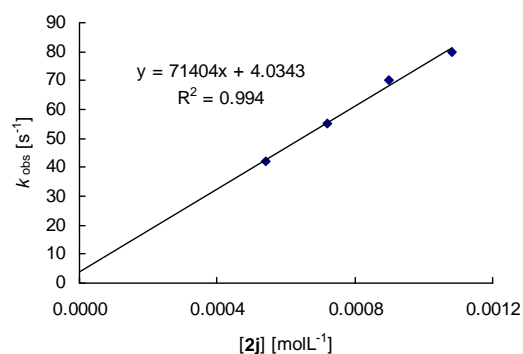
[E] [mol L ⁻¹]	[Nu] [mol L ⁻¹]	[Nu]/[E]	<i>k</i> _{obs} [s ⁻¹]
4.85 × 10 ⁻⁵	5.41 × 10 ⁻⁴	11.1	76.5
4.85 × 10 ⁻⁵	7.21 × 10 ⁻⁴	14.9	103
4.85 × 10 ⁻⁵	9.01 × 10 ⁻⁴	18.6	138
4.85 × 10 ⁻⁵	1.08 × 10 ⁻³	22.3	170

$$k_2 = 1.76 \times 10^5 \text{ L mol}^{-1} \text{ s}^{-1}$$

Table 38: Kinetics of the reaction of **2j** (generated in situ by addition of 1.11 equivalents P₂-*t*Bu-base) with **1h** (20 °C, in DMSO, stopped-flow, at 635 nm).

[E] [mol L ⁻¹]	[Nu] [mol L ⁻¹]	[Nu]/[E]	<i>k</i> _{obs} [s ⁻¹]
3.33 × 10 ⁻⁵	5.41 × 10 ⁻⁴	16.2	42.2
3.33 × 10 ⁻⁵	7.21 × 10 ⁻⁴	21.7	55.3
3.33 × 10 ⁻⁵	9.01 × 10 ⁻⁴	27.1	70.2
3.33 × 10 ⁻⁵	1.08 × 10 ⁻³	32.5	80.0

$$k_2 = 7.14 \times 10^4 \text{ L mol}^{-1} \text{ s}^{-1}$$

Table 39: Kinetics of the reaction of **2j** (generated in situ by addition of 1.11 equivalents P₂-*t*Bu-base) with **1i** (20 °C, in DMSO, stopped-flow, at 630 nm).

[E] [mol L ⁻¹]	[Nu] [mol L ⁻¹]	[Nu]/[E]	<i>k</i> _{obs} [s ⁻¹]
2.35 × 10 ⁻⁵	5.41 × 10 ⁻⁴	23.0	20.1
2.35 × 10 ⁻⁵	7.21 × 10 ⁻⁴	30.6	24.6
2.35 × 10 ⁻⁵	9.01 × 10 ⁻⁴	38.3	31.2
2.35 × 10 ⁻⁵	1.08 × 10 ⁻³	46.0	34.7

$$k_2 = 2.81 \times 10^4 \text{ L mol}^{-1} \text{ s}^{-1}$$

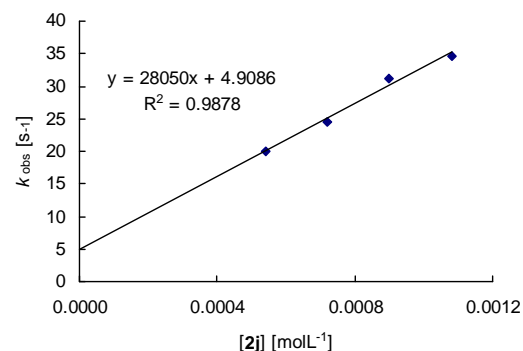
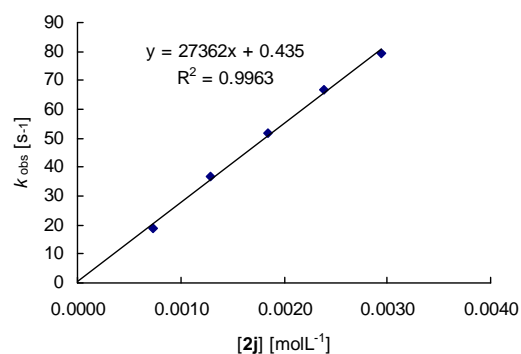


Table 40: Kinetics of the reaction of **2j-K** with **1i** (20 °C, in DMSO, stopped-flow, at 630 nm).

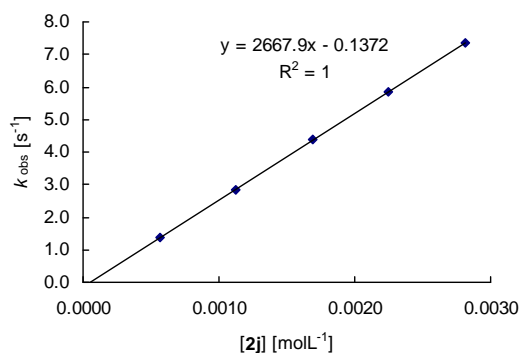
[E] [mol L ⁻¹]	[Nu] [mol L ⁻¹]	[Nu]/[E]	<i>k</i> _{obs} [s ⁻¹]
1.71 × 10 ⁻⁵	7.36 × 10 ⁻⁴	43.0	18.9
1.71 × 10 ⁻⁵	1.29 × 10 ⁻³	75.4	37.0
1.71 × 10 ⁻⁵	1.84 × 10 ⁻³	108	51.8
1.71 × 10 ⁻⁵	2.39 × 10 ⁻³	140	66.7
1.71 × 10 ⁻⁵	2.94 × 10 ⁻³	172	79.4

$$k_2 = 2.74 \times 10^4 \text{ L mol}^{-1} \text{ s}^{-1}$$

Table 41: Kinetics of the reaction of **2j-K** with **1j** (20 °C, in DMSO, stopped-flow, at 422 nm).

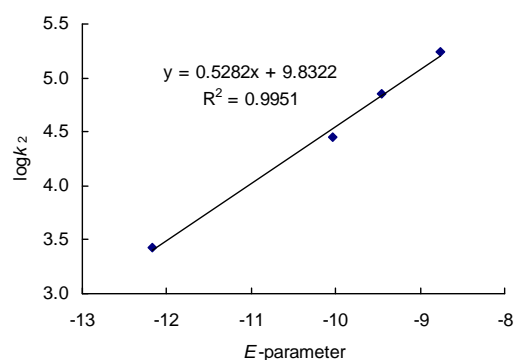
[E] [mol L ⁻¹]	[Nu] [mol L ⁻¹]	[Nu]/[E]	<i>k</i> _{obs} [s ⁻¹]
5.13 × 10 ⁻⁵	5.62 × 10 ⁻⁴	11.0	1.36
5.13 × 10 ⁻⁵	1.12 × 10 ⁻³	21.8	2.86
5.13 × 10 ⁻⁵	1.69 × 10 ⁻³	32.9	4.37
5.13 × 10 ⁻⁵	2.25 × 10 ⁻³	43.9	5.85
5.13 × 10 ⁻⁵	2.81 × 10 ⁻³	54.8	7.37

$$k_2 = 2.67 \times 10^3 \text{ L mol}^{-1} \text{ s}^{-1}$$

Table 42: Determination of *N*- and *s*-parameters for **2j** at 20 °C in DMSO.

Electrophile	<i>E</i> -parameter	<i>k</i> ₂ [L mol ⁻¹ s ⁻¹]	log <i>k</i> ₂
1g	-8.76	1.76 × 10 ⁵	5.25
1h	-9.45	7.14 × 10 ⁴	4.85
1i	-10.04	2.81 × 10 ⁴	4.45
1j	-12.18	2.67 × 10 ³	3.43

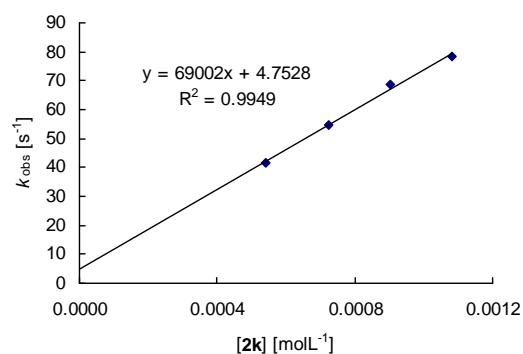
$$N = 18.61; s = 0.53$$



Anion of Hydantoin (2k)Table 43: Kinetics of the reaction of **2k** (generated in situ by addition of 1.11 equivalents P₂-*t*Bu-base) with **1g** (20 °C, in DMSO, stopped-flow, at 627 nm).

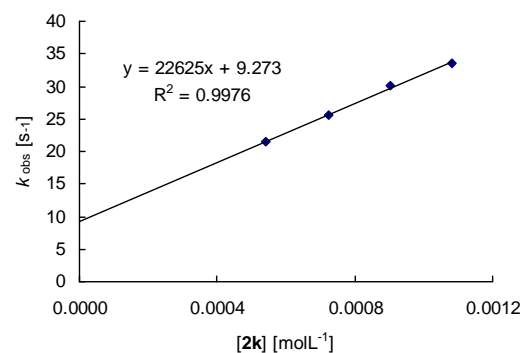
[E] [mol L ⁻¹]	[Nu] [mol L ⁻¹]	[Nu]/[E]	<i>k</i> _{obs} [s ⁻¹]
4.85 × 10 ⁻⁵	5.42 × 10 ⁻⁴	11.2	41.6
4.85 × 10 ⁻⁵	7.23 × 10 ⁻⁴	14.9	54.7
4.85 × 10 ⁻⁵	9.04 × 10 ⁻⁴	18.6	68.7
4.85 × 10 ⁻⁵	1.08 × 10 ⁻³	22.3	78.2

$$k_2 = 6.90 \times 10^4 \text{ L mol}^{-1} \text{ s}^{-1}$$

Table 44: Kinetics of the reaction of **2k** (generated in situ by addition of 1.11 equivalents P₂-*t*Bu-base) with **1h** (20 °C, in DMSO, stopped-flow, at 635 nm).

[E] [mol L ⁻¹]	[Nu] [mol L ⁻¹]	[Nu]/[E]	<i>k</i> _{obs} [s ⁻¹]
3.33 × 10 ⁻⁵	5.42 × 10 ⁻⁴	16.3	21.5
3.33 × 10 ⁻⁵	7.23 × 10 ⁻⁴	21.7	25.5
3.33 × 10 ⁻⁵	9.04 × 10 ⁻⁴	27.1	30.1
3.33 × 10 ⁻⁵	1.08 × 10 ⁻³	32.6	33.5

$$k_2 = 2.26 \times 10^4 \text{ L mol}^{-1} \text{ s}^{-1}$$

Table 45: Kinetics of the reaction of **2k** (generated in situ by addition of 1.11 equivalents P₂-*t*Bu-base) with **1i** (20 °C, in DMSO, stopped-flow, at 630 nm).

[E] [mol L ⁻¹]	[Nu] [mol L ⁻¹]	[Nu]/[E]	<i>k</i> _{obs} [s ⁻¹]
2.35 × 10 ⁻⁵	5.42 × 10 ⁻⁴	23.0	9.72
2.35 × 10 ⁻⁵	7.23 × 10 ⁻⁴	30.7	12.5
2.35 × 10 ⁻⁵	9.04 × 10 ⁻⁴	38.4	15.0
2.35 × 10 ⁻⁵	1.08 × 10 ⁻³	46.1	17.2

$$k_2 = 1.39 \times 10^4 \text{ L mol}^{-1} \text{ s}^{-1}$$

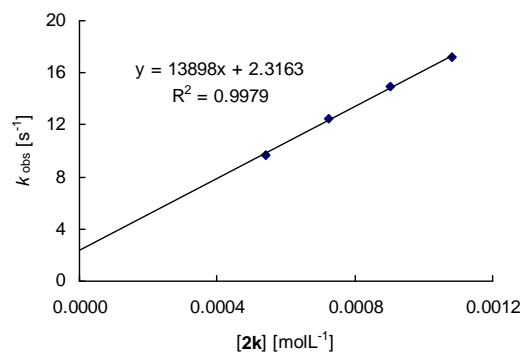
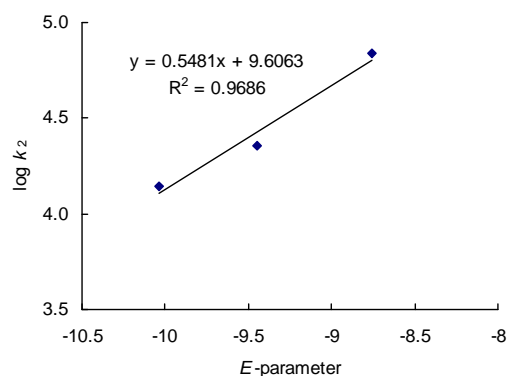


Table 46: Determination of *N*- and *s*-parameters for **2k** at 20 °C in DMSO.

Electrophile	<i>E</i> -parameter	k_2 [L mol ⁻¹ s ⁻¹]	log k_2
1g	-8.76	6.90×10^4	4.84
1h	-9.45	2.26×10^4	4.35
1i	-10.04	1.39×10^4	4.14

$$N = 17.52; s = 0.55$$

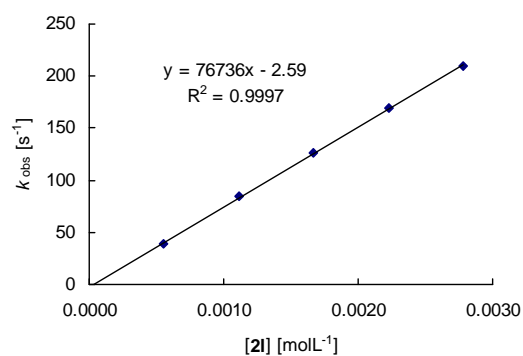


Potassium Salt of 2-Oxazolidinone (**2I-K**)

Table 47: Kinetics of the reaction of **2I-K** with **1k** (20 °C, additive: 1.21 eq. 18-crown-6, in DMSO, stopped-flow, at 533 nm).

[E] [mol L ⁻¹]	[Nu] [mol L ⁻¹]	[Nu]/[E]	k_{obs} [s ⁻¹]
2.07×10^{-5}	5.57×10^{-4}	26.9	38.7
2.07×10^{-5}	1.11×10^{-3}	53.9	84.3
2.07×10^{-5}	1.67×10^{-3}	80.8	126
2.07×10^{-5}	2.23×10^{-3}	108	169
2.07×10^{-5}	2.78×10^{-3}	135	210

$$k_2 = 7.67 \times 10^4 \text{ L mol}^{-1} \text{ s}^{-1}$$

Table 48: Kinetics of the reaction of **2I-K** with **1l** (20 °C, additive: 1.24 eq. 18-crown-6, in DMSO, stopped-flow, at 374 nm).

[E] [mol L ⁻¹]	[Nu] [mol L ⁻¹]	[Nu]/[E]	k_{obs} [s ⁻¹]
2.58×10^{-5}	5.50×10^{-4}	21.3	57.0
2.58×10^{-5}	1.10×10^{-3}	42.7	118
2.58×10^{-5}	1.65×10^{-3}	64.0	171
2.58×10^{-5}	2.20×10^{-3}	85.3	213
2.58×10^{-5}	2.75×10^{-3}	107	263

$$k_2 = 9.21 \times 10^4 \text{ L mol}^{-1} \text{ s}^{-1}$$

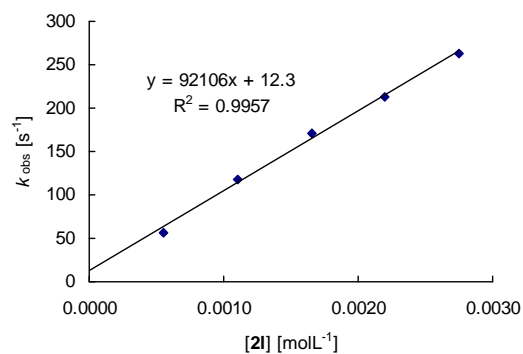
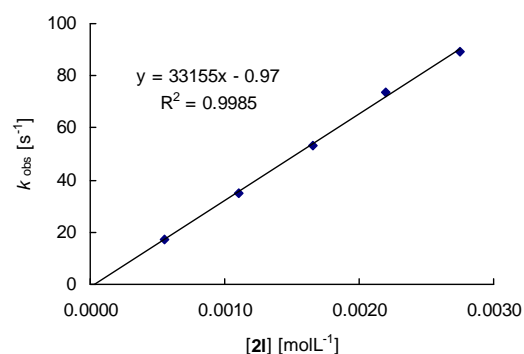


Table 49: Kinetics of the reaction of **2I-K** with **1m** (20 °C, additive: 1.24 eq. 18-crown-6, in DMSO, stopped-flow, at 354 nm).

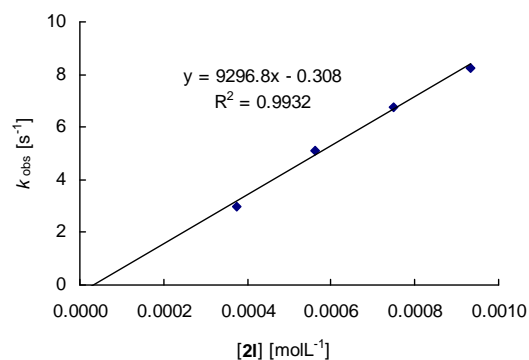
[E] [mol L ⁻¹]	[Nu] [mol L ⁻¹]	[Nu]/[E]	<i>k</i> _{obs} [s ⁻¹]
2.80 × 10 ⁻⁵	5.50 × 10 ⁻⁴	19.6	17.4
2.80 × 10 ⁻⁵	1.10 × 10 ⁻³	39.3	35.0
2.80 × 10 ⁻⁵	1.65 × 10 ⁻³	58.9	53.4
2.80 × 10 ⁻⁵	2.20 × 10 ⁻³	78.5	73.9
2.80 × 10 ⁻⁵	2.75 × 10 ⁻³	98.2	89.2

$$k_2 = 3.32 \times 10^4 \text{ L mol}^{-1} \text{ s}^{-1}$$

Table 50: Kinetics of the reaction of **2I-K** with **1n** (20 °C, in DMSO, stopped-flow, at 371 nm).

[E] [mol L ⁻¹]	[Nu] [mol L ⁻¹]	[Nu]/[E]	<i>k</i> _{obs} [s ⁻¹]
1.93 × 10 ⁻⁵	3.74 × 10 ⁻⁴	19.3	3.00
1.93 × 10 ⁻⁵	5.61 × 10 ⁻⁴	29.0	5.09
1.93 × 10 ⁻⁵	7.48 × 10 ⁻⁴	38.7	6.78
1.93 × 10 ⁻⁵	9.35 × 10 ⁻⁴	48.4	8.23

$$k_2 = 9.30 \times 10^3 \text{ L mol}^{-1} \text{ s}^{-1}$$

Table 51: Kinetics of the reaction of **2I-K** with **1o** (20 °C, in DMSO, stopped-flow, at 393 nm).

[E] [mol L ⁻¹]	[Nu] [mol L ⁻¹]	[Nu]/[E]	<i>k</i> _{obs} [s ⁻¹]
3.39 × 10 ⁻⁵	3.74 × 10 ⁻⁴	11.0	1.68
3.39 × 10 ⁻⁵	5.61 × 10 ⁻⁴	16.5	2.92
3.39 × 10 ⁻⁵	7.48 × 10 ⁻⁴	22.1	4.03
3.39 × 10 ⁻⁵	9.35 × 10 ⁻⁴	27.6	5.01

$$k_2 = 5.94 \times 10^3 \text{ L mol}^{-1} \text{ s}^{-1}$$

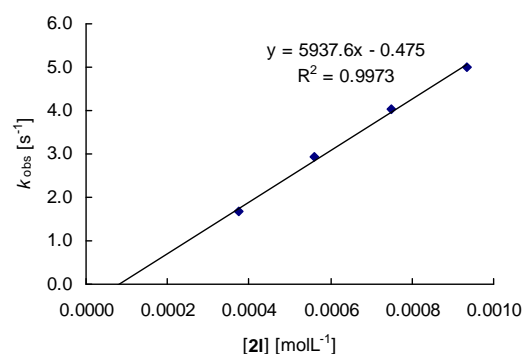
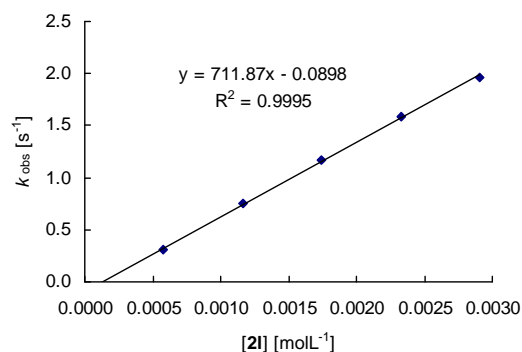


Table 52: Kinetics of the reaction of **2l-K** with **1p** (20 °C, additive: 18-crown-6, in DMSO, stopped-flow, at 486 nm).

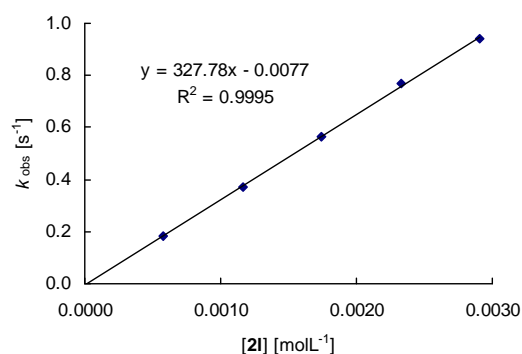
[E] [mol L ⁻¹]	[Nu] [mol L ⁻¹]	[18-crown-6] [mol L ⁻¹]	[Nu]/[E]	<i>k</i> _{obs} [s ⁻¹]
2.61 × 10 ⁻⁵	5.82 × 10 ⁻⁴	6.99 × 10 ⁻⁴	22.3	0.310
2.61 × 10 ⁻⁵	1.16 × 10 ⁻³	1.40 × 10 ⁻³	44.7	0.749
2.61 × 10 ⁻⁵	1.75 × 10 ⁻³	2.10 × 10 ⁻³	67.0	1.16
2.61 × 10 ⁻⁵	2.33 × 10 ⁻³	2.80 × 10 ⁻³	89.3	1.58
2.61 × 10 ⁻⁵	2.91 × 10 ⁻³	3.49 × 10 ⁻³	112	1.97

$$k_2 = 7.12 \times 10^2 \text{ L mol}^{-1} \text{ s}^{-1}$$

Table 53: Kinetics of the reaction of **2l-K** with **1q** (20 °C, additive: 18-crown-6, in DMSO, stopped-flow, at 521 nm).

[E] [mol L ⁻¹]	[Nu] [mol L ⁻¹]	[18-crown-6] [mol L ⁻¹]	[Nu]/[E]	<i>k</i> _{obs} [s ⁻¹]
2.62 × 10 ⁻⁵	5.82 × 10 ⁻⁴	6.99 × 10 ⁻⁴	22.2	0.183
2.62 × 10 ⁻⁵	1.16 × 10 ⁻³	1.40 × 10 ⁻³	44.5	0.372
2.62 × 10 ⁻⁵	1.75 × 10 ⁻³	2.10 × 10 ⁻³	66.7	0.563
2.62 × 10 ⁻⁵	2.33 × 10 ⁻³	2.80 × 10 ⁻³	89.0	0.767
2.62 × 10 ⁻⁵	2.91 × 10 ⁻³	3.49 × 10 ⁻³	112	0.940

$$k_2 = 3.28 \times 10^2 \text{ L mol}^{-1} \text{ s}^{-1}$$

Table 54: Kinetics of the reaction of **2l-K** with **4b** (20 °C, in DMSO, stopped-flow, at 480 nm).

[E] [mol L ⁻¹]	[Nu] [mol L ⁻¹]	[Nu]/[E]	<i>k</i> _{obs} [s ⁻¹]
3.88 × 10 ⁻⁵	3.74 × 10 ⁻⁴	9.6	17.6
3.88 × 10 ⁻⁵	6.37 × 10 ⁻⁴	16.4	38.7
3.88 × 10 ⁻⁵	7.01 × 10 ⁻⁴	18.1	41.9
3.88 × 10 ⁻⁵	9.35 × 10 ⁻⁴	24.1	60.1

$$k_2 = 7.55 \times 10^4 \text{ L mol}^{-1} \text{ s}^{-1}$$

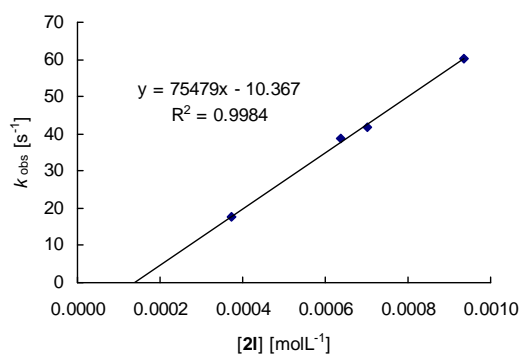
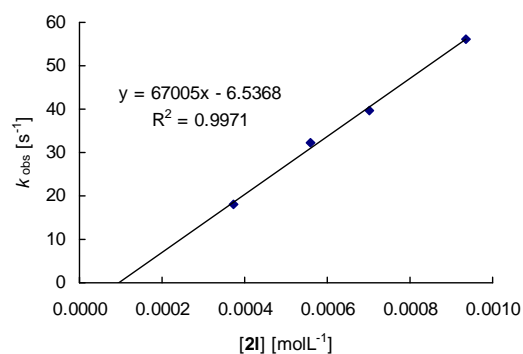


Table 55: Kinetics of the reaction of **2l-K** with **4a** (20 °C, in DMSO, stopped-flow, at 500 nm).

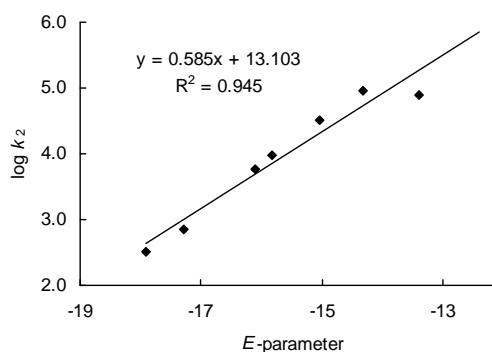
[E] [mol L ⁻¹]	[Nu] [mol L ⁻¹]	[Nu]/[E]	k_{obs} [s ⁻¹]
2.92×10^{-5}	3.74×10^{-4}	12.8	18.1
2.92×10^{-5}	5.61×10^{-4}	19.2	32.2
2.92×10^{-5}	7.01×10^{-4}	24.0	39.6
2.92×10^{-5}	9.35×10^{-4}	32.0	56.2

$$k_2 = 6.70 \times 10^4 \text{ L mol}^{-1} \text{ s}^{-1}$$

Table 56: Determination of *N*- and *s*-parameters for **2l** at 20 °C in DMSO.

Electrophile	<i>E</i> -parameter	k_2 [L mol ⁻¹ s ⁻¹]	log k_2
1k	-13.39	7.67×10^4	4.88
1l	-14.32	9.21×10^4	4.96
1m	-15.03	3.32×10^4	4.52
1n	-15.83	9.30×10^3	3.97
1o	-16.11	5.94×10^3	3.77
1p	-17.29	7.12×10^2	2.85
1q	-17.90	3.28×10^2	2.52

$$N = 22.40; s = 0.59$$



Potassium Salt of (*S*)-4-Benzyloxazolidin-2-one (**2m-K**)

Table 57: Kinetics of the reaction of **2m-K** with **1j** (20 °C, additive: 18-crown-6, in DMSO, stopped-flow, at 422 nm).

[E] [mol L ⁻¹]	[Nu] [mol L ⁻¹]	[18-crown-6] [mol L ⁻¹]	[Nu]/[E]	k_{obs} [s ⁻¹]
3.13×10^{-5}	3.18×10^{-4}	–	10.2	94.0
3.13×10^{-5}	4.77×10^{-4}	7.44×10^{-4}	15.2	142
3.13×10^{-5}	6.35×10^{-4}	–	20.3	194
3.13×10^{-5}	7.94×10^{-4}	9.56×10^{-4}	25.4	238
3.13×10^{-5}	9.53×10^{-4}	–	30.5	307

$$k_2 = 3.29 \times 10^5 \text{ L mol}^{-1} \text{ s}^{-1}$$

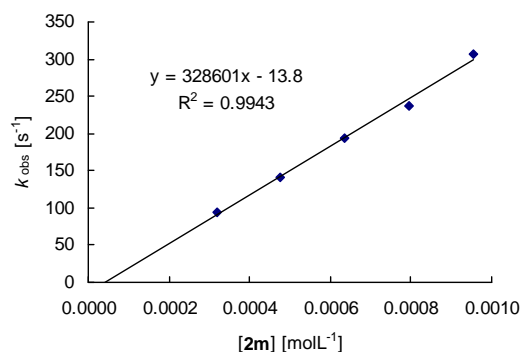
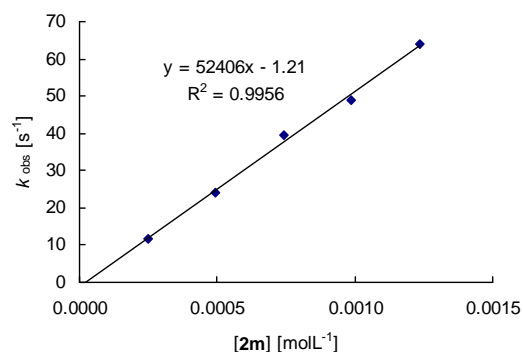


Table 58: Kinetics of the reaction of **2m-K** with **1k** (20 °C, additive: 18-crown-6, in DMSO, stopped-flow, at 533 nm).

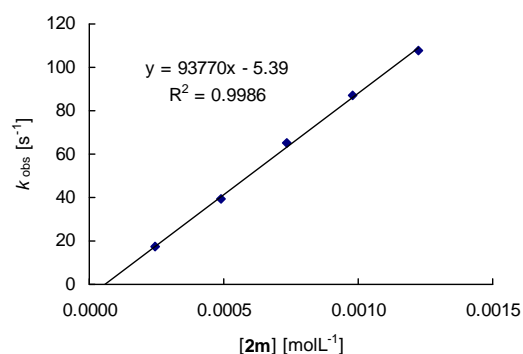
[E] [mol L ⁻¹]	[Nu] [mol L ⁻¹]	[18-crown-6] [mol L ⁻¹]	[Nu]/[E]	<i>k</i> _{obs} [s ⁻¹]
2.07 × 10 ⁻⁵	2.47 × 10 ⁻⁴	–	12.0	11.7
2.07 × 10 ⁻⁵	4.94 × 10 ⁻⁴	6.41 × 10 ⁻⁴	23.9	24.0
2.07 × 10 ⁻⁵	7.41 × 10 ⁻⁴	–	35.9	39.6
2.07 × 10 ⁻⁵	9.88 × 10 ⁻⁴	1.28 × 10 ⁻³	47.8	48.9
2.07 × 10 ⁻⁵	1.24 × 10 ⁻³	–	59.8	64.0

$$k_2 = 5.24 \times 10^4 \text{ L mol}^{-1} \text{ s}^{-1}$$

Table 59: Kinetics of the reaction of **2m-K** with **1l** (20 °C, additive: 18-crown-6, in DMSO, stopped-flow, at 374 nm).

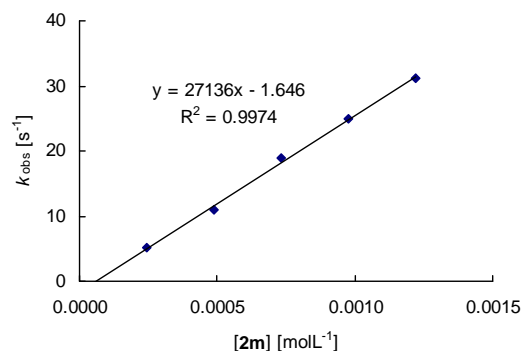
[E] [mol L ⁻¹]	[Nu] [mol L ⁻¹]	[18-crown-6] [mol L ⁻¹]	[Nu]/[E]	<i>k</i> _{obs} [s ⁻¹]
2.62 × 10 ⁻⁵	2.44 × 10 ⁻⁴	–	9.3	17.2
2.62 × 10 ⁻⁵	4.89 × 10 ⁻⁴	6.43 × 10 ⁻⁴	18.7	39.3
2.62 × 10 ⁻⁵	7.33 × 10 ⁻⁴	–	28.0	65.4
2.62 × 10 ⁻⁵	9.77 × 10 ⁻³	1.29 × 10 ⁻³	37.4	86.8
2.62 × 10 ⁻⁵	1.22 × 10 ⁻³	–	46.7	108

$$k_2 = 9.38 \times 10^4 \text{ L mol}^{-1} \text{ s}^{-1}$$

Table 60: Kinetics of the reaction of **2m-K** with **1m** (20 °C, additive: 18-crown-6, in DMSO, stopped-flow, at 354 nm).

[E] [mol L ⁻¹]	[Nu] [mol L ⁻¹]	[18-crown-6] [mol L ⁻¹]	[Nu]/[E]	<i>k</i> _{obs} [s ⁻¹]
2.80 × 10 ⁻⁵	2.44 × 10 ⁻⁴	–	8.7	5.08
2.80 × 10 ⁻⁵	4.89 × 10 ⁻⁴	6.43 × 10 ⁻⁴	17.4	10.9
2.80 × 10 ⁻⁵	7.33 × 10 ⁻⁴	–	26.1	19.0
2.80 × 10 ⁻⁵	9.77 × 10 ⁻⁴	1.29 × 10 ⁻³	34.9	25.0
2.80 × 10 ⁻⁵	1.22 × 10 ⁻³	–	43.6	31.2

$$k_2 = 2.71 \times 10^4 \text{ L mol}^{-1} \text{ s}^{-1}$$



Chapter 4: Nucleophilic Reactivities of Imide and Amide Anions

Table 61: Kinetics of the reaction of **2m-K** with **1n** (20 °C, additive: 18-crown-6, in DMSO, stopped-flow, at 371 nm).

[E] [mol L ⁻¹]	[Nu] [mol L ⁻¹]	[18-crown-6] [mol L ⁻¹]	[Nu]/[E]	<i>k</i> _{obs} [s ⁻¹]
2.43 × 10 ⁻⁵	3.00 × 10 ⁻⁴	–	12.3	1.34
2.43 × 10 ⁻⁵	5.99 × 10 ⁻⁴	7.44 × 10 ⁻⁴	24.6	3.29
2.43 × 10 ⁻⁵	8.99 × 10 ⁻⁴	–	37.0	5.16
2.43 × 10 ⁻⁵	1.20 × 10 ⁻³	1.49 × 10 ⁻³	49.3	6.73
2.43 × 10 ⁻⁵	1.50 × 10 ⁻³	–	61.6	8.82

$$k_2 = 6.14 \times 10^3 \text{ L mol}^{-1} \text{ s}^{-1}$$

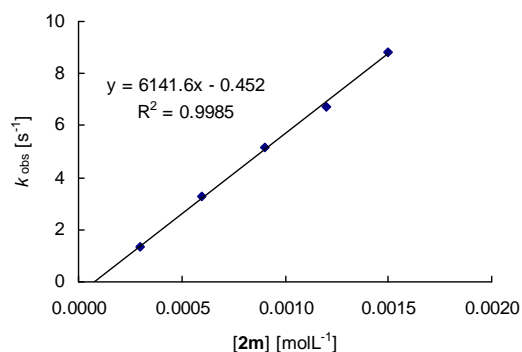


Table 62: Kinetics of the reaction of **2m-K** with **1o** (20 °C, additive: 18-crown-6, in DMSO, stopped-flow, at 393 nm).

[E] [mol L ⁻¹]	[Nu] [mol L ⁻¹]	[18-crown-6] [mol L ⁻¹]	[Nu]/[E]	<i>k</i> _{obs} [s ⁻¹]
2.98 × 10 ⁻⁵	3.00 × 10 ⁻⁴	–	10.1	0.923
2.98 × 10 ⁻⁵	5.99 × 10 ⁻⁴	7.44 × 10 ⁻⁴	20.1	1.93
2.98 × 10 ⁻⁵	8.99 × 10 ⁻⁴	–	30.2	3.26
2.98 × 10 ⁻⁵	1.20 × 10 ⁻³	1.49 × 10 ⁻³	40.3	4.40
2.98 × 10 ⁻⁵	1.50 × 10 ⁻³	–	50.3	5.69

$$k_2 = 4.01 \times 10^3 \text{ L mol}^{-1} \text{ s}^{-1}$$

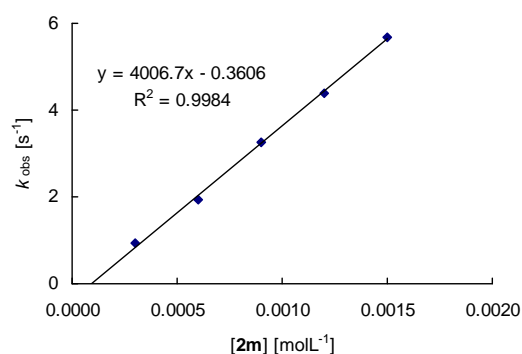


Table 63: Kinetics of the reaction of **2m-K** with **1p** (20 °C, additive: 18-crown-6, in DMSO, stopped-flow, at 486 nm).

[E] [mol L ⁻¹]	[Nu] [mol L ⁻¹]	[18-crown-6] [mol L ⁻¹]	[Nu]/[E]	<i>k</i> _{obs} [s ⁻¹]
2.73 × 10 ⁻⁵	3.18 × 10 ⁻⁴	–	11.7	0.146
2.73 × 10 ⁻⁵	6.35 × 10 ⁻⁴	7.44 × 10 ⁻⁴	23.3	0.322
2.73 × 10 ⁻⁵	9.53 × 10 ⁻⁴	–	35.0	0.520
2.73 × 10 ⁻⁵	1.27 × 10 ⁻³	1.49 × 10 ⁻³	46.6	0.680
2.73 × 10 ⁻⁵	1.59 × 10 ⁻³	–	58.3	0.890

$$k_2 = 5.81 \times 10^2 \text{ L mol}^{-1} \text{ s}^{-1}$$

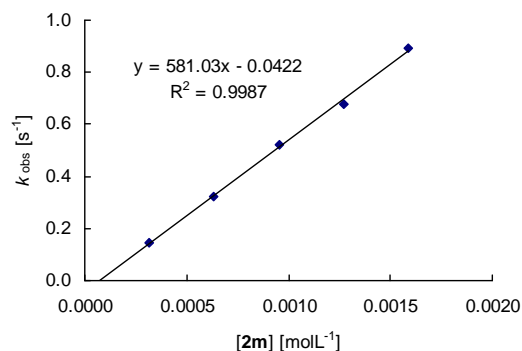
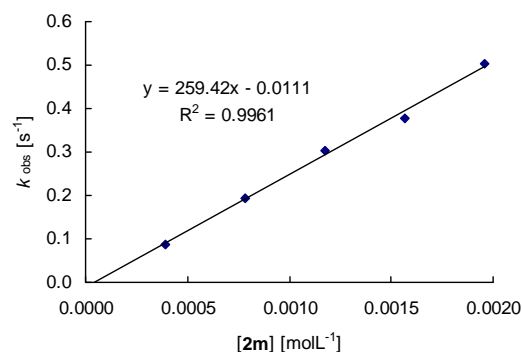


Table 64: Kinetics of the reaction of **2m-K** with **1q** (20 °C, additive: 18-crown-6, in DMSO, stopped-flow, at 521 nm).

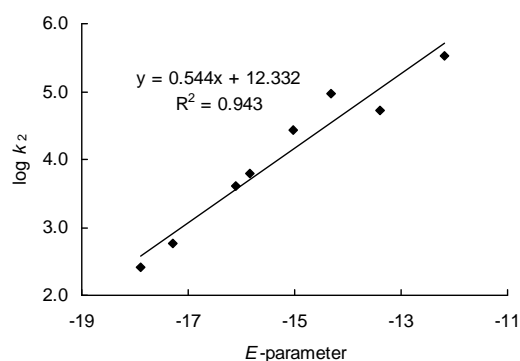
[E] [mol L ⁻¹]	[Nu] [mol L ⁻¹]	[18-crown-6] [mol L ⁻¹]	[Nu]/[E]	<i>k</i> _{obs} [s ⁻¹]
2.67 × 10 ⁻⁵	3.92 × 10 ⁻⁴	5.21 × 10 ⁻⁴	14.7	0.0881
2.67 × 10 ⁻⁵	7.83 × 10 ⁻⁴	1.04 × 10 ⁻³	29.3	0.195
2.67 × 10 ⁻⁵	1.17 × 10 ⁻³	1.56 × 10 ⁻³	44.0	0.302
2.67 × 10 ⁻⁵	1.57 × 10 ⁻³	2.08 × 10 ⁻³	58.7	0.379
2.67 × 10 ⁻⁵	1.96 × 10 ⁻³	2.60 × 10 ⁻³	73.3	0.504

$$k_2 = 2.59 \times 10^2 \text{ L mol}^{-1} \text{ s}^{-1}$$

Table 65: Determination of *N*- and *s*-parameters for **2m** at 20 °C in DMSO.

Electrophile	<i>E</i> -parameter	<i>k</i> ₂ [L mol ⁻¹ s ⁻¹]	log <i>k</i> ₂
1j	-12.18	3.29 × 10 ⁵	5.52
1k	-13.39	5.24 × 10 ⁴	4.72
1l	-14.32	9.38 × 10 ⁴	4.97
1m	-15.03	2.71 × 10 ⁴	4.43
1n	-15.83	6.14 × 10 ³	3.79
1o	-16.11	4.01 × 10 ³	3.60
1p	-17.29	5.81 × 10 ²	2.76
1q	-17.90	2.59 × 10 ²	2.41

$$N = 22.67; s = 0.54$$



Potassium Salt of Cyanamide (**2n-K**)

Table 66: Kinetics of the reaction of **2n-K** with **1j** (20 °C, in DMSO, stopped-flow, at 422 nm).

[E] [mol L ⁻¹]	[Nu] [mol L ⁻¹]	[Nu]/[E]	<i>k</i> _{obs} [s ⁻¹]
5.10 × 10 ⁻⁵	4.50 × 10 ⁻⁴	8.8	73.6
5.10 × 10 ⁻⁵	6.75 × 10 ⁻⁴	13.2	112
5.10 × 10 ⁻⁵	9.00 × 10 ⁻⁴	17.6	145
5.10 × 10 ⁻⁵	1.13 × 10 ⁻³	22.2	183
5.10 × 10 ⁻⁵	1.35 × 10 ⁻³	26.5	222

$$k_2 = 1.63 \times 10^5 \text{ L mol}^{-1} \text{ s}^{-1}$$

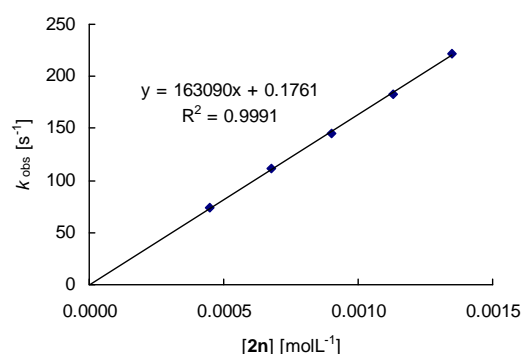
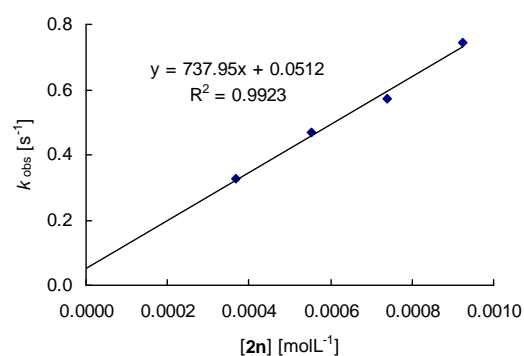


Table 67: Kinetics of the reaction of **2n-K** with **1n** (20 °C, in DMSO, stopped-flow, at 371 nm).

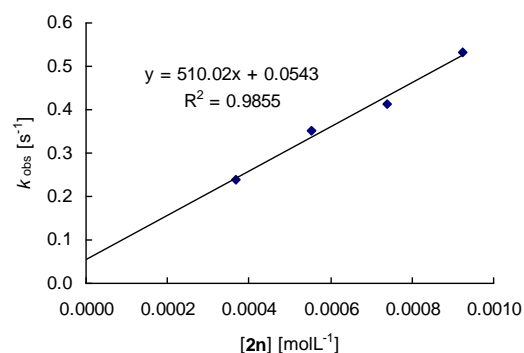
[E] [mol L ⁻¹]	[Nu] [mol L ⁻¹]	[Nu]/[E]	<i>k</i> _{obs} [s ⁻¹]
2.54 × 10 ⁻⁵	3.69 × 10 ⁻⁴	14.5	0.326
2.54 × 10 ⁻⁵	5.54 × 10 ⁻⁴	21.8	0.468
2.54 × 10 ⁻⁵	7.39 × 10 ⁻⁴	29.0	0.574
2.54 × 10 ⁻⁵	9.23 × 10 ⁻⁴	36.3	0.745

$$k_2 = 7.38 \times 10^2 \text{ L mol}^{-1} \text{ s}^{-1}$$

Table 68: Kinetics of the reaction of **2n-K** with **1o** (20 °C, in DMSO, stopped-flow, at 393 nm).

[E] [mol L ⁻¹]	[Nu] [mol L ⁻¹]	[Nu]/[E]	<i>k</i> _{obs} [s ⁻¹]
1.66 × 10 ⁻⁵	3.69 × 10 ⁻⁴	22.2	0.238
1.66 × 10 ⁻⁵	5.54 × 10 ⁻⁴	33.3	0.353
1.66 × 10 ⁻⁵	7.39 × 10 ⁻⁴	44.4	0.413
1.66 × 10 ⁻⁵	9.23 × 10 ⁻⁴	55.5	0.532

$$k_2 = 5.10 \times 10^2 \text{ L mol}^{-1} \text{ s}^{-1}$$

Table 69: Kinetics of the reaction of **2n-K** with **4b** (20 °C, in DMSO, stopped-flow, at 480 nm).

[E] [mol L ⁻¹]	[Nu] [mol L ⁻¹]	[Nu]/[E]	<i>k</i> _{obs} [s ⁻¹]
2.92 × 10 ⁻⁵	3.22 × 10 ⁻⁴	11.0	57.4
2.92 × 10 ⁻⁵	4.29 × 10 ⁻⁴	14.7	80.5
2.92 × 10 ⁻⁵	5.11 × 10 ⁻⁴	17.5	92.5
2.92 × 10 ⁻⁵	6.44 × 10 ⁻⁴	22.1	124

$$k_2 = 2.04 \times 10^5 \text{ L mol}^{-1} \text{ s}^{-1}$$

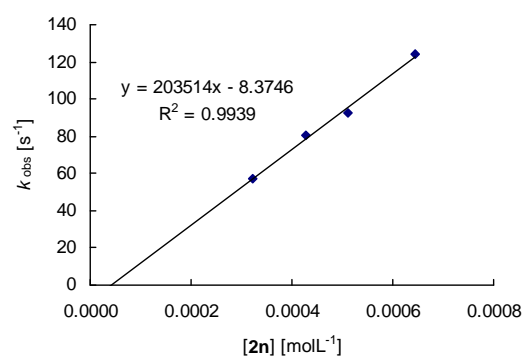
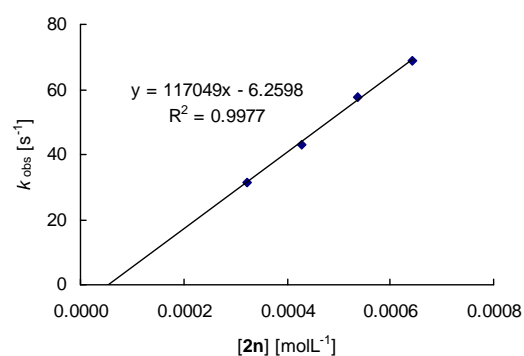


Table 70: Kinetics of the reaction of **2n-K** with **4a** (20 °C, in DMSO, stopped-flow, at 500 nm).

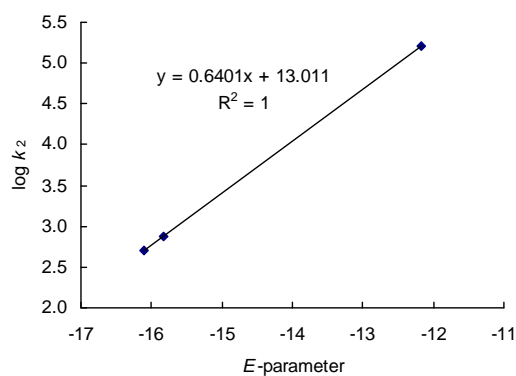
[E] [mol L ⁻¹]	[Nu] [mol L ⁻¹]	[Nu]/[E]	<i>k</i> _{obs} [s ⁻¹]
3.88 × 10 ⁻⁵	3.22 × 10 ⁻⁴	8.3	31.6
3.88 × 10 ⁻⁵	4.29 × 10 ⁻⁴	11.1	43.2
3.88 × 10 ⁻⁵	5.37 × 10 ⁻⁴	13.8	57.6
3.88 × 10 ⁻⁵	6.44 × 10 ⁻⁴	16.6	68.7



$$k_2 = 1.17 \times 10^5 \text{ L mol}^{-1} \text{ s}^{-1}$$

Table 71: Determination of *N*- and *s*-parameters for **2n** at 20 °C in DMSO.

Electrophile	<i>E</i> -parameter	<i>k</i> ₂ [L mol ⁻¹ s ⁻¹]	log <i>k</i> ₂
1j	-12.18	1.64 × 10 ⁵	5.21
1n	-15.83	7.38 × 10 ²	2.87
1o	-16.11	5.10 × 10 ²	2.71



$$N = 20.33; s = 0.64$$

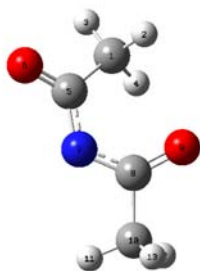
5.7 Quantum Chemical Calculations

General

All quantum chemical calculations were carried out using Gaussian 03.^[45] Density functional calculations used the B3LYP (Becke-Lee-Yang-Parr) functional.^[63] Free energies were calculated at B3LYP/6-31+G(d,p) level.

Structures

Sickle-Conformation of the Anion of Diacetamide (2g-I)

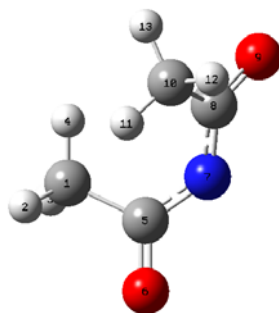


```
1 | 1 | UNPC-UNK | FOpt | RB3LYP | 6-31+G(d,p) | C4H6N1O2(1-) | PCUSER | 14-Apr-2010 | 0
| #p b3lyp/6-31+g(d,p) opt freq | Diacetamid-Anion - Sichel-Konformatio
n | -1, 1 | C, 1.5643402476, 1.1294243429, 0.4345342081 | H, 1.5722154699, 1.7676
261172, -0.4551849633 | H, 2.5622802896, 1.1350282078, 0.8854139439 | H, 0.8238
822957, 1.5544482197, 1.1172306951 | C, 1.2326106484, -0.3118967917, 0.011913
1946 | O, 2.1905781439, -1.0492478235, -0.2882755398 | N, -0.0511020698, -0.764
5892125, 0.0507064151 | C, -1.1092887859, 0.0529341744, -0.0935137428 | O, -1.1
441298822, 1.2256867924, -0.5424986491 | C, -2.4510771738, -0.5909077284, 0.2
872682205 | H, -2.3153777871, -1.577480022, 0.7379559412 | H, -2.9838585107, 0.
0701940611, 0.9816177459 | H, -3.0760918856, -0.6856753375, -0.6098094692 | | V
ersi on=I A32W-G03RevE.01 | State=1-A | HF=-361.335027 | RMSD=8.871e-009 | RMSF=
1.595e-005 | Thermal=0. | Dipole=-0.810657, 0.5689176, 0.7017554 | PG=C01 [X(C
4H6N1O2)] | @
```

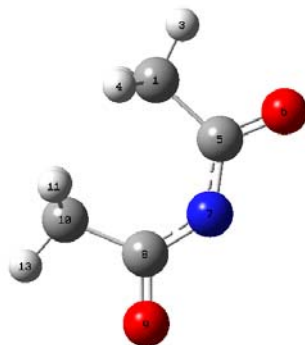
W-Conformation of the Anion of Diacetamide (2g-III)



```
1 | 1 | UNPC-UNK | FOpt | RB3LYP | 6-31+G(d,p) | C4H6N1O2(1-) | PCUSER | 14-Apr-2010 | 0
| #p b3lyp/6-31+g(d,p) opt freq | Diacetamid-Anion - W-Form | -1, 1 | C, -2.
3924068932, -0.7708521166, -0.3517355296 | H, -3.195998607, -0.7402186738, 0.
3931794652 | H, -2.1190250111, -1.8065586048, -0.5719996023 | H, -2.7781800264
, -0.3040382624, -1.2677142848 | C, -1.1875276239, 0.0499740284, 0.1409415229
| O, -1.4189469958, 1.1528607853, 0.6727816459 | N, -0.0011156822, -0.58367700
36, -0.0022668 | C, 1.1866730714, 0.049057671, -0.1393849167 | O, 1.4207076263,
1.1542804365, -0.6649922107 | C, 2.3885454532, -0.7756220293, 0.3540932083 | H
, 2.1183556983, -1.8183318369, 0.5431828104 | H, 3.2058693553, -0.7199380247,
-0.3740620672 | H, 2.7526016352, -0.330797369, 1.2898087586 | | Versi on=I A32W-
G03RevE.01 | State=1-A | HF=-361.3304457 | RMSD=8.447e-009 | RMSF=8.943e-006 | T
hermal=0. | Dipole=-0.0002311, -1.478403, -0.0010304 | PG=C01 [X(C4H6N1O2)] |
| @
```

U-Conformation of the Anion of Diacetamide (2g-VII)

```
1|1|UNPC-UNK|FOpt|RB3LYP|6-31+G(d,p)|C4H6N1O2(1-)|PCUSER|14-Apr-2010|0
|#p opt freq B3LYP/6-31+G(d,p)||Di acetami d-Ani on - U-Form||-1,1|C,-1.
1950760537,-3.1082267644,0.2419196711|H,-1.679706353,-3.6448039501,1.0
651528316|H,-0.5769917245,-3.8341437475,-0.3000294629|H,-1.9514859816,
-2.7216593593,-0.4474226567|C,-0.2523969932,-2.0216993955,0.8160242491
|O,0.526914795,-2.3963685923,1.7177388861|N,-0.2214313695,-0.812675349
6,0.2347923087|C,-1.2580362977,-0.1342362124,-0.2806084314|O,-1.177760
6051,0.6680656812,-1.2349104618|C,-2.6298151459,-0.1985537887,0.435560
119|H,-2.7075042036,-0.9995169038,1.1766463256|H,-2.784046538,0.758517
0868,0.9483099576|H,-3.4272176161,-0.3003046293,-0.3089530187||Versi on
=|A32W-G03RevE.01|State=1-A|HF=-361.3268364|RMSD=9.428e-009|RMSF=6.305
e-006|Thermal=0.|Di pol e=-1.8679588,-0.9291437,0.1147585|PG=C01 [X(C4H6
N1O2)]||@
```

Planar W-Conformation of the Anion of Diacetamide (2g-VII)

```
1|1|UNPC-UNK|FOpt|RB3LYP|6-31+G(d,p)|C4H6N1O2(1-)|PCUSER|18-May-2010|0
|#P B3LYP/6-31+G(d,p) opt=modredundant freq||W-Form Planar||-1,1|C,-1
.4865468727,1.2456546487,0.000083176|H,-1.0651707645,1.737838889,0.883
0497969|H,-2.569321757,1.3878289818,0.0000453052|H,-1.065082049,1.7379
776615,-0.8827605153|C,-1.2233534531,-0.2853206293,-0.0000287916|O,-2.
26254982,-0.9803295673,0.0001339858|N,-0.0000183528,-0.8615447456,0.00
00074344|C,1.2233640275,-0.285423728,-0.0001447142|O,2.2625018655,-0.9
805219453,-0.0000805249|C,1.4866862144,1.2455295346,-0.0000331918|H,1.
0653497526,1.7378451233,-0.8829455987|H,1.0652609164,1.7377915255,0.88
286367|H,2.5694722928,1.3876142512,0.0000169683||Versi on=|A32W-G03RevE
.01|State=1-A|HF=-361.3186267|RMSD=4.191e-009|RMSF=6.992e-005|Thermal =
0.|Di pol e=0.0001056,2.6346899,-0.0000884|PG=C01 [X(C4H6N1O2)]||@
```

Relaxed Potential Energy Surface Scan (ϕ -Scan)

ϕ	Energy / Hartree	ΔE / kJ mol ⁻¹	ϕ	Energy / Hartree	ΔE / kJ mol ⁻¹
-180.0	-361.3338126	3.18	5.0	-361.3288419	16.23
-175.0	-361.3340623	2.52	10.0	-361.3294142	14.72
-170.0	-361.3344607	1.48	15.0	-361.3298857	13.49
-165.0	-361.3347857	0.62	20.0	-361.3302078	12.64
-160.0	-361.3349807	0.11	25.0	-361.3303836	12.18
-155.0	-361.3350226	0.00	30.0	-361.3304449	12.02
-150.0	-361.3349034	0.31	35.0	-361.3304097	12.11
-145.0	-361.3346242	1.05	40.0	-361.3302993	12.40
-140.0	-361.3342766	1.96	45.0	-361.3301088	12.90
-135.0	-361.3339312	2.87	50.0	-361.3298611	13.55
-130.0	-361.3334755	4.06	55.0	-361.3295807	14.29
-125.0	-361.3329287	5.50	60.0	-361.3292976	15.03
-120.0	-361.3323143	7.11	65.0	-361.329044	15.70
-115.0	-361.3316602	8.83	70.0	-361.3288439	16.22
-110.0	-361.3309977	10.57	75.0	-361.3287115	16.57
-105.0	-361.3303609	12.24	80.0	-361.3286721	16.67
-100.0	-361.3297937	13.73	85.0	-361.3287664	16.43
-95.0	-361.3293285	14.95	90.0	-361.3289786	15.87
-90.0	-361.3289777	15.87	95.0	-361.3293285	14.95
-85.0	-361.3287664	16.43	100.0	-361.3297937	13.73
-80.0	-361.3286721	16.67	105.0	-361.3303609	12.24
-75.0	-361.3287114	16.57	110.0	-361.3309977	10.57
-70.0	-361.3288439	16.22	115.0	-361.3316602	8.83
-65.0	-361.329044	15.70	120.0	-361.3323143	7.11
-60.0	-361.3292976	15.03	125.0	-361.3329287	5.50
-55.0	-361.3295806	14.29	130.0	-361.3334755	4.06
-50.0	-361.3298611	13.55	135.0	-361.3339312	2.87
-45.0	-361.3301086	12.90	140.0	-361.3342765	1.96
-40.0	-361.3302992	12.40	145.0	-361.3346242	1.05
-35.0	-361.3304092	12.11	150.0	-361.3349034	0.31
-30.0	-361.3304449	12.02	155.0	-361.3350226	0.00
-25.0	-361.3303835	12.18	160.0	-361.3349806	0.11
-20.0	-361.3302078	12.64	165.0	-361.3347856	0.62
-15.0	-361.3298857	13.49	170.0	-361.3344607	1.48
-10.0	-361.3294142	14.72	175.0	-361.3340623	2.52
-5.0	-361.328842	16.23	180.0	-361.3338126	3.18
0.0	-361.3284696	17.20			

Relaxed Potential Energy Surface Scan (ϕ -Scan)

ϕ	Energy / Hartree	ΔE / kJ mol ⁻¹	ϕ	Energy / Hartree	ΔE / kJ mol ⁻¹
-175.0	-361.324708	27.08	5.0	-361.334509	1.35
-170.0	-361.325501	25.00	10.0	-361.334869	0.40
-165.0	-361.326108	23.40	15.0	-361.335022	0.00
-160.0	-361.326525	22.31	20.0	-361.334961	0.16
-155.0	-361.326761	21.69	25.0	-361.334682	0.89
-150.0	-361.326836	21.49	30.0	-361.334199	2.16
-145.0	-361.326771	21.66	35.0	-361.333354	3.89
-140.0	-361.326584	22.15	40.0	-361.332734	6.01
-135.0	-361.326299	22.90	45.0	-361.331832	8.38
-130.0	-361.325953	23.81	50.0	-361.330879	10.88
-125.0	-361.325579	24.79	55.0	-361.329907	13.43
-120.0	-361.325209	25.76	60.0	-361.328922	16.02
-115.0	-361.324873	26.65	65.0	-361.327972	18.51
-110.0	-361.324561	27.47	70.0	-361.327082	20.85
-105.0	-361.32439	27.91	75.0	-361.326282	22.95
-100.0	-361.324302	28.15	80.0	-361.325597	24.75
-95.0	-361.324369	27.97	85.0	-361.325044	26.20
-90.0	-361.324581	27.41	90.0	-361.324642	27.25
-85.0	-361.325044	26.20	95.0	-361.3244	27.89
-80.0	-361.325597	24.75	100.0	-361.324336	28.06
-75.0	-361.326282	22.95	105.0	-361.324379	27.94
-70.0	-361.327082	20.85	110.0	-361.324586	27.40
-65.0	-361.327972	18.51	115.0	-361.324873	26.65
-60.0	-361.328923	16.01	120.0	-361.325209	25.76
-55.0	-361.329907	13.43	125.0	-361.325579	24.79
-50.0	-361.33088	10.87	130.0	-361.325953	23.81
-45.0	-361.331831	8.38	135.0	-361.326299	22.90
-40.0	-361.332734	6.01	140.0	-361.326584	22.15
-35.0	-361.33354	3.89	145.0	-361.326771	21.66
-30.0	-361.334199	2.16	150.0	-361.326836	21.49
-25.0	-361.334682	0.89	155.0	-361.326761	21.69
-20.0	-361.33496	0.16	160.0	-361.326525	22.31
-15.0	-361.335022	0.00	165.0	-361.326108	23.40
-10.0	-361.334869	0.40	170.0	-361.325501	25.00
-5.0	-361.334509	1.35	175.0	-361.324708	27.08
0.0	-361.333981	2.73			

6 References

- [1] S. Gabriel, *Ber. Dtsch. Chem. Ges.* **1887**, *20*, 2224–2236.
- [2] M. S. Gibson, R. W. Bradshaw, *Angew. Chem.* **1968**, *80*, 986–996; *Angew. Chem. Int. Ed. Engl.* **1968**, *7*, 919–930.
- [3] a) J. B. Hendrickson, R. Bergeron, D. D. Sternbach, *Tetrahedron* **1975**, *31*, 2517–2521; b) U. Ragnarsson, L. Grehn, *Acc. Chem. Res.* **1991**, *24*, 285–289.
- [4] a) R. A. W. Johnstone, D. W. Payling, C. Thomas, *J. Chem. Soc. C* **1969**, *16*, 2223–2224; b) P. A. Harland, P. Hodge, W. Maughan, E. Wildsmith, *Synthesis* **1984**, 941–943.
- [5] U. Ragnarsson, *Chem. Soc. Rev.* **2001**, *30*, 205–213.
- [6] a) A. Kubo, H. Kubota, M. Takahashi, K.-i. Nunami, *Tetrahedron Lett.* **1996**, *37*, 4957–4960; b) D. Albanese, D. Landini, V. Lupi, M. Penso, *Eur. J. Org. Chem.* **2000**, 1443–1449.
- [7] H. Fujisawa, E. Takahashi, T. Mukaiyama, *Chem. Eur. J.* **2006**, *12*, 5082–5093.
- [8] a) J. F. Bunnett, J. H. Beale, *J. Org. Chem.* **1971**, *36*, 1659–1661; b) J. H. Beale, *J. Org. Chem.* **1972**, *37*, 3871–3872; c) F. Bordwell, D. L. Hughes, *J. Am. Chem. Soc.* **1984**, *106*, 3234–3240.
- [9] a) Y. Kondo, K. Kondo, S. Kusabayashi, *J. Chem. Soc. Perkin Trans. 2* **1993**, 1141–1145; b) Y. Kondo, T. Tsukamoto, C. Moriguchi, *J. Chem. Soc., Perkin Trans. 2* **1996**, 1699–1704; c) Y. Kondo, T. Tsukamoto, N. Kimura, *J. Chem. Soc., Perkin Trans. 2* **1997**, 1765–1769.
- [10] H. Mayr, T. Bug, M. F. Gotta, N. Hering, B. Irrgang, B. Janker, B. Kempf, R. Loos, A. R. Ofial, G. Remennikov, H. Schimmel, *J. Am. Chem. Soc.* **2001**, *123*, 9500–9512.
- [11] H. Mayr, B. Kempf, A. R. Ofial, *Acc. Chem. Res.* **2003**, *36*, 66–77.
- [12] a) R. Lucius, H. Mayr, *Angew. Chem.* **2000**, *112*, 2086–2089; *Angew. Chem. Int. Ed.* **2000**, *39*, 1995–1997; b) T. Bug, T. Lemek, H. Mayr, *J. Org. Chem.* **2004**, *69*, 7565–7576.
- [13] a) F. Brotzel, Y. C. Chu, H. Mayr, *J. Org. Chem.* **2007**, *72*, 3679–3688; b) T. Kanzian, T. A. Nigst, A. Maier, S. Pichl, H. Mayr, *Eur. J. Org. Chem.* **2009**, *2009*, 6379–6385.
- [14] a) S. Minegishi, S. Kobayashi, H. Mayr, *J. Am. Chem. Soc.* **2004**, *126*, 5174–5181; b) T. B. Phan, H. Mayr, *Can. J. Chem.* **2005**, *83*, 1554–1560.
- [15] a) E.-U. Würthwein, G. Lang, L. H. Schappele, H. Mayr, *J. Am. Chem. Soc.* **2002**, *124*, 4084–4092; b) H. Mayr, G. Lang, A. R. Ofial, *J. Am. Chem. Soc.* **2002**, *124*,

- 4076–4083; c) D. Richter, H. Mayr, *Angew. Chem.* **2009**, *121*, 1992–1995; *Angew. Chem. Int. Ed.* **2009**, *48*, 1958–1961; d) D. Richter, Y. Tan, A. Antipova, X.-Q. Zhu, H. Mayr, *Chem. Asian J.* **2009**, *4*, 1824–1829.
- [16] H. Mayr, M. Patz, *Angew. Chem.* **1994**, *106*, 990–1010; Patz, *Angew. Chem. Int. Ed. Engl.* **1994**, *33*, 938–957.
- [17] For a comprehensive listing of nucleophilicity parameters N and electrophilicity parameters E , see <http://www.cup.uni-muenchen.de/oc/mayr/DBintro.html>.
- [18] a) R. Lucius, R. Loos, H. Mayr, *Angew. Chem.* **2002**, *114*, 97–102; *Angew. Chem. Int. Ed.* **2002**, *41*, 91–95; b) D. Richter, N. Hampel, T. Singer, A. R. Ofial, H. Mayr, *Eur. J. Org. Chem.* **2009**, *2009*, 3203–3211.
- [19] I. Koppel, J. Koppel, F. Degerbeck, L. Grehn, U. Ragnarsson, *J. Org. Chem.* **1991**, *56*, 7172–7174.
- [20] F. G. Bordwell, *Acc. Chem. Res.* **1988**, *21*, 456–463.
- [21] H. Falk, A. Leodolter, *Monatsh. Chem.* **1978**, *109*, 883–897.
- [22] R. G. Barradas, S. Fletcher, J. D. Porter, *Can. J. Chem.* **1976**, *54*, 1400–1404.
- [23] M. M. Hansen, A. R. Harkness, D. S. Coffey, F. G. Bordwell, Y. Zhao, *Tetrahedron Lett.* **1995**, *36*, 8949–8952.
- [24] W. H. Wang, C. C. Cheng, *Bull. Chem. Soc. Jpn.* **1994**, *67*, 1054–1057.
- [25] E. M. Arnett, J. A. Harrelson, Jr., *J. Am. Chem. Soc.* **1987**, *109*, 809–812.
- [26] A. Albert, *J. Chem. Soc. Perkin Trans. 1* **1975**, 345–349.
- [27] I. A. Koppel, J. Koppel, I. Leito, I. Koppel, M. Mishima, L. M. Yagupolskii, *J. Chem. Soc., Perkin Trans. 2* **2001**, 229–232.
- [28] A. V. Willi, *Helv. Chim. Acta* **1956**, *39*, 46–53.
- [29] R. L. Hinman, B. E. Hoogenboom, *J. Org. Chem.* **1961**, *26*, 3461–3467.
- [30] R. Schwesinger, H. Schlemper, C. Hasenfratz, J. Willaredt, T. Dambacher, T. Breuer, C. Ottaway, M. Fletschinger, J. Boele, H. Fritz, D. Putzas, H. W. Rotter, F. G. Bordwell, A. V. Satish, G.-Z. Ji, E.-M. Peters, K. Peters, H. G. V. Schnering, L. Walz, *Liebigs Ann. Chem.* **1996**, 1055–1081.
- [31] M. J. Bausch, B. David, P. Dobrowolski, V. Prasad, *J. Org. Chem.* **1990**, *55*, 5806–5808.
- [32] M. Zief, J. T. Edsall, *J. Am. Chem. Soc.* **1937**, *59*, 2245–2248.
- [33] X.-M. Zhang, F. G. Bordwell, *J. Org. Chem.* **1994**, *59*, 6456–6458.
- [34] F. G. Bordwell, G. E. Drucker, H. E. Fried, *J. Org. Chem.* **1981**, *46*, 632–635.

- [35] I. Leito, I. Kaljurand, I. A. Koppel, L. M. Yagupolskii, V. M. Vlasov, *J. Org. Chem.* **1998**, *63*, 7868–7874.
- [36] F. Seeliger, S. T. A. Berger, G. Y. Remennikov, K. Polborn, H. Mayr, *J. Org. Chem.* **2007**, *72*, 9170–9180.
- [37] T. B. Phan, M. Breugst, H. Mayr, *Angew. Chem.* **2006**, *118*, 3954–3959; *Angew. Chem. Int. Ed.* **2006**, *45*, 3869–3874.
- [38] a) B. C. Challis, J. Challis, in *The Chemistry of Amides* (Ed.: J. Zabicky), Interscience Publisher, London, **1970**, pp. 731–858; b) C. J. M. Stirling, *J. Chem. Soc.* **1960**, 255–262.
- [39] D. Döpp, H. Döpp, in *Methoden der organischen Chemie (Houben-Weyl)*, Thieme, Stuttgart, **1985**.
- [40] a) T. H. Koch, R. J. Sluski, R. H. Moseley, *J. Am. Chem. Soc.* **1973**, *95*, 3957–3963; b) D. R. Anderson, J. S. Keute, T. H. Koch, R. H. Moseley, *J. Am. Chem. Soc.* **1977**, *99*, 6332–6340.
- [41] N. Kornblum, R. A. Smiley, R. K. Blackwood, D. C. Iffland, *J. Am. Chem. Soc.* **1955**, *77*, 6269–6280.
- [42] a) W. Khayata, D. Baylocq, F. Pellerin, N. Rodier, *Acta Crystallogr., Sect. C: Cryst. Struct. Commun.* **1984**, *C40*, 765–767; b) J. Perron, A. L. Beauchamp, *Inorg. Chem.* **1984**, *23*, 2853–2859; c) D. R. Whitcomb, M. Rajeswaran, *J. Chem. Crystallogr.* **2006**, *36*, 587–598; d) D. R. Whitcomb, M. Rajeswaran, *Acta Crystallogr., Sect. E: Struct. Rep. Online* **2007**, *E63*, m2753; e) X. Tao, Y.-Q. Li, H.-H. Xu, N. Wang, F.-L. Du, Y.-Z. Shen, *Polyhedron* **2009**, *28*, 1191–1195.
- [43] A. A. Tishkov, H. Mayr, *Angew. Chem.* **2005**, *117*, 145–148; *Angew. Chem. Int. Ed.* **2005**, *44*, 142–145.
- [44] a) F. Seeliger, H. Mayr, *Org. Biomol. Chem.* **2008**, *6*, 3052–3058; b) O. Kaumanns, R. Appel, T. Lemek, F. Seeliger, H. Mayr, *J. Org. Chem.* **2009**, *74*, 75–81.
- [45] Gaussian 03, Revision D.01, M. J. Frisch, G. W. Trucks, H. B. Schlegel, G. E. Scuseria, M. A. Robb, J. R. Cheeseman, J. A. Montgomery, Jr., T. Vreven, K. N. Kudin, J. C. Burant, J. M. Millam, S. S. Iyengar, J. Tomasi, V. Barone, B. Mennucci, M. Cossi, G. Scalmani, N. Rega, G. A. Petersson, H. Nakatsuji, M. Hada, M. Ehara, K. Toyota, R. Fukuda, J. Hasegawa, M. Ishida, T. Nakajima, Y. Honda, O. Kitao, H. Nakai, M. Klene, X. Li, J. E. Knox, H. P. Hratchian, J. B. Cross, V. Bakken, C. Adamo, J. Jaramillo, R. Gomperts, R. E. Stratmann, O. Yazyev, A. J. Austin, R. Cammi, C. Pomelli, J. W. Ochterski, P. Y. Ayala, K. Morokuma, G. A. Voth, P.

- Salvador, J. J. Dannenberg, V. G. Zakrzewski, S. Dapprich, A. D. Daniels, M. C. Strain, O. Farkas, D. K. Malick, A. D. Rabuck, K. Raghavachari, J. B. Foresman, J. V. Ortiz, Q. Cui, A. G. Baboul, S. Clifford, J. Cioslowski, B. B. Stefanov, G. Liu, A. Liashenko, P. Piskorz, I. Komaromi, R. L. Martin, D. J. Fox, T. Keith, M. A. Al-Laham, C. Y. Peng, A. Nanayakkara, M. Challacombe, P. M. W. Gill, B. Johnson, W. Chen, M. W. Wong, C. Gonzalez, J. A. Pople, Gaussian, Inc., Wallingford CT, **2004**.
- [46] a) W. Funke, E.-U. Würthwein, *Chem. Ber.* **1992**, *125*, 1967–1968; b) N. Heße, R. Fröhlich, I. Humelnicu, E.-U. Würthwein, *Eur. J. Inorg. Chem.* **2005**, *2005*, 2189–2197.
- [47] F. G. Bordwell, T. A. Cripe, D. L. Hughes, in *Nucleophilicity, Vol. 215* (Eds.: J. M. Harris, S. P. McManus), American Chemical Society, Chicago, **1987**, pp. 137–153.
- [48] F. G. Bordwell, J. C. Branca, J. E. Bares, R. Filler, *J. Org. Chem.* **1988**, *53*, 780–782.
- [49] S. Hoz, H. Basch, J. L. Wolk, T. Hoz, E. Rozental, *J. Am. Chem. Soc.* **1999**, *121*, 7724–7725.
- [50] J. B. Pedley, R. D. Naylor, S. P. Kirby, *Thermochemical Data of Organic Compounds*, 2nd ed., Chapman and Hall, London, **1986**.
- [51] J. Hine, R. D. Weimar, *J. Am. Chem. Soc.* **1965**, *87*, 3387–3396.
- [52] M. R. Atkinson, J. B. Polya, *J. Chem. Soc.* **1954**, 3319–3324.
- [53] R. S. Neale, *Ind. Eng. Chem. Prod. Res. Dev.* **1980**, *19*, 648–654.
- [54] C. Hansch, A. Leo, D. Hoekman, *Exploring QSAR Hydrophobic, Electronic, and Steric Constants*, American Chemical Society, Washington, D.C., **1995**.
- [55] S. Bradamante, G. A. Pagani, *J. Org. Chem.* **1980**, *45*, 114–122.
- [56] M. Charton, *J. Org. Chem.* **1964**, *29*, 1222–1227.
- [57] C. Y. Meyers, B. Cremonini, L. Maioli, *J. Am. Chem. Soc.* **1964**, *86*, 2944–2945.
- [58] H. H. Szmant, G. Suld, *J. Am. Chem. Soc.* **1956**, *78*, 3400–3403.
- [59] D. D. Perrin, B. Dempsey, E. P. Serjeant, *pKa Prediction for Organic Acids and Bases*, Chapman and Hall, London, **1981**.
- [60] D. S. McDaniel, H. C. Brown, *J. Org. Chem.* **1958**, *23*, 420–427.
- [61] F. G. Bordwell, H. M. Andersen, *J. Am. Chem. Soc.* **1953**, *75*, 6019–6022.
- [62] J. D. Roberts, E. A. McElhill, *J. Am. Chem. Soc.* **1950**, *72*, 628.
- [63] a) Becke, A. D. *J. Chem. Phys.* **1993**, *98*, 5648–5652; b) Lee, C.; Yang, W.; Parr, R. G. *Phys. Rev. B* **1988**, *37*, 785–789.

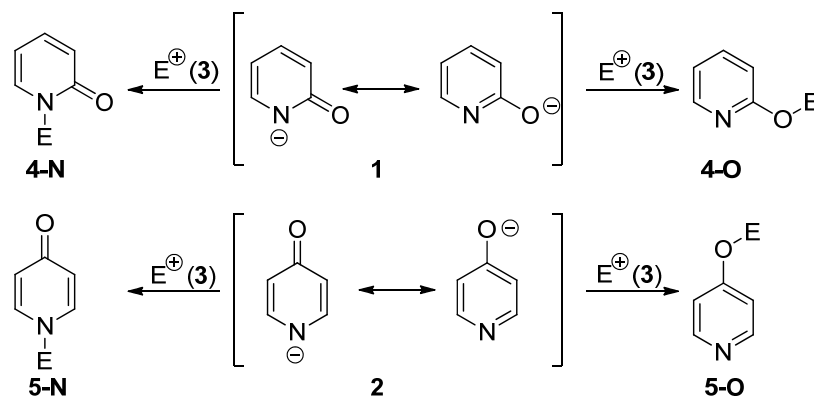
Chapter 5: Ambident Reactivities of Pyridone Anions

Martin Breugst and Herbert Mayr

J. Am. Chem. Soc. **2010**, *132*, 15380-15389.

1 Introduction

The anions of 2-pyridone (**1**) and 4-pyridone (**2**) are possibly the least understood ambident nucleophiles. As the selective formation of *N*-alkylated pyridones and alkoxy-pyridines according to Scheme 1 is of eminent importance for the synthesis of many biologically active compounds,^[1] control of the regioselectivity of electrophilic attack at **1** and **2** has intrigued chemists for many decades.^[2]



Scheme 1: Ambident reactivities of pyridone anions.

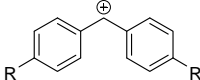
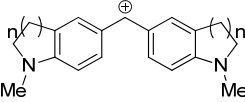
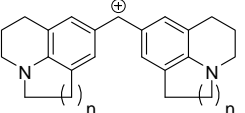
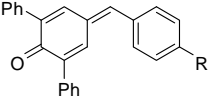
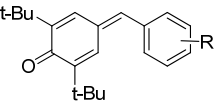
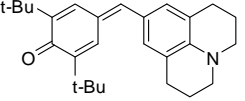
Kornblum rationalized the predominant formation of 2-ethoxypyridine from the silver salt of 2-pyridone with ethyl iodide by the “great carbonium character” of the electrophile in the presence of silver ions.^[3] Systematic investigations of the alkylations of 2-pyridone salts by Tieckelmann^[4] showed “that the results are completely consistent with Kornblum’s proposal that the silver ion enhances unimolecular character in the silver salt reactions, thereby favoring alkylation at the more electronegative oxygen atom”.^[4a] However, at the end of his thorough investigation, Tieckelmann stated: “The mechanism which leads to oxygen alkylation of the silver salts of 2-pyridones also needs further examination and may be more related to heterogeneous reaction than to the ability of the silver ion to promote unimolecular reaction as previously suggested”.^[4a]

Kornblum’s rule was later integrated in Pearson’s concept of “Hard and Soft Acids and Bases” (HSAB) which became the best known approach to rationalize ambident reactivity in

general.^[5] Remarkably few investigators have employed the HSAB model on the pyridone anions^[6] and a consistent rationalization of the large diversity of experimental results with **1** and **2** is lacking despite the great importance of these anions in synthesis.

Systematic experimental investigations of the reactivities of cyanide,^[7] cyanate,^[8] thiocyanate,^[9] nitrite,^[10] and phenyl sulfinate^[11] demonstrated that not even the behavior of the prototypes of ambident nucleophiles can be explained by the HSAB model^[5] or the related Klopman-Salem concept of charge and orbital controlled reactions.^[12] Recently, we have shown that Marcus theory^[13] provides a consistent rationalization of the ambident reactivities of these nucleophiles.^[14] We now report on a systematic experimental and quantum chemical investigation of the ambident reactivities of **1** and **2**, and demonstrate that Marcus theory also provides a consistent rationalization of the ambident reactivities of pyridone anions.

Table 1: Reference Electrophiles Employed in this Work and Wavelengths Monitored in the Kinetic Experiments.

Electrophile		E^a	$\lambda_{\text{eval}} / \text{nm}$
	R = H	3a 5.90	-
	R = Me	3b 3.63	-
	R = NMe ₂	3c -7.02	613
	R = N(CH ₂) ₄	3d -7.69	620
	n = 2	3e -8.22	618
	n = 1	3f -8.76	627
	n = 2	3g -9.45	635
	n = 1	3h -10.04	630
	R = OMe	3i -12.18	422
	R = NMe ₂	3j -13.39	533
	R = 4-NO ₂	3k -14.32	374
	R = 4-Me	3l -15.83	371
	R = 4-OMe	3m -16.11	393
	R = 4-NMe ₂	3n -17.29	486
		3o -17.90	521

^a Electrophilicity parameters from ref^[15].

In previous work, we have shown that the benzhydrylium ions **3a–h** and the structurally related quinone methides **3i–o** (Table 1) are electrophiles, which differ by approximately 20 orders of magnitude in reactivity while the steric surroundings of the reaction center are kept constant.^[15] We now use these compounds as reference electrophiles to investigate the influence of electrophilicity on regioselectivity and kinetics of the reactions of the pyridone anions **1** and **2**.

2 Results

Kinetic Investigations

The reactions of the pyridone anions **1** and **2** with the quinone methides **3i–o** and the benzhydrylium ions **3d–h** were performed in DMSO, acetonitrile, or water at 20 °C and monitored by UV-Vis spectroscopy at or close to the absorption maxima of the electrophiles ($354 < \lambda < 635$ nm) (Table 1). While the anions of 2-pyridone (**1**) reacted smoothly with the quinone methides **3k–o**, no reactions were observed when the anion of 4-pyridone (**2**) was employed. Reactivities of the more electrophilic benzhydrylium ions **3a–c** could not be determined, because the laser-flash-photolytic generation of benzhydrylium ions, which we usually employ for studying fast reactions, was not applicable due to the absorption of the pyridone anions **1** and **2** ($\epsilon = 1.85 \times 10^3$ L mol⁻¹ cm⁻¹) at 266 nm, i.e., the excitation wavelength of the laser.

By using the nucleophiles **1** and **2** in large excess over the electrophiles, their concentrations remained almost constant throughout the reactions, and pseudo-first-order kinetics were obtained in all runs. The first-order rate constants k_{obs} were then derived by least-squares fitting of the time-dependent absorbances A_t of the electrophiles to the exponential function $A_t = A_0 \exp(-k_{\text{obs}}t) + C$. Second-order rate constants were obtained as the slopes of the plots of k_{obs} versus the concentration of the nucleophiles (Figure 1).

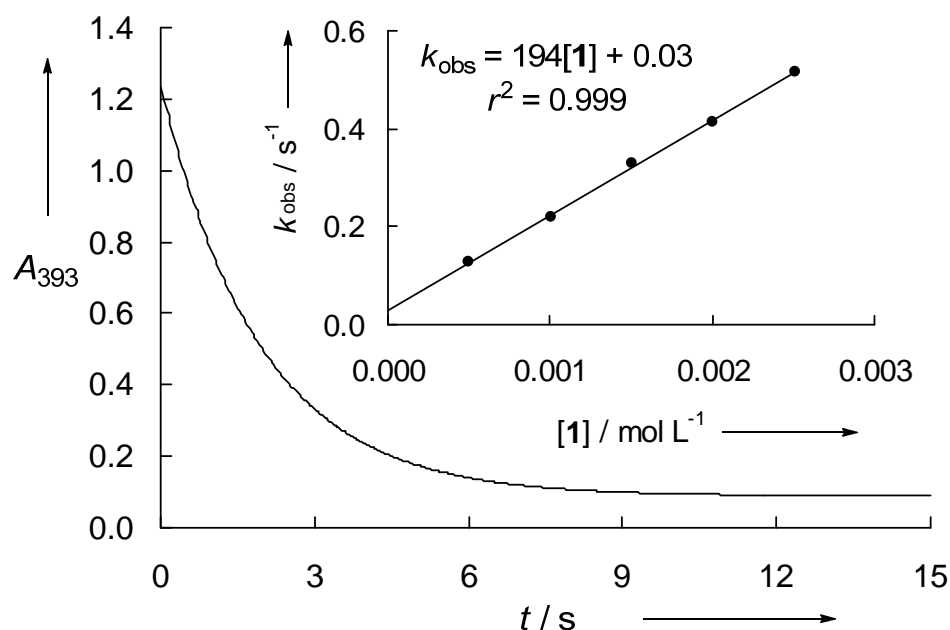


Figure 1: Plot of the absorbance at 393 nm, A_{393} , vs. time for the reaction of **3m** with the anion of 2-pyridone (**1**) in DMSO at 20 °C and correlation of the first-order rate constants k_{obs} with the concentration of **1** (insert).

Due to the low acidities of the pyridones **1-H** ($\text{p}K_{\text{a}} = 11.74$)^[16] and **2-H** ($\text{p}K_{\text{a}} = 11.12$)^[16] aqueous solutions of the pyridone anions **1** and **2** are partially hydrolyzed and contain hydroxide anions. For that reason, three competing reactions may account for the decay of the benzhydrylium ions in water and the observed rate constants k_{obs} for the consumption of the electrophiles in water reflect the sum of their reactions with the pyridone anions **1** or **2** (k_2), hydroxide ($k_{2,\text{OH}}$)^[17] and water (k_{w}) [Eq. (1)].

$$k_{\text{obs}} = k_2[\mathbf{1} \text{ or } \mathbf{2}] + k_{2,\text{OH}}[\text{OH}^-] + k_{\text{w}} \quad (1)$$

$$k_{\text{eff}} = k_{\text{obs}} - k_{2,\text{OH}}[\text{OH}^-] = k_2[\mathbf{1} \text{ or } \mathbf{2}] + k_{\text{w}} \quad (2)$$

All equilibrium concentrations in equation (2) were calculated from the initial concentrations and the $\text{p}K_{\text{aH}}$ values, as described in the Experimental Section. Rearrangement of equation (1), i.e., subtraction of the contribution of hydroxide from the observed rate constant k_{obs} , yields equation (2), and the second-order rate constants for the reactions of the benzhydrylium ions with **1** and **2** can then be obtained from plots of k_{eff} versus the concentration of the nucleophiles. By combining the pyridones **1-H** and **2-H**, which are used in high excess over the electrophiles **3** (pseudo-first-order conditions), with only 0.02 to 0.2 equivalents of KOH,

we were able to realize conditions, where the correction term $k_{2,\text{OH}}[\text{OH}^-]$ never exceeded 10 % of k_{obs} , thus giving rise to highly reliable values of k_2 . The intercepts of these plots correspond to the reactions of the electrophiles with water and are generally negligible in agreement with previous work, where water ($N = 5.20$)^[18] was demonstrated to react much slower with benzhydrylium ions than the nucleophiles investigated in this work.

Table 2: Second-Order Rate Constants for the Reactions of the 2-Pyridone Anion **1** with Reference Electrophiles at 20 °C.

Solvent	N/s	Electrophile	$k_2 / \text{L mol}^{-1} \text{s}^{-1}$	
DMSO	19.91 / 0.60	3o	1.51×10^1	
		3n	3.68×10^1	
		3m	1.94×10^2	
		3l	2.44×10^2	
			$1.66 \times 10^{2,a}$	
		3k	3.06×10^3	
		3j	6.49×10^3	
		3i	4.05×10^4	
			$2.64 \times 10^{4,a}$	
			3h	8.69×10^5
CH ₃ CN	20.11 / 0.57	3g	1.65×10^6	
		3o	1.94×10^1	
		3n	3.84×10^1	
		3m	1.72×10^2	
		3l	2.38×10^2	
		3k	2.34×10^3	
		3j	5.79×10^3	
		3i	3.12×10^4	
			3h	2.04×10^1
			3g	3.42×10^1
Water	12.47 / 0.52	3f	8.50×10^1	
		3e	1.56×10^2	
		3d	3.37×10^2	

^a Li⁺ as counterion.

As shown for several examples in the Experimental Section, k_{obs} values obtained for **1-K** and **2-K** in the presence and in the absence of 18-crown-6 are on the same k_{obs} vs. [**1**] or k_{obs} vs. [**2**] plots, indicating that in the concentration range under investigation ($c < 4 \times 10^{-3}$ M) reactivities of the free anions **1** (Table 2) and **2** (Table 3) are observed.

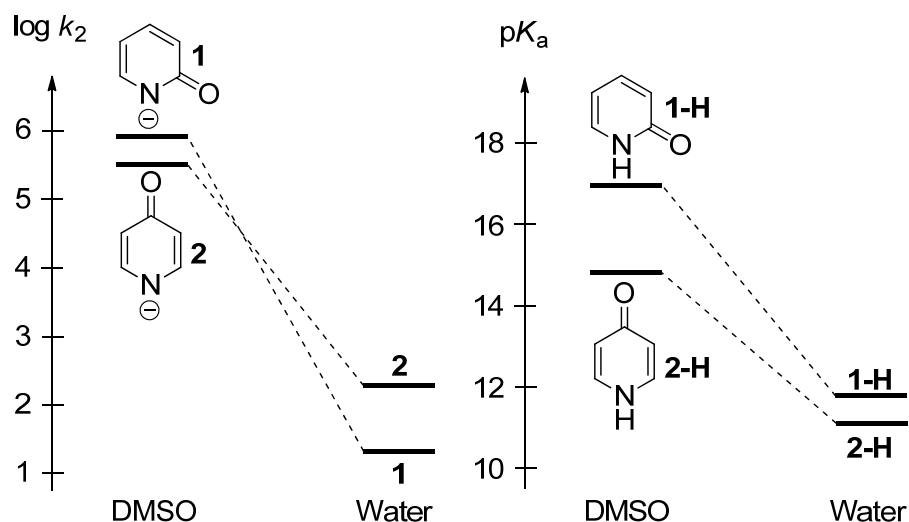
Furthermore, an exchange of K⁺ by Li⁺ only moderately reduces the rate constant in DMSO by a factor of 0.65 (Table 2), in line with previous findings by Tieckelmann.^[4]

Table 3: Second-Order Rate Constants for the Reactions of the 4-Pyridone Anion **2** with Reference Electrophiles at 20 °C.

Solvent	<i>N</i> / <i>s</i>	Electrophile	<i>k</i> ₂ / L mol ⁻¹ s ⁻¹
DMSO	18.97 / 0.62	3k	7.28 × 10 ²
		3j	2.75 × 10 ³
		3i	1.34 × 10 ⁴
		3h	3.26 × 10 ⁵
		3g	7.45 × 10 ⁵
CH ₃ CN	20.22 / 0.49	3l	1.61 × 10 ²
		3k	5.53 × 10 ²
		3j	2.25 × 10 ³
		3i	9.14 × 10 ³
		3h	1.93 × 10 ²
Water	14.76 / 0.48	3g	2.99 × 10 ²
		3f	6.61 × 10 ²
		3e	1.35 × 10 ³
		3d	2.34 × 10 ³

Solvent Effects

Tables 2 and 3 show that the reactivities of **1** and **2** towards benzhydrylium ions and quinone methides (**3**) are almost identical in DMSO and CH₃CN. The rate constants in these solvents differ by less than a factor of 1.5 and we can neglect differential solvent effects when comparing rate constants determined in DMSO and CH₃CN. The rate constants for the reactions of **1** and **2** with benzhydrylium ions show a different order in DMSO and water. As depicted in Scheme 2 for the reactions with **3h**, 2-pyridone anion (**1**) reacts approximately 48000 times faster in DMSO than in water, while the reactions of 4-pyridone anion (**2**) differ by a factor of only ca 2000. The resulting reversal of the relative reactivities of **1** and **2** in the two solvents indicates that the 2-pyridone anion **1** is better stabilized by hydrogen bonding in water than the 4-pyridone anion **2**. In line with this interpretation the significant difference between the acidities of 2-pyridone (**1-H**) and 4-pyridone (**2-H**) in DMSO is almost cancelled in aqueous solution (Scheme 2, right).



Scheme 2: Solvent dependence of the rate constant of the reactions of **1-K** and **2-K** with **3h** at 20 °C and the corresponding pK_a values (pK_a from refs ^[16, 19]).

Correlation Analysis

In line with the linear free-energy relationship [Eq. (3)], where the second-order rate constant ($\log k_2$) is described by the nucleophile-specific parameters s and N and the electrophile-specific parameter E ,^[20] plots of $\log k_2$ for the reactions of the pyridone anions **1** and **2** with the reference electrophiles **3d–o** versus their electrophilicity parameters E were linear.

$$\log k_2 = s (N + E) \quad (3)$$

The slopes of these correlations correspond to the nucleophile-specific sensitivity parameters s , whereas the negative intercepts on the abscissa yield the nucleophilicity parameters N . For reasons of clarity the rate constants determined in CH_3CN are not shown in Figure 2, but all individual correlations are depicted in the Experimental Section. The almost parallel correlation lines in Figure 2 which refer to N -attack (see below) imply that the relative reactivities of 2- and 4-pyridone anions (**1** and **2**) are nearly independent of the reactivities of the electrophiles.

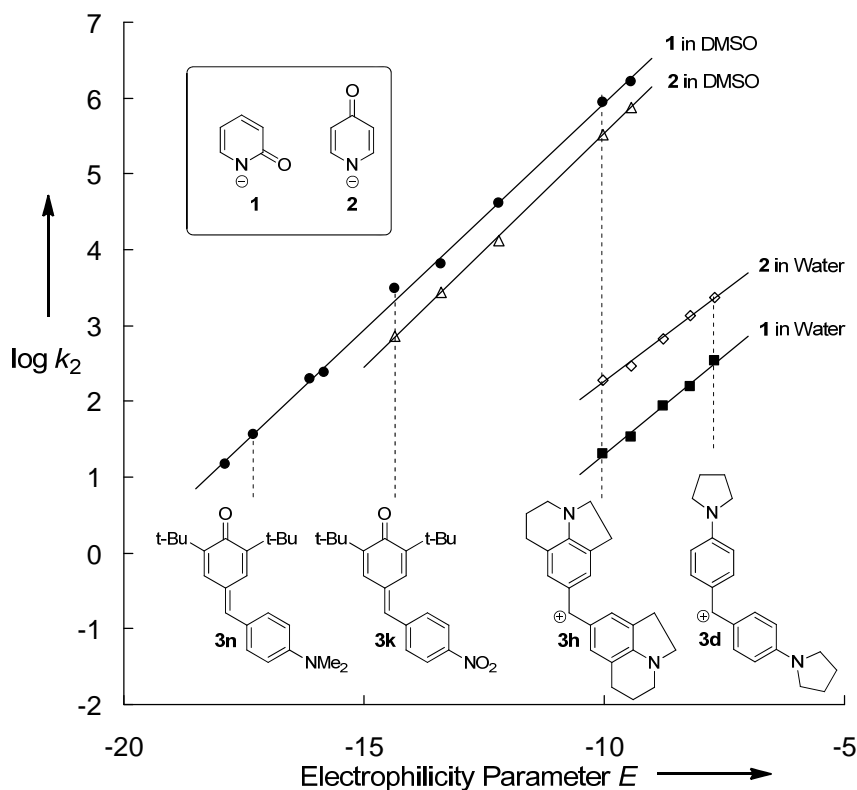
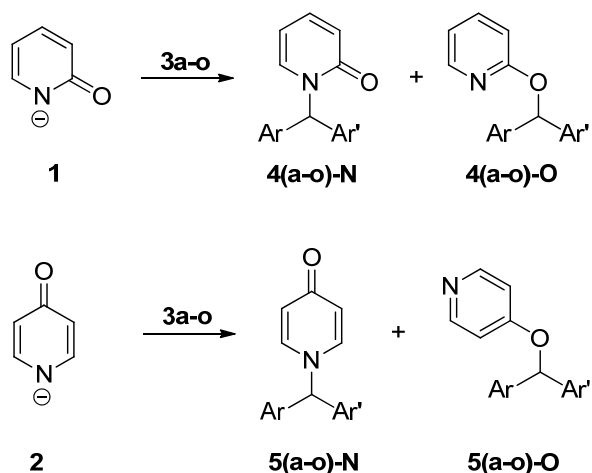


Figure 2: Plots of the rate constants $\log k_2$ for the reaction of the pyridone anions **1** and **2** with reference electrophiles versus their electrophilicity parameters E (correlation in CH_3CN are shown in the Experimental Section).

Reaction Products

Scheme 3 specifies the general Scheme 1 for the reaction of the pyridone anions **1** and **2** with the benzhydrylium ions **3a–h** and the quinone methides **3i–o**. The letters in the products **4** and **5** identify their origin; thus **4k–N** is formed from **1** and **3k** via *N*-attack.



Scheme 3: Reaction of pyridone anions **1** and **2** with the electrophiles **3a-o** in DMSO.

When the potassium salts of **1** or **2** (1 to 5 equivalents) were combined with the quinone methides **3l** and **3k** in dry DMSO or dry CH₃CN, the solutions remained colored indicating incomplete reactions. Equilibria and non-optimized work-up procedures account for the fact that some reaction products were only obtained in moderate yields (Table 5). The reactions of **1** and **2** with the weakly stabilized benzhydrylium ions **3c–h** resulted in colorless solutions, but as the investigated pyridone anions **1** and **2** are weak bases in water ($pK_{\text{aH}}(\mathbf{1}) = 11.74$ and $pK_{\text{aH}}(\mathbf{2}) = 11.12$),^[16] the resulting products undergo heterolytic cleavage during aqueous workup. In these cases, product studies were performed by NMR-spectroscopy in *d*⁶-DMSO solution.

The carbonyl carbon of the 4-pyridones (δ 177.4 for **5g–N**) is considerably more deshielded than the oxy-substituted 4-position of the 4-oxy substituted pyridines (δ 164 for **5a–O** and **5b–O**) which allows a straightforward differentiation of the two isomers.

In contrast, the carbonyl group of the 2-pyridones **4(a–o)–N** and the alkoxy substituted ring carbon in the pyridines **4(a–o)–O** have similar ¹³C-NMR chemical shifts. Therefore, the site of attack at the 2-pyridone anion **1** cannot directly be derived from the appearance of a ¹³C-NMR signal for the carbonyl group, and the differentiation between *N*- and *O*-alkylated products was based on 2D-NMR experiments.

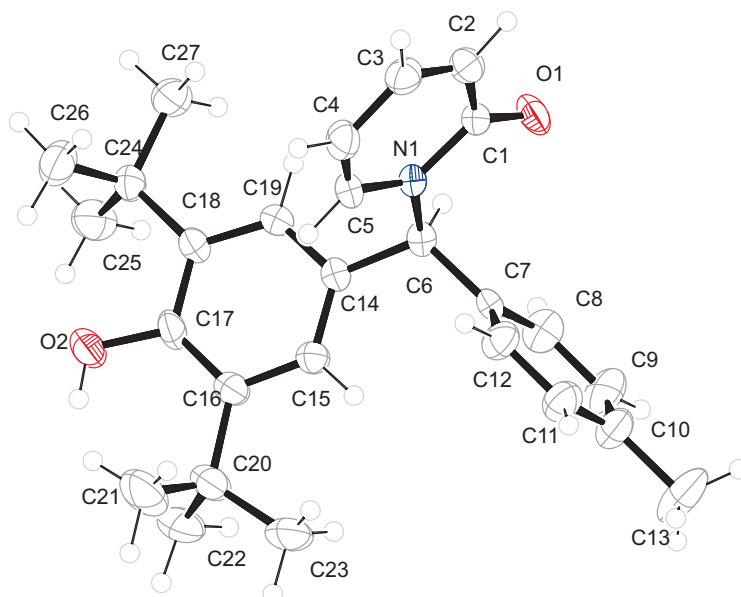


Figure 3: Crystal structure of the reaction product **4l–N** obtained from **1a–K** and **2l** (50 % probability ellipsoids).

In cases where the reaction products are isolable, the structural assignment can be confirmed by IR-spectroscopy. While the *N*-alkylated pyridones **4l-N**, **4k-N**, **4b-N**, and **4a-N** show a strong band at ca 1660 cm⁻¹, the alkoxy pyridines **4a-O** and **5a-O** absorb at ca 1590 cm⁻¹. Further structural evidence comes from the crystal structure of **4l-N** (Figure 3, Table 4).

Table 4: Crystallographic Data of **4l-N**.

Empirical Formula	C ₂₇ H ₃₃ NO ₂
<i>M_r</i> / g mol ⁻¹	403.556
Crystal size/mm	0.41 × 0.10 × 0.09
<i>T</i> / K	173(2)
Radiation	MoKα
Diffractionmeter	'Oxford XCalibur'
Crystal system	monoclinic
Space group	<i>P</i> 2 ₁ / <i>c</i>
<i>a</i> / Å	10.6093(6)
<i>b</i> / Å	10.9456(8)
<i>c</i> / Å	20.9242(13)
α / °	90
β / °	94.074(5)
γ / °	90
<i>V</i> / Å ³	2423.7(3)
<i>Z</i>	4
Calc. density / g cm ⁻³	1.10596(14)
μ / mm ⁻¹	0.069
Absorption correction	'multi-scan'
Transmission factor range	0.95407–1.00000
Refls. measured	9587
<i>R</i> _{int}	0.0884
Mean σ(<i>I</i>)/ <i>I</i>	0.1934
θ range	4.19–25.37
Observed refls.	1693
<i>x</i> , <i>y</i> (weighting scheme)	0.0293, 0
Hydrogen refinement	constr
Refls in refinement	4391
Parameters	278
Restraints	0
<i>R</i> (<i>F</i> _{obs})	0.0563
<i>R</i> _w (<i>F</i> ²)	0.1005
<i>S</i>	0.776
Shift/error _{max}	0.001
Max electron density / e Å ⁻³	0.153
Min electron density / e Å ⁻³	-0.147

Independent of the counterion and the solvent, the anion of 2-pyridone (**1**) gives exclusive *N*-alkylation with the quinone methides **3l** and **3k** and with the weakly electrophilic benzhydrylium ions **3c** and **3g** (Table 5, entries 1–7). Mixtures resulting from *O*- and *N*-attack

were obtained, when **1** was treated with the tetrafluoroborate of the more electrophilic ditolylcarbenium ion **3b** (entry 8) or the corresponding benzhydryl bromides **3b-Br** and **3a-Br** (entries 9–10, 12). Only when the silver salt of **1** was treated with **3b-Br**, exclusive *O*-attack took place (entry 11).

A different behavior was found for the 4-pyridone anion (**2**). While the weakly electrophilic benzhydrylium ion **3g** gave exclusive *N*-attack (entry 14), only alkoxy pyridines were isolated in the reactions of **2** with the more electrophilic benzhydrylium ion **3b** or the corresponding benzhydrylium bromides **3b-Br** and **3a-Br** (entries 15–18).

Table 5: Products of the Reactions of the Pyridone Salts (**1** and **2**) with Electrophiles.

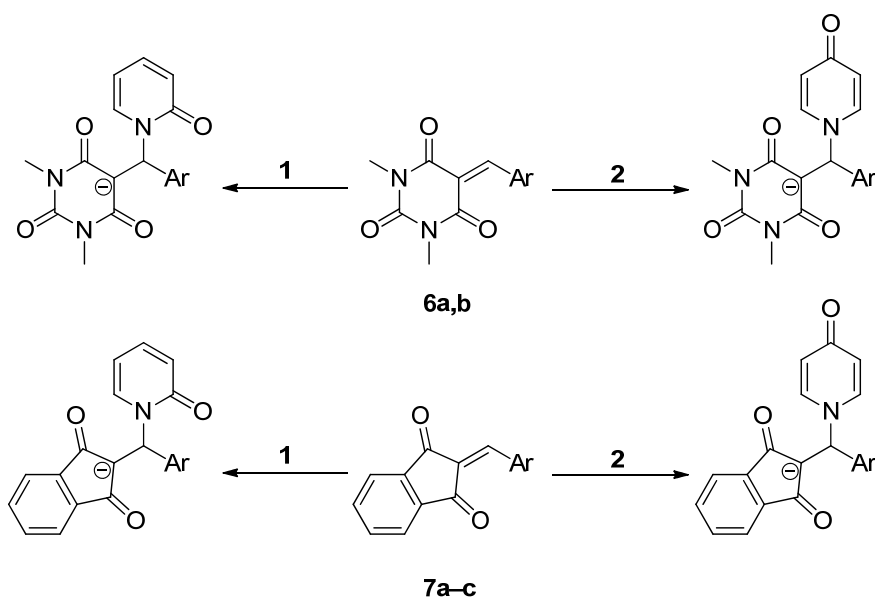
Entry	Pyridone	Electrophile		Solvent	Product (Yield)	
		No.	E^a		<i>N</i> -attack	<i>O</i> -attack
1	1-K	3l	-15.83	DMSO	4l-N (88 %)	-
2	1-Li	3l	-15.83	DMSO	4l-N (80 %)	-
3	1-K	3l	-15.83	CH ₃ CN	4l-N (79 %)	-
4	1-NBu₄	3l	-15.83	CH ₃ CN	4l-N (89 %)	-
5	1-K	3k	-14.32	DMSO	4k-N (84 %)	-
6	1-K	3g	-9.45	DMSO	4g-N (NMR)	-
7	1-K	3c	-7.02	DMSO	4c-N (NMR)	-
8	1-K	3b^b	+3.63	CH ₃ CN / CH ₂ Cl ₂	4b-N (49 %) ^c	4b-O (17 %)
9	1-NBu₄	3b-Br	+3.63	CH ₃ CN	4b-N (50 %)	4b-O (38 %)
10	1-NBu₄	3b-Br	+3.63	CH ₃ CN/ H ₂ O (9:1)	4b-N (53 %)	4b-O (41 %)
11	1-Ag^d	3b-Br	+3.63	CH ₃ CN	-	4b-O (92 %)
12	1-NBu₄	3a-Br	+5.90	CH ₃ CN	4a-N (60 %)	4a-O (38 %)
13	2-K	3l	-15.83	DMSO	no reaction	
14	2-K	3g	-9.45	DMSO	5g-N (NMR)	-
15	2-K	3b	+3.63	CH ₃ CN / CH ₂ Cl ₂	-	5b-O (74 %)
16	2-NBu₄	3b-Br	+3.63	CH ₃ CN	-	5b-O (71 %)
17	2-Ag^d	3b-Br	+3.63	CH ₃ CN	-	5b-O (72 %)
18	2-NBu₄	3a-Br	+5.90	CH ₃ CN	-	5a-O (77 %)

^a Empirical electrophilicity parameters from ref^[15]. ^b **3b-Br** was ionized with 1 equiv. AgOTf; as AgBr precipitates, there are no Ag⁺ ions in solution. ^c Along with 31 % (tol₂CH)₂O. ^d **3b-Br** was added to heterogeneous systems obtained by treatment of **1-NBu₄** or **2-NBu₄** with AgNO₃.

Reactions with Other Types of Michael Acceptors

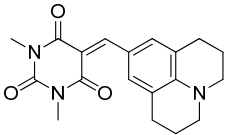
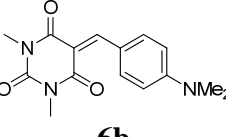
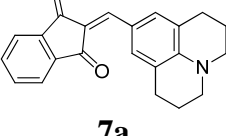
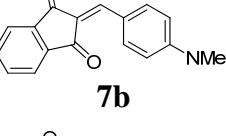
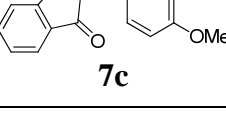
NMR studies showed that the Michael acceptors **6a,b** and **7a–c** also exclusively attack the nitrogen atom of the pyridone anions **1** and **2** and that oxygen attack did not occur (Scheme 4). Comparison of the experimentally determined rate constants (Table 6) with those calculated by equation 3 from the *N/s*-parameters of **1** and **2** (Table 2 and Table 3) and the previously published electrophilicity parameters^[21] of **6a,b** and **7a–c** is an impressive demonstration of the predictive power of the 3-parameter equation (3), which presently covers

40 orders of magnitude. While the calculated rate constants for **1** are 1.5 to 3 times larger than the experimental values, k_{calc} for **2** are 2.5 to 7 times smaller than the experimental numbers.



Scheme 4: Reactions of pyridone anions **1** and **2** with the electrophiles **6** and **7** in DMSO.

Table 6: Rate Constants (in $\text{L mol}^{-1} \text{s}^{-1}$) for the Reactions of **1** and **2** with Michael Acceptors **6** and **7** at 20 °C.

Electrophile	E^a	Pyridone	Solvent	$k_{2,\text{exp}}$	$k_{2,\text{calc}}$
 6a	-13.97	1	DMSO	1.27×10^3	3.7×10^3
			CH ₃ CN	1.35×10^3	3.2×10^3
		2	DMSO	6.51×10^3	1.3×10^3
			CH ₃ CN	7.58×10^3	1.2×10^3
 6b	-12.76	1	DMSO	7.54×10^3	1.9×10^4
			CH ₃ CN	8.98×10^3	1.5×10^4
		2	DMSO	3.02×10^4	7.1×10^3
			CH ₃ CN	3.10×10^4	4.5×10^3
 7a	-14.68	1	DMSO	8.03×10^2	1.4×10^3
			CH ₃ CN	5.79×10^2	1.2×10^3
		2	DMSO	2.45×10^3	4.6×10^2
			CH ₃ CN	1.51×10^3	5.2×10^2
 7b	-13.56	1	DMSO	3.59×10^3	6.5×10^3
			CH ₃ CN	2.73×10^3	5.4×10^3
		2	DMSO	8.02×10^3	2.3×10^3
			CH ₃ CN	6.64×10^3	1.8×10^3
 7c	-11.32	1	DMSO	7.60×10^4	1.4×10^5
			CH ₃ CN	6.50×10^4	1.0×10^5
		2	DMSO	1.37×10^5	5.5×10^4
			CH ₃ CN	7.98×10^4	2.3×10^4

^a Electrophilicities E from ref^[21].

Equilibrium Constants and Intrinsic Barriers

In DMSO the pyridone anions **1** and **2** reacted quantitatively with all investigated benzhydrylium ions and with quinone methides of $E > -14$, while incomplete reactions were observed with less reactive electrophiles. As the quinone methides are colored and the reaction products are colorless, we were able to determine equilibrium constants for these reactions (Table 7) by UV/Vis spectrometry as described in the Experimental Section.

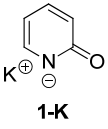
The availability of rate and equilibrium constants allows us to employ Marcus theory^[13] [Eq. (4)] for calculating the intrinsic barriers ΔG_0^\ddagger (defined as the activation energy for a thermoneutral reaction, Table 7) from the Gibbs energy of activation ΔG^\ddagger [derived from the rate constants, Eq. (5)] and the Gibbs energy of reaction ΔG^0 [derived from the equilibrium constants, Eq. (6)].

$$\Delta G^\ddagger = \Delta G_0^\ddagger + 0.5 \Delta G^0 + [(\Delta G^0)^2 / 16 \Delta G_0^\ddagger] \quad (4)$$

$$\Delta G^\ddagger = -RT \ln[(k h)/(k_b T)] \quad (5)$$

$$\Delta G^0 = -RT \ln K \quad (6)$$

Table 7: Equilibrium Constants, Gibbs Reaction Energies ΔG^0 , Gibbs Activation Energies ΔG^\ddagger , and Intrinsic Barriers ΔG_0^\ddagger for the Reactions of Pyridone Anions with Electrophiles in DMSO at 20 °C (all energies in kJ mol⁻¹).

Nucleophile	Electrophile	$K / \text{L mol}^{-1}$	ΔG^0	$\Delta G^\ddagger, ^a$	$\Delta G_0^\ddagger, ^b$
 1-K	3l	$(1.40 \pm 0.09) \times 10^4$	-23.3	58.4	69.6
	3m	$(6.15 \pm 0.24) \times 10^3$	-21.3	58.9	69.1
	3n	$(3.56 \pm 0.30) \times 10^2$	-14.3	63.0	70.0
	3o	$(9.91 \pm 0.66) \times 10^1$	-11.2	65.1	70.6
 2-K	3k	$(1.27 \pm 0.06) \times 10^3$	-17.4	55.7	64.1
	3l	$(8.18 \pm 0.49) \times 10^1$	-10.7	~ 61 ^c	~ 66
	3m	$(4.27 \pm 0.23) \times 10^1$	-9.2	~ 62 ^c	~ 66
	7a	$(1.82 \pm 0.05) \times 10^3$	-18.3	52.7	61.5

^a From Tables 2, 3, and 6 using the Eyring equation [Eq. (5)]. ^b From Eq. (4). ^c ΔG^\ddagger was calculated from k_2 obtained from Eq. (3) with N/s from Table 3 and $E(\mathbf{3})$ from Table 1.

Table 7 shows that the equilibrium constants for the reactions of **1** with quinone methides in DMSO are more than two orders of magnitude larger than those of analogous reactions of **2**. On the other hand, **1** reacts only 2–4 times faster than **2** with neutral (**3i–k**) and charged electrophiles (**3g,h**) in DMSO. Obviously, the reactions of the 2-pyridone anion **1** require a

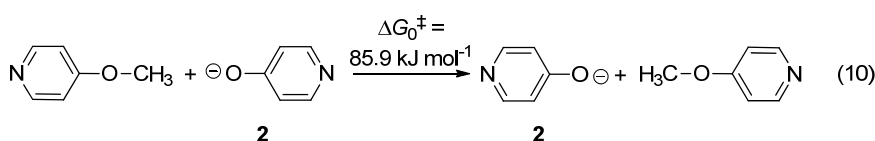
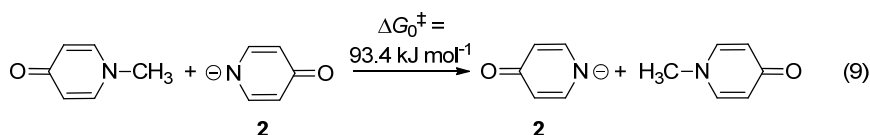
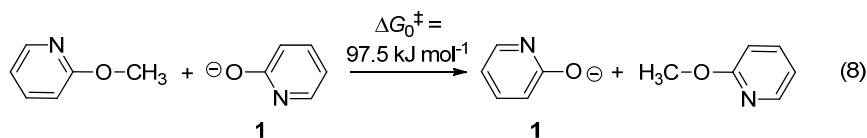
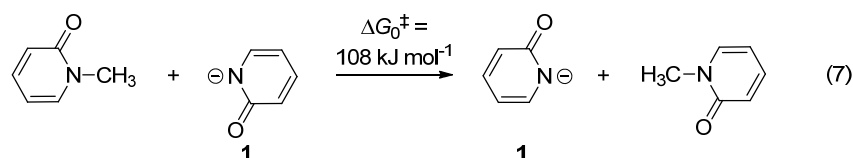
considerably higher reorganization energy than the analogous reactions of the 4-pyridone anion **2**, as quantitatively expressed by the intrinsic barriers ΔG_0^\ddagger in the last column of Table 7.

Quantum Chemical Calculations

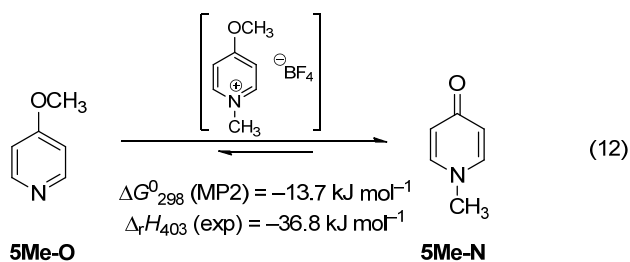
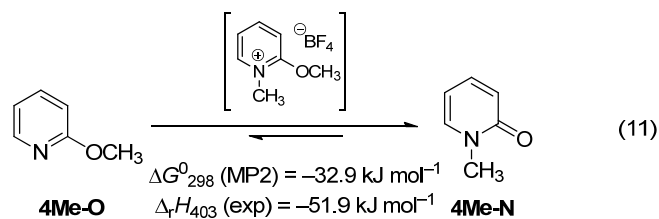
Extending earlier work by Wolfe and Schlegel,^[22] as well as by Schaefer III,^[23] we have recently demonstrated that the directly calculated activation energies of *C*- and *O*-alkylation of enolate anions with methyl halides agree well with those derived from Eq. (4) using calculated Gibbs reaction energies ΔG° and intrinsic barriers ΔG_0^\ddagger which were obtained as the arithmetic mean of the corresponding identity reactions.^[14] Calculated values of ΔG° and ΔG_0^\ddagger for the methylation of enolate, cyanide, cyanate, thiocyanate, and nitrite in combination with the Marcus equation were reported to provide a consistent rationalization of the ambident reactivities of these nucleophiles.^[14]

In order to employ this method also on the ambident reactivities of the pyridone anions **1** and **2**, we have calculated the Gibbs energies of activation for the identity methyl-transfer reactions in equations (7) – (10) at the MP2/6-311+G(2d,p) level, as this basis set was found to give similar results as G3(+) calculations of related systems.^[14] The barriers for *O*-attack [97.5 and 85.9 kJ mol⁻¹, Eqs (8) and (10)] are smaller than the corresponding barriers for the attack at nitrogen [108 and 93.4 kJ mol⁻¹, Eqs (7) and (9)] which is in agreement with Hoz' findings that the barriers of identity S_N2 reactions decrease when the center of nucleophilicity is positioned further right in the periodic table.^[24] Intrinsically preferred is, hence, oxygen attack in the reactions of 2- and 4-pyridone anions.

Comparison of equations (7) and (9) as well of equations (8) and (10) furthermore shows that the reactions of the 4-pyridone anion **2** are intrinsically favored over the corresponding reactions of the 2-pyridone anion **1**, a trend which is also observed experimentally in reactions with the electrophiles **3** (see Table 7).



Furthermore, we have calculated the Gibbs reaction energies for the methylation of the ambident pyridone anions **1** and **2** with methyl chloride at MP2/6-311+G(2d,p) level of theory. Table 8 shows that the *N*-methyl pyridones are thermodynamically favored over the corresponding methoxypyridines by 32.9 kJ mol⁻¹ (for 2-pyridone) and 13.7 kJ mol⁻¹ (for 4-pyridone). In agreement with these calculations, calorimetric measurements by Beak showed that the rearrangement **4Me-O** → **4Me-N** [Eq. (11)] is considerably more exothermic than the analogous rearrangement in the 4-pyridone series [Eq. (12)].^[25] The absolute values of the experimental enthalpies of rearrangement are considerably larger than the calculated numbers as specified in equations (11) and (12), but the differences of the two series ($\Delta\Delta_rH$) are similar (19.2 kJ mol⁻¹ calculated gas phase vs. 15.1 kJ mol⁻¹ calorimetric).

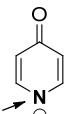
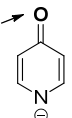


Using Marcus' additivity rule,^[26] which yields the intrinsic barriers for non-identity reactions as the arithmetic means of the corresponding identity reactions, ΔG_0^\ddagger for the reactions of **1** and **2** with CH_3Cl (Table 8) are obtained from the identity reactions in equations (7) – (10) and the intrinsic barrier for the chloride exchange in CH_3Cl (38.2 kJ mol^{-1})^[14] as formulated in the footnote of Table 8.

The Gibbs energies of activation for the methylation of the pyridone anions **1** and **2** by methyl chloride (ΔG^\ddagger) have then been calculated by the Marcus equation [Eq. (4)] from the corresponding intrinsic barriers ΔG_0^\ddagger and the Gibbs energies of reaction ΔG^0 (Table 8).

Table 8: Intrinsic Barriers, Reaction Free Energies, and Activation Free Energies for the Methylation of Pyridone Anions **1** and **2** by Methyl Chloride in the Gas Phase

(MP2/6-311+G(2d,p), in kJ mol^{-1}).

	ΔG_0^\ddagger ^a	ΔG^0	ΔG^\ddagger
	+72.9	-66.7	+43.4
	+67.9	-33.8	+52.1
	+65.8	-12.8	+59.6
	+62.0	+0.9	+62.4

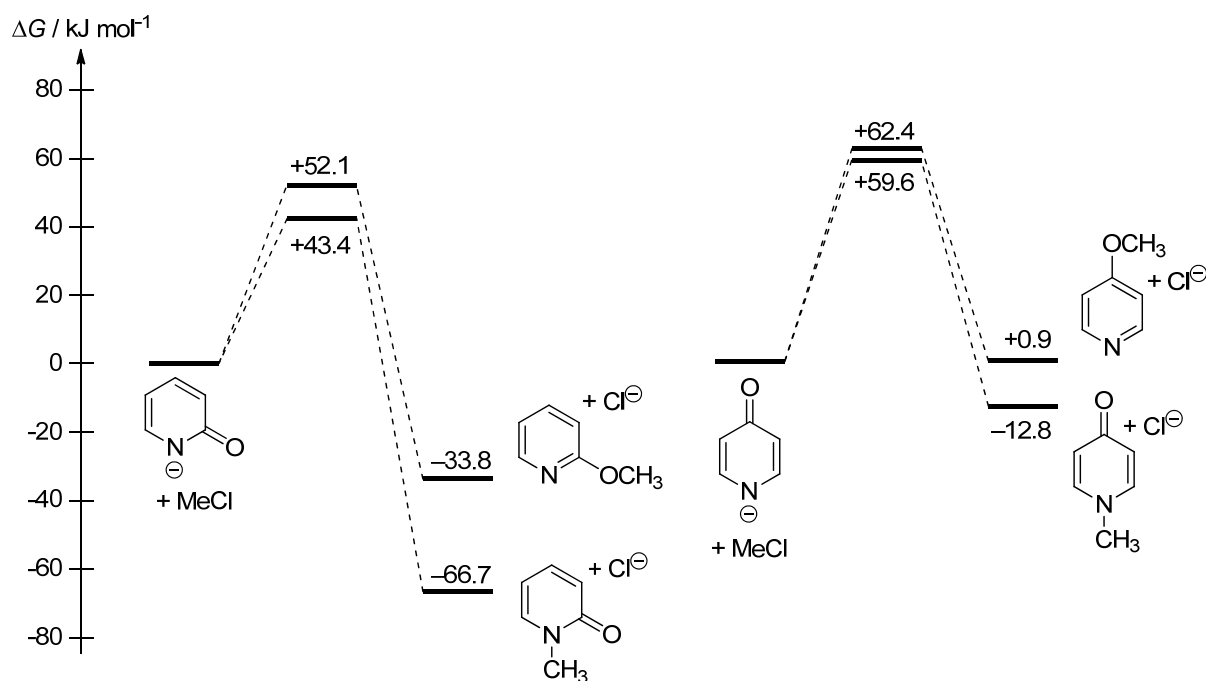
$$^a \Delta G_0^\ddagger = 0.5 [\Delta G_0^\ddagger [\text{Eqs (7)–(10)}] + \Delta G_0^\ddagger (\text{Cl}^- + \text{MeCl})].$$

3 Discussion

Alkylation of Alkali Salts

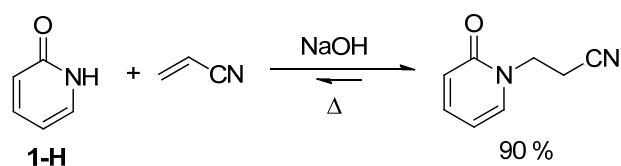
Scheme 5, which summarizes the results presented in Table 8, can now be used to rationalize the experimental findings on the reactivities of pyridone anions. In the case of both pyridones, *N*-alkylation is generally preferred thermodynamically, but the preference of the *N*-alkylated pyridone over the isomeric alkoxy pyridine is considerably greater in the 2-pyridone than in the 4-pyridone series. The exclusive observation of *N*-attack with highly stabilized carbenium ions ($E < -7$) and Michael acceptors ($-17 < E < -11$) reported in Table 6 and Scheme 4 can be explained by the reversibility of these reactions and the formation of the thermodynamically more stable product. Support for this interpretation comes from the fast dissociation reactions of the adducts which can be calculated from the equilibrium constants in Table 7 and the rate

constants of the reactions of the pyridone anions with the quinone methides reported in Tables 2 and 3. Furthermore, the adducts **4-N** and **5-N** obtained from amino substituted benzhydrylium ions were observed to dissociate into the carbenium ions **3** and the pyridone anions **1** and **2** when treated with water.



Scheme 5: Gibbs Energy Profile for the methylation of the pyridone anions with methyl chloride [MP2/6-311+G(2d,p), all in kJ mol^{-1}].

The exclusive formation of *N*-alkylated products from 2-pyridone anions with acrylonitrile^[27] or with related Michael acceptors^[16] can analogously be rationalized by the reversibility of these additions (Scheme 6).



Scheme 6: Selective *N*-alkylation of the 2-pyridone anion with acrylonitrile.^[27]

According to Scheme 5, the higher thermodynamic stabilities of the *N*-methylated pyridones ($\Delta\Delta G^0$ term) are also responsible for the lower transition state for *N*-attack, i.e., for the preferred *N*-alkylations of the pyridone anions under conditions of kinetic control. As reported by Tieckelmann,^[4] the sodium and potassium salt of **1** react with 92–98% nitrogen attack

when treated with methyl iodide and different benzyl halides in DMF at room temperature (entries 1–5, Table 9).

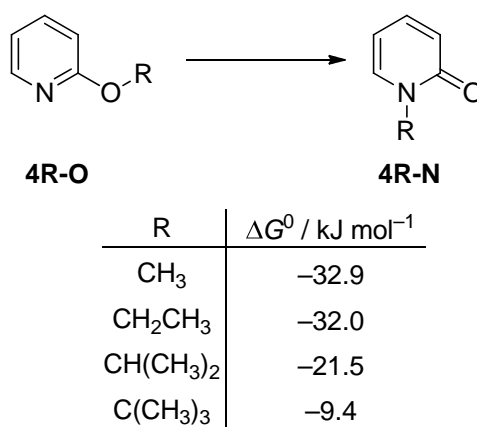
Table 9: Effect of Alkylating Agent and Counterion on the *N/O*-Alkylation Ratio in DMF.^[4]

Entry	Electrophile	Salt	<i>N/O</i> -ratio
1	MeI	1-Na	95:5
2	MeI	1-K	92:8
3	PhCH ₂ Cl	1-Na	94:6
4	PhCH ₂ Br	1-Na	97:3
5	PhCH ₂ I	1-Na	98:2
6	EtI	1-Na	69:31
7	<i>i</i> PrI	1-Na	30:61 ^a

^a 2-pyridone was partially recovered

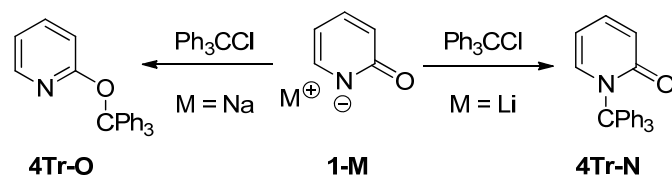
MP2/6-311+G(2d,p) calculations show that the thermodynamic preference for *N*-attack shrinks when the steric bulk of the alkylation agent is increased (Scheme 7).

The decreasing *N/O* ratio when turning from MeI to EtI and *i*PrI (entries 6, 7 in Table 9) can therefore be explained by the fact that the intrinsically preferred *O*-attack is gaining importance as the $\Delta\Delta G^0$ term, which favors *N*-attack, decreases. Qualitatively speaking: An increase of the size of R introduces more strain into the *N*-alkylated product **4R-N** than in the *O*-alkylated product **4R-O**, and a fraction of this effect is already noted in the corresponding transition states.



Scheme 7: Calculated thermodynamic difference ΔG^0 for *O*- and *N*-alkylated 2-pyridones in the gas phase [MP2/6-311+G(2d,p)].

Exclusive *O*-attack was observed, when **1-Na** was treated with the even bulkier trityl chloride, while **1-Li** gave exclusive *N*-attack under the same conditions (Scheme 8).^[28] Since **4Tr-O** was found to isomerize into **4Tr-N** in the presence of Lewis acids, one can conclude that also for tritylations, *N*-attack is thermodynamically favored over *O*-attack. The smaller $\Delta\Delta G^0$ term in favor of *N*-attack (extrapolate data in Scheme 7) cannot any longer overcome the intrinsic preference for *O*-attack.



Scheme 8: Selective *O*- and *N*-tritylation of pyridone salts in acetonitrile.^[28]

The exclusive *N*-tritylation of **1-Li** (Scheme 8) cannot be the result of thermodynamic product control because the rearrangement **4Tr-O** to **4Tr-N** is very slow under the reaction conditions. We therefore join Effenberger's rationalization that Li^+ blocks the attack at oxygen; obviously this ion-pairing plays a role in the more concentrated solutions used for the synthesis of **4Tr-N**,^[28] though in the highly dilute solutions of **1-K** and **1-Li** in DMSO used for the kinetic investigations, only a slight difference of reactivity was observed (**1** + **3l**, **3i**, Table 2).

Almost exclusive *N*-attack in the reactions of 2- and 4-pyridone anions with 6-(mesyloxymethyl)purines in THF and acetonitrile^[29] is also in line with the Marcus model illustrated in Scheme 5. Analogously, R ath obtained *N*-alkylated pyridones in 30–85% yield from the potassium salt of 2-pyridone (**1-K**) and various alkyl halides or dimethyl sulfate (Scheme 9).^[30]

Extrapolation of the correlations shown in Figure 2 shows that the reactions of **1** and **2** with carbocations will be diffusion controlled, when their electrophilicity exceeds -2 (Figure 4). As the mechanism of the reactions of the pyridone anions **1** and **2** with the benzhydryl bromides **3a-Br** and **3b-Br** was not clear ($\text{S}_{\text{N}}1$ or $\text{S}_{\text{N}}2$), we have treated **3b-Br** with AgOTf before the pyridone anion was added in order to study the selectivity of the free ditolylcarbenium ion **3b**. The observation of comparable amounts of *O*- and *N*-attack in the reactions of **1** with **3a** ($E = 5.90$) and **3b** ($E = 3.63$) (entries 9, 10, 12 in Table 5) therefore reflects the result of barrierless reactions and cannot be explained by transition state models. Surprisingly, the

diffusion-controlled reaction of **2** with **3a** and **3b** occurs exclusively at oxygen, indicating that site-selectivity is not necessarily lost when both competing reactions proceed without barrier.

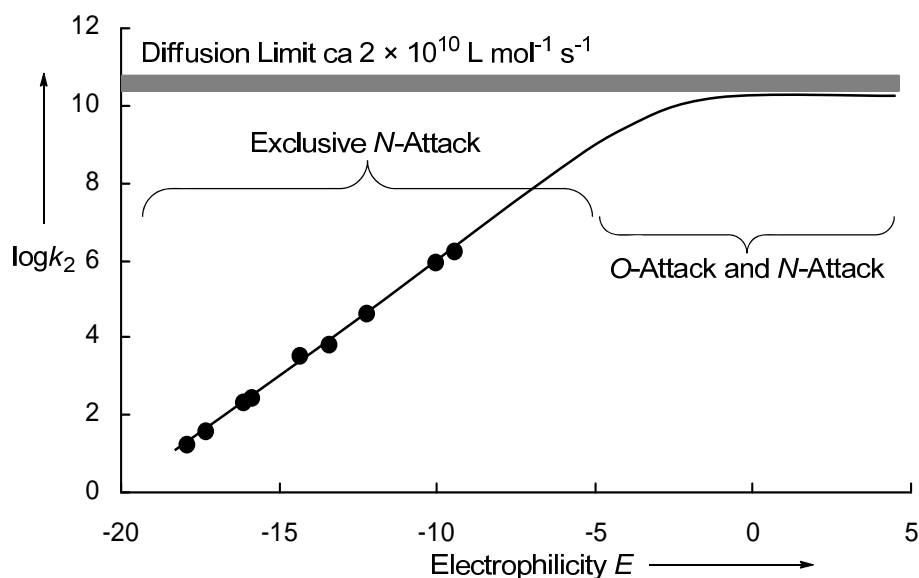
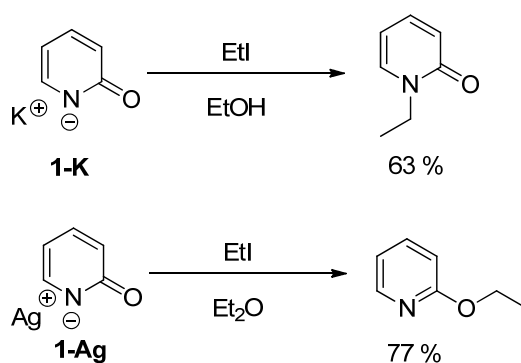


Figure 4: Estimated influence of the diffusion limit on the rate of the reactions of **1** with carbocations and Michael acceptors in DMSO.

Alkylation of Silver Salts

Already in 1891, von Pechmann and Baltzer^[31] reported that exclusive *N*-attack took place when 2-pyridone was heated with an excess of ethyl iodide, whereas 2-ethoxypyridine (*O*-attack) was isolated when the silver salt of 2-pyridone (**1-Ag**) was employed (Scheme 9). Analogously, Takahasi and Yoneda reported that phenacyl bromide in ethanol react at nitrogen of **1-Na** and at oxygen of **1-Ag**.^[32]

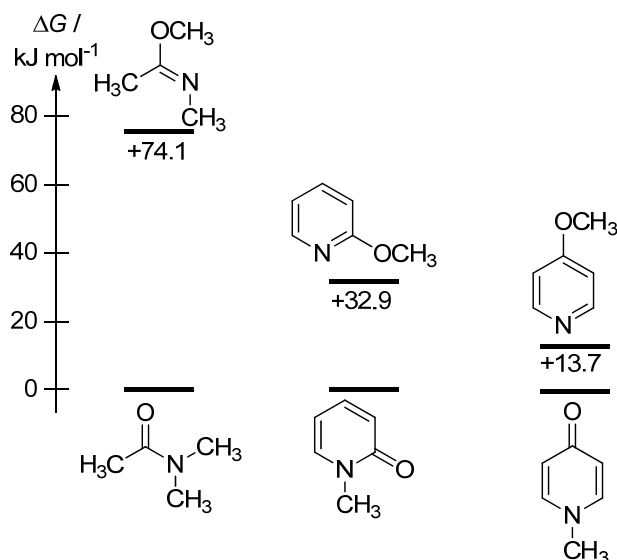


Scheme 9: Regioselectivities in the alkylation of potassium^[30b] and silver^[31] salts of pyridones.

Since we have shown that carbocations also give significant amounts of *N*-alkylated pyridones, Kornblum's rationalization^[3] that the preferred *O*-attack in the presence of silver ions is due to the increased charge of the electrophile cannot hold. As in the case of the ordinary amide anions,^[33] silver ions may coordinate to the nitrogen atom of **1** and thus direct the electrophile to the oxygen.^[34] The same reason, which is responsible for the formation of isonitriles from alkyl halides and silver cyanide (Ag^+ blocks C),^[7] thus also controls the site of alkylation of amide and pyridone anions in the presence of silver ions. However, the blocking of nitrogen by silver ions does not occur in the vinylogous amide **2**, as **2-Ag** is attacked at nitrogen by methyl iodide and phenacyl bromide in ethanol.^[32]

4 Conclusion

The large thermodynamic preference of amides over imidates is strongly reduced in the pyridone analogues due to the aromatic character of the *O*-alkylated compounds (Scheme 10). However, *N*-alkylated pyridones are still thermodynamically favored over alkoxy pyridines that Michael additions and other reversible reactions generally give *N*-alkylated pyridones.



Scheme 10: Comparison of the thermodynamic differences of *N*- and *O*-methylated ordinary amides, 2-pyridones, and 4-pyridones [gas phase, MP2/6-311+G(2d,p)].

In kinetically-controlled reactions of pyridone anions, *N*-attack is mostly preferred because the thermodynamic contribution to the Gibbs energy of activation, which favors *N*-attack, outmatches the contribution of the intrinsic barriers which favor *O*-attack. Only when $\Delta\Delta G^0$

for *O*- and *N*-attack is becoming small, which is the case for bulky alkylating agents, *O*-attack becomes more favorable.

While diffusion-controlled reactions of the 2-pyridone anion **1** give mixtures of *O*- and *N*-attack, exclusive *O*-attack was observed in diffusion-controlled reactions with the 4-pyridone anion **2**. The *O*-directing effect of silver ions is not due to the increased positive charge in the electrophile but due to blocking of *N*-attack by coordination with the silver ion.

5 Experimental Section

5.1 General

Materials

Commercially available DMSO and acetonitrile (both: H₂O content < 50 ppm) were used without further purification. Water passed through a Milli-Q water purification system. The reference electrophiles used in this work were synthesized according to literature procedures.^[15]

NMR spectroscopy

In the ¹H- and ¹³C-NMR spectra chemical shifts are given in ppm and refer to tetramethylsilane ($\delta_{\text{H}} = 0.00$, $\delta_{\text{C}} = 0.0$), *d*⁶-DMSO ($\delta_{\text{H}} = 2.50$, $\delta_{\text{C}} = 39.5$), or to CDCl₃ ($\delta_{\text{H}} = 7.26$, $\delta_{\text{C}} = 77.0$) as internal standards. The coupling constants are given in Hz. For reasons of simplicity, the ¹H-NMR signals of AA'BB'-spin systems of *p*-disubstituted aromatic rings are treated as doublets. Signal assignments are based on additional COSY, gHSQC, and gHMBC experiments.

Kinetics

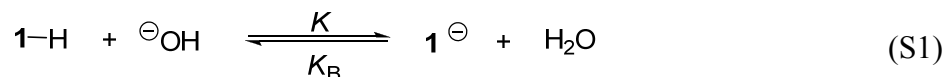
As the reactions of colored benzhydrylium ions or quinone methides with colorless pyridone anions **1** and **2** result in colorless products, the reactions could be followed by UV-Vis spectroscopy. Slow reactions ($\tau_{1/2} > 10$ s) were determined by using conventional UV-Vis-spectrophotometers. Stopped-flow techniques were used for the investigation of rapid reactions ($\tau_{1/2} < 10$ s). The temperature of all solutions was kept constant at 20.0 ± 0.1 °C during all kinetic studies by using a circulating bath thermostat. In all runs the nucleophile concentration was at least 10 times higher than the concentration of the electrophile, resulting in pseudo-first-order kinetics with an exponential decay of the electrophile's concentration.

First-order rate constants k_{obs} were obtained by least-squares fitting of the absorbance data to a single-exponential $A_t = A_0 \exp(-k_{\text{obs}}t) + C$. The second-order rate constants k_2 were obtained from the slopes of the linear plots of k_{obs} against the nucleophile's concentration.

Determination of rate constants in water:

The combination reactions of **1** and **2** with benzhydrylium ions **3d–h** were also studied in water. Due to the low acidities of the pyridones **1-H** ($\text{p}K_{\text{a}} = 11.74$)^[16] and **2-H** ($\text{p}K_{\text{a}} = 11.12$)^[16] aqueous solutions of the pyridone anions **1** and **2** are partially hydrolyzed and contain hydroxide anions. Therefore, the pyridones **1-H** and **2-H**, which are used in high excess over the electrophiles **3** (pseudo-first-order conditions), were deprotonated with only 0.02 to 0.2 equivalents of KOH.

For these deprotonation reactions [Eq. (S1) shows only 2-pyridone **1-H**], one can calculate the equilibrium constants as shown in equation (S2). Applying the mass balances [Eq. (S3) and (S4)], where the index “0” stands for the initial concentration and “eff” for the equilibrium concentration, equation (S2) can be rewritten as a quadratic equation (S5) with its positive solution (S6).



$$K = [\mathbf{1}^{\ominus}]_{\text{eff}} / ([\mathbf{1-H}]_{\text{eff}} [\text{OH}^{\ominus}]_{\text{eff}}) = 1 / K_{\text{B}} \quad (\text{S2})$$

$$[\text{OH}^{\ominus}]_0 = [\text{OH}^{\ominus}]_{\text{eff}} + [\mathbf{1}^{\ominus}]_{\text{eff}} \quad (\text{S3})$$

$$[\mathbf{1-H}]_0 = [\mathbf{1}^{\ominus}]_{\text{eff}} + [\mathbf{1-H}]_{\text{eff}} \quad (\text{S4})$$

$$[\text{OH}^{\ominus}]_{\text{eff}}^2 - [\text{OH}^{\ominus}]_{\text{eff}} ([\mathbf{1-H}]_0 - [\text{OH}^{\ominus}]_0 + K_{\text{B}}) - K_{\text{B}}[\text{OH}^{\ominus}]_0 = 0 \quad (\text{S5})$$

$$[\text{OH}^{\ominus}]_{\text{eff}} = 0.5 (-[\mathbf{1-H}]_0 - [\text{OH}^{\ominus}]_0 + K_{\text{B}} + (([\mathbf{1-H}]_0 - [\text{OH}^{\ominus}]_0 + K_{\text{B}})^2 + 4K_{\text{B}}[\text{OH}^{\ominus}]_0)^{1/2}) \quad (\text{S6})$$

The observed rate constants k_{obs} for the reactions in water reflect the sum of the reaction of the electrophiles with the pyridone anions **1** and **2** (k_2), with hydroxide ($k_{2,\text{OH}}$)^[17] and with water (k_{w}) [Eq. (S7)]. Rearrangement of Eq. (S7), i.e., subtracting the contribution of hydroxide from the observed rate constant k_{obs} , yields equation (S8). The second-order rate constants for the reactions of the benzhydrylium ions with **1** and **2** can then be obtained from plots of k_{eff}

versus the concentration of the nucleophiles. The intercepts of these plots correspond to the reactions of the electrophiles with water and are generally negligible in agreement with previous work, showing that water ($N = 5.20$)^[18] reacts much slower with benzhydrylium ions than the nucleophiles investigated in this work.

$$k_{\text{obs}} = k_2[\mathbf{1} \text{ or } \mathbf{2}] + k_{2,\text{OH}}[\text{OH}^-] + k_{\text{w}} \quad (\text{S7})$$

$$k_{\text{eff}} = k_{\text{obs}} - k_{2,\text{OH}}[\text{OH}^-] = k_2[\mathbf{1} \text{ or } \mathbf{2}] + k_{\text{w}} \quad (\text{S8})$$

Determination of Equilibrium Constants:

Equilibrium constants were determined by UV/Vis spectroscopy by adding small volumes of stock solutions of the potassium salts of 2- or 4-pyridone (**1-K** and **2-K**) to solutions of the quinone methides in DMSO. The decay of the electrophiles' absorbances was monitored and when the absorbance was constant (typically after less than a minute), another portion of the nucleophile was added. This procedure was repeated several times. In order to determine the equilibrium constants K , the molar absorptivities ε of the electrophiles were determined from the initial absorbance assuming the validity of Lambert-Beer's law. Then, the equilibrium constants for the reaction depicted in equation (S9) were determined according to equation (S10). The equilibrium concentrations of the electrophile $[\text{E}]_{\text{eq}}$, the nucleophiles $[\text{Nu}]_{\text{eq}}$, and the product $[\text{P}]_{\text{eq}}$ were calculated from the initial concentrations $[\text{E}]_0$ and $[\text{Nu}]_0$ and from the absorptivities of the electrophile.



$$K = [\text{P}]_{\text{eq}} / ([\text{E}]_{\text{eq}} [\text{Nu}]_{\text{eq}}) = ([\text{E}]_0 - [\text{E}]_{\text{eq}}) / (([\text{E}]_{\text{eq}} ([\text{Nu}]_0 - [\text{E}]_0 + [\text{E}]_{\text{eq}}))) \quad (\text{S10})$$

5.2 Synthesis of Pyridone Salts

2-Pyridone-Potassium (**1-K**)

2-Pyridone (1.80 g, 18.9 mmol) was added to a solution of KO t Bu (2.00 g, 17.8 mmol) in 25 mL dry ethanol and stirred for 30 min. The solvent was evaporated at low pressure and the solid residue was washed several times with dry diethyl ether to afford 2-pyridone potassium (**1-K**, 2.20 g, 16.5 mmol, 93%) as a colorless solid.

¹H-NMR (d_6 -DMSO, 400 MHz) δ = 5.81-5.84 (m, 2 H), 6.94-6.98 (m, 1 H), 7.60-7.62 (m, 1 H). ¹³C-NMR (d_6 -DMSO, 101 MHz) δ = 103.9 (d), 113.8 (d), 136.0 (d), 147.7 (d), 173.0 (s).

2-Pyridone-Tetrabutylammonium (1-NBu₄)

2-Pyridone (1.03 g, 10.8 mmol) was added to a solution of 40 wt% aqueous tetrabutylammonium hydroxide (7.00 g, 10.8 mmol) in 10 mL water and stirred for 15 min. The solvent was evaporated at low pressure and the solid residue was dried at 60 °C at 0.01 mbar to afford 2-pyridone tetrabutylammonium (**1-NBu₄**, 3.56 g, 10.6 mmol, 98%) as a colorless solid.

¹H-NMR (d₆-DMSO, 400 MHz) δ = 0.90-0.93 (m, 12 H), 1.25-1.34 (m, 8 H), 1.52-1.60 (m, 8 H), 3.18-3.22 (m, 8 H), 5.62-5.68 (m, 2 H), 6.80-6.84 (m, 1 H), 7.53-7.55 (m, 1 H). ¹³C-NMR (d₆-DMSO, 101 MHz) δ = 13.5 (q), 19.2 (t), 23.1 (t), 57.5 (t), 102.6 (d), 113.5 (d), 135.1 (d), 148.3 (d), 172.9 (s).

4-Pyridone-Potassium (2-K)

4-Pyridone (3.10 g, 32.6 mmol) was added to a solution of KO^tBu (3.60 g, 32.1 mmol) in 25 mL dry ethanol and stirred for 30 min. The solvent was evaporated at low pressure and the solid residue was washed several times with dry ether to afford 4-pyridone potassium (**2-K**, 4.05 g, 30.4 mmol, 95%) as a colorless solid.

¹H-NMR (d₆-DMSO, 400 MHz) δ = 5.95 (d, ³J = 6.4 Hz, 2 H), 7.60 (d, ³J = 6.4 Hz, 2 H). ¹³C-NMR (d₆-DMSO, 101 MHz) δ = 116.4 (d), 148.9 (d), 175.3 (s).

4-Pyridone-Tetrabutylammonium (2-NBu₄)

4-Pyridone (1.03 g, 10.8 mmol) was added to a solution of 40 wt% aqueous tetrabutylammonium hydroxide (7.00 g, 10.8 mmol) in 10 mL water and stirred for 15 min. The solvent was evaporated at low pressure and the solid residue was dried at 60 °C at 0.01 mbar to afford 4-pyridone tetrabutylammonium (**2-NBu₄**, 3.50 g, 10.4 mmol, 96%) as a colorless solid.

¹H-NMR (d₆-DMSO, 400 MHz) δ = 0.90-0.94 (m, 12 H), 1.25-1.34 (m, 8 H), 1.52-1.59 (m, 8 H), 3.15-3.19 (m, 8 H), 5.78 (d, ³J = 6.4 Hz, 2 H), 7.49 (d, ³J = 6.4 Hz, 2 H). ¹³C-NMR (d₆-DMSO, 101 MHz) δ = 13.5 (q), 19.2 (t), 23.1 (t), 57.5 (t), 116.6 (d), 148.7 (d), 175.7 (s).

5.3 Reaction Products

5.3.1 Isolated reaction products

General Procedure 1 (GP1):

The pyridone salts were dissolved in dry DMSO or CH₃CN and a solution of the electrophile in the same solvent (with ca. 5–10 % CH₂Cl₂ as cosolvent) was added. The mixture was stirred for 15 min before 0.5 % acetic acid was added. The mixture was extracted with dichloromethane or ethyl acetate, and the combined organic phases were washed with saturated NaCl-solution, dried over Na₂SO₄ and evaporated under reduced pressure. The crude reaction products were purified by column chromatography on silica gel and subsequently characterized by NMR, IR, and MS.

General Procedure 2 (GP2):

The tetrabutylammonium salts **1-NBu₄** and **2-NBu₄** were dissolved in dry CH₃CN and the benzhydryl bromide was added. After some time the solvent was removed and the crude reaction products were purified by column chromatography on silica gel.

General Procedure 3 (GP3):

In the case of the highly reactive benzhydrylium ion **3b**, a solution of 1 equiv. silver triflate in CH₃CN was cooled to –40 °C. Dropwise addition of a solution of the benzhydryl bromide **3b-Br** in dry CH₂Cl₂ to the reaction mixture was accompanied by the appearance of a yellow color. Then, a solution of the potassium salts **1-K** or **2-K** and 18-crown-6 in dry CH₂Cl₂ was added. The mixture was stirred for 15 min before warming to room temperature. The solvent was removed, and the crude reaction products were purified by column chromatography on silica gel.

5.3.2 Products of the Reaction of the 2-Pyridone Anion (1)

Reactions with 3I

MB201:

According to GP1, 2-pyridone-potassium (**1-K**, 63.8 mg, 0.479 mmol) and **3I** (147 mg, 0.477 mmol) furnished 1-((3,5-di-*tert*-butyl-4-hydroxyphenyl)(*p*-tolyl)methyl)pyridin-2(1*H*)-one (**4I-N**, 170 mg, 0.421 mmol, 88%) in DMSO as colorless crystals.

MB204:

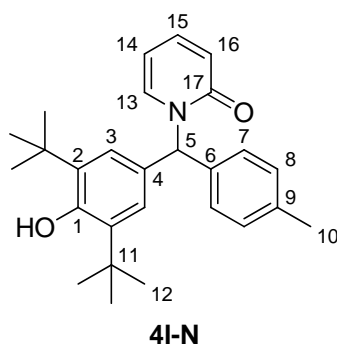
According to GP1, 2-pyridone-potassium (**1-K**, 116 mg 0.871 mmol), 18-crown-6 (230 mg, 0.870 mmol), and **3I** (135 mg, 0.438 mmol) furnished 1-((3,5-di-*tert*-butyl-4-hydroxyphenyl)(*p*-tolyl)methyl)pyridin-2(1*H*)-one (**4I-N**, 140 mg, 0.347 mmol, 79%) in CH₃CN.

MB218:

According to GP1, 2-pyridone (104 mg, 1.09 mmol), LiOtBu (87.0 mg, 1.09 mmol), and **3I** (120 mg, 0.389 mmol) yielded 1-((3,5-di-*tert*-butyl-4-hydroxyphenyl)(*p*-tolyl)methyl)pyridin-2(1*H*)-one (**4I-N**, 125 mg, 0.310 mmol, 80%) in DMSO.

MB284:

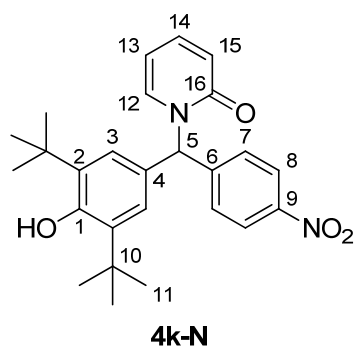
According to GP1, 2-pyridone-NBu₄ (**1-NBu₄**, 275 mg, 0.817 mmol) and **3I** (120 mg, 0.389 mmol) yielded 1-((3,5-di-*tert*-butyl-4-hydroxyphenyl)(*p*-tolyl)methyl)pyridin-2(1*H*)-one (**4I-N**, 140 mg, 0.347 mmol, 89%) in CH₃CN.



Melting point: 164.1-165.1 °C (from CHCl₃/pentane). ¹H-NMR (CDCl₃, 599 MHz) δ = 1.35 (s, 18 H, 12-H), 2.33 (s, 3 H, 10-H), 5.23 (s, OH), 6.10-6.12 (m, 1 H, 14-H), 6.62 (d, ³J = 9.1 Hz, 1H, 16-H), 6.90 (s, 2 H, 3-H), 7.01 (d, ³J = 8.0 Hz, 2 H, 7-H), 7.12-7.16 (m, 3 H, 8-H, 13-H), 7.29-7.32 (m, 1 H, 15-H), 7.38 (s, 1H, 5-H). ¹³C-NMR (CDCl₃, 151 MHz) δ = 21.1 (q, C-10), 30.2 (q, C-12), 34.4 (s, C-11), 61.9 (d, C-5), 105.5 (d, C-14), 120.7 (d, C-16), 125.6 (d, C-3), 128.5 (d, C-7), 129.1 (s, C-4), 129.3 (d, C-8), 136.0 (d, C-13), 136.1 (s, C-2), 136.5 (d, C-13), 137.3 (s, C-9), 138.9 (d, C-15), 153.4 (s, C-1), 162.7 (s, C-17). IR (neat, ATR) $\tilde{\nu}$ = 3377 (w), 2959 (m), 2922 (m), 2870 (m), 1658 (vs), 1574 (m), 1538 (m), 1432 (m), 1230 (m), 1222 (m), 1142 (w), 1065 (m), 1020 (w), 892 (w), 874 (w), 796 (w), 760 (m), 732 (w). HR-MS (ESI) [M-H]⁻: *m/z* calcd for C₂₇H₃₂NO₂⁻: 402.2439 found: 402.2447.

Reactions with **3k****MB209:**

According to GP1, 2-pyridone-potassium (**1-K**, 160 mg, 1.20 mmol) and **3k** (200 mg, 0.589 mmol) furnished 1-((3,5-di-*tert*-butyl-4-hydroxyphenyl)(4-nitrophenyl)methyl)-pyridin-2(1*H*)-one (**4k-N**, 215 mg, 0.495 mmol, 84%) in DMSO.



Melting point: 254.1-255.2 °C (from CHCl₃/pentane). ¹H-NMR (CDCl₃, 300 MHz) δ = 1.36 (s, 18 H, 11-H), 5.37 (s, OH), 6.17-6.22 (m, 1 H, 13-H), 6.65 (d, ³J = 8.5 Hz, 1 H, 15-H), 6.88 (s, 2 H, 3-H), 7.11 (dd, ³J = 7.0 Hz, ⁴J = 2.0 Hz, 1 H, 12-H), 7.28 (d, ³J = 7.9 Hz, 2 H, 7-H), 7.35-7.41 (m, 2 H, 5-H, 14-H), 8.21 (d, ³J = 8.8 Hz, 2 H, 8-H). ¹³C-NMR (CDCl₃, 75.5 MHz) δ = 30.1

(q, C-11), 34.4 (s, C-10), 62.3 (d, C-5), 106.1 (d, C-13), 121.0 (d, C-15), 123.8 (d, C-8), 126.4 (d, C-3), 127.4 (s, C-4), 128.7 (d, C-7), 135.3 (d, C-12), 136.7 (s, C-2), 139.4 (d, C-14), 147.2 (s, C-6 and C-9 superimposed), 154.2 (s, C-1), 162.5 (s, C-16). IR (neat, ATR) $\tilde{\nu}$ = 3378 (w), 3108 (w), 3081 (w), 3002 (w), 2955 (m), 2925 (m), 2872 (w), 2856 (w), 1657 (vs), 1572 (s), 1541 (m), 1516 (s), 1434 (m), 1346 (vs), 1273 (w), 1232 (w), 1221 (m), 1146 (w), 1108 (w), 1063 (m), 1020 (w), 1009 (w), 896 (w), 868 (w), 844 (w), 764 (m), 746 (w), 736 (w), 709 (w). HR-MS (ESI) [M-H]⁻: *m/z* calcd for C₂₆H₂₉N₂O₄⁻: 433.2133 found: 433.2137.

Reactions with tol₂CHBr (**3b-Br**) and with tol₂CH⁺ (**3b**)

MB287:

According to GP2, 2-pyridone-NBu₄ (**1-NBu₄**, 200 mg, 0.594 mmol) and tol₂CHBr (**3b-Br**, 100 mg, 0.363 mmol) yielded 2-(di-*p*-tolylmethoxy)pyridine (**4b-O**, 40 mg, 0.14 mmol, 39%) and 1-(di-*p*-tolylmethyl)-pyridin-2(1*H*)-one (**4b-N**, 52 mg, 0.18 mmol, 50%) in CH₃CN as colorless oils.

MB327:

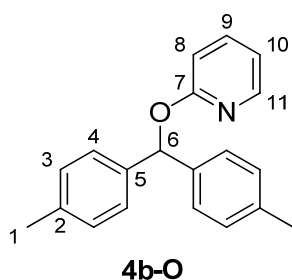
According to GP2, 2-pyridone-NBu₄ (**1-NBu₄**, 210 mg, 0.624 mmol) and tol₂CHBr (**3b-Br**, 100 mg, 0.363 mmol) furnished 2-(di-*p*-tolylmethoxy)pyridine (**4b-O**, 43 mg, 0.15 mmol, 41%) and 1-(di-*p*-tolylmethyl)-pyridin-2(1*H*)-one (**4b-N**, 56 mg, 0.19 mmol, 52%) in 90% aqueous CH₃CN as colorless oils.

MB291:

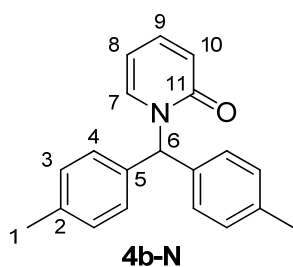
According to GP2, 2-pyridone-NBu₄ (**1-NBu₄**, 203 mg, 0.603 mmol), AgNO₃ (105 mg, 0.618 mmol), and tol₂CHBr (**3b-Br**, 100 mg, 0.363 mmol) yielded 2-(di-*p*-tolylmethoxy)pyridine (**4b-O**, 97.0 mg, 0.34 mmol, 94%) in CH₃CN as colorless oil.

MB344:

According to GP3, 2-pyridone-potassium (**1-K**, 70.0 mg, 0.526 mmol), 18-crown-6 (162 mg, 0.613 mmol), tol_2CHBr (**3b-Br**, 122 mg, 0.443 mmol) and silver triflate (114 mg, 0.444 mmol) furnished 2-(di-*p*-tolylmethoxy)pyridine (**4b-O**, 22.1 mg, 0.0764 mmol, 17%) and 1-(di-*p*-tolyl-methyl)pyridin-2(1*H*)-one (**4b-N**, 62.9 mg, 0.217 mmol, 49 %) and bis(4,4'-dimethyl-benzhydryl)ether (28.3 mg, 0.0696 mmol, 31%) in $\text{CH}_3\text{CN}/\text{CH}_2\text{Cl}_2$ as colorless oils.



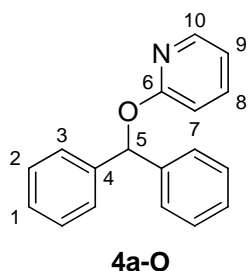
$^1\text{H-NMR}$ (CDCl_3 , 300 MHz) $\delta = 2.30$ (s, 6 H, 1-H), 6.77-6.81 (m, 1 H, 10-H), 6.82-6.85 (m, 1 H, 8-H), 7.11 (d, $^3J = 7.8$ Hz, 4 H, 3-H), 7.20 (s, 1 H, 6-H), 7.32 (d, $^3J = 8.0$ Hz, 4 H, 4-H), 7.49-7.55 (m, 1 H, 9-H), 8.07-8.10 (m, 1 H, 11-H). $^{13}\text{C-NMR}$ (CDCl_3 , 75.5 MHz) $\delta = 21.1$ (q, C-1), 77.3 (d, C-6), 111.6 (d, C-8), 116.8 (d, C-10), 127.1 (d, C-4), 129.0 (d, C-3), 137.0 (s, C-2), 138.6 (d, C-9), 138.8 (s, C-5), 146.9 (d, C-11), 163.1 (s, C-7). HR-MS (EI) $[\text{M}]^+$: m/z calcd for $\text{C}_{20}\text{H}_{19}\text{NO}$: 289.1467 found: 289.1452. MS (EI) $m/z = 289$ (16) $[\text{M}^+]$, 196 (16), 195 (100) $[\text{M}-\text{C}_5\text{H}_4\text{NO}^+]$, 180 (17), 179 (18), 178 (12), 165 (20).



$^1\text{H-NMR}$ (CDCl_3 , 300 MHz) $\delta = 2.33$ (s, 6 H, 1-H), 6.06-6.11 (m, 1 H, 8-H), 6.58-6.62 (m, 1 H, 10-H), 7.02 (d, $^3J = 8.1$ Hz, 4 H, 4-H), 7.13-7.16 (m, 5 H, 3-H 7-H), 7.25-7.32 (m, 1 H, 9-H), 7.42 (s, 1 H, 6-H). $^{13}\text{C-NMR}$ (CDCl_3 , 75.5 MHz) $\delta = 21.1$ (q, C-1), 61.5 (d, C-6), 105.5 (d, C-8), 120.8 (d, C-10), 128.7 (d, C-4), 129.4 (d, C-3), 135.9 (s, C-5), 136.0 (d, C-7), 137.7 (s, C-2), 138.9 (d, C-9), 162.5 (s, C-11). IR (neat, ATR) $\tilde{\nu} = 3284$ (w), 3130 (w), 3052 (w), 3024 (m), 2922 (m), 2860 (m), 2364 (w), 1906 (vw), 1654 (vs), 1610 (s), 1592 (s), 1568 (m), 1542 (m), 1512 (m), 1468 (vs), 1428 (vs), 1378 (w), 1308 (m), 1284 (s), 1246 (s), 1174 (m), 1112 (w), 1036 (m), 988 (s), 940 (w), 894 (m), 848 (m), 806 (s), 766 (s), 722 (m), 614 (w). HR-MS (EI) $[\text{M}]^+$: m/z calcd for $\text{C}_{20}\text{H}_{19}\text{NO}$: 289.1467 found: 289.1459. MS (EI) $m/z = 289$ (30) $[\text{M}^+]$, 196 (15), 195 (100) $[\text{M}-\text{C}_5\text{H}_4\text{NO}^+]$, 180 (17), 179 (18), 178 (13), 165 (19).

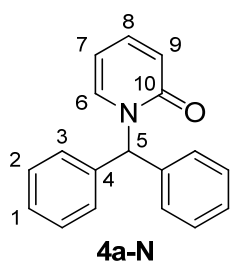
Reactions with Ph_2CHBr (3a-Br**)****MB292:**

According to GP2, 2-pyridone- NBu_4 (**1-NBu₄**, 298 mg, 0.885 mmol) and Ph_2CHBr (**3a-Br**, 100 mg, 0.405 mmol) furnished 2-(benzhydryloxy)pyridine (**4a-O**, 40 mg, 0.15 mmol, 37%) and 1-benzhydrylpyridin-2(1*H*)-one (**4a-N**, 63 mg, 0.24 mmol, 59%) in CH_3CN as colorless oils.



$^1\text{H-NMR}$ (CDCl_3 , 300 MHz) δ = 6.78-6.82 (m, 1 H, 9-H), 6.84-6.87 (m, 1 H, 7-H), 7.20-7.34 (m, 7 H, 1-H, 2-H, 5-H), 7.42-7.45 (m, 4 H, 3-H), 7.51-7.57 (m, 1 H, 8-H), 8.07-8.10 (m, 1 H, 10-H). $^{13}\text{C-NMR}$ (CDCl_3 , 75.5 MHz) δ = 77.5 (d, C-5), 111.6 (d, C-7), 117.0 (d, C-9), 127.2 (d, C-3), 127.4 (d, C-1), 128.3 (d, C-2),

138.6 (d, C-8), 141.6 (s, C-4), 146.9 (d, C-10), 162.9 (s, C-6). IR (neat, ATR) $\tilde{\nu}$ = 3088 (w), 3062 (w), 3030 (w), 2958 (w), 2918 (m), 2850 (m), 2362 (vw), 1738 (w), 1596 (s), 1570 (m), 1494 (w), 1468 (s), 1430 (vs), 1308 (m), 1284 (m), 1262 (s), 1248 (s), 1186 (w), 1142 (w), 1080 (w), 1040 (m), 988 (m), 918 (w), 886 (w), 800 (w), 778 (m), 740 (m), 696 (s), 664 (w).



$^1\text{H-NMR}$ (CDCl_3 , 300 MHz) δ = 6.08-6.13 (m, 1 H, 7-H), 6.60-6.64 (m, 1 H, 9-H), 7.12-7.15 (m, 5 H, 3-H, 6-H), 7.27-7.37 (m, 7 H, 1-H, 2-H, 8-H), 7.52 (s, 1 H, 5-H). $^{13}\text{C-NMR}$ (CDCl_3 , 75.5 MHz) δ = 61.8 (d, C-5), 105.7 (d, C-7), 120.9 (d, C-9), 128.0 (d, C-1), 128.8 (2 d, C-2, C-3), 135.9 (d, C-6), 138.8 (s, C-4), 139.0

(d, C-8), 162.5 (s, C-10). IR (neat, ATR) $\tilde{\nu}$ = 3082 (w), 3064 (w), 3028 (w), 3010 (w), 2940 (w), 2360 (w), 2332 (w), 1810 (vw), 1652 (vs), 1572 (vs), 1528 (s), 1496 (m), 1450 (m), 1400 (w), 1336 (w), 1238 (w), 1148 (m), 888 (w), 778 (m), 756 (w), 730 (m), 696 (m). HR-MS (ESI) $[\text{M-H}]^-$: $[\text{M}+\text{Na}]^+$: m/z calcd for $\text{C}_{18}\text{H}_{15}\text{NONa}$: 284.1051 found: 284.1045.

5.3.3 Products of the Reaction of the 4-Pyridone Anion (2)

Reactions with tol_2CHBr (**3b-Br**) and tol_2CH^+ (**3b**)

MB299:

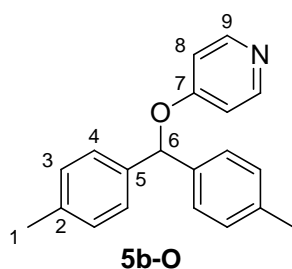
According to GP2, 4-pyridone-NBu₄ (**2-NBu₄**, 266 mg, 0.790 mmol) and tol_2CHBr (**3b-Br**, 103 mg, 0.374 mmol) yielded 4-(di-*p*-tolylmethoxy)pyridine (**5b-O**, 77.0 mg, 0.266 mmol, 71%) in CH_3CN as colorless oil.

MB300:

According to GP2, 4-pyridone-NBu₄ (**2-NBu₄**, 199 mg, 0.591 mmol), AgNO_3 (107 mg, 0.630 mmol), and tol_2CHBr (**3-Br**, 92.0 mg, 0.334 mmol) furnished 4-(di-*p*-tolylmethoxy)pyridine (**5b-O**, 70.0 mg, 0.242 mmol, 72%) in CH_3CN as colorless oil.

MB340:

According to GP3, 4-pyridone-potassium (**2-K**, 118 mg, 0.886 mmol), 18-crown-6 (240 mg, 0.908 mmol), silver triflate (149 mg, 0.580 mmol), and tol_2CHBr (**3b-Br**, 160 mg, 0.581 mmol) yielded 4-(di-*p*-tolylmethoxy)pyridine (**5b-O**, 124 mg, 0.429 mmol, 74%) and bis(4,4'-dimethyl-benzhydryl)ether (29 mg, 0.071 mmol, 24%) in $\text{CH}_3\text{CN}/\text{CH}_2\text{Cl}_2$ as colorless oils.

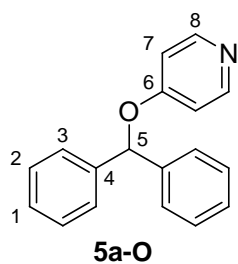


$^1\text{H-NMR}$ (CDCl_3 , 300 MHz) δ = 2.31 (s, 6 H, 1-H), 6.22 (s, 1 H, 6-H), 6.83 (d, 3J = 6.4 Hz, 2 H, 8-H), 7.14 (d, 3J = 7.9 Hz, 4 H, 3-H), 7.26 (d, 3J = 8.1 Hz, 4 H, 4-H), 8.34 (d, 3J = 6.0 Hz, 2 H, 9-H). $^{13}\text{C-NMR}$ (CDCl_3 , 75.5 MHz) δ = 21.1 (q, C-1), 81.4 (d, C-6), 111.6 (d, C-8), 126.7 (d, C-4), 129.4 (d, C-3), 137.2 (s, C-

5), 137.9 (s, C-2), 151.0 (d, C-9), 164.1 (s, C-7). HR-MS (EI) $[\text{M}]^+$: m/z calcd for $\text{C}_{20}\text{H}_{19}\text{NO}$: 289.1467 found: 289.1445. MS (EI) m/z = 289 (26) $[\text{M}^+]$, 196 (14), 195 (100) $[\text{M}-\text{C}_5\text{H}_4\text{NO}^+]$, 180 (14), 179 (10), 165 (15).

Reactions with Ph_2CHBr (3a-Br**)****MB298:**

According to GP2, 4-pyridone- NBu_4 (**2-NBu₄**, 306 mg, 0.909 mmol) and Ph_2CHBr (**3a-Br**, 102 mg, 0.413 mmol) furnished 4-(benzhydryloxy)pyridine (**5a-O**, 83.1 mg, 0.318 mmol, 77%) in CH_3CN as colorless oil.



$^1\text{H-NMR}$ (CDCl_3 , 300 MHz) δ = 6.27 (s, 1 H, 5-H), 6.84 (d, 3J = 6.4 Hz, 2 H, 7-H), 7.24-7.41 (m, 10 H, 1-H, 2-H, and 3-H), 8.36 (d, 3J = 6.4 Hz, 2 H, 8-H). $^{13}\text{C-NMR}$ (CDCl_3 , 75.5 MHz) δ = 81.5 (d, C-5), 111.6 (d, C-7), 126.8 (d, C-3), 128.1 (d, C-1), 128.8 (d, C-2), 140.0 (s, C-4), 151.0 (d, C-8), 164.0 (s, C-6). IR

(neat, ATR) $\tilde{\nu}$ = 3384 (vw), 3088 (w), 3064 (w), 3030 (w), 2922 (w), 2367 (vw), 1590 (vs), 1568 (s), 1496 (s), 1454 (m), 1418 (w), 1266 (s), 1210 (s), 1184 (w), 1082 (w), 1002 (s), 910 (w), 884 (m), 830 (m), 812 (m), 740 (m), 696 (s), 650 (w), 630 (w). HR-MS (EI) $[\text{M}]^+$: m/z calcd for $\text{C}_{18}\text{H}_{15}\text{NO}$: 261.1154 found: 261.1153. MS (EI) m/z = 261 (1) $[\text{M}^+]$, 168 (13), 167 (100) $[\text{M}-\text{C}_5\text{H}_4\text{NO}^+]$, 165 (25), 152 (12).

5.4 NMR reaction products

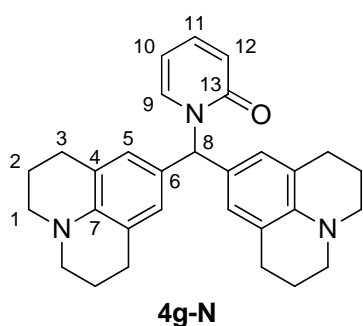
5.4.1 General Procedure:

In an NMR tube equimolar amounts (approx. 10–30 mg) of the pyridone-salt and the electrophile were mixed in 1 mL d_6 -DMSO. NMR spectra were recorded shortly after the mixing.

5.4.2 Products of the Reaction of the 2-Pyridone Anion (1)

MB229

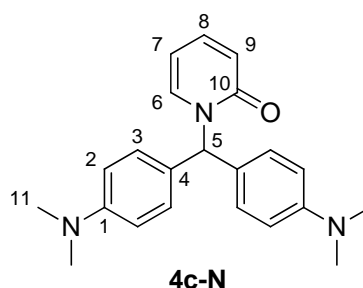
2-pyridone-potassium (**1-K**, 10.9 mg, 81.8 μ mol) and $jul_2CH^+BF_4^-$ (**3g**, 35.7 mg, 80.3 μ mol) were mixed in 1 mL d_6 -DMSO.



1H -NMR (d_6 -DMSO, 400 MHz) δ = 1.79-1.85 (m, 8 H, 2-H), 2.57-2.60 (m, 8 H, 3-H), 3.06-3.08 (m, 8 H, 1-H), 6.16-6.20 (m, 1 H, 10-H), 6.35-6.38 (m, 1 H, 12-H), 6.41 (s, 4 H, 5-H), 6.85 (s, 1 H, 8-H), 7.31-7.39 (m, 2 H, 9-H, 11-H). ^{13}C -NMR (d_6 -DMSO, 101 MHz) δ = 21.5 (t, C-2), 27.2 (t, C-3), 49.2 (t, C-1), 60.7 (d, C-8), 105.1 (d, C-10), 119.4 (d, C-12), 120.8 (s, C-4), 125.8 (s, C-6), 126.7 (d, C-5), 136.6 (d, C-9), 139.3 (d, C-11), 142.0 (s, C-7), 161.2 (s, C-13).

MB230

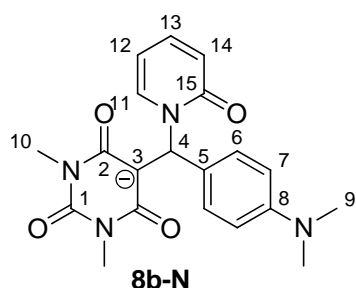
2-pyridone-potassium (**1-K**, 15.3 mg, 0.115 mmol) and $dma_2CH^+BF_4^-$ (**3c**, 38.6 mg, 0.113 mmol) were mixed in 1 mL d_6 -DMSO.



1H -NMR (d_6 -DMSO, 400 MHz) δ = 2.87 (s, 12 H, 11-H), 6.17-6.20 (m, 1 H, 7-H), 6.40-6.43 (m, 1 H, 9-H), 6.70 (d, 3J = 8.9 Hz, 4 H, 2-H), 6.89 (d, 3J = 8.4 Hz, 4 H, 3-H), 7.09 (s, 1 H, 5-H), 7.26-7.28 (m, 1 H, 6-H), 7.37-7.41 (m, 1 H, 8-H). ^{13}C -NMR (d_6 -DMSO, 101 MHz) δ = 40.1 (q, C-11), 60.4 (d, 5-H), 105.2 (d, C-7), 112.3 (d, C-2), 119.5 (d, C-9), 126.5 (s, C-4), 129.1 (d, C-3), 136.4 (d, C-6), 139.4 (d, C-8), 149.7 (s, C-1), 161.3 (s, C-10).

MB206

2-pyridone-potassium (**1-K**, 17.1 mg, 0.128 mmol) and **6b** (36.8 mg, 0.128 mmol) were mixed in 1 mL d_6 -DMSO.



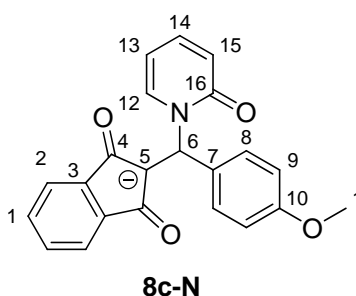
$^1\text{H-NMR}$ (d_6 -DMSO, 400 MHz) δ = 2.82 (s, 6 H, 9-H), 3.06 (s, 6 H, 10-H), 6.07-6.11 (m, 1 H, 12-H), 6.26-6.29 (m, 1 H, 14-H), 6.57 (d, 3J = 8.9 Hz, 2 H, 7-H), 6.74-6.77 (m, 2 H, 6-H), 7.25 (s, 1 H, 4-H), 7.30-7.34 (m, 1 H, 13-H), 8.19-8.22 (m, 1 H, 11-H).

$^{13}\text{C-NMR}$ (d_6 -DMSO, 101 MHz) δ = 27.0 (q, C-10), 40.5 (q, C-9), 55.8 (d, C-4), 85.3 (s, C-3), 103.7 (d, C-12), 112.0 (d, C-7),

118.4 (d, C-14), 127.3 (d, C-6), 130.5 (s, C-5), 138.8 (d, C-13), 140.0 (d, C-11), 148.5 (s, C-8), 152.9 (s, C-1), 161.6 (s, C-15), 162.8 (s, C-2).

MB210

2-pyridone-potassium (**1-K**, 20.6 mg, 0.155 mmol) and **7c** (41.0 mg, 0.155 mmol) were mixed in 1 mL d_6 -DMSO.



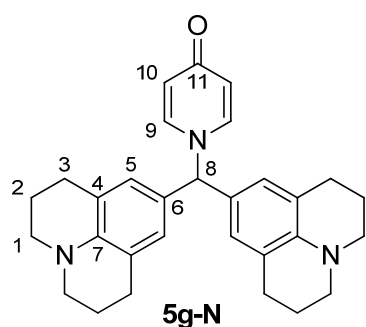
$^1\text{H-NMR}$ (d_6 -DMSO, 400 MHz) δ = 3.69 (s, 3 H, 11-H), 6.13-6.16 (m, 1 H, 13-H), 6.31-6.34 (m, 1 H, 15-H), 6.76-6.78 (m, 2 H, 9-H), 7.00 (s, 1 H, 6-H), 7.04-7.06 (m, 2 H, 8-H), 7.10-7.12 (m, 2 H, 2-H), 7.24-7.26 (m, 2 H, 1-H), 7.31-7.35 (m, 1 H, 14-H), 8.50-8.53 (m, 1 H, 12 H).

$^{13}\text{C-NMR}$ (d_6 -DMSO, 101 MHz) δ = 52.9 (d, C-6), 55.0 (q, C-11), 103.1 (s, C-5), 104.6 (d, C-13),

113.0 (d, C-9), 117.0 (d, C-2), 118.7 (d, C-15), 128.1 (d, C-8), 129.3 (d, C-1), 134.6 (s, C-7), 139.0 (d, C-14), 139.9 (s + d, C-3 and C-12 superimposed), 157.3 (s, C-10), 161.4 (s, C-16), 189.0 (s, C-4).

5.4.3 Products of the Reaction of the 4-Pyridone Anion (2)**MB223**

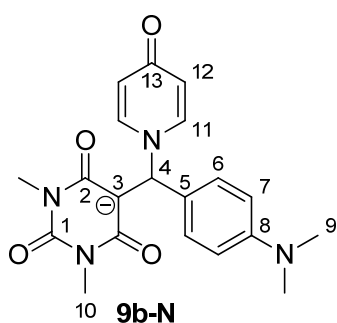
4-pyridone-potassium (**2-K**, 13 mg, 0.10 mmol) and $\text{jul}_2\text{CH}^+\text{BF}_4^-$ (**3g**, 44 mg, 0.10 mmol) were mixed in 1 mL d_6 -DMSO.



$^1\text{H-NMR}$ (d_6 -DMSO, 400 MHz) δ = 1.81-1.84 (m, 8 H, 2-H), 2.58-2.61 (m, 8 H, 3-H), 3.07-3.10 (m, 8 H, 1-H), 6.08 (d, 3J = 7.7 Hz, 2 H, 10-H), 6.16 (s, 1 H, 8-H), 6.46 (s, 4 H, 5-H), 7.52 (d, 3J = 7.7 Hz, 2 H, 9-H). $^{13}\text{C-NMR}$ (d_6 -DMSO, 101 MHz) δ = 21.4 (t, C-2), 27.2 (t, C-3), 49.2 (t, C-1), 71.0 (d, C-8), 117.3 (d, C-10), 120.9 (s, C-4), 125.0 (s, C-6), 126.4 (d, C-5), 140.0 (d, C-9), 142.4 (s, C-7), 177.4 (s, C-11).

MB213

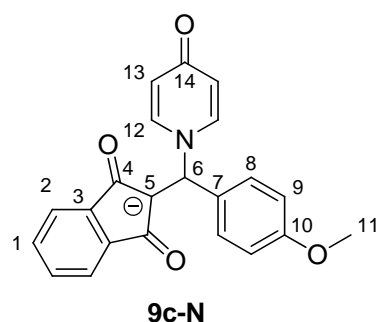
4-pyridone-potassium (**2-K**, 28.7 mg, 0.215 mmol) and **6b** (61.5 mg, 0.214 mmol) were mixed in 1 mL d_6 -DMSO.



$^1\text{H-NMR}$ (d_6 -DMSO, 400 MHz) δ = 2.84 (s, 6 H, 9-H), 3.07 (s, 6 H, 10-H), 6.01 (d, 3J = 7.7 Hz, 2 H, 12-H), 6.40 (s, 1 H, 4-H), 6.61 (d, 3J = 8.9 Hz, 2 H, 7-H), 6.87 (d, 3J = 8.3 Hz, 2 H, 6-H), 7.80 (d, 3J = 7.8 Hz, 2 H, 11-H). $^{13}\text{C-NMR}$ (d_6 -DMSO, 101 MHz) δ = 27.0 (q, C-10), 40.3 (q, C-9), 66.1 (d, C-4), 84.8 (s, C-3), 112.0 (d, C-7), 116.4 (d, C-12), 127.6 (d, C-6), 128.8 (s, C-5), 141.3 (d, C-11), 149.0 (s, C-8), 152.9 (s, C-1), 162.4 (s, C-2), 177.5 (s, C-13).

MB212

4-pyridone-potassium (**2-K**, 28.7 mg, 0.215 mmol) and **7c** (56.9 mg, 0.215 mmol) were mixed in 1 mL d_6 -DMSO.



$^1\text{H-NMR}$ (d_6 -DMSO, 400 MHz) δ = 3.71 (s, 3 H, 11-H), 6.04 (s, 1 H, 6-H), 6.06 (d, 3J = 7.7 Hz, 2 H, 13-H), 6.84 (d, 3J = 8.8 Hz, 2 H, 9-H), 7.14-7.18 (m, 4 H, 2-H and 8-H), 7.26-7.28 (m, 2 H, 1-H), 8.03 (d, 3J = 7.7 Hz, 2 H, 12-H). $^{13}\text{C-NMR}$ (d_6 -DMSO, 101 MHz) δ = 55.0 (q, C-11), 63.8 (d, C-6), 102.0 (s, C-5), 113.4 (d, C-9), 116.8 (d, C-13), 117.3 (d, C-2), 128.3 (d, C-8), 129.5 (d, C-1), 133.7 (s, C-7), 139.8 (s, C-3), 141.1 (d, C-12), 158.0 (s, C-10), 177.3 (s, C-14), 188.5 (s, C-4).

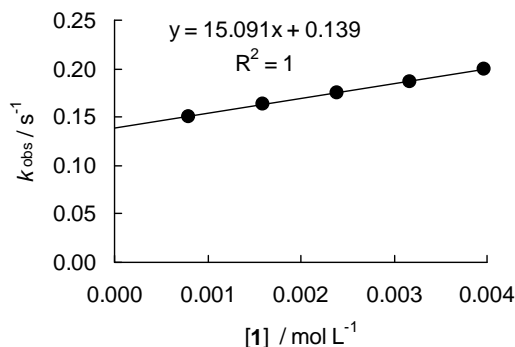
5.5 Determination of the Nucleophilicity of Pyridone Anions

5.5.1 Reactions of the Potassium Salt of 2-Pyridone (1-K) in DMSO

Table 1: Kinetics of the reaction of **1-K** with **3o** (20 °C, stopped-flow, at 521 nm)

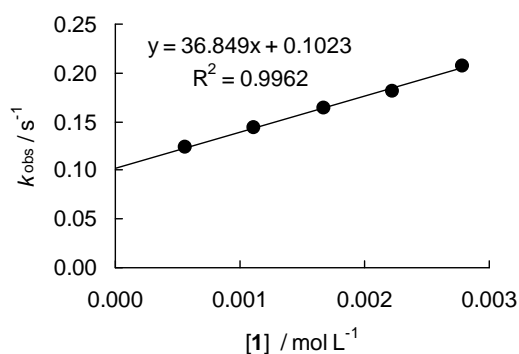
[E] / mol L ⁻¹	[Nu] / mol L ⁻¹	[18-crown-6] / mol L ⁻¹	[Nu]/[E]	<i>k</i> _{obs} / s ⁻¹
2.98 × 10 ⁻⁵	7.95 × 10 ⁻⁴		26.7	0.151
2.98 × 10 ⁻⁵	1.59 × 10 ⁻³	2.14 × 10 ⁻³	53.4	0.163
2.98 × 10 ⁻⁵	2.39 × 10 ⁻³		80.1	0.175
2.98 × 10 ⁻⁵	3.18 × 10 ⁻³	4.28 × 10 ⁻³	107	0.187
2.98 × 10 ⁻⁵	3.98 × 10 ⁻³		134	0.199

$$k_2 = 1.51 \times 10^1 \text{ L mol}^{-1} \text{ s}^{-1}$$

Table 2: Kinetics of the reaction of **1-K** with **3n** (20 °C, stopped-flow, at 533 nm)

[E] / mol L ⁻¹	[Nu] / mol L ⁻¹	[18-crown-6] / mol L ⁻¹	[Nu]/[E]	<i>k</i> _{obs} / s ⁻¹
2.61 × 10 ⁻⁵	5.56 × 10 ⁻⁴		21.3	0.123
2.61 × 10 ⁻⁵	1.11 × 10 ⁻³	1.34 × 10 ⁻³	42.7	0.144
2.61 × 10 ⁻⁵	1.67 × 10 ⁻³		64.0	0.164
2.61 × 10 ⁻⁵	2.23 × 10 ⁻³	2.68 × 10 ⁻³	85.3	0.181
2.61 × 10 ⁻⁵	2.78 × 10 ⁻³		107	0.207

$$k_2 = 3.68 \times 10^1 \text{ L mol}^{-1} \text{ s}^{-1}$$

Table 3: Kinetics of the reaction of **1-K** with **3m** (20 °C, stopped-flow, at 393 nm)

[E] / mol L ⁻¹	[Nu] / mol L ⁻¹	[18-crown-6] / mol L ⁻¹	[Nu]/[E]	<i>k</i> _{obs} / s ⁻¹
2.86 × 10 ⁻⁵	5.02 × 10 ⁻⁴		17.5	0.128
2.86 × 10 ⁻⁵	1.00 × 10 ⁻³	1.26 × 10 ⁻³	35.1	0.221
2.86 × 10 ⁻⁵	1.51 × 10 ⁻³		52.6	0.328
2.86 × 10 ⁻⁵	2.01 × 10 ⁻³	2.53 × 10 ⁻³	70.1	0.414
2.86 × 10 ⁻⁵	2.51 × 10 ⁻³		87.7	0.517

$$k_2 = 1.94 \times 10^2 \text{ L mol}^{-1} \text{ s}^{-1}$$

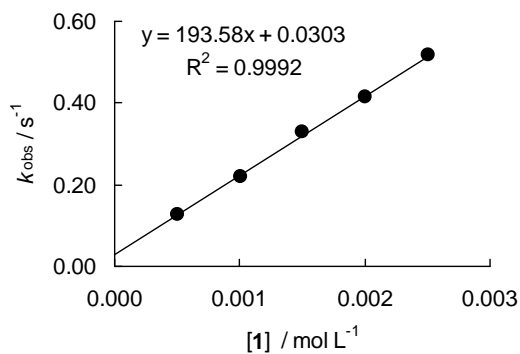
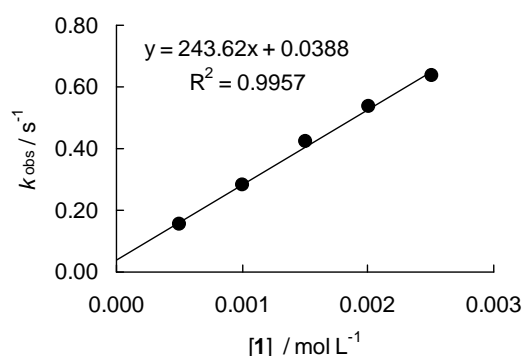


Table 4: Kinetics of the reaction of **1-K** with **3l** (20 °C, stopped-flow, at 371 nm)

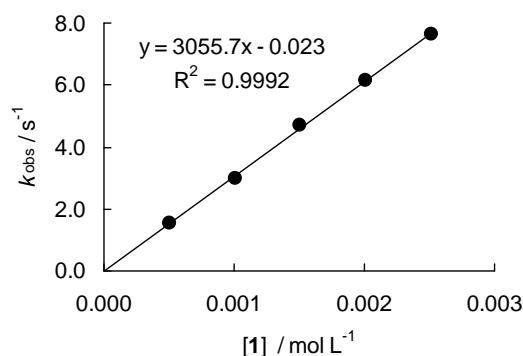
[E] / mol L ⁻¹	[Nu] / mol L ⁻¹	[18-crown-6] / mol L ⁻¹	[Nu]/[E]	<i>k</i> _{obs} / s ⁻¹
3.32 × 10 ⁻⁵	5.02 × 10 ⁻⁴		15.1	0.153
3.32 × 10 ⁻⁵	1.00 × 10 ⁻³	1.26 × 10 ⁻³	30.2	0.280
3.32 × 10 ⁻⁵	1.51 × 10 ⁻³		45.3	0.421
3.32 × 10 ⁻⁵	2.01 × 10 ⁻³	2.53 × 10 ⁻³	60.4	0.538
3.32 × 10 ⁻⁵	2.51 × 10 ⁻³		75.5	0.635

$$k_2 = 2.44 \times 10^2 \text{ L mol}^{-1} \text{ s}^{-1}$$

Table 5: Kinetics of the reaction of **1-K** with **3k** (20 °C, stopped-flow, at 374 nm)

[E] / mol L ⁻¹	[Nu] / mol L ⁻¹	[18-crown-6] / mol L ⁻¹	[Nu]/[E]	<i>k</i> _{obs} / s ⁻¹
3.96 × 10 ⁻⁵	5.03 × 10 ⁻⁴		12.7	1.52
3.96 × 10 ⁻⁵	1.01 × 10 ⁻³	1.35 × 10 ⁻³	25.4	2.97
3.96 × 10 ⁻⁵	1.51 × 10 ⁻³		38.1	4.69
3.96 × 10 ⁻⁵	2.01 × 10 ⁻³	2.71 × 10 ⁻³	50.8	6.14
3.96 × 10 ⁻⁵	2.52 × 10 ⁻³		63.5	7.62

$$k_2 = 3.06 \times 10^3 \text{ L mol}^{-1} \text{ s}^{-1}$$

Table 6: Kinetics of the reaction of **1-K** with **3j** (20 °C, stopped-flow, at 533 nm)

[E] / mol L ⁻¹	[Nu] / mol L ⁻¹	[18-crown-6] / mol L ⁻¹	[Nu]/[E]	<i>k</i> _{obs} / s ⁻¹
2.67 × 10 ⁻⁵	3.45 × 10 ⁻⁴		12.9	2.04
2.67 × 10 ⁻⁵	6.89 × 10 ⁻⁴	1.07 × 10 ⁻³	25.8	4.02
2.67 × 10 ⁻⁵	1.03 × 10 ⁻³		38.7	6.49
2.67 × 10 ⁻⁵	1.38 × 10 ⁻³	2.14 × 10 ⁻³	51.6	8.47
2.67 × 10 ⁻⁵	1.72 × 10 ⁻³		64.5	11.0

$$k_2 = 6.49 \times 10^3 \text{ L mol}^{-1} \text{ s}^{-1}$$

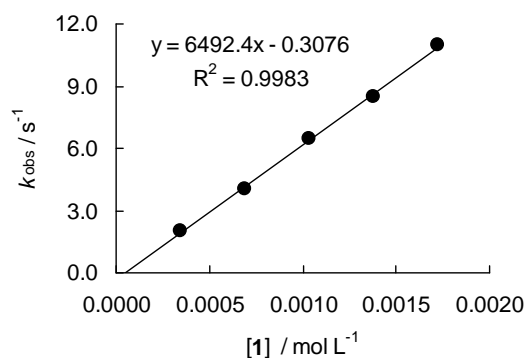
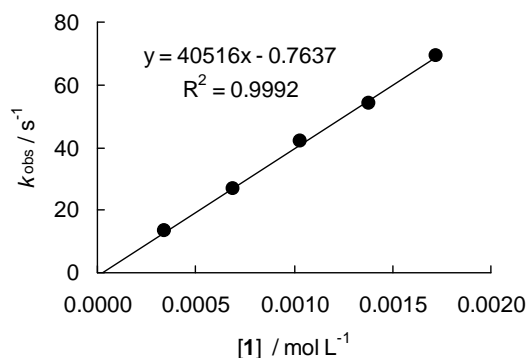


Table 7: Kinetics of the reaction of **1-K** with **3i** (20 °C stopped-flow, at 422 nm)

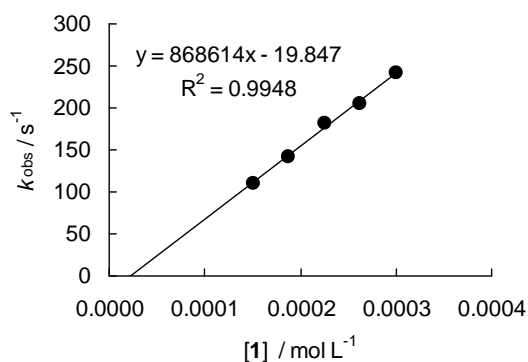
[E] / mol L ⁻¹	[Nu] / mol L ⁻¹	[18-crown-6] / mol L ⁻¹	[Nu]/[E]	<i>k</i> _{obs} / s ⁻¹
2.85 × 10 ⁻⁵	3.45 × 10 ⁻⁴		12.1	13.3
2.85 × 10 ⁻⁵	6.89 × 10 ⁻⁴	1.07 × 10 ⁻³	24.1	26.7
2.85 × 10 ⁻⁵	1.03 × 10 ⁻³		36.2	42.0
2.85 × 10 ⁻⁵	1.38 × 10 ⁻³	2.14 × 10 ⁻³	48.3	54.3
2.85 × 10 ⁻⁵	1.72 × 10 ⁻³		60.4	69.3

$$k_2 = 4.05 \times 10^4 \text{ L mol}^{-1} \text{ s}^{-1}$$

Table 8: Kinetics of the reaction of **1-K** with **3h** (20 °C, stopped-flow, at 630 nm)

[E] / mol L ⁻¹	[Nu] / mol L ⁻¹	[18-crown-6] / mol L ⁻¹	[Nu]/[E]	<i>k</i> _{obs} / s ⁻¹
1.37 × 10 ⁻⁵	1.50 × 10 ⁻⁴		11.0	110
1.37 × 10 ⁻⁵	1.88 × 10 ⁻⁴	2.15 × 10 ⁻⁴	13.7	141
1.37 × 10 ⁻⁵	2.25 × 10 ⁻⁴		16.4	182
1.37 × 10 ⁻⁵	2.63 × 10 ⁻⁴	3.23 × 10 ⁻⁴	19.2	205
1.37 × 10 ⁻⁵	3.00 × 10 ⁻⁴		21.9	241

$$k_2 = 8.69 \times 10^5 \text{ L mol}^{-1} \text{ s}^{-1}$$

Table 9: Kinetics of the reaction of **1-K** with **3g** (20 °C, stopped-flow, at 635 nm)

[E] / mol L ⁻¹	[Nu] / mol L ⁻¹	[18-crown-6] / mol L ⁻¹	[Nu]/[E]	<i>k</i> _{obs} / s ⁻¹
1.22 × 10 ⁻⁵	1.50 × 10 ⁻⁴		12.4	204
1.22 × 10 ⁻⁵	1.88 × 10 ⁻⁴	2.15 × 10 ⁻⁴	15.4	258
1.22 × 10 ⁻⁵	2.25 × 10 ⁻⁴		18.5	335
1.22 × 10 ⁻⁵	2.63 × 10 ⁻⁴	3.23 × 10 ⁻⁴	21.6	378
1.22 × 10 ⁻⁵	3.00 × 10 ⁻⁴		24.7	454

$$k_2 = 1.65 \times 10^6 \text{ L mol}^{-1} \text{ s}^{-1}$$

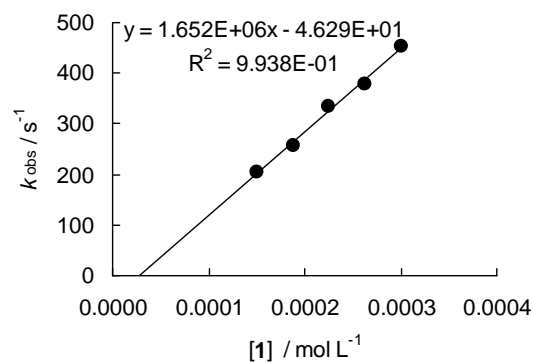
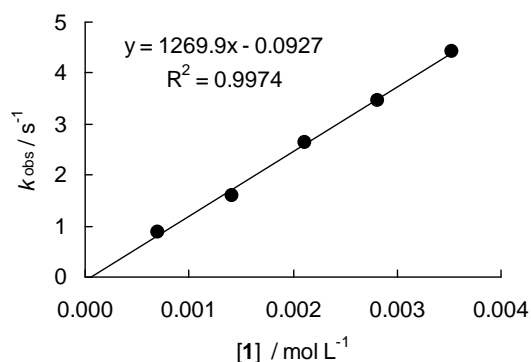


Table 10: Kinetics of the reaction of **1-K** with **6a** (20 °C, stopped-flow, at 487 nm)

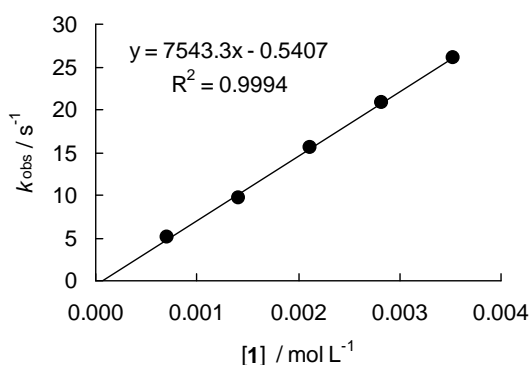
[E] / mol L ⁻¹	[Nu] / mol L ⁻¹	[18-crown-6] / mol L ⁻¹	[Nu]/[E]	<i>k</i> _{obs} / s ⁻¹
4.13 × 10 ⁻⁵	7.06 × 10 ⁻⁴		17.1	0.869
4.13 × 10 ⁻⁵	1.41 × 10 ⁻³	1.83 × 10 ⁻³	34.2	1.59
4.13 × 10 ⁻⁵	2.12 × 10 ⁻³		51.4	2.65
4.13 × 10 ⁻⁵	2.82 × 10 ⁻³	3.79 × 10 ⁻³	68.4	3.45
4.13 × 10 ⁻⁵	3.53 × 10 ⁻³		85.6	4.42

$$k_2 = 1.27 \times 10^3 \text{ L mol}^{-1} \text{ s}^{-1}$$

Table 11: Kinetics of the reaction of **1-K** with **6b** (20 °C, stopped-flow, at 487 nm)

[E] / mol L ⁻¹	[Nu] / mol L ⁻¹	[18-crown-6] / mol L ⁻¹	[Nu]/[E]	<i>k</i> _{obs} / s ⁻¹
4.87 × 10 ⁻⁵	7.06 × 10 ⁻⁴		14.5	5.01
4.87 × 10 ⁻⁵	1.41 × 10 ⁻³	1.83 × 10 ⁻³	28.9	9.74
4.87 × 10 ⁻⁵	2.12 × 10 ⁻³		43.5	15.5
4.87 × 10 ⁻⁵	2.82 × 10 ⁻³	3.79 × 10 ⁻³	57.9	20.8
4.87 × 10 ⁻⁵	3.53 × 10 ⁻³		72.4	26.1

$$k_2 = 7.54 \times 10^3 \text{ L mol}^{-1} \text{ s}^{-1}$$

Table 12: Kinetics of the reaction of **1-K** with **7a** (20 °C, stopped-flow, at 490 nm)

[E] / mol L ⁻¹	[Nu] / mol L ⁻¹	[18-crown-6] / mol L ⁻¹	[Nu]/[E]	<i>k</i> _{obs} / s ⁻¹
2.91 × 10 ⁻⁵	5.03 × 10 ⁻⁴		17.3	0.406
2.91 × 10 ⁻⁵	1.01 × 10 ⁻³	1.35 × 10 ⁻³	34.7	0.776
2.91 × 10 ⁻⁵	1.51 × 10 ⁻³		51.8	1.23
2.91 × 10 ⁻⁵	2.01 × 10 ⁻³	2.71 × 10 ⁻³	69.0	1.61
2.91 × 10 ⁻⁵	2.52 × 10 ⁻³		86.5	2.01

$$k_2 = 8.03 \times 10^2 \text{ L mol}^{-1} \text{ s}^{-1}$$

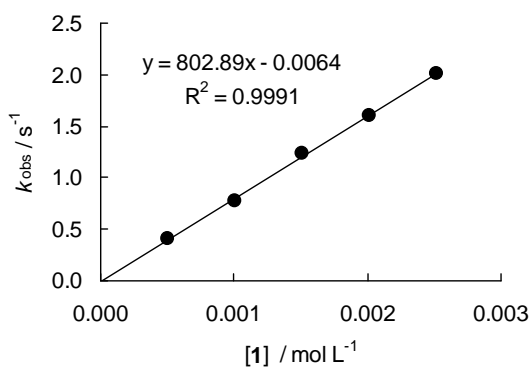
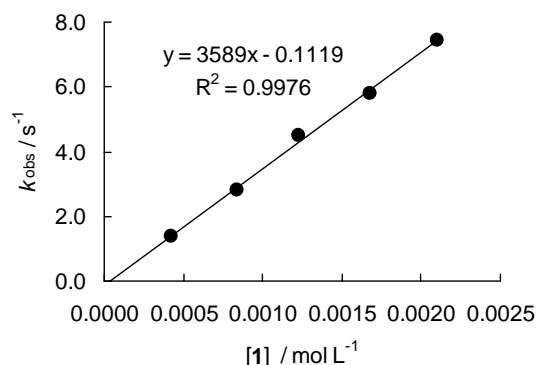


Table 13: Kinetics of the reaction of **1-K** with **7b** (20 °C, stopped-flow, at 490 nm)

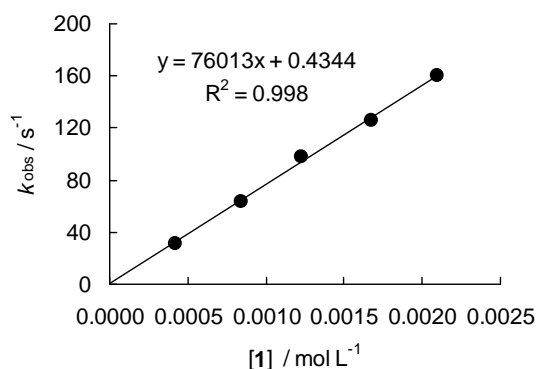
[E] / mol L ⁻¹	[Nu] / mol L ⁻¹	[18-crown-6] / mol L ⁻¹	[Nu]/[E]	<i>k</i> _{obs} / s ⁻¹
2.55 × 10 ⁻⁵	4.20 × 10 ⁻⁴		16.5	1.40
2.55 × 10 ⁻⁵	8.39 × 10 ⁻⁴	1.08 × 10 ⁻³	32.9	2.81
2.55 × 10 ⁻⁵	1.23 × 10 ⁻³		48.2	4.48
2.55 × 10 ⁻⁵	1.68 × 10 ⁻³	2.16 × 10 ⁻³	65.8	5.80
2.55 × 10 ⁻⁵	2.10 × 10 ⁻³		82.3	7.45

$$k_2 = 3.59 \times 10^3 \text{ L mol}^{-1} \text{ s}^{-1}$$

Table 14: Kinetics of the reaction of **1-K** with **7c** (20 °C, stopped-flow, at 390 nm)

[E] / mol L ⁻¹	[Nu] / mol L ⁻¹	[18-crown-6] / mol L ⁻¹	[Nu]/[E]	<i>k</i> _{obs} / s ⁻¹
3.31 × 10 ⁻⁵	4.20 × 10 ⁻⁴		12.7	31.4
3.31 × 10 ⁻⁵	8.39 × 10 ⁻⁴	1.08 × 10 ⁻³	25.3	63.6
3.31 × 10 ⁻⁵	1.23 × 10 ⁻³		37.2	97.7
3.31 × 10 ⁻⁵	1.68 × 10 ⁻³	2.16 × 10 ⁻³	50.8	126
3.31 × 10 ⁻⁵	2.10 × 10 ⁻³		63.4	160

$$k_2 = 7.60 \times 10^4 \text{ L mol}^{-1} \text{ s}^{-1}$$

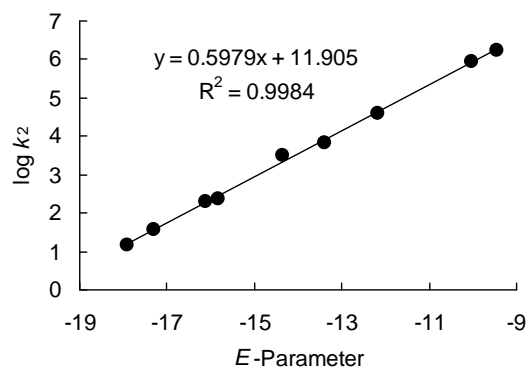


Determination of Reactivity Parameters *N* and *s* for the anion of 2-pyridone (**1**) in DMSO

Table 15: Rate Constants for the reactions of **1-K** with different electrophiles (20 °C)

Electrophile	<i>E</i>	<i>k</i> ₂ / L mol ⁻¹ s ⁻¹	log <i>k</i> ₂
jul-tBu (3o)	-17.90	1.51 × 10 ¹	1.18
dma-tBu (3n)	-17.29	3.68 × 10 ¹	1.57
OMe-tBu (3m)	-16.11	1.94 × 10 ²	2.29
Me-tBu (3l)	-15.83	2.44 × 10 ²	2.39
NO ₂ -tBu (3k)	-14.36	3.06 × 10 ³	3.49
dma-Ph (3j)	-13.39	6.49 × 10 ³	3.81
OMe-Ph (3i)	-12.18	4.05 × 10 ⁴	4.61
(lil) ₂ CH ⁺ (3h)	-10.04	8.69 × 10 ⁵	5.94
(jul) ₂ CH ⁺ (3g)	-9.45	1.65 × 10 ⁶	6.22

$$N = 19.91, s = 0.60$$

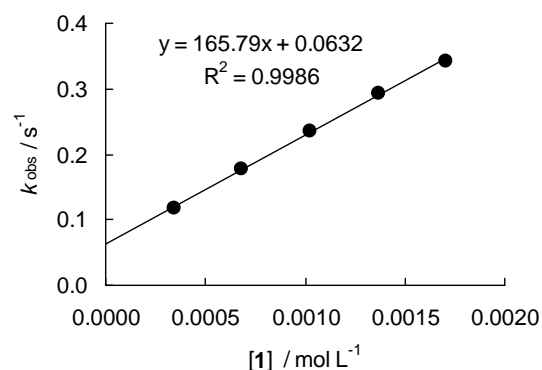


5.5.2 Reactions of the Lithium Salt of 2-Pyridone (1-Li) in DMSO

Table 16: Kinetics of the reaction of **1-Li** with **3i** (20 °C, stopped-flow, at 371 nm)

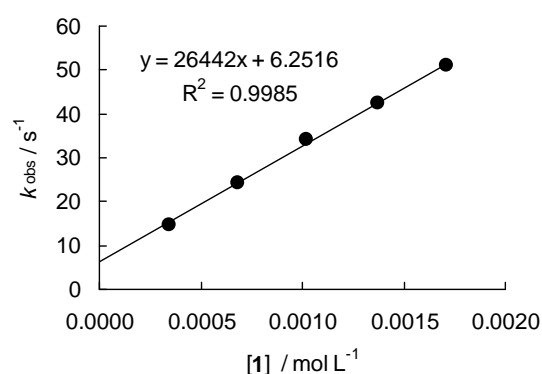
[E] / mol L ⁻¹	[Nu] / mol L ⁻¹	[LiOtBu] / mol L ⁻¹	[Nu]/[E]	<i>k</i> _{obs} / s ⁻¹
3.32 × 10 ⁻⁵	3.42 × 10 ⁻⁴	3.59 × 10 ⁻⁴	10.3	0.117
3.32 × 10 ⁻⁵	6.83 × 10 ⁻⁴	7.17 × 10 ⁻⁴	20.6	0.177
3.32 × 10 ⁻⁵	1.02 × 10 ⁻³	1.08 × 10 ⁻³	30.8	0.236
3.32 × 10 ⁻⁵	1.37 × 10 ⁻³	1.43 × 10 ⁻³	41.1	0.293
3.32 × 10 ⁻⁵	1.72 × 10 ⁻³	1.79 × 10 ⁻³	51.4	0.342

$$k_2 = 1.66 \times 10^2 \text{ L mol}^{-1} \text{ s}^{-1}$$

Table 17: Kinetics of the reaction of **1-Li** with **3i** (20 °C, stopped-flow, at 422 nm)

[E] / mol L ⁻¹	[Nu] / mol L ⁻¹	[LiOtBu] / mol L ⁻¹	[Nu]/[E]	<i>k</i> _{obs} / s ⁻¹
2.47 × 10 ⁻⁵	3.42 × 10 ⁻⁴	3.59 × 10 ⁻⁴	13.9	14.8
2.47 × 10 ⁻⁵	6.83 × 10 ⁻³	7.17 × 10 ⁻⁴	27.7	24.4
2.47 × 10 ⁻⁵	1.02 × 10 ⁻³	1.08 × 10 ⁻³	41.3	34.1
2.47 × 10 ⁻⁵	1.37 × 10 ⁻³	1.43 × 10 ⁻³	55.5	42.5
2.47 × 10 ⁻⁵	1.72 × 10 ⁻³	1.79 × 10 ⁻³	69.3	51.0

$$k_2 = 2.64 \times 10^4 \text{ L mol}^{-1} \text{ s}^{-1}$$



5.5.3 Reactions of the Potassium Salt of 4-Pyridone (2-K) in DMSO

Table 18: Kinetics of the reaction of **2-K** with **3k** (20 °C, stopped-flow, at 374 nm)

[E] / mol L ⁻¹	[Nu] / mol L ⁻¹	[18-crown-6] / mol L ⁻¹	[Nu]/[E]	<i>k</i> _{obs} / s ⁻¹
5.09 × 10 ⁻⁵	4.94 × 10 ⁻⁴		9.7	1.41
5.09 × 10 ⁻⁵	9.88 × 10 ⁻⁴	1.35 × 10 ⁻³	19.4	1.80
5.09 × 10 ⁻⁵	1.48 × 10 ⁻³		29.1	2.16
5.09 × 10 ⁻⁵	1.98 × 10 ⁻³	2.71 × 10 ⁻³	38.9	2.56
5.09 × 10 ⁻⁵	2.47 × 10 ⁻³		48.5	2.83

$$k_2 = 7.28 \times 10^2 \text{ L mol}^{-1} \text{ s}^{-1}$$

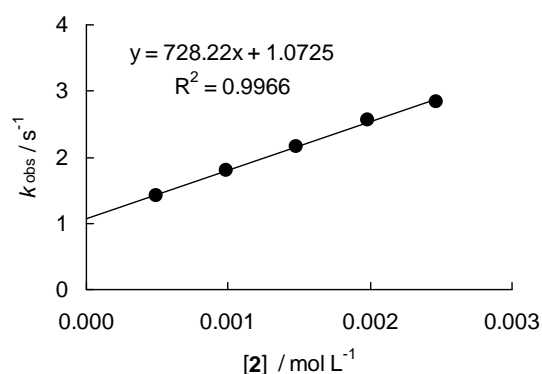
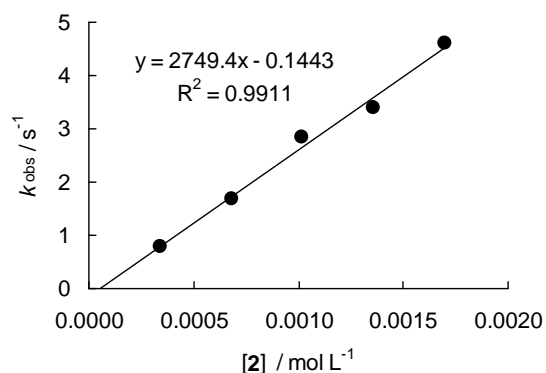


Table 19: Kinetics of the reaction of **2-K** with **3j** (20 °C, stopped-flow, at 533 nm)

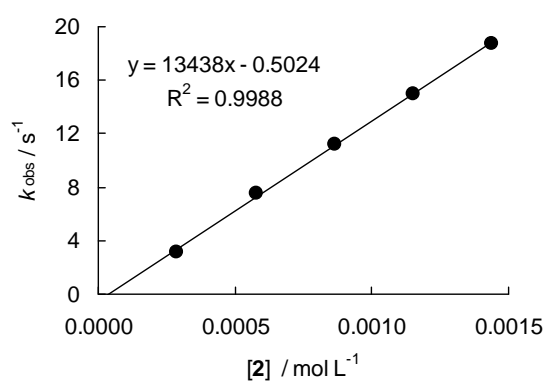
[E] / mol L ⁻¹	[Nu] / mol L ⁻¹	[18-crown-6] / mol L ⁻¹	[Nu]/[E]	<i>k</i> _{obs} / s ⁻¹
2.12 × 10 ⁻⁵	3.40 × 10 ⁻⁴		16.1	0.784
2.12 × 10 ⁻⁵	6.80 × 10 ⁻⁴	8.13 × 10 ⁻³	32.1	1.69
2.12 × 10 ⁻⁵	1.02 × 10 ⁻³		48.1	2.83
2.12 × 10 ⁻⁵	1.36 × 10 ⁻³	1.63 × 10 ⁻³	64.2	3.39
2.12 × 10 ⁻⁵	1.70 × 10 ⁻³		80.3	4.61

$$k_2 = 2.75 \times 10^3 \text{ L mol}^{-1} \text{ s}^{-1}$$

Table 20: Kinetics of the reaction of **2-K** with **3i** (20 °C stopped-flow, at 422 nm)

[E] / mol L ⁻¹	[Nu] / mol L ⁻¹	[18-crown-6] / mol L ⁻¹	[Nu]/[E]	<i>k</i> _{obs} / s ⁻¹
2.61 × 10 ⁻⁵	2.88 × 10 ⁻⁴		11.0	3.10
2.61 × 10 ⁻⁵	5.77 × 10 ⁻⁴	7.53 × 10 ⁻⁴	22.1	7.54
2.61 × 10 ⁻⁵	8.65 × 10 ⁻⁴		33.1	11.2
2.61 × 10 ⁻⁵	1.15 × 10 ⁻³	1.51 × 10 ⁻³	44.1	15.0
2.61 × 10 ⁻⁵	1.44 × 10 ⁻³		55.2	18.7

$$k_2 = 1.34 \times 10^4 \text{ L mol}^{-1} \text{ s}^{-1}$$

Table 21: Kinetics of the reaction of **2-K** with **3h** (20 °C, stopped-flow, at 630 nm)

[E] / mol L ⁻¹	[Nu] / mol L ⁻¹	[18-crown-6] / mol L ⁻¹	[Nu]/[E]	<i>k</i> _{obs} / s ⁻¹
1.44 × 10 ⁻⁵	1.29 × 10 ⁻⁴		9.0	37.8
1.44 × 10 ⁻⁵	1.94 × 10 ⁻⁴	2.33 × 10 ⁻⁴	13.5	59.6
1.44 × 10 ⁻⁵	2.59 × 10 ⁻⁴		18.0	82.2
1.44 × 10 ⁻⁵	3.24 × 10 ⁻⁴	4.19 × 10 ⁻⁴	22.5	102
1.44 × 10 ⁻⁵	3.88 × 10 ⁻⁴		26.9	122

$$k_2 = 3.26 \times 10^5 \text{ L mol}^{-1} \text{ s}^{-1}$$

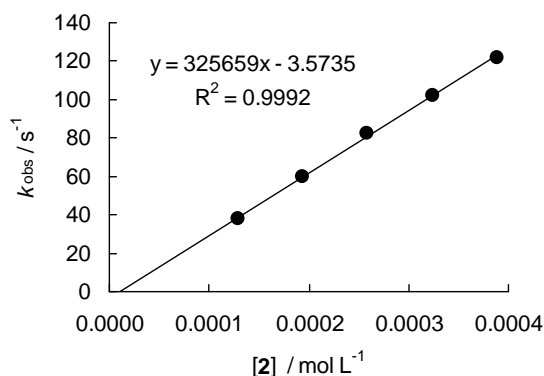
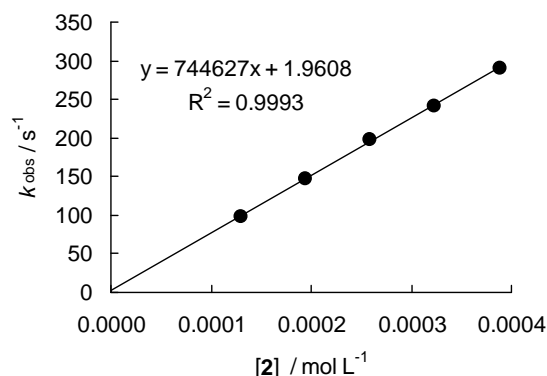


Table 22: Kinetics of the reaction of **2-K** with **3g** (20 °C, stopped-flow, at 635 nm)

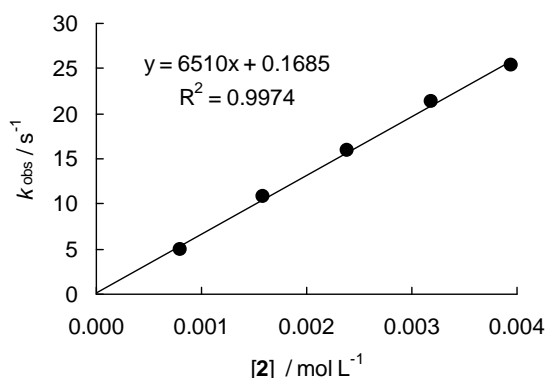
[E] / mol L ⁻¹	[Nu] / mol L ⁻¹	[18-crown-6] / mol L ⁻¹	[Nu]/[E]	<i>k</i> _{obs} / s ⁻¹
1.30 × 10 ⁻⁵	1.29 × 10 ⁻⁴		10.0	97.5
1.30 × 10 ⁻⁵	1.94 × 10 ⁻⁴	2.33 × 10 ⁻⁴	15.0	146
1.30 × 10 ⁻⁵	2.59 × 10 ⁻⁴		20.0	198
1.30 × 10 ⁻⁵	3.24 × 10 ⁻⁴	4.19 × 10 ⁻⁴	25.0	241
1.30 × 10 ⁻⁵	3.88 × 10 ⁻⁴		30.0	291

$$k_2 = 7.45 \times 10^5 \text{ L mol}^{-1} \text{ s}^{-1}$$

Table 23: Kinetics of the reaction of **2-K** with **6a** (20 °C, stopped-flow, at 487 nm)

[E] / mol L ⁻¹	[Nu] / mol L ⁻¹	[18-crown-6] / mol L ⁻¹	[Nu]/[E]	<i>k</i> _{obs} / s ⁻¹
4.30 × 10 ⁻⁵	7.96 × 10 ⁻⁴		18.5	4.95
4.30 × 10 ⁻⁵	1.59 × 10 ⁻³	1.88 × 10 ⁻³	37.0	10.8
4.30 × 10 ⁻⁵	2.39 × 10 ⁻³		55.6	15.9
4.30 × 10 ⁻⁵	3.18 × 10 ⁻³	3.75 × 10 ⁻³	74.0	21.3
4.30 × 10 ⁻⁵	3.95 × 10 ⁻³		91.9	25.4

$$k_2 = 6.51 \times 10^3 \text{ L mol}^{-1} \text{ s}^{-1}$$

Table 24: Kinetics of the reaction of **2-K** with **6b** (20 °C, stopped-flow, at 487 nm)

[E] / mol L ⁻¹	[Nu] / mol L ⁻¹	[18-crown-6] / mol L ⁻¹	[Nu]/[E]	<i>k</i> _{obs} / s ⁻¹
3.95 × 10 ⁻⁵	5.74 × 10 ⁻⁴		14.5	15.9
3.95 × 10 ⁻⁵	1.15 × 10 ⁻³	1.35 × 10 ⁻³	29.1	33.1
3.95 × 10 ⁻⁵	1.72 × 10 ⁻³		43.5	52.0
3.95 × 10 ⁻⁵	2.30 × 10 ⁻³	2.71 × 10 ⁻³	58.2	66.7
3.95 × 10 ⁻⁵	2.87 × 10 ⁻³		72.7	85.9

$$k_2 = 3.02 \times 10^4 \text{ L mol}^{-1} \text{ s}^{-1}$$

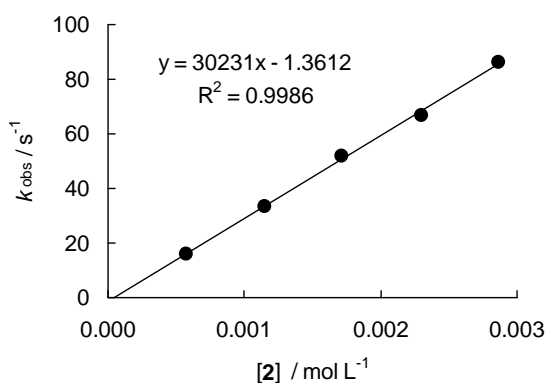
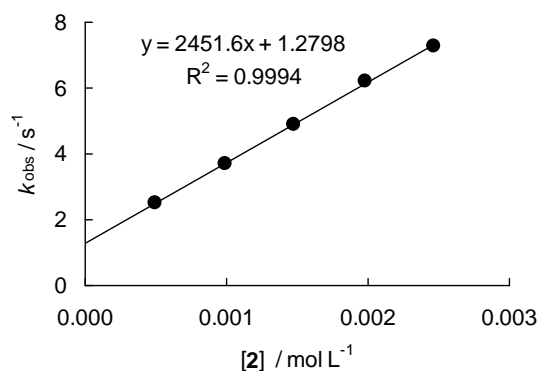


Table 25: Kinetics of the reaction of **2-K** with **7a** (20 °C, stopped-flow, at 490 nm)

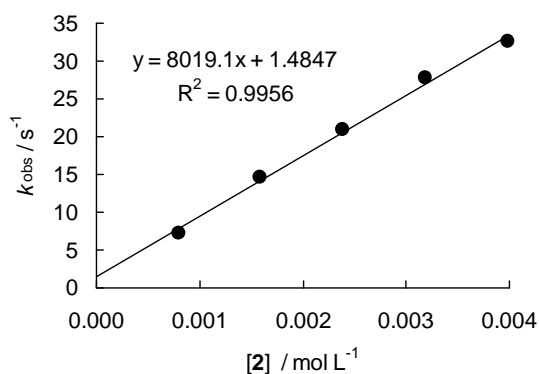
[E] / mol L ⁻¹	[Nu] / mol L ⁻¹	[18-crown-6] / mol L ⁻¹	[Nu]/[E]	<i>k</i> _{obs} / s ⁻¹
3.52 × 10 ⁻⁵	4.94 × 10 ⁻⁴		14.0	2.49
3.52 × 10 ⁻⁵	9.88 × 10 ⁻⁴	1.35 × 10 ⁻³	28.1	3.69
3.52 × 10 ⁻⁵	1.48 × 10 ⁻³		42.0	4.98
3.52 × 10 ⁻⁵	1.98 × 10 ⁻³	2.71 × 10 ⁻³	56.3	6.21
3.52 × 10 ⁻⁵	2.47 × 10 ⁻³		70.2	7.29

$$k_2 = 2.45 \times 10^3 \text{ L mol}^{-1} \text{ s}^{-1}$$

Table 26: Kinetics of the reaction of **2-K** with **7b** (20 °C, stopped-flow, at 490 nm)

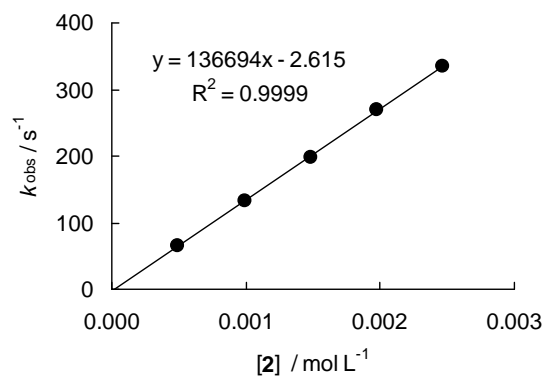
[E] / mol L ⁻¹	[Nu] / mol L ⁻¹	[18-crown-6] / mol L ⁻¹	[Nu]/[E]	<i>k</i> _{obs} / s ⁻¹
2.88 × 10 ⁻⁵	7.96 × 10 ⁻⁴		27.6	7.24
2.88 × 10 ⁻⁵	1.59 × 10 ⁻³	1.88 × 10 ⁻³	55.2	14.6
2.88 × 10 ⁻⁵	2.39 × 10 ⁻³		83.0	21.0
2.88 × 10 ⁻⁵	3.18 × 10 ⁻³	3.75 × 10 ⁻³	110	27.7
2.88 × 10 ⁻⁵	3.98 × 10 ⁻³		138	32.6

$$k_2 = 8.02 \times 10^3 \text{ L mol}^{-1} \text{ s}^{-1}$$

Table 27: Kinetics of the reaction of **2-K** with **7c** (20 °C, stopped-flow, at 390 nm)

[E] / mol L ⁻¹	[Nu] / mol L ⁻¹	[18-crown-6] / mol L ⁻¹	[Nu]/[E]	<i>k</i> _{obs} / s ⁻¹
4.63 × 10 ⁻⁵	4.94 × 10 ⁻⁴		10.7	65.1
4.63 × 10 ⁻⁵	9.88 × 10 ⁻⁴	1.35 × 10 ⁻³	21.3	133
4.63 × 10 ⁻⁵	1.48 × 10 ⁻³		32.0	198
4.63 × 10 ⁻⁵	1.98 × 10 ⁻³	2.71 × 10 ⁻³	42.8	269
4.63 × 10 ⁻⁵	2.47 × 10 ⁻³		53.3	335

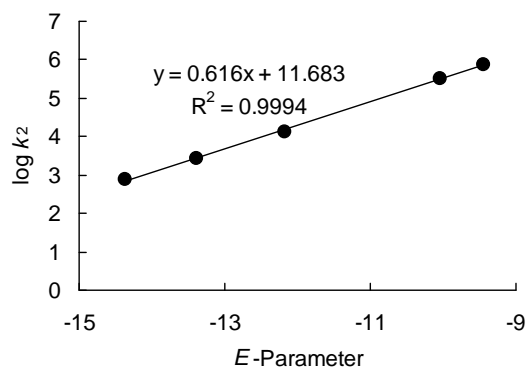
$$k_2 = 1.37 \times 10^5 \text{ L mol}^{-1} \text{ s}^{-1}$$



Determination of Reactivity Parameters N and s for the anion of 4-pyridone (**2**) in DMSOTable 28: Rate Constants for the reactions of **2-K** with different electrophiles (20 °C)

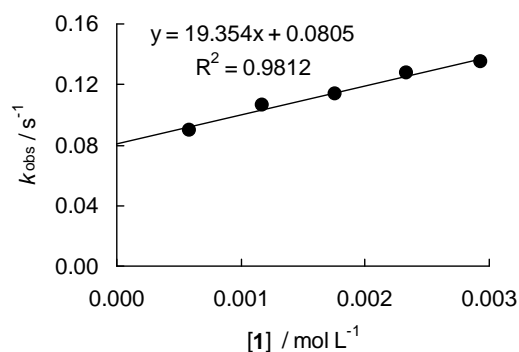
Electrophile	E	$k_2 / \text{L mol}^{-1} \text{s}^{-1}$	$\log k_2$
$\text{NO}_2\text{-tBu}$ (3k)	-14.36	7.28×10^2	2.86
dma-Ph (3j)	-13.39	2.75×10^3	3.44
OMe-Ph (3i)	-12.18	1.34×10^4	4.13
$(\text{il})_2\text{CH}^+$ (3h)	-10.04	3.26×10^5	5.51
$(\text{jul})_2\text{CH}^+$ (3g)	-9.45	7.45×10^5	5.87

$$N = 18.97, s = 0.62$$

5.5.4 Reactions of the Potassium Salt of 2-Pyridone (**1-K**) in CH_3CN Table 29: Kinetics of the reaction of **1-K** with **3o** (20 °C, stopped-flow, at 521 nm)

[E] / mol L ⁻¹	[Nu] / mol L ⁻¹	[18-crown-6] / mol L ⁻¹	[Nu]/[E]	$k_{\text{obs}} /$ s ⁻¹
2.79×10^{-5}	5.86×10^{-4}	7.44×10^{-4}	21.0	0.0893
2.79×10^{-5}	1.17×10^{-3}	1.49×10^{-3}	41.9	0.106
2.79×10^{-5}	1.76×10^{-3}	2.24×10^{-3}	63.1	0.114
2.79×10^{-5}	2.34×10^{-3}	2.97×10^{-3}	83.9	0.128
2.79×10^{-5}	2.93×10^{-3}	3.72×10^{-3}	105	0.135

$$k_2 = 1.94 \times 10^1 \text{ L mol}^{-1} \text{ s}^{-1}$$

Table 30: Kinetics of the reaction of **1-K** with **3n** (20 °C, stopped-flow, at 533 nm)

[E] / mol L ⁻¹	[Nu] / mol L ⁻¹	[18-crown-6] / mol L ⁻¹	[Nu]/[E]	$k_{\text{obs}} /$ s ⁻¹
3.83×10^{-5}	6.78×10^{-4}	8.41×10^{-4}	17.7	0.0854
3.83×10^{-5}	1.36×10^{-3}	1.69×10^{-3}	35.5	0.109
3.83×10^{-5}	2.03×10^{-3}	2.52×10^{-3}	53.0	0.142
3.83×10^{-5}	2.71×10^{-3}	3.36×10^{-3}	70.8	0.168
3.83×10^{-5}	3.39×10^{-3}	4.20×10^{-3}	88.5	0.186

$$k_2 = 3.84 \times 10^1 \text{ L mol}^{-1} \text{ s}^{-1}$$

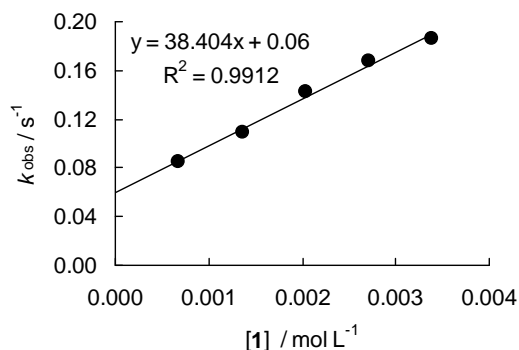
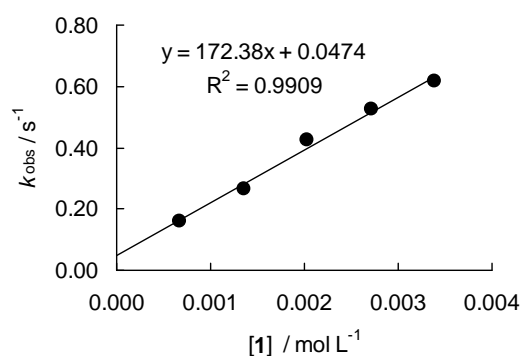


Table 31: Kinetics of the reaction of **1-K** with **3m** (20 °C, stopped-flow, at 393 nm)

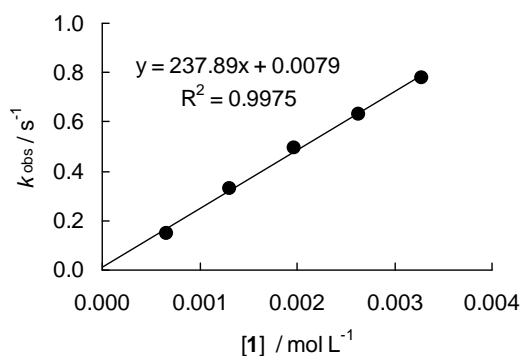
[E] / mol L ⁻¹	[Nu] / mol L ⁻¹	[18-crown-6] / mol L ⁻¹	[Nu]/[E]	k_{obs} / s ⁻¹
3.95×10^{-5}	6.78×10^{-4}	8.41×10^{-4}	17.2	0.161
3.95×10^{-5}	1.36×10^{-3}	1.69×10^{-3}	34.5	0.266
3.95×10^{-5}	2.03×10^{-3}	2.52×10^{-3}	51.5	0.423
3.95×10^{-5}	2.71×10^{-3}	3.36×10^{-3}	68.7	0.524
3.95×10^{-5}	3.39×10^{-3}	4.20×10^{-3}	85.9	0.616

$$k_2 = 1.72 \times 10^2 \text{ L mol}^{-1} \text{ s}^{-1}$$

Table 32: Kinetics of the reaction of **1-K** with **3l** (20 °C, stopped-flow, at 371 nm)

[E] / mol L ⁻¹	[Nu] / mol L ⁻¹	[18-crown-6] / mol L ⁻¹	[Nu]/[E]	k_{obs} / s ⁻¹
3.03×10^{-5}	6.57×10^{-4}	8.34×10^{-4}	21.7	0.150
3.03×10^{-5}	1.31×10^{-3}	1.66×10^{-3}	43.2	0.329
3.03×10^{-5}	1.97×10^{-3}	2.50×10^{-3}	64.9	0.492
3.03×10^{-5}	2.63×10^{-3}	3.34×10^{-3}	86.7	0.631
3.03×10^{-5}	3.28×10^{-3}	4.17×10^{-3}	108	0.780

$$k_2 = 2.38 \times 10^2 \text{ L mol}^{-1} \text{ s}^{-1}$$

Table 33: Kinetics of the reaction of **1-K** with **3k** (20 °C, stopped-flow, at 374 nm)

[E] / mol L ⁻¹	[Nu] / mol L ⁻¹	[18-crown-6] / mol L ⁻¹	[Nu]/[E]	k_{obs} / s ⁻¹
5.60×10^{-5}	6.78×10^{-4}	8.41×10^{-4}	12.1	1.97
5.60×10^{-5}	1.36×10^{-3}	1.69×10^{-3}	24.3	3.38
5.60×10^{-5}	2.03×10^{-3}	2.52×10^{-3}	36.3	5.45
5.60×10^{-5}	2.71×10^{-3}	3.36×10^{-3}	48.4	6.88
5.60×10^{-5}	3.39×10^{-3}	4.20×10^{-3}	60.6	8.15

$$k_2 = 2.34 \times 10^3 \text{ L mol}^{-1} \text{ s}^{-1}$$

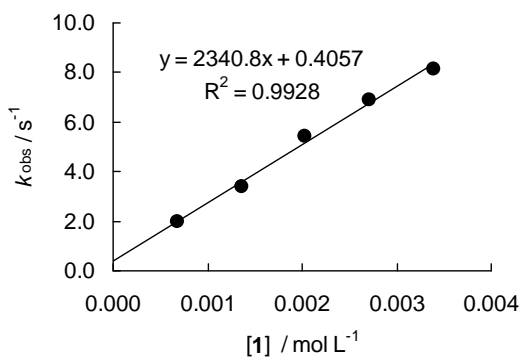
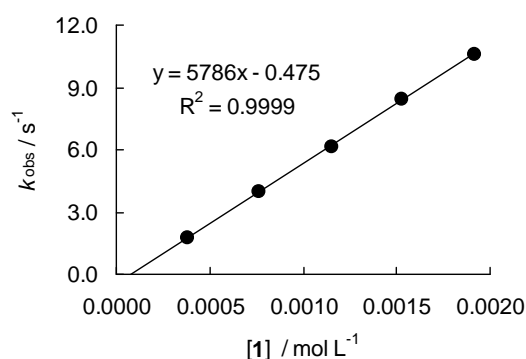


Table 34: Kinetics of the reaction of **1-K** with **3j** (20 °C, stopped-flow, at 533 nm)

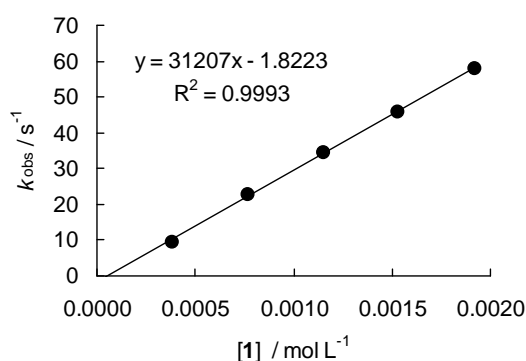
[E] / mol L ⁻¹	[Nu] / mol L ⁻¹	[18-crown-6] / mol L ⁻¹	[Nu]/[E]	<i>k</i> _{obs} / s ⁻¹
2.96 × 10 ⁻⁵	3.84 × 10 ⁻⁴	6.11 × 10 ⁻⁴	13.0	1.73
2.96 × 10 ⁻⁵	7.67 × 10 ⁻⁴	1.22 × 10 ⁻³	25.9	3.98
2.96 × 10 ⁻⁵	1.15 × 10 ⁻³	1.83 × 10 ⁻³	38.8	6.16
2.96 × 10 ⁻⁵	1.53 × 10 ⁻³	2.43 × 10 ⁻³	51.6	8.43
2.96 × 10 ⁻⁵	1.92 × 10 ⁻³	3.05 × 10 ⁻³	64.8	10.6

$$k_2 = 5.79 \times 10^3 \text{ L mol}^{-1} \text{ s}^{-1}$$

Table 35: Kinetics of the reaction of **1-K** with **3i** (20 °C, stopped-flow, at 422 nm)

[E] / mol L ⁻¹	[Nu] / mol L ⁻¹	[18-crown-6] / mol L ⁻¹	[Nu]/[E]	<i>k</i> _{obs} / s ⁻¹
2.80 × 10 ⁻⁵	3.84 × 10 ⁻⁴	6.11 × 10 ⁻⁴	13.7	9.56
2.80 × 10 ⁻⁵	7.67 × 10 ⁻⁴	1.22 × 10 ⁻³	27.4	22.8
2.80 × 10 ⁻⁵	1.15 × 10 ⁻³	1.83 × 10 ⁻³	41.1	34.3
2.80 × 10 ⁻⁵	1.53 × 10 ⁻³	2.43 × 10 ⁻³	54.7	45.8
2.80 × 10 ⁻⁵	1.92 × 10 ⁻³	3.05 × 10 ⁻³	68.6	57.9

$$k_2 = 3.12 \times 10^4 \text{ L mol}^{-1} \text{ s}^{-1}$$

Table 36: Kinetics of the reaction of **1-K** with **6a** (20 °C, stopped-flow, at 487 nm)

[E] / mol L ⁻¹	[Nu] / mol L ⁻¹	[18-crown-6] / mol L ⁻¹	[Nu]/[E]	<i>k</i> _{obs} / s ⁻¹
2.37 × 10 ⁻⁵	4.15 × 10 ⁻⁴	5.27 × 10 ⁻⁴	17.5	0.425
2.37 × 10 ⁻⁵	8.30 × 10 ⁻⁴	1.05 × 10 ⁻³	35.0	1.00
2.37 × 10 ⁻⁵	1.23 × 10 ⁻³	1.56 × 10 ⁻³	51.9	1.58
2.37 × 10 ⁻⁵	1.66 × 10 ⁻³	2.11 × 10 ⁻³	70.0	2.13
2.37 × 10 ⁻⁵	2.08 × 10 ⁻³	2.64 × 10 ⁻³	87.8	2.66

$$k_2 = 1.35 \times 10^3 \text{ L mol}^{-1} \text{ s}^{-1}$$

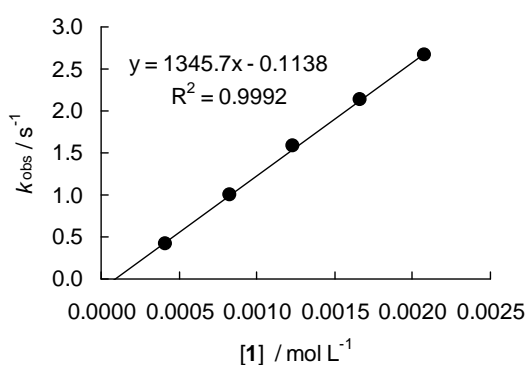
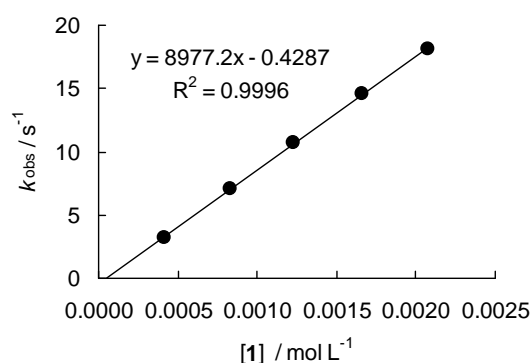


Table 37: Kinetics of the reaction of **1-K** with **6b** (20 °C, stopped-flow, at 487 nm)

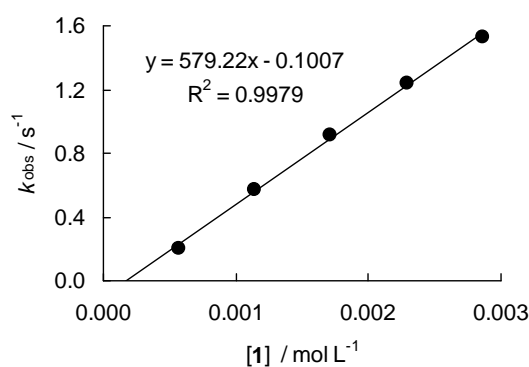
[E] / mol L ⁻¹	[Nu] / mol L ⁻¹	[18-crown-6] / mol L ⁻¹	[Nu]/[E]	<i>k</i> _{obs} / s ⁻¹
2.48 × 10 ⁻⁵	4.15 × 10 ⁻⁴	5.27 × 10 ⁻⁴	16.7	3.20
2.48 × 10 ⁻⁵	8.30 × 10 ⁻⁴	1.05 × 10 ⁻³	33.5	7.05
2.48 × 10 ⁻⁵	1.23 × 10 ⁻³	1.56 × 10 ⁻³	49.6	10.7
2.48 × 10 ⁻⁵	1.66 × 10 ⁻³	2.11 × 10 ⁻³	66.9	14.6
2.48 × 10 ⁻⁵	2.08 × 10 ⁻³	2.64 × 10 ⁻³	83.9	18.1

$$k_2 = 8.98 \times 10^3 \text{ L mol}^{-1} \text{ s}^{-1}$$

Table 38: Kinetics of the reaction of **1-K** with **7a** (20 °C, stopped-flow, at 490 nm)

[E] / mol L ⁻¹	[Nu] / mol L ⁻¹	[18-crown-6] / mol L ⁻¹	[Nu]/[E]	<i>k</i> _{obs} / s ⁻¹
2.37 × 10 ⁻⁵	5.71 × 10 ⁻⁴	6.57 × 10 ⁻⁴	24.1	0.204
2.37 × 10 ⁻⁵	1.14 × 10 ⁻³	1.31 × 10 ⁻³	48.1	0.574
2.37 × 10 ⁻⁵	1.71 × 10 ⁻³	1.97 × 10 ⁻³	72.2	0.913
2.37 × 10 ⁻⁵	2.29 × 10 ⁻³	2.63 × 10 ⁻³	96.6	1.24
2.37 × 10 ⁻⁵	2.86 × 10 ⁻³	3.29 × 10 ⁻³	121	1.53

$$k_2 = 5.79 \times 10^2 \text{ L mol}^{-1} \text{ s}^{-1}$$

Table 39: Kinetics of the reaction of **1-K** with **7b** (20 °C, stopped-flow, at 490 nm)

[E] / mol L ⁻¹	[Nu] / mol L ⁻¹	[18-crown-6] / mol L ⁻¹	[Nu]/[E]	<i>k</i> _{obs} / s ⁻¹
1.50 × 10 ⁻⁵	5.71 × 10 ⁻⁴	6.57 × 10 ⁻⁴	38.1	1.44
1.50 × 10 ⁻⁵	1.14 × 10 ⁻³	1.31 × 10 ⁻³	76.0	3.20
1.50 × 10 ⁻⁵	1.71 × 10 ⁻³	1.97 × 10 ⁻³	114	4.56
1.50 × 10 ⁻⁵	2.29 × 10 ⁻³	2.63 × 10 ⁻³	153	6.33
1.50 × 10 ⁻⁵	2.86 × 10 ⁻³	3.29 × 10 ⁻³	191	7.71

$$k_2 = 2.74 \times 10^3 \text{ L mol}^{-1} \text{ s}^{-1}$$

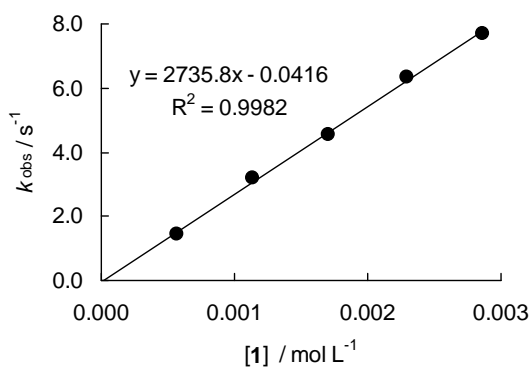
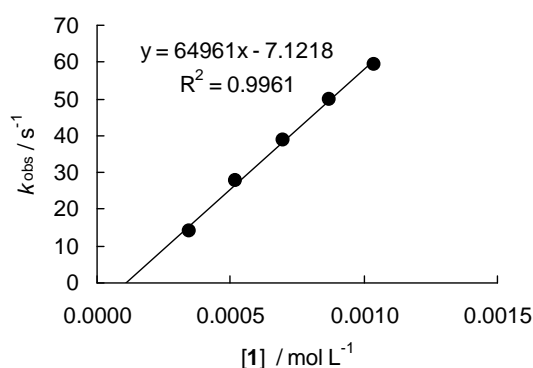


Table 40: Kinetics of the reaction of **1-K** with **7c** (20 °C, stopped-flow, at 390 nm)

[E] / mol L ⁻¹	[Nu] / mol L ⁻¹	[18-crown-6] / mol L ⁻¹	[Nu]/[E]	<i>k</i> _{obs} / s ⁻¹
3.56 × 10 ⁻⁵	3.48 × 10 ⁻⁴	4.84 × 10 ⁻⁴	9.8	14.2
3.56 × 10 ⁻⁵	5.21 × 10 ⁻⁴	7.24 × 10 ⁻⁴	14.6	27.7
3.56 × 10 ⁻⁵	6.95 × 10 ⁻⁴	9.66 × 10 ⁻⁴	19.5	38.8
3.56 × 10 ⁻⁵	8.69 × 10 ⁻⁴	1.21 × 10 ⁻³	24.4	50.0
3.56 × 10 ⁻⁵	1.04 × 10 ⁻³	1.45 × 10 ⁻³	29.2	59.3

$$k_2 = 6.50 \times 10^4 \text{ L mol}^{-1} \text{ s}^{-1}$$

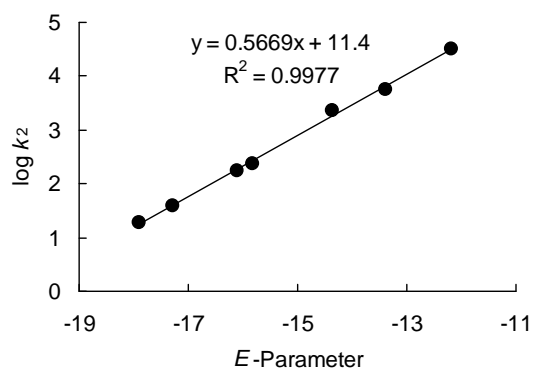


Determination of Reactivity Parameters *N* and *s* for the anion of 2-pyridone (**1**) in CH₃CN

Table 41: Rate Constants for the reactions of **1-K** with different electrophiles (20 °C)

Electrophile	<i>E</i>	<i>k</i> ₂ / L mol ⁻¹ s ⁻¹	log <i>k</i> ₂
jul-tBu (3o)	-17.90	1.94 × 10 ¹	1.29
dma-tBu (3n)	-17.29	3.84 × 10 ¹	1.58
OMe-tBu (3m)	-16.11	1.72 × 10 ²	2.24
Me-tBu (3l)	-15.83	2.38 × 10 ²	2.38
NO ₂ -tBu (3k)	-14.36	2.34 × 10 ³	3.37
dma-Ph (3j)	-13.39	5.79 × 10 ³	3.76
OMe-Ph (3i)	-12.18	3.12 × 10 ⁴	4.49

$$N = 20.11, s = 0.57$$



5.5.5 Reactions of the Potassium Salt of 4-Pyridone (**2-K**) in CH₃CN

Table 42: Kinetics of the reaction of **2-K** with **3l** (20 °C, stopped-flow, at 371 nm)

[E] / mol L ⁻¹	[Nu] / mol L ⁻¹	[18-crown-6] / mol L ⁻¹	[Nu]/[E]	<i>k</i> _{obs} / s ⁻¹
4.95 × 10 ⁻⁵	1.20 × 10 ⁻³	1.61 × 10 ⁻³	24.2	1.20
4.95 × 10 ⁻⁵	1.80 × 10 ⁻³	2.41 × 10 ⁻³	36.4	1.31
4.95 × 10 ⁻⁵	2.41 × 10 ⁻³	3.23 × 10 ⁻³	48.7	1.41
4.95 × 10 ⁻⁵	3.01 × 10 ⁻³	4.03 × 10 ⁻³	60.8	1.49

$$k_2 = 1.61 \times 10^2 \text{ L mol}^{-1} \text{ s}^{-1}$$

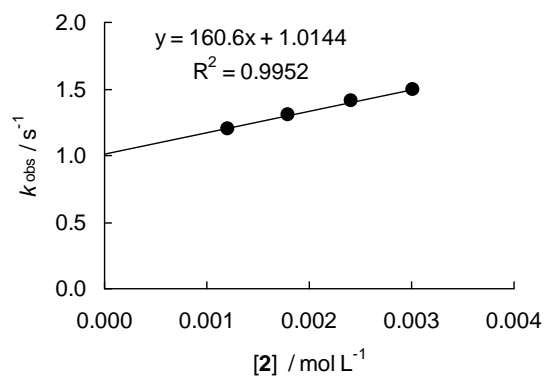
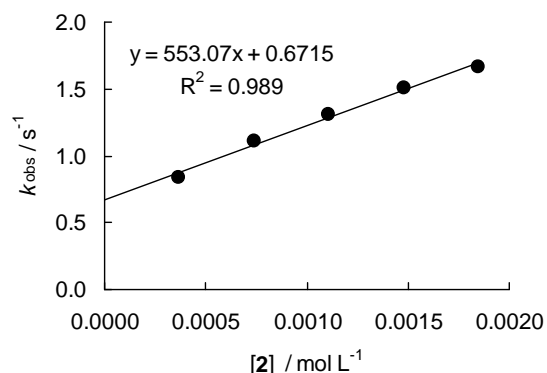


Table 43: Kinetics of the reaction of **2-K** with **3k** (20 °C, stopped-flow, at 374 nm)

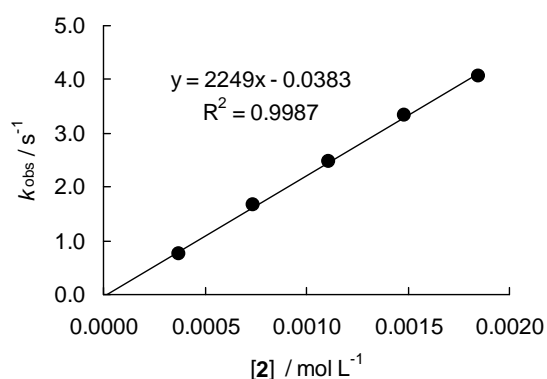
[E] / mol L ⁻¹	[Nu] / mol L ⁻¹	[18-crown-6] / mol L ⁻¹	[Nu]/[E]	<i>k</i> _{obs} / s ⁻¹
4.60 × 10 ⁻⁵	3.69 × 10 ⁻⁴	6.16 × 10 ⁻⁴	8.0	0.836
4.60 × 10 ⁻⁵	7.39 × 10 ⁻⁴	1.23 × 10 ⁻³	16.1	1.11
4.60 × 10 ⁻⁵	1.11 × 10 ⁻³	1.85 × 10 ⁻³	24.1	1.31
4.60 × 10 ⁻⁵	1.48 × 10 ⁻³	2.47 × 10 ⁻³	32.2	1.51
4.60 × 10 ⁻⁵	1.85 × 10 ⁻³	3.09 × 10 ⁻³	40.2	1.66

$$k_2 = 5.53 \times 10^2 \text{ L mol}^{-1} \text{ s}^{-1}$$

Table 44: Kinetics of the reaction of **2-K** with **3j** (20 °C, stopped-flow, at 533 nm)

[E] / mol L ⁻¹	[Nu] / mol L ⁻¹	[18-crown-6] / mol L ⁻¹	[Nu]/[E]	<i>k</i> _{obs} / s ⁻¹
4.28 × 10 ⁻⁵	3.69 × 10 ⁻⁴	6.16 × 10 ⁻⁴	8.6	0.746
4.28 × 10 ⁻⁵	7.39 × 10 ⁻⁴	1.23 × 10 ⁻³	17.3	1.66
4.28 × 10 ⁻⁵	1.11 × 10 ⁻³	1.85 × 10 ⁻³	25.9	2.47
4.28 × 10 ⁻⁵	1.48 × 10 ⁻³	2.47 × 10 ⁻³	34.6	3.34
4.28 × 10 ⁻⁵	1.85 × 10 ⁻³	3.09 × 10 ⁻³	43.2	4.07

$$k_2 = 2.25 \times 10^3 \text{ L mol}^{-1} \text{ s}^{-1}$$

Table 45: Kinetics of the reaction of **2-K** with **3i** (20 °C, stopped-flow, at 422 nm)

[E] / mol L ⁻¹	[Nu] / mol L ⁻¹	[18-crown-6] / mol L ⁻¹	[Nu]/[E]	<i>k</i> _{obs} / s ⁻¹
4.12 × 10 ⁻⁵	3.69 × 10 ⁻⁴	6.16 × 10 ⁻⁴	9.0	3.09
4.12 × 10 ⁻⁵	7.39 × 10 ⁻⁴	1.23 × 10 ⁻³	17.9	6.79
4.12 × 10 ⁻⁵	1.11 × 10 ⁻³	1.85 × 10 ⁻³	26.9	10.2
4.12 × 10 ⁻⁵	1.48 × 10 ⁻³	2.47 × 10 ⁻³	35.9	13.6
4.12 × 10 ⁻⁵	1.85 × 10 ⁻³	3.09 × 10 ⁻³	44.9	16.6

$$k_2 = 9.14 \times 10^3 \text{ L mol}^{-1} \text{ s}^{-1}$$

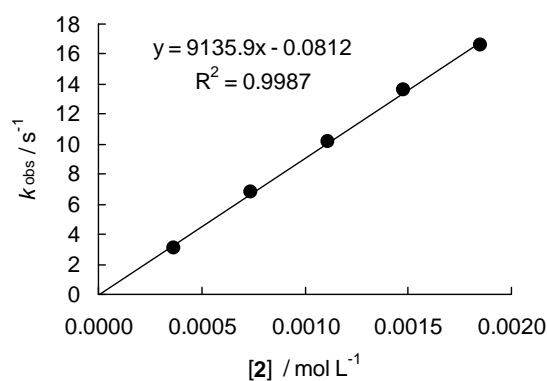
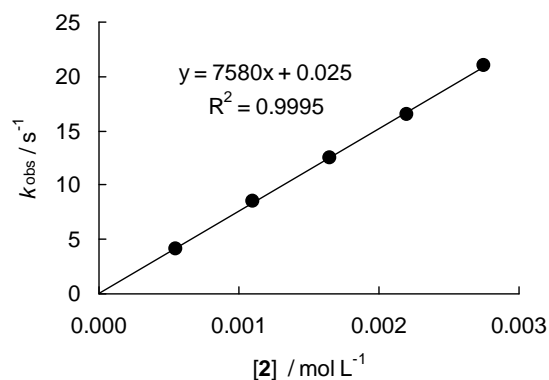


Table 46: Kinetics of the reaction of **2-K** with **6a** (20 °C, stopped-flow, at 487 nm)

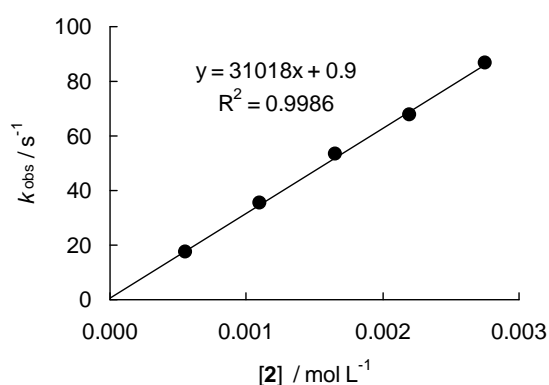
[E] / mol L ⁻¹	[Nu] / mol L ⁻¹	[18-crown-6] / mol L ⁻¹	[Nu]/[E]	<i>k</i> _{obs} / s ⁻¹
2.25 × 10 ⁻⁵	5.50 × 10 ⁻⁴	7.32 × 10 ⁻⁴	24.4	4.15
2.25 × 10 ⁻⁵	1.10 × 10 ⁻³	1.46 × 10 ⁻³	48.9	8.51
2.25 × 10 ⁻⁵	1.65 × 10 ⁻³	2.19 × 10 ⁻³	73.3	12.5
2.25 × 10 ⁻⁵	2.20 × 10 ⁻³	2.93 × 10 ⁻³	97.8	16.5
2.25 × 10 ⁻⁵	2.75 × 10 ⁻³	3.66 × 10 ⁻³	122	21.0

$$k_2 = 7.58 \times 10^3 \text{ L mol}^{-1} \text{ s}^{-1}$$

Table 47: Kinetics of the reaction of **2-K** with **6b** (20 °C, stopped-flow, at 487 nm)

[E] / mol L ⁻¹	[Nu] / mol L ⁻¹	[18-crown-6] / mol L ⁻¹	[Nu]/[E]	<i>k</i> _{obs} / s ⁻¹
3.20 × 10 ⁻⁵	5.50 × 10 ⁻⁴	7.32 × 10 ⁻⁴	17.2	17.5
3.20 × 10 ⁻⁵	1.10 × 10 ⁻³	1.46 × 10 ⁻³	34.4	35.3
3.20 × 10 ⁻⁵	1.65 × 10 ⁻³	2.19 × 10 ⁻³	51.6	53.3
3.20 × 10 ⁻⁵	2.20 × 10 ⁻³	2.93 × 10 ⁻³	68.8	67.7
3.20 × 10 ⁻⁵	2.75 × 10 ⁻³	3.66 × 10 ⁻³	85.9	86.6

$$k_2 = 3.10 \times 10^4 \text{ L mol}^{-1} \text{ s}^{-1}$$

Table 48: Kinetics of the reaction of **2-K** with **7a** (20 °C, stopped-flow, at 490 nm)

[E] / mol L ⁻¹	[Nu] / mol L ⁻¹	[18-crown-6] / mol L ⁻¹	[Nu]/[E]	<i>k</i> _{obs} / s ⁻¹
3.40 × 10 ⁻⁵	5.46 × 10 ⁻⁴	6.99 × 10 ⁻⁴	16.1	2.51
3.40 × 10 ⁻⁵	1.09 × 10 ⁻³	1.40 × 10 ⁻³	32.1	3.30
3.40 × 10 ⁻⁵	1.64 × 10 ⁻³	2.10 × 10 ⁻³	48.2	4.12
3.40 × 10 ⁻⁵	2.18 × 10 ⁻³	2.79 × 10 ⁻³	64.1	4.98
3.40 × 10 ⁻⁵	2.73 × 10 ⁻³	3.49 × 10 ⁻³	80.3	5.78

$$k_2 = 1.51 \times 10^3 \text{ L mol}^{-1} \text{ s}^{-1}$$

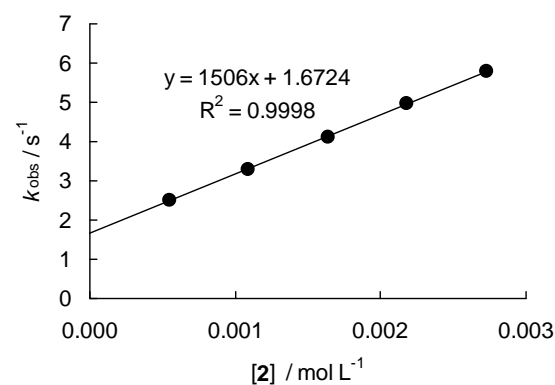
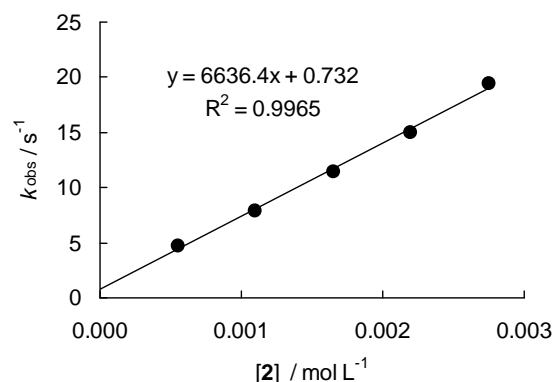


Table 49: Kinetics of the reaction of **2-K** with **7b** (20 °C, stopped-flow, at 490 nm)

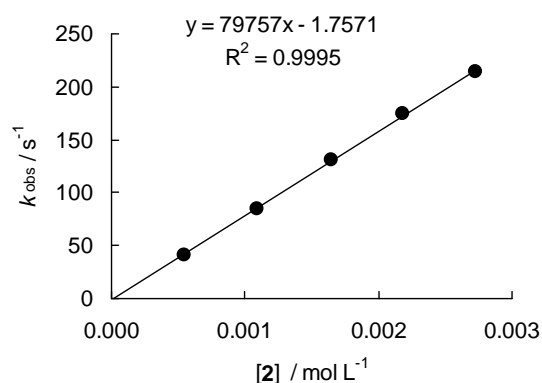
[E] / mol L ⁻¹	[Nu] / mol L ⁻¹	[18-crown-6] / mol L ⁻¹	[Nu]/[E]	<i>k</i> _{obs} / s ⁻¹
1.44 × 10 ⁻⁵	5.50 × 10 ⁻⁴	7.26 × 10 ⁻⁴	38.2	4.69
1.44 × 10 ⁻⁵	1.10 × 10 ⁻³	1.45 × 10 ⁻³	76.4	7.92
1.44 × 10 ⁻⁵	1.65 × 10 ⁻³	2.18 × 10 ⁻³	115	11.4
1.44 × 10 ⁻⁵	2.20 × 10 ⁻³	2.90 × 10 ⁻³	153	15.0
1.44 × 10 ⁻⁵	2.75 × 10 ⁻³	3.63 × 10 ⁻³	191	19.4

$$k_2 = 6.64 \times 10^3 \text{ L mol}^{-1} \text{ s}^{-1}$$

Table 50: Kinetics of the reaction of **2-K** with **7c** (20 °C, stopped-flow, at 390 nm)

[E] / mol L ⁻¹	[Nu] / mol L ⁻¹	[18-crown-6] / mol L ⁻¹	[Nu]/[E]	<i>k</i> _{obs} / s ⁻¹
3.56 × 10 ⁻⁵	5.46 × 10 ⁻⁴	6.99 × 10 ⁻⁴	15.3	40.8
3.56 × 10 ⁻⁵	1.09 × 10 ⁻³	1.40 × 10 ⁻³	30.6	85.1
3.56 × 10 ⁻⁵	1.64 × 10 ⁻³	2.10 × 10 ⁻³	46.3	131
3.56 × 10 ⁻⁵	2.18 × 10 ⁻³	2.79 × 10 ⁻³	61.2	174
3.56 × 10 ⁻⁵	2.73 × 10 ⁻³	3.49 × 10 ⁻³	76.7	214

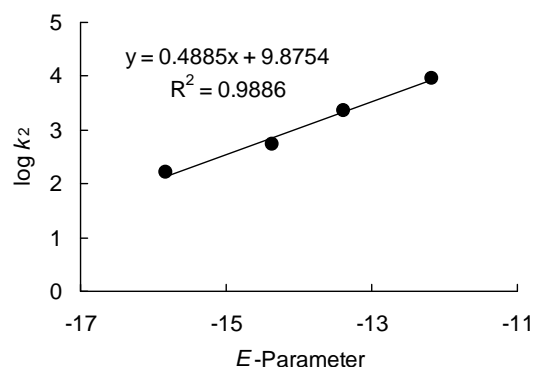
$$k_2 = 7.98 \times 10^4 \text{ L mol}^{-1} \text{ s}^{-1}$$



Determination of Reactivity Parameters *N* and *s* for the anion of 4-pyridone (**2**) in CH₃CN

Table 51: Rate Constants for the reactions of **2-K** with different electrophiles (20 °C)

Electrophile	<i>E</i>	<i>k</i> ₂ / L mol ⁻¹ s ⁻¹	log <i>k</i> ₂
Me-tBu (3l)	-15.83	1.61 × 10 ²	2.21
NO ₂ -tBu (3k)	-14.36	5.53 × 10 ²	2.74
dma-Ph (3j)	-13.39	2.25 × 10 ³	3.35
OMe-Ph (3i)	-12.18	9.14 × 10 ³	3.96

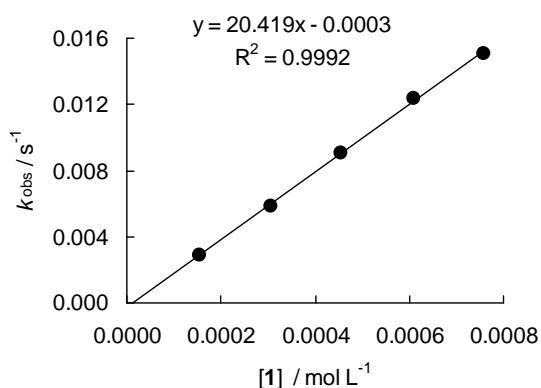


$$N = 20.22, s = 0.49$$

5.5.6 Reactions of the Potassium Salt of 2-Pyridone (1-K) in Water

Table 52: Kinetics of the reaction of **1-K** with **3h** (20 °C, Conventional UV/Vis, at 630 nm)

[E] / mol L ⁻¹	[1-H] ₀ / mol L ⁻¹	[KOH] ₀ / mol L ⁻¹	[1-K] _{eff} / mol L ⁻¹	[KOH] _{eff} / mol L ⁻¹	[Nu]/[E]	k _{obs} / s ⁻¹	k _{OH⁻} / s ⁻¹	k _{eff} / s ⁻¹
1.87 × 10 ⁻⁵	1.18 × 10 ⁻²	2.27 × 10 ⁻⁴	1.54 × 10 ⁻⁴	7.30 × 10 ⁻⁵	8.2	3.05 × 10 ⁻³	1.58 × 10 ⁻⁴	2.89 × 10 ⁻³
1.87 × 10 ⁻⁵	1.18 × 10 ⁻²	4.55 × 10 ⁻⁴	3.07 × 10 ⁻⁴	1.48 × 10 ⁻⁴	16.4	6.15 × 10 ⁻³	3.20 × 10 ⁻⁴	5.83 × 10 ⁻³
1.87 × 10 ⁻⁵	1.18 × 10 ⁻²	6.38 × 10 ⁻⁴	4.56 × 10 ⁻⁴	1.82 × 10 ⁻⁴	24.4	9.46 × 10 ⁻³	3.93 × 10 ⁻⁴	9.07 × 10 ⁻³
1.87 × 10 ⁻⁵	1.18 × 10 ⁻²	9.09 × 10 ⁻⁴	6.10 × 10 ⁻⁴	2.99 × 10 ⁻⁴	32.6	1.30 × 10 ⁻²	6.46 × 10 ⁻⁴	1.24 × 10 ⁻²
1.87 × 10 ⁻⁵	1.18 × 10 ⁻²	1.14 × 10 ⁻³	7.59 × 10 ⁻⁴	3.81 × 10 ⁻⁴	40.6	1.59 × 10 ⁻²	8.23 × 10 ⁻⁴	1.51 × 10 ⁻²



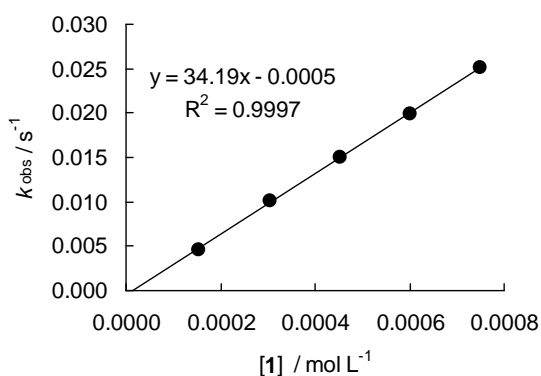
$$k_2(OH^-)^{[17]} = 2.16\ L\ mol^{-1}\ s^{-1}$$

$$pK_a(\mathbf{1-H})^{[16]} = 11.74$$

$$k_2 = 2.04 \times 10^1\ L\ mol^{-1}\ s^{-1}$$

Table 53: Kinetics of the reaction of **1-K** with **3g** (20 °C, Conventional UV/Vis, at 635 nm)

[E] / mol L ⁻¹	[1-H] ₀ / mol L ⁻¹	[KOH] ₀ / mol L ⁻¹	[1-K] _{eff} / mol L ⁻¹	[KOH] _{eff} / mol L ⁻¹	[Nu]/[E]	k _{obs} / s ⁻¹	k _{OH⁻} / s ⁻¹	k _{eff} / s ⁻¹
1.44 × 10 ⁻⁵	1.14 × 10 ⁻²	2.27 × 10 ⁻⁴	1.53 × 10 ⁻⁴	7.40 × 10 ⁻⁵	10.6	4.87 × 10 ⁻³	2.55 × 10 ⁻⁴	4.62 × 10 ⁻³
1.44 × 10 ⁻⁵	1.14 × 10 ⁻²	4.55 × 10 ⁻⁴	3.04 × 10 ⁻⁴	1.51 × 10 ⁻⁴	21.1	1.06 × 10 ⁻²	5.19 × 10 ⁻⁴	1.01 × 10 ⁻²
1.44 × 10 ⁻⁵	1.14 × 10 ⁻²	6.38 × 10 ⁻⁴	4.53 × 10 ⁻⁴	1.85 × 10 ⁻⁴	31.5	1.57 × 10 ⁻²	6.36 × 10 ⁻⁴	1.51 × 10 ⁻²
1.44 × 10 ⁻⁵	1.14 × 10 ⁻²	9.09 × 10 ⁻⁴	6.02 × 10 ⁻⁴	3.07 × 10 ⁻⁴	41.8	2.10 × 10 ⁻²	1.06 × 10 ⁻³	1.99 × 10 ⁻²
1.44 × 10 ⁻⁵	1.14 × 10 ⁻²	1.14 × 10 ⁻³	7.49 × 10 ⁻⁴	3.91 × 10 ⁻⁴	52.0	2.65 × 10 ⁻²	1.35 × 10 ⁻³	2.52 × 10 ⁻²



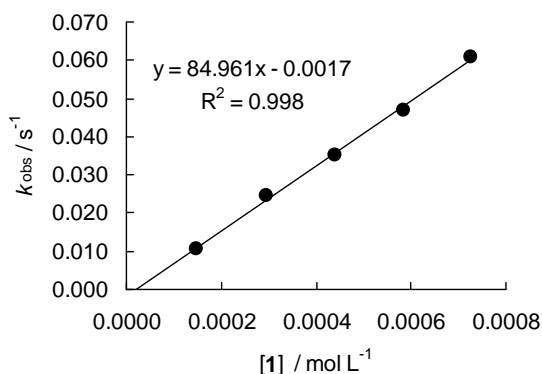
$$k_2(OH^-)^{[17]} = 3.44\ L\ mol^{-1}\ s^{-1}$$

$$pK_a(\mathbf{1-H})^{[16]} = 11.74$$

$$k_2 = 3.42 \times 10^1\ L\ mol^{-1}\ s^{-1}$$

Table 54: Kinetics of the reaction of **1-K** with **3f** (20 °C, Conventional UV/Vis, at 627 nm)

[E] / mol L ⁻¹	[1-H] ₀ / mol L ⁻¹	[KOH] ₀ / mol L ⁻¹	[1-K] _{eff} / mol L ⁻¹	[KOH] _{eff} / mol L ⁻¹	[Nu]/[E]	k _{obs} / s ⁻¹	k _{OH⁻} / s ⁻¹	k _{eff} / s ⁻¹
1.25 × 10 ⁻⁵	1.05 × 10 ⁻²	2.27 × 10 ⁻⁴	1.48 × 10 ⁻⁴	7.90 × 10 ⁻⁵	11.8	1.16 × 10 ⁻²	8.55 × 10 ⁻⁴	1.07 × 10 ⁻²
1.25 × 10 ⁻⁵	1.05 × 10 ⁻²	4.55 × 10 ⁻⁴	2.95 × 10 ⁻⁴	1.60 × 10 ⁻⁴	23.6	2.61 × 10 ⁻²	1.73 × 10 ⁻³	2.44 × 10 ⁻²
1.25 × 10 ⁻⁵	1.05 × 10 ⁻²	6.38 × 10 ⁻⁴	4.40 × 10 ⁻⁴	1.98 × 10 ⁻⁴	35.2	3.72 × 10 ⁻²	2.14 × 10 ⁻³	3.51 × 10 ⁻²
1.25 × 10 ⁻⁵	1.05 × 10 ⁻²	9.09 × 10 ⁻⁴	5.84 × 10 ⁻⁴	3.25 × 10 ⁻⁴	46.7	5.05 × 10 ⁻²	3.51 × 10 ⁻³	4.70 × 10 ⁻²
1.25 × 10 ⁻⁵	1.05 × 10 ⁻²	1.14 × 10 ⁻³	7.26 × 10 ⁻⁴	4.14 × 10 ⁻⁴	58.1	6.53 × 10 ⁻²	4.47 × 10 ⁻³	6.08 × 10 ⁻²



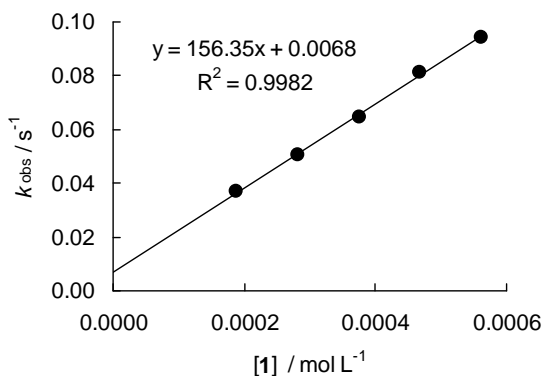
$$k_2(\text{OH}^-)^{[17]} = 10.8 \text{ L mol}^{-1} \text{ s}^{-1}$$

$$\text{p}K_{\text{a}}(\mathbf{1-H})^{[16]} = 11.74$$

$$k_2 = 8.50 \times 10^1 \text{ L mol}^{-1} \text{ s}^{-1}$$

Table 55: Kinetics of the reaction of **1-K** with **3e** (20 °C, Stopped-flow, at 618 nm)

[E] / mol L ⁻¹	[1-H] ₀ / mol L ⁻¹	[KOH] ₀ / mol L ⁻¹	[1-K] _{eff} / mol L ⁻¹	[KOH] _{eff} / mol L ⁻¹	[Nu]/[E]	k _{obs} / s ⁻¹	k _{OH⁻} / s ⁻¹	k _{eff} / s ⁻¹
1.12 × 10 ⁻⁵	1.69 × 10 ⁻²	2.50 × 10 ⁻⁴	1.88 × 10 ⁻⁴	6.20 × 10 ⁻⁵	16.8	3.84 × 10 ⁻²	1.46 × 10 ⁻³	3.68 × 10 ⁻²
1.12 × 10 ⁻⁵	1.69 × 10 ⁻²	3.75 × 10 ⁻⁴	2.82 × 10 ⁻⁴	9.30 × 10 ⁻⁵	25.2	5.25 × 10 ⁻²	2.19 × 10 ⁻³	5.03 × 10 ⁻²
1.12 × 10 ⁻⁵	1.69 × 10 ⁻²	5.00 × 10 ⁻⁴	3.75 × 10 ⁻⁴	1.25 × 10 ⁻⁴	33.5	6.74 × 10 ⁻²	2.94 × 10 ⁻³	6.45 × 10 ⁻²
1.12 × 10 ⁻⁵	1.69 × 10 ⁻²	6.25 × 10 ⁻⁴	4.68 × 10 ⁻⁴	1.57 × 10 ⁻⁴	41.8	8.51 × 10 ⁻²	3.69 × 10 ⁻³	8.14 × 10 ⁻²
1.12 × 10 ⁻⁵	1.69 × 10 ⁻²	7.50 × 10 ⁻⁴	5.61 × 10 ⁻⁴	1.89 × 10 ⁻⁴	50.1	9.86 × 10 ⁻²	4.44 × 10 ⁻³	9.42 × 10 ⁻²



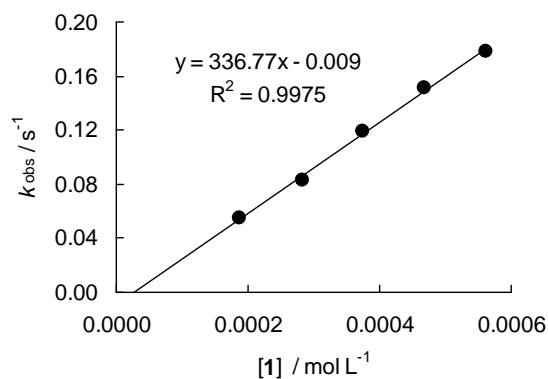
$$k_2(\text{OH}^-)^{[17]} = 23.5 \text{ L mol}^{-1} \text{ s}^{-1}$$

$$\text{p}K_{\text{a}}(\mathbf{1-H})^{[16]} = 11.74$$

$$k_2 = 1.56 \times 10^2 \text{ L mol}^{-1} \text{ s}^{-1}$$

Table 56: Kinetics of the reaction of **1-K** with **3d** (20 °C, Stopped-flow, at 620 nm)

[E] / mol L ⁻¹	[1-H] ₀ / mol L ⁻¹	[KOH] ₀ / mol L ⁻¹	[1-K] _{eff} / mol L ⁻¹	[KOH] _{eff} / mol L ⁻¹	[Nu]/[E]	<i>k</i> _{obs} / s ⁻¹	<i>k</i> _{OH⁻} / s ⁻¹	<i>k</i> _{eff} / s ⁻¹
1.08 × 10 ⁻⁵	1.69 × 10 ⁻²	2.50 × 10 ⁻⁴	1.88 × 10 ⁻⁴	6.20 × 10 ⁻⁵	17.4	5.81 × 10 ⁻²	3.01 × 10 ⁻³	5.51 × 10 ⁻²
1.08 × 10 ⁻⁵	1.69 × 10 ⁻²	3.75 × 10 ⁻⁴	2.82 × 10 ⁻⁴	9.30 × 10 ⁻⁵	26.1	8.75 × 10 ⁻²	4.51 × 10 ⁻³	8.30 × 10 ⁻²
1.08 × 10 ⁻⁵	1.69 × 10 ⁻²	5.00 × 10 ⁻⁴	3.75 × 10 ⁻⁴	1.25 × 10 ⁻⁴	34.7	1.25 × 10 ⁻¹	6.06 × 10 ⁻³	1.19 × 10 ⁻¹
1.08 × 10 ⁻⁵	1.69 × 10 ⁻²	6.25 × 10 ⁻⁴	4.68 × 10 ⁻⁴	1.57 × 10 ⁻⁴	43.3	1.59 × 10 ⁻¹	7.61 × 10 ⁻³	1.51 × 10 ⁻¹
1.08 × 10 ⁻⁵	1.69 × 10 ⁻²	7.50 × 10 ⁻⁴	5.61 × 10 ⁻⁴	1.89 × 10 ⁻⁴	51.9	1.87 × 10 ⁻¹	9.17 × 10 ⁻³	1.78 × 10 ⁻¹



$$k_2(\text{OH}^-)^{[17]} = 48.5 \text{ L mol}^{-1} \text{ s}^{-1}$$

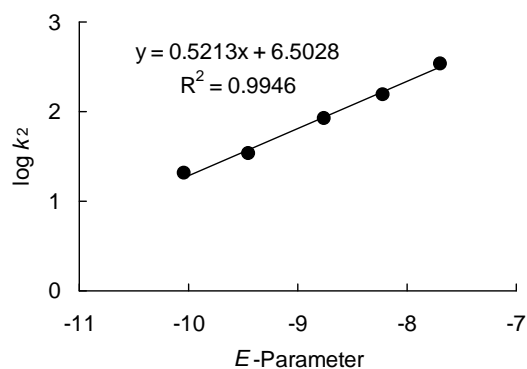
$$\text{p}K_a(\mathbf{1-H})^{[16]} = 11.74$$

$$k_2 = 3.37 \times 10^2 \text{ L mol}^{-1} \text{ s}^{-1}$$

Determination of Reactivity Parameters *N* and *s* for the anion of 2-pyridone (**1**) in Water

Table 57: Rate Constants for the reactions of **1-K** with different electrophiles (20 °C)

Electrophile	<i>E</i>	<i>k</i> ₂ / L mol ⁻¹ s ⁻¹	log <i>k</i> ₂
lil ₂ CH ⁺ (3h)	-10.04	2.04 × 10 ¹	1.31
jul ₂ CH ⁺ (3g)	-9.45	3.42 × 10 ¹	1.53
ind ₂ CH ⁺ (3f)	-8.76	8.50 × 10 ¹	1.93
thq ₂ CH ⁺ (3e)	-8.22	1.56 × 10 ²	2.19
pyr ₂ CH ⁺ (3d)	-7.69	3.37 × 10 ²	2.53

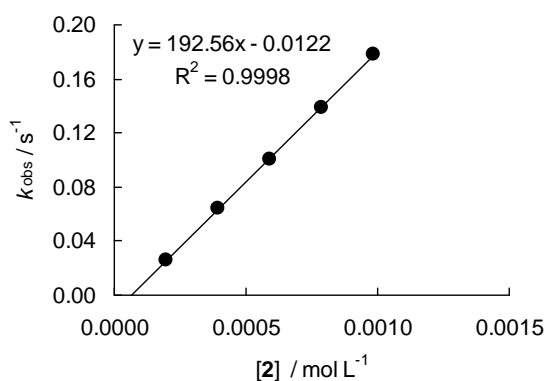


$$N = 12.47, s = 0.52$$

5.6 Reactions of the Potassium Salt of 4-Pyridone (2-K) in Water

Table 58: Kinetics of the reaction of 2-K with 3h (20 °C, Conventional UV/Vis, at 630 nm)

[E] / mol L ⁻¹	[2-H] ₀ / mol L ⁻¹	[KOH] ₀ / mol L ⁻¹	[2-K] _{eff} / mol L ⁻¹	[KOH] _{eff} / mol L ⁻¹	[Nu]/[E]	k _{obs} / s ⁻¹	k _{OH⁻} / s ⁻¹	k _{eff} / s ⁻¹
1.84 × 10 ⁻⁵	1.10 × 10 ⁻²	2.22 × 10 ⁻⁴	1.98 × 10 ⁻⁴	2.40 × 10 ⁻⁵	10.8	2.63 × 10 ⁻²	5.18 × 10 ⁻⁵	2.62 × 10 ⁻²
1.84 × 10 ⁻⁵	1.10 × 10 ⁻²	4.44 × 10 ⁻⁴	3.95 × 10 ⁻⁴	4.90 × 10 ⁻⁵	21.5	6.44 × 10 ⁻²	1.06 × 10 ⁻⁴	6.43 × 10 ⁻²
1.84 × 10 ⁻⁵	1.10 × 10 ⁻²	6.67 × 10 ⁻⁴	5.92 × 10 ⁻⁴	7.50 × 10 ⁻⁵	32.2	1.01 × 10 ⁻¹	1.62 × 10 ⁻⁴	1.01 × 10 ⁻¹
1.84 × 10 ⁻⁵	1.10 × 10 ⁻²	8.89 × 10 ⁻⁴	7.87 × 10 ⁻⁴	1.02 × 10 ⁻⁴	42.8	1.39 × 10 ⁻¹	2.20 × 10 ⁻⁴	1.39 × 10 ⁻¹
1.84 × 10 ⁻⁵	1.10 × 10 ⁻²	1.11 × 10 ⁻³	9.82 × 10 ⁻⁴	1.28 × 10 ⁻⁴	53.4	1.78 × 10 ⁻¹	2.76 × 10 ⁻⁴	1.78 × 10 ⁻¹



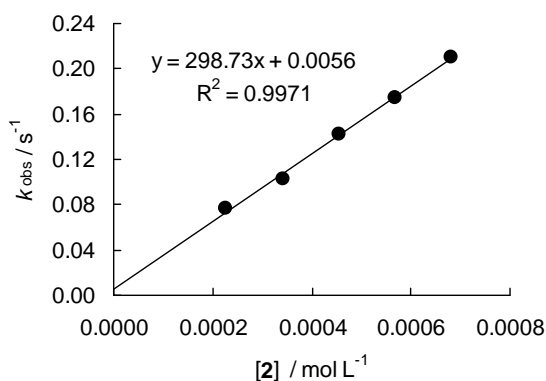
$$k_2(\text{OH}^-)^{[17]} = 2.16 \text{ L mol}^{-1} \text{ s}^{-1}$$

$$\text{p}K_{\text{a}}(\text{2-H})^{[16]} = 11.12$$

$$k_2 = 1.93 \times 10^2 \text{ L mol}^{-1} \text{ s}^{-1}$$

Table 59: Kinetics of the reaction of 2-K with 3g (20 °C, Stopped-Flow, at 635 nm)

[E] / mol L ⁻¹	[2-H] ₀ / mol L ⁻¹	[KOH] ₀ / mol L ⁻¹	[2-K] _{eff} / mol L ⁻¹	[KOH] _{eff} / mol L ⁻¹	[Nu]/[E]	k _{obs} / s ⁻¹	k _{OH⁻} / s ⁻¹	k _{eff} / s ⁻¹
1.17 × 10 ⁻⁵	1.35 × 10 ⁻²	2.50 × 10 ⁻⁴	2.27 × 10 ⁻⁴	2.30 × 10 ⁻⁵	19.4	7.67 × 10 ⁻²	7.91 × 10 ⁻⁵	7.66 × 10 ⁻²
1.17 × 10 ⁻⁵	1.35 × 10 ⁻²	3.75 × 10 ⁻⁴	3.41 × 10 ⁻⁴	3.40 × 10 ⁻⁵	29.1	1.03 × 10 ⁻¹	1.17 × 10 ⁻⁴	1.03 × 10 ⁻¹
1.17 × 10 ⁻⁵	1.35 × 10 ⁻²	5.00 × 10 ⁻⁴	4.54 × 10 ⁻⁴	4.60 × 10 ⁻⁵	38.8	1.42 × 10 ⁻¹	1.58 × 10 ⁻⁴	1.42 × 10 ⁻¹
1.17 × 10 ⁻⁵	1.35 × 10 ⁻²	6.25 × 10 ⁻⁴	5.67 × 10 ⁻⁴	5.80 × 10 ⁻⁵	48.5	1.75 × 10 ⁻¹	2.00 × 10 ⁻⁴	1.75 × 10 ⁻¹
1.17 × 10 ⁻⁵	1.35 × 10 ⁻²	7.50 × 10 ⁻⁴	6.80 × 10 ⁻⁴	7.00 × 10 ⁻⁵	58.1	2.10 × 10 ⁻¹	2.41 × 10 ⁻⁴	2.10 × 10 ⁻¹



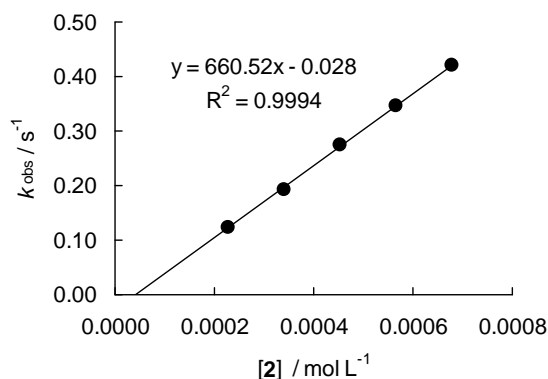
$$k_2(\text{OH}^-)^{[17]} = 3.44 \text{ L mol}^{-1} \text{ s}^{-1}$$

$$\text{p}K_{\text{a}}(\text{2-H})^{[16]} = 11.12$$

$$k_2 = 2.99 \times 10^2 \text{ L mol}^{-1} \text{ s}^{-1}$$

Table 60: Kinetics of the reaction of **2-K** with **3f** (20 °C, Stopped-Flow, at 627 nm)

[E] / mol L ⁻¹	[2-H] ₀ / mol L ⁻¹	[KOH] ₀ / mol L ⁻¹	[2-K] _{eff} / mol L ⁻¹	[KOH] _{eff} / mol L ⁻¹	[Nu]/[E]	<i>k</i> _{obs} / s ⁻¹	<i>k</i> _{OH⁻} / s ⁻¹	<i>k</i> _{eff} / s ⁻¹
9.34 × 10 ⁻⁶	1.35 × 10 ⁻²	2.50 × 10 ⁻⁴	2.27 × 10 ⁻⁴	2.30 × 10 ⁻⁵	24.3	1.24 × 10 ⁻¹	2.48 × 10 ⁻⁴	1.24 × 10 ⁻¹
9.34 × 10 ⁻⁶	1.35 × 10 ⁻²	3.75 × 10 ⁻⁴	3.41 × 10 ⁻⁴	3.40 × 10 ⁻⁵	36.5	1.93 × 10 ⁻¹	3.67 × 10 ⁻⁴	1.93 × 10 ⁻¹
9.34 × 10 ⁻⁶	1.35 × 10 ⁻²	5.00 × 10 ⁻⁴	4.54 × 10 ⁻⁴	4.60 × 10 ⁻⁵	48.6	2.75 × 10 ⁻¹	4.97 × 10 ⁻⁴	2.75 × 10 ⁻¹
9.34 × 10 ⁻⁶	1.35 × 10 ⁻²	6.25 × 10 ⁻⁴	5.67 × 10 ⁻⁴	5.80 × 10 ⁻⁵	60.7	3.48 × 10 ⁻¹	6.26 × 10 ⁻⁴	3.47 × 10 ⁻¹
9.34 × 10 ⁻⁶	1.35 × 10 ⁻²	7.50 × 10 ⁻⁴	6.80 × 10 ⁻⁴	7.00 × 10 ⁻⁵	72.8	4.21 × 10 ⁻¹	7.56 × 10 ⁻⁴	4.20 × 10 ⁻¹



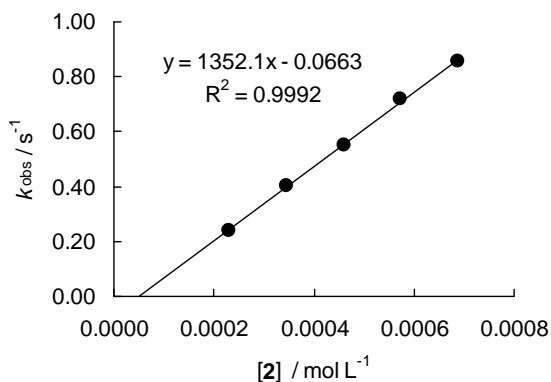
$$k_2(\text{OH}^-)^{[17]} = 10.8 \text{ L mol}^{-1} \text{ s}^{-1}$$

$$\text{p}K_a(\mathbf{2-H})^{[16]} = 11.12$$

$$k_2 = 6.61 \times 10^2 \text{ L mol}^{-1} \text{ s}^{-1}$$

Table 61: Kinetics of the reaction of **2-K** with **3e** (20 °C, Stopped-flow, at 618 nm)

[E] / mol L ⁻¹	[2-H] ₀ / mol L ⁻¹	[KOH] ₀ / mol L ⁻¹	[2-K] _{eff} / mol L ⁻¹	[KOH] _{eff} / mol L ⁻¹	[Nu]/[E]	<i>k</i> _{obs} / s ⁻¹	<i>k</i> _{OH⁻} / s ⁻¹	<i>k</i> _{eff} / s ⁻¹
1.12 × 10 ⁻⁵	1.51 × 10 ⁻²	2.50 × 10 ⁻⁴	2.30 × 10 ⁻⁴	2.00 × 10 ⁻⁵	20.5	2.40 × 10 ⁻¹	4.70 × 10 ⁻⁴	2.40 × 10 ⁻¹
1.12 × 10 ⁻⁵	1.51 × 10 ⁻²	3.75 × 10 ⁻⁴	3.44 × 10 ⁻⁴	3.10 × 10 ⁻⁵	30.7	4.05 × 10 ⁻¹	7.29 × 10 ⁻⁴	4.04 × 10 ⁻¹
1.12 × 10 ⁻⁵	1.51 × 10 ⁻²	5.00 × 10 ⁻⁴	4.59 × 10 ⁻⁴	4.10 × 10 ⁻⁵	41.0	5.53 × 10 ⁻¹	9.64 × 10 ⁻⁴	5.52 × 10 ⁻¹
1.12 × 10 ⁻⁵	1.51 × 10 ⁻²	6.25 × 10 ⁻⁴	5.73 × 10 ⁻⁴	5.20 × 10 ⁻⁵	51.2	7.19 × 10 ⁻¹	1.22 × 10 ⁻³	7.18 × 10 ⁻¹
1.12 × 10 ⁻⁵	1.51 × 10 ⁻²	7.50 × 10 ⁻⁴	6.87 × 10 ⁻⁴	6.30 × 10 ⁻⁵	61.3	8.57 × 10 ⁻¹	1.48 × 10 ⁻³	8.56 × 10 ⁻¹



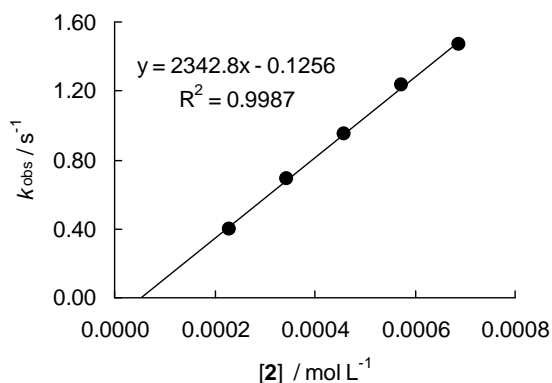
$$k_2(\text{OH}^-)^{[17]} = 23.5 \text{ L mol}^{-1} \text{ s}^{-1}$$

$$\text{p}K_a(\mathbf{2-H})^{[16]} = 11.12$$

$$k_2 = 1.35 \times 10^3 \text{ L mol}^{-1} \text{ s}^{-1}$$

Table 62: Kinetics of the reaction of **2-K** with **3d** (20 °C, Stopped-Flow, at 620 nm)

[E] / mol L ⁻¹	[2-H] ₀ / mol L ⁻¹	[KOH] ₀ / mol L ⁻¹	[2-K] _{eff} / mol L ⁻¹	[KOH] _{eff} / mol L ⁻¹	[Nu]/[E]	<i>k</i> _{obs} / s ⁻¹	<i>k</i> _{OH⁻} / s ⁻¹	<i>k</i> _{eff} / s ⁻¹
1.08 × 10 ⁻⁵	1.51 × 10 ⁻²	2.50 × 10 ⁻⁴	2.30 × 10 ⁻⁴	2.00 × 10 ⁻⁵	21.3	4.03 × 10 ⁻¹	9.70 × 10 ⁻⁴	4.02 × 10 ⁻¹
1.08 × 10 ⁻⁵	1.51 × 10 ⁻²	3.75 × 10 ⁻⁴	3.44 × 10 ⁻⁴	3.10 × 10 ⁻⁵	31.9	6.91 × 10 ⁻¹	1.50 × 10 ⁻³	6.89 × 10 ⁻¹
1.08 × 10 ⁻⁵	1.51 × 10 ⁻²	5.00 × 10 ⁻⁴	4.59 × 10 ⁻⁴	4.10 × 10 ⁻⁵	42.5	9.50 × 10 ⁻¹	1.99 × 10 ⁻³	9.48 × 10 ⁻¹
1.08 × 10 ⁻⁵	1.51 × 10 ⁻²	6.25 × 10 ⁻⁴	5.73 × 10 ⁻⁴	5.20 × 10 ⁻⁵	53.1	1.24 × 10 ⁰	2.52 × 10 ⁻³	1.24 × 10 ⁰
1.08 × 10 ⁻⁵	1.51 × 10 ⁻²	7.50 × 10 ⁻⁴	6.87 × 10 ⁻⁴	6.30 × 10 ⁻⁵	63.6	1.47 × 10 ⁰	3.06 × 10 ⁻³	1.47 × 10 ⁰



$$k_2(\text{OH}^-)^{[17]} = 48.5 \text{ L mol}^{-1} \text{ s}^{-1}$$

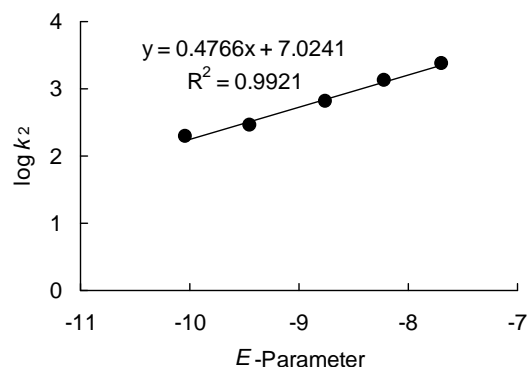
$$\text{p}K_a(\mathbf{2-H})^{[16]} = 11.12$$

$$k_2 = 2.34 \times 10^3 \text{ L mol}^{-1} \text{ s}^{-1}$$

Determination of Reactivity Parameters *N* and *s* for the anion of 4-pyridone (**2**) in Water

Table 63: Rate Constants for the reactions of **2-K** with different electrophiles (20 °C)

Electrophile	<i>E</i>	<i>k</i> ₂ / L mol ⁻¹ s ⁻¹	log <i>k</i> ₂
liI ₂ CH ⁺ (3h)	-10.04	1.93 × 10 ²	2.29
juI ₂ CH ⁺ (3g)	-9.45	2.99 × 10 ²	2.47
ind ₂ CH ⁺ (3f)	-8.76	6.61 × 10 ²	2.82
thq ₂ CH ⁺ (3e)	-8.22	1.35 × 10 ³	3.13
pyr ₂ CH ⁺ (3d)	-7.69	2.34 × 10 ³	3.37



$$N = 14.76, s = 0.48$$

5.7 Determination of Equilibrium Constants in DMSO

5.7.1 Equilibrium Constants for Reactions of the Potassium Salt of 2-Pyridone (1-K)

Table 64: Equilibrium constant for the reaction of **1-K** with **3o** (20 °C, at 521 nm)

No.	[E] ₀ / mol L ⁻¹	[Nu] ₀ / mol L ⁻¹	A ₀	A _{eq}	[E] _{eq} / mol L ⁻¹	[Nu] _{eq} / mol L ⁻¹	[E-Nu] _{eq} / mol L ⁻¹	K / L mol ⁻¹
0	3.65 × 10 ⁻⁵	-	0.724	-	3.65 × 10 ⁻⁵	-	-	-
1	3.61 × 10 ⁻⁵	5.00 × 10 ⁻⁴	0.716	0.685	3.45 × 10 ⁻⁵	4.99 × 10 ⁻⁴	1.54 × 10 ⁻⁶	8.94 × 10 ¹
2	3.58 × 10 ⁻⁵	8.27 × 10 ⁻⁴	0.710	0.656	3.31 × 10 ⁻⁵	8.24 × 10 ⁻⁴	2.72 × 10 ⁻⁶	9.98 × 10 ¹
3	3.55 × 10 ⁻⁵	1.15 × 10 ⁻³	0.705	0.629	3.17 × 10 ⁻⁵	1.15 × 10 ⁻³	3.81 × 10 ⁻⁶	1.05 × 10 ²
4	3.52 × 10 ⁻⁵	1.47 × 10 ⁻³	0.699	0.605	3.05 × 10 ⁻⁵	1.46 × 10 ⁻³	4.74 × 10 ⁻⁶	1.07 × 10 ²
5	3.50 × 10 ⁻⁵	1.78 × 10 ⁻³	0.694	0.582	2.93 × 10 ⁻⁵	1.77 × 10 ⁻³	5.64 × 10 ⁻⁶	1.08 × 10 ²
6	3.47 × 10 ⁻⁵	2.09 × 10 ⁻³	0.689	0.560	2.82 × 10 ⁻⁵	2.08 × 10 ⁻³	6.48 × 10 ⁻⁶	1.11 × 10 ²
7	3.44 × 10 ⁻⁵	2.39 × 10 ⁻³	0.684	0.543	2.74 × 10 ⁻⁵	2.38 × 10 ⁻³	7.08 × 10 ⁻⁶	1.09 × 10 ²
0	4.19 × 10 ⁻⁵	-	0.824	-	4.19 × 10 ⁻⁵	-	-	-
1	4.10 × 10 ⁻⁵	9.47 × 10 ⁻⁴	0.806	0.757	3.85 × 10 ⁻⁵	9.45 × 10 ⁻⁴	2.48 × 10 ⁻⁶	(6.81 × 10 ¹)
2	4.01 × 10 ⁻⁵	1.85 × 10 ⁻³	0.788	0.675	3.43 × 10 ⁻⁵	1.84 × 10 ⁻³	5.76 × 10 ⁻⁶	9.08 × 10 ¹
3	3.92 × 10 ⁻⁵	2.72 × 10 ⁻³	0.772	0.612	3.11 × 10 ⁻⁵	2.71 × 10 ⁻³	8.11 × 10 ⁻⁶	9.61 × 10 ¹
4	3.84 × 10 ⁻⁵	3.55 × 10 ⁻³	0.755	0.561	2.85 × 10 ⁻⁵	3.54 × 10 ⁻³	9.89 × 10 ⁻⁶	9.79 × 10 ¹
5	3.76 × 10 ⁻⁵	4.35 × 10 ⁻³	0.740	0.520	2.64 × 10 ⁻⁵	4.34 × 10 ⁻³	1.12 × 10 ⁻⁵	9.75 × 10 ¹
6	3.69 × 10 ⁻⁵	5.12 × 10 ⁻³	0.725	0.485	2.47 × 10 ⁻⁵	5.10 × 10 ⁻³	1.22 × 10 ⁻⁵	9.71 × 10 ¹
7	3.62 × 10 ⁻⁵	5.85 × 10 ⁻³	0.711	0.455	2.31 × 10 ⁻⁵	5.84 × 10 ⁻³	1.30 × 10 ⁻⁵	9.64 × 10 ¹
8	3.55 × 10 ⁻⁵	6.56 × 10 ⁻³	0.697	0.430	2.19 × 10 ⁻⁵	6.55 × 10 ⁻³	1.36 × 10 ⁻⁵	9.50 × 10 ¹
9	3.48 × 10 ⁻⁵	7.24 × 10 ⁻³	0.684	0.407	2.07 × 10 ⁻⁵	7.23 × 10 ⁻³	1.41 × 10 ⁻⁵	9.43 × 10 ¹
10	3.42 × 10 ⁻⁵	7.90 × 10 ⁻³	0.672	0.387	1.97 × 10 ⁻⁵	7.88 × 10 ⁻³	1.45 × 10 ⁻⁵	9.33 × 10 ¹

Data in parenthesis were not used for the calculation of equilibrium constants.

$$\underline{K = (9.91 \pm 0.66) \times 10^1 \text{ L mol}^{-1}}$$

Table 65: Equilibrium constant for the reaction of **1-K** with **3n** (20 °C, at 533 nm)

No.	[E] ₀ / mol L ⁻¹	[Nu] ₀ / mol L ⁻¹	A ₀	A _{eq}	[E] _{eq} / mol L ⁻¹	[Nu] _{eq} / mol L ⁻¹	[E-Nu] _{eq} / mol L ⁻¹	K / L mol ⁻¹
0	4.47 × 10 ⁻⁵	-	0.748	-	4.47 × 10 ⁻⁵	-	-	-
1	4.39 × 10 ⁻⁵	1.05 × 10 ⁻³	0.734	0.515	3.08 × 10 ⁻⁵	1.04 × 10 ⁻³	1.31 × 10 ⁻⁵	4.08 × 10 ²
2	4.31 × 10 ⁻⁵	2.07 × 10 ⁻³	0.720	0.399	2.39 × 10 ⁻⁵	2.05 × 10 ⁻³	1.92 × 10 ⁻⁵	3.93 × 10 ²
3	4.23 × 10 ⁻⁵	3.05 × 10 ⁻³	0.707	0.330	1.97 × 10 ⁻⁵	3.02 × 10 ⁻³	2.25 × 10 ⁻⁵	3.78 × 10 ²
4	4.15 × 10 ⁻⁵	3.99 × 10 ⁻³	0.694	0.284	1.70 × 10 ⁻⁵	3.96 × 10 ⁻³	2.45 × 10 ⁻⁵	3.64 × 10 ²
5	4.08 × 10 ⁻⁵	4.90 × 10 ⁻³	0.682	0.251	1.50 × 10 ⁻⁵	4.87 × 10 ⁻³	2.58 × 10 ⁻⁵	3.52 × 10 ²
6	4.01 × 10 ⁻⁵	5.78 × 10 ⁻³	0.670	0.226	1.35 × 10 ⁻⁵	5.75 × 10 ⁻³	2.66 × 10 ⁻⁵	3.42 × 10 ²
7	3.94 × 10 ⁻⁵	6.62 × 10 ⁻³	0.659	0.206	1.23 × 10 ⁻⁵	6.60 × 10 ⁻³	2.71 × 10 ⁻⁵	3.33 × 10 ²
8	3.87 × 10 ⁻⁵	7.44 × 10 ⁻³	0.648	0.190	1.14 × 10 ⁻⁵	7.41 × 10 ⁻³	2.74 × 10 ⁻⁵	3.25 × 10 ²
9	3.81 × 10 ⁻⁵	8.23 × 10 ⁻³	0.637	0.177	1.06 × 10 ⁻⁵	8.21 × 10 ⁻³	2.75 × 10 ⁻⁵	3.17 × 10 ²
0	4.47 × 10 ⁻⁵	-	0.756	-	4.47 × 10 ⁻⁵	-	-	-
1	4.39 × 10 ⁻⁵	1.54 × 10 ⁻³	0.736	0.459	2.72 × 10 ⁻⁵	1.53 × 10 ⁻³	1.67 × 10 ⁻⁵	4.03 × 10 ²
2	4.31 × 10 ⁻⁵	3.03 × 10 ⁻³	0.716	0.339	2.01 × 10 ⁻⁵	3.01 × 10 ⁻³	2.30 × 10 ⁻⁵	3.81 × 10 ²
3	4.23 × 10 ⁻⁵	4.46 × 10 ⁻³	0.698	0.273	1.62 × 10 ⁻⁵	4.44 × 10 ⁻³	2.61 × 10 ⁻⁵	3.64 × 10 ²
4	4.15 × 10 ⁻⁵	5.85 × 10 ⁻³	0.680	0.231	1.37 × 10 ⁻⁵	5.82 × 10 ⁻³	2.78 × 10 ⁻⁵	3.50 × 10 ²
5	4.08 × 10 ⁻⁵	7.18 × 10 ⁻³	0.664	0.202	1.20 × 10 ⁻⁵	7.15 × 10 ⁻³	2.88 × 10 ⁻⁵	3.37 × 10 ²
6	4.01 × 10 ⁻⁵	8.46 × 10 ⁻³	0.648	0.181	1.07 × 10 ⁻⁵	8.43 × 10 ⁻³	2.94 × 10 ⁻⁵	3.25 × 10 ²
7	3.94 × 10 ⁻⁵	9.71 × 10 ⁻³	0.633	0.164	9.70 × 10 ⁻⁶	9.68 × 10 ⁻³	2.97 × 10 ⁻⁵	3.16 × 10 ²

$$K = (3.56 \pm 0.30) \times 10^2 \text{ L mol}^{-1}$$

Table 66: Equilibrium constant for the reaction of **1-K** with **3m** (20 °C, at 393 nm)

No.	[E] ₀ / mol L ⁻¹	[Nu] ₀ / mol L ⁻¹	A ₀	A _{eq}	[E] _{eq} / mol L ⁻¹	[Nu] _{eq} / mol L ⁻¹	[E-Nu] _{eq} / mol L ⁻¹	K / L mol ⁻¹
0	4.19 × 10 ⁻⁵	-	0.844	-	4.19 × 10 ⁻⁵	-	-	-
1	4.17 × 10 ⁻⁵	1.11 × 10 ⁻⁴	0.840	0.527	2.62 × 10 ⁻⁵	9.55 × 10 ⁻⁴	1.55 × 10 ⁻⁵	6.22 × 10 ³
2	4.15 × 10 ⁻⁵	2.21 × 10 ⁻⁴	0.836	0.370	1.84 × 10 ⁻⁵	1.98 × 10 ⁻⁴	2.21 × 10 ⁻⁵	6.36 × 10 ³
3	4.13 × 10 ⁻⁵	3.30 × 10 ⁻⁴	0.832	0.285	1.42 × 10 ⁻⁵	3.03 × 10 ⁻⁴	2.72 × 10 ⁻⁵	6.34 × 10 ³
4	4.11 × 10 ⁻⁵	4.38 × 10 ⁻⁴	0.828	0.232	1.15 × 10 ⁻⁵	4.08 × 10 ⁻⁴	2.96 × 10 ⁻⁵	6.29 × 10 ³
5	4.09 × 10 ⁻⁵	5.45 × 10 ⁻⁴	0.824	0.197	9.78 × 10 ⁻⁶	5.13 × 10 ⁻⁴	3.11 × 10 ⁻⁵	6.20 × 10 ³
6	4.07 × 10 ⁻⁵	6.50 × 10 ⁻⁴	0.820	0.173	8.59 × 10 ⁻⁶	6.18 × 10 ⁻⁴	3.21 × 10 ⁻⁵	6.05 × 10 ³
7	4.05 × 10 ⁻⁵	7.55 × 10 ⁻⁴	0.816	0.156	7.75 × 10 ⁻⁶	7.22 × 10 ⁻⁴	3.28 × 10 ⁻⁵	5.86 × 10 ³
8	4.03 × 10 ⁻⁵	8.59 × 10 ⁻⁴	0.812	0.143	7.10 × 10 ⁻⁶	8.26 × 10 ⁻⁴	3.32 × 10 ⁻⁵	5.67 × 10 ³

Table 66: Continued

No.	[E] ₀ / mol L ⁻¹	[Nu] ₀ / mol L ⁻¹	A ₀	A _{eq}	[E] _{eq} / mol L ⁻¹	[Nu] _{eq} / mol L ⁻¹	[E-Nu] _{eq} / mol L ⁻¹	K / L mol ⁻¹
0	4.60 × 10 ⁻⁵	-	0.849	-	4.60 × 10 ⁻⁵	-	-	-
1	4.56 × 10 ⁻⁵	1.18 × 10 ⁻⁴	0.842	0.517	2.80 × 10 ⁻⁵	1.00 × 10 ⁻⁴	1.76 × 10 ⁻⁵	6.27 × 10 ³
2	4.52 × 10 ⁻⁵	2.33 × 10 ⁻⁴	0.834	0.358	1.94 × 10 ⁻⁵	2.07 × 10 ⁻⁴	2.58 × 10 ⁻⁵	6.41 × 10 ³
3	4.48 × 10 ⁻⁵	3.47 × 10 ⁻⁴	0.827	0.274	1.48 × 10 ⁻⁵	3.17 × 10 ⁻⁴	3.00 × 10 ⁻⁵	6.37 × 10 ³
4	4.44 × 10 ⁻⁵	4.59 × 10 ⁻⁴	0.820	0.222	1.20 × 10 ⁻⁵	4.26 × 10 ⁻⁴	3.24 × 10 ⁻⁵	6.32 × 10 ³
5	4.39 × 10 ⁻⁵	6.22 × 10 ⁻⁴	0.809	0.173	9.37 × 10 ⁻⁶	5.88 × 10 ⁻⁴	3.45 × 10 ⁻⁵	6.26 × 10 ³
6	4.33 × 10 ⁻⁵	7.82 × 10 ⁻⁴	0.799	0.144	7.80 × 10 ⁻⁶	7.47 × 10 ⁻⁴	3.55 × 10 ⁻⁵	6.09 × 10 ³
7	4.28 × 10 ⁻⁵	9.38 × 10 ⁻⁴	0.789	0.125	6.77 × 10 ⁻⁶	9.02 × 10 ⁻⁴	3.60 × 10 ⁻⁵	5.89 × 10 ³
8	4.23 × 10 ⁻⁵	1.09 × 10 ⁻³	0.780	0.111	6.01 × 10 ⁻⁶	1.05 × 10 ⁻³	3.62 × 10 ⁻⁵	5.72 × 10 ³

$$K = (6.15 \pm 0.24) \times 10^3 \text{ L mol}^{-1}$$

Table 67: Equilibrium constant for the reaction of **1-K** with **3I** (20 °C, at 371 nm)

No.	[E] ₀ / mol L ⁻¹	[Nu] ₀ / mol L ⁻¹	A ₀	A _{eq}	[E] _{eq} / mol L ⁻¹	[Nu] _{eq} / mol L ⁻¹	[E-Nu] _{eq} / mol L ⁻¹	K / L mol ⁻¹
0	3.89 × 10 ⁻⁵	-	0.725	-	3.89 × 10 ⁻⁵	-	-	-
1	3.87 × 10 ⁻⁵	1.02 × 10 ⁻⁴	0.722	0.329	1.76 × 10 ⁻⁵	8.05 × 10 ⁻⁵	2.11 × 10 ⁻⁵	1.48 × 10 ⁴
2	3.85 × 10 ⁻⁵	2.02 × 10 ⁻⁴	0.719	0.199	1.07 × 10 ⁻⁵	1.74 × 10 ⁻⁴	2.79 × 10 ⁻⁵	1.50 × 10 ⁴
3	3.84 × 10 ⁻⁵	3.02 × 10 ⁻⁴	0.715	0.146	7.83 × 10 ⁻⁶	2.72 × 10 ⁻⁴	3.05 × 10 ⁻⁵	1.44 × 10 ⁴
4	3.82 × 10 ⁻⁵	4.01 × 10 ⁻⁴	0.712	0.116	6.22 × 10 ⁻⁶	3.69 × 10 ⁻⁴	3.20 × 10 ⁻⁵	1.39 × 10 ⁴
5	3.80 × 10 ⁻⁵	4.99 × 10 ⁻⁴	0.709	0.098	5.26 × 10 ⁻⁶	4.66 × 10 ⁻⁴	3.28 × 10 ⁻⁵	1.34 × 10 ⁴
6	3.79 × 10 ⁻⁵	5.96 × 10 ⁻⁴	0.706	0.086	4.61 × 10 ⁻⁶	5.63 × 10 ⁻⁴	3.33 × 10 ⁻⁵	1.28 × 10 ⁴
0	3.89 × 10 ⁻⁵	-	0.680	-	3.89 × 10 ⁻⁵	-	-	-
1	3.85 × 10 ⁻⁵	1.18 × 10 ⁻⁴	0.674	0.278	1.59 × 10 ⁻⁵	9.50 × 10 ⁻⁵	2.26 × 10 ⁻⁵	1.50 × 10 ⁴
2	3.82 × 10 ⁻⁵	2.33 × 10 ⁻⁴	0.668	0.166	9.49 × 10 ⁻⁶	2.05 × 10 ⁻⁴	2.87 × 10 ⁻⁵	1.48 × 10 ⁴
3	3.79 × 10 ⁻⁵	3.47 × 10 ⁻⁴	0.662	0.122	6.98 × 10 ⁻⁶	3.16 × 10 ⁻⁴	3.09 × 10 ⁻⁵	1.40 × 10 ⁴
4	3.76 × 10 ⁻⁵	4.59 × 10 ⁻⁴	0.657	0.098	5.60 × 10 ⁻⁶	4.27 × 10 ⁻⁴	3.20 × 10 ⁻⁵	1.34 × 10 ⁴
5	3.71 × 10 ⁻⁵	6.22 × 10 ⁻⁴	0.648	0.078	4.46 × 10 ⁻⁶	5.90 × 10 ⁻⁴	3.26 × 10 ⁻⁵	1.24 × 10 ⁴

$$K = (1.40 \pm 0.09) \times 10^4 \text{ L mol}^{-1}$$

5.7.2 Equilibrium Constants for Reactions of the Potassium Salt of 4-Pyridone (2-K)

Table 68: Equilibrium constant for the reaction of 2-K with 3k (20 °C, at 374 nm)

No.	[E] ₀ / mol L ⁻¹	[Nu] ₀ / mol L ⁻¹	A ₀	A _{eq}	[E] _{eq} / mol L ⁻¹	[Nu] _{eq} / mol L ⁻¹	[E-Nu] _{eq} / mol L ⁻¹	K / L mol ⁻¹
0	3.86 × 10 ⁻⁵	-	0.667	-	3.86 × 10 ⁻⁵	-	-	-
1	3.84 × 10 ⁻⁵	2.55 × 10 ⁻⁴	0.664	0.501	2.90 × 10 ⁻⁵	2.45 × 10 ⁻⁴	9.43 × 10 ⁻⁶	1.33 × 10 ³
2	3.82 × 10 ⁻⁵	5.07 × 10 ⁻⁴	0.661	0.402	2.32 × 10 ⁻⁵	4.92 × 10 ⁻⁴	1.50 × 10 ⁻⁵	1.31 × 10 ³
3	3.81 × 10 ⁻⁵	7.57 × 10 ⁻⁴	0.658	0.341	1.97 × 10 ⁻⁵	7.39 × 10 ⁻⁴	1.83 × 10 ⁻⁵	1.26 × 10 ³
4	3.79 × 10 ⁻⁵	1.01 × 10 ⁻³	0.655	0.301	1.74 × 10 ⁻⁵	9.85 × 10 ⁻⁴	2.05 × 10 ⁻⁵	1.20 × 10 ³

$$K = (1.27 \pm 0.06) \times 10^3 \text{ L mol}^{-1}$$

Table 69: Equilibrium constant for the reaction of 2-K with 3l (20 °C, at 371 nm)

No.	[E] ₀ / mol L ⁻¹	[Nu] ₀ / mol L ⁻¹	A ₀	A _{eq}	[E] _{eq} / mol L ⁻¹	[Nu] _{eq} / mol L ⁻¹	[E-Nu] _{eq} / mol L ⁻¹	K / L mol ⁻¹
0	3.51 × 10 ⁻⁵	-	0.662	-	3.51 × 10 ⁻⁵	-	-	-
1	3.47 × 10 ⁻⁵	1.42 × 10 ⁻³	0.654	0.580	3.07 × 10 ⁻⁵	1.41 × 10 ⁻³	3.91 × 10 ⁻⁶	9.01 × 10 ¹
2	3.42 × 10 ⁻⁵	2.80 × 10 ⁻³	0.646	0.521	2.76 × 10 ⁻⁵	2.79 × 10 ⁻³	6.61 × 10 ⁻⁶	8.58 × 10 ¹
3	3.38 × 10 ⁻⁵	4.15 × 10 ⁻³	0.638	0.473	2.51 × 10 ⁻⁵	4.14 × 10 ⁻³	8.74 × 10 ⁻⁶	8.43 × 10 ¹
4	3.34 × 10 ⁻⁵	5.46 × 10 ⁻³	0.630	0.432	2.29 × 10 ⁻⁵	5.45 × 10 ⁻³	1.05 × 10 ⁻⁵	8.42 × 10 ¹
5	3.29 × 10 ⁻⁵	7.17 × 10 ⁻³	0.620	0.391	2.07 × 10 ⁻⁵	7.15 × 10 ⁻³	1.22 × 10 ⁻⁵	8.20 × 10 ¹
6	3.24 × 10 ⁻⁵	8.82 × 10 ⁻³	0.611	0.356	1.89 × 10 ⁻⁵	8.81 × 10 ⁻³	1.35 × 10 ⁻⁵	8.13 × 10 ¹
7	3.19 × 10 ⁻⁵	1.04 × 10 ⁻²	0.601	0.332	1.76 × 10 ⁻⁵	1.04 × 10 ⁻²	1.43 × 10 ⁻⁵	7.80 × 10 ¹
8	3.14 × 10 ⁻⁵	1.20 × 10 ⁻²	0.592	0.308	1.63 × 10 ⁻⁵	1.20 × 10 ⁻²	1.51 × 10 ⁻⁵	7.72 × 10 ¹

No.	[E] ₀ / mol L ⁻¹	[Nu] ₀ / mol L ⁻¹	A ₀	A _{eq}	[E] _{eq} / mol L ⁻¹	[Nu] _{eq} / mol L ⁻¹	[E-Nu] _{eq} / mol L ⁻¹	K
0	3.37 × 10 ⁻⁵	-	0.629	-	3.37 × 10 ⁻⁵	-	-	-
1	3.31 × 10 ⁻⁵	2.38 × 10 ⁻³	0.619	0.512	2.74 × 10 ⁻⁵	2.73 × 10 ⁻³	5.73 × 10 ⁻⁶	8.83 × 10 ¹
2	3.26 × 10 ⁻⁵	4.68 × 10 ⁻³	0.610	0.434	2.32 × 10 ⁻⁵	4.67 × 10 ⁻³	9.40 × 10 ⁻⁶	8.66 × 10 ¹
3	3.21 × 10 ⁻⁵	6.91 × 10 ⁻³	0.600	0.380	2.03 × 10 ⁻⁵	6.90 × 10 ⁻³	1.18 × 10 ⁻⁵	8.40 × 10 ¹
4	3.17 × 10 ⁻⁵	9.07 × 10 ⁻³	0.591	0.340	1.82 × 10 ⁻⁵	9.06 × 10 ⁻³	1.35 × 10 ⁻⁵	8.16 × 10 ¹
5	3.11 × 10 ⁻⁵	1.17 × 10 ⁻²	0.580	0.301	1.61 × 10 ⁻⁵	1.17 × 10 ⁻²	1.50 × 10 ⁻⁵	7.95 × 10 ¹
6	3.05 × 10 ⁻⁵	1.42 × 10 ⁻²	0.570	0.271	1.45 × 10 ⁻⁵	1.42 × 10 ⁻²	1.60 × 10 ⁻⁵	7.77 × 10 ¹
7	3.00 × 10 ⁻⁵	1.66 × 10 ⁻²	0.560	0.249	1.33 × 10 ⁻⁵	1.66 × 10 ⁻²	1.66 × 10 ⁻⁵	7.51 × 10 ¹
8	2.94 × 10 ⁻⁵	1.90 × 10 ⁻²	0.550	0.231	1.24 × 10 ⁻⁵	1.90 × 10 ⁻²	1.71 × 10 ⁻⁵	7.28 × 10 ¹

$$K = (8.18 \pm 0.49) \times 10^1 \text{ L mol}^{-1}$$

Table 70: Equilibrium constant for the reaction of **2-K** with **3m** (20 °C, at 393 nm)

No.	[E] ₀ / mol L ⁻¹	[Nu] ₀ / mol L ⁻¹	A ₀	A _{eq}	[E] _{eq} / mol L ⁻¹	[Nu] _{eq} / mol L ⁻¹	[E-Nu] _{eq} / mol L ⁻¹	K / L mol ⁻¹
0	2.99 × 10 ⁻⁵	-	0.549	-	2.99 × 10 ⁻⁵	-	-	-
1	2.94 × 10 ⁻⁵	1.83 × 10 ⁻³	0.540	0.501	2.73 × 10 ⁻⁵	1.83 × 10 ⁻³	2.13 × 10 ⁻⁶	4.27 × 10 ¹
2	2.90 × 10 ⁻⁵	3.61 × 10 ⁻³	0.532	0.460	2.51 × 10 ⁻⁵	3.60 × 10 ⁻³	3.90 × 10 ⁻⁶	4.32 × 10 ¹
3	2.85 × 10 ⁻⁵	5.33 × 10 ⁻³	0.523	0.427	2.33 × 10 ⁻⁵	5.32 × 10 ⁻³	5.25 × 10 ⁻⁶	4.24 × 10 ¹
4	2.81 × 10 ⁻⁵	6.99 × 10 ⁻³	0.515	0.400	2.18 × 10 ⁻⁵	6.99 × 10 ⁻³	6.28 × 10 ⁻⁶	4.13 × 10 ¹
5	2.75 × 10 ⁻⁵	9.01 × 10 ⁻³	0.506	0.369	2.01 × 10 ⁻⁵	9.00 × 10 ⁻³	7.44 × 10 ⁻⁶	4.11 × 10 ¹
6	2.70 × 10 ⁻⁵	1.09 × 10 ⁻²	0.496	0.344	1.87 × 10 ⁻⁵	1.09 × 10 ⁻²	8.29 × 10 ⁻⁶	4.05 × 10 ¹
7	2.65 × 10 ⁻⁵	1.28 × 10 ⁻²	0.487	0.322	1.75 × 10 ⁻⁵	1.28 × 10 ⁻²	9.00 × 10 ⁻⁶	4.01 × 10 ¹
8	2.61 × 10 ⁻⁵	1.46 × 10 ⁻²	0.479	0.302	1.64 × 10 ⁻⁵	1.46 × 10 ⁻²	9.62 × 10 ⁻⁶	4.00 × 10 ¹
0	3.97 × 10 ⁻⁵	-	0.692	-	3.97 × 10 ⁻⁵	-	-	-
1	3.89 × 10 ⁻⁵	3.01 × 10 ⁻³	0.678	0.592	3.40 × 10 ⁻⁵	3.01 × 10 ⁻³	4.95 × 10 ⁻⁶	4.85 × 10 ¹
2	3.82 × 10 ⁻⁵	5.90 × 10 ⁻³	0.665	0.523	3.00 × 10 ⁻⁵	5.89 × 10 ⁻³	8.14 × 10 ⁻⁶	4.60 × 10 ¹
3	3.74 × 10 ⁻⁵	8.68 × 10 ⁻³	0.652	0.471	2.70 × 10 ⁻⁵	8.67 × 10 ⁻³	1.04 × 10 ⁻⁵	4.44 × 10 ¹
4	3.67 × 10 ⁻⁵	1.14 × 10 ⁻²	0.640	0.426	2.44 × 10 ⁻⁵	1.13 × 10 ⁻³	1.23 × 10 ⁻⁵	4.42 × 10 ¹
5	3.60 × 10 ⁻⁵	1.39 × 10 ⁻²	0.628	0.391	2.24 × 10 ⁻⁵	1.39 × 10 ⁻³	1.36 × 10 ⁻⁵	4.35 × 10 ¹
6	3.54 × 10 ⁻⁵	1.64 × 10 ⁻²	0.617	0.365	2.09 × 10 ⁻⁵	1.64 × 10 ⁻²	1.44 × 10 ⁻⁵	4.20 × 10 ¹
7	3.48 × 10 ⁻⁵	1.88 × 10 ⁻²	0.606	0.340	1.95 × 10 ⁻⁵	1.88 × 10 ⁻²	1.52 × 10 ⁻⁵	4.16 × 10 ¹
8	3.41 × 10 ⁻⁵	2.11 × 10 ⁻²	0.595	0.319	1.83 × 10 ⁻⁵	2.11 × 10 ⁻²	1.58 × 10 ⁻⁵	4.10 × 10 ¹

$$K = (4.27 \pm 0.23) \times 10^1 \text{ L mol}^{-1}$$

Table 71: Equilibrium constant for the reaction of **2-K** with **7a** (20 °C, at 525 nm)

No.	[E] ₀ / mol L ⁻¹	[Nu] ₀ / mol L ⁻¹	A ₀	A _{eq}	[E] _{eq} / mol L ⁻¹	[Nu] _{eq} / mol L ⁻¹	[E-Nu] _{eq} / mol L ⁻¹	K / L mol ⁻¹
0	2.68 × 10 ⁻⁵	-	1.204	-	2.68 × 10 ⁻⁵	-	-	-
1	2.66 × 10 ⁻⁵	3.61 × 10 ⁻⁴	1.198	0.732	1.63 × 10 ⁻⁵	3.51 × 10 ⁻⁴	1.04 × 10 ⁻⁵	1.82 × 10 ³
2	2.65 × 10 ⁻⁵	7.18 × 10 ⁻⁴	1.192	0.516	1.15 × 10 ⁻⁵	7.03 × 10 ⁻⁴	1.50 × 10 ⁻⁵	1.86 × 10 ³
3	2.64 × 10 ⁻⁵	1.07 × 10 ⁻³	1.187	0.401	8.92 × 10 ⁻⁶	1.05 × 10 ⁻³	1.75 × 10 ⁻⁵	1.86 × 10 ³
4	2.63 × 10 ⁻⁵	1.42 × 10 ⁻³	1.181	0.323	7.18 × 10 ⁻⁶	1.40 × 10 ⁻³	1.91 × 10 ⁻⁵	1.89 × 10 ³
5	2.61 × 10 ⁻⁵	1.77 × 10 ⁻³	1.175	0.277	6.16 × 10 ⁻⁶	1.75 × 10 ⁻³	2.00 × 10 ⁻⁵	1.85 × 10 ³
6	2.60 × 10 ⁻⁵	2.11 × 10 ⁻³	1.170	0.239	5.32 × 10 ⁻⁶	2.09 × 10 ⁻³	2.07 × 10 ⁻⁵	1.86 × 10 ³
7	2.59 × 10 ⁻⁵	2.45 × 10 ⁻³	1.164	0.209	4.65 × 10 ⁻⁶	2.43 × 10 ⁻³	2.12 × 10 ⁻⁵	1.88 × 10 ³
8	2.58 × 10 ⁻⁵	2.79 × 10 ⁻³	1.159	0.188	4.18 × 10 ⁻⁶	2.77 × 10 ⁻³	2.16 × 10 ⁻⁵	1.86 × 10 ³

Table 71: Continued

No.	$[E]_0 / \text{mol L}^{-1}$	$[\text{Nu}]_0 / \text{mol L}^{-1}$	A_0	A_{eq}	$[E]_{\text{eq}} / \text{mol L}^{-1}$	$[\text{Nu}]_{\text{eq}} / \text{mol L}^{-1}$	$[E\text{-Nu}]_{\text{eq}} / \text{mol L}^{-1}$	$K / \text{L mol}^{-1}$
0	2.65×10^{-5}	-	1.198	-	2.65×10^{-5}	-	-	-
1	2.64×10^{-5}	5.35×10^{-4}	1.189	0.606	1.34×10^{-5}	5.22×10^{-4}	1.29×10^{-5}	1.84×10^3
2	2.62×10^{-5}	1.06×10^{-3}	1.181	0.404	8.95×10^{-6}	1.05×10^{-3}	1.72×10^{-5}	1.84×10^3
3	2.60×10^{-5}	1.58×10^{-3}	1.172	0.306	6.78×10^{-6}	1.56×10^{-3}	1.92×10^{-5}	1.81×10^3
4	2.58×10^{-5}	2.10×10^{-3}	1.164	0.246	5.45×10^{-6}	2.08×10^{-3}	2.03×10^{-5}	1.80×10^3
5	2.56×10^{-5}	2.60×10^{-3}	1.156	0.207	4.59×10^{-6}	2.58×10^{-3}	2.10×10^{-5}	1.78×10^3
6	2.54×10^{-5}	3.10×10^{-3}	1.148	0.179	3.97×10^{-6}	3.08×10^{-3}	2.15×10^{-5}	1.76×10^3
7	2.53×10^{-5}	3.59×10^{-3}	1.140	0.157	3.48×10^{-6}	3.57×10^{-3}	2.18×10^{-5}	1.75×10^3
8	2.51×10^{-5}	4.08×10^{-3}	1.132	0.141	3.12×10^{-6}	4.05×10^{-3}	2.20×10^{-5}	1.73×10^3
9	2.49×10^{-5}	4.56×10^{-3}	1.124	0.128	2.84×10^{-6}	4.53×10^{-3}	2.21×10^{-5}	1.72×10^3

$$K = (1.82 \pm 0.05) \times 10^3 \text{ L mol}^{-1}$$

5.8 Quantum Chemical Calculations

5.8.1 General

Free energies G_{298} were calculated at MP2/6-311+G(2d,p) or B3LYP/6-31+G(d,p) level of theory. Thermal corrections to 298.15 K have been calculated using unscaled harmonic vibrational frequencies. All calculations were performed with Gaussian 03.^[35]

5.8.2 Archive Entries for Geometry Optimization at MP2/6-311+G(2d,p)

2-Pyridone-Anion

```
1\1\G1 NC-NODE24\F0pt\RMP2-FC\6-311+G(2d,p)\C5H4N101(1-)\MAY04\19-Mar-2010\0\#p opt freq mp2/6-311+g(2d,p)\Pyridon-Anion\1,1\C,-0.507815922,0.3174712691,-0.00033035\C,0.5557416285,1.3019612731,0.0000758494\C,1.8879337699,0.9384730937,0.0003572117\C,2.2306011548,-0.4240841715,0.0002423715\C,1.1721886819,-1.3323685826,-0.0001599317\H,0.2611295773,2.3488173802,0.0001506027\H,2.6622721506,1.7058380009,0.000664958\H,3.2614385647,-0.765713842,0.0004488693\H,1.3968516613,-2.4029447266,-0.0002590387\N,-0.1308382566,-1.0235221694,-0.0004400782\O,-1.7220580103,0.653721475,-0.000637464\Version=AM64L-G03RevD.01\State=1-A\HF=-321.0809963\MP2=-322.2072908\RMSD=7.440e-09\RMSF=9.657e-06\Thermal=0.\Dipole=2.1998222,0.2395337,0.0006167\PG=C01 [X(C5H4N101)]\@
```

N-Methyl-2-Pyridone

```
1\1\G1 NC-NODE25\F0pt\RMP2-FC\6-311+G(2d,p)\C6H7N101\MAY04\20-Mar-2010\0\#p MP2/6-311+g(2d,p) Opt Freq\N-Methyl pyridon\0,1\C,0.4057042647,0.8927231118,-0.0097223337\C,-0.9900639327,1.2563002782,-0.0274225168\C,-1.9878478387,0.3184624305,-0.014843361\C,-1.6747527429,-1.0619878637,0.0164352824\C,-0.3571664832,-1.4274481577,0.0335783167\H,-1.2053292752,2.3184265347,-0.0513445123\H,-3.0257327306,0.6376768849,-0.0290276898\H,-2.4412077624,-1.8257230348,0.0269661245\H,-0.0369310245,-2.4630679501,0.0575976998\N,0.6380935621,-0.4978044423,0.0211569405\O,1.3641266144,1.6723740322,-0.0192033424\C,2.0420860226,-0.897869622,0.0396811555\H,2.5442466637,-0.5103071861,-0.8465886383\H,2.5314640794,-0.4736
```

439197, 0. 916257822\H, 2. 0970315835, -1. 9847230959, 0. 0626750529\\Version=AM64L-G03RevD. 01\State=1-A\HF=-360. 6950389\MP2=-361. 9672936\RMSD=5. 332e-09\RMSF=3. 466e-06\Thermal=0. \Di pol e=-0. 5957751, -1. 4773101, 0. 0267229\PG=C01 [X(C6H7N101)]\@

N-Ethyl-2-Pyridone

1\1\GINC-NODE13\FOpt\RMP2-FC\6-311+G(2d,p)\C7H9N101\MAY04\08-Sep-2010\0\#p opt freq mp2/6-311+g(2d,p)\N-Ethyl-2-pyridon\0,1\C, -0. 7706645612, -1. 092548964, 0. 1624416081\C, -2. 2061822191, -0. 9519756332, 0. 1393549294\C, -2. 8206634165, 0. 2625871743, -0. 0122704131\C, -2. 0511077713, 1. 4433528949, -0. 1442513239\C, -0. 6883892546, 1. 3330613316, -0. 1136135013\H, -2. 7745978039, -1. 8692995531, 0. 2426788149\H, -3. 9051097122, 0. 3180506544, -0. 0292722322\H, -2. 507201174, 2. 417736145, -0. 2609788287\H, -0. 0290499565, 2. 1898509719, -0. 2035088584\N, -0. 0723428211, 0. 1278353743, 0. 0386185201\O, -0. 1486943521, -2. 1546920751, 0. 2771612234\C, 1. 3912166557, 0. 0454089997, 0. 0306257602\C, 1. 9136238081, -0. 3525144101, -1. 3417499248\H, 3. 0037741829, -0. 4164174468, -1. 3234462775\H, 1. 5134386964, -1. 3269810495, -1. 6218337985\H, 1. 6227187453, 0. 3837382222, -2. 0942192441\H, 1. 6746822448, -0. 6967604225, 0. 7772081603\H, 1. 7729917193, 1. 0211795161, 0. 3369039061\\Version=AM64L-G03RevD. 01\State=1-A\HF=-399. 7425449\MP2=-401. 1740124\RMSD=3. 199e-09\RMSF=1. 340e-05\Thermal=0. \Di pol e=-0. 0106398, 1. 5237767, -0. 2324537\PG=C01 [X(C7H9N101)]\@

N-iso-Propyl-2-Pyridone

1\1\GINC-NODE20\FOpt\RMP2-FC\6-311+G(2d,p)\C8H11N101\MAY04\08-Sep-2010\0\#p MP2/6-311+G(2d,p) opt freq\N-iso-Propyl-2-pyridon\0,1\C, -0. 7064654594, -1. 0170065077, 0. 2679255994\C, -2. 1444943698, -0. 9239353899, 0. 3185232149\C, -2. 8151457833, 0. 2354438611, 0. 0340494306\C, -2. 0984952845, 1. 4052699806, -0. 3095218782\C, -0. 7315963018, 1. 3468479594, -0. 3342611252\H, -2. 6680363165, -1. 836659348, 0. 5796534286\H, -3. 9003137435, 0. 2538009506, 0. 0727254421\H, -2. 5962659785, 2. 3370110126, -0. 5450876311\H, -0. 1264534868, 2. 2089281253, -0. 5832844468\N, -0. 0559284657, 0. 2017622933, -0. 0393368294\O, -0. 0483292669, -2. 0448993026, 0. 4669460571\C, 1. 4186504317, 0. 1405235534, -0. 1146498151\C, 1. 8322544693, -0. 3070009587, -1. 511177378\H, 2. 9179769887, -0. 4178316367, -1. 564826364\H, 1. 3735646101, -1. 2669096239, -1. 7518637124\H, 1. 5232877862, 0. 434299967, -2. 2539001081\C, 2. 0768465361, 1. 4484987573, 0. 2973496157\H, 1. 9631358105, 2. 230239793, -0. 4572514152\H, 1. 6809230314, 1. 8130031974, 1. 2476555342\H, 3. 1472284595, 1. 2710670708, 0. 4197173815\H, 1. 6888013732, -0. 6407011543, 0. 5977011693\\Version=AM64L-G03RevD. 01\State=1-A\HF=-438. 785751\MP2=-440. 3797554\RMSD=6. 687e-09\RMSF=2. 027e-05\Thermal=0. \Di pol e=0. 0247395, 1. 4954189, -0. 3629996\PG=C01 [X(C8H11N101)]\@

N-tert-Butyl-2-Pyridone

1\1\GINC-NODE9\FOpt\RMP2-FC\6-311+G(2d,p)\C9H13N101\MAY04\24-Jul-2010\0\#p MP2/6-311+g(2d,p) opt freq\N-Tert-butyl-2-pyridon\0,1\C, 0. 4445232792, 0. 9250113362, -0. 0021139613\C, -0. 9210343962, 1. 3911232793, -0. 0026021764\C, -1. 9969214628, 0. 5480397551, -0. 002574695\C, -1. 7820074969, -0. 8472741564, -0. 0017057753\C, -0. 4958559327, -1. 313813622, -0. 0005979611\H, -1. 0376604666, 2. 4690575806, -0. 0033120205\H, -3. 0054101953, 0. 9507793063, -0. 0031836423\H, -2. 5984758582, -1. 5580160798, -0. 0018215299\H, -0. 2984888532, -2. 3740479203, 0. 0002658805\N, 0. 5947006387, -0. 4883232924, -0. 0003762716\O, 1. 4222255313, 1. 6828901049, -0. 0029896347\C, 1. 9892017157, -1. 0526433033, 0. 000995329\C, 2. 7072885555, -0. 5887189913, 1. 2709792598\H, 3. 7097481635, -1. 0241945722, 1. 2895640698\H, 2. 7911453367, 0. 4948100359, 1. 3069636996\H, 2. 1661954802, -0. 9383356389, 2. 1546972279\C, 2. 7082682663, -0. 5927320927, -1. 2698734005\H, 2. 7922745592, 0. 4906792833, -1. 3090827086\H, 3. 7106457893, -1. 0284700578, -1. 2864771508\H, 2. 1676961865, -0. 9448843522, -2. 1529197405\C, 1. 9683424822, -2. 5802478203, 0. 003506451\H, 1. 4900422285, -2. 9905735804, 0. 8959254389\H, 1. 4916012798, -2. 9935963933, -0. 8883496653\H, 3. 0077118493, -2. 9139807083, 0. 0049529811\\Version=AM64L-G03RevD. 01\State=1-A\HF=-477. 8210652\MP2=-479. 5818994\RMSD=8. 455e-09\RMSF=5. 176e-06\Thermal=0. \Di pol e=-0. 485659, -1. 4006597, 0. 0016584\PG=C01 [X(C9H13N101)]\@

N-Acetyl-2-Pyridone

```

1\1\GI NC-NODE25\F0pt\RMP2-FC\6-311+G(2d, p)\C7H7N1O2\MAY04\24-Jun-2010\
O\#\#p MP2/6-311+g(2d, p) opt=tight freq\N-Acetyl-2-pyridon - Geometrie
1-\0, 1\C, -0. 5133914903, 0. 7639683195, -0. 57851882\C, -1. 9536163318, 0. 62
77209746, -0. 4828828209\C, -2. 5561682521, -0. 4705644437, 0. 0498525861\C, -1
. 7661750927, -1. 5568448486, 0. 5219099657\C, -0. 415527078, -1. 4847849845, 0.
4118014894\H, -2. 5204865813, 1. 4795204457, -0. 8407148439\H, -3. 6390160368,
-0. 5153895597, 0. 1159723187\H, -2. 2141389522, -2. 4416054983, 0. 9553841585\
H, 0. 2565777393, -2. 2666346128, 0. 7384382023\N, 0. 2133957181, -0. 3869142946
, -0. 1487116656\O, 0. 0476763611, 1. 7820360246, -0. 9760680277\C, 1. 663489559
1, -0. 4789903309, -0. 2407946429\O, 2. 2268088617, -1. 3533517719, 0. 381197459
6\C, 2. 3894501968, 0. 4724643798, -1. 1421060036\H, 1. 870459085, 0. 6028885759
, -2. 0904278156\H, 2. 4479343845, 1. 4571225893, -0. 679049751\H, 3. 3876530596
, 0. 0625188157, -1. 2883171789\Versi on=AM64L-G03RevD. 01\State=1-A\HF=-47
3. 4690243\MP2=-475. 082377\RMSD=8. 174e-09\RMSF=8. 470e-08\Thermal =0. \Di p
ol e=-0. 8273705, -0. 5630999, -0. 0310119\PG=C01 [X(C7H7N1O2)]\#@

```

Transition State: Methyl-Transfer N-Methyl-2-Pyridone to 2-Pyridone (N-attack)

```

1\1\GI NC-NODE10\FTS\RMP2-FC\6-311+G(2d, p)\C11H11N2O2(1-)\MAY04\30-Mar-
2010\O\#\#p GEOM=ALLCHECK GUESS=READ SCRF=CHECK MP2/6-311+G(2d, p) opt=(
readfc, ts, noigentest) freq\Methyl Transfer N->N\ -1, 1\C, 2. 6701033499
, -1. 0402261676, 0. 0774184025\C, 4. 1075133446, -0. 8891697153, 0. 0767767274\
C, 4. 7068714587, 0. 3509494463, 0. 0345365808\C, 3. 9158128714, 1. 515710358, -0
. 0095339829\C, 2. 5423769284, 1. 3441997586, -0. 0078740231\H, 4. 6980963664, -
1. 8002895588, 0. 1111997258\H, 5. 7927192489, 0. 4262071165, 0. 0354038208\H, 4
. 3489672073, 2. 509130552, -0. 0434760867\H, 1. 8697589412, 2. 2025298228, -0. 0
40586723\N, 1. 9443025248, 0. 1446209976, 0. 0328429029\O, 2. 0835392227, -2. 14
80406587, 0. 1149091673\C, -0. 0066647318, 0. 0232704345, 0. 0310589668\H, 0. 03
65231346, -0. 5553812433, -0. 8755339064\H, 0. 0320518344, -0. 5029516124, 0. 96
92452191\H, -0. 0903122061, 1. 098080399, -0. 0001819256\N, -1. 9465779877, -0.
0924663577, 0. 0296055125\C, -2. 4986187633, -1. 3145867048, 0. 0692869483\C, -
2. 7145985774, 1. 0655331644, -0. 0115923211\C, -3. 8641223816, -1. 537054536, 0
. 0729690928\H, -1. 7907765587, -2. 1442519085, 0. 0992363315\C, -4. 1452514205
, 0. 8591325437, -0. 0085430279\C, -4. 6980471464, -0. 4022156778, 0. 0324163663
\H, -4. 2599334656, -2. 545908326, 0. 1058868378\H, -4. 7693481113, 1. 747690114
, -0. 040187401\H, -5. 7803314846, -0. 5174533951, 0. 0333121724\O, -2. 17456559
81, 2. 1970061548, -0. 0483143773\Versi on=AM64L-G03RevD. 01\State=1-A\HF=-
681. 7293888\MP2=-684. 1487151\RMSD=8. 258e-09\RMSF=2. 229e-06\Thermal =0. \
Di pol e=-0. 0044181, -0. 0463367, -0. 0011731\PG=C01 [X(C11H11N2O2)]\#@

```

O-Methyl-2-Pyridone

```

1\1\GI NC-NODE25\F0pt\RMP2-FC\6-311+G(2d, p)\C6H7N1O1\MAY04\19-Mar-2010\
O\#\#p MP2/6-311+g(2d, p) Opt Freq\2-Methoxy pyridin - Geometrie 1\0, 1\
C, -0. 4275608987, 0. 2982722807, 0. 0001742738\C, 0. 5419376236, 1. 3130012732,
0. 0000958739\C, 1. 8742254402, 0. 9369074348, 0. 0000689395\C, 2. 1973489502, -
0. 4254778067, 0. 0001375677\C, 1. 1600840073, -1. 3460311302, 0. 0002286999\H,
0. 2306355748, 2. 3514355012, 0. 0000634895\H, 2. 6535570014, 1. 6923098682, 0. 0
000129719\H, 3. 227867371, -0. 7617818472, 0. 0001182275\H, 1. 3621990817, -2. 4
135007477, 0. 0002943575\N, -0. 1436057782, -0. 9988134401, 0. 0002408514\O, -1
. 7218766096, 0. 6986134149, 0. 0001507805\C, -2. 6976406062, -0. 3510944388, 0.
0005784017\H, -3. 6591905904, 0. 1569021786, 0. 0008486734\H, -2. 594610704, -0
. 9765714367, -0. 8866673556\H, -2. 594013863, -0. 9764101042, 0. 8878662475\
Versi on=AM64L-G03RevD. 01\State=1-A\HF=-360. 6887837\MP2=-361. 954828\RMSD
=5. 305e-09\RMSF=5. 931e-05\Thermal =0. \Di pol e=0. 3068339, 0. 0859297, 0. 0001
569\PG=C01 [X(C6H7N1O1)]\#@

```

O-Ethyl-2-Pyridone

```

1\1\GI NC-NODE9\F0pt\RMP2-FC\6-311+G(2d, p)\C7H9N1O1\MAY04\08-Sep-2010\
O\#\#p opt freq mp2/6-311+g(2d, p)\O-Ethyl -2-pyri don\0, 1\C, -0. 564329492
8, 0. 3962877981, -0. 005722908\C, -1. 5762592955, 1. 3649083647, -0. 0954721112
\C, -2. 8926004951, 0. 9387446198, -0. 0440159004\C, -3. 1606814889, -0. 4282914
678, 0. 0934152637\C, -2. 0861312492, -1. 3018698636, 0. 1717315062\H, -1. 30743
05756, 2. 4100744397, -0. 1988842792\H, -3. 701441109, 1. 6595654727, -0. 109321

```

286\H, -4. 1764360541, -0. 8043976893, 0. 1366815855\H, -2. 2447529149, -2. 3716
221252, 0. 277051229\N, -0. 7977107913, -0. 9057752728, 0. 121640453\O, 0. 71018
53211, 0. 8560922104, -0. 0427997899\C, 1. 7601327029, -0. 1314669649, -0. 00450
19506\C, 1. 9759041339, -0. 765541837, -1. 3634733894\H, 2. 8273751667, -1. 4495
58446, -1. 3194878851\H, 1. 0950729639, -1. 3300377877, -1. 6681683165\H, 2. 186
8386498, 0. 001322022, -2. 110867759\H, 1. 5249390415, -0. 8819034994, 0. 751390
9214\H, 2. 6378302865, 0. 4340005163, 0. 3091864266\Version=AM64L-G03RevD. 0
1\State=1-A\HF=-399. 7368783\MP2=-401. 1614286\RMSD=9. 361e-09\RMSF=1. 310
e-05\Thermal=0. \Di pol e=-0. 2770722, 0. 0398121, -0. 0642896\PG=C01 [X(C7H9N
101)]\@

O-iso-Propyl-2-Pyridone

1\1\GINC-NODE15\FOpt\RMP2-FC\6-311+G(2d, p)\C8H11N101\MAY04\08-Sep-2010
\0\#p MP2/6-311+G(2d, p) opt freq\0-iso-Propyl-2-pyridon\0, 1\C, -0. 56
73827751, 0. 4449765878, -0. 0853266435\C, -1. 617923514, 1. 3683602427, -0. 207
5053011\C, -2. 9148356064, 0. 9040979917, -0. 0680362966\C, -3. 127035726, -0. 4
559900994, 0. 186009687\C, -2. 0186441326, -1. 2838783042, 0. 2865248188\H, -1.
3919103988, 2. 4104751752, -0. 4033966081\H, -3. 7514146831, 1. 5901410946, -0.
1553709696\H, -4. 1257983232, -0. 8614765681, 0. 3008438707\H, -2. 1337759799,
-2. 3467304412, 0. 4810184372\N, -0. 7483004821, -0. 8506534661, 0. 1525562719\
O, 0. 6856220852, 0. 9462223549, -0. 2085682945\C, 1. 7899846747, 0. 0091594444,
-0. 1510093261\C, 1. 9281002437, -0. 7067191287, -1. 4814306853\H, 2. 774170959
6, -1. 3978536995, -1. 4463582323\H, 1. 0275244448, -1. 2765738792, -1. 70995955
86\H, 2. 105371463, 0. 0203055594, -2. 2778626293\C, 3. 0031752142, 0. 848144209
, 0. 1904604953\H, 3. 8883229246, 0. 2120850117, 0. 2600084781\H, 3. 1743221626,
1. 598319433, -0. 5848306175\H, 2. 8632807074, 1. 3583620806, 1. 1444864898\H, 1
. 5829808814, -0. 7119091486, 0. 6429654137\Version=AM64L-G03RevD. 01\State
=1-A\HF=-438. 7865398\MP2=-440. 370898\RMSD=5. 268e-09\RMSF=3. 285e-06\The
rmal=0. \Di pol e=-0. 2422936, 0. 0518936, -0. 0286164\PG=C01 [X(C8H11N101)]\@
@

O-tert-Butyl-2-Pyridone

1\1\GINC-NODE26\FOpt\RMP2-FC\6-311+G(2d, p)\C9H13N101\MAY04\24-Jul-2010
\0\#p MP2/6-311+g(2d, p) opt freq\0-Tert-butyl-2-pyridon\0, 1\C, 0. 339
7866894, -0. 1847144374, 0. 0000038959\C, -0. 5782525486, -1. 2494489021, -0. 00
07218817\C, -1. 9303774846, -0. 9530381245, -0. 0016057475\C, -2. 3319491556, 0
. 38763019, -0. 0017836896\C, -1. 3466210816, 1. 3635059847, -0. 001088221\H, -0
. 2087457685, -2. 2687018307, -0. 0005754492\H, -2. 6635442382, -1. 7534795675,
-0. 0021642713\H, -3. 3796108626, 0. 666139115, -0. 00245185\H, -1. 6094911785,
2. 4180629093, -0. 0012239491\N, -0. 0244146832, 1. 0946873203, -0. 0001983235\
O, 1. 6429855206, -0. 5515144335, 0. 0008801002\C, 2. 7298947301, 0. 4265223181,
0. 0011443448\C, 2. 6987471719, 1. 2722792021, 1. 2676491321\H, 3. 6211196286, 1
. 8564715116, 1. 3281203161\H, 1. 8495680386, 1. 9528182784, 1. 2726850319\H, 2.
6452858526, 0. 624887617, 2. 1466011564\C, 2. 7000723211, 1. 2712637925, -1. 266
0664812\H, 3. 622406944, 1. 8555613273, -1. 3260063818\H, 2. 6476554667, 0. 6231
703106, -2. 1445647654\H, 1. 8508187453, 1. 9517115132, -1. 2725479086\C, 3. 958
0904239, -0. 4718399054, 0. 0022258344\H, 4. 8650360313, 0. 1366028407, 0. 00260
17139\H, 3. 9608982487, -1. 10856897, 0. 8892285136\H, 3. 9619920087, -1. 109103
1298, -0. 8843859494\Version=AM64L-G03RevD. 01\State=1-A\HF=-477. 8275661
\MP2=-479. 5763112\RMSD=9. 082e-09\RMSF=6. 639e-06\Thermal=0. \Di pol e=-0. 1
946945, -0. 0903042, -0. 0003887\PG=C01 [X(C9H13N101)]\@

O-Acetyl-2-Pyridone

1\1\GINC-NODE24\FOpt\RMP2-FC\6-311+G(2d, p)\C7H7N102\MAY04\18-Jun-2010\
O\#p MP2/6-311+g(2d, p) opt freq\0-Acetyl-2-pyridon - Geometrie 1-\0
, 1\C, 1. 647985794, -1. 2669664601, -1. 3127617101\C, 0. 3537751168, -1. 7693772
196, -1. 2362986901\C, -0. 2461576145, -2. 181427283, -2. 4220140688\C, 0. 47336
97601, -2. 0674758579, -3. 6113104561\C, 1. 7652834569, -1. 5495649026, -3. 5627
171031\H, -0. 1518212316, -1. 8274276683, -0. 2793822871\H, -1. 2555862411, -2.
5793181621, -2. 4170365028\H, 0. 0451895211, -2. 3741074884, -4. 5591347729\H,
2. 3587154459, -1. 4469636157, -4. 4664975822\N, 2. 3580461287, -1. 1516307451,
-2. 4235326032\O, 2. 2917139243, -0. 900913669, -0. 1316612601\C, 2. 3048002412
, 0. 4543059287, 0. 1179331216\O, 1. 7023434613, 1. 2536650822, -0. 5532847804\C
, 3. 1568375585, 0. 7447868675, 1. 3171692116\H, 2. 8699090489, 0. 0987072543, 2.
1471275756\H, 4. 1982566921, 0. 5306306924, 1. 0706236323\H, 3. 0493402174, 1. 7
210

910479766, 1. 5923838359\\Version=AM64L-G03RevD. 01\\State=1-A\\HF=-473. 475
4351\\MP2=-475. 0856131\\RMSD=4. 448e-09\\RMSF=1. 725e-05\\Thermal =0. \\Di pol e=
-0. 4933718, -0. 706197, 0. 2268334\\PG=C01 [X(C7H7N1O2)]\\@

Transition State: Methyl-Transfer *O*-Methyl-2-Pyridone to 2-Pyridone (*O*-attack)

1\\1\\GI NC-NODE13\\F0pt\\RMP2-FC\\6-311+G(2d,p)\\C11H11N2O2(1-)\\MAY04\\02-Apr-
2010\\0\\#P GEOM=ALLCHECK GUESS=READ SCRF=CHECK MP2/6-311+G(2d,p) opt=(
readfc,ts,noigentest) freq\\Methyl Transfer 0->0\\-1,1\\C, 0. 0360817534
, -0. 6878947508, -0. 3715986698\\C, -1. 1058387781, -1. 5482604313, -0. 38556646
91\\C, -2. 3030985411, -1. 1317518768, 0. 1643492325\\C, -2. 3856988274, 0. 146180
3082, 0. 7371913115\\C, -1. 2362722681, 0. 92731036, 0. 7151459874\\H, -0. 9979905
06, -2. 5295331715, -0. 8378047888\\H, -3. 1679959772, -1. 7918905168, 0. 1508679
799\\H, -3. 3020926573, 0. 5196367144, 1. 1825368506\\H, -1. 2536543791, 1. 927354
7803, 1. 1495382981\\N, -0. 0589533929, 0. 551302666, 0. 1884733868\\O, 1. 1475460
945, -1. 0940859063, -0. 892735817\\C, 2. 6412641901, 0. 1086748432, -0. 83657011
99\\H, 3. 1914069302, -0. 6581332693, -1. 3485968688\\H, 2. 0940415927, 0. 8570106
467, -1. 3782013542\\H, 2. 6383301889, 0. 1275221707, 0. 2368774627\\O, 4. 1354050
205, 1. 3088139509, -0. 9267136206\\C, 5. 2440889729, 0. 9210622026, -0. 38596419
68\\C, 6. 3861773995, 1. 7804880011, -0. 4239034502\\C, 7. 580504173, 1. 383427263
7, 0. 1463870214\\H, 6. 2807990009, 2. 7454384313, -0. 9105382608\\C, 6. 510568126
1, -0. 6552855209, 0. 7629242675\\C, 7. 6599621909, 0. 1261935158, 0. 7637553343\\
H, 8. 4455445772, 2. 0427431446, 0. 1144493687\\H, 6. 5255582253, -1. 6396079186,
1. 2319361003\\H, 8. 5739805424, -0. 2314965028, 1. 2265821107\\N, 5. 3360483888,
-0. 2978892943, 0. 2173692138\\Version=AM64L-G03RevD. 01\\State=1-A\\HF=-681
. 7317594\\MP2=-684. 1399159\\RMSD=3. 422e-09\\RMSF=2. 499e-06\\Thermal =0. \\Di pol e=
-0. 0010445, 0. 0073131, 0. 4202548\\PG=C01 [X(C11H11N2O2)]\\@

4-Pyridone-Anion

1\\1\\GI NC-NODE10\\F0pt\\RMP2-FC\\6-311+G(2d,p)\\C5H4N1O1(1-)\\MAY04\\21-Mar-2
010\\0\\#p opt freq mp2/6-311+g(2d,p)\\4-Pyri don-Ani on\\-1,1\\C, 0. 008894
5736, 0. 0174432153, 0. 0000285182\\C, 1. 3955278289, 0. 0090319809, -0. 00014185
56\\C, 2. 1600894272, 1. 2296653974, -0. 0008636546\\C, 1. 3086297644, 2. 39134998
99, -0. 0004708493\\C, -0. 0737069639, 2. 2819328864, -0. 0002744718\\N, -0. 77201
04936, 1. 122710646, -0. 0001640815\\H, -0. 5277291084, -0. 9333671668, 0. 000295
3427\\H, 1. 9325521743, -0. 9377558724, 0. 0001833321\\H, 1. 7752409857, 3. 374750
538, -0. 0004184283\\H, -0. 6781756463, 3. 191121406, -0. 000275753\\O, 3. 4288604
681, 1. 2759433892, -0. 0003729288\\Version=AM64L-G03RevD. 01\\State=1-A\\HF=
-321. 0857162\\MP2=-322. 211157\\RMSD=3. 336e-09\\RMSF=4. 134e-05\\Thermal =0. \\
Di pol e=-0. 8817997, -0. 0321658, 0. 0000995\\PG=C01 [X(C5H4N1O1)]\\@

N-Methyl-2-Pyridone

1\\1\\GI NC-NODE24\\F0pt\\RMP2-FC\\6-311+G(2d,p)\\C6H7N1O1\\MAY04\\21-Mar-2010\\
0\\#p opt freq mp2/6-311+g(2d,p)\\N-Methyl -4-pyri don\\O, 1\\C, 0. 01852227
72, -0. 0265303101, -0. 0296568324\\C, 1. 3811774245, -0. 0139008173, 0. 00092464
94\\C, 2. 1392181771, 1. 2288908081, 0. 0211153327\\C, 1. 2926411258, 2. 413132408
7, 0. 0000542256\\C, -0. 0673115942, 2. 3264213478, -0. 0305006948\\N, -0. 7192806
076, 1. 1245876721, -0. 0549924357\\H, -0. 5538542071, -0. 9481131114, -0. 042473
6614\\H, 1. 9212262214, -0. 9540430415, 0. 0066652042\\H, 1. 7627541983, 3. 390128
4307, 0. 0051072191\\H, -0. 7053143072, 3. 2038410199, -0. 043962732\\O, 3. 379585
4726, 1. 2741481539, 0. 0481598621\\C, -2. 17420616, 1. 0715404447, 0. 021239364\\
H, -2. 5295319421, 0. 1730802053, -0. 4822873737\\H, -2. 5117441137, 1. 059599914
5, 1. 0602069901\\H, -2. 5940375187, 1. 9413621494, -0. 4829215273\\Version=AM6
4L-G03RevD. 01\\State=1-A\\HF=-360. 6787482\\MP2=-361. 9488497\\RMSD=9. 022e-0
9\\RMSF=2. 653e-05\\Thermal =0. \\Di pol e=-2. 9584176, -0. 1079333, -0. 0349639\\PG
=C01 [X(C6H7N1O1)]\\@

N-Acetyl-4-Pyridone

1\\1\\GI NC-NODE22\\F0pt\\RMP2-FC\\6-311+G(2d,p)\\C7H7N1O2\\MAY04\\19-Jun-2010\\
0\\#p MP2/6-311+g(2d,p) opt freq\\N-Acetyl -4-pyri don - Geometrie 1-\\O
, 1\\C, -0. 6035425574, -1. 1624685443, 0. 0051332053\\C, 0. 7488931045, -1. 219909
8737, -0. 0291232643\\C, 1. 5767688725, -0. 0167252452, -0. 0295366668\\C, 0. 8037
561747, 1. 2217508854, 0. 0097184818\\C, -0. 5512302051, 1. 2206883744, 0. 043098

1289\N, -1. 2822127999, 0. 0458843177, 0. 0417876\H, -1. 2441158616, -2. 0344851658, 0. 006456392\H, 1. 2396269524, -2. 1862601937, -0. 057158275\H, 1. 3354793615, 2. 1665457402, 0. 0121374658\H, -1. 1201571129, 2. 1388730108, 0. 0722877635\O, 2. 8124778296, -0. 0415603908, -0. 0602526025\C, -2. 7071252254, 0. 0201877766, 0. 0763633421\O, -3. 2967896299, -1. 0403013182, 0. 0733465941\C, -3. 4136794839, 1. 3506949695, 0. 1157282969\H, -4. 4810904882, 1. 1443721181, 0. 1385753682\H, -3. 1372569203, 1. 9203358932, 1. 0048828268\H, -3. 1808766007, 1. 949659956, -0. 7666127869\Version=AM64L-G03RevD. 01\State=1-A\HF=-473. 4609962\MP2=-475. 0733717\RMSD=4. 510e-09\RMSF=1. 127e-05\Thermal =0. \Di pol e=-1. 7432342, 1. 0320723, 0. 059811\PG=C01 [X(C7H7N102)]\@

Transition State: Methyl-Transfer *N*-Methyl-4-Pyridone 4-Pyridone (*N*-attack)

1\1\GINC-NODE25\FTS\RMP2-FC\6-311+G(2d,p)\C11H11N2O2(1-)\MAY04\06-Apr-2010\O\#p GEOM=ALLCHECK GUESS=READ SCRF=CHECK MP2/6-311+G(2d,p) opt=(readfc,ts,noigentest) freq\4-Pyridon-Anion: Methyl Transfer N->N\ -1, 1\C, -0. 9650618931, 0. 5038648693, -1. 0368346282\C, 0. 4105287443, 0. 4935045632, -1. 1124869238\C, 1. 2261542096, -0. 0167884541, -0. 0312835854\C, 0. 4345266802, -0. 4915957252, 1. 0832608262\C, -0. 9421922017, -0. 4402786904, 1. 065315553\N, -1. 6584142721, 0. 0513048587, 0. 0307627986\H, -1. 5674424623, 0. 8902690522, -1. 859673823\H, 0. 907121334, 0. 8766194574, -1. 9996266545\H, 0. 9502051025, -0. 8963288345, 1. 9496648113\H, -1. 525998582, -0. 8045012475, 1. 9113333662\O, 2. 4831882921, -0. 0441157413, -0. 0573758474\C, -3. 582793628, 0. 0013797588, 0. 0233479302\H, -3. 6013950614, 0. 9082583119, -0. 5584706456\H, -3. 5642767107, -0. 9557039286, -0. 4715621524\H, -3. 5827099037, 0. 0516532263, 1. 101479162\N, -5. 5071712564, -0. 0477007562, 0. 0356575958\C, -6. 2233009575, 0. 5384237381, 1. 0198065488\C, -6. 2006336573, -0. 5984179569, -0. 9846977675\C, -7. 6000270932, 0. 5908889364, 1. 0331801963\H, -5. 6394079545, 0. 9803926763, 1. 827869651\C, -7. 576244338, -0. 5954941163, -1. 0606752786\H, -5. 5983309145, -1. 0600492087, -1. 7678730834\C, -8. 3917706105, 0. 0136254756, -0. 0318258895\H, -8. 1156260946, 1. 0748561768, 1. 8579969202\H, -8. 0729252039, -1. 0601164798, -1. 9079250243\O, -9. 6488165873, 0. 0381127285, -0. 060073316\Version=AM64L-G03RevD. 01\State=1-A\HF=-681. 717635\MP2=-684. 1385766\RMSD=9. 466e-09\RMSF=5. 508e-07\Thermal =0. \Di pol e=0. 0000329, 0. 0036456, 0. 0673108\PG=C01 [X(C11H11N2O2)]\@

O-Methyl-2-Pyridone

1\1\GINC-NODE10\F0pt\RMP2-FC\6-311+G(2d,p)\C6H7N101\MAY04\21-Mar-2010\O\#p opt freq mp2/6-311+g(2d,p)\O-Methyl -4-pyridon\O, 1\C, -0. 0933741011, 0. 0293953075, -0. 0007357738\C, 1. 3013950102, -0. 0533111809, 0. 0085965946\C, 2. 0318321042, 1. 1357102058, 0. 0101159073\C, 1. 3274926233, 2. 3424868476, 0. 0022263485\C, -0. 0599120183, 2. 3077397572, -0. 0067887499\N, -0. 7869089668, 1. 1741413976, -0. 0084190914\H, -0. 6802537351, -0. 885663756, -0. 0020229674\H, 1. 775535815, -1. 0266307466, 0. 0142797926\H, 1. 8696404018, 3. 2820367654, 0. 0032711176\H, -0. 6239818692, 3. 2363773688, -0. 0130066465\O, 3. 3876539643, 1. 2223749368, 0. 0188220029\C, 4. 1041967, -0. 0101251925, 0. 0275342111\H, 3. 8824387415, -0. 5990018338, -0. 8663613487\H, 5. 1569376242, 0. 2607615583, 0. 0343341949\H, 3. 8695643862, -0. 5938209553, 0. 9215329181\Version=AM64L-G03RevD. 01\State=1-A\HF=-360. 6782949\MP2=-361. 944965\RMSD=4. 128e-09\RMSF=3. 106e-05\Thermal =0. \Di pol e=1. 189993, -0. 550956, 0. 0096189\PG=C01 [X(C6H7N101)]\@

O-Acetyl-4-Pyridone

1\1\GINC-NODE13\F0pt\RMP2-FC\6-311+G(2d,p)\C7H7N102\MAY04\23-Jun-2010\O\#p MP2/6-311+g(2d,p) opt=readfc freq geom=Check Guess=Read SCRF=Check\O-Acetyl -4-pyridon - Geometrie 1-\O, 1\C, 2. 0450385794, 1. 1628633579, 0. 9038691411\C, 0. 6734519395, 0. 9197171283, 0. 9624083915\C, 0. 2308400529, -0. 3518523871, 0. 6214786807\C, 1. 1480230491, -1. 322176263, 0. 244445854\C, 2. 4976876165, -0. 9735488068, 0. 2252658278\N, 2. 9580888668, 0. 246042912, 0. 5448036146\H, 2. 4301104955, 2. 1459911534, 1. 1595823088\H, -0. 0192228857, 1. 697636516, 1. 2596076882\H, 0. 8154128765, -2. 3198924451, -0. 0200518299\H, 3. 244845637, -1. 7083973986, -0. 0611955836\O, -1. 1061654938, -0. 7263581816, 0. 7190620758\C, -2. 0276363933, 0. 0155400183, 0. 0071825787\O, -1. 7329964688, 0. 9440024152, -0. 7010844068\C, -3. 4037142838, -0. 5278494053, 0. 2535744052\H, -3. 4485644097, -1. 5692387958, -0. 0680802248\H, -3. 6241354347, -0. 4995036115, 1. 3214960342\H, -4. 1287644033, 0. 0657879535, -0. 2973925354\Version=AM64

L-G03RevD. 01\State=1-A\HF=-473. 4689483\MP2=-475. 0797218\RMSD=5. 436e-09
 \RMSF=3. 443e-06\Thermal =0. \Di pol e=-1. 1275639, -0. 6300417, 0. 3811495\PG=C
 01 [X(C7H7N102)]\@

Transition State: Methyl-Transfer *O*-Methyl-4-Pyridone 4-Pyridone (*O*-attack)

1\1\GI NC-NODE13\FTS\RMP2-FC\6-311+G(2d,p)\C11H11N202(1-)\MAY04\24-Apr-
 2010\0\#P GEOM=ALLCHECK GUESS=READ SCRF=CHECK MP2/6-311+G(2d,p) opt=(
 readfc,ts,noigentest) freq\4-Pyri don-Ani on: Methyl Transfer 0->0\1-
 , 1\C, 5. 0452093062, -0. 5686764755, -0. 2125048035\C, 3. 9175009914, -1. 127072
 1445, 0. 3692375396\C, 2. 6721896882, -0. 4455109158, 0. 3438776782\C, 2. 710166
 2629, 0. 8124446171, -0. 3145814098\C, 3. 9010936251, 1. 2778590157, -0. 8646377
 356\N, 5. 0787934885, 0. 6279518892, -0. 8368444671\H, 5. 9893575021, -1. 111177
 3247, -0. 1797411945\H, 3. 9694179579, -2. 0974816026, 0. 8551139523\H, 1. 82102
 6932, 1. 4271536391, -0. 3992784102\H, 3. 9082080475, 2. 2454344381, -1. 3652539
 906\0, 1. 6162768578, -0. 9766298118, 0. 895427877\C, -0. 0000277877, -0. 000571
 5721, 0. 8447982118\H, -0. 4338300834, -0. 8230307842, 1. 3848171141\H, 0. 43377
 52603, 0. 8212159045, 1. 3858373828\H, -0. 0000247618, 0. 0000987828, -0. 231258
 5202\0, -1. 6163348315, 0. 9754175752, 0. 896650133\C, -2. 6722139557, 0. 445040
 6547, 0. 3443215819\C, -3. 9175152983, 1. 1265898181, 0. 3704769644\C, -2. 71016
 04407, -0. 8120501603, -0. 3157882751\C, -5. 0451874552, 0. 5689768442, -0. 2120
 856257\H, -3. 9694536727, 2. 0963624399, 0. 8576209473\C, -3. 9010523844, -1. 27
 67222647, -0. 8665483039\H, -1. 8210254186, -1. 4266639391, -0. 4012185941\N, -
 5. 0787430873, -0. 6268314271, -0. 8379961496\H, -5. 9893288281, 1. 1114507337,
 -0. 1786852845\H, -3. 9081442697, -2. 2436406867, -1. 3684326742\Version=AM6
 4L-G03RevD. 01\State=1-A\HF=-681. 727558\MP2=-684. 13997\RMSD=8. 493e-09\R
 MSF=2. 468e-06\Thermal =0. \Di pol e=-0. 0000132, -0. 0001495, 0. 2197337\PG=C01
 X(C11H11N202)]\@

N,N-Dimethylacetamide

1\1\GI NC-NODE22\FOpt\RMP2-FC\6-311+G(2d,p)\C4H9N101\MAY04\30-Jul -2010\
 0\#P MP2/6-311+G(2d,p) opt=(cal cfc, ti ght) freq\N, N-Di methyl acetami de
 \0, 1\C, 0. 721847793, -0. 2915530156, 0. 0242399327\0, 1. 0624934946, -1. 47073
 30505, 0. 1072826699\N, -0. 5906222902, 0. 0779214696, -0. 1078906492\C, 1. 7547
 383346, 0. 8188346118, 0. 0447611632\H, 1. 7184137358, 1. 4210395956, -0. 865412
 8897\H, 1. 6115305709, 1. 4831059963, 0. 8997972954\H, 2. 7314515527, 0. 3470928
 421, 0. 1208334668\C, -1. 6200748473, -0. 9444474772, -0. 0435792625\H, -2. 1246
 265798, -0. 9298271558, 0. 9287208843\H, -2. 362876731, -0. 765322721, -0. 82461
 7924\H, -1. 1577932544, -1. 9172861803, -0. 1894495653\C, -1. 0659619281, 1. 445
 1287937, -0. 0331223466\H, -1. 4651502327, 1. 6747239906, 0. 9620556139\H, -0. 2
 713198023, 2. 1496585158, -0. 2614727629\H, -1. 8675508157, 1. 589408785, -0. 76
 21404801\Version=AM64L-G03RevD. 01\State=1-A\HF=-286. 1143736\MP2=-287.
 139049\RMSD=6. 901e-09\RMSF=6. 768e-08\Thermal =0. \Di pol e=-0. 8018771, 1. 32
 14479, -0. 0485465\PG=C01 [X(C4H9N101)]\@

(*E*)-Methyl *N*-Methylacetimidate

1\1\GI NC-NODE28\FOpt\RMP2-FC\6-311+G(2d,p)\C4H9N101\MAY04\31-Jul -2010\
 0\#p MP2/6-311+G(2d,p) opt=(cal cfc) freq\N-methyl N-methyl acetimi d
 ate\0, 1\C, 0. 025242, 0. 324903, -0. 002182\0, -1. 31683, 0. 524673, -0. 003458\N
 , 0. 508092, -0. 854207, -0. 000636\C, 0. 773709, 1. 626335, 0. 000915\H, 1. 351711,
 1. 724995, 0. 923018\H, 1. 477766, 1. 659113, -0. 833344\H, 0. 082162, 2. 46285, -0.
 076853\C, 1. 962585, -0. 969761, 0. 00075\H, 2. 231094, -2. 021352, 0. 090808\H, 2.
 398147, -0. 588978, -0. 929704\H, 2. 422482, -0. 42874, 0. 835258\C, -2. 105374, -0
 . 67286, 0. 002417\H, -3. 139017, -0. 334896, 0. 002771\H, -1. 893129, -1. 274707, -
 0. 881527\H, -1. 890192, -1. 267927, 0. 890286\Version=AM64L-G03RevD. 01\Stat
 e=1-A\HF=-286. 0871077\MP2=-287. 1104209\RMSD=6. 608e-09\RMSF=3. 167e-07\T
 hermal =0. \Di pol e=0. 2738638, 0. 2734628, 0. 0027267\Pol ar=72. 3349119, -2. 154
 8826, 63. 1233237, -0. 0405999, 0. 1000207, 47. 0289656\PG=C01 [X(C4H9N101)]\@

6 References

- [1] a) D. L. Comins, M. F. Baevsky, H. Hong, *J. Am. Chem. Soc.* **1992**, *114*, 10971–10972; b) H. Liu, S.-B. Ko, H. Josien, D. P. Curran, *Tetrahedron Lett.* **1995**, *36*, 8917–8920; c) D. Conreux, E. Bossharth, N. Monteiro, P. Desbordes, G. Balme, *Tetrahedron Lett.* **2005**, *46*, 7917–7920; d) S. K. Tipparaju, S. Joyasawal, S. Forrester, D. C. Mulhearn, S. Pegan, M. E. Johnson, A. D. Mesecar, A. P. Kozikowski, *Bioorg. Med. Chem. Lett.* **2008**, *18*, 3565–3569.
- [2] a) H. Meislich, in *Pyridine and Its Derivatives, Part III* (Ed.: E. Klingsberg), Interscience Publisher, New York, London, **1962**; b) P. A. Keller, *Science of Synthesis* **2005**, *15*, 285–387.
- [3] N. Kornblum, R. A. Smiley, R. K. Blackwood, D. C. Iffland, *J. Am. Chem. Soc.* **1955**, *77*, 6269–6280.
- [4] a) G. C. Hopkins, J. P. Jonak, H. J. Minnemeyer, H. Tieckelmann, *J. Org. Chem.* **1967**, *32*, 4040–4044; b) N. M. Chung, H. Tieckelmann, *J. Org. Chem.* **1970**, *35*, 2517–2520.
- [5] a) R. G. Pearson, *J. Am. Chem. Soc.* **1963**, *85*, 3533–3539; b) R. G. Pearson, *Science* **1966**, *151*, 172–177; c) R. G. Pearson, *J. Chem. Educ.* **1968**, *45*, 581–587; d) R. G. Pearson, *J. Chem. Educ.* **1968**, *45*, 643–648; e) R. G. Pearson, *Chemical Hardness*, Wiley-VCH, Weinheim, **1997**.
- [6] a) F. Zaragoza Dörwald, *Side Reactions in Organic Synthesis*, WILEY-VCH, Weinheim, **2005**; b) T.-L. Ho, *Chem. Rev.* **1975**, *75*, 1–20.
- [7] A. A. Tishkov, H. Mayr, *Angew. Chem.* **2005**, *117*, 145–148; *Angew. Chem. Int. Ed.* **2005**, *44*, 142–145.
- [8] H. F. Schaller, U. Schmidhammer, E. Riedle, H. Mayr, *Chem. Eur. J.* **2008**, *14*, 3866–3868.
- [9] R. Loos, S. Kobayashi, H. Mayr, *J. Am. Chem. Soc.* **2003**, *125*, 14126–14132.
- [10] A. A. Tishkov, U. Schmidhammer, S. Roth, E. Riedle, H. Mayr, *Angew. Chem.* **2005**, *117*, 4699–4703; *Angew. Chem. Int. Ed.* **2005**, *44*, 4623–4626.
- [11] M. Baidya, S. Kobayashi, H. Mayr, *J. Am. Chem. Soc.* **2010**, *132*, 4796–4805.
- [12] a) G. Klopman, *J. Am. Chem. Soc.* **1968**, *90*, 223–234; b) L. Salem, *J. Am. Chem. Soc.* **1968**, *90*, 543–552.
- [13] a) R. A. Marcus, *Annu. Rev. Phys. Chem.* **1964**, *15*, 155–196; b) R. A. Marcus, *Pure Appl. Chem.* **1997**, *69*, 13–29.

- [14] M. Breugst, H. Zipse, J. P. Guthrie, H. Mayr, *Angew. Chem.* **2010**, *122*, 5291–5295; *Angew. Chem. Int. Ed.* **2010**, *49*, 5165–5169.
- [15] a) H. Mayr, T. Bug, M. F. Gotta, N. Hering, B. Irrgang, B. Janker, B. Kempf, R. Loos, A. R. Ofial, G. Remennikov, H. Schimmel, *J. Am. Chem. Soc.* **2001**, *123*, 9500–9512; b) R. Lucius, R. Loos, H. Mayr, *Angew. Chem.* **2002**, *114*, 97–102; *Angew. Chem. Int. Ed.* **2002**, *41*, 91–95; c) D. Richter, N. Hampel, T. Singer, A. R. Ofial, H. Mayr, *Eur. J. Org. Chem.* **2009**, 3203–3211.
- [16] a) J. W. Bunting, A. Toth, C. K. M. Heo, R. G. Moors, *J. Am. Chem. Soc.* **1990**, *112*, 8878–8885; b) C. K. M. Heo, J. W. Bunting, *J. Org. Chem.* **1992**, *57*, 3570–3578.
- [17] S. Minegishi, H. Mayr, *J. Am. Chem. Soc.* **2003**, *125*, 286–295.
- [18] S. Minegishi, S. Kobayashi, H. Mayr, *J. Am. Chem. Soc.* **2004**, *126*, 5174–5181.
- [19] F. G. Bordwell, *Acc. Chem. Res.* **1988**, *21*, 456–463.
- [20] H. Mayr, M. Patz, *Angew. Chem.* **1994**, *106*, 990–1010; *Angew. Chem. Int. Ed. Engl.* **1994**, *33*, 938–957.
- [21] a) F. Seeliger, S. T. A. Berger, G. Y. Remennikov, K. Polborn, H. Mayr, *J. Org. Chem.* **2007**, *72*, 9170–9180; b) S. T. A. Berger, F. H. Seeliger, F. Hofbauer, H. Mayr, *Org. Biomol. Chem.* **2007**, *5*, 3020–3026.
- [22] a) S. Wolfe, D. J. Mitchell, H. B. Schlegel, *J. Am. Chem. Soc.* **1981**, *103*, 7692–7694; b) S. Wolfe, D. J. Mitchell, H. B. Schlegel, *J. Am. Chem. Soc.* **1981**, *103*, 7694–7696.
- [23] a) J. M. Gonzales, R. S. Cox III, S. T. Brown, W. D. Allen, H. F. Schaefer III, *J. Phys. Chem. A* **2001**, *105*, 11327–11346; b) J. M. Gonzales, C. Pak, R. S. Cox, W. D. Allen, H. F. Schaefer III, A. G. Csaszar, G. Tarczay, *Chem. Eur. J.* **2003**, *9*, 2173–2192; c) J. M. Gonzales, W. D. Allen, H. F. Schaefer III, *J. Phys. Chem. A* **2005**, *109*, 10613–10628.
- [24] S. Hoz, H. Basch, J. L. Wolk, T. Hoz, E. Rozental, *J. Am. Chem. Soc.* **1999**, *121*, 7724–7725.
- [25] P. Beak, J. Bonham, J. T. Lee, Jr., *J. Am. Chem. Soc.* **1968**, *90*, 1569–1582.
- [26] a) R. A. Marcus, *J. Am. Chem. Soc.* **1969**, *91*, 7224–7225; b) W. J. Albery, M. M. Kreevoy, *Adv. Phys. Org. Chem.* **1978**, *16*, 87–157; c) S. S. Shaik, H. B. Schlegel, P. Wolfe, *Theoretical Aspects of Physical Organic Chemistry: The S_N2 Mechanism*, John Wiley & Sons, New York, Chichester, Brisbane, Toronto, Singapore, **1992**.
- [27] R. Adams, V. V. Jones, *J. Am. Chem. Soc.* **1947**, *69*, 1803–1805.
- [28] F. Effenberger, W. Brodt, J. Zinczuk, *Chem. Ber.* **1983**, *116*, 3011–3026.

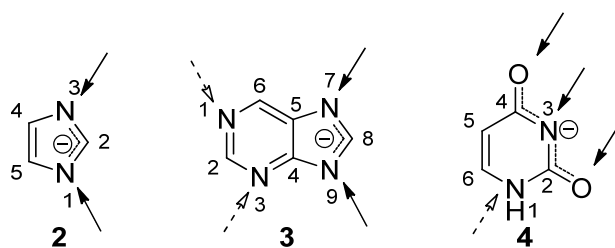
- [29] P. Silhár, M. Hocek, R. Pohl, I. Votruba, I. h. Shih, E. Mabery, R. Mackman, *Bioorg. Med. Chem.* **2008**, *16*, 2329–2366.
- [30] a) C. Rãth, *Liebigs Ann. Chem.* **1930**, *484*, 52–64; b) C. Rãth, *Liebigs Ann. Chem.* **1931**, *489*, 107–118.
- [31] H. v. Pechmann, O. Baltzer, *Ber. Dtsch. Chem. Ges.* **1891**, *24*, 3144–3153.
- [32] T. Takahashi, F. Yoneda, *Chem. Pharm. Bull.* **1958**, *6*, 365–369.
- [33] M. Breugst, T. Tokuyasu, H. Mayr, *J. Org. Chem.* **2010**, *75*, 5250–5258.
- [34] a) D. P. Bancroft, F. A. Cotton, L. R. Falvello, W. Schwotzer, *Inorg. Chem.* **1986**, *25*, 763–770; b) D. P. Bancroft, F. A. Cotton, *Inorg. Chem.* **1988**, *27*, 1633–1637; c) J. M. Rawson, R. E. P. Winpenny, *Coord. Chem. Rev.* **1995**, *139*, 313–374.
- [35] Gaussian 03, Revision D.01, M. J. Frisch, G. W. Trucks, H. B. Schlegel, G. E. Scuseria, M. A. Robb, J. R. Cheeseman, J. A. Montgomery, Jr., T. Vreven, K. N. Kudin, J. C. Burant, J. M. Millam, S. S. Iyengar, J. Tomasi, V. Barone, B. Mennucci, M. Cossi, G. Scalmani, N. Rega, G. A. Petersson, H. Nakatsuji, M. Hada, M. Ehara, K. Toyota, R. Fukuda, J. Hasegawa, M. Ishida, T. Nakajima, Y. Honda, O. Kitao, H. Nakai, M. Klene, X. Li, J. E. Knox, H. P. Hratchian, J. B. Cross, V. Bakken, C. Adamo, J. Jaramillo, R. Gomperts, R. E. Stratmann, O. Yazyev, A. J. Austin, R. Cammi, C. Pomelli, J. W. Ochterski, P. Y. Ayala, K. Morokuma, G. A. Voth, P. Salvador, J. J. Dannenberg, V. G. Zakrzewski, S. Dapprich, A. D. Daniels, M. C. Strain, O. Farkas, D. K. Malick, A. D. Rabuck, K. Raghavachari, J. B. Foresman, J. V. Ortiz, Q. Cui, A. G. Baboul, S. Clifford, J. Cioslowski, B. B. Stefanov, G. Liu, A. Liashenko, P. Piskorz, I. Komaromi, R. L. Martin, D. J. Fox, T. Keith, M. A. Al-Laham, C. Y. Peng, A. Nanayakkara, M. Challacombe, P. M. W. Gill, B. Johnson, W. Chen, M. W. Wong, C. Gonzalez, J. A. Pople, Gaussian, Inc., Wallingford CT, **2004**.

Chapter 6: Ambident Reactivities of the Anions of Nucleobases and Their Subunits

1 Introduction

Imidazoles and their derivatives like purines or xanthenes as well as pyrimidines are omnipresent in chemistry, biology, and medicine and are of tremendous importance for many syntheses.^[1] The imidazole moiety in histidine plays an important role in the active center of several enzymes,^[2] and Staab was among the first to realize that imidazoles are very effective catalysts in acylation reactions and ester hydrolysis.^[3] While the neutral imidazole is typically involved in the hydrolysis of esters with good leaving groups (e.g., *p*-nitrophenyl acetate), the imidazole anion is an effective catalyst in the hydrolysis of esters with poor leaving groups (e.g., *p*-cresol acetate).^[1a, 1b]

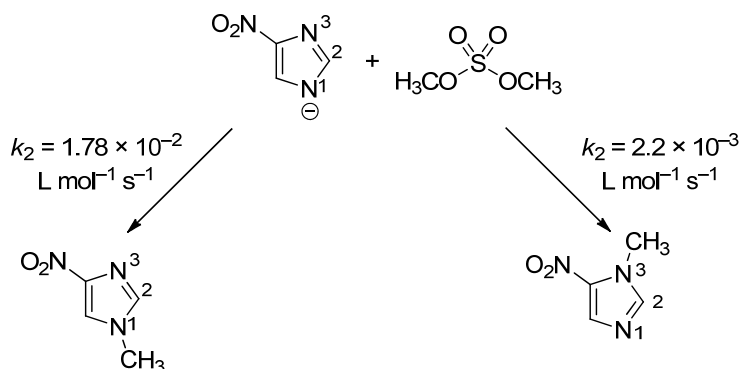
In general, imidazoles, purines, and pyrimidines have to be considered as ambident nucleophiles with several competing reaction centers and these multiple reaction pathways complicate their use in organic synthesis. A similar situation is found for the anions of these compounds, although some reaction pathways can be neglected for these compounds due to the higher reactivity of the negative charged fragments (Scheme 1).



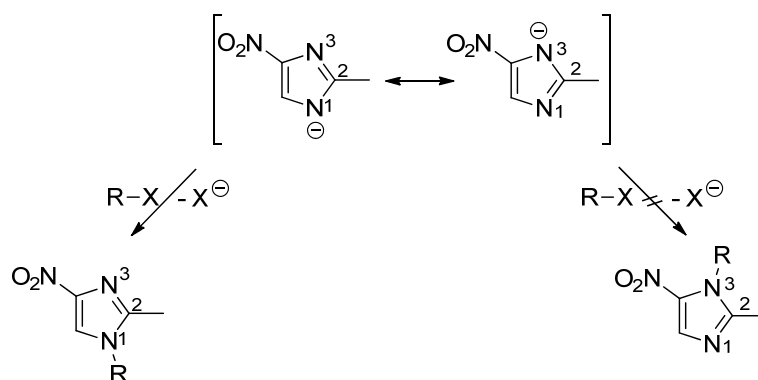
Scheme 1: Conceivable reaction pathways of the ambident heterocyclic anions (solid arrows) and additional reaction pathways in the neutral compounds (dashed arrows).

The reactions of imidazoles with alkyl halides or methyl sulfate under basic conditions, i.e., the alkylations of the imidazole anions, yield *N*-alkylated imidazoles. In the case of unsymmetrically substituted imidazoles, the ratio of both isomers depends on the substituents and on steric effects.^[1a, 1b] The methylation of 4-nitroimidazole by dimethyl sulfate in aqueous NaOH occurs 8 times faster at *N*1 than at *N*3 (Scheme 2)^[4] and a selective *N*1-attack was observed in the reactions of 2-methyl-4-nitroimidazole with alkyl halides or sulfates under

alkaline conditions (Scheme 3). These findings indicated the higher nucleophilicity of the *N1* compared to *N3* atom.^[5]

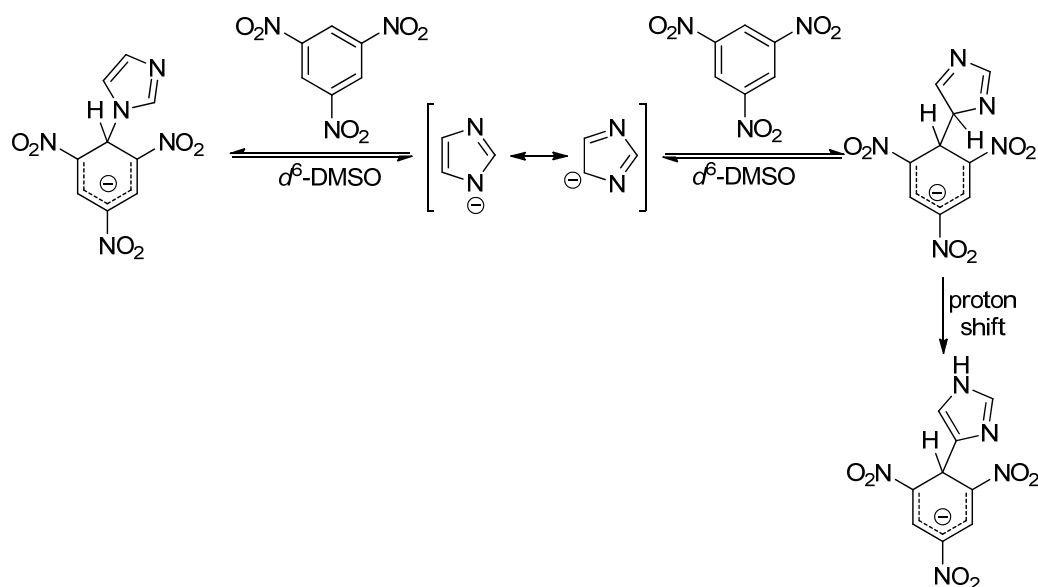


Scheme 2: Alkylation of the anion of 4-nitroimidazole with methyl sulfate in 90% water 10 % ethanol.^[4]



Scheme 3: Alkylation of the 2-methyl-5-nitroimidazole anion.^[5]

Furthermore, imidazole anions can also react as C-nucleophiles. A detailed analysis of the ambident reactivity (*N*- vs. *C*-attack) of imidazole anions was performed by Terrier and co-workers.^[6] The authors showed that the imidazole anion attacks trinitrobenzene under conditions of kinetic control at one of the two equivalent nitrogen atoms, but the attack at the carbon atom leads, after proton transfer, to the thermodynamically more stable product.^[6a] In the case of unsymmetrical imidazole anions (e.g., 4-methylimidazole), attack at both nitrogen atoms (*N1* : *N3* = 4 : 1) was observed under conditions of kinetic control and after several days, rearrangement, again including proton transfer, to the thermodynamically more stable product of *C*-attack was observed.^[6b]

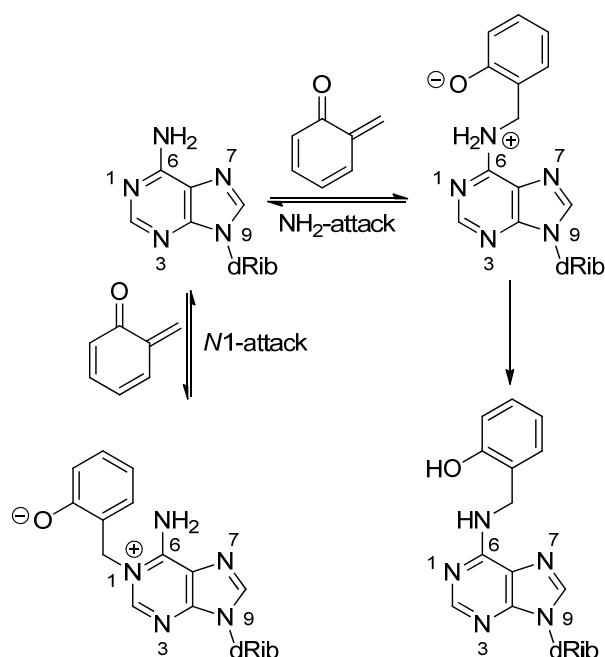


Scheme 4: Ambident reactivity of the imidazole anion toward trinitrobenzene.^[6]

The problem of ambident reactivity becomes even more complicated when purine derivatives are considered. In extensive studies, the groups of Freccero and Rokita examined the selectivities of the alkylation of purine bases by the parent *ortho*-quinone methide (Scheme 5).^[7]

Quantum-chemical calculations at B3LYP/6-311+G(d,p) level of theory predicted the following nucleophilic (i.e., kinetic) reactivity scale for adenine in water: $N3 > N7 \approx N1 \gg \text{NH}_2$, while a different sorting is obtained according to thermodynamic product stability ($\text{NH}_2 > N3 \approx N7 \gg N1$).^[7e] The time-dependent analysis of the adduct formation in the reaction of deoxyadenosine with the quinone methide showed a fast and reversible attack at $N1$. However, in a much slower but irreversible reaction at the amino group which additionally involves proton transfer, the thermodynamically more stable reaction product was obtained (Scheme 5).^[7c]

Some rare studies of purine anions, where the reactivity of the $N1$ - and $N3$ -position can be neglected, showed that the anions of purine nucleobases exclusively attack epoxides with $N9$,^[8] while mixtures resulting from $N9$ - and $N7$ -attack on dimethyl propargyl chloride in HMPT were observed.^[9]



Scheme 5: Alkylation of deoxyadenosine with the parent *ortho*-quinone methide in water.^[7c]

The control of *N1*- vs. *N3*-alkylation (see Scheme 1 for numbering) in uracil derivatives is very important for medical applications, and several strategies involving protective groups can be employed for the synthesis of the desired alkylation product.^[10] In reactions of uracil anions, preferred *N1*-alkylation was observed with methoxymethyloxirane,^[11] alkyl halides,^[12] or lactones^[13] in DMF and also Michael reactions of uracil anions with acrolein resulted in the predominant formation of the *N1*-alkylated product.^[14] However, *N1,N3*-dialkylated compounds are typically formed as side products in these reactions. The lack of *N3*-monoalkylated products cannot be attributed to the higher acidity of *N1*H in comparison with *N3*H, as Wittenburg^[15] as well as Ganguly and Kundu^[16] showed that thymine is first deprotonated at *N3* but this anion is in equilibrium with the anion bearing the negative charge at *N1*.

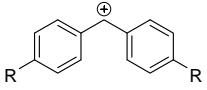
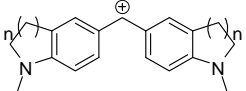
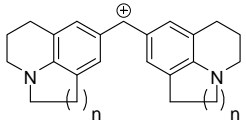
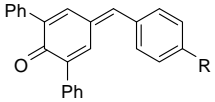
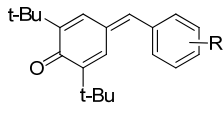
Gambacorta and co-workers explained the different *N/O* alkylation ratios with a qualitative hardness scale ($N1 < N3 < O4$) in uracil derivatives,^[17] employing the HSAB principle^[18] or the related Klopman-Salem concept of charge and orbital controlled reactions.^[19] However, we have recently shown that the ambident reactivity of other imide and amide anions cannot be explained with these concepts.^[20] Free amide and imide anions are selectively attacked at nitrogen by benzhydrylium ions and quinone methide and the attack at the oxygen terminus does only occur when the diffusion limit is reached or the nitrogen atom is blocked (e.g., by silver ions).

The fact that only little quantitative data on the reactivities of these important classes of heterocycles is known in the literature tempted us to study the nucleophilic reactivities of these compounds in detail. In earlier work, we have shown that benzhydrylium ions and structurally related quinone methides can be used as reference electrophiles with tunable reactivity for characterizing a large variety of nucleophiles.^[21] The second-order rate constants at 20 °C of the reactions of these nucleophiles have been described by Eq. (1),^[22] where s and N are nucleophiles-specific parameters and E is an electrophile-specific parameter.

$$\log k_2 = s(N + E) \quad (1)$$

To reduce the possible sites of nucleophilic attack (Scheme 1), we have only investigated the kinetics of the anions of several imidazoles (**2**), purines (**3**), and pyrimidines (**4**) (see Tables 2 and 3 for structures) with the reference electrophiles listed in Table 1 in DMSO and water in order to determine the nucleophilicities (N and s) of these nucleophiles and to include them into our comprehensive nucleophilicity scale.^[21e]

Table 1: Reference Electrophiles Employed in this Work and their Wavelengths Monitored in the Kinetic Experiments.

Electrophile		E^a	λ_{eval}	
	R = N(CH ₂ CH ₂) ₂ O	1a	-5.53	620
	R = NMe ₂	1b	-7.02	613
	R = N(CH ₂) ₄	1c	-7.69	620
	n = 2	1d	-8.22	618
	n = 1	1e	-8.76	627
	n = 2	1f	-9.45	635
	n = 1	1g	-10.04	630
	R = OMe	1h	-12.18	422
	R = NMe ₂	1i	-13.39	533
	R = 4-NO ₂	1j	-14.32	374
	R = 4-Me	1k	-15.83	371
	R = 4-OMe	1l	-16.11	393
	R = 4-NMe ₂	1m	-17.29	486

^a: Electrophilicity parameters from ref. ^[21a,b,g]

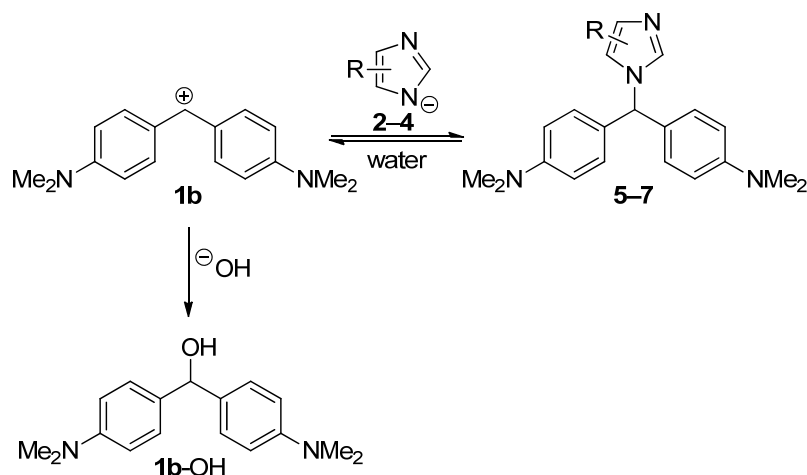
2 Results and Discussion

Reaction Products

In general, the anions of imidazoles **2a–g**, purines **3a–h**, and pyrimidines **4a–c** can react via different atoms and several reaction products may be obtained in the reactions of electrophiles with the anions of imidazoles (*N*1- vs. *N*3-attack), purine (*N*7- vs. *N*9-attack), and pyrimidine (*N*- vs. *O*-attack) (Scheme 1). As only anionic nucleophiles are investigated in this work, products resulting from attack at the *N*1/*N*3 nitrogen atoms in the purine compounds or at the *N*1 position in the pyrimidines are not among the expected reaction products.

When the potassium salts of **2–4** (between 1 and 5 equivalents) and the representative electrophile were combined in dry DMSO, complete decolorization of the solutions was observed in all cases (exception: reaction of **2e** with **1k**), indicating quantitative consumption of the electrophiles. The fact that some reaction products were only obtained in moderate yields after acidic work-up can be explained by non-optimized work-up procedures, or in the case of the reaction of **2e** with **1k** due to an equilibrium. Quinone methides were used as reaction partners for the more reactive imidazole anions **2a–e** and the blue benzhydrylium ion **1b** was employed for anions of lower reactivity. While the products formed from quinone methides are stable under the reaction conditions, most products formed from the benzhydrylium ion **1b** are unstable and are rapidly hydrolysed during aqueous work-up. Therefore, no further purification by means of chromatography or recrystallization was carried out for these compounds and the differentiation between different regioisomers was based on 2D-NMR experiments. The letters in the products **5–7** identify their origin; thus **5ak–I** is formed from **2a** and **1k**, while the ending **I** or **II** specifies which atom in the nucleophile was alkylated.

Complete decolorization of the reaction mixture was also observed, when the potassium salts of **2–4** were combined with the benzhydrylium ion **1b** in water. However, we were not able to isolate these reaction products in water, as the initially formed adducts undergo heterolysis and the regenerated benzhydrylium ions **1b** are then trapped by hydroxide to yield the benzhydrol **1b-OH** (Scheme 6).

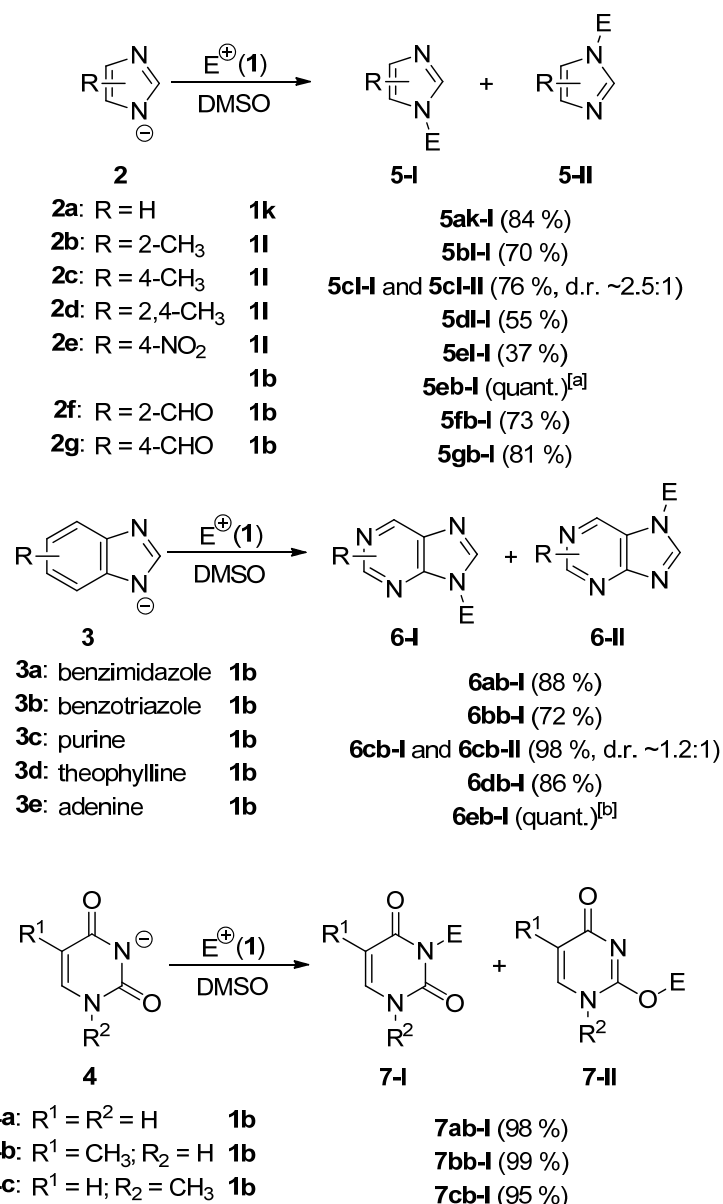


Scheme 6: Reversible reaction of the benzhydrylium ion **1b** with the nucleophiles **2–4**.

Scheme 7 shows that only one reaction product was obtained from symmetrically substituted heterocyclic anions. The unsymmetrically substituted anions of 4-methylimidazole (**2c**, 2.5 : 1) and of purine (**3c**, 1.2 : 1) yielded mixtures of two different regioisomers, whereas the anions of 2,4-dimethylimidazole (**2d**), 4-nitroimidazole (**2e**), 4-formylimidazole (**2g**), theophylline (**3d**), and adenine (**3e**), i.e., other unsymmetrically substituted anions, gave only one regioisomer. To exclude the fact that one isomer of the reaction with the benzhydrylium ion **1b** is lost under the employed reaction and work-up conditions, the combination reaction of **1b** with the best nucleofuge among the studied nucleophiles, i.e., the anion of 4-nitroimidazole (**2e**), which is therefore most likely reversible, was studied in d^6 -DMSO by means of NMR-spectroscopy. As here again, only one reaction product is observed, one has to conclude that the found regioselectivities are not due to partial decomposition.

Ambident Reactivity of Heterocyclic Anions

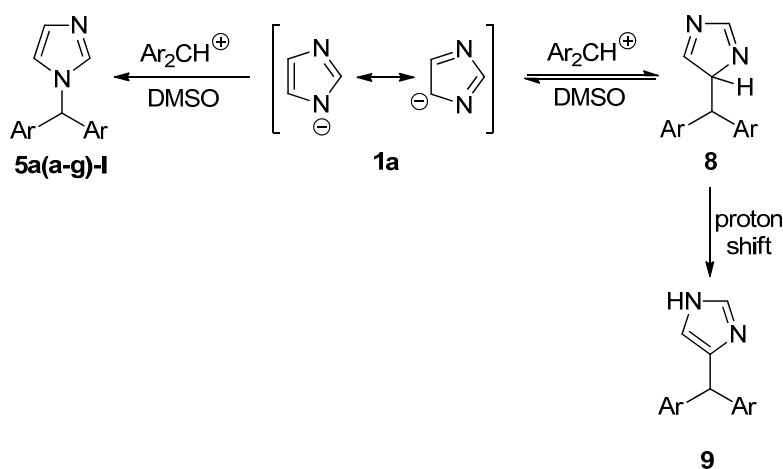
Due to symmetry, only one reaction product is obtained in the reactions of the imidazole anions **2a**, **2b**, and **2f** with the quinone methides **1k** or **1l** or the benzhydrylium ion **1b**. While most unsymmetrically substituted anions give rise only to one reaction product, the anions of 4-methylimidazole (**2c**) and of purine (**3c**) yielded mixtures of two isomers. In previous studies on neutral azoles a similar ratio for 4-methylimidazole **2c-H** (2.5 : 1) was found and a 1:1 mixture was obtained for 5-methylbenzimidazole which is structurally similar to purine, where a 1.2 : 1 ratio was observed.^[23] These findings are in line with previous studies on the methylation of 4-nitroimidazole by dimethyl sulfate in aqueous NaOH yielding a 9:1 ratio of *N*1- and *N*3-methylated imidazole,^[4] while selective *N*1-attack was observed in the reactions of 2-methyl-4-nitroimidazole with alkyl halides or sulfates under alkaline conditions.^[5]



Scheme 7: Isolated products of the reactions of the heterocyclic anions **2–4** with the reference electrophiles **1** in DMSO (for detailed structures see Table 2); ^[a]: not isolated, determined by ¹H-NMR, ^[b]: contains DMSO as impurity.

One has to conclude from the instability of the reaction products with **1b** that the products are obtained by thermodynamic product control and do not necessary reflect the initial kinetic distribution. In line with the thermodynamic product control is the fact that the higher steric repulsion in the minor isomer **5cl-II** leads to a higher product ratio than the smaller repulsion in **6cb-II** that gives almost equal amounts of both isomers.

The reactions of the azole anions **2** and **3** with benzhydrylium ions (Scheme 8) yielded only the products of nitrogen attack and no *C*-alkylation could be detected under these conditions in line with previous reports by Terrier for trinitrobenzene.^[6] **5a(a-g)-I** is thermodynamically favored over **8**, as the imidazole moiety in **8** no longer has an aromatic character. Furthermore, as nitrogen is more electronegative compared to carbon, the formation of **5a(a-g)-I** should also be favored by the intrinsic barrier.^[24] *C*-attack can be observed with trinitrobenzene as this arene is a better electrofuge than the studied benzhydrylium ions and therefore, *N*-alkylation is more reversible for trinitrobenzene.



Scheme 8: *C*- vs. *N*-alkylation of the imidazole anion **2a** with benzhydrylium ions in DMSO.

In line with earlier studies on imide and amide anions that are exclusively attacked by benzhydrylium ions and quinone methides,^[20] the pyrimidine anions **4a–c** are also selectively attacked at nitrogen by the studied electrophiles. While alkylation reactions of neutral amides often give rise to mixtures of *N*- and *O*-attack,^[25] amide anions are typically attacked at nitrogen.^[26] Oxygen-alkylation of amide anions has only been observed when the nitrogen terminus was blocked by silver ions.^[27]

Kinetic Investigations

The reactions of the heterocyclic anions **2–4** with benzhydrylium ions **1a–g** and structurally related quinone methides **1h–m** were performed in DMSO (Table 2) and water (Table 3) at 20 °C and were monitored by UV-Vis spectroscopy at or close to the absorption maxima of the electrophiles (Table 1, 371 < λ < 635 nm). To simplify the evaluation of the kinetic experiments, the nucleophiles were generally used in large excess over the electrophiles. Therefore, the concentrations of **2–4** remained almost constant throughout the reactions, and

pseudo-first-order kinetics were obtained in all runs. The first-order rate constants k_{obs} were then derived by least-squares fitting of the time-dependent absorbances A_t of the electrophiles to the exponential function $A_t = A_0 \exp(-k_{\text{obs}}t) + C$. Second-order rate constants were obtained as the slopes of plots of k_{obs} versus the concentration of the nucleophile (Figure 1).

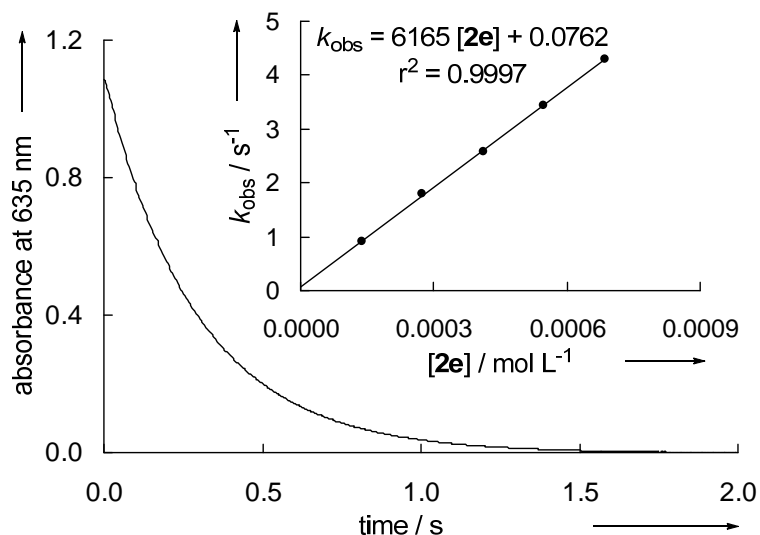
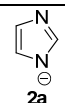
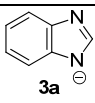
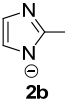
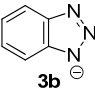
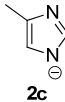
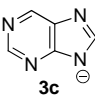
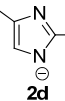
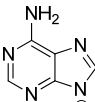
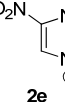
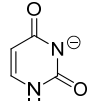
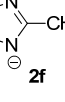
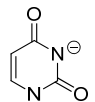
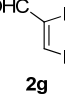
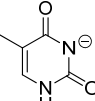


Figure 1: Plot of the absorbance (635 nm) vs. time for the reaction of **1e** with the anion of 4-nitroimidazole (**2e**) in DMSO at 20 °C and correlation of the first-order rate constants k_{obs} values with the concentration of **2e** (insert).

For the investigations in DMSO solution, the potassium salts of the nucleophiles **2–4** were used. As the presence of 18-crown-6 does not significantly change the observed kinetics (see the Experimental Section), one can conclude that the reactivities of the free anions were determined.

Due to their high reactivities, the imidazole potassium salts **2a–c-K** were not isolated in substance, but were generated by deprotonation of the corresponding imidazoles **2a–c-H** with $\text{KO}t\text{Bu}$ (typically 1.05 equivalents) in DMSO in the flasks used for the kinetic investigations. The fact that almost the same rate constants (for the reactions of **2b** with **1i,k** and of **2c** with **1h,i**, Table 2) were obtained when stoichiometric and substoichiometric (typically 0.7 equivalents) amounts of the base were used, indicates the complete deprotonation of the imidazoles by $\text{KO}t\text{Bu}$ ($\text{p}K_{\text{aH}} = 32.2$ in DMSO)^[28] in line with their much smaller $\text{p}K_{\text{aH}}$ -values compared to $\text{KO}t\text{Bu}$ (Figure 6).

Table 2: Second-Order Rate Constants for the Reactions of 2–4 with the Reference Electrophiles 1 in DMSO at 20 °C.

Nu	<i>N</i> / <i>s</i>	Electro- phile	<i>k</i> ₂ / L mol ⁻¹ s ⁻¹	Nu	<i>N</i> / <i>s</i>	Electro- phile	<i>k</i> ₂ / L mol ⁻¹ s ⁻¹
	21.09/ 0.51	1m	7.69×10^1		19.13/ 0.55	1k	6.88×10^1
		1l	3.82×10^2			1j	4.91×10^2
		1k	4.49×10^2			1i	9.32×10^2
		1j	3.97×10^3			1h	6.05×10^3
		1i	5.88×10^3			1g	9.17×10^4
		1h	3.28×10^4			1f	2.11×10^5
	21.32/ 0.50	1m	7.83×10^1		16.29/ 0.65	1i	7.11×10^1
		1l	4.54×10^2			1h	4.86×10^2
		1k	5.28×10^2			1g	1.18×10^4
			$5.25 \times 10^{2, a}$			1f	2.91×10^4
			6.72×10^3			1e	6.09×10^4
		1j	6.72×10^3			1d	1.81×10^5
		1i	7.20×10^3			1i	1.92×10^1
			$7.67 \times 10^{3, a}$			1h	1.43×10^2
			3.95×10^4			1g	9.23×10^3
			4.13×10^5			1f	2.16×10^4
	21.29/ 0.51	1m	9.47×10^1		15.03/ 0.77	1e	5.26×10^4
		1l	4.47×10^2			1d	1.51×10^5
		1k	6.74×10^2			1c	6.07×10^5
		1j	6.88×10^3			1i	1.05×10^1
		1i	7.40×10^3			1h	6.70×10^1
			$7.33 \times 10^{3, a}$			1g	2.32×10^3
			4.04×10^4			1f	5.81×10^3
			$3.98 \times 10^{4, a}$			1e	1.34×10^4
			6.38×10^5			1d	3.63×10^4
			9.19×10^1			1c	1.57×10^5
	20.69/ 0.60	1m	9.19×10^1		18.00/ 0.55	1h	1.51×10^3
		1l	5.80×10^2			1g	2.40×10^4
		1k	9.67×10^2			1f	5.02×10^4
		1j	1.03×10^4			1e	1.09×10^5
		1i	1.50×10^4			1i	2.15×10^2
		1h	1.43×10^5			1h	9.73×10^2
	14.81/ 0.71	1g	2.50×10^3		17.04/ 0.63	1g	3.66×10^4
		1f	6.16×10^3			1f	7.30×10^4
		1e	1.41×10^4			1e	1.56×10^5
		1d	4.60×10^4			1d	3.43×10^5
		1c	1.52×10^5			1i	9.71×10^1
		1b	2.66×10^5			1h	7.88×10^2
	16.06/ 0.68	1i	6.54×10^1		16.37/ 0.69	1h	7.88×10^2
		1h	4.04×10^2			1g	3.18×10^4
		1g	1.29×10^4			1f	5.32×10^4
		1f	3.02×10^4			1e	1.74×10^5
		1e	6.03×10^4			1d	3.25×10^5
		1d	1.65×10^5			1i	4.12×10^2
	16.40/ 0.67	1c	6.20×10^5		17.62/ 0.62	1h	2.20×10^3
		1i	1.22×10^2			1g	4.94×10^4
		1h	7.01×10^2			1f	1.05×10^5
		1g	1.82×10^4			1e	2.56×10^5
		1f	4.16×10^4			1d	6.93×10^5
		1e	1.13×10^5				
1d	3.13×10^5						
1c	1.10×10^6						

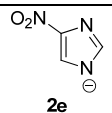
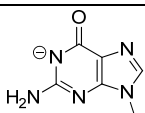
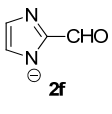
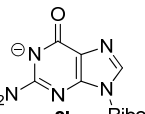
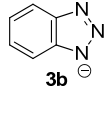
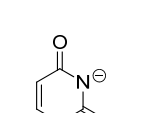
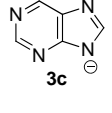
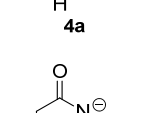
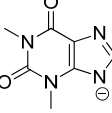
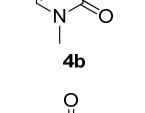
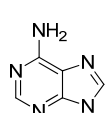
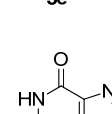
^a: KO^tBu was used as minor component.

Several combinations of heterocyclic anions **2–4** with the benzhydrylium ions **1b–g** were also studied in water (Table 3) and due to the low acidities of the heterocycles, aqueous solutions of these anions are partially hydrolyzed and contain hydroxide anions. Therefore, three competing reactions may account for the decay of the benzhydrylium ions in water and the observed rate constants k_{obs} for the consumption of the electrophiles in water reflect the sum of the reactions with the ambident nucleophiles **2–4** (k_2), with hydroxide ($k_{2,\text{OH}}$),^[29] and with water (k_w) [Eq. (1)].

$$k_{\text{obs}} = k_2[\mathbf{2-4}] + k_{2,\text{OH}}[\text{OH}^-] + k_w \quad (2)$$

$$k_{\text{eff}} = k_{\text{obs}} - k_{2,\text{OH}}[\text{OH}^-] = k_2[\mathbf{2-4}] + k_w \quad (3)$$

Table 3: Second-Order Rate Constants for the Reactions of **2–4** with the Reference Electrophiles **1** in Water at 20 °C.

Nu	<i>N</i> / <i>s</i>	p <i>K</i> _{aH}	Electro- phile	<i>k</i> ₂ / L mol ⁻¹ s ⁻¹	Nu	<i>N</i> / <i>s</i>	p <i>K</i> _{aH}	Electro- phile	<i>k</i> ₂ / L mol ⁻¹ s ⁻¹
 2e	11.37/ 0.53	9.10 ^[31]	1g	4.53 × 10 ⁰	 3g	10.76/ 0.65	9.80 ^[32]	1g	3.26 × 10 ⁰
			1f	1.27 × 10 ¹				1f	6.75 × 10 ⁰
			1e	1.98 × 10 ¹				1e	1.76 × 10 ¹
			1d	4.75 × 10 ¹				1b	2.79 × 10 ²
 2f	11.07/ 0.50	10.5 ^[33]	1g	3.27 × 10 ⁰	 3h Ribose	12.09/ 0.52	9.31 ^[34]	1g	1.41 × 10 ¹
			1f	6.21 × 10 ⁰				1f	1.73 × 10 ¹
			1e	1.49 × 10 ¹				1e	5.74 × 10 ¹
			1d	2.55 × 10 ¹				1d	9.48 × 10 ¹
 3b	11.52/ 0.67	8.57 ^[35]	1g	1.42 × 10 ¹	 4a	10.75/ 0.53	9.45 ^[36]	1c	2.07 × 10 ²
			1e	5.32 × 10 ¹				1g	2.71 × 10 ⁰
			1b	7.16 × 10 ²				1f	4.26 × 10 ⁰
			1a	1.56 × 10 ⁴				1e	1.08 × 10 ¹
 3c	11.00/ 0.54	8.93 ^[37]	1g	3.49 × 10 ⁰	 4b	8.54/ 0.77	9.99 ^[36]	1d	2.12 × 10 ¹
			1f	6.75 × 10 ⁰				1c	4.54 × 10 ¹
			1e	1.45 × 10 ¹				1e	7.26 × 10 ⁻¹
			1d	3.50 × 10 ¹				1d	1.41 × 10 ⁰
 3d	10.06/ 0.71	8.52 ^[38]	1g	1.07 × 10 ⁰	 4c	11.17/ 0.51	9.94 ^[36]	1c	5.57 × 10 ⁰
			1f	2.69 × 10 ⁰				1g	3.86 × 10 ⁰
			1e	8.01 × 10 ⁰				1f	6.92 × 10 ⁰
			1d	2.09 × 10 ¹				1e	1.80 × 10 ¹
 3e	10.93/ 0.61	9.80 ^[39]	1g	3.68 × 10 ⁰				1d	2.89 × 10 ¹
			1e	1.93 × 10 ¹				1c	1.06 × 10 ²
			1d	4.13 × 10 ¹				1b	2.40 × 10 ²
			1c	1.06 × 10 ²				1e	5.09 × 10 ¹
 3f	11.62/ 0.59	9.21 ^[40]	1b	2.40 × 10 ²				1d	1.09 × 10 ²
			1e	5.09 × 10 ¹				1c	1.60 × 10 ²
			1d	1.09 × 10 ²				1b	5.92 × 10 ²
			1c	1.60 × 10 ²					

All equilibrium concentrations in equation (2) were calculated from the initial concentrations and the pK_{aH} values, as described in the Experimental Section. Rearrangement of equation (1), i.e., subtraction of the contribution of hydroxide from the observed rate constant k_{obs} , yields equation (2), and the second-order rate constants for the reactions of the benzhydrylium ions with **2–4** can then be obtained from plots of k_{eff} versus the concentration of the nucleophiles. Usually, we were able to realize conditions, where the correction term did not exceed 10 % of k_{obs} by combining a large excess of the heterocycles (**2–4**)-H with only 0.02 to 0.2 equivalents of KOH. In rare cases, where the neutral species was almost insoluble in water, larger corrections had to be made, as here, 1 equivalent of KOH was needed to give clear solutions. The intercepts of these plots correspond to the reactions of the electrophiles with water and are generally negligible in agreement with previous work, where water ($N = 5.20$)^[30] was demonstrated to react much slower with benzhydrylium ions than the nucleophiles investigated in this work.

Furthermore, we have studied the influence of the solvent composition in the binary system DMSO/water. For that investigation we have systematically varied the DMSO/water ratio from 3 % v/v DMSO in water to pure DMSO and determined the second-order rate constants for the reaction of **1e** with **3d** in these mixtures. As the pK_{aH} value of **3d** is not known in these mixtures and as the corrections made by the consideration of the contribution of hydroxide (see Experimental Section) are typically very small for **3d**, the values in Figure 2 do not include a correction for hydroxide.

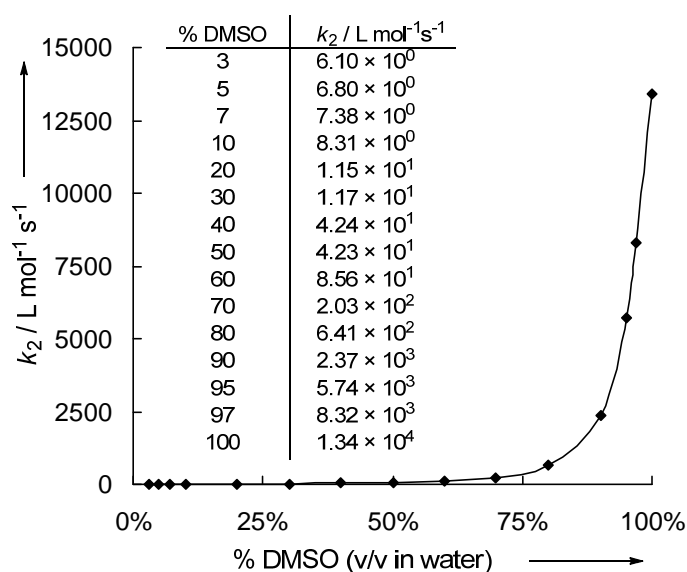


Figure 2: Dependence of the second-order rate constant k_2 of the reaction of the anion of theophylline (**3d**) with **1d** in DMSO-water-mixtures at 20 °C.

Correlation Analysis

Linear correlations were obtained in all cases, when $\log k_2$ for the reactions of the anionic nucleophiles **2–4** with the reference electrophiles **1** were plotted against the electrophilicity parameters E , as shown for some representative examples in Figure 3. As depicted in the Experimental Section, all other reactions investigated in this work followed analogous linear correlations indicating that equation (1) is applicable to these classes of nucleophiles. The slopes of these correlations are the nucleophile-specific parameter s , whereas the negative intercepts on the abscissa ($\log k_2 = 0$) correspond to the nucleophilicity parameters N .

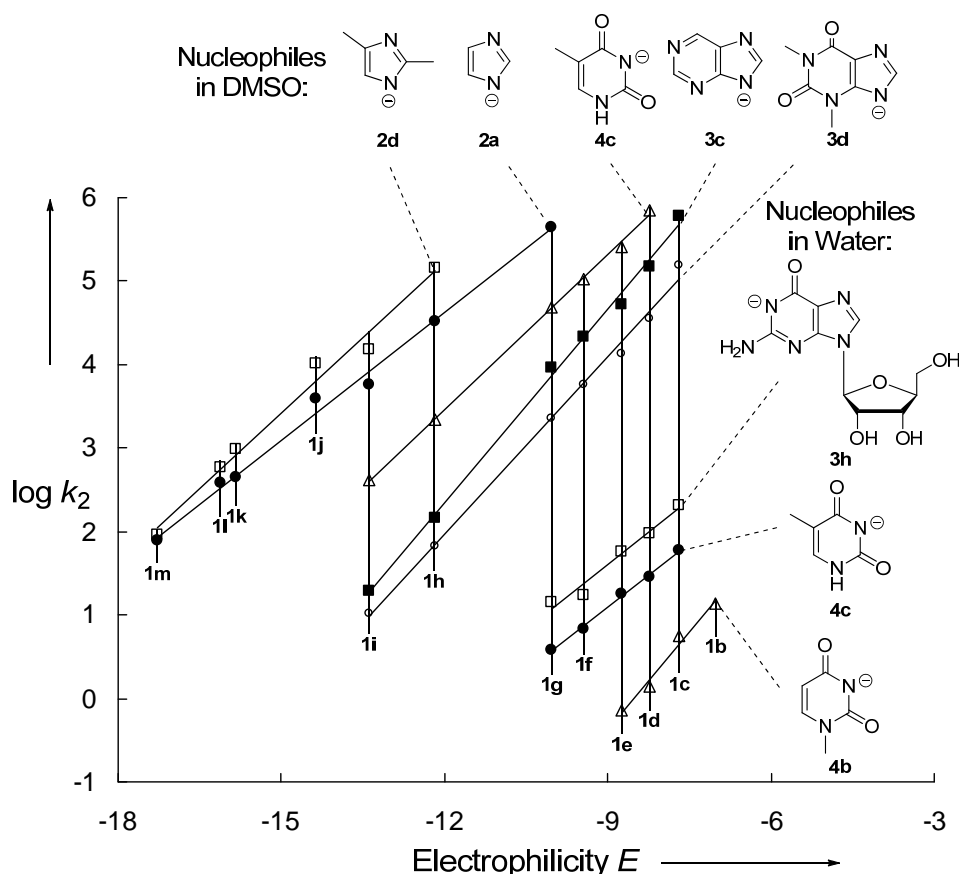
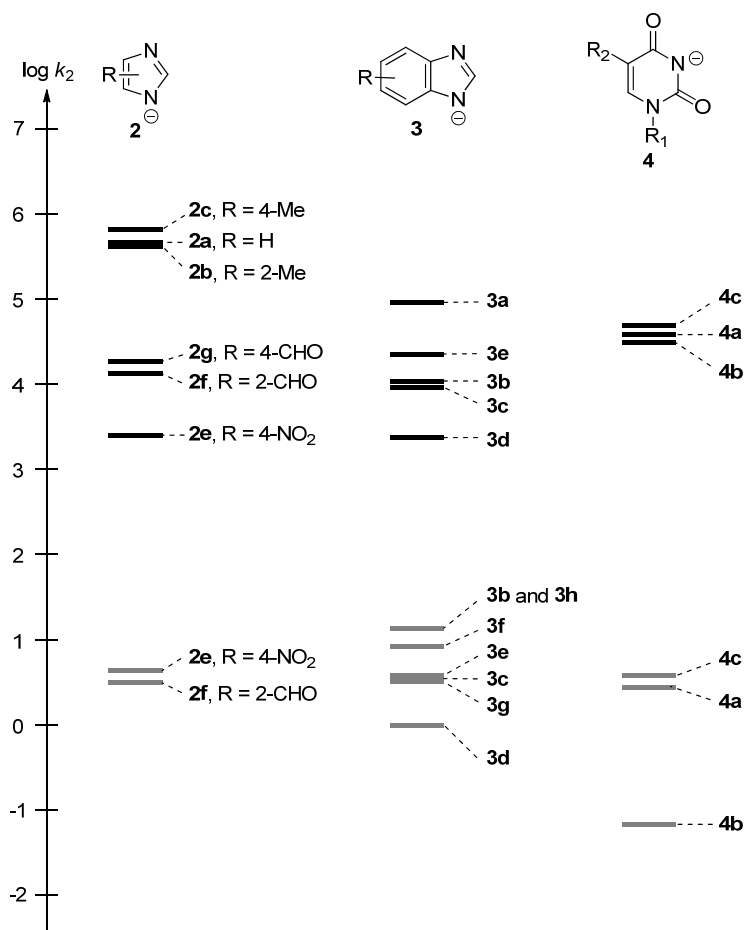


Figure 3: Plots of the rate constants $\log k_2$ for the reactions of the heterocyclic anions **2–4** with reference electrophiles **1** in DMSO and water versus their electrophilicity parameters E .

Structure Reactivity Relationships

The narrow range of s for all nucleophiles listed in Table 2 and Table 3 ($0.51 < s < 0.77$ in DMSO and $0.50 < s < 0.77$ in water), which is illustrated by the almost parallel correlation lines in Figure 3 implies that the relative reactivities of these anions depend only slightly on the electrophilicity of the reaction partner. The reactivities towards the benzhydrylium ion **1g**, for which most rate constants have directly been measured, therefore, reflect general structure reactivity trends (Scheme 9).



Scheme 9: Comparison of the gross reactivities of azole anions with the benzhydrylium ion **1g** in DMSO (black) and water (grey) (20 °C) [Entries for **3f** and **4b** in water were calculated using Eq. (1)].

The decreasing nucleophilicities of the imidazole anions **2** in the left column of Scheme 9 can be explained by a better stabilization of the negative charge by electron-withdrawing substituents. This is also reflected by the correlation with the Hammett parameters σ_p , σ_p^- , and σ_m plots depicted in Figure 4. The slopes of these correlations, i.e., the negative reaction constants ρ , show that electron-withdrawing substituents are decelerating the reaction and that there are fewer electrons at the reaction center in the transition state than in the starting material. As linear correlations are obtained for all Hammett parameters, one can conclude that inductive effects (σ_m) are more important for imidazole anions than mesomeric effects (σ_p and σ_p^-).

Furthermore, a comparison of the reactivities of **2b** and **2c** as well as of **2f** and **2g** (Scheme 9) reveals that the relative position of the substituent, i.e., whether the substituent is in 2- or in 4-position, is of minor relevance for the nucleophilicity of imidazole anions.

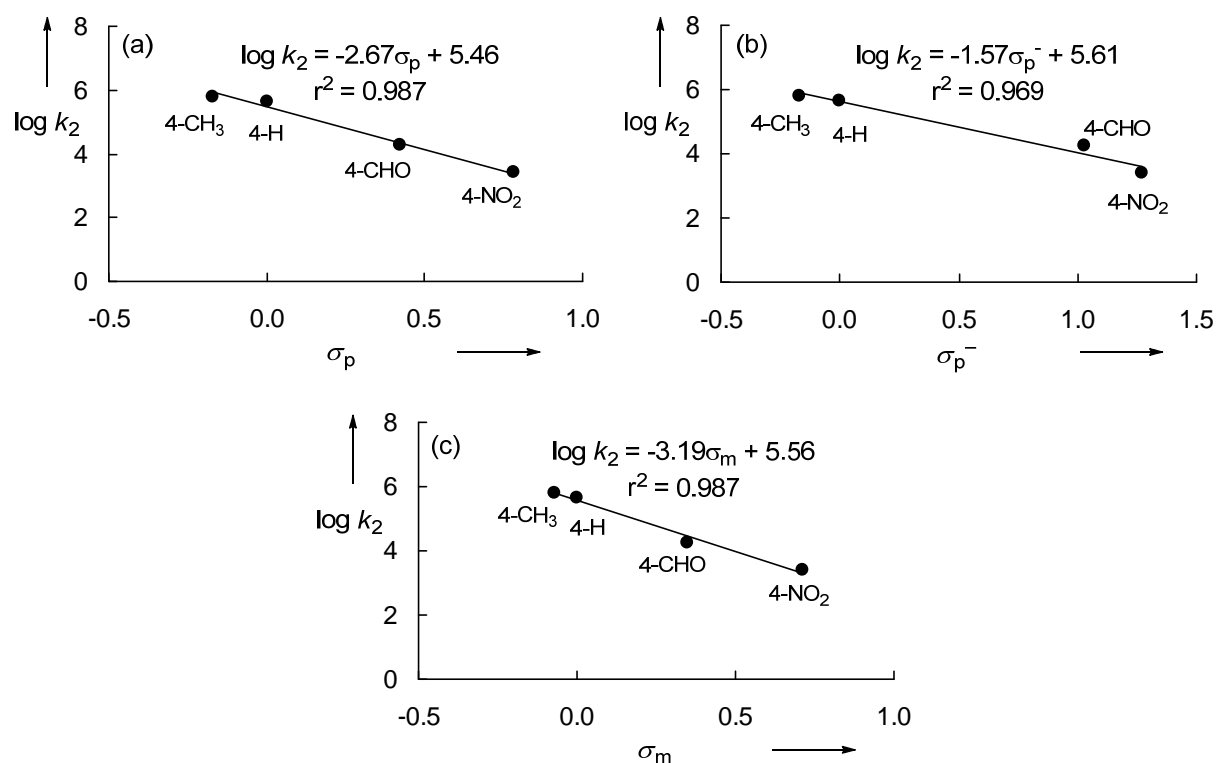


Figure 4: Correlation of Hammett substitution constants σ_p (a), σ_p^- (b), and σ_m (c) vs. the rate constant ($\log k_2$) for the reactions of different 4-substituted imidazole anions **2** with the benzhydrylium ion **1g** in DMSO at 20 °C.

A comparison of the reactivities of the anions of imidazole (**2a**), benzimidazole (**3a**), and benzotriazole (**3b**) shows that the annelation of a benzene ring (**2a** \rightarrow **3a**) reduces the nucleophilicity by a factor of 4.8 and furthermore by a factor of 37 when an additional nitrogen is incorporated in the five-membered ring (**2a** \rightarrow **3b**). A ten-fold decrease is found when the phenyl ring in **3a** is exchanged by the more electron-withdrawing pyrimidine ring in **3c**, which is partially compensated by the additional amino group in the adenine anion **3e**. Annelation of an uracil ring causes an even stronger reduction in reactivity and the anion of theophylline (**3d**) is even less reactive than the 2- or 4-formyl substituted imidazole anions **2f** and **2g**.

The degree of methylation of the anions of pyrimidones **4** does not strongly affect their nucleophilicities (right column in Scheme 9) and the anions of uracil (**4a**), 1-methyluracil (**4b**), and thymine (**4c**) are positioned between the anions of benzimidazole (**3a**) and adenine (**3e**) in Scheme 9.

Due to their low solubility in DMSO even in the presence of 18-crown-6, the purine anions **3f–3h** were only studied in water. In this solvent, all compounds were found within a very small reactivity range that only covers 1 order of magnitude. The guanine anion **3f** where the carbamate structure of theophylline is replaced by a guanidinium structure is 8 times more reactive than **3d**. A change from the imidazole anion in guanidine to the amide anion in 9-methyl guanine (**3f** → **3g**) goes along with a decrease of reactivity by a factor of 2.6. However, when the methyl group is exchanged by ribose in the anion of guanosine (**3h**), an increase of reactivity by a factor of 4.3 is found.

Solvent Effects

A large decrease of reactivity is found when DMSO is replaced by water as the solvent (Figure 3, Table 2, and Table 3). While the pyrimidine anions **4a** and **4c** react approximately 10000 times slower in water than in DMSO, a factor of only 500 – 5000 is found for the azole anions **2** and **3**. Furthermore, Figure 2 reveals that the addition of 20 % DMSO to water has almost no effect on the second-order rate constant of the reaction of **3d** with **1d**, while the addition of 20 % water to DMSO reduces the reactivity by a factor of 20. These effects can be rationalized by the formation of hydrogen bonds of the anions **2–4** towards water which reduces the negative charge and thereby the reactivity of the anionic nucleophile. Obviously, a relatively small portion of water is sufficient for the formation of hydrogen bonds and already leads to a lowered nucleophilicity.

However, a remarkable difference can be found in the behavior of the anion of 1-methyluracil (**4b**) in comparison to the other pyrimidine anions uracil (**4a**) and thymine (**4c**). While **4a** and **4c** react only 13000 times slower in water than in DMSO, a decrease of reactivity by a factor of 450000 is found for the anion of 1-methyluracil **4b**. A possible explanation for this deviation can be derived from the findings of Wittenburg^[15] and Ganguly and Kundu^[16] who showed that thymine is first deprotonated at *N3* but this anion is in equilibrium with the anion bearing the negative charge at *N1*. As no product studies are available in water due to the instability of the formed adducts, it might be possible, that the anions of uracil (**4a**) and thymine (**4c**) are also attacked at *N1* while this reaction center is blocked in the anion of 1-methyluracil (**4b**).

Comparison with Neutral Nucleophiles

Figure 5 shows that the azole anions **2** and **3** are approximately 20000 times more nucleophilic in DMSO than their conjugate acids. As several neutral imidazoles have previously been demonstrated to be equally reactive in DMSO and acetonitrile, rate constants for neutral azoles in acetonitrile have been employed for the comparison in Figure 5 when data in DMSO were not available.

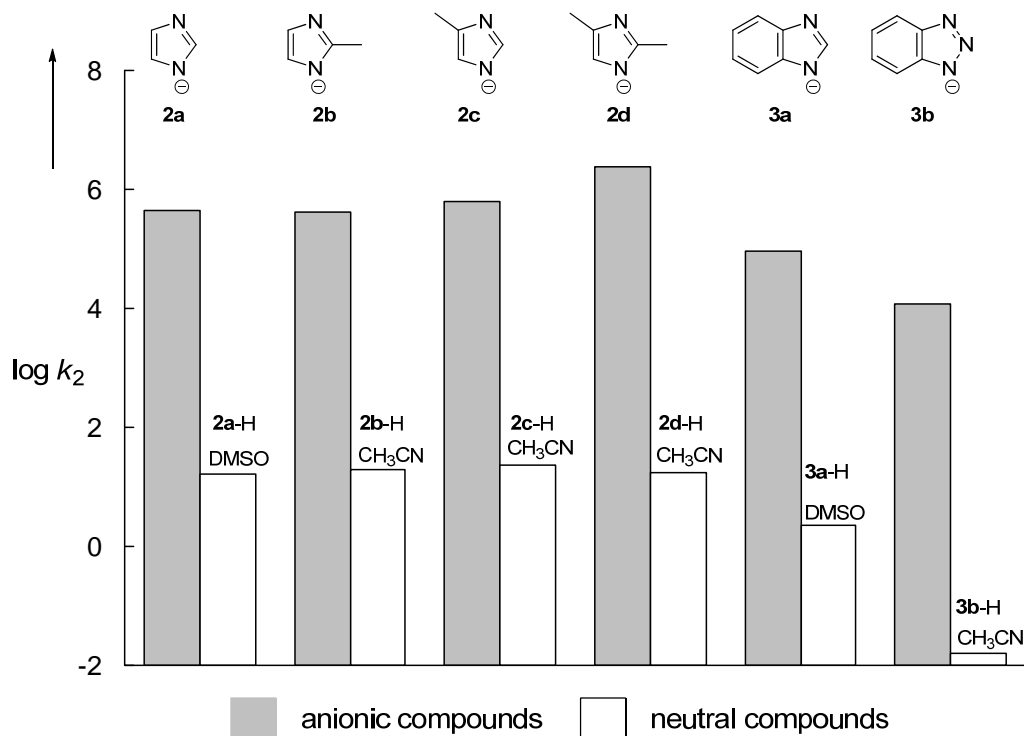


Figure 5: Comparison of the second-order rate constants of the reaction of **1g** with either the heterocyclic anions **2** and **3** or with their neutral analogues **2-H** or **3-H** (from ref. [23]) in DMSO or CH₃CN.

Correlation with Brønsted Basicities

Brønsted basicity is often used as a tool to estimate the nucleophilic reactivity despite the poor quality that is often obtained in these correlations. Figure 6 shows that the correlation between reactivity towards the benzhydrylium ion **1g** and Brønsted basicity in DMSO is remarkably good whereas no relation between basicity and nucleophilicity is found in water. Though only few pK_{aH} values for the anions **2–4** are available in DMSO, the slope obtained for the heterocyclic anions **2–4** is similar to that obtained for other amide and imide anions.^[20]

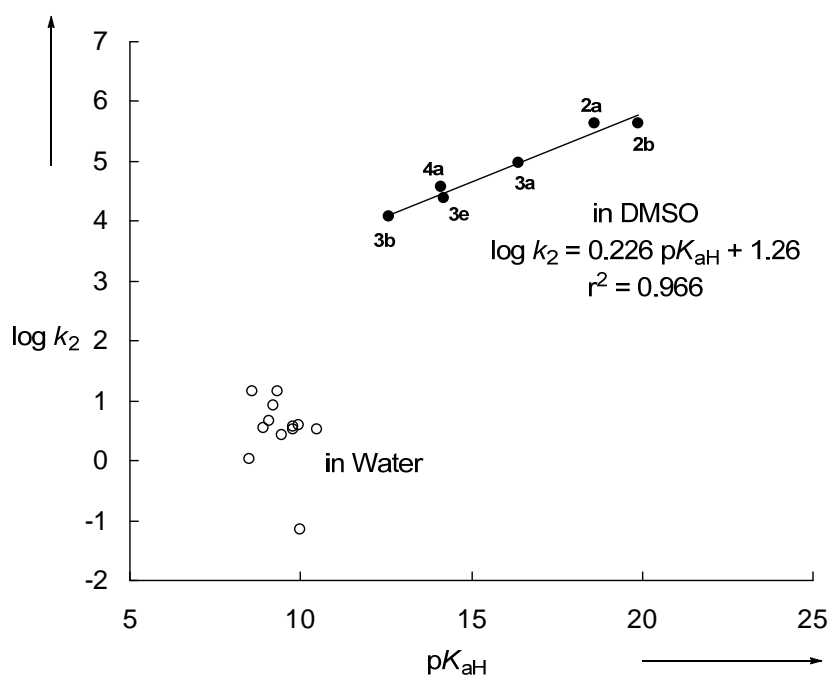


Figure 6: Relationship between Brønsted basicity and $\log k_2$ for the reaction of **1g** with several heterocyclic nucleophiles in DMSO (●) and Water (○). [pK_{aH} in DMSO: **2a**: 18.6 (ref. ^[41]), **2b**: 19.9 (ref. ^[42]), **3a**: 16.4 (ref. ^[41]), **3b**: 12.6 (ref. ^[42]), **3e**: 14.2 (ref. ^[41]), **4a**: 14.1 (ref. ^[41]); pK_{aH} in water: see Table 3].

3 Conclusion

The rate constants for the reactions of imidazole, purine, and pyrimidine anions with quinone methides and benzhydrylium ions follow the linear free-energy relationship (1), which allows us to include these compounds into our comprehensive nucleophilicity scales and compare their nucleophilicity with those of other nucleophiles (Figure 7). In DMSO, these heterocyclic anions cover more than 6 order of reactivity and are comparable to carbanions, amide and imide anions or amines while in water, a smaller range of reactivity is observed. The poor correlation between Brønsted basicity and nucleophilicity in water shows that pK_{aH} values cannot be used for the prediction of relative reactivities. This deviation may be due to the fact that pK_{aH} values refer to reactions with the proton, while the nucleophilicity parameters N refer to reactions with carbon electrophiles. The knowledge of carbon basicities is needed to elucidate the reason for the breakdown of the Brønsted correlations.

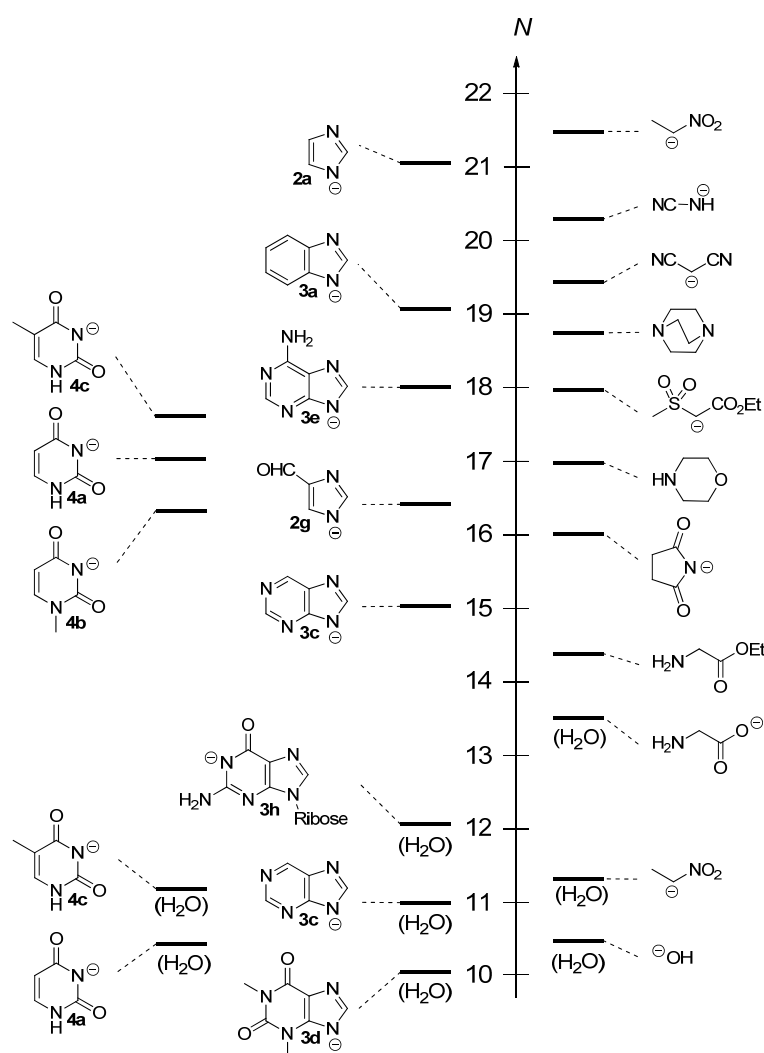


Figure 7: Comparison of the nucleophilicities N of heterocyclic anions with other C- and N nucleophiles in DMSO and water (data in water are marked).^[21e]

4 Experimental Section

In order to identify my contributions to this part, the Experimental Sections exclusively consist of the experiments performed by me.

4.1 General

Materials

Commercially available DMSO and acetonitrile (both: H₂O content < 50 ppm) were used without further purification. Water was distilled and passed through a Milli-Q water purification system. The reference electrophiles used in this work were synthesized according to literature procedures.^[21a,b,g]

NMR spectroscopy

In the ^1H - and ^{13}C -NMR spectra chemical shifts are given in ppm and refer to tetramethylsilane ($\delta_{\text{H}} = 0.00$, $\delta_{\text{C}} = 0.0$), d^6 -DMSO ($\delta_{\text{H}} = 2.50$, $\delta_{\text{C}} = 39.5$), CDCl_3 ($\delta_{\text{H}} = 7.26$, $\delta_{\text{C}} = 77.0$), or to D_2O ($\delta_{\text{H}} = 4.79$, ^{13}C spectra in D_2O refer to a few droplets of CD_3OD ($\delta_{\text{C}} = 49.5$) or d^6 -acetone ($\delta_{\text{C}} = 30.9$))^[43] as internal standards. The coupling constants are given in Hz. For reasons of simplicity, the ^1H -NMR signals of AA'BB'-spin systems of *p*-disubstituted aromatic rings are treated as doublets. Signal assignments are based on additional COSY, gHSQC, and gHMBC experiments.

Kinetics

As the reactions of colored benzhydrylium ions or quinone methides with colorless nucleophiles result in colorless products, the reactions could be followed by UV-Vis spectroscopy. Slow reactions ($\tau_{1/2} > 10$ s) were determined by using conventional UV-Vis-spectrophotometers. Stopped-flow techniques were used for the investigation of rapid reactions ($\tau_{1/2} < 10$ s). The temperature of all solutions was kept constant at 20.0 ± 0.1 °C during all kinetic studies by using a circulating bath thermostat. In all runs the nucleophile concentration was at least 10 times higher than the concentration of the electrophile, resulting in pseudo-first-order kinetics with an exponential decay of the electrophile's concentration. First-order rate constants k_{obs} were obtained by least-squares fitting of the absorbance data to a single-exponential $A_t = A_0 \exp(-k_{\text{obs}}t) + C$. The second-order rate constants k_2 were obtained from the slopes of the linear plots of k_{obs} against the nucleophile's concentration.

Determination of rate constants in water:

The combination reactions of the anionic nucleophiles **2–4** with benzhydrylium ions were also studied in water. Due to the low acidities of the neutral heterocycles ($8.5 < \text{p}K_{\text{a}} < 10.5$, Table 2), aqueous solutions of the anions **2–4** are partially hydrolyzed and contain hydroxide anions. Therefore, the neutral heterocycles, which are used in high excess over the electrophiles (pseudo-first-order conditions), were deprotonated with only 0.02 to 0.2 equivalents of KOH. For these deprotonation reactions [Eq. (S1)], one can calculate the equilibrium constants as shown in equation (S2). Applying the mass balances [Eqs (S3) and (S4)], where the index “0” stands for the initial concentration and “eff” for the equilibrium concentration, equation (S2) can be rewritten as a quadratic equation (S5) with its positive solution (S6).



$$K = [\text{Nu}^-]_{\text{eff}} / ([\text{Nu-H}]_{\text{eff}} [\text{OH}^-]_{\text{eff}}) = 1 / K_B \quad (\text{S2})$$

$$[\text{OH}^-]_0 = [\text{OH}^-]_{\text{eff}} + [\text{Nu}^-]_{\text{eff}} \quad (\text{S3})$$

$$[\text{Nu-H}]_0 = [\text{Nu}^-]_{\text{eff}} + [\text{1-Nu}]_{\text{eff}} \quad (\text{S4})$$

$$[\text{OH}^-]_{\text{eff}}^2 - [\text{OH}^-]_{\text{eff}} ([\text{Nu-H}]_0 - [\text{OH}^-]_0 + K_B) - K_B [\text{OH}^-]_0 = 0 \quad (\text{S5})$$

$$[\text{OH}^-]_{\text{eff}} = 0.5 (-[\text{Nu-H}]_0 - [\text{OH}^-]_0 + K_B + (([\text{Nu-H}]_0 - [\text{OH}^-]_0 + K_B)^2 + 4K_B[\text{OH}^-]_0)^{1/2}) \quad (\text{S6})$$

The observed rate constants k_{obs} for the reactions in water reflect the sum of the reaction of the electrophiles with the heterocyclic anions **2–4** (k_2), with hydroxide ($k_{2,\text{OH}}$) and with water (k_w) [Eq. (S7)]. Rearrangement of equation (S7), i.e., subtracting the contribution of hydroxide from the observed rate constant k_{obs} , yields equation (S8). The second-order rate constants for the reactions of the benzhydrylium ions with **2–4** can then be obtained from plots of k_{eff} versus the concentration of the nucleophiles. The intercepts of these plots correspond to the reactions of the electrophiles with water and are generally negligible in agreement with previous work, showing that water ($N = 5.20$)^[30] reacts much slower with benzhydrylium ions than the nucleophiles investigated in this work.

$$k_{\text{obs}} = k_2[\text{Nu}^-] + k_{2,\text{OH}}[\text{OH}^-] + k_w \quad (\text{S7})$$

$$k_{\text{eff}} = k_{\text{obs}} - k_{2,\text{OH}}[\text{OH}^-] = k_2[\text{Nu}^-] + k_w \quad (\text{S8})$$

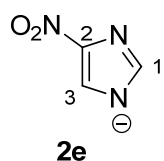
4.2 Synthesis of the Heterocyclic Potassium Salts

General Procedure

The NH-acid was added to a solution of KO t Bu in dry ethanol or to a solution of KOH in water and the mixture was stirred for 10 minutes. The solvent was subsequently evaporated under reduced pressure and the solid residue was washed several times with dry ether and filtrated under N₂. The benzimidazole-potassium salt **3b-K** was prepared as already described for the sodium salt.^[44] 1-Methyuracil was synthesized according to ref. ^[45].

Potassium Salt of 4-Nitroimidazole (2e-K)

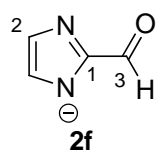
4-Nitroimidazole (2.00 g, 17.7 mmol) and KO t Bu (1.98 g, 17.6 mmol) furnished 4-nitroimidazol-potassium **2e-K** (2.60 g, 17.2 mmol, 97 %).



$^1\text{H-NMR}$ (d_6 -DMSO, 400 MHz) δ = 7.10 (s, 1 H, 1-H), 7.72 (s, 1 H, 3-H).
 $^{13}\text{C-NMR}$ (d_6 -DMSO, 101 MHz) δ = 132.0 (d, C-3), 146.3 (d, C-1), 148.2 (s, C-2).

Potassium Salt of 2-Formylimidazole (2f-K)

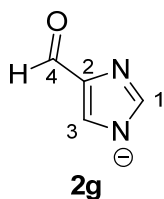
2-Formylimidazole (2.00 g, 25.4 mmol) and KO t Bu (2.30 g, 20.5 mmol) gave 2-formylimidazol-potassium **2f-K** (2.50 g, 18.6 mmol, 91 %).



$^1\text{H-NMR}$ (d_6 -DMSO, 400 MHz) δ = 7.07 (s, 2 H, 2-H), 9.35 (s, 1 H, 3-H).
 $^{13}\text{C-NMR}$ (d_6 -DMSO, 101 MHz) δ = 133.1 (d, C-2), 156.1 (s, C-1), 182.4 (s, C-3).

Potassium Salt of 4-Formylimidazole (2g-K)

4-Formylimidazole (1.50 g, 15.6 mmol) and KO t Bu (1.70 g, 15.2 mmol) yielded 4-formylimidazol-potassium **2g-K** (1.90 g, 14.2 mmol, 93 %).



$^1\text{H-NMR}$ (d_6 -DMSO, 400 MHz) δ = 7.34 (s, 1 H, 1-H), 7.61 (s, 1 H, 3-H), 9.43 (s, 1 H, 4-H). $^{13}\text{C-NMR}$ (d_6 -DMSO, 101 MHz) δ = 140.8 (s, C-2), 142.2 (d, C-3), 149.3 (d, C-1), 181.5 (s, C-4).

Potassium Salt of Benzotriazole (3a-K)

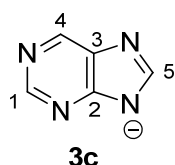
Benzotriazole (2.12 g, 17.8 mmol) and KOH (1.00 g, 17.8 mmol) furnished benzotriazole-potassium **3a-K** (2.74 g, 17.4 mmol, 98 %).



$^1\text{H-NMR}$ (d_6 -DMSO, 400 MHz) δ = 6.95-6.98 (m, 2 H, 2-H), 7.68-7.70 (m, 2 H, 3-H). $^{13}\text{C-NMR}$ (d_6 -DMSO, 101 MHz) δ = 115.8 (d, C-3), 119.7 (d, C-2), 144.8 (s, C-1).

Potassium Salt of Purine (3c-K)

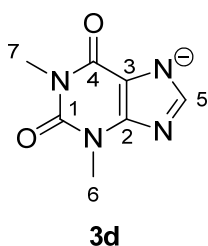
Purine (306 mg, 2.55 mmol) and KOH (143 mg, 2.55 mmol) yielded purine-potassium **3c-K** (390 mg, 2.47 mmol, 97 %).



$^1\text{H-NMR}$ (d_6 -DMSO, 400 MHz) $\delta = 7.95$ (s, 1 H, 5-H), 8.45 (s, 1 H, 1-H), 8.63 (s, 1 H, 4-H). $^{13}\text{C-NMR}$ (d_6 -DMSO, 101 MHz) $\delta = 136.7$ (s, C-3), 142.1 (d, C-4), 147.8 (d, C-1), 157.6 (d, C-5), 163.4 (s, C-2).

Potassium Salt of Theophylline (3d-K)

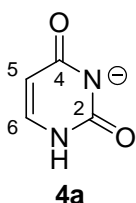
Theophylline (2.25 g, 12.5 mmol) and KOH (700 mg, 12.5 mmol) gave theophylline-potassium **3d-K** (2.65 g, 12.1 mmol, 98 %).



$^1\text{H-NMR}$ (D_2O , 400 MHz) $\delta = 3.17$ (s, 3 H, 7-H), 3.29 (s, 3 H, 6-H), 7.43 (s, 1 H, 5-H). $^{13}\text{C-NMR}$ ($\text{D}_2\text{O}/\text{CD}_3\text{OD}$, 101 MHz) $\delta = 29.4$ (q, C-7), 31.7 (q, C-6), 115.2 (s, C-3), 148.6 (d, C-5), 150.8 (s, C-2), 153.8 (s, C-1), 195.9 (s, C-4).

Potassium Salt of Uracil (4a-K)

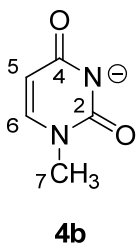
Uracil (1.51 g, 13.5 mmol) and KOH (756 mg, 13.5 mmol) yielded uracil-potassium **4a-K** (1.98 g, 13.2 mmol, 98 %).



Melting point: 310 – 312 °C (from EtOH/water). $^1\text{H-NMR}$ (D_2O , 400 MHz) $\delta = 5.70$ (dd, $^3J = 6.8$ Hz, $^4J = 0.6$ Hz, 1 H, 5-H), 7.58 (dd, $^3J = 6.8$ Hz, $^3J = 0.7$ Hz, 1 H, 6-H). $^{13}\text{C-NMR}$ ($\text{D}_2\text{O}/d^6$ -acetone, 101 MHz) $\delta = 101.4$ (d, C-5), 152.3 (d, C-6), 162.6 (s, C-2), 174.6 (s, C-4).

Potassium Salt of 1-Methyluracil (4b-K)

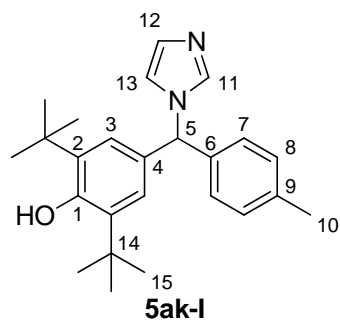
1-Methyluracil (900 mg, 7.14 mmol) and KOH (400 mg, 7.13 mmol) afforded 1-methyluracil-potassium **4b-K** (1.12 g, 6.82 mmol, 96 %).



$^1\text{H-NMR}$ (D_2O , 400 MHz) $\delta = 3.36$ (s, 3 H, 7-H), 5.75 (d, $^3J = 7.3$ Hz, 1 H, 5-H), 7.50 (d, $^3J = 6.8$ Hz, 1 H, 6-H). $^{13}\text{C-NMR}$ ($\text{D}_2\text{O}/d^6$ -acetone, 101 MHz) $\delta = 38.1$ (q, C-7), 103.0 (d, C-5), 148.0 (d, C-6), 160.8 (s, C-2), 177.1 (s, C-4).

Potassium Salt of Thymine (4c-K)

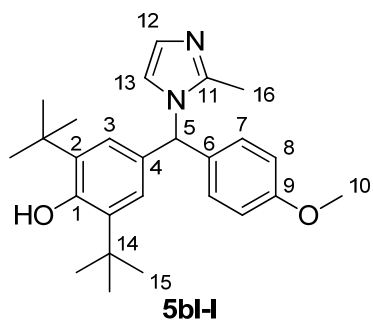
Thymine (1.26 mg, 9.99 mmol) and 0.5 M aqueous KOH solution (20.0 mL, 10.0 mmol) yielded thymine-potassium **4c-K** (1.60 g, 9.74 mmol, 97 %).



Melting point: 148–150 °C (from CH₂Cl₂/pentane). ¹H-NMR (CDCl₃, 300 MHz) δ = 1.37 (s, 18 H, 15-H), 2.35 (s, 3 H, C-10), 5.34 (s, 1 H, OH), 6.37 (s, 1 H, 5-H), 6.83 (s, 1 H, 13-H), 6.91 (s, 2 H, 3-H), 6.98 (d, ³*J* = 8.1 Hz, 2 H, 7-H), 7.07 (s, 1 H, 12-H), 7.15 (d, ³*J* = 7.9 Hz, 2 H, 8-H), 7.37 (s, 1 H, 11-H). ¹³C-NMR (CDCl₃, 75.5 MHz) δ = 21.1 (q, C-10), 30.2 (q, C-15), 34.4 (s, C-14), 65.2 (d, C-5), 119.4 (d, C-13), 125.0 (d, C-3), 127.7 (d, C-7), 129.0 (d, C-12), 129.3 (d, C-8), 129.6 (s, C-4), 136.3 (s, C-2), 137.1 (s, C-6), 137.4 (s, C-9), 137.8 (d, C-11), 153.7 (s, C-1). HR-MS (ESI) [M-H]⁻: *m/z* calcd for C₂₅H₃₁N₂O⁻: 375.2442 found: 375.2448.

Product of the Reaction of 2-Methylimidazole-Potassium (2b-K) with the Quinone Methide 11

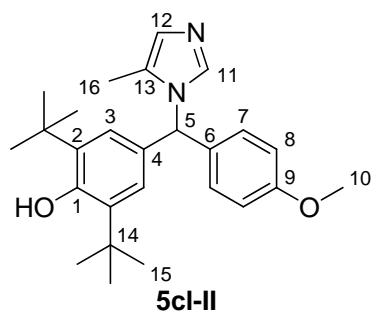
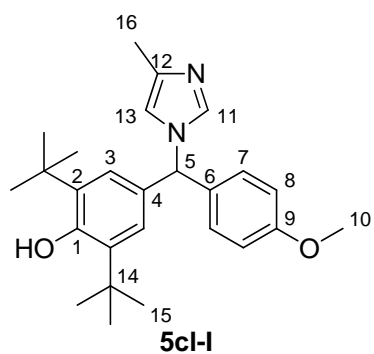
According to GP1, 2-methylimidazole (127 mg, 1.55 mmol), KO^tBu (176 mg, 1.57 mmol) and **11** (103 mg, 0.317 mmol) afforded 2,6-di-*tert*-butyl-4-((4-methoxyphenyl)(2-methyl-1*H*-imidazol-1-yl)methyl)phenol **5bl-I** (90.0 mg, 0.230 mmol, 70 %) as colorless crystals.



Melting point: 141–143 °C (from CH₂Cl₂/pentane). ¹H-NMR (CDCl₃, 300 MHz) δ = 1.36 (s, 18 H, 15-H), 2.31 (s, 3 H, 16-H), 3.81 (s, 3 H, 10-H), 5.29 (s, 1 H, OH), 6.30 (s, 1 H, 5-H), 6.52 (d, ³*J* = 1.4 Hz, 1 H, 13-H), 6.84–6.88 (m, 5 H, 3-H, 8-H, and 12-H), 6.93–6.96 (m, 2 H, 7-H). ¹³C-NMR (CDCl₃, 75.5 MHz) δ = 13.5 (q, C-16), 30.2 (q, C-15), 34.4 (s, C-14), 55.3 (q, C-10), 63.4 (d, C-5), C-12), 129.1 (d, C-7), 132.0 (s, C-6), 136.2 (s, C-2), 145.0 (s, 114.0 (d, C-8), 118.6 (d, C- C-11), 153.5 (s, C-1), 159.1 (s, C-9). HR-MS (ESI) [M+H]⁺: 13), 125.1 (d, C-3), 126.3 (d, *m/z* calcd for C₂₆H₃₅N₂O₂⁺: 407.2693 found: 407.2695.

Product of the Reaction of 4-Methylimidazole-Potassium (2c-K) with the Quinone Methide 11

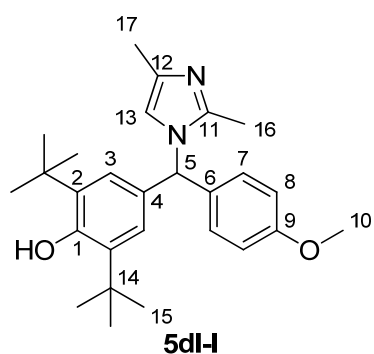
According to GP1, 4-methylimidazole (76.0 mg, 0.926 mmol), KO^tBu (110 mg, 0.998 mmol), and **11** (102 mg, 0.314 mmol) furnished a 2.5 : 1 mixture (based on ¹H-integrals) of 2,6-di-*tert*-butyl-4-((2,4-dimethyl-1*H*-imidazol-1-yl)(4-methoxyphenyl)methyl)phenol **5cl-I** and 2,6-di-*tert*-butyl-4-((2,5-dimethyl-1*H*-imidazol-1-yl)(4-methoxyphenyl)methyl)phenol **5cl-II** (in total: 97.5 mg, 0.240 mmol, 76 %) as yellow oil.



Major isomer: $^1\text{H-NMR}$ (CDCl_3 , 300 MHz) δ = 1.37 (s, 18 H, 15-H), 2.21 (d, 3J = 0.9 Hz, 3 H, 16-H), 3.81 (s, 3 H, 10-H), 5.37 (s, 1 H, OH), 6.28 (s, 1 H, 5-H), 6.54 (s, 1 H, 13-H), 6.84-6.88 (m, 4 H, 8-H), 6.90 (s, 2 H, 3-H), 7.00-7.05 (m, 2 H, 7-H), 7.23 (d, 1 H, 3J = 1.3 Hz, 11-H). Additionally, the following chemical shifts were found for the minor isomer: δ = 1.36 (s, 18 H, 15-H), 2.05 (d, 3J = 0.9 Hz, 3 H, 14-H), 6.22 (s, 1 H, 5-H). $^{13}\text{C-NMR}$ (CDCl_3 , 75.5 MHz) δ = 13.8 (q, C-16), 30.2 (q, C-15), 34.36 (s, C-14), 55.27 (q, C-10), 64.7 (d, C-5), 113.9 (d, C-8), 115.8 (d, C-13), 124.9 (d, C-3), 129.0 (d, C-7), 129.8 (s, C-4), 132.2 (s, C-6), 136.2 (s, C-2), 136.4 (d, C-11), 138.0 (s, C-12), 153.59 (s, C-1), 159.2 (s, C-9). Additionally, the following chemical shifts were found for the minor isomer: δ = 9.67 (q, C-16), 34.35 (s, C-14), 55.26 (q, C-10), 62.9 (d, C-5), 114.0 (d, C-8), 153.64 (s, C-1), 159.1 (s, C-9). HR-MS (ESI) $[\text{M}+\text{H}]^+$: m/z calcd for $\text{C}_{26}\text{H}_{35}\text{N}_2\text{O}_2^+$: 407.2693 found: 407.2694.

Product of the Reaction of 2,4-Dimethylimidazole-Potassium (2d-K) with the Quinone Methide **11**

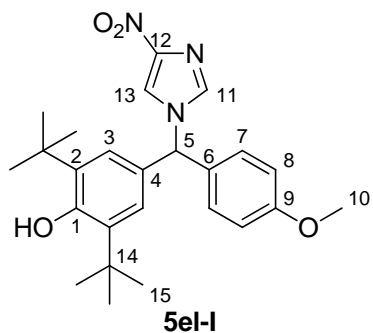
According to GP1, 2,4-dimethylimidazole (96.0 mg, 0.999 mmol), $\text{KO}t\text{Bu}$ (115 mg, 1.02 mmol), and **11** (100 mg, 0.308 mmol) yielded 2,6-di-*tert*-butyl-4-((2,4-dimethyl-1*H*-imidazol-1-yl)(4-methoxyphenyl)methyl)phenol **5dl-I** (71.0 mg, 0.169 mmol, 55 %) as colorless crystals.



Melting point: 164.2-166.8 °C (from CH_2Cl_2 /pentane). $^1\text{H-NMR}$ (CDCl_3 , 300 MHz) δ = 1.37 (s, 18 H, 15-H), 2.13 (s, 3 H, 17-H), 2.27 (s, 3 H, 16-H), 3.81 (s, 3 H, 10-H), 5.28 (s, 1 H, OH), 6.21 (d, 3J = 1.0 Hz, 1 H, 13-H), 6.23 (s, 1 H, 5-H), 6.84-6.87 (m, 4 H, 3-H and 8-H), 6.93-6.96 (m, 2 H, 7-H). $^{13}\text{C-NMR}$ (CDCl_3 , 75.5 MHz) δ = 13.5 (q, C-16), 13.7 (q, C-17), 30.2 (q, C-15), 34.4 (s, C-14), 55.3 (q, C-10), 63.2 (d, C-5), 113.9 (d, C-8), 114.7 (d, C-13), 125.1 (d, C-3), 129.0 (d, C-7), 132.2 (s, C-6), 135.1 (s, C-12), 136.1 (s, C-2), 144.2 (s, C-11), 153.4 (s, C-1), 159.0 (s, C-9). HR-MS (ESI) $[\text{M}+\text{H}]^+$: m/z calcd for $\text{C}_{27}\text{H}_{37}\text{N}_2\text{O}_2^+$: 421.2850 found: 421.2851.

Product of the Reaction of 4-Nitroimidazole-Potassium (2e-K) with the Quinone Methide 11

According to GP1, 4-nitroimidazole (114 mg, 1.00 mmol), KO t Bu (120 mg, 1.07 mmol), and **11** (101 mg, 0.311 mmol) afforded 2,6-di-*tert*-butyl-4-((4-methoxyphenyl)(4-nitro-1*H*-imidazol-1-yl)methyl)phenol **5el-I** (50.0 mg, 0.114 mmol, 37 %) as light yellow oil.

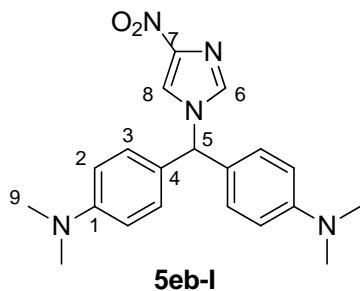


$^1\text{H-NMR}$ (CDCl_3 , 300 MHz) δ = 1.38 (s, 18 H, 15-H), 3.83 (s, 3 H, 10-H), 5.37 (s, 1 H, OH), 6.42 (s, 1 H, 5-H), 6.91-6.94 (m, 4 H, 3-H and 8-H), 7.06 (d, 3J = 8.8 Hz, 2 H, 7-H), 7.34 (d, 3J = 1.4 Hz, 1 H, 11-H), 7.62 (d, 3J = 1.3 Hz, 1 H, 13-H). $^{13}\text{C-NMR}$ (CDCl_3 , 75.5 MHz) δ = 30.1 (q, C15), 34.4 (s, C-14), 55.4 (q, C-10), 66.4 (d, C-5), 114.5 (d, C-8), 119.6 (d, C-13), 124.7 (d,

C-3), 127.8 (s, C-4), 129.1 (d, C-7), 129.8 (s, C-6), 136.2 (d, C-11), 136.8 (s, C-2), 147.7 (s, C-12), 154.3 (s, C-1), 159.9 (s, C-9).

Product of the Reaction of 4-Nitroimidazole-Potassium (2e-K) with the Benzhydrylium Ion 1b-BF $_4$

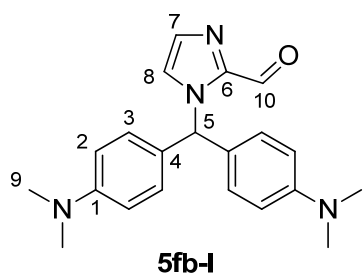
4-Nitroimidazole-potassium (16.6 mg, 0.110 mmol) and **1b-BF $_4$** (dma) (37.3 mg, 0.110 mmol) were combined in 1 mL d^6 -DMSO.



$^1\text{H-NMR}$ (d^6 -DMSO, 400 MHz) δ = 2.89 (s, 12 H, 9-H), 6.70-6.72 (m, 5 H, 2-H and 5-H), 7.02 (d, 3J = 8.5 Hz, 4 H, 3-H), 7.80 (s, 1 H, 8-H), 8.13 (s, 1 H, 6-H). $^{13}\text{C-NMR}$ (d^6 -DMSO, 101 MHz) δ = 39.9 (q, C-9), 64.3 (d, C-5), 112.2 (d, C-2), 120.6 (d, C-6), 125.9 (s, C-4), 128.5 (d, C-3), 136.9 (d, C-8), 146.8 (s, C-7), 150.0 (s, C-1).

Product of the Reaction of 2-Formylimidazole-Potassium (2f-K) with the Benzhydrylium Ion 1b-BF $_4$

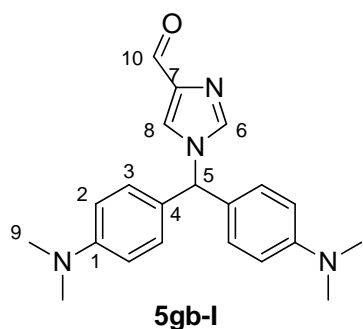
According to GP2, 2-formylimidazole (56.0 mg, 0.583 mmol), KO t Bu (66.0 mg, 0.588 mmol), and **1b-BF $_4$** (95.0 mg, 0.279 mmol) furnished 1-(bis(4-(dimethylamino)phenyl)methyl)-1*H*-imidazole-2-carbaldehyde **5fb-I** (71.0 mg, 0.204 mmol, 73 %) as colorless oil.



$^1\text{H-NMR}$ ($\text{d}^6\text{-DMSO}$, 400 MHz) δ = 2.87 (s, 12 H, 9-H), 6.68 (d, 3J = 8.9 Hz, 4 H, 2-H), 6.69 (d, 3J = 8.7 Hz, 4 H, 3-H), 7.23 (s, 1 H, 8-H), 7.27 (s, 1 H, 7-H), 9.70 (s, 1 H, 10-H). $^{13}\text{C-NMR}$ ($\text{d}^6\text{-DMSO}$, 101 MHz) δ = 39.9 (q, C-9), 62.5 (d, C-5), 112.1 (d, C-2), 125.6 (d, C-8), 126.7 (s, C-4), 128.5 (d, C-3), 131.1 (d, C-7), 143.1 (s, C-6), 149.8 (s, C-1), 181.7 (d, C-10).

Product of the Reaction of 4-Formylimidazole-Potassium (2g-K) with the Benzhydrylium Ion 1b-BF₄

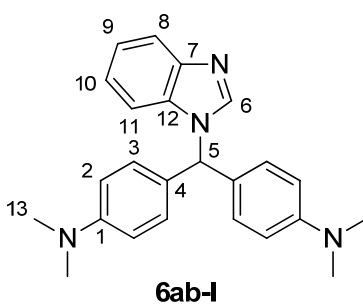
According to GP2, 4-formylimidazole (90.0 mg, 0.937 mmol), KO t Bu (110 mg, 0.980 mmol), and **1b-BF₄** (90.0 mg, 0.265 mmol) gave 1-(bis(4-(dimethylamino)phenyl)methyl)-1H-imidazole-4-carbaldehyde **5gb-I** (75.0 mg, 0.215 mmol, 81 %) as colorless oil.



$^1\text{H-NMR}$ ($\text{d}^6\text{-DMSO}$, 400 MHz) δ = 2.88 (s, 12 H, 9-H), 6.68 (s, 1 H, 5-H), 6.71 (d, 3J = 8.9 Hz, 4 H, 2-H), 6.97 (d, 3J = 8.5 Hz, 4 H, 3-H), 7.82 (d, 3J = 1.0 Hz, 1 H, 6-H), 7.85 (d, 3J = 1.2 Hz, 1 H, 8-H), 9.69 (s, 1 H, 10-H). $^{13}\text{C-NMR}$ ($\text{d}^6\text{-DMSO}$, 101 MHz) δ = 40.0 (q, C-9), 63.3 (d, C-5), 112.2 (d, C-2), 126.7 (s, C-4), 127.4 (d, C-8), 128.4 (d, C-3), 139.6 (d, C-6), 141.3 (s, C-7), 149.9 (s, C-1), 185.2 (s, C-10).

Product of the Reaction of Benzimidazole-Potassium (3a-K) with the Benzhydrylium Ion 1b-BF₄

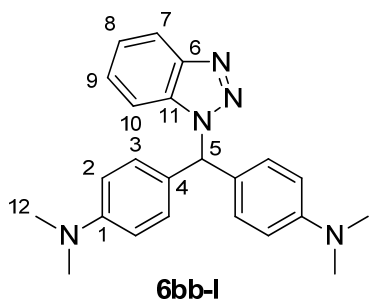
According to GP2, benzimidazole (47.0 mg, 0.398 mmol), KO t Bu, (46.6 mg, 0.415 mmol) and **1b-BF₄** (95.0 mg, 0.279 mmol) yielded 4,4'-((1H-benzo[d]imidazol-1-yl)-methylene)-bis(*N,N*-dimethyl-aniline) **6ab-I** (91.0 mg, 0.246 mmol, 88 %) as colorless oil.



$^1\text{H-NMR}$ ($\text{d}^6\text{-DMSO}$, 400 MHz) δ = 2.86 (s, 12 H, 13-H), 6.69 (d, 3J = 8.9 Hz, 4 H, 2-H), 6.85 (s, 1 H, 5-H), 7.01 (d, 3J = 8.6 Hz, 4 H, 3-H), 7.12-7.20 (m, 2 H, 9-H, 10-H), 7.30-7.33 (m, 1 H, 11-H), 7.65-7.68 (m, 1 H, 8-H), 7.84 (s, 1 H, 6-H). $^{13}\text{C-NMR}$ ($\text{d}^6\text{-DMSO}$, 101 MHz) δ = 40.0 (q, C-13), 61.6 (d, C-5), 111.5 (d, C-11), 112.2 (d, C-2), 119.5 (d, C-8), 121.5 (d, C-9), 122.2 (d, C-10), 126.4 (s, C-4), 128.6 (d, C-3), 133.9 (s, C-12), 142.7 (d, C-6), 143.8 (s, C-7), 149.8 (s, C-1).

Product of the Reaction of Benzotriazole-Potassium (3b-K) with the Benzhydrylium Ion**1b-BF₄**

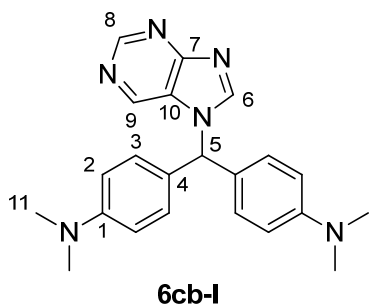
According to GP2, benzotriazole (54.6 mg, 0.458 mmol), KO^tBu (52.9 mg, 0.471 mmol), and **1b-BF₄** (100 mg, 0.294 mmol) furnished 4,4'-((1*H*-benzo[*d*][1,2,3]triazol-1-yl)-methylene)-bis(*N,N*-di-methylaniline) **6bb-I** (79.0 mg, 0.213 mmol, 72 %) as colorless oil.



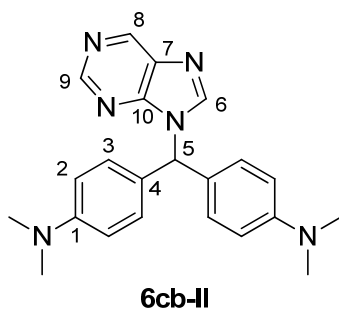
¹H-NMR (d⁶-DMSO, 400 MHz) δ = 2.86 (s, 12 H, 12-H), 6.68 (d, ³*J* = 9.0 Hz, 4 H, 2-H), 7.07 (³*J* = 8.5 Hz, 4 H, 3-H), 7.34-7.38 (m, 2 H, 5-H and 8-H), 7.43-7.47 (m, 1 H, 9-H), 7.58 (dt, ³*J* = 8.4 Hz, ⁴*J* = 1.0 Hz, 1 H, 10-H), 8.04 (dt, ³*J* = 8.3 Hz, ⁴*J* = 1.0 Hz, 1 H, 7-H). ¹³C-NMR (d⁶-DMSO, 101 MHz) δ = 40.0 (q, C-12), 64.8 (d, C-5), 111.1 (d, C-10), 112.1 (d, C-2), 119.2 (d, C-7), 123.9 (d, C-8), 126.2 (s, C-4), 127.1 (d, C-9), 128.8 (d, C-3), 132.8 (s, C-11), 145.3 (s, C-6), 149.9 (s, C-1).

Product of the Reaction of Purine-Potassium (3c-K) with the Benzhydrylium Ion 1b-BF₄

According to GP2, purine (71.8 mg, 0.598 mmol), KO^tBu (72.1 mg, 0.643 mmol), and **1b-BF₄** (100 mg, 0.294 mmol) yielded a 1.2 : 1 mixture (based on ¹H-integrals) of 4,4'-((7*H*-purin-7-yl)methylene)bis(*N,N*-dimethylaniline) **6cb-I** and 4,4'-((9*H*-purin-9-yl)-methylene)-bis(*N,N*-dimethyl-aniline) **6cb-II** (in total: 107 mg, 0.287 mmol, 98 %) as light blue oil.



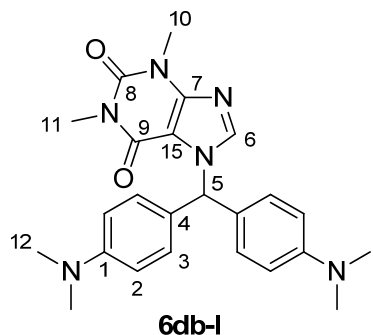
Major isomer **6cb-I**: ¹H-NMR (d⁶-DMSO, 400 MHz) δ = 2.86 (s, 18 H, 11-H), 6.66-6.71 (m, 4 H, 2-H), 7.04-7.07 (m, 5 H, 3-H and 5-H), 8.46 (s, 1 H, 6-H), 8.60 (s, 1 H, 9-H), 8.94 (s, 1 H, 8-H). ¹³C-NMR (d⁶-DMSO, 101 MHz) δ = 39.9 (q, C-11), 62.8 (d, C-5), 112.22 (d, C-2), 125.2 (s, C-10), 125.3 (s, C-4), 128.7 (d, C-3), 141.5 (d, C-9), 148.4 (d, C-6), 150.0 (d, C-8), 152.2 (s, C-1), 160.3 (s, C-7). HR-MS (EI) [M]⁺: *m/z* calcd for C₂₂H₂₄N₆: 372.2062 found: 372.2056. MS (EI) *m/z* = 372 (32) [M⁺], 254 (44), 253 (100), 237 (18), 126 (13).



Minor isomer **6cb-II**: ¹H-NMR (d⁶-DMSO, 400 MHz) δ = 2.85 (s, 18 H, 11-H), 6.66-6.71 (m, 4 H, 2-H), 6.99 (s, 1 H, 5-H), 7.04-7.07 (m, 4 H, 3-H), 8.41 (s, 1 H, 6-H), 8.91 (s, 1 H, 9-H), 9.81 (s, 1 H, 8-H). ¹³C-NMR (d⁶-DMSO, 101 MHz) δ = 40.0 (q, C-11), 60.5 (d, C-5), 112.19 (d, C-2), 126.0 (s, C-4), 128.6 (d, C-3), 133.8 (s, C-7), 145.8 (d, C-6), 148.1 (d, C-8), 149.9 (d, C-9), 150.8 (s, C-10), 152.1 (s, C-1).

Product of the Reaction of Theophylline-Potassium (3d-K) with the Benzhydrylium Ion**1b-BF₄**

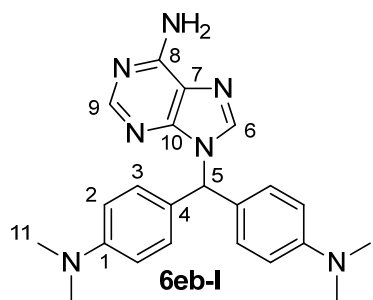
According to GP2, theophylline-potassium **3d-K** (177 mg, 0.811 mmol) and **1b-BF₄** (275 mg, 0.808 mmol) afforded 7-(bis(4-(dimethylamino)phenyl)methyl)-1,3-dimethyl-1*H*-purine-2,6-(3*H*,7*H*)-dione **6db-I** (300 mg, 0.694 mmol, 86 %) as colorless oil.



¹H-NMR (CD₂Cl₂, 400 MHz) δ = 2.94 (s, 12 H, 12-H), 3.29 (s, 3 H, 11-H), 3.53 (s, 3 H, 10-H), 6.68 (d, ³*J* = 8.9 Hz, 4 H, 2-H), 6.97 (d, ³*J* = 8.5 Hz, 4 H, 3-H), 7.14 (s, 1 H, 5-H), 7.34 (s, 1 H, 6-H). ¹³C-NMR (CD₂Cl₂, 101 MHz) δ = 28.2 (q, C-11), 30.0 (q, C-10), 40.8 (q, C-12), 64.3 (d, C-5), 107.8 (s, C-15), 112.7 (d, C-2), 126.9 (s, C-4), 129.3 (d, C-3), 141.3 (d, C-6), 149.7 (s, C-7), 150.9 (s, C-1), 152.2 (s, C-8), 155.5 (s, C-9).

Product of the Reaction of Adenine-Potassium (3e-K) with the Benzhydrylium Ion 1b-BF₄

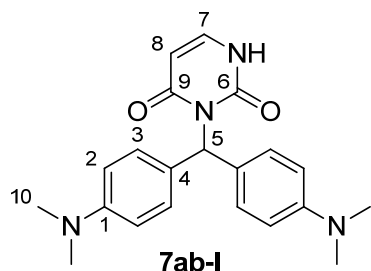
According to GP2, adenine (80.7 mg, 0.597 mmol), KO*t*Bu (70.6 mg, 0.629 mmol), and **1b-BF₄** (100 mg, 0.294 mmol) furnished 4,4'-((6-amino-9*H*-purin-9-yl)methylene)-bis(*N,N*-dimethylaniline) **6eb-I** (126 mg, 0.325 mmol, 111 %) as light blue oil, that still contains DMSO and ethyl acetate as impurities.



¹H-NMR (d⁶-DMSO, 400 MHz) δ = 2.84 (s, 12 H, 11-H), 6.67 (d, ³*J* = 8.8 Hz, 4 H, 2-H), 6.82 (s, 1 H, 5-H), 6.99 (d, ³*J* = 8.7 Hz, 4 H, 3-H), 7.34 (s, 2 H, NH₂), 7.87 (s, 1 H, 6-H), 8.13 (s, 9-H). ¹³C-NMR (d⁶-DMSO, 101 MHz) δ = 40.0 (1, C-11), 60.1 (d, C-5), 112.2 (d, C-2), 118.8 (s, C-7), 126.8 (s, C-4), 128.6 (d, C-3), 139.7 (d, C-6), 149.4 (s, C-10), 149.8 (s, C-1), 152.5 (d, C-9), 156.0 (s, C-8). HR-MS (EI) [M]⁺: *m/z* calcd for C₂₂H₂₅N₇: 387.2171 found: 387.2171. MS (EI) *m/z* = 387 (12) [M⁺], 254 (48), 253 (100), 239 (10), 237 (29), 210 (10), 135 (13), 134 (13), 126 (15), 118 (11).

Product of the Reaction of Uracil-Potassium (4a-K) with the Benzhydrylium Ion 1b-BF₄

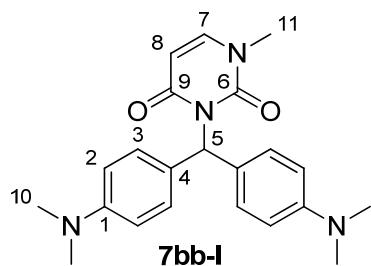
According to GP2, uracil-potassium **4a-K** (87.2 mg, 0.581 mmol), 18-crown-6 (160 mg, 0.605 mmol), and **1b-BF₄** (100 mg, 0.294 mmol) afforded 3-(bis(4-(dimethylamino)phenyl)-methyl)pyrimidine-2,4(1*H*,3*H*)-dione **7ab-I** (105 mg, 0.288 mmol, 98 %) as light green oil.



$^1\text{H-NMR}$ ($\text{d}^6\text{-DMSO}$, 400 MHz) δ = 2.88 (s, 12 H, 10-H), 5.54 (dd, $^3J = 8.0$ Hz and $^4J = 2.3$ Hz, 1 H, 8-H), 6.67 (s, 1 H, 5-H), 6.71 (d, $^3J = 8.9$ Hz, 4 H, 2-H), 6.95 (d, $^3J = 8.8$ Hz, 4 H, 3-H), 7.23 (d, $^3J = 8.0$ Hz, 1 H, 7-H), 11.4 (s, 1 H, NH). $^{13}\text{C-NMR}$ ($\text{d}^6\text{-DMSO}$, 101 MHz) δ = 40.0 (q, C-10), 60.8 (d, C-5), 101.0 (d, C-8), 112.3 (d, C-2), 125.6 (s, C-4), 128.9 (d, C-3), 142.8 (d, C-7), 149.8 (s, C-1), 151.0 (s, C-6), 163.2 (s, C-9). HR-MS (EI) $[\text{M}+\text{H}]^+$: m/z calcd for $\text{C}_{21}\text{H}_{24}\text{N}_4\text{O}_2^+$: 364.1899 found: 364.1898. MS (EI) m/z = 264 (19) $[\text{M}^+]$, 255 (15), 254 (100), 253 (72) $[\text{M}-\text{C}_4\text{H}_3\text{N}_2\text{O}_2^+]$, 240 (35), 239 (30), 238 (16), 237 (21), 226 (10), 210 (23), 134 (23).

Product of the Reaction of 1-Methyluracil-Potassium (4b-K) with the Benzhydrylium Ion 1b-BF₄

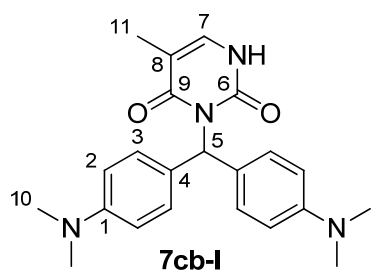
According to GP2, 1-methyluracil (77.1 mg, 0.611 mmol), $\text{KO}t\text{Bu}$ (74.0 mg, 0.659 mmol), 18-crown-6 (190 mg, 0.719 mmol), and **1b-BF₄** (100 mg, 0.294 mmol) yielded 3-(bis(4-(dimethylamino)phenyl)methyl)-1-methylpyrimidine-2,4(1*H*,3*H*)-dione **7bb-I** (110 mg, 0.291 mmol, 99 %) as colorless oil.



$^1\text{H-NMR}$ ($\text{d}^6\text{-DMSO}$, 400 MHz) δ = 2.86 (s, 12 H, 10-H), 3.23 (s, 3 H, 11-H), 5.66 (d, $^3J = 7.8$ Hz, 1 H, 8-H), 6.64 (d, $^3J = 8.9$ Hz, 4 H, 2-H), 7.06–7.08 (m, 5 H, 3-H and 5-H), 7.69 (d, $^3J = 7.8$ Hz, 1 H, 7-H). $^{13}\text{C-NMR}$ ($\text{d}^6\text{-DMSO}$, 101 MHz) δ = 36.4 (q, C-11), 40.2 (q, C-10), 57.3 (d, C-5), 99.9 (d, C-8), 111.8 (d, C-2), 126.4 (s, C-4), 129.1 (d, C-3), 145.1 (d, C-7), 149.3 (s, C-1), 150.9 (s, C-6), 162.9 (s, C-9). HR-MS (EI) $[\text{M}+\text{H}]^+$: m/z calcd for $\text{C}_{22}\text{H}_{26}\text{N}_4\text{O}_2^+$: 378.2056 found: 378.2050. MS (EI) m/z = 378 (4) $[\text{M}^+]$, 255 (20), 254 (100), 253 (68) $[\text{M}-\text{C}_5\text{H}_5\text{N}_2\text{O}_2^+]$, 238 (13), 237 (20), 210 (19), 134 (10), 126 (44), 83 (16), 42 (15).

Product of the Reaction of Thymine-Potassium (4c-K) with the Benzhydrylium Ion 1b-BF₄

According to GP2, thymine (70.4 mg, 0.558 mmol), $\text{KO}t\text{Bu}$ (65.0 mg, 0.579 mmol), 18-crown-6 (160 mg, 0.605 mmol), and **1b-BF₄** (100 mg, 0.294 mmol) furnished 3-(bis(4-(dimethylamino)phenyl)methyl)-5-methylpyrimidine-2,4(1*H*,3*H*)-dione **7cb-I** (106 mg, 0.280 mmol, 95 %) as light blue oil.



$^1\text{H-NMR}$ (d^6 -DMSO, 400 MHz) δ = 1.69 (s, 3 H, 11-H), 2.88 (s, 12 H, 10-H), 6.69–6.71 (m, 5 H, 2-H and 5-H), 6.98 (d, 3J = 8.7 Hz, 4 H, 3-H), 7.13 (d, 3J = 1.2 Hz, 1 H, 7-H), 11.4 (s, 1 H, NH). $^{13}\text{C-NMR}$ (d^6 -DMSO, 101 MHz) δ = 12.3 (q, C-11), 40.0 (q, C-10), 60.4 (d, C-5), 108.8 (s, C-8), 112.3 (d, C-2), 125.8 (s, C-4), 129.0 (d, C-3), 138.2 (d, C-7), 149.8 (s, C-1), 151.1 (s, C-6), 163.8 (s, C-9).

4.4 Determination of the Nucleophilicities of Heterocyclic Anions in DMSO

Reactions of the Potassium Salt of Imidazole (**2a-K**)

Table 4: Kinetics of the reaction of **2a** (generated in situ by addition of 1.03 equivalents KO t Bu) with **1m** (20 °C, stopped-flow, at 486 nm).

[E] / mol L ⁻¹	[2a] / mol L ⁻¹	[18-crown-6] / mol L ⁻¹	[2a]/[E]	k_{obs} / s ⁻¹
1.81×10^{-5}	7.29×10^{-4}		40.3	0.0312
1.81×10^{-5}	1.46×10^{-3}	1.81×10^{-3}	80.7	0.0853
1.81×10^{-5}	2.19×10^{-3}		121	0.129
1.81×10^{-5}	2.91×10^{-3}	3.62×10^{-3}	161	0.195
1.81×10^{-5}	3.64×10^{-3}		201	0.256

$$k_2 = 7.69 \times 10^1 \text{ L mol}^{-1} \text{ s}^{-1}$$

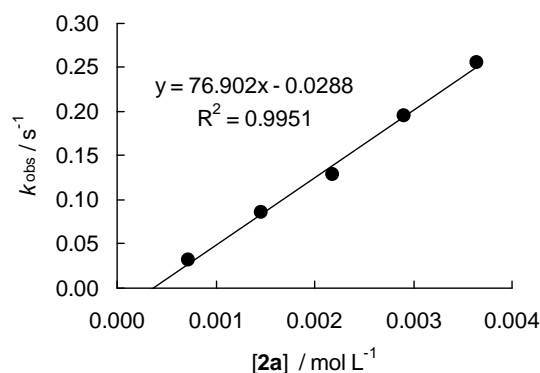


Table 5: Kinetics of the reaction of **2a** (generated in situ by addition of 1.03 equivalents KO t Bu) with **1l** (20 °C, stopped-flow, at 393 nm).

[E] / mol L ⁻¹	[2a] / mol L ⁻¹	[18-crown-6] / mol L ⁻¹	[2a]/[E]	k_{obs} / s ⁻¹
1.63×10^{-5}	7.29×10^{-4}		44.7	0.168
1.63×10^{-5}	1.46×10^{-3}	1.81×10^{-3}	89.6	0.459
1.63×10^{-5}	2.19×10^{-3}		134	0.666
1.63×10^{-5}	2.91×10^{-3}	3.62×10^{-3}	179	1.01
1.63×10^{-5}	3.64×10^{-3}		223	1.28

$$k_2 = 3.82 \times 10^2 \text{ L mol}^{-1} \text{ s}^{-1}$$

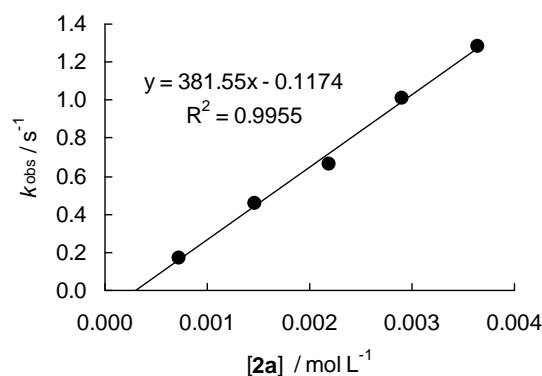
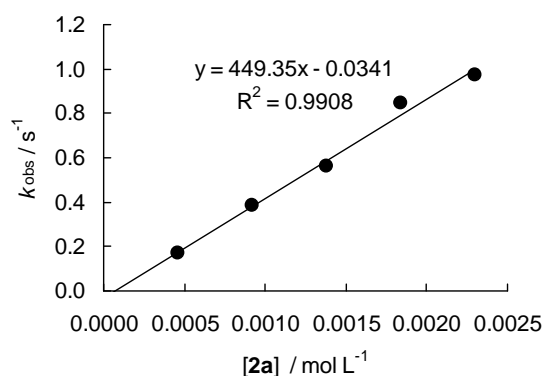


Table 6: Kinetics of the reaction of **2a** (generated in situ by addition of 1.09 equivalents KO^tBu) with **1k** (20 °C, stopped-flow, at 371 nm).

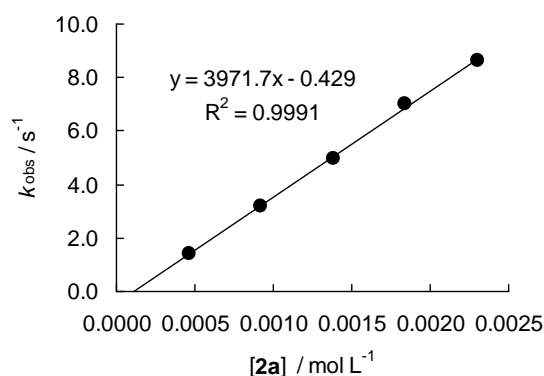
[E] / mol L ⁻¹	[2a] / mol L ⁻¹	[18-crown-6] / mol L ⁻¹	[2a]/[E]	<i>k</i> _{obs} / s ⁻¹
2.41 × 10 ⁻⁵	4.60 × 10 ⁻⁴		19.1	0.169
2.41 × 10 ⁻⁵	9.20 × 10 ⁻⁴	1.07 × 10 ⁻³	38.2	0.383
2.41 × 10 ⁻⁵	1.38 × 10 ⁻³		57.3	0.562
2.41 × 10 ⁻⁵	1.84 × 10 ⁻³	2.15 × 10 ⁻³	76.3	0.844
2.41 × 10 ⁻⁵	2.30 × 10 ⁻³		95.4	0.972

$$k_2 = 4.49 \times 10^2 \text{ L mol}^{-1} \text{ s}^{-1}$$

Table 7: Kinetics of the reaction of **2a** (generated in situ by addition of 1.09 equivalents KO^tBu) with **1j** (20 °C, stopped-flow, at 374 nm).

[E] / mol L ⁻¹	[2a] / mol L ⁻¹	[18-crown-6] / mol L ⁻¹	[2a]/[E]	<i>k</i> _{obs} / s ⁻¹
2.22 × 10 ⁻⁵	4.60 × 10 ⁻⁴		20.7	1.43
2.22 × 10 ⁻⁵	9.20 × 10 ⁻⁴	1.07 × 10 ⁻³	41.4	3.17
2.22 × 10 ⁻⁵	1.38 × 10 ⁻³		62.2	5.00
2.22 × 10 ⁻⁵	1.84 × 10 ⁻³	2.15 × 10 ⁻³	82.9	7.02
2.22 × 10 ⁻⁵	2.30 × 10 ⁻³		104	8.64

$$k_2 = 3.97 \times 10^3 \text{ L mol}^{-1} \text{ s}^{-1}$$

Table 8: Kinetics of the reaction of **2a** (generated in situ by addition of 1.03 equivalents KO^tBu) with **1i** (20 °C, stopped-flow, at 533 nm).

[E] / mol L ⁻¹	[2a] / mol L ⁻¹	[18-crown-6] / mol L ⁻¹	[2a]/[E]	<i>k</i> _{obs} / s ⁻¹
1.34 × 10 ⁻⁵	2.73 × 10 ⁻⁴		20.4	1.68
1.34 × 10 ⁻⁵	5.45 × 10 ⁻⁴	6.70 × 10 ⁻⁴	40.7	3.46
1.34 × 10 ⁻⁵	8.18 × 10 ⁻⁴		61.0	4.93
1.34 × 10 ⁻⁵	1.09 × 10 ⁻³	1.34 × 10 ⁻³	81.3	6.56
1.34 × 10 ⁻⁵	1.36 × 10 ⁻³		101	8.12

$$k_2 = 5.88 \times 10^3 \text{ L mol}^{-1} \text{ s}^{-1}$$

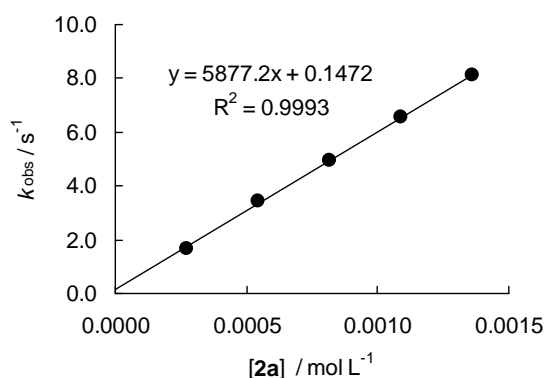
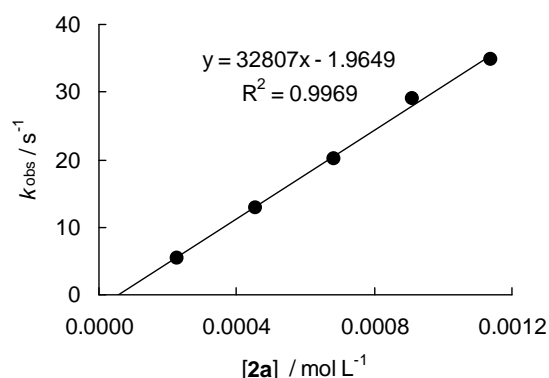


Table 9: Kinetics of the reaction of **2a** (generated in situ by addition of 1.02 equivalents KO^tBu) with **1h** (20 °C, stopped-flow, at 421 nm).

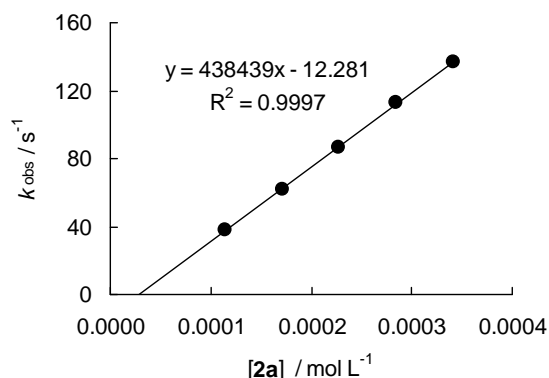
[E] / mol L ⁻¹	[2a] / mol L ⁻¹	[18-crown-6] / mol L ⁻¹	[2a]/[E]	<i>k</i> _{obs} / s ⁻¹
1.81 × 10 ⁻⁵	2.27 × 10 ⁻⁴		12.5	5.48
1.81 × 10 ⁻⁵	4.55 × 10 ⁻⁴	5.76 × 10 ⁻⁴	25.1	12.8
1.81 × 10 ⁻⁵	6.82 × 10 ⁻⁴		37.7	20.1
1.81 × 10 ⁻⁵	9.10 × 10 ⁻⁴	1.15 × 10 ⁻³	50.3	29.0
1.81 × 10 ⁻⁵	1.14 × 10 ⁻³		63.0	34.8

$$k_2 = 3.28 \times 10^4 \text{ L mol}^{-1} \text{ s}^{-1}$$

Table 10: Kinetics of the reaction of **2a** (generated in situ by addition of 1.02 equivalents KO^tBu) with **1g** (20 °C, stopped-flow, at 630 nm).

[E] / mol L ⁻¹	[2a] / mol L ⁻¹	[18-crown-6] / mol L ⁻¹	[2a]/[E]	<i>k</i> _{obs} / s ⁻¹
1.18 × 10 ⁻⁵	1.14 × 10 ⁻⁴		9.7	38.3
1.18 × 10 ⁻⁵	1.71 × 10 ⁻⁴	2.16 × 10 ⁻⁴	14.5	61.8
1.18 × 10 ⁻⁵	2.27 × 10 ⁻⁴		19.2	87.0
1.18 × 10 ⁻⁵	2.84 × 10 ⁻⁴	3.60 × 10 ⁻⁴	24.1	113
1.18 × 10 ⁻⁵	3.41 × 10 ⁻⁴		28.9	137

$$k_2 = 4.38 \times 10^5 \text{ L mol}^{-1} \text{ s}^{-1}$$

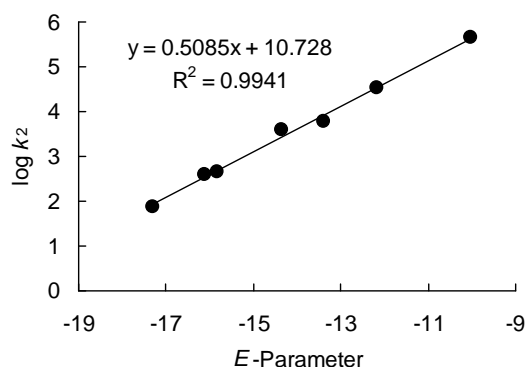


Determination of Reactivity Parameters *N* and *s* for the anion of imidazole (**2a**) in DMSO

Table 11: Rate Constants for the reactions of **2a** with different electrophiles (20 °C).

Electrophile	<i>E</i>	<i>k</i> ₂ / L mol ⁻¹ s ⁻¹	log <i>k</i> ₂
1m	-17.29	7.69 × 10 ¹	1.89
1l	-16.11	3.82 × 10 ²	2.58
1k	-15.83	4.49 × 10 ²	2.65
1j	-14.36	3.97 × 10 ³	3.60
1i	-13.39	5.88 × 10 ³	3.77
1h	-12.18	3.28 × 10 ⁴	4.52
1g	-10.04	4.38 × 10 ⁵	5.64

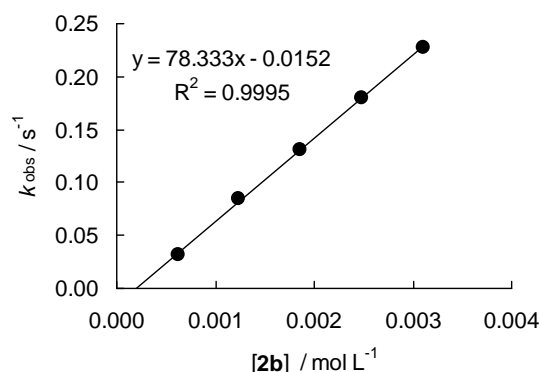
$$N = 21.09, s = 0.51$$



Reactions of the Potassium Salt of 2-Methylimidazole (2b-K)Table 12: Kinetics of the reaction of **2b** (generated in situ by addition of 1.02 equivalents KO t Bu) with **1m** (20 °C, stopped-flow, at 486 nm).

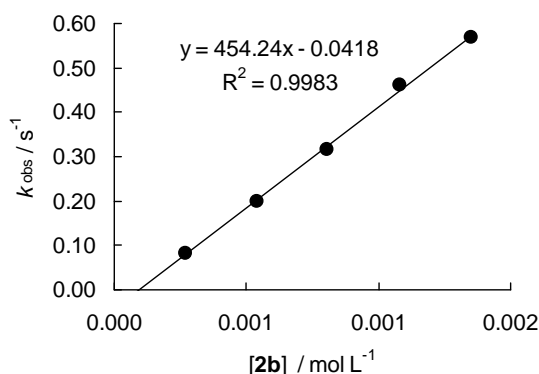
[E] / mol L ⁻¹	[2b] / mol L ⁻¹	[18-crown-6] / mol L ⁻¹	[2b]/[E]	k_{obs} / s ⁻¹
1.92×10^{-5}	6.21×10^{-4}		32.3	0.0314
1.92×10^{-5}	1.24×10^{-3}	1.37×10^{-3}	64.6	0.0841
1.92×10^{-5}	1.86×10^{-3}		96.9	0.131
1.92×10^{-5}	2.48×10^{-3}	2.73×10^{-3}	129	0.180
1.92×10^{-5}	3.11×10^{-3}		162	0.227

$$k_2 = 7.83 \times 10^1 \text{ L mol}^{-1} \text{ s}^{-1}$$

Table 13: Kinetics of the reaction of **2b** (generated in situ by addition of 1.05 equivalents KO t Bu) with **1l** (20 °C, stopped-flow, at 393 nm).

[E] / mol L ⁻¹	[2b] / mol L ⁻¹	[2b]/[E]	k_{obs} / s ⁻¹
1.38×10^{-5}	2.69×10^{-4}	19.5	0.0834
1.38×10^{-5}	5.38×10^{-4}	39.0	0.200
1.38×10^{-5}	8.08×10^{-4}	58.6	0.317
1.38×10^{-5}	1.08×10^{-3}	78.3	0.461
1.38×10^{-5}	1.35×10^{-3}	97.8	0.567

$$k_2 = 4.54 \times 10^2 \text{ L mol}^{-1} \text{ s}^{-1}$$

Table 14: Kinetics of the reaction of **2b** (generated in situ by addition of 1.04 equivalents KO t Bu) with **1k** (20 °C, stopped-flow, at 371 nm).

[E] / mol L ⁻¹	[2b] / mol L ⁻¹	[18-crown-6] / mol L ⁻¹	[2b]/[E]	k_{obs} / s ⁻¹
2.06×10^{-5}	4.29×10^{-4}		20.8	0.145
2.06×10^{-5}	8.57×10^{-4}	9.78×10^{-4}	41.6	0.408
2.06×10^{-5}	1.29×10^{-3}		62.6	0.615
2.06×10^{-5}	1.71×10^{-3}	1.96×10^{-3}	83.0	0.834
2.06×10^{-5}	2.14×10^{-3}		104	1.06

$$k_2 = 5.28 \times 10^2 \text{ L mol}^{-1} \text{ s}^{-1}$$

(with 1.04 eq KO t Bu)

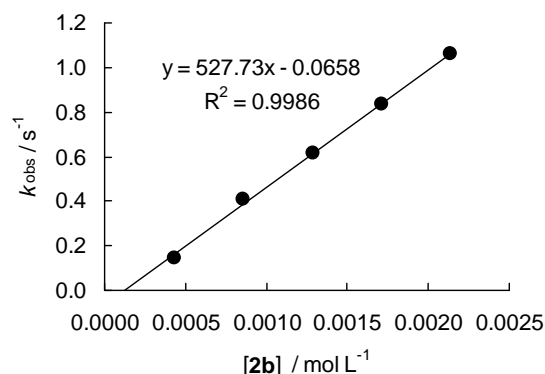
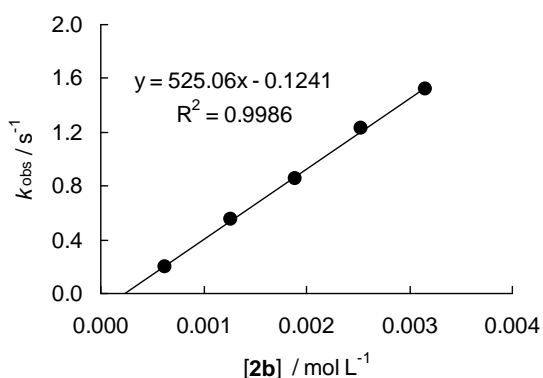


Table 15: Kinetics of the reaction of **2b** (generated in situ by addition of 0.70 equivalents KOtBu) with **1k** (20 °C, stopped-flow, at 371 nm).

[E] / mol L ⁻¹	[2b] / mol L ⁻¹	[2b]/[E]	$k_{\text{obs}} /$ s ⁻¹
1.73×10^{-5}	6.32×10^{-4}	36.5	0.202
1.73×10^{-5}	1.27×10^{-3}	73.2	0.553
1.73×10^{-5}	1.90×10^{-3}	110	0.852
1.73×10^{-5}	2.53×10^{-3}	146	1.23
1.73×10^{-5}	3.16×10^{-3}	182	1.52

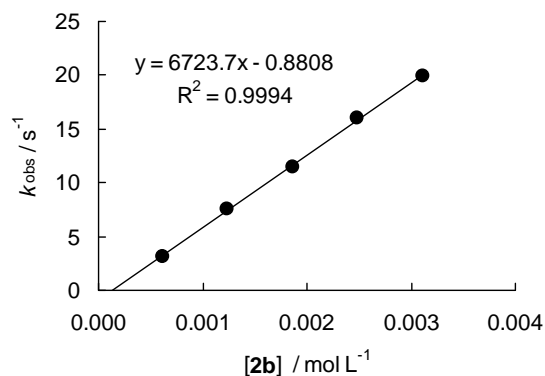
$$k_2 = 5.25 \times 10^2 \text{ L mol}^{-1} \text{ s}^{-1}$$

(with 0.70 eq KOtBu)

Table 16: Kinetics of the reaction of **2b** (generated in situ by addition of 1.02 equivalents KOtBu) with **1j** (20 °C, stopped-flow, at 375 nm).

[E] / mol L ⁻¹	[2b] / mol L ⁻¹	[18-crown-6] / mol L ⁻¹	[2b]/[E]	$k_{\text{obs}} /$ s ⁻¹
2.02×10^{-5}	6.21×10^{-4}		30.7	3.19
2.02×10^{-5}	1.24×10^{-3}	1.37×10^{-3}	61.4	7.61
2.02×10^{-5}	1.86×10^{-3}		92.1	11.5
2.02×10^{-5}	2.48×10^{-3}	2.73×10^{-3}	123	16.0
2.02×10^{-5}	3.11×10^{-3}		154	19.9

$$k_2 = 6.72 \times 10^3 \text{ L mol}^{-1} \text{ s}^{-1}$$

Table 17: Kinetics of the reaction of **2b** (generated in situ by addition of 1.02 equivalents KOtBu) with **1i** (20 °C, stopped-flow, at 533 nm).

[E] / mol L ⁻¹	[2b] / mol L ⁻¹	[18-crown-6] / mol L ⁻¹	[2b]/[E]	$k_{\text{obs}} /$ s ⁻¹
1.59×10^{-5}	4.38×10^{-4}		27.5	1.99
1.59×10^{-5}	8.77×10^{-4}	9.76×10^{-4}	55.2	4.80
1.59×10^{-5}	1.32×10^{-3}		83.0	7.94
1.59×10^{-5}	1.75×10^{-3}	1.95×10^{-3}	110	11.1
1.59×10^{-5}	2.19×10^{-3}		138	14.6

$$k_2 = 7.20 \times 10^3 \text{ L mol}^{-1} \text{ s}^{-1}$$

(with 1.02 eq KOtBu)

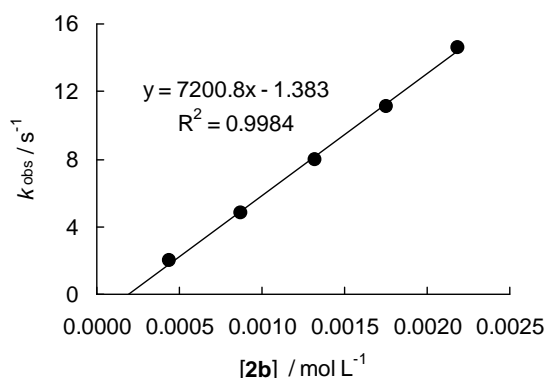
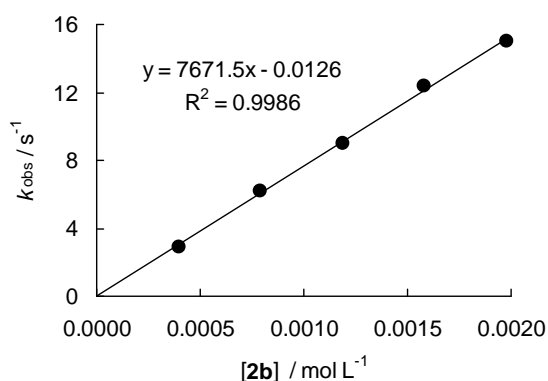


Table 18: Kinetics of the reaction of **2b** (generated in situ by addition of 0.72 equivalents KOtBu) with **1i** (20 °C, stopped-flow, at 533 nm).

[E] / mol L ⁻¹	[2b] / mol L ⁻¹	[2b]/[E]	$k_{\text{obs}} /$ s ⁻¹
1.11×10^{-5}	3.95×10^{-4}	35.6	2.92
1.11×10^{-5}	7.92×10^{-4}	71.4	6.17
1.11×10^{-5}	1.19×10^{-3}	107	9.01
1.11×10^{-5}	1.58×10^{-3}	143	12.4
1.11×10^{-5}	1.98×10^{-3}	178	15.0

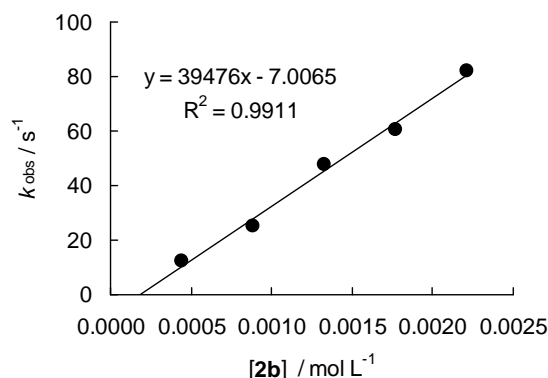
$$k_2 = 7.67 \times 10^3 \text{ L mol}^{-1} \text{ s}^{-1}$$

(with 0.72 eq KOtBu)

Table 19: Kinetics of the reaction of **2b** (generated in situ by addition of 1.02 equivalents KOtBu) with **1h** (20 °C, stopped-flow, at 422 nm).

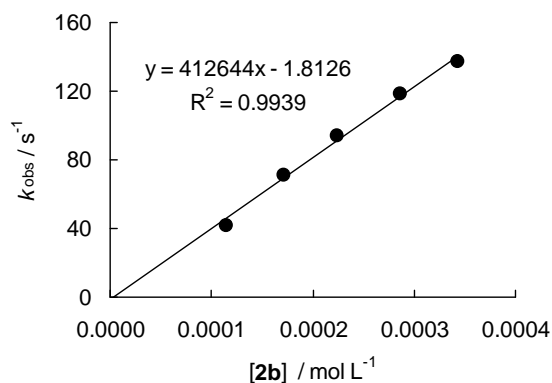
[E] / mol L ⁻¹	[2b] / mol L ⁻¹	[18-crown-6] / mol L ⁻¹	[2b]/[E]	$k_{\text{obs}} /$ s ⁻¹
2.15×10^{-5}	4.35×10^{-4}		20.2	12.2
2.15×10^{-5}	8.70×10^{-4}	9.85×10^{-4}	40.5	25.0
2.15×10^{-5}	1.30×10^{-3}		60.5	47.8
2.15×10^{-5}	1.74×10^{-3}	1.97×10^{-3}	80.9	60.4
2.15×10^{-5}	2.17×10^{-3}		101	81.9

$$k_2 = 3.95 \times 10^4 \text{ L mol}^{-1} \text{ s}^{-1}$$

Table 20: Kinetics of the reaction of **2b** (generated in situ by addition of 1.02 equivalents KOtBu) with **1g** (20 °C, stopped-flow, at 630 nm).

[E] / mol L ⁻¹	[2b] / mol L ⁻¹	[18-crown-6] / mol L ⁻¹	[2b]/[E]	$k_{\text{obs}} /$ s ⁻¹
1.21×10^{-5}	1.12×10^{-4}		9.3	42.0
1.21×10^{-5}	1.68×10^{-4}	1.97×10^{-4}	13.9	70.8
1.21×10^{-5}	2.20×10^{-4}		18.2	93.7
1.21×10^{-5}	2.81×10^{-4}	3.28×10^{-4}	23.2	118
1.21×10^{-5}	3.37×10^{-4}		27.9	137

$$k_2 = 4.13 \times 10^5 \text{ L mol}^{-1} \text{ s}^{-1}$$

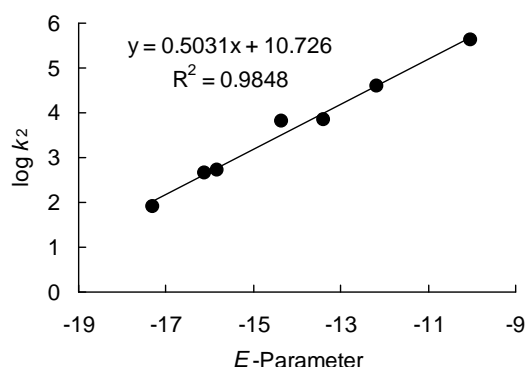


Determination of Reactivity Parameters N and s for the Anion of 2-Methyl Imidazole (**2b**) in DMSO

Table 21: Rate Constants for the reactions of **2b** with different electrophiles (20 °C).

Electrophile	E	$k_2 / \text{L mol}^{-1} \text{s}^{-1}$	$\log k_2$
1m	-17.29	7.83×10^1	1.89
1l	-16.11	4.54×10^2	2.66
1k	-15.83	5.28×10^2	2.72
1j	-14.36	6.72×10^3	3.83
1i	-13.39	7.20×10^3	3.86
1h	-12.18	3.95×10^4	4.61
1g	-10.04	4.13×10^5	5.62

$$N = 21.32, s = 0.50$$

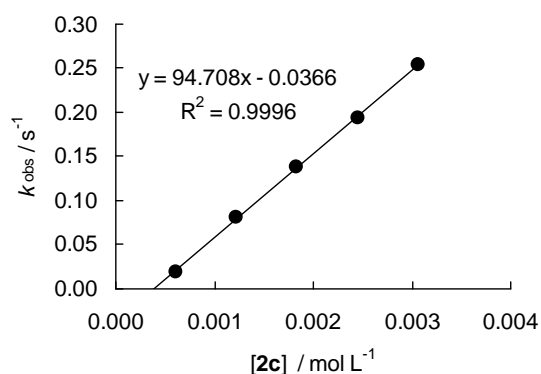


Reactions of the Potassium Salt of 4-Methylimidazole (**2c-K**)

Table 22: Kinetics of the reaction of **2c** (generated in situ by addition of 1.04 equivalents KO t Bu) with **1m** (20 °C, stopped-flow, at 486 nm).

[E] / mol L ⁻¹	[2c] / mol L ⁻¹	[18-crown-6] / mol L ⁻¹	[2c]/[E]	$k_{\text{obs}} / \text{s}^{-1}$
1.85×10^{-5}	6.11×10^{-4}		33.0	0.0198
1.85×10^{-5}	1.22×10^{-3}	1.36×10^{-3}	65.9	0.0810
1.85×10^{-5}	1.83×10^{-3}		98.9	0.138
1.85×10^{-5}	2.45×10^{-3}	2.73×10^{-3}	132	0.193
1.85×10^{-5}	3.06×10^{-3}		165	0.254

$$k_2 = 9.47 \times 10^1 \text{ L mol}^{-1} \text{ s}^{-1}$$

Table 23: Kinetics of the reaction of **2c** (generated in situ by addition of 1.04 equivalents KO t Bu) with **1l** (20 °C, stopped-flow, at 393 nm).

[E] / mol L ⁻¹	[2c] / mol L ⁻¹	[18-crown-6] / mol L ⁻¹	[2c]/[E]	$k_{\text{obs}} / \text{s}^{-1}$
2.00×10^{-5}	4.26×10^{-4}		21.3	0.127
2.00×10^{-5}	8.53×10^{-4}	9.65×10^{-4}	42.7	0.303
2.00×10^{-5}	1.28×10^{-3}		64.0	0.501
2.00×10^{-5}	1.71×10^{-3}	1.93×10^{-3}	85.5	0.696
2.00×10^{-5}	2.13×10^{-3}		107	0.883

$$k_2 = 4.47 \times 10^2 \text{ L mol}^{-1} \text{ s}^{-1}$$

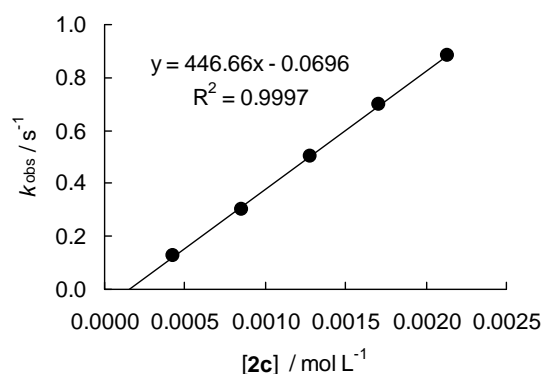
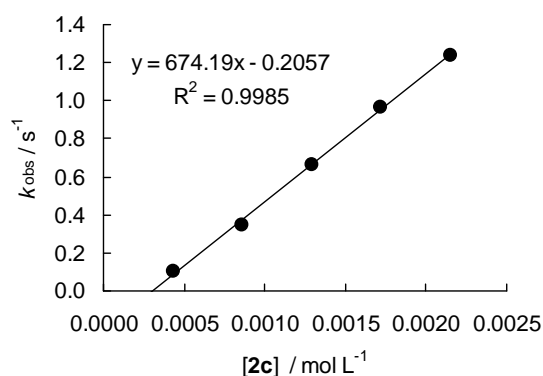


Table 24: Kinetics of the reaction of **2c** (generated in situ by addition of 1.03 equivalents KO t Bu) with **1k** (20 °C, stopped-flow, at 371 nm).

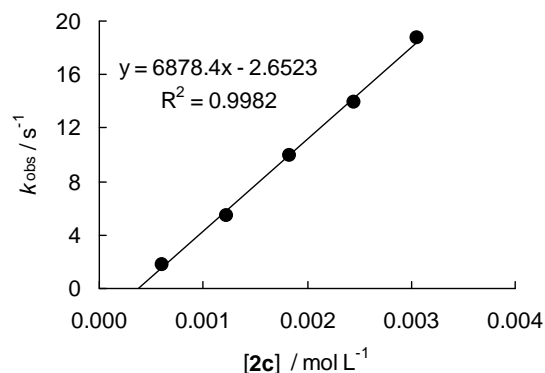
[E] / mol L ⁻¹	[2c] / mol L ⁻¹	[18-crown-6] / mol L ⁻¹	[2c]/[E]	k_{obs} / s ⁻¹
2.10×10^{-5}	4.30×10^{-4}		20.5	0.101
2.10×10^{-5}	8.60×10^{-4}	9.73×10^{-4}	41.0	0.347
2.10×10^{-5}	1.29×10^{-3}		61.4	0.664
2.10×10^{-5}	1.72×10^{-3}	1.95×10^{-3}	81.9	0.968
2.10×10^{-5}	2.15×10^{-3}		102	1.24

$$k_2 = 6.74 \times 10^2 \text{ L mol}^{-1} \text{ s}^{-1}$$

Table 25: Kinetics of the reaction of **2c** (generated in situ by addition of 1.04 equivalents KO t Bu) with **1j** (20 °C, stopped-flow, at 375 nm).

[E] / mol L ⁻¹	[2c] / mol L ⁻¹	[18-crown-6] / mol L ⁻¹	[2c]/[E]	k_{obs} / s ⁻¹
1.91×10^{-5}	6.11×10^{-4}		32.0	1.83
1.91×10^{-5}	1.22×10^{-3}	1.36×10^{-3}	63.9	5.49
1.91×10^{-5}	1.83×10^{-3}		95.8	9.90
1.91×10^{-5}	2.45×10^{-3}	2.73×10^{-3}	128	13.9
1.91×10^{-5}	3.06×10^{-3}		160	18.7

$$k_2 = 6.88 \times 10^3 \text{ L mol}^{-1} \text{ s}^{-1}$$

Table 26: Kinetics of the reaction of **2c** (generated in situ by addition of 1.03 equivalents KO t Bu) with **1i** (20 °C, stopped-flow, at 533 nm).

[E] / mol L ⁻¹	[2c] / mol L ⁻¹	[18-crown-6] / mol L ⁻¹	[2c]/[E]	k_{obs} / s ⁻¹
1.72×10^{-5}	4.30×10^{-4}		25.0	2.12
1.72×10^{-5}	8.60×10^{-4}	9.73×10^{-4}	50.0	5.44
1.72×10^{-5}	1.29×10^{-3}		75.0	9.24
1.72×10^{-5}	1.72×10^{-3}	1.95×10^{-3}	100	12.3
1.72×10^{-5}	2.15×10^{-3}		125	14.6

$$k_2 = 7.40 \times 10^3 \text{ L mol}^{-1} \text{ s}^{-1}$$

(with 1.03 eq KO t Bu)

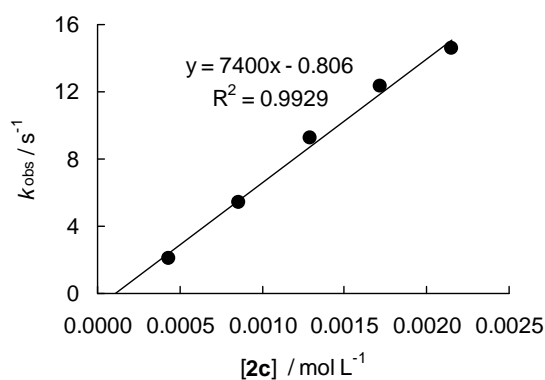
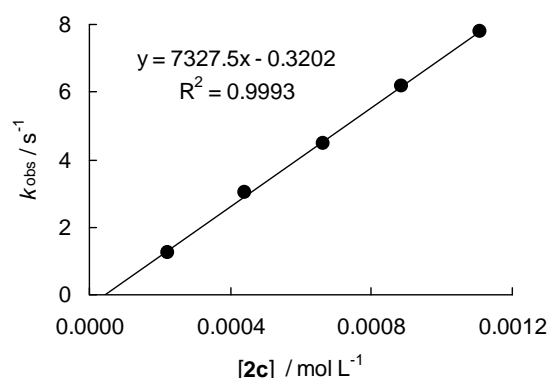


Table 27: Kinetics of the reaction of **2c** (generated in situ by addition of 0.70 equivalents KO t Bu) with **1i** (20 °C, stopped-flow, at 533 nm).

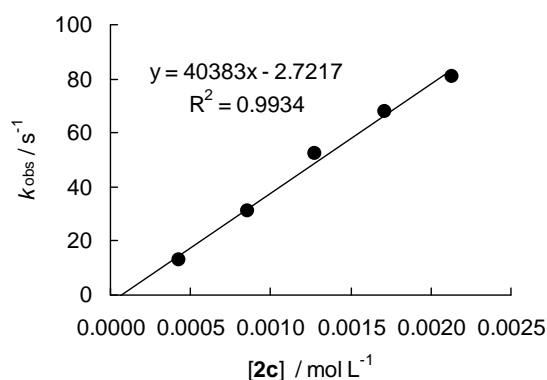
[E] / mol L ⁻¹	[2c] / mol L ⁻¹	[18-crown-6] / mol L ⁻¹	[2c]/[E]	$k_{\text{obs}} / \text{s}^{-1}$
1.15×10^{-5}	2.22×10^{-4}		19.3	1.26
1.15×10^{-5}	4.43×10^{-4}	5.32×10^{-4}	38.5	3.03
1.15×10^{-5}	6.65×10^{-4}		57.8	4.48
1.15×10^{-5}	8.86×10^{-4}	1.06×10^{-3}	77.0	6.19
1.15×10^{-5}	1.11×10^{-3}		96.5	7.81

$$k_2 = 7.33 \times 10^3 \text{ L mol}^{-1} \text{ s}^{-1}$$

 (with 0.70 eq KO t Bu)

 Table 28: Kinetics of the reaction of **2c** (generated in situ by addition of 1.04 equivalents KO t Bu) with **1h-Ph** (20 °C, stopped-flow, at 422 nm).

[E] / mol L ⁻¹	[2c] / mol L ⁻¹	[18-crown-6] / mol L ⁻¹	[2c]/[E]	$k_{\text{obs}} / \text{s}^{-1}$
2.00×10^{-5}	4.26×10^{-4}		21.3	13.2
2.00×10^{-5}	8.53×10^{-4}	9.65×10^{-4}	42.7	30.9
2.00×10^{-5}	1.28×10^{-3}		64.0	52.1
2.00×10^{-5}	1.71×10^{-3}	1.93×10^{-3}	85.5	67.7
2.00×10^{-5}	2.13×10^{-3}		107	80.9

$$k_2 = 4.04 \times 10^4 \text{ L mol}^{-1} \text{ s}^{-1}$$

 (with 1.04 eq KO t Bu)

 Table 29: Kinetics of the reaction of **2c** (generated in situ by addition of 0.71 equivalents KO t Bu) with **1h** (20 °C, stopped-flow, at 422 nm).

[E] / mol L ⁻¹	[2c] / mol L ⁻¹	[18-crown-6] / mol L ⁻¹	[2c]/[E]	$k_{\text{obs}} / \text{s}^{-1}$
1.15×10^{-5}	2.53×10^{-4}		21.8	8.75
1.15×10^{-5}	5.02×10^{-4}	6.17×10^{-4}	43.7	20.2
1.15×10^{-5}	7.53×10^{-4}		65.5	29.5
1.15×10^{-5}	1.00×10^{-3}	1.23×10^{-3}	87.0	39.3
1.15×10^{-5}	1.26×10^{-3}		110	49.3

$$k_2 = 3.98 \times 10^4 \text{ L mol}^{-1} \text{ s}^{-1}$$

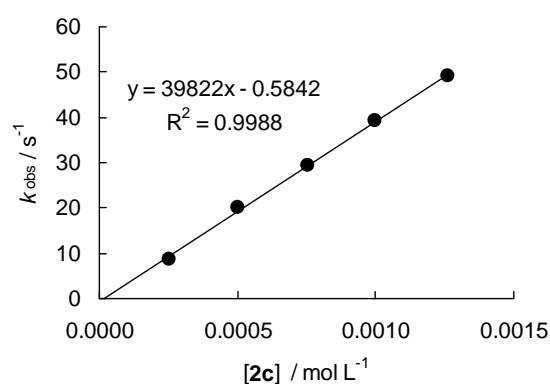
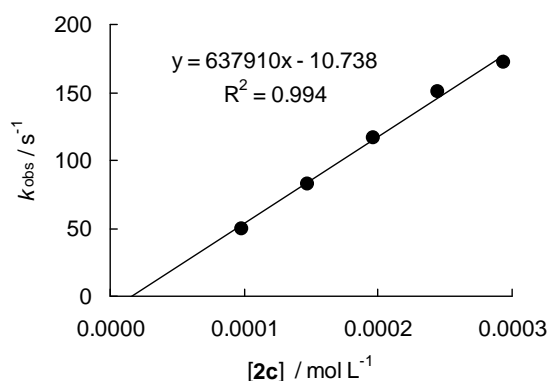
 (with 0.71 eq KO t Bu)


Table 30: Kinetics of the reaction of **2c** (generated in situ by addition of 1.04 equivalents KOtBu) with **1g** (20 °C, stopped-flow, at 630 nm).

[E] / mol L ⁻¹	[2c] / mol L ⁻¹	[2c]/[E]	k_{obs} / s ⁻¹
6.63×10^{-6}	9.79×10^{-5}	14.8	49.9
6.63×10^{-6}	1.47×10^{-4}	22.2	82.5
6.63×10^{-6}	1.96×10^{-4}	29.6	116
6.63×10^{-6}	2.45×10^{-4}	37.0	151
6.63×10^{-6}	2.94×10^{-4}	44.3	172

$$k_2 = 6.38 \times 10^5 \text{ L mol}^{-1} \text{ s}^{-1}$$

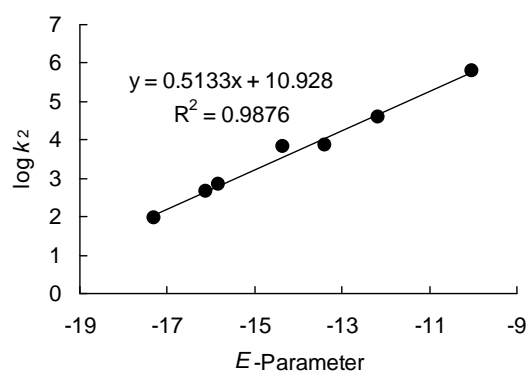


Determination of Reactivity Parameters N and s for the Anion of 4-Methyl Imidazole (**2c**) in DMSO

Table 31: Rate Constants for the reactions of **2c** with different electrophiles (20 °C).

Electrophile	E	$k_2 / \text{L mol}^{-1} \text{ s}^{-1}$	$\log k_2$
1m	-17.29	9.47×10^1	1.98
1l	-16.11	4.47×10^2	2.65
1k	-15.83	6.74×10^2	2.83
1j	-14.36	6.88×10^3	3.84
1i	-13.39	7.40×10^3	3.87
1h	-12.18	4.04×10^4	4.61
1g	-10.04	6.38×10^5	5.80

$$N = 21.29, s = 0.51$$



Reactions of the Potassium Salt of 2,4-Dimethylimidazole (**2d-K**)

Table 32: Kinetics of the reaction of **2d** with **1m** (20 °C, stopped-flow, at 486 nm).

[E] / mol L ⁻¹	[2d] / mol L ⁻¹	[18-crown-6] / mol L ⁻¹	[2d]/[E]	k_{obs} / s ⁻¹
2.37×10^{-5}	6.59×10^{-4}		27.8	0.0258
2.37×10^{-5}	1.32×10^{-3}	1.60×10^{-3}	55.7	0.0827
2.37×10^{-5}	1.98×10^{-3}		83.5	0.141
2.37×10^{-5}	2.63×10^{-3}	3.21×10^{-3}	111	0.202
2.37×10^{-5}	3.29×10^{-3}		139	0.268

$$k_2 = 9.19 \times 10^1 \text{ L mol}^{-1} \text{ s}^{-1}$$

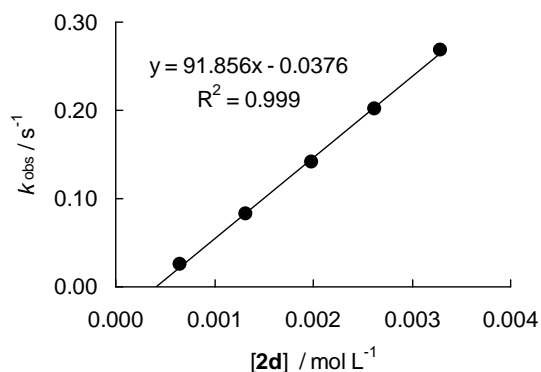
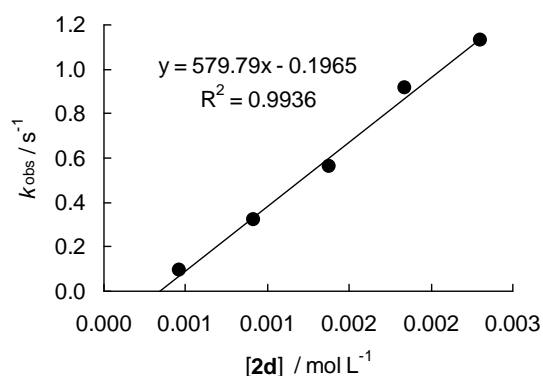


Table 33: Kinetics of the reaction of **2d** with **1l** (20 °C, stopped-flow, at 393 nm).

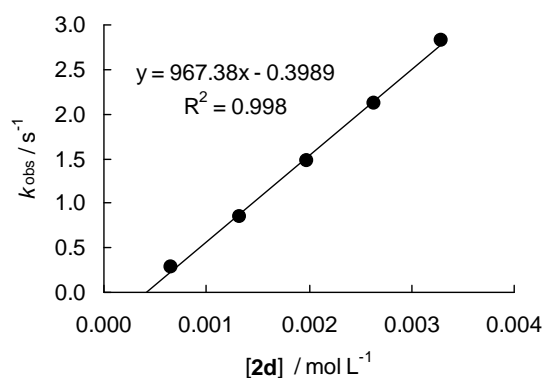
[E] / mol L ⁻¹	[2d] / mol L ⁻¹	[18-crown-6] / mol L ⁻¹	[2d]/[E]	<i>k</i> _{obs} / s ⁻¹
2.77 × 10 ⁻⁵	4.60 × 10 ⁻⁴		16.6	0.0917
2.77 × 10 ⁻⁵	9.19 × 10 ⁻⁴	1.15 × 10 ⁻³	33.2	0.323
2.77 × 10 ⁻⁵	1.38 × 10 ⁻³		49.8	0.559
2.77 × 10 ⁻⁵	1.84 × 10 ⁻³	2.30 × 10 ⁻³	66.4	0.914
2.77 × 10 ⁻⁵	2.30 × 10 ⁻³		83.0	1.13

$$k_2 = 5.80 \times 10^2 \text{ L mol}^{-1} \text{ s}^{-1}$$


 Table 34: Kinetics of the reaction of **2d** with **1k** (20 °C, stopped-flow, at 371 nm).

[E] / mol L ⁻¹	[2d] / mol L ⁻¹	[18-crown-6] / mol L ⁻¹	[2d]/[E]	<i>k</i> _{obs} / s ⁻¹
2.98 × 10 ⁻⁵	6.59 × 10 ⁻⁴		22.1	0.290
2.98 × 10 ⁻⁵	1.32 × 10 ⁻³	1.60 × 10 ⁻³	44.3	0.842
2.98 × 10 ⁻⁵	1.98 × 10 ⁻³		66.4	1.48
2.98 × 10 ⁻⁵	2.63 × 10 ⁻³	3.21 × 10 ⁻³	88.3	2.12
2.98 × 10 ⁻⁵	3.29 × 10 ⁻³		110.4	2.83

$$k_2 = 9.67 \times 10^2 \text{ L mol}^{-1} \text{ s}^{-1}$$


 Table 35: Kinetics of the reaction of **2d** with **1j** (20 °C, stopped-flow, at 375 nm).

[E] / mol L ⁻¹	[2d] / mol L ⁻¹	[18-crown-6] / mol L ⁻¹	[2d]/[E]	<i>k</i> _{obs} / s ⁻¹
2.28 × 10 ⁻⁵	4.90 × 10 ⁻⁴	6.32 × 10 ⁻⁴	21.5	1.36
2.28 × 10 ⁻⁵	7.35 × 10 ⁻⁴		32.2	3.58
2.28 × 10 ⁻⁵	9.80 × 10 ⁻⁴	1.26 × 10 ⁻³	43.0	6.73
2.28 × 10 ⁻⁵	1.23 × 10 ⁻³		53.9	8.75

$$k_2 = 1.03 \times 10^4 \text{ L mol}^{-1} \text{ s}^{-1}$$

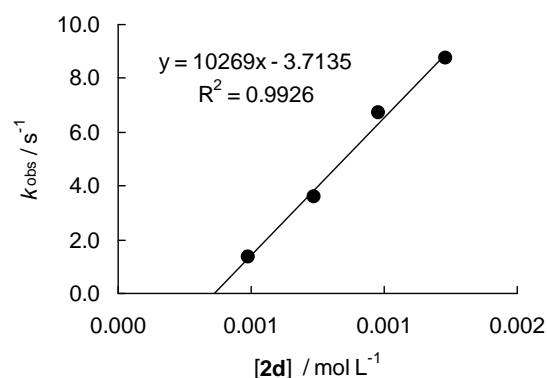
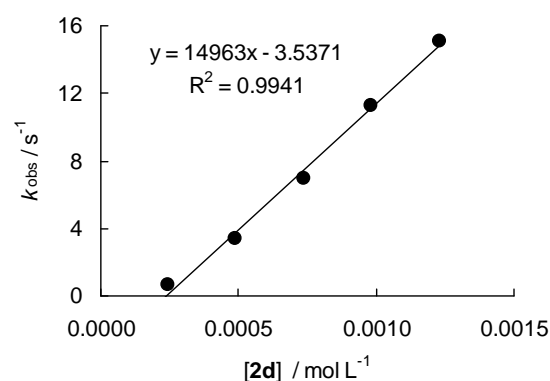


Table 36: Kinetics of the reaction of **2d** with **1i** (20 °C, stopped-flow, at 533 nm).

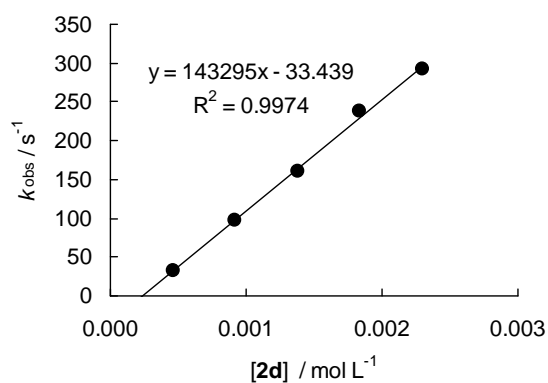
[E] / mol L ⁻¹	[2d] / mol L ⁻¹	[18-crown-6] / mol L ⁻¹	[2d]/[E]	<i>k</i> _{obs} / s ⁻¹
1.75 × 10 ⁻⁵	2.45 × 10 ⁻⁴		14.0	0.658
1.75 × 10 ⁻⁵	4.90 × 10 ⁻⁴	6.32 × 10 ⁻⁴	28.0	3.38
1.75 × 10 ⁻⁵	7.35 × 10 ⁻⁴		42.0	6.94
1.75 × 10 ⁻⁵	9.80 × 10 ⁻⁴	1.26 × 10 ⁻³	56.0	11.3
1.75 × 10 ⁻⁵	1.23 × 10 ⁻³		70.3	15.1

$$k_2 = 1.50 \times 10^4 \text{ L mol}^{-1} \text{ s}^{-1}$$

Table 37: Kinetics of the reaction of **2d** with **1h** (20 °C, stopped-flow, at 422 nm).

[E] / mol L ⁻¹	[2d] / mol L ⁻¹	[18-crown-6] / mol L ⁻¹	[2d]/[E]	<i>k</i> _{obs} / s ⁻¹
2.76 × 10 ⁻⁵	4.60 × 10 ⁻⁴		16.7	33.3
2.76 × 10 ⁻⁵	9.19 × 10 ⁻⁴	1.15 × 10 ⁻³	33.3	97.1
2.76 × 10 ⁻⁵	1.38 × 10 ⁻³		50.0	160
2.76 × 10 ⁻⁵	1.84 × 10 ⁻³	2.30 × 10 ⁻³	66.7	239
2.76 × 10 ⁻⁵	2.30 × 10 ⁻³		83.3	292

$$k_2 = 1.43 \times 10^5 \text{ L mol}^{-1} \text{ s}^{-1}$$

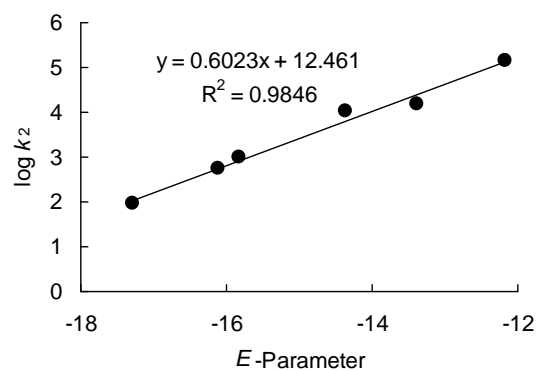


Determination of Reactivity Parameters *N* and *s* for the Anion of 2,4-Dimethyl Imidazole (**2d**) in DMSO

Table 38: Rate Constants for the reactions of **2d** with different electrophiles (20 °C).

Electrophile	<i>E</i>	<i>k</i> ₂ / L mol ⁻¹ s ⁻¹	log <i>k</i> ₂
1m	-17.29	9.19 × 10 ¹	1.96
1l	-16.11	5.80 × 10 ²	2.76
1k	-15.83	9.67 × 10 ²	2.99
1j	-14.36	1.04 × 10 ⁴	4.02
1i	-13.39	1.50 × 10 ⁴	4.18
1h	-12.18	1.43 × 10 ⁵	5.16

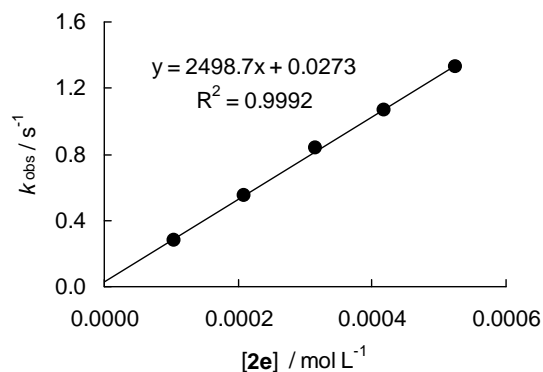
$$N = 20.69, s = 0.60$$



Reactions of the Potassium Salt of 4-Nitroimidazole (2e-K)Table 39: Kinetics of the reaction of **2e** with **1g** (20 °C, stopped-flow, at 630 nm).

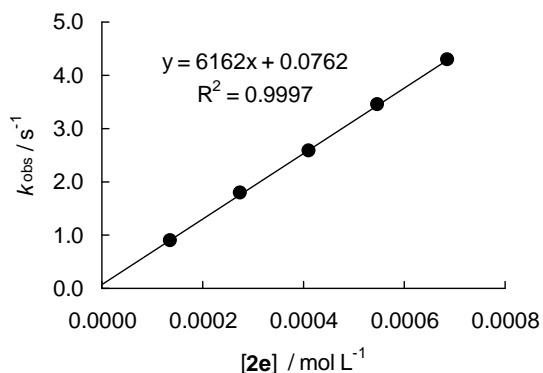
[E] / mol L ⁻¹	[2e] / mol L ⁻¹	[18-crown-6] / mol L ⁻¹	[2e]/[E]	<i>k</i> _{obs} / s ⁻¹
1.22 × 10 ⁻⁵	1.05 × 10 ⁻⁴		8.6	0.281
1.22 × 10 ⁻⁵	2.10 × 10 ⁻⁴	3.72 × 10 ⁻⁴	17.2	0.552
1.22 × 10 ⁻⁵	3.15 × 10 ⁻⁴		25.8	0.834
1.22 × 10 ⁻⁵	4.19 × 10 ⁻⁴	7.44 × 10 ⁻⁴	34.3	1.07
1.22 × 10 ⁻⁵	5.24 × 10 ⁻⁴		43.0	1.33

$$k_2 = 2.50 \times 10^3 \text{ L mol}^{-1} \text{ s}^{-1}$$

Table 40: Kinetics of the reaction of **2e** with **1f** (20 °C, stopped-flow, at 635 nm).

[E] / mol L ⁻¹	[2e] / mol L ⁻¹	[18-crown-6] / mol L ⁻¹	[2e]/[E]	<i>k</i> _{obs} / s ⁻¹
1.01 × 10 ⁻⁵	1.37 × 10 ⁻⁴		13.6	0.904
1.01 × 10 ⁻⁵	2.74 × 10 ⁻⁴	3.72 × 10 ⁻⁴	27.1	1.80
1.01 × 10 ⁻⁵	4.11 × 10 ⁻⁴		40.7	2.59
1.01 × 10 ⁻⁵	5.48 × 10 ⁻⁴	7.44 × 10 ⁻⁴	54.3	3.45
1.01 × 10 ⁻⁵	6.85 × 10 ⁻⁴		67.8	4.30

$$k_2 = 6.16 \times 10^3 \text{ L mol}^{-1} \text{ s}^{-1}$$

Table 41: Kinetics of the reaction of **2e** with **1e** (20 °C, stopped-flow, at 627 nm).

[E] / mol L ⁻¹	[2e] / mol L ⁻¹	[18-crown-6] / mol L ⁻¹	[2e]/[E]	<i>k</i> _{obs} / s ⁻¹
1.24 × 10 ⁻⁵	1.37 × 10 ⁻⁴		11.0	2.03
1.24 × 10 ⁻⁵	2.74 × 10 ⁻⁴	3.72 × 10 ⁻⁴	22.1	4.01
1.24 × 10 ⁻⁵	4.11 × 10 ⁻⁴		33.1	5.86
1.24 × 10 ⁻⁵	5.48 × 10 ⁻⁴	7.44 × 10 ⁻⁴	44.2	7.81
1.24 × 10 ⁻⁵	6.85 × 10 ⁻⁴		55.2	9.78

$$k_2 = 1.41 \times 10^4 \text{ L mol}^{-1} \text{ s}^{-1}$$

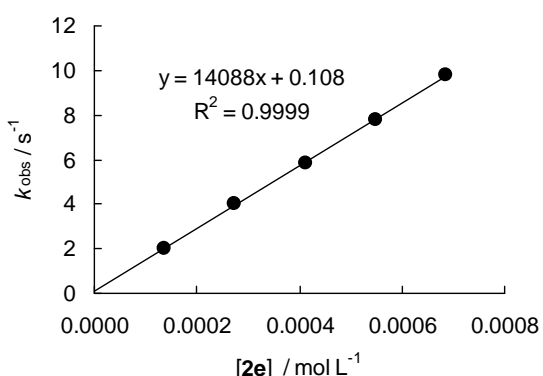
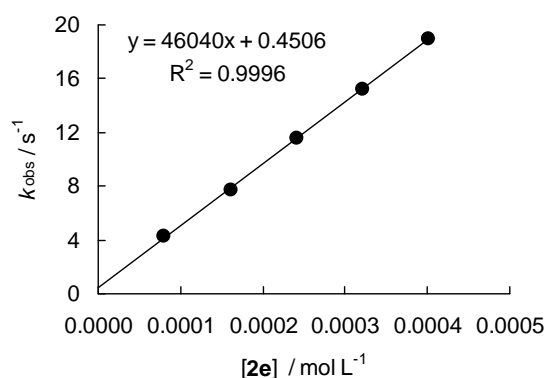


Table 42: Kinetics of the reaction of **2e** with **1d** (20 °C, stopped-flow, at 618 nm).

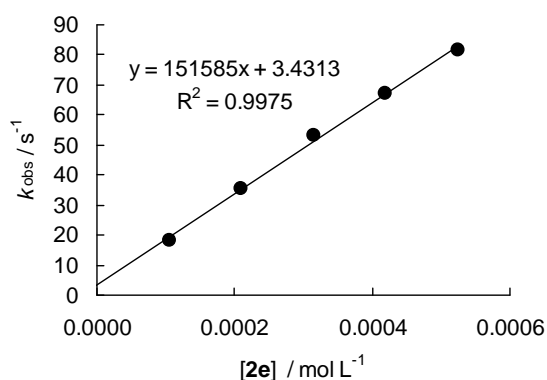
[E] / mol L ⁻¹	[2e] / mol L ⁻¹	[18-crown-6] / mol L ⁻¹	[2e]/[E]	<i>k</i> _{obs} / s ⁻¹
7.95 × 10 ⁻⁶	8.04 × 10 ⁻⁵		10.1	4.27
7.95 × 10 ⁻⁶	1.61 × 10 ⁻⁴	2.79 × 10 ⁻⁴	20.3	7.68
7.95 × 10 ⁻⁶	2.41 × 10 ⁻⁴		30.3	11.6
7.95 × 10 ⁻⁶	3.21 × 10 ⁻⁴	5.58 × 10 ⁻⁴	40.4	15.2
7.95 × 10 ⁻⁶	4.02 × 10 ⁻⁴		50.6	19.0

$$k_2 = 4.60 \times 10^4 \text{ L mol}^{-1} \text{ s}^{-1}$$


 Table 43: Kinetics of the reaction of **2e** with **1c** (20 °C, stopped-flow, at 620 nm).

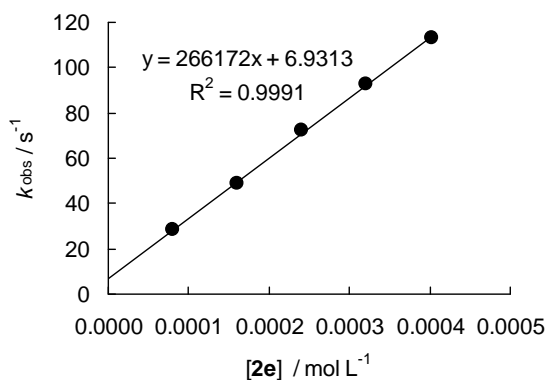
[E] / mol L ⁻¹	[2e] / mol L ⁻¹	[18-crown-6] / mol L ⁻¹	[2e]/[E]	<i>k</i> _{obs} / s ⁻¹
1.28 × 10 ⁻⁵	1.05 × 10 ⁻⁴		8.2	18.3
1.28 × 10 ⁻⁵	2.10 × 10 ⁻⁴	3.72 × 10 ⁻⁴	16.4	35.3
1.28 × 10 ⁻⁵	3.15 × 10 ⁻⁴		24.6	53.2
1.28 × 10 ⁻⁵	4.19 × 10 ⁻⁴	7.44 × 10 ⁻⁴	32.7	67.0
1.28 × 10 ⁻⁵	5.24 × 10 ⁻⁴		40.9	81.8

$$k_2 = 1.52 \times 10^5 \text{ L mol}^{-1} \text{ s}^{-1}$$


 Table 44: Kinetics of the reaction of **2e** with **1b** (20 °C, stopped-flow, at 613 nm).

[E] / mol L ⁻¹	[2e] / mol L ⁻¹	[18-crown-6] / mol L ⁻¹	[2e]/[E]	<i>k</i> _{obs} / s ⁻¹
6.00 × 10 ⁻⁶	8.04 × 10 ⁻⁵		13.4	28.2
6.00 × 10 ⁻⁶	1.61 × 10 ⁻⁴	2.79 × 10 ⁻⁴	26.8	48.8
6.00 × 10 ⁻⁶	2.41 × 10 ⁻⁴		40.2	72.5
6.00 × 10 ⁻⁶	3.21 × 10 ⁻⁴	5.58 × 10 ⁻⁴	53.5	93.0
6.00 × 10 ⁻⁶	4.02 × 10 ⁻⁴		67.0	113

$$k_2 = 2.66 \times 10^5 \text{ L mol}^{-1} \text{ s}^{-1}$$

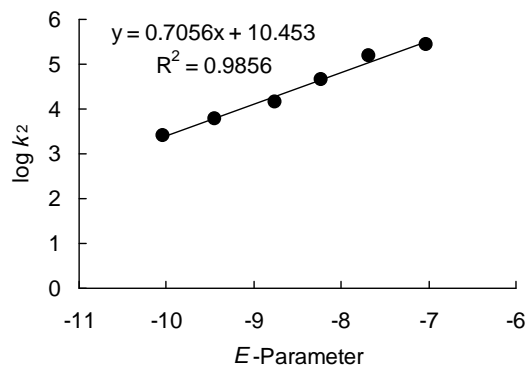


Determination of Reactivity Parameters N and s for the Anion of 4-Nitro Imidazole (**2e**) in DMSO

Table 45: Rate Constants for the reactions of **2e** with different electrophiles (20 °C).

Electrophile	E	$k_2 / \text{L mol}^{-1} \text{s}^{-1}$	$\log k_2$
1g	-10.04	2.50×10^3	3.40
1f	-9.45	6.16×10^3	3.79
1e	-8.76	1.41×10^4	4.15
1d	-8.22	4.60×10^4	4.66
1c	-7.69	1.52×10^5	5.18
1b	-7.02	2.66×10^5	5.42

$$N = 14.81, s = 0.71$$

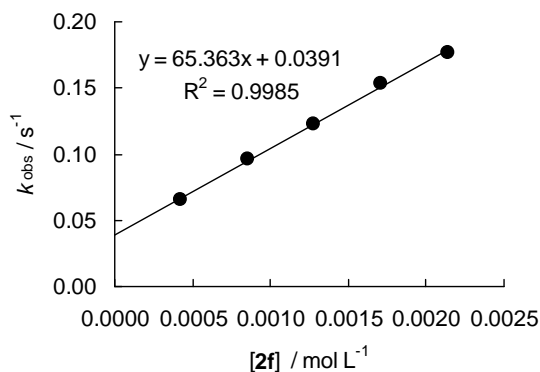


Reactions of the Potassium Salt of 2-Formylimidazole (**2f-K**)

Table 46: Kinetics of the reaction of **2f** with **1i** (20 °C, stopped-flow, at 533 nm).

$[\text{E}] / \text{mol L}^{-1}$	$[\mathbf{2f}] / \text{mol L}^{-1}$	$[\text{18-crown-6}] / \text{mol L}^{-1}$	$[\mathbf{2f}]/[\text{E}]$	$k_{\text{obs}} / \text{s}^{-1}$
1.43×10^{-5}	4.27×10^{-4}		29.9	0.0656
1.43×10^{-5}	8.54×10^{-4}	8.95×10^{-4}	59.7	0.0959
1.43×10^{-5}	1.28×10^{-3}		89.5	0.123
1.43×10^{-5}	1.71×10^{-3}	1.79×10^{-3}	120	0.153
1.43×10^{-5}	2.14×10^{-3}		150	0.177

$$k_2 = 6.54 \times 10^1 \text{ L mol}^{-1} \text{ s}^{-1}$$

Table 47: Kinetics of the reaction of **2f** with **1h** (20 °C, stopped-flow, at 422 nm).

$[\text{E}] / \text{mol L}^{-1}$	$[\mathbf{2f}] / \text{mol L}^{-1}$	$[\text{18-crown-6}] / \text{mol L}^{-1}$	$[\mathbf{2f}]/[\text{E}]$	$k_{\text{obs}} / \text{s}^{-1}$
1.73×10^{-5}	1.75×10^{-4}		10.1	0.0718
1.73×10^{-5}	3.50×10^{-4}	4.77×10^{-4}	20.2	0.143
1.73×10^{-5}	5.25×10^{-4}		30.3	0.210
1.73×10^{-5}	7.01×10^{-4}	9.53×10^{-4}	40.5	0.286
1.73×10^{-5}	8.76×10^{-4}		50.6	0.354

$$k_2 = 4.04 \times 10^2 \text{ L mol}^{-1} \text{ s}^{-1}$$

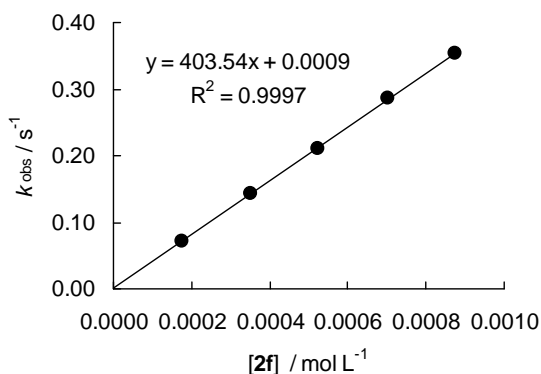
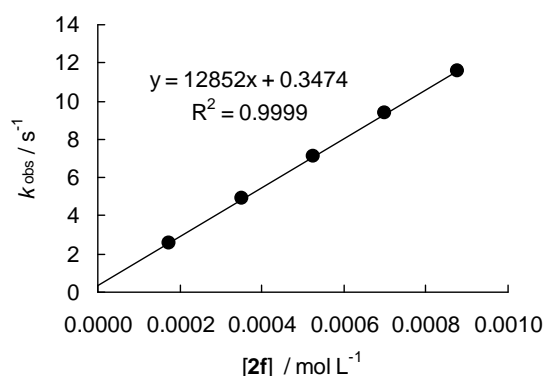


Table 48: Kinetics of the reaction of **2f** with **1g** (20 °C, stopped-flow, at 630 nm).

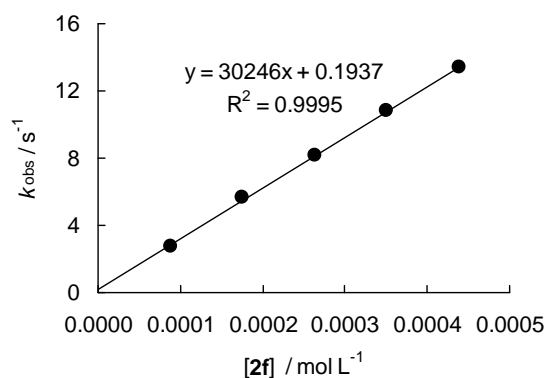
[E] / mol L ⁻¹	[2f] / mol L ⁻¹	[18-crown-6] / mol L ⁻¹	[2f]/[E]	<i>k</i> _{obs} / s ⁻¹
1.75 × 10 ⁻⁵	1.75 × 10 ⁻⁴		10.0	2.57
1.75 × 10 ⁻⁵	3.50 × 10 ⁻⁴	4.77 × 10 ⁻⁴	20.0	4.89
1.75 × 10 ⁻⁵	5.25 × 10 ⁻⁴		30.0	7.08
1.75 × 10 ⁻⁵	7.01 × 10 ⁻⁴	9.53 × 10 ⁻⁴	40.1	9.36
1.75 × 10 ⁻⁵	8.76 × 10 ⁻⁴		50.1	11.6

$$k_2 = 1.29 \times 10^4 \text{ L mol}^{-1} \text{ s}^{-1}$$

Table 49: Kinetics of the reaction of **2f** with **1f** (20 °C, stopped-flow, at 635 nm).

[E] / mol L ⁻¹	[2f] / mol L ⁻¹	[18-crown-6] / mol L ⁻¹	[2f]/[E]	<i>k</i> _{obs} / s ⁻¹
9.99 × 10 ⁻⁶	8.76 × 10 ⁻⁵		8.8	2.74
9.99 × 10 ⁻⁶	1.75 × 10 ⁻⁴	2.38 × 10 ⁻⁴	17.5	5.63
9.99 × 10 ⁻⁶	2.63 × 10 ⁻⁴		26.3	8.13
9.99 × 10 ⁻⁶	3.50 × 10 ⁻⁴	4.77 × 10 ⁻⁴	35.0	10.8
9.99 × 10 ⁻⁶	4.38 × 10 ⁻⁴		43.8	13.4

$$k_2 = 3.02 \times 10^4 \text{ L mol}^{-1} \text{ s}^{-1}$$

Table 50: Kinetics of the reaction of **2f** with **1e** (20 °C, stopped-flow, at 627 nm).

[E] / mol L ⁻¹	[2f] / mol L ⁻¹	[18-crown-6] / mol L ⁻¹	[2f]/[E]	<i>k</i> _{obs} / s ⁻¹
1.24 × 10 ⁻⁵	2.11 × 10 ⁻⁴		17.0	16.2
1.24 × 10 ⁻⁵	4.22 × 10 ⁻⁴	5.49 × 10 ⁻⁴	34.0	30.7
1.24 × 10 ⁻⁵	6.33 × 10 ⁻⁴		51.0	43.3
1.24 × 10 ⁻⁵	8.44 × 10 ⁻⁴	1.10 × 10 ⁻³	68.1	56.3
1.24 × 10 ⁻⁵	1.05 × 10 ⁻³		84.7	66.7

$$k_2 = 6.03 \times 10^4 \text{ L mol}^{-1} \text{ s}^{-1}$$

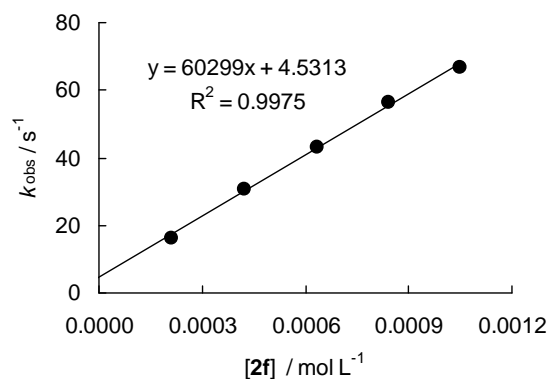
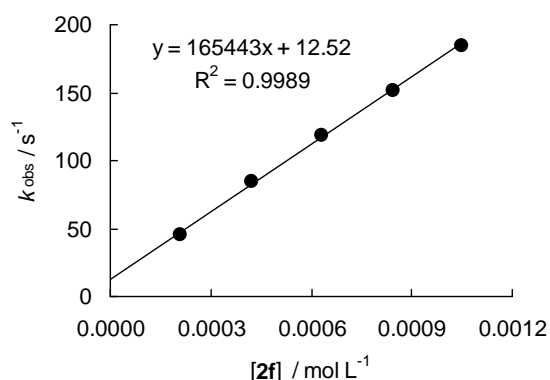


Table 51: Kinetics of the reaction of **2f** with **1d** (20 °C, stopped-flow, at 618 nm).

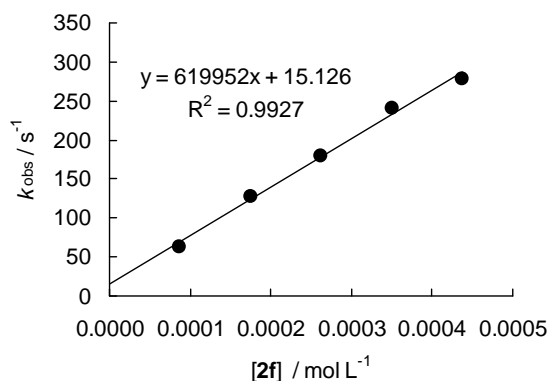
[E] / mol L ⁻¹	[2f] / mol L ⁻¹	[18-crown-6] / mol L ⁻¹	[2f]/[E]	<i>k</i> _{obs} / s ⁻¹
1.25 × 10 ⁻⁵	2.11 × 10 ⁻⁴		16.9	45.2
1.25 × 10 ⁻⁵	4.22 × 10 ⁻⁴	5.49 × 10 ⁻⁴	33.8	84.2
1.25 × 10 ⁻⁵	6.33 × 10 ⁻⁴		50.6	119
1.25 × 10 ⁻⁵	8.44 × 10 ⁻⁴	1.10 × 10 ⁻³	67.5	152
1.25 × 10 ⁻⁵	1.05 × 10 ⁻³		84.0	185

$$k_2 = 1.65 \times 10^5 \text{ L mol}^{-1} \text{ s}^{-1}$$


 Table 52: Kinetics of the reaction of **2f** with **1c** (20 °C, stopped-flow, at 620 nm).

[E] / mol L ⁻¹	[2f] / mol L ⁻¹	[18-crown-6] / mol L ⁻¹	[2f]/[E]	<i>k</i> _{obs} / s ⁻¹
1.10 × 10 ⁻⁵	8.76 × 10 ⁻⁵		8.0	63.0
1.10 × 10 ⁻⁵	1.75 × 10 ⁻⁴	2.38 × 10 ⁻⁴	15.9	128
1.10 × 10 ⁻⁵	2.63 × 10 ⁻⁴		23.9	180
1.10 × 10 ⁻⁵	3.50 × 10 ⁻⁴	4.77 × 10 ⁻⁴	31.8	241
1.10 × 10 ⁻⁵	4.38 × 10 ⁻⁴		39.8	278

$$k_2 = 6.20 \times 10^5 \text{ L mol}^{-1} \text{ s}^{-1}$$

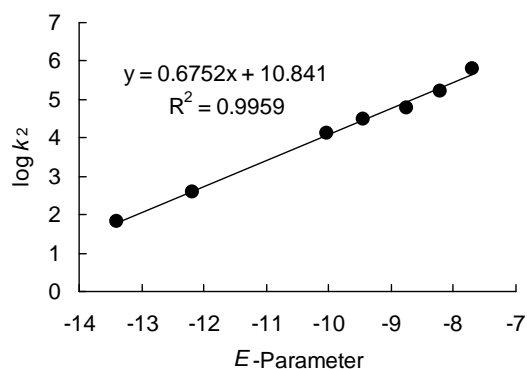


Determination of Reactivity Parameters *N* and *s* for the Anion of 2-Formyl Imidazole (**2f**) in DMSO

 Table 53: Rate Constants for the reactions of **2f** with different electrophiles (20 °C).

Electrophile	<i>E</i>	<i>k</i> ₂ / L mol ⁻¹ s ⁻¹	log <i>k</i> ₂
1i	-13.39	6.54 × 10 ¹	1.82
1h	-12.18	4.04 × 10 ²	2.61
1g	-10.04	1.29 × 10 ⁴	4.11
1f	-9.45	3.02 × 10 ⁴	4.48
1e	-8.76	6.03 × 10 ⁴	4.78
1d	-8.22	1.65 × 10 ⁵	5.22
1c	-7.69	6.20 × 10 ⁵	5.79

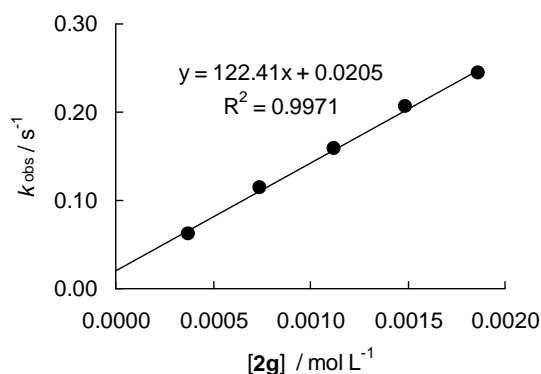
$$N = 16.06, s = 0.68$$



Reactions of the Potassium Salt of 4-Formylimidazole (2g-K)Table 54: Kinetics of the reaction of **2g** with **1i** (20 °C, stopped-flow, at 533 nm).

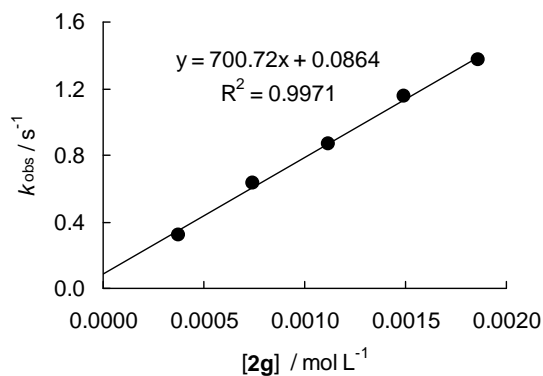
[E] / mol L ⁻¹	[2g] / mol L ⁻¹	[18-crown-6] / mol L ⁻¹	[2g]/[E]	$k_{\text{obs}} /$ s ⁻¹
1.17×10^{-5}	3.72×10^{-4}		31.8	0.0622
1.17×10^{-5}	7.44×10^{-4}	9.61×10^{-4}	63.6	0.115
1.17×10^{-5}	1.12×10^{-3}		95.7	0.158
1.17×10^{-5}	1.49×10^{-3}	1.92×10^{-3}	127	0.207
1.17×10^{-5}	1.86×10^{-3}		159	0.244

$$k_2 = 1.22 \times 10^2 \text{ L mol}^{-1} \text{ s}^{-1}$$

Table 55: Kinetics of the reaction of **2g** with **1h** (20 °C, stopped-flow, at 422 nm).

[E] / mol L ⁻¹	[2g] / mol L ⁻¹	[18-crown-6] / mol L ⁻¹	[2g]/[E]	$k_{\text{obs}} /$ s ⁻¹
1.21×10^{-5}	3.72×10^{-4}		30.7	0.324
1.21×10^{-5}	7.44×10^{-4}	9.61×10^{-4}	61.5	0.634
1.21×10^{-5}	1.12×10^{-3}		92.6	0.868
1.21×10^{-5}	1.49×10^{-3}	1.92×10^{-3}	123	1.15
1.21×10^{-5}	1.86×10^{-3}		154	1.37

$$k_2 = 7.01 \times 10^2 \text{ L mol}^{-1} \text{ s}^{-1}$$

Table 56: Kinetics of the reaction of **2g** with **1g** (20 °C, stopped-flow, at 630 nm).

[E] / mol L ⁻¹	[2g] / mol L ⁻¹	[18-crown-6] / mol L ⁻¹	[2g]/[E]	$k_{\text{obs}} /$ s ⁻¹
1.30×10^{-5}	2.97×10^{-4}		22.8	8.04
1.30×10^{-5}	5.93×10^{-4}	8.01×10^{-4}	45.6	12.6
1.30×10^{-5}	8.90×10^{-4}		68.5	19.2
1.30×10^{-5}	1.19×10^{-3}	1.60×10^{-3}	91.5	24.7
1.30×10^{-5}	1.48×10^{-3}		114	29.0

$$k_2 = 1.82 \times 10^4 \text{ L mol}^{-1} \text{ s}^{-1}$$

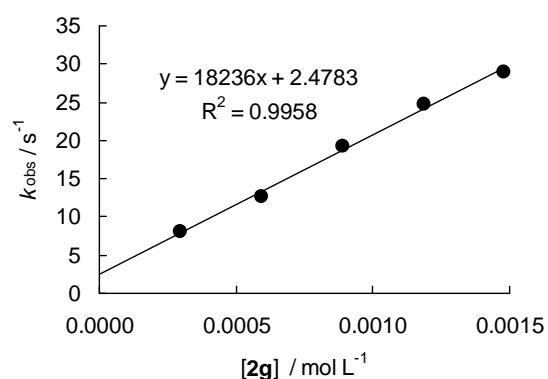
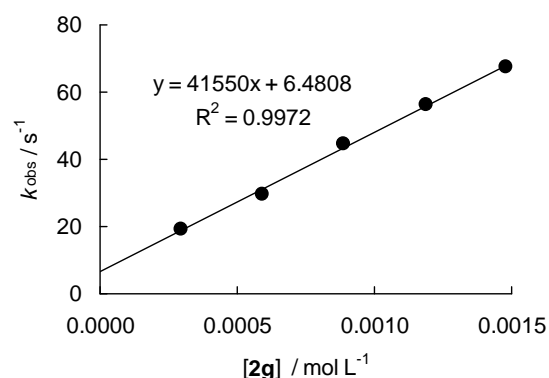


Table 57: Kinetics of the reaction of **2g** with **1f** (20 °C, stopped-flow, at 635 nm).

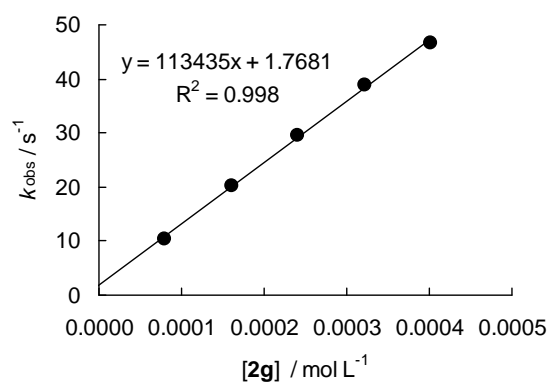
[E] / mol L ⁻¹	[2g] / mol L ⁻¹	[18-crown-6] / mol L ⁻¹	[2g]/[E]	<i>k</i> _{obs} / s ⁻¹
8.82 × 10 ⁻⁶	2.97 × 10 ⁻⁴		33.7	19.3
8.82 × 10 ⁻⁶	5.93 × 10 ⁻⁴	8.01 × 10 ⁻⁴	67.2	29.6
8.82 × 10 ⁻⁶	8.90 × 10 ⁻⁴		101	44.6
8.82 × 10 ⁻⁶	1.19 × 10 ⁻³	1.60 × 10 ⁻³	135	56.3
8.82 × 10 ⁻⁶	1.48 × 10 ⁻³		168	67.5

$$k_2 = 4.16 \times 10^4 \text{ L mol}^{-1} \text{ s}^{-1}$$


 Table 58: Kinetics of the reaction of **2g** with **1e** (20 °C, stopped-flow, at 627 nm).

[E] / mol L ⁻¹	[2g] / mol L ⁻¹	[18-crown-6] / mol L ⁻¹	[2g]/[E]	<i>k</i> _{obs} / s ⁻¹
7.58 × 10 ⁻⁶	8.05 × 10 ⁻⁵		10.6	10.3
7.58 × 10 ⁻⁶	1.61 × 10 ⁻⁴	2.40 × 10 ⁻⁴	21.2	20.3
7.58 × 10 ⁻⁶	2.41 × 10 ⁻⁴		31.8	29.6
7.58 × 10 ⁻⁶	3.22 × 10 ⁻⁴	4.84 × 10 ⁻⁴	42.5	38.9
7.58 × 10 ⁻⁶	4.02 × 10 ⁻⁴		53.0	46.6

$$k_2 = 1.13 \times 10^5 \text{ L mol}^{-1} \text{ s}^{-1}$$


 Table 59: Kinetics of the reaction of **2g** with **1d** (20 °C, stopped-flow, at 618 nm).

[E] / mol L ⁻¹	[2g] / mol L ⁻¹	[18-crown-6] / mol L ⁻¹	[2g]/[E]	<i>k</i> _{obs} / s ⁻¹
8.13 × 10 ⁻⁶	8.05 × 10 ⁻⁵		9.9	29.8
8.13 × 10 ⁻⁶	1.61 × 10 ⁻⁴	2.40 × 10 ⁻⁴	19.8	56.4
8.13 × 10 ⁻⁶	2.41 × 10 ⁻⁴		29.6	80.7
8.13 × 10 ⁻⁶	3.22 × 10 ⁻⁴	4.84 × 10 ⁻⁴	39.6	106
8.13 × 10 ⁻⁶	4.02 × 10 ⁻⁴		49.4	131

$$k_2 = 3.13 \times 10^5 \text{ L mol}^{-1} \text{ s}^{-1}$$

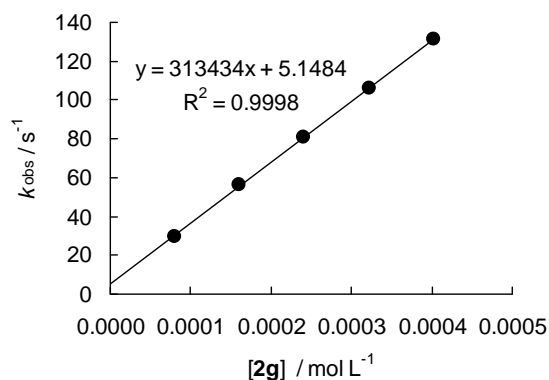
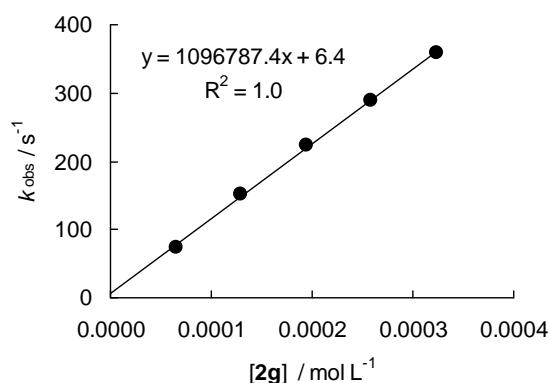


Table 60: Kinetics of the reaction of **2g** with **1c** (20 °C, stopped-flow, at 620 nm).

[E] / mol L ⁻¹	[2g] / mol L ⁻¹	[2g]/[E]]	<i>k</i> _{obs} / s ⁻¹
7.34 × 10 ⁻⁶	6.47 × 10 ⁻⁵	8.8	73.4
7.34 × 10 ⁻⁶	1.19 × 10 ⁻⁴	17.6	151
7.34 × 10 ⁻⁶	1.94 × 10 ⁻⁴	26.4	223
7.34 × 10 ⁻⁶	2.59 × 10 ⁻⁴	35.3	289
7.34 × 10 ⁻⁶	3.23 × 10 ⁻⁴	44.0	359

$$k_2 = 1.10 \times 10^6 \text{ L mol}^{-1} \text{ s}^{-1}$$

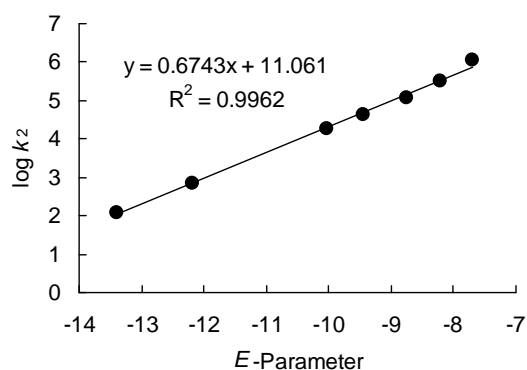


Determination of Reactivity Parameters *N* and *s* for the Anion of 4-Formyl Imidazole (**2g**) in DMSO

Table 61: Rate Constants for the reactions of **2g** with different electrophiles (20 °C).

Electrophile	<i>E</i>	<i>k</i> ₂ / L mol ⁻¹ s ⁻¹	log <i>k</i> ₂
1i	-13.39	1.22 × 10 ²	2.09
1h	-12.18	7.01 × 10 ²	2.85
1g	-10.04	1.84 × 10 ⁴	4.26
1f	-9.45	4.16 × 10 ⁴	4.62
1e	-8.76	1.13 × 10 ⁵	5.05
1d	-8.22	3.13 × 10 ⁵	5.50
1c	-7.69	1.10 × 10 ⁶	6.04

$$N = 16.40, s = 0.67$$



Reactions of the Potassium Salt of Benzimidazole (**3a-K**)

Table 62: Kinetics of the reaction of **3a** with **1k** (20 °C, stopped-flow, at 371 nm).

[E] / mol L ⁻¹	[3a] / mol L ⁻¹	[18-crown-6] / mol L ⁻¹	[3a]/[E]	<i>k</i> _{obs} / s ⁻¹
1.85 × 10 ⁻⁵	3.52 × 10 ⁻⁴		19.0	0.0268
1.85 × 10 ⁻⁵	7.04 × 10 ⁻⁴	9.08 × 10 ⁻⁴	38.1	0.0511
1.85 × 10 ⁻⁵	1.06 × 10 ⁻³		57.3	0.0757
1.85 × 10 ⁻⁵	1.41 × 10 ⁻³	1.82 × 10 ⁻³	76.2	0.0989
1.85 × 10 ⁻⁵	1.76 × 10 ⁻³		95.1	0.124

$$k_2 = 6.88 \times 10^1 \text{ L mol}^{-1} \text{ s}^{-1}$$

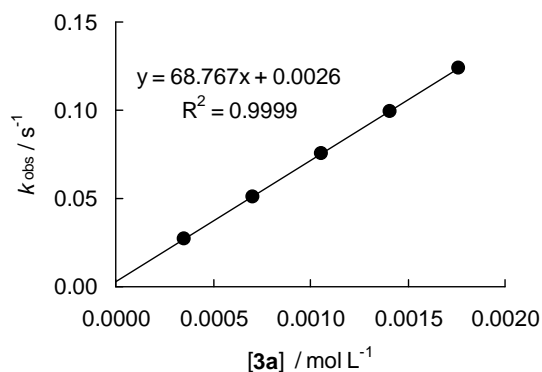
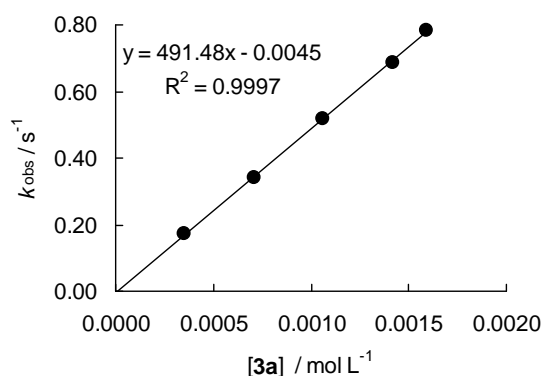


Table 63: Kinetics of the reaction of **3a** with **1j** (20 °C, stopped-flow, at 375 nm).

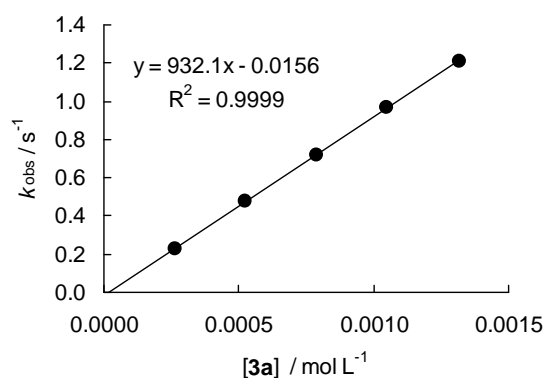
[E] / mol L ⁻¹	[3a] / mol L ⁻¹	[18-crown-6] / mol L ⁻¹	[3a]/[E]	<i>k</i> _{obs} / s ⁻¹
1.74 × 10 ⁻⁵	3.54 × 10 ⁻⁴		20.3	0.171
1.74 × 10 ⁻⁵	7.08 × 10 ⁻⁴	9.68 × 10 ⁻⁴	40.7	0.343
1.74 × 10 ⁻⁵	1.06 × 10 ⁻³		60.9	0.516
1.74 × 10 ⁻⁵	1.42 × 10 ⁻³	1.94 × 10 ⁻³	81.6	0.687
1.74 × 10 ⁻⁵	1.59 × 10 ⁻³		91.4	0.783

$$k_2 = 4.91 \times 10^2 \text{ L mol}^{-1} \text{ s}^{-1}$$

Table 64: Kinetics of the reaction of **3a** with **1i** (20 °C, stopped-flow, at 533 nm).

[E] / mol L ⁻¹	[3a] / mol L ⁻¹	[18-crown-6] / mol L ⁻¹	[3a]/[E]	<i>k</i> _{obs} / s ⁻¹
1.38 × 10 ⁻⁵	2.63 × 10 ⁻⁴		19.1	0.225
1.38 × 10 ⁻⁵	5.26 × 10 ⁻⁴	6.56 × 10 ⁻⁴	38.1	0.479
1.38 × 10 ⁻⁵	7.89 × 10 ⁻⁴		57.2	0.720
1.38 × 10 ⁻⁵	1.05 × 10 ⁻³	1.30 × 10 ⁻³	76.1	0.968
1.38 × 10 ⁻⁵	1.32 × 10 ⁻³		95.7	1.21

$$k_2 = 9.32 \times 10^2 \text{ L mol}^{-1} \text{ s}^{-1}$$

Table 65: Kinetics of the reaction of **3a** with **1h** (20 °C, stopped-flow, at 422 nm).

[E] / mol L ⁻¹	[3a] / mol L ⁻¹	[18-crown-6] / mol L ⁻¹	[3a]/[E]	<i>k</i> _{obs} / s ⁻¹
1.40 × 10 ⁻⁵	2.63 × 10 ⁻⁴		18.8	1.47
1.40 × 10 ⁻⁵	5.26 × 10 ⁻⁴	6.56 × 10 ⁻⁴	37.6	3.04
1.40 × 10 ⁻⁵	7.89 × 10 ⁻⁴		56.4	4.71
1.40 × 10 ⁻⁵	1.05 × 10 ⁻³	1.30 × 10 ⁻³	75.0	6.22
1.40 × 10 ⁻⁵	1.32 × 10 ⁻³		94.3	7.86

$$k_2 = 6.05 \times 10^3 \text{ L mol}^{-1} \text{ s}^{-1}$$

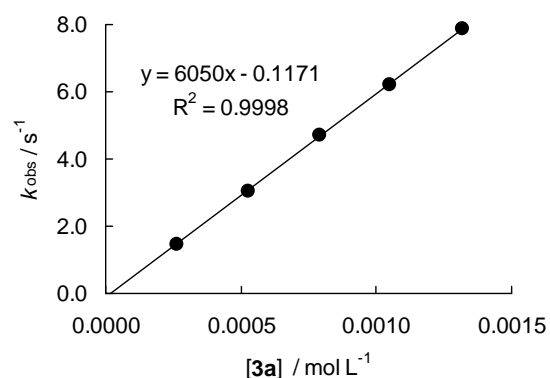
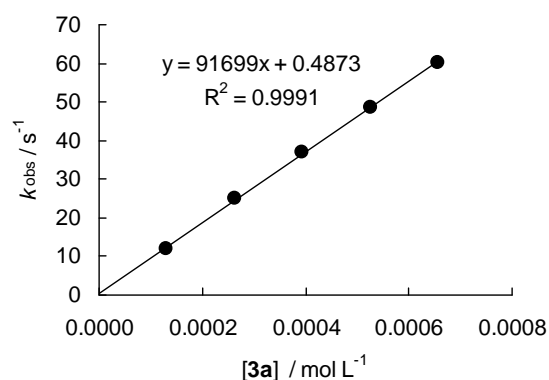


Table 66: Kinetics of the reaction of **3a** with **1g** (20 °C, stopped-flow, at 630 nm).

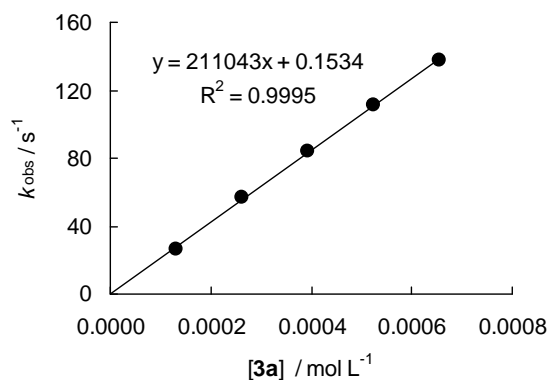
[E] / mol L ⁻¹	[3a] / mol L ⁻¹	[18-crown-6] / mol L ⁻¹	[3a]/[E]	<i>k</i> _{obs} / s ⁻¹
1.23 × 10 ⁻⁵	1.31 × 10 ⁻⁴		10.7	11.8
1.23 × 10 ⁻⁵	2.62 × 10 ⁻⁴	3.26 × 10 ⁻⁴	21.3	25.1
1.23 × 10 ⁻⁵	3.94 × 10 ⁻⁴		32.0	37.1
1.23 × 10 ⁻⁵	5.25 × 10 ⁻⁴	6.52 × 10 ⁻⁴	42.7	48.7
1.23 × 10 ⁻⁵	6.56 × 10 ⁻⁴		53.3	60.2

$$k_2 = 9.17 \times 10^4 \text{ L mol}^{-1} \text{ s}^{-1}$$

Table 67: Kinetics of the reaction of **3a** with **1f** (20 °C, stopped-flow, at 635 nm).

[E] / mol L ⁻¹	[3a] / mol L ⁻¹	[18-crown-6] / mol L ⁻¹	[3a]/[E]	<i>k</i> _{obs} / s ⁻¹
1.30 × 10 ⁻⁵	1.31 × 10 ⁻⁴		10.1	26.6
1.30 × 10 ⁻⁵	2.62 × 10 ⁻⁴	3.26 × 10 ⁻⁴	20.2	56.7
1.30 × 10 ⁻⁵	3.94 × 10 ⁻⁴		30.3	83.8
1.30 × 10 ⁻⁵	5.25 × 10 ⁻⁴	6.52 × 10 ⁻⁴	40.4	111
1.30 × 10 ⁻⁵	6.56 × 10 ⁻⁴		50.5	138

$$k_2 = 2.11 \times 10^5 \text{ L mol}^{-1} \text{ s}^{-1}$$

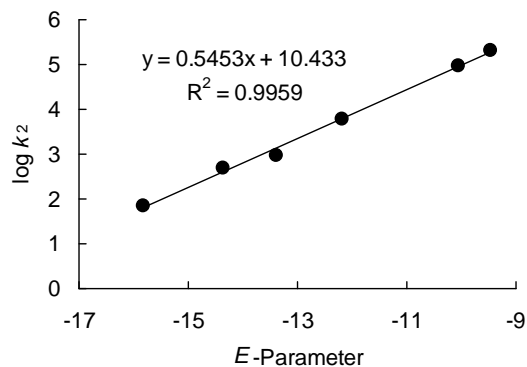


Determination of Reactivity Parameters *N* and *s* for the Benzimidazole Anion (**3a**) in DMSO

Table 68: Rate Constants for the reactions of **3a** with different electrophiles (20 °C).

Electrophile	<i>E</i>	<i>k</i> ₂ / L mol ⁻¹ s ⁻¹	log <i>k</i> ₂
1k	-15.83	6.88 × 10 ¹	1.84
1j	-14.36	4.91 × 10 ²	2.69
1i	-13.39	9.32 × 10 ²	2.97
1h	-12.18	6.05 × 10 ³	3.78
1g	-10.04	9.17 × 10 ⁴	4.96
1f	-9.45	2.11 × 10 ⁵	5.32

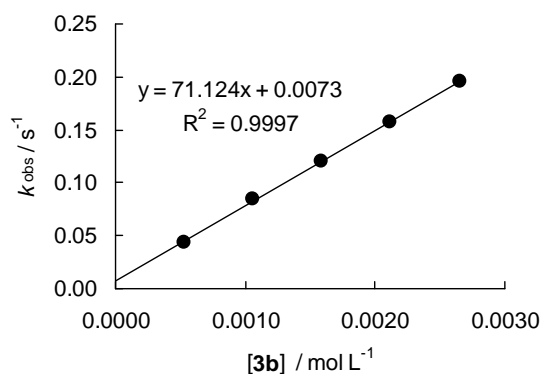
$$N = 19.13, s = 0.55$$



Reactions of the Potassium Salt of Benzotriazole (3b-K)Table 69: Kinetics of the reaction of **3b** with **1i** (20 °C, stopped-flow, at 533 nm).

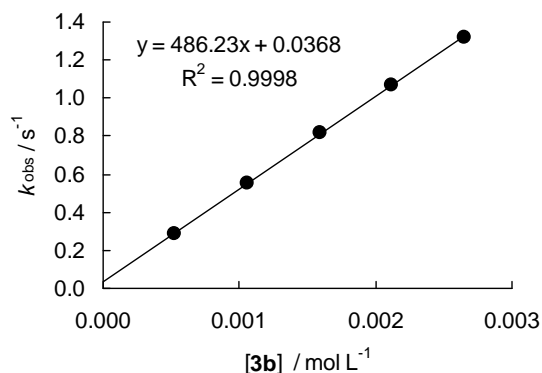
[E] / mol L ⁻¹	[3b] / mol L ⁻¹	[18-crown-6] / mol L ⁻¹	[3b]/[E]	<i>k</i> _{obs} / s ⁻¹
1.91 × 10 ⁻⁵	5.29 × 10 ⁻⁴		27.7	0.0439
1.91 × 10 ⁻⁵	1.06 × 10 ⁻³	1.21 × 10 ⁻³	55.5	0.0841
1.91 × 10 ⁻⁵	1.59 × 10 ⁻³		83.2	0.121
1.91 × 10 ⁻⁵	2.12 × 10 ⁻³	2.42 × 10 ⁻³	111	0.157
1.91 × 10 ⁻⁵	2.65 × 10 ⁻³		139	0.196

$$k_2 = 7.11 \times 10^1 \text{ L mol}^{-1} \text{ s}^{-1}$$

Table 70: Kinetics of the reaction of **3b** with **1h** (20 °C, stopped-flow, at 422 nm).

[E] / mol L ⁻¹	[3b] / mol L ⁻¹	[18-crown-6] / mol L ⁻¹	[3b]/[E]	<i>k</i> _{obs} / s ⁻¹
2.14 × 10 ⁻⁵	5.29 × 10 ⁻⁴		24.7	0.288
2.14 × 10 ⁻⁵	1.06 × 10 ⁻³	1.21 × 10 ⁻³	49.5	0.556
2.14 × 10 ⁻⁵	1.59 × 10 ⁻³		74.3	0.815
2.14 × 10 ⁻⁵	2.12 × 10 ⁻³	2.42 × 10 ⁻³	99.1	1.07
2.14 × 10 ⁻⁵	2.65 × 10 ⁻³		124	1.32

$$k_2 = 4.86 \times 10^2 \text{ L mol}^{-1} \text{ s}^{-1}$$

Table 71: Kinetics of the reaction of **3b** with **1g** (20 °C, stopped-flow, at 630 nm).

[E] / mol L ⁻¹	[3b] / mol L ⁻¹	[18-crown-6] / mol L ⁻¹	[3b]/[E]	<i>k</i> _{obs} / s ⁻¹
1.31 × 10 ⁻⁵	1.72 × 10 ⁻⁴		13.1	2.08
1.31 × 10 ⁻⁵	3.45 × 10 ⁻⁴	4.37 × 10 ⁻⁴	26.3	3.98
1.31 × 10 ⁻⁵	5.17 × 10 ⁻⁴		39.5	6.17
1.31 × 10 ⁻⁵	6.90 × 10 ⁻⁴	8.74 × 10 ⁻⁴	52.7	8.08
1.31 × 10 ⁻⁵	8.62 × 10 ⁻⁴		65.8	10.2

$$k_2 = 1.18 \times 10^4 \text{ L mol}^{-1} \text{ s}^{-1}$$

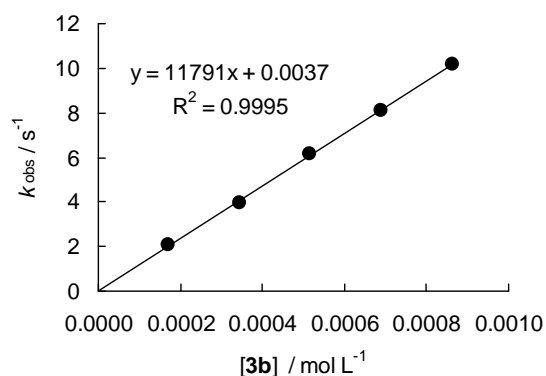
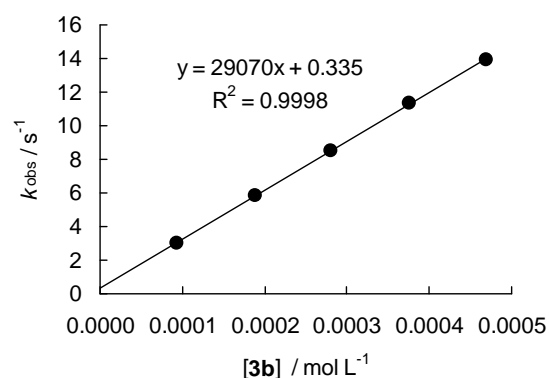


Table 72: Kinetics of the reaction of **3b** with **1f** (20 °C, stopped-flow, at 635 nm).

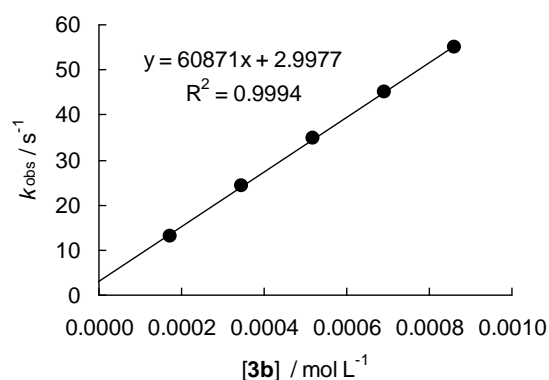
[E] / mol L ⁻¹	[3b] / mol L ⁻¹	[18-crown-6] / mol L ⁻¹	[3b]/[E]	<i>k</i> _{obs} / s ⁻¹
8.46 × 10 ⁻⁶	9.38 × 10 ⁻⁵		11.1	3.02
8.46 × 10 ⁻⁶	1.88 × 10 ⁻⁴	2.51 × 10 ⁻⁴	22.2	5.81
8.46 × 10 ⁻⁶	2.81 × 10 ⁻⁴		33.2	8.54
8.46 × 10 ⁻⁶	3.75 × 10 ⁻³	5.02 × 10 ⁻³	44.3	11.3
8.46 × 10 ⁻⁶	4.69 × 10 ⁻³		55.4	13.9

$$k_2 = 2.91 \times 10^4 \text{ L mol}^{-1} \text{ s}^{-1}$$

Table 73: Kinetics of the reaction of **3b** with **1e** (20 °C, stopped-flow, at 627 nm).

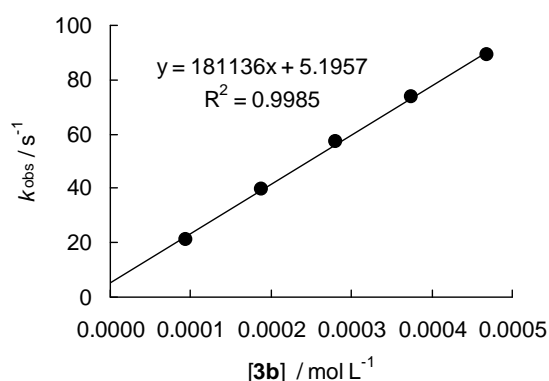
[E] / mol L ⁻¹	[3b] / mol L ⁻¹	[18-crown-6] / mol L ⁻¹	[3b]/[E]	<i>k</i> _{obs} / s ⁻¹
1.35 × 10 ⁻⁵	1.72 × 10 ⁻⁴		12.7	13.0
1.35 × 10 ⁻⁵	3.45 × 10 ⁻⁴	4.37 × 10 ⁻⁴	25.6	24.4
1.35 × 10 ⁻⁵	5.17 × 10 ⁻⁴		38.3	34.7
1.35 × 10 ⁻⁵	6.90 × 10 ⁻³	8.74 × 10 ⁻⁴	51.1	45.2
1.35 × 10 ⁻⁵	8.62 × 10 ⁻³		63.9	55.1

$$k_2 = 6.09 \times 10^4 \text{ L mol}^{-1} \text{ s}^{-1}$$

Table 74: Kinetics of the reaction of **3b** with **1d** (20 °C, stopped-flow, at 618 nm).

[E] / mol L ⁻¹	[3b] / mol L ⁻¹	[18-crown-6] / mol L ⁻¹	[3b]/[E]	<i>k</i> _{obs} / s ⁻¹
9.43 × 10 ⁻⁶	9.38 × 10 ⁻⁵		9.9	21.1
9.43 × 10 ⁻⁶	1.88 × 10 ⁻⁴	2.51 × 10 ⁻⁴	19.9	39.8
9.43 × 10 ⁻⁶	2.81 × 10 ⁻⁴		29.8	57.1
9.43 × 10 ⁻⁶	3.75 × 10 ⁻³	5.02 × 10 ⁻³	39.8	73.8
9.43 × 10 ⁻⁶	4.69 × 10 ⁻³		49.7	89.0

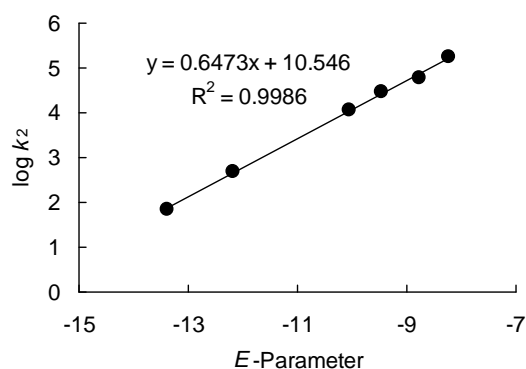
$$k_2 = 1.81 \times 10^5 \text{ L mol}^{-1} \text{ s}^{-1}$$



Determination of Reactivity Parameters N and s for the Benzotriazole Anion (**3b**) in DMSOTable 75: Rate Constants for the reactions of **3b** with different electrophiles (20 °C).

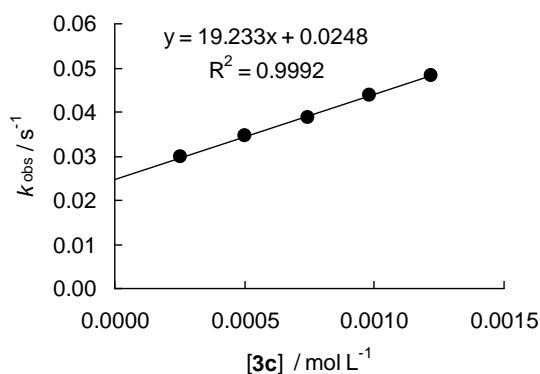
Electrophile	E	$k_2 / \text{L mol}^{-1} \text{s}^{-1}$	$\log k_2$
1i	-13.39	7.11×10^1	1.85
1h	-12.18	4.86×10^2	2.69
1g	-10.04	1.18×10^4	4.07
1f	-9.45	2.91×10^4	4.46
1e	-8.76	6.09×10^4	4.78
1d	-8.22	1.81×10^5	5.26

$$N = 16.29, s = 0.65$$

Reactions of the Potassium Salt of Purine (**3c-K**)Table 76: Kinetics of the reaction of **3c** with **1i** (20 °C, Conventional UV/Vis, at 533 nm).

$[\text{E}] / \text{mol L}^{-1}$	$[\text{3c}] / \text{mol L}^{-1}$	$[\text{3c}]/[\text{E}]$	$k_{\text{obs}} / \text{s}^{-1}$
2.30×10^{-5}	2.54×10^{-4}	10.6	0.0298
2.31×10^{-5}	5.03×10^{-4}	21.3	0.0346
2.33×10^{-5}	7.46×10^{-4}	32.0	0.0388
2.36×10^{-5}	9.83×10^{-4}	42.6	0.0438
2.39×10^{-5}	1.22×10^{-3}	53.0	0.0484

$$k_2 = 1.92 \times 10^1 \text{ L mol}^{-1} \text{ s}^{-1}$$

Table 77: Kinetics of the reaction of **3c** with **1h** (20 °C, stopped-flow, at 422 nm).

$[\text{E}] / \text{mol L}^{-1}$	$[\text{3c}] / \text{mol L}^{-1}$	$[\text{18-crown-6}] / \text{mol L}^{-1}$	$[\text{3c}]/[\text{E}]$	$k_{\text{obs}} / \text{s}^{-1}$
1.48×10^{-5}	2.66×10^{-4}		18.0	0.0442
1.48×10^{-5}	5.32×10^{-4}	6.80×10^{-4}	35.9	0.0812
1.48×10^{-5}	7.98×10^{-4}		53.9	0.121
1.48×10^{-5}	1.05×10^{-3}	1.36×10^{-3}	71.6	0.159
1.48×10^{-5}	1.33×10^{-3}		89.9	0.195

$$k_2 = 1.43 \times 10^2 \text{ L mol}^{-1} \text{ s}^{-1}$$

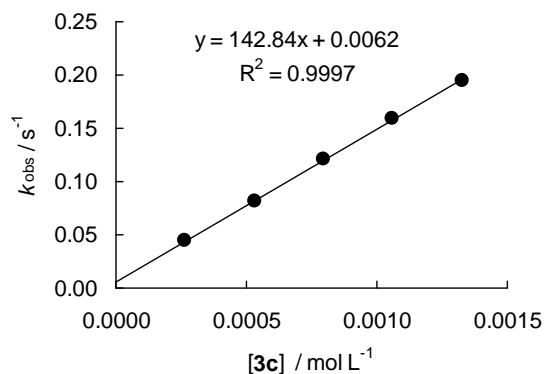
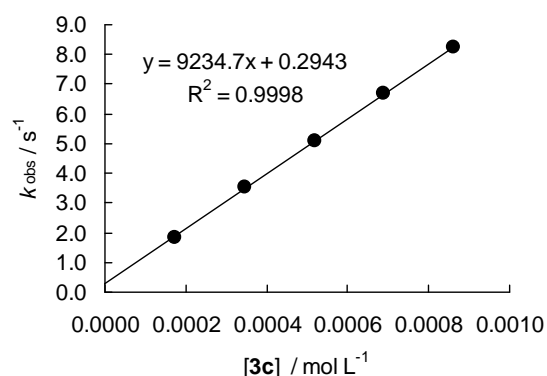


Table 78: Kinetics of the reaction of **3c** with **1g** (20 °C, stopped-flow, at 630 nm).

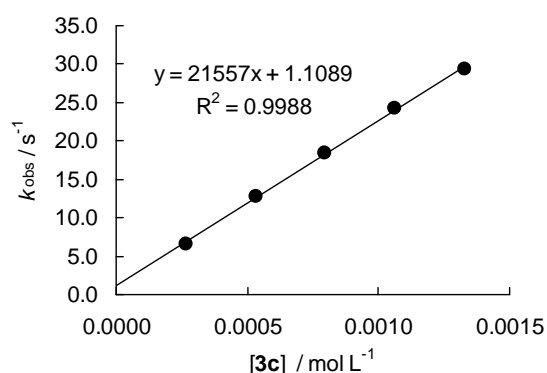
[E] / mol L ⁻¹	[3c] / mol L ⁻¹	[18-crown-6] / mol L ⁻¹	[3c]/[E]	<i>k</i> _{obs} / s ⁻¹
8.94 × 10 ⁻⁶	1.73 × 10 ⁻⁴		19.4	1.85
8.94 × 10 ⁻⁶	3.45 × 10 ⁻⁴	4.25 × 10 ⁻⁴	38.6	3.52
8.94 × 10 ⁻⁶	5.18 × 10 ⁻⁴		57.9	5.10
8.94 × 10 ⁻⁶	6.90 × 10 ⁻⁴	8.50 × 10 ⁻³	77.2	6.67
8.94 × 10 ⁻⁶	8.63 × 10 ⁻⁴		96.5	8.24

$$k_2 = 9.23 \times 10^3 \text{ L mol}^{-1} \text{ s}^{-1}$$

Table 79: Kinetics of the reaction of **3c** with **1f** (20 °C, stopped-flow, at 635 nm).

[E] / mol L ⁻¹	[3c] / mol L ⁻¹	[18-crown-6] / mol L ⁻¹	[3c]/[E]	<i>k</i> _{obs} / s ⁻¹
1.13 × 10 ⁻⁵	2.66 × 10 ⁻⁴		23.5	6.57
1.13 × 10 ⁻⁵	5.32 × 10 ⁻⁴	6.80 × 10 ⁻⁴	47.1	12.7
1.13 × 10 ⁻⁵	7.98 × 10 ⁻⁴		70.6	18.5
1.13 × 10 ⁻⁵	1.05 × 10 ⁻³	1.36 × 10 ⁻³	93.8	24.3
1.13 × 10 ⁻⁵	1.33 × 10 ⁻³		118	29.4

$$k_2 = 2.16 \times 10^4 \text{ L mol}^{-1} \text{ s}^{-1}$$

Table 80: Kinetics of the reaction of **3c** with **1e** (20 °C, stopped-flow, at 627 nm).

[E] / mol L ⁻¹	[3c] / mol L ⁻¹	[18-crown-6] / mol L ⁻¹	[3c]/[E]	<i>k</i> _{obs} / s ⁻¹
6.75 × 10 ⁻⁶	7.87 × 10 ⁻⁵		11.7	4.59
6.75 × 10 ⁻⁶	1.57 × 10 ⁻⁴	1.99 × 10 ⁻⁴	23.3	9.64
6.75 × 10 ⁻⁶	2.36 × 10 ⁻⁴		35.0	13.2
6.75 × 10 ⁻⁶	3.15 × 10 ⁻⁴	3.98 × 10 ⁻⁴	46.7	17.4
6.75 × 10 ⁻⁶	3.93 × 10 ⁻⁴		58.2	21.4

$$k_2 = 5.26 \times 10^4 \text{ L mol}^{-1} \text{ s}^{-1}$$

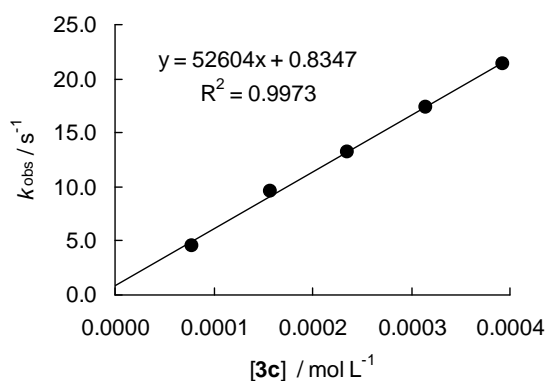
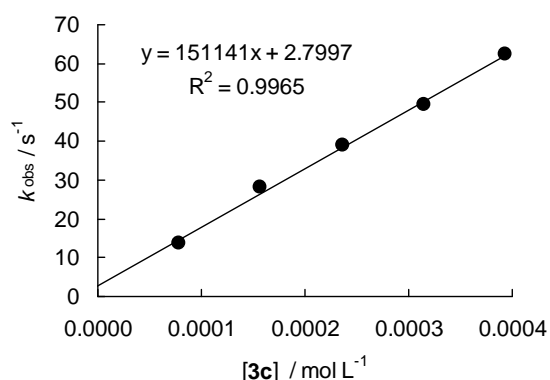


Table 81: Kinetics of the reaction of **3c** with **1d** (20 °C, stopped-flow, at 618 nm).

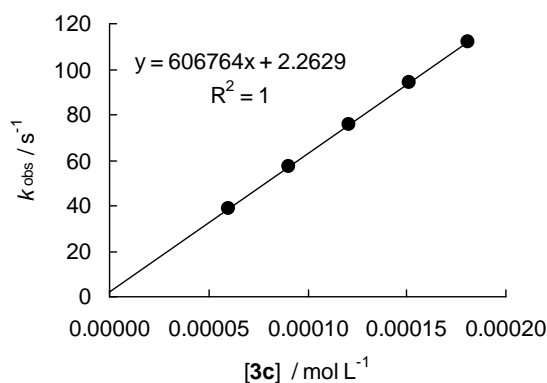
[E] / mol L ⁻¹	[3c] / mol L ⁻¹	[18-crown-6] / mol L ⁻¹	[3c]/[E]	<i>k</i> _{obs} / s ⁻¹
6.73 × 10 ⁻⁶	7.87 × 10 ⁻⁵		11.7	13.6
6.73 × 10 ⁻⁶	1.57 × 10 ⁻⁴	1.99 × 10 ⁻⁴	23.3	28.0
6.73 × 10 ⁻⁶	2.36 × 10 ⁻⁴		35.1	39.0
6.73 × 10 ⁻⁶	3.15 × 10 ⁻⁴	3.98 × 10 ⁻⁴	46.8	49.3
6.73 × 10 ⁻⁶	3.93 × 10 ⁻⁴		58.4	62.4

$$k_2 = 1.51 \times 10^5 \text{ L mol}^{-1} \text{ s}^{-1}$$

Table 82: Kinetics of the reaction of **3c** with **1c** (20 °C, stopped-flow, at 620 nm).

[E] / mol L ⁻¹	[3c] / mol L ⁻¹	[3c]/[E]	<i>k</i> _{obs} / s ⁻¹
6.58 × 10 ⁻⁶	6.04 × 10 ⁻⁵	9.2	38.8
6.58 × 10 ⁻⁶	9.06 × 10 ⁻⁵	13.8	57.4
6.58 × 10 ⁻⁶	1.21 × 10 ⁻⁴	18.4	75.6
6.58 × 10 ⁻⁶	1.51 × 10 ⁻⁴	22.9	94.0
6.58 × 10 ⁻⁶	1.81 × 10 ⁻⁴	27.5	112

$$k_2 = 6.07 \times 10^5 \text{ L mol}^{-1} \text{ s}^{-1}$$

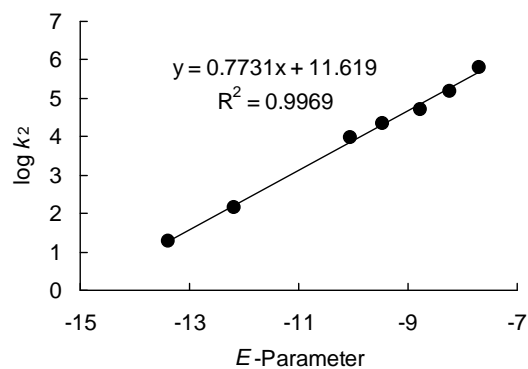


Determination of Reactivity Parameters *N* and *s* for the Purine Anion (**3c**) in DMSO

Table 83: Rate Constants for the reactions of **3c** with different electrophiles (20 °C).

Electrophile	<i>E</i>	<i>k</i> ₂ / L mol ⁻¹ s ⁻¹	log <i>k</i> ₂
1i	-13.39	1.92 × 10 ¹	1.28
1h	-12.18	1.43 × 10 ²	2.16
1g	-10.04	9.23 × 10 ³	3.97
1f	-9.45	2.16 × 10 ⁴	4.33
1e	-8.76	5.26 × 10 ⁴	4.72
1d	-8.22	1.51 × 10 ⁵	5.18
1c	-7.69	6.07 × 10 ⁵	5.78

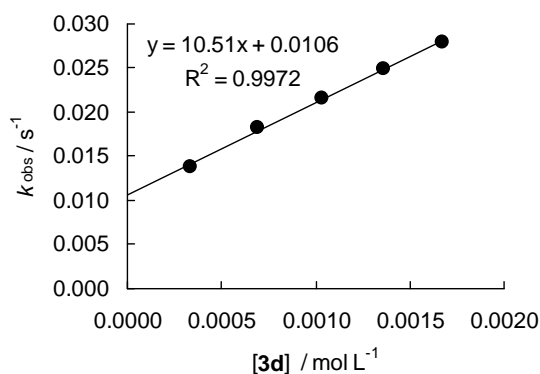
$$N = 15.03, s = 0.77$$



Reactions of the Potassium Salt of Theophylline (3d-K)Table 84: Kinetics of the reaction of **3d** with **1i** (20 °C, J&M, at 533 nm).

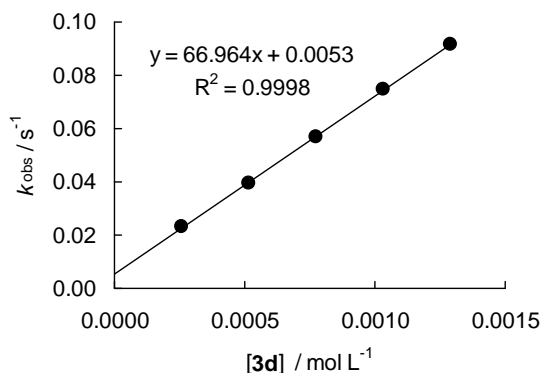
[E] / mol L ⁻¹	[3d] / mol L ⁻¹	[3d]/[E]	k_{obs} / s ⁻¹
2.30×10^{-5}	3.38×10^{-4}	14.7	0.0138
2.34×10^{-5}	6.90×10^{-4}	29.5	0.0182
2.33×10^{-5}	1.03×10^{-3}	44.2	0.0216
2.32×10^{-5}	1.36×10^{-3}	58.6	0.0250
2.27×10^{-5}	1.67×10^{-3}	73.6	0.0279

$$k_2 = 1.05 \times 10^1 \text{ L mol}^{-1} \text{ s}^{-1}$$

Table 85: Kinetics of the reaction of **3d** with **1h** (20 °C, stopped-flow, at 422 nm).

[E] / mol L ⁻¹	[3d] / mol L ⁻¹	[18-crown-6] / mol L ⁻¹	[3d]/[E]	k_{obs} / s ⁻¹
1.15×10^{-5}	2.58×10^{-4}		22.4	0.0229
1.15×10^{-5}	5.15×10^{-4}	6.17×10^{-4}	44.8	0.0394
1.15×10^{-5}	7.73×10^{-4}		67.2	0.0567
1.15×10^{-5}	1.03×10^{-3}	1.23×10^{-3}	89.6	0.0747
1.15×10^{-5}	1.29×10^{-3}		112	0.0916

$$k_2 = 6.70 \times 10^1 \text{ L mol}^{-1} \text{ s}^{-1}$$

Table 86: Kinetics of the reaction of **3d** with **1g** (20 °C, stopped-flow, at 630 nm).

[E] / mol L ⁻¹	[3d] / mol L ⁻¹	[3d]/[E]	k_{obs} / s ⁻¹
2.42×10^{-5}	3.00×10^{-4}	12.4	0.680
2.42×10^{-5}	4.50×10^{-4}	18.6	0.940
2.42×10^{-5}	5.99×10^{-4}	24.8	1.39
2.42×10^{-5}	7.49×10^{-4}	31.0	1.78
2.42×10^{-5}	8.99×10^{-4}	37.1	2.00

$$k_2 = 2.32 \times 10^3 \text{ L mol}^{-1} \text{ s}^{-1}$$

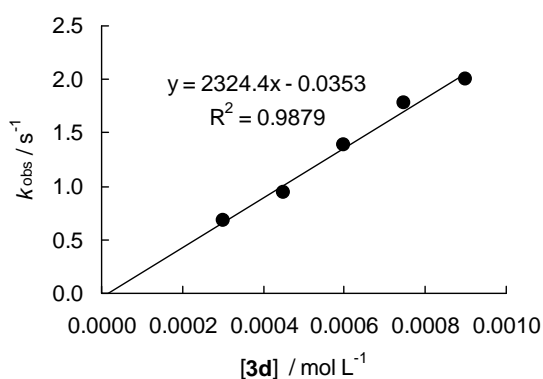
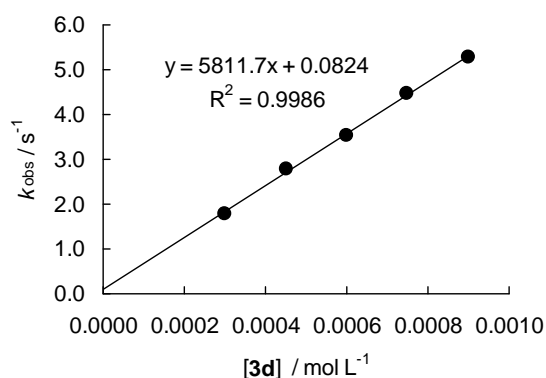


Table 87: Kinetics of the reaction of **3d** with **1f** (20 °C, stopped-flow, at 635 nm).

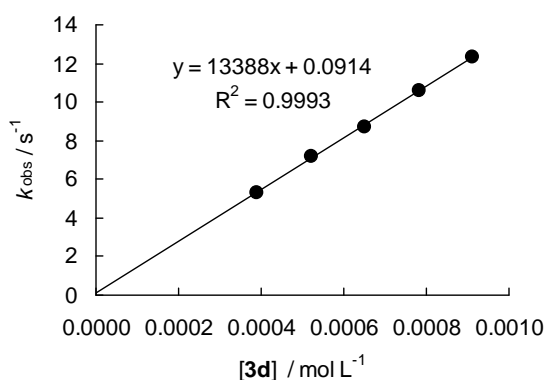
[E] / mol L ⁻¹	[3d] / mol L ⁻¹	[3d]/[E]	k_{obs} / s ⁻¹
2.57×10^{-5}	3.00×10^{-4}	11.7	1.78
2.57×10^{-5}	4.50×10^{-4}	17.5	2.77
2.57×10^{-5}	5.99×10^{-4}	23.3	3.53
2.57×10^{-5}	7.49×10^{-4}	29.1	4.47
2.57×10^{-5}	8.99×10^{-4}	35.0	5.28

$$k_2 = 5.81 \times 10^3 \text{ L mol}^{-1} \text{ s}^{-1}$$

Table 88: Kinetics of the reaction of **3d** with **1e** (20 °C, stopped-flow, at 627 nm).

[E] / mol L ⁻¹	[3d] / mol L ⁻¹	[3d]/[E]	k_{obs} / s ⁻¹
3.30×10^{-5}	3.91×10^{-4}	11.8	5.28
3.30×10^{-5}	5.21×10^{-4}	15.8	7.17
3.30×10^{-5}	6.50×10^{-4}	19.7	8.71
3.30×10^{-5}	7.82×10^{-4}	23.7	10.6
3.30×10^{-5}	9.13×10^{-4}	27.7	12.3

$$k_2 = 1.34 \times 10^4 \text{ L mol}^{-1} \text{ s}^{-1}$$

Table 89: Kinetics of the reaction of **3d** with **1d** (20 °C, stopped-flow, at 618 nm).

[E] / mol L ⁻¹	[3d] / mol L ⁻¹	[3d]/[E]	k_{obs} / s ⁻¹
2.02×10^{-5}	2.74×10^{-4}	13.6	15.6
2.02×10^{-5}	4.10×10^{-4}	20.3	20.1
2.02×10^{-5}	5.47×10^{-4}	27.1	24.4
2.02×10^{-5}	6.84×10^{-4}	33.9	30.0
2.02×10^{-5}	8.21×10^{-4}	40.6	35.5

$$k_2 = 3.63 \times 10^4 \text{ L mol}^{-1} \text{ s}^{-1}$$

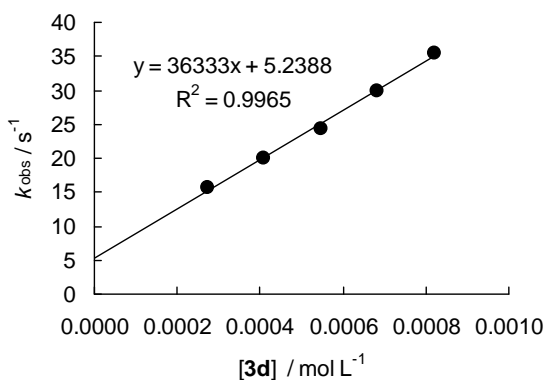
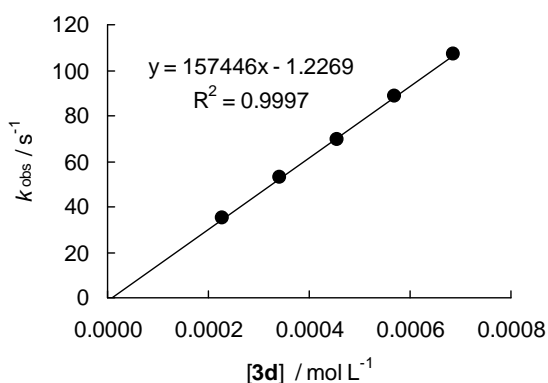


Table 90: Kinetics of the reaction of **3d** with **1c** (20 °C, stopped-flow, at 620 nm).

[E] / mol L ⁻¹	[3d] / mol L ⁻¹	[3d]/[E]	<i>k</i> _{obs} / s ⁻¹
2.33 × 10 ⁻⁵	2.28 × 10 ⁻⁴	9.8	35.0
2.33 × 10 ⁻⁵	3.42 × 10 ⁻⁴	14.7	52.7
2.33 × 10 ⁻⁵	4.56 × 10 ⁻⁴	19.6	69.8
2.33 × 10 ⁻⁵	5.70 × 10 ⁻⁴	24.5	88.5
2.33 × 10 ⁻⁵	6.85 × 10 ⁻⁴	29.4	107

$$k_2 = 1.57 \times 10^5 \text{ L mol}^{-1} \text{ s}^{-1}$$

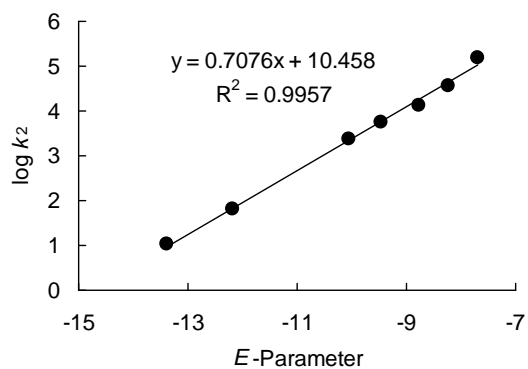


Determination of Reactivity Parameters *N* and *s* for the Theophylline Anion (**3d**) in DMSO

Table 91: Rate Constants for the reactions of **3d** with different electrophiles (20 °C).

Electrophile	<i>E</i>	<i>k</i> ₂ / L mol ⁻¹ s ⁻¹	log <i>k</i> ₂
1i	-13.39	1.05 × 10 ¹	1.02
1h	-12.18	6.70 × 10 ¹	1.83
1g	-10.04	2.32 × 10 ³	3.37
1f	-9.45	5.81 × 10 ³	3.76
1e	-8.76	1.34 × 10 ⁴	4.13
1d	-8.22	3.63 × 10 ⁴	4.56
1c	-7.69	1.57 × 10 ⁵	5.20

$$N = 14.78, s = 0.71$$



Reactions of the Potassium Salt of Adenin (**3e-K**)

Table 92: Kinetics of the reaction of **3e** (generated in situ by addition of 1.05 equivalents KOtBu) with **1h** (20 °C, stopped-flow, at 422 nm).

[E] / mol L ⁻¹	[3e] / mol L ⁻¹	[3e]/[E]	<i>k</i> _{obs} / s ⁻¹
2.28 × 10 ⁻⁵	6.84 × 10 ⁻⁴	30.0	1.08
2.28 × 10 ⁻⁵	1.03 × 10 ⁻³	45.2	1.53
2.28 × 10 ⁻⁵	1.37 × 10 ⁻³	60.1	2.15
2.28 × 10 ⁻⁵	1.71 × 10 ⁻³	75.0	2.59

$$k_2 = 1.51 \times 10^3 \text{ L mol}^{-1} \text{ s}^{-1}$$

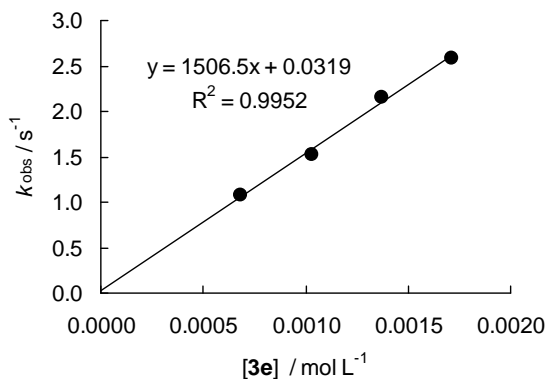
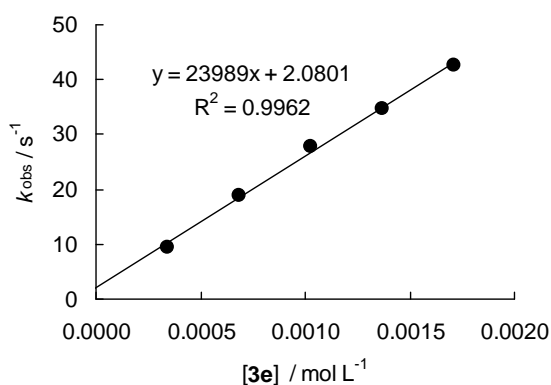


Table 93: Kinetics of the reaction of **3e** (generated in situ by addition of 1.0 equivalents KO^tBu) with **1g** (20 °C; stopped-flow, at 630 nm).

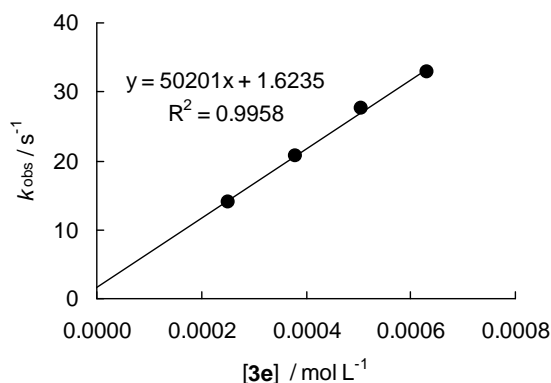
[E] / mol L ⁻¹	[3e] / mol L ⁻¹	[3e]/[E]	<i>k</i> _{obs} / s ⁻¹
1.33 × 10 ⁻⁵	3.42 × 10 ⁻⁴	25.7	9.41
1.33 × 10 ⁻⁵	6.84 × 10 ⁻⁴	51.4	19.0
1.33 × 10 ⁻⁵	1.03 × 10 ⁻³	77.4	27.9
1.33 × 10 ⁻⁵	1.37 × 10 ⁻³	103	34.7
1.33 × 10 ⁻⁵	1.71 × 10 ⁻³	129	42.6

$$k_2 = 2.40 \times 10^4 \text{ L mol}^{-1} \text{ s}^{-1}$$

Table 94: Kinetics of the reaction of **3e** (generated in situ by addition of 1.05 equivalents KO^tBu) with **1f** (20 °C, stopped-flow, at 635 nm).

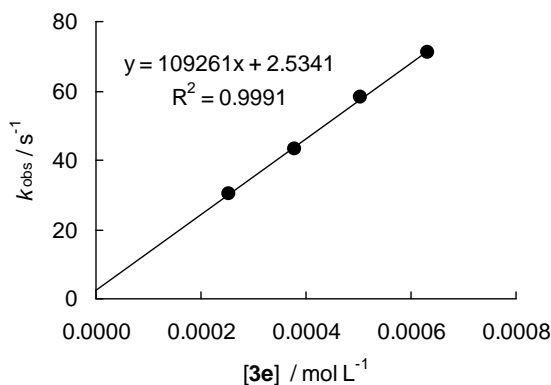
[E] / mol L ⁻¹	[3e] / mol L ⁻¹	[3e]/[E]	<i>k</i> _{obs} / s ⁻¹
1.13 × 10 ⁻⁵	2.52 × 10 ⁻⁴	22.3	14.0
1.13 × 10 ⁻⁵	3.79 × 10 ⁻⁴	33.5	20.7
1.13 × 10 ⁻⁵	5.05 × 10 ⁻⁴	44.7	27.7
1.13 × 10 ⁻⁵	6.31 × 10 ⁻⁴	55.8	32.8

$$k_2 = 5.02 \times 10^4 \text{ L mol}^{-1} \text{ s}^{-1}$$

Table 95: Kinetics of the reaction of **3e** (generated in situ by addition of 1.05 equivalents KO^tBu) with **1e** (20 °C, stopped-flow, at 627 nm).

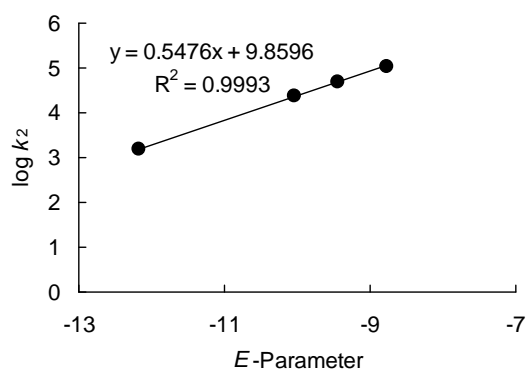
[E] / mol L ⁻¹	[3e] / mol L ⁻¹	[3e]/[E]	<i>k</i> _{obs} / s ⁻¹
1.29 × 10 ⁻⁵	2.52 × 10 ⁻⁴	19.5	30.3
1.29 × 10 ⁻⁵	3.79 × 10 ⁻⁴	29.4	43.3
1.29 × 10 ⁻⁵	5.05 × 10 ⁻⁴	39.1	58.3
1.29 × 10 ⁻⁵	6.31 × 10 ⁻⁴	48.9	71.3

$$k_2 = 1.09 \times 10^5 \text{ L mol}^{-1} \text{ s}^{-1}$$



Determination of Reactivity Parameters N and s for the Adenine Anion (**3e**) in DMSOTable 96: Rate Constants for the reactions of **3e** with different electrophiles (20 °C).

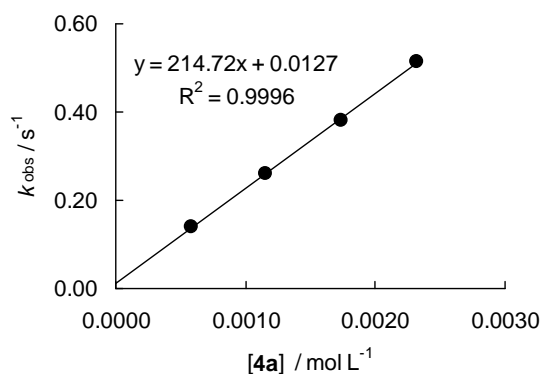
Electrophile	E	$k_2 / \text{L mol}^{-1} \text{s}^{-1}$	$\log k_2$
1h	-12.18	1.51×10^3	3.18
1g	-10.04	2.40×10^4	4.38
1f	-9.45	5.02×10^4	4.70
1e	-8.76	1.09×10^5	5.04



$$N = 18.00, s = 0.55$$

Reactions of the Potassium Salt of Uracile (**4a-K**)Table 97: Kinetics of the reaction of **4a** with **1i** (20 °C, stopped-flow, at 533 nm).

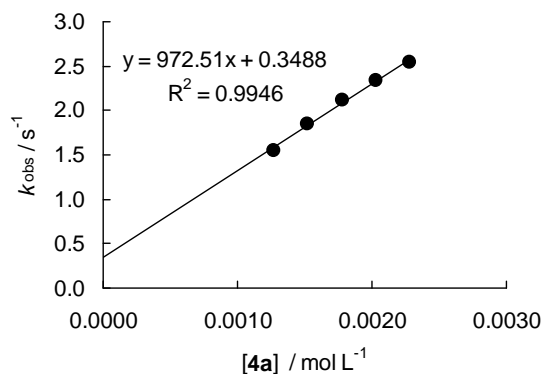
$[\text{E}] / \text{mol L}^{-1}$	$[\mathbf{4a}] / \text{mol L}^{-1}$	$[\text{18-crown-6}] / \text{mol L}^{-1}$	$[\mathbf{4a}]/[\text{E}]$	$k_{\text{obs}} / \text{s}^{-1}$
2.76×10^{-5}	5.79×10^{-4}		21.0	0.139
2.76×10^{-5}	1.16×10^{-3}	1.53×10^{-3}	42.0	0.261
2.76×10^{-5}	1.74×10^{-3}		63.0	0.382
2.76×10^{-5}	2.32×10^{-3}	3.06×10^{-3}	84.1	0.514



$$k_2 = 2.15 \times 10^2 \text{ L mol}^{-1} \text{ s}^{-1}$$

Table 98: Kinetics of the reaction of **4a** with **1h** (20 °C, stopped-flow, at 422 nm).

$[\text{E}] / \text{mol L}^{-1}$	$[\mathbf{4a}] / \text{mol L}^{-1}$	$[\mathbf{4a}]/[\text{E}]$	$k_{\text{obs}} / \text{s}^{-1}$
4.94×10^{-5}	1.27×10^{-4}	25.7	1.55
4.94×10^{-5}	1.52×10^{-3}	30.8	1.85
4.94×10^{-5}	1.78×10^{-3}	36.0	2.11
4.94×10^{-5}	2.03×10^{-3}	41.1	2.33
4.94×10^{-5}	2.28×10^{-3}	46.2	2.54

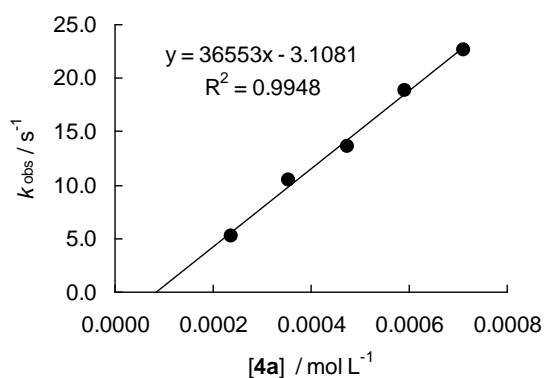


$$k_2 = 9.73 \times 10^2 \text{ L mol}^{-1} \text{ s}^{-1}$$

Table 99: Kinetics of the reaction of **4a** with **1g** (20 °C, stopped-flow, at 630 nm).

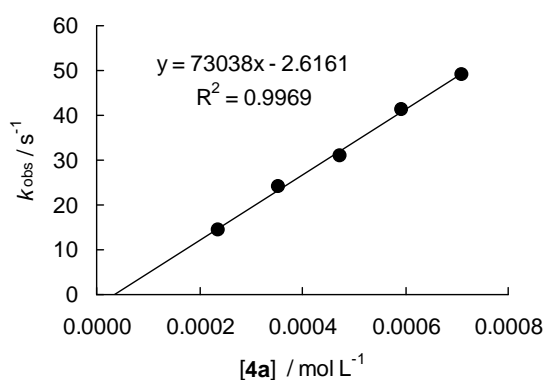
[E] / mol L ⁻¹	[4a] / mol L ⁻¹	[4a]/[E]	k_{obs} / s ⁻¹
1.88×10^{-5}	2.37×10^{-4}	12.6	5.28
1.88×10^{-5}	3.55×10^{-4}	18.9	10.5
1.88×10^{-5}	4.73×10^{-4}	25.2	13.6
1.88×10^{-5}	5.92×10^{-4}	31.5	18.9
1.88×10^{-5}	7.10×10^{-4}	37.8	22.7

$$k_2 = 3.66 \times 10^4 \text{ L mol}^{-1} \text{ s}^{-1}$$

Table 100: Kinetics of the reaction of **4a** with **1f** (20 °C, stopped-flow, at 635 nm).

[E] / mol L ⁻¹	[4a] / mol L ⁻¹	[4a]/[E]	k_{obs} / s ⁻¹
1.84×10^{-5}	2.37×10^{-4}	12.9	14.4
1.84×10^{-5}	3.55×10^{-4}	19.3	24.2
1.84×10^{-5}	4.73×10^{-4}	25.7	30.9
1.84×10^{-5}	5.92×10^{-4}	32.2	41.2
1.84×10^{-5}	7.10×10^{-4}	38.6	49.1

$$k_2 = 7.30 \times 10^4 \text{ L mol}^{-1} \text{ s}^{-1}$$

Table 101: Kinetics of the reaction of **4a** with **1e** (20 °C, stopped-flow, at 627 nm).

[E] / mol L ⁻¹	[4a] / mol L ⁻¹	[4a]/[E]	k_{obs} / s ⁻¹
2.11×10^{-5}	2.37×10^{-4}	11.2	34.1
2.11×10^{-5}	3.55×10^{-4}	16.8	50.7
2.11×10^{-5}	4.73×10^{-4}	22.4	69.5
2.11×10^{-5}	5.92×10^{-4}	28.1	90.0
2.11×10^{-5}	7.10×10^{-4}	33.6	107

$$k_2 = 1.56 \times 10^5 \text{ L mol}^{-1} \text{ s}^{-1}$$

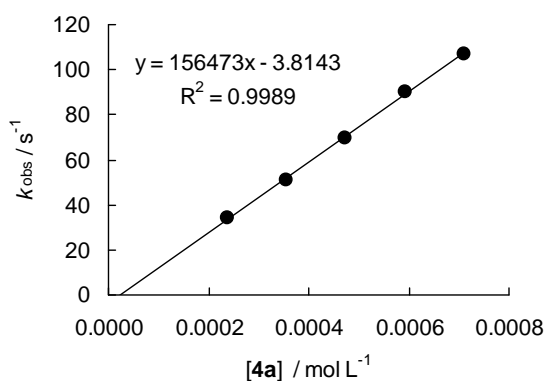
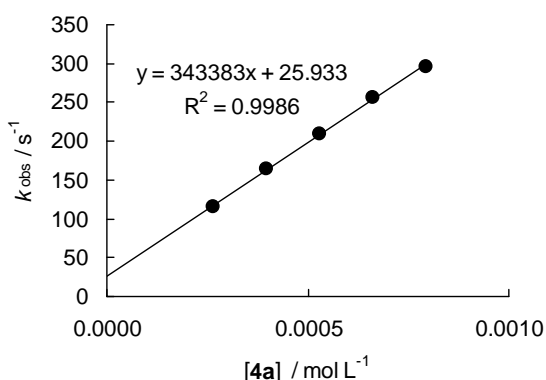


Table 102: Kinetics of the reaction of **4a** with **1d** (20 °C, stopped-flow, at 618 nm).

[E] / mol L ⁻¹	[4a] / mol L ⁻¹	[4a]/[E]	<i>k</i> _{obs} / s ⁻¹
1.85 × 10 ⁻⁵	2.66 × 10 ⁻⁴	14.4	115
1.85 × 10 ⁻⁵	3.98 × 10 ⁻⁴	21.5	164
1.85 × 10 ⁻⁵	5.31 × 10 ⁻⁴	28.7	209
1.85 × 10 ⁻⁵	6.63 × 10 ⁻⁴	35.8	257
1.85 × 10 ⁻⁵	7.96 × 10 ⁻⁴	43.0	296

$$k_2 = 3.43 \times 10^5 \text{ L mol}^{-1} \text{ s}^{-1}$$

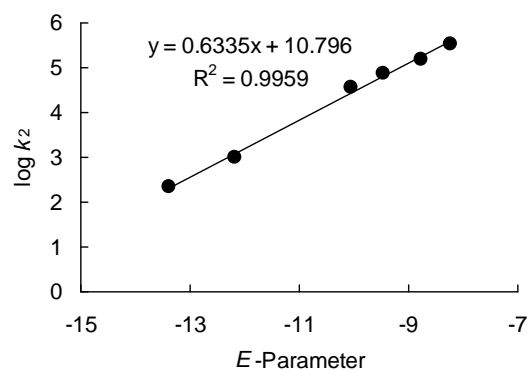


Determination of Reactivity Parameters *N* and *s* for the Uracile Anion (**4a**) in DMSO

Table 103: Rate Constants for the reactions of **4a** with different electrophiles (20 °C).

Electrophile	<i>E</i>	<i>k</i> ₂ / L mol ⁻¹ s ⁻¹	log <i>k</i> ₂
1i	-13.39	2.15 × 10 ²	2.33
1h	-12.18	9.73 × 10 ²	2.99
1g	-10.04	3.66 × 10 ⁴	4.56
1f	-9.45	7.30 × 10 ⁴	4.86
1e	-8.76	1.56 × 10 ⁵	5.19
1d	-8.22	3.43 × 10 ⁵	5.54

$$N = 17.04, s = 0.63$$



Reactions of the Potassium Salt of 1-Methyluracile (**4b-K**)

Table 104: Kinetics of the reaction of **4b** with **1i** (20 °C, stopped-flow, at 533 nm).

[E] / mol L ⁻¹	[4b] / mol L ⁻¹	[18-crown-6] / mol L ⁻¹	[4b]/[E]	<i>k</i> _{obs} / s ⁻¹
2.70 × 10 ⁻⁵	2.73 × 10 ⁻⁴	5.02 × 10 ⁻⁴	10.1	0.0790
2.70 × 10 ⁻⁵	5.46 × 10 ⁻⁴	1.00 × 10 ⁻³	20.2	0.109
2.70 × 10 ⁻⁵	8.19 × 10 ⁻⁴	1.51 × 10 ⁻³	30.3	0.134
2.70 × 10 ⁻⁵	1.09 × 10 ⁻³	2.01 × 10 ⁻³	40.4	0.159
2.70 × 10 ⁻⁵	1.36 × 10 ⁻³	2.50 × 10 ⁻³	50.4	0.186

$$k_2 = 9.71 \times 10^1 \text{ L mol}^{-1} \text{ s}^{-1}$$

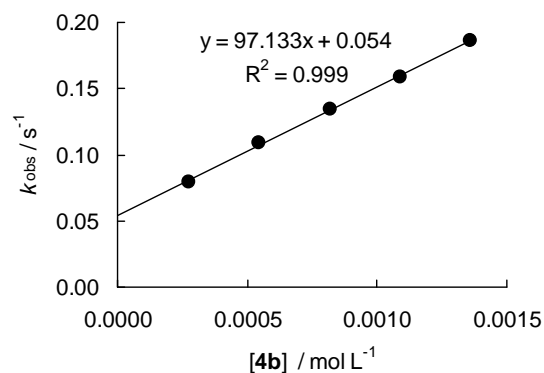
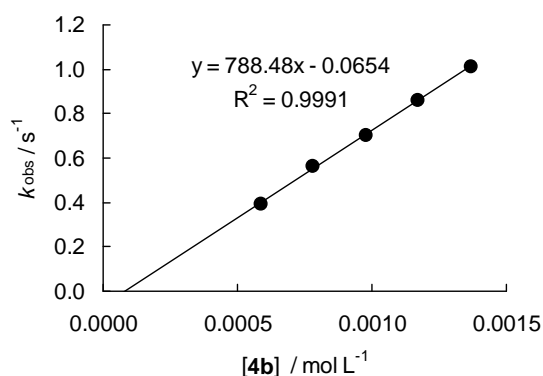


Table 105: Kinetics of the reaction of **4b** with **1h** (20 °C, stopped-flow, at 422 nm).

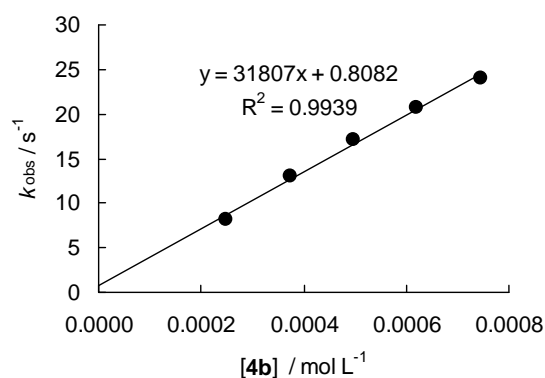
[E] / mol L ⁻¹	[4b] / mol L ⁻¹	[18-crown-6] / mol L ⁻¹	[4b]/[E]	<i>k</i> _{obs} / s ⁻¹
4.83 × 10 ⁻⁵	5.87 × 10 ⁻⁴	7.54 × 10 ⁻⁴	12.2	0.390
4.83 × 10 ⁻⁵	7.83 × 10 ⁻⁴	1.01 × 10 ⁻³	16.2	0.562
4.83 × 10 ⁻⁵	9.79 × 10 ⁻⁴	1.26 × 10 ⁻³	20.3	0.704
4.83 × 10 ⁻⁵	1.17 × 10 ⁻³	1.51 × 10 ⁻³	24.2	0.862
4.83 × 10 ⁻⁵	1.37 × 10 ⁻³	1.77 × 10 ⁻³	28.4	1.01

$$k_2 = 7.88 \times 10^2 \text{ L mol}^{-1} \text{ s}^{-1}$$


 Table 106: Kinetics of the reaction of **4b** with **1g** (20 °C, stopped-flow, at 630 nm).

[E] / mol L ⁻¹	[4b] / mol L ⁻¹	[18-crown-6] / mol L ⁻¹	[4b]/[E]	<i>k</i> _{obs} / s ⁻¹
1.99 × 10 ⁻⁵	2.48 × 10 ⁻⁴	3.08 × 10 ⁻⁴	12.5	8.15
1.99 × 10 ⁻⁵	3.73 × 10 ⁻⁴	4.63 × 10 ⁻⁴	18.7	13.0
1.99 × 10 ⁻⁵	4.97 × 10 ⁻⁴	6.16 × 10 ⁻⁴	25.0	17.1
1.99 × 10 ⁻⁵	6.21 × 10 ⁻⁴	7.70 × 10 ⁻⁴	31.2	20.8
1.99 × 10 ⁻⁵	7.45 × 10 ⁻⁴	9.24 × 10 ⁻⁴	37.4	24.0

$$k_2 = 3.18 \times 10^4 \text{ L mol}^{-1} \text{ s}^{-1}$$


 Table 107: Kinetics of the reaction of **4b** with **1f** (20 °C, stopped-flow, at 635 nm).

[E] / mol L ⁻¹	[4b] / mol L ⁻¹	[18-crown-6] / mol L ⁻¹	[4b]/[E]	<i>k</i> _{obs} / s ⁻¹
2.02 × 10 ⁻⁵	2.48 × 10 ⁻⁴	3.08 × 10 ⁻⁴	12.3	12.8
2.02 × 10 ⁻⁵	3.73 × 10 ⁻⁴	4.63 × 10 ⁻⁴	18.5	20.8
2.02 × 10 ⁻⁵	4.97 × 10 ⁻⁴	6.16 × 10 ⁻⁴	24.6	27.5
2.02 × 10 ⁻⁵	6.21 × 10 ⁻⁴	7.70 × 10 ⁻⁴	30.7	33.9
2.02 × 10 ⁻⁵	7.45 × 10 ⁻⁴	9.24 × 10 ⁻⁴	36.9	39.3

$$k_2 = 5.32 \times 10^4 \text{ L mol}^{-1} \text{ s}^{-1}$$

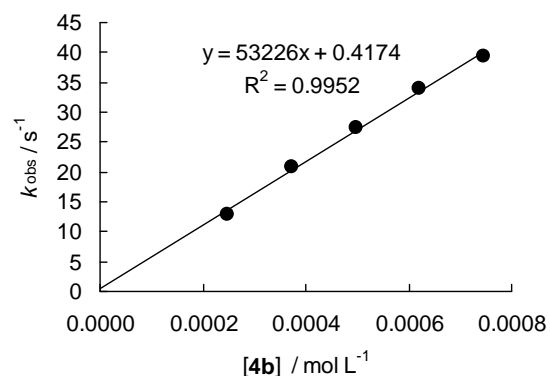
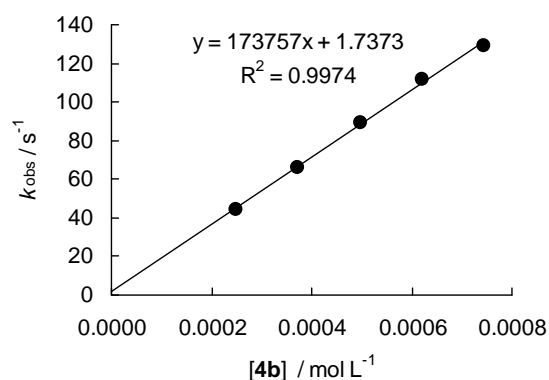


Table 108: Kinetics of the reaction of **4b** with **1e** (20 °C, stopped-flow, at 627 nm).

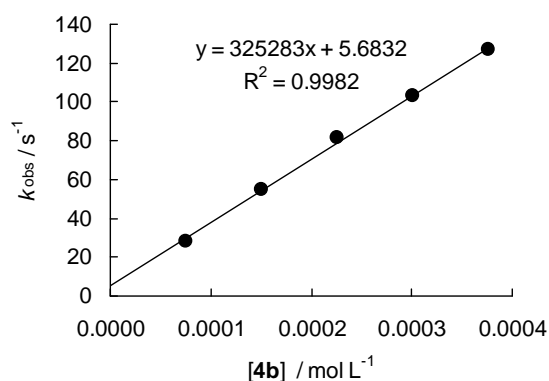
[E] / mol L ⁻¹	[4b] / mol L ⁻¹	[18-crown-6] / mol L ⁻¹	[4b]/[E]	<i>k</i> _{obs} / s ⁻¹
1.94 × 10 ⁻⁵	2.48 × 10 ⁻⁴	3.08 × 10 ⁻⁴	12.8	44.0
1.94 × 10 ⁻⁵	3.73 × 10 ⁻⁴	4.63 × 10 ⁻⁴	19.2	66.2
1.94 × 10 ⁻⁵	4.97 × 10 ⁻⁴	6.16 × 10 ⁻⁴	25.6	89.1
1.94 × 10 ⁻⁵	6.21 × 10 ⁻⁴	7.70 × 10 ⁻⁴	32.0	112
1.94 × 10 ⁻⁵	7.45 × 10 ⁻⁴	9.24 × 10 ⁻⁴	38.4	129

$$k_2 = 1.74 \times 10^5 \text{ L mol}^{-1} \text{ s}^{-1}$$

Table 109: Kinetics of the reaction of **4b** with **1d** (20 °C, stopped-flow, at 618 nm).

[E] / mol L ⁻¹	[4b] / mol L ⁻¹	[18-crown-6] / mol L ⁻¹	[4b]/[E]	<i>k</i> _{obs} / s ⁻¹
7.34 × 10 ⁻⁶	7.52 × 10 ⁻⁵	1.23 × 10 ⁻⁴	10.2	28.5
7.34 × 10 ⁻⁶	1.50 × 10 ⁻⁴	2.46 × 10 ⁻⁴	20.4	55.2
7.34 × 10 ⁻⁶	2.26 × 10 ⁻⁴	3.71 × 10 ⁻⁴	30.8	81.7
7.34 × 10 ⁻⁶	3.01 × 10 ⁻⁴	4.94 × 10 ⁻⁴	41.0	103
7.34 × 10 ⁻⁶	3.76 × 10 ⁻⁴	6.17 × 10 ⁻⁴	51.2	127

$$k_2 = 3.25 \times 10^5 \text{ L mol}^{-1} \text{ s}^{-1}$$

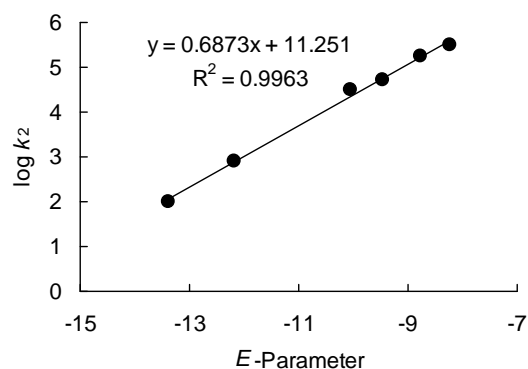


Determination of Reactivity Parameters *N* and *s* for the 1-Methyluracile Anion (**4b**) in DMSO

Table 110: Rate Constants for the reactions of **4b** with different electrophiles (20 °C).

Electrophile	<i>E</i>	<i>k</i> ₂ / L mol ⁻¹ s ⁻¹	log <i>k</i> ₂
1i	-13.39	9.71 × 10 ¹	1.99
1h	-12.18	7.88 × 10 ²	2.90
1g	-10.04	3.18 × 10 ⁴	4.50
1f	-9.45	5.32 × 10 ⁴	4.73
1e	-8.76	1.74 × 10 ⁵	5.24
1d	-8.22	3.25 × 10 ⁵	5.51

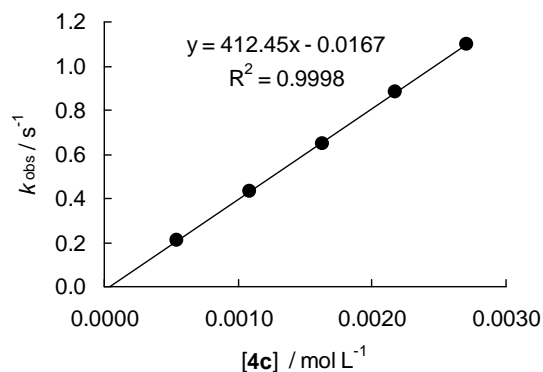
$$N = 16.37, s = 0.69$$



Reactions of the Potassium Salt of Thymine (4c-K)Table 111: Kinetics of the reaction of **4c** with **1i** (20 °C, stopped-flow, at 533 nm).

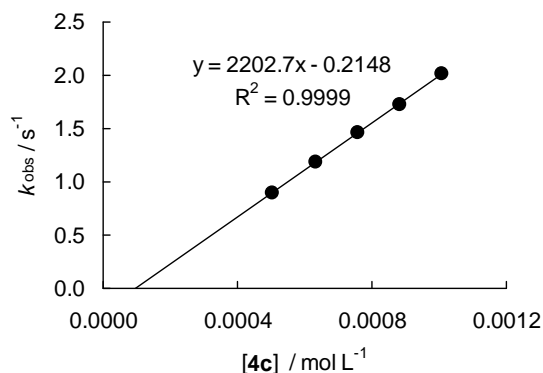
[E] / mol L ⁻¹	[4c] / mol L ⁻¹	[18-crown-6] / mol L ⁻¹	[4c]/[E]	$k_{\text{obs}} /$ s ⁻¹
2.23×10^{-5}	5.43×10^{-4}	8.31×10^{-4}	24.3	0.209
2.23×10^{-5}	1.09×10^{-3}	1.67×10^{-3}	48.9	0.433
2.23×10^{-5}	1.63×10^{-3}	2.49×10^{-3}	73.1	0.649
2.23×10^{-5}	2.17×10^{-3}	3.32×10^{-3}	97.3	0.884
2.23×10^{-5}	2.71×10^{-3}	4.15×10^{-3}	122	1.10

$$k_2 = 4.12 \times 10^2 \text{ L mol}^{-1} \text{ s}^{-1}$$

Table 112: Kinetics of the reaction of **4c** with **1h** (20 °C, stopped-flow, at 422 nm).

[E] / mol L ⁻¹	[4c] / mol L ⁻¹	[18-crown-6] / mol L ⁻¹	[4c]/[E]	$k_{\text{obs}} /$ s ⁻¹
4.83×10^{-5}	5.05×10^{-4}	6.62×10^{-4}	10.5	0.894
4.83×10^{-5}	6.32×10^{-4}	8.28×10^{-4}	13.1	1.18
4.83×10^{-5}	7.58×10^{-4}	9.93×10^{-4}	15.7	1.46
4.83×10^{-5}	8.85×10^{-4}	1.16×10^{-3}	18.3	1.73
4.83×10^{-5}	1.01×10^{-3}	1.32×10^{-3}	20.9	2.01

$$k_2 = 2.20 \times 10^3 \text{ L mol}^{-1} \text{ s}^{-1}$$

Table 113: Kinetics of the reaction of **4c** with **1g** (20 °C, stopped-flow, at 630 nm).

[E] / mol L ⁻¹	[4c] / mol L ⁻¹	[18-crown-6] / mol L ⁻¹	[4c]/[E]	$k_{\text{obs}} /$ s ⁻¹
2.15×10^{-5}	2.66×10^{-4}	3.67×10^{-4}	12.4	11.7
2.15×10^{-5}	3.99×10^{-4}	5.51×10^{-4}	18.6	19.7
2.15×10^{-5}	5.32×10^{-4}	7.34×10^{-4}	24.7	25.4
2.15×10^{-5}	6.65×10^{-4}	9.18×10^{-4}	30.9	32.0
2.15×10^{-5}	7.98×10^{-4}	1.10×10^{-3}	37.1	38.4

$$k_2 = 4.94 \times 10^4 \text{ L mol}^{-1} \text{ s}^{-1}$$

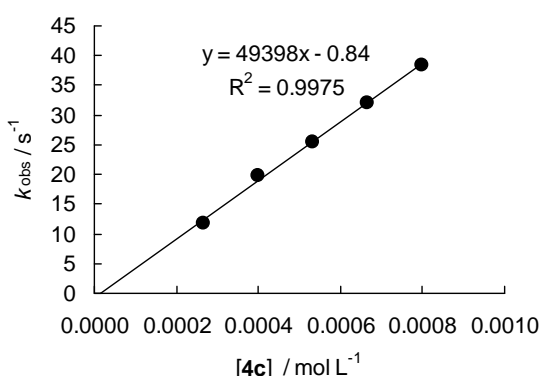
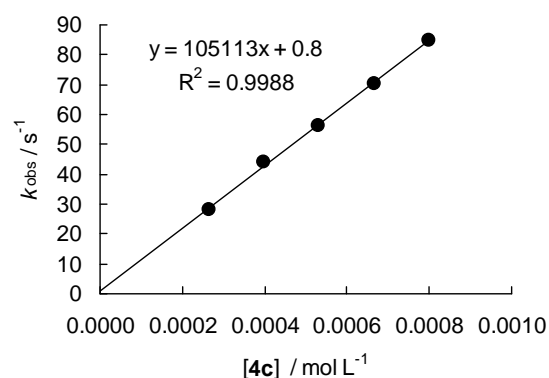


Table 114: Kinetics of the reaction of **4c** with **1f** (20 °C, stopped-flow, at 635 nm).

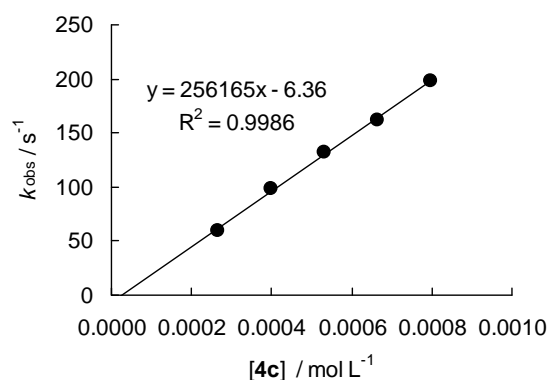
[E] / mol L ⁻¹	[4c] / mol L ⁻¹	[18-crown-6] / mol L ⁻¹	[4c]/[E]	<i>k</i> _{obs} / s ⁻¹
1.92 × 10 ⁻⁵	2.66 × 10 ⁻⁴	3.67 × 10 ⁻⁴	13.9	28.1
1.92 × 10 ⁻⁵	3.99 × 10 ⁻⁴	5.51 × 10 ⁻⁴	20.8	44.0
1.92 × 10 ⁻⁵	5.32 × 10 ⁻⁴	7.34 × 10 ⁻⁴	27.7	56.3
1.92 × 10 ⁻⁵	6.65 × 10 ⁻⁴	9.18 × 10 ⁻⁴	34.6	70.4
1.92 × 10 ⁻⁵	7.98 × 10 ⁻⁴	1.10 × 10 ⁻³	41.6	84.8

$$k_2 = 1.05 \times 10^5 \text{ L mol}^{-1} \text{ s}^{-1}$$

Table 115: Kinetics of the reaction of **4c** with **1e** (20 °C, stopped-flow, at 627 nm).

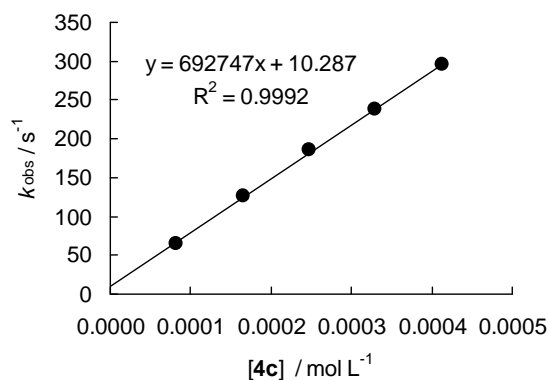
[E] / mol L ⁻¹	[4c] / mol L ⁻¹	[18-crown-6] / mol L ⁻¹	[4c]/[E]	<i>k</i> _{obs} / s ⁻¹
2.24 × 10 ⁻⁵	2.66 × 10 ⁻⁴	3.67 × 10 ⁻⁴	11.9	59.7
2.24 × 10 ⁻⁵	3.99 × 10 ⁻⁴	5.51 × 10 ⁻⁴	17.8	97.9
2.24 × 10 ⁻⁵	5.32 × 10 ⁻⁴	7.34 × 10 ⁻⁴	23.8	132
2.24 × 10 ⁻⁵	6.65 × 10 ⁻⁴	9.18 × 10 ⁻⁴	29.7	162
2.24 × 10 ⁻⁵	7.98 × 10 ⁻⁴	1.10 × 10 ⁻³	35.6	198

$$k_2 = 2.56 \times 10^5 \text{ L mol}^{-1} \text{ s}^{-1}$$

Table 116: Kinetics of the reaction of **4c** with **1d** (20 °C, stopped-flow, at 618 nm).

[E] / mol L ⁻¹	[4c] / mol L ⁻¹	[18-crown-6] / mol L ⁻¹	[4c]/[E]	<i>k</i> _{obs} / s ⁻¹
7.34 × 10 ⁻⁶	8.25 × 10 ⁻⁵	1.47 × 10 ⁻⁴	11.2	64.4
7.34 × 10 ⁻⁶	1.65 × 10 ⁻⁴	2.94 × 10 ⁻⁴	22.5	127
7.34 × 10 ⁻⁶	2.48 × 10 ⁻⁴	4.41 × 10 ⁻⁴	33.8	185
7.34 × 10 ⁻⁶	3.30 × 10 ⁻⁴	5.87 × 10 ⁻⁴	45.0	238
7.34 × 10 ⁻⁶	4.13 × 10 ⁻⁴	7.35 × 10 ⁻⁴	56.3	295

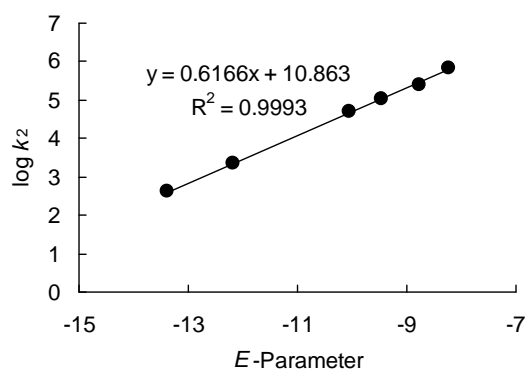
$$k_2 = 6.93 \times 10^5 \text{ L mol}^{-1} \text{ s}^{-1}$$



Determination of Reactivity Parameters N and s for the Thymine Anion (**4c**) in DMSOTable 117: Rate Constants for the reactions of **4c** with different electrophiles (20 °C).

Electrophile	E	$k_2 / \text{L mol}^{-1} \text{s}^{-1}$	$\log k_2$
1i	-13.39	4.12×10^2	2.61
1h	-12.18	2.20×10^3	3.34
1g	-10.04	4.94×10^4	4.69
1f	-9.45	1.05×10^5	5.02
1e	-8.76	2.56×10^5	5.41
1d	-8.22	6.93×10^5	5.84

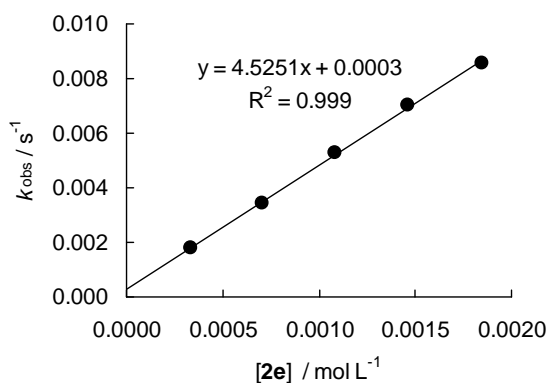
$$N = 17.62, s = 0.62$$



4.5 Reactions in Water

Reactions of the Potassium Salt of 4-Nitroimidazole (**2e**)Table 118: Kinetics of the reaction of **2e** with **1g** (20 °C, Conventional UV/Vis, at 630 nm).

$[E] / \text{mol L}^{-1}$	$[2\mathbf{e}\text{-H}]_0 / \text{mol L}^{-1}$	$[\text{KOH}]_0 / \text{mol L}^{-1}$	$[2\mathbf{e}]_{\text{eff}} / \text{mol L}^{-1}$	$[\text{KOH}]_{\text{eff}} / \text{mol L}^{-1}$	$[\text{Nu}]/[E]$	$k_{\text{obs}} / \text{s}^{-1}$	$k_{\text{OH}^-} / \text{s}^{-1}$	$k_{\text{eff}} / \text{s}^{-1}$
1.21×10^{-5}	3.95×10^{-4}	4.07×10^{-4}	3.35×10^{-4}	7.11×10^{-5}	27.7	1.93×10^{-3}	1.54×10^{-4}	1.78×10^{-3}
1.21×10^{-5}	7.89×10^{-4}	8.13×10^{-4}	7.06×10^{-4}	1.07×10^{-4}	58.4	3.68×10^{-3}	2.31×10^{-4}	3.45×10^{-3}
1.21×10^{-5}	1.18×10^{-3}	1.22×10^{-3}	1.08×10^{-3}	1.36×10^{-4}	89.6	5.56×10^{-3}	2.93×10^{-4}	5.27×10^{-3}
1.21×10^{-5}	1.58×10^{-3}	1.63×10^{-3}	1.46×10^{-3}	1.61×10^{-4}	121	7.37×10^{-3}	3.49×10^{-4}	7.02×10^{-3}
1.21×10^{-5}	1.97×10^{-3}	2.03×10^{-3}	1.85×10^{-3}	1.85×10^{-4}	153	8.95×10^{-3}	3.99×10^{-4}	8.55×10^{-3}



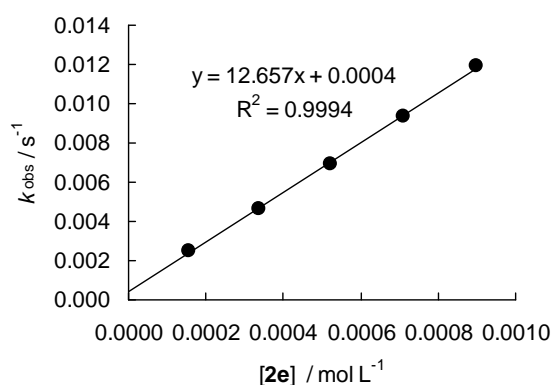
$$k_2(\text{OH}^-)^{[29]} = 2.16$$

$$\text{p}K_{\text{A}}(\mathbf{2e}\text{-H})^{[31]} = 9.10$$

$$k_2 = 4.53 \times 10^0 \text{ L mol}^{-1} \text{ s}^{-1}$$

Table 119: Kinetics of the reaction of **2e** with **1f** (20 °C, Conventional UV/Vis, at 635 nm).

[E] / mol L ⁻¹	[2e-H] ₀ / mol L ⁻¹	[KOH] ₀ / mol L ⁻¹	[2e] _{eff} / mol L ⁻¹	[KOH] _{eff} / mol L ⁻¹	[Nu]/[E]	k _{obs} / s ⁻¹	k _{OH⁻} / s ⁻¹	k _{eff} / s ⁻¹
1.35 × 10 ⁻⁵	1.99 × 10 ⁻⁴	2.03 × 10 ⁻⁴	1.57 × 10 ⁻⁴	4.67 × 10 ⁻⁵	11.6	2.69 × 10 ⁻³	1.61 × 10 ⁻⁴	2.53 × 10 ⁻³
1.35 × 10 ⁻⁵	3.98 × 10 ⁻⁴	4.07 × 10 ⁻⁴	3.37 × 10 ⁻⁴	6.97 × 10 ⁻⁵	24.9	4.87 × 10 ⁻³	2.40 × 10 ⁻⁴	4.63 × 10 ⁻³
1.35 × 10 ⁻⁵	5.96 × 10 ⁻⁴	6.10 × 10 ⁻⁴	5.22 × 10 ⁻⁴	8.80 × 10 ⁻⁵	38.5	7.25 × 10 ⁻³	3.03 × 10 ⁻⁴	6.95 × 10 ⁻³
1.35 × 10 ⁻⁵	7.95 × 10 ⁻⁴	8.13 × 10 ⁻⁴	7.09 × 10 ⁻⁴	1.04 × 10 ⁻⁴	52.4	9.74 × 10 ⁻³	3.57 × 10 ⁻⁴	9.38 × 10 ⁻³
1.35 × 10 ⁻⁵	9.94 × 10 ⁻⁴	1.02 × 10 ⁻³	8.98 × 10 ⁻⁴	1.18 × 10 ⁻⁴	66.3	1.23 × 10 ⁻²	4.06 × 10 ⁻⁴	1.19 × 10 ⁻²



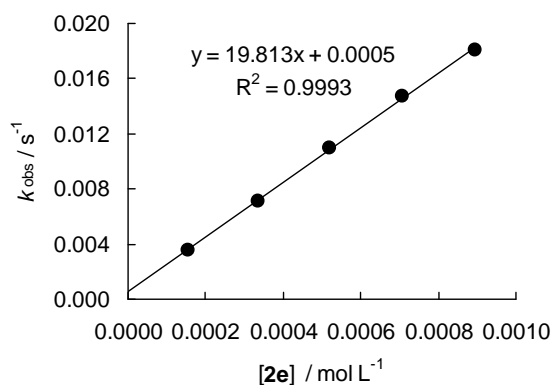
$$k_2(\text{OH}^-)^{[29]} = 3.44$$

$$\text{p}K_{\text{A}}(\text{2e-H})^{[31]} = 9.10$$

$$k_2 = 1.27 \times 10^1 \text{ L mol}^{-1} \text{ s}^{-1}$$

Table 120: Kinetics of the reaction of **2e** with **1e** (20 °C, Conventional UV/Vis, at 627 nm).

[E] / mol L ⁻¹	[2e-H] ₀ / mol L ⁻¹	[KOH] ₀ / mol L ⁻¹	[2e] _{eff} / mol L ⁻¹	[KOH] _{eff} / mol L ⁻¹	[Nu]/[E]	k _{obs} / s ⁻¹	k _{OH⁻} / s ⁻¹	k _{eff} / s ⁻¹
1.56 × 10 ⁻⁵	1.97 × 10 ⁻⁴	2.03 × 10 ⁻⁴	1.56 × 10 ⁻⁴	4.73 × 10 ⁻⁵	10.0	4.11 × 10 ⁻³	5.11 × 10 ⁻⁴	3.60 × 10 ⁻³
1.56 × 10 ⁻⁵	3.95 × 10 ⁻⁴	4.07 × 10 ⁻⁴	3.35 × 10 ⁻⁴	7.11 × 10 ⁻⁵	21.5	7.87 × 10 ⁻³	7.68 × 10 ⁻⁴	7.10 × 10 ⁻³
1.56 × 10 ⁻⁵	5.92 × 10 ⁻⁴	6.10 × 10 ⁻⁴	5.20 × 10 ⁻⁴	9.02 × 10 ⁻⁵	33.2	1.19 × 10 ⁻²	9.74 × 10 ⁻⁴	1.09 × 10 ⁻²
1.56 × 10 ⁻⁵	7.89 × 10 ⁻⁴	8.13 × 10 ⁻⁴	7.06 × 10 ⁻⁴	1.07 × 10 ⁻⁴	45.2	1.59 × 10 ⁻²	1.15 × 10 ⁻³	1.47 × 10 ⁻²
1.56 × 10 ⁻⁵	9.87 × 10 ⁻⁴	1.02 × 10 ⁻³	8.94 × 10 ⁻⁴	1.22 × 10 ⁻⁴	57.2	1.94 × 10 ⁻²	1.32 × 10 ⁻³	1.81 × 10 ⁻²



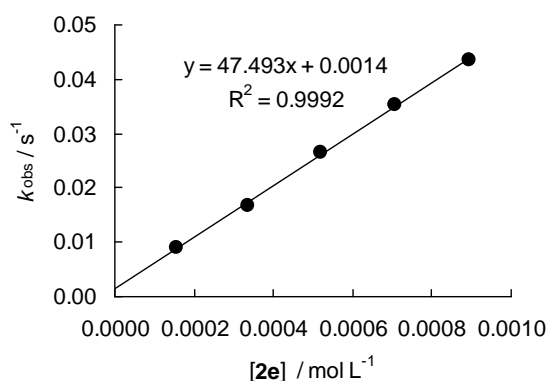
$$k_2(\text{OH}^-)^{[29]} = 10.8$$

$$\text{p}K_{\text{A}}(\text{2e-H})^{[31]} = 9.10$$

$$k_2 = 1.98 \times 10^1 \text{ L mol}^{-1} \text{ s}^{-1}$$

Table 121: Kinetics of the reaction of **2e** with **1d** (20 °C, Conventional UV/Vis, at 618 nm).

[E] / mol L ⁻¹	[2e-H] ₀ / mol L ⁻¹	[KOH] ₀ / mol L ⁻¹	[2e] _{eff} / mol L ⁻¹	[KOH] _{eff} / mol L ⁻¹	[Nu]/[E]	k _{obs} / s ⁻¹	k _{OH⁻} / s ⁻¹	k _{eff} / s ⁻¹
1.33 × 10 ⁻⁵	1.97 × 10 ⁻⁴	2.03 × 10 ⁻⁴	1.56 × 10 ⁻⁴	4.73 × 10 ⁻⁵	11.8	1.01 × 10 ⁻²	1.11 × 10 ⁻³	8.99 × 10 ⁻³
1.33 × 10 ⁻⁵	3.95 × 10 ⁻⁴	4.07 × 10 ⁻⁴	3.35 × 10 ⁻⁴	7.11 × 10 ⁻⁵	25.3	1.85 × 10 ⁻²	1.67 × 10 ⁻³	1.68 × 10 ⁻²
1.33 × 10 ⁻⁵	5.92 × 10 ⁻⁴	6.10 × 10 ⁻⁴	5.20 × 10 ⁻⁴	9.02 × 10 ⁻⁵	39.2	2.86 × 10 ⁻²	2.12 × 10 ⁻³	2.65 × 10 ⁻²
1.33 × 10 ⁻⁵	7.89 × 10 ⁻⁴	8.13 × 10 ⁻⁴	7.06 × 10 ⁻⁴	1.07 × 10 ⁻⁴	53.2	3.78 × 10 ⁻²	2.51 × 10 ⁻³	3.53 × 10 ⁻²
1.33 × 10 ⁻⁵	9.87 × 10 ⁻⁴	1.02 × 10 ⁻³	8.94 × 10 ⁻⁴	1.22 × 10 ⁻⁴	67.4	4.65 × 10 ⁻²	2.86 × 10 ⁻³	4.36 × 10 ⁻²



$$k_2(\text{OH}^-)^{[29]} = 23.5$$

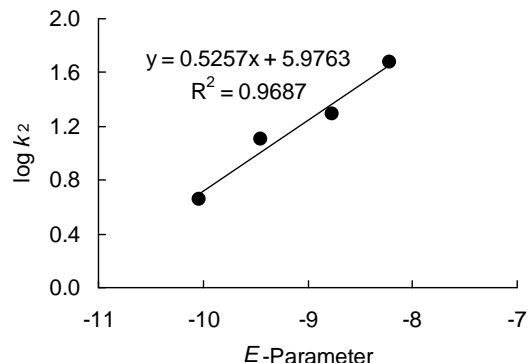
$$\text{p}K_A(\mathbf{2e-H})^{[31]} = 9.10$$

$$k_2 = 4.75 \times 10^1 \text{ L mol}^{-1} \text{ s}^{-1}$$

Determination of Reactivity Parameters N and s for the 4-Nitroimidazole Anion (**2e**) in Water

 Table 122: Rate Constants for the reactions of **2e** with different electrophiles (20 °C).

Electrophile	E	$k_2 / \text{L mol}^{-1} \text{ s}^{-1}$	$\log k_2$
1g	-10.04	4.53×10^0	0.66
1f	-9.45	1.27×10^1	1.10
1e	-8.76	1.98×10^1	1.30
1d	-8.22	4.75×10^1	1.68

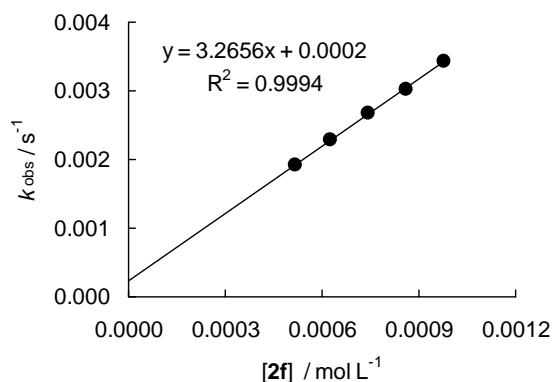


$$N = 11.37, s = 0.53$$

Reactions of the Potassium Salt of 2-Formylimidazole (**2f**)

 Table 123: Kinetics of the reaction of **2f** with **1g** (20 °C, Conventional UV/Vis, at 630 nm).

[E] / mol L ⁻¹	[2f] ₀ / mol L ⁻¹	[2f] _{eff} / mol L ⁻¹	[KOH] _{eff} / mol L ⁻¹	[Nu]/[E]	k _{obs} / s ⁻¹	k _{OH⁻} / s ⁻¹	k _{eff} / s ⁻¹
1.92 × 10 ⁻⁵	9.20 × 10 ⁻⁴	5.16 × 10 ⁻⁴	4.04 × 10 ⁻⁴	26.9	2.79 × 10 ⁻³	8.73 × 10 ⁻⁴	1.92 × 10 ⁻³
1.92 × 10 ⁻⁵	1.07 × 10 ⁻³	6.28 × 10 ⁻⁴	4.46 × 10 ⁻⁴	32.7	3.24 × 10 ⁻³	9.63 × 10 ⁻⁴	2.28 × 10 ⁻³
1.92 × 10 ⁻⁵	1.23 × 10 ⁻³	7.43 × 10 ⁻⁴	4.85 × 10 ⁻⁴	38.6	3.73 × 10 ⁻³	1.05 × 10 ⁻³	2.68 × 10 ⁻³
1.92 × 10 ⁻⁵	1.38 × 10 ⁻³	8.59 × 10 ⁻⁴	5.21 × 10 ⁻⁴	44.7	4.15 × 10 ⁻³	1.13 × 10 ⁻³	3.02 × 10 ⁻³
1.92 × 10 ⁻⁵	1.53 × 10 ⁻³	9.78 × 10 ⁻⁴	5.56 × 10 ⁻⁴	50.9	4.63 × 10 ⁻³	1.20 × 10 ⁻³	3.43 × 10 ⁻³



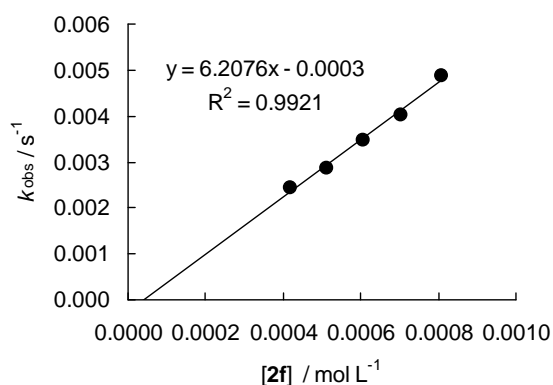
$$k_2(\text{OH}^-)^{[29]} = 2.16$$

$$\text{p}K_{\text{A}}(\text{2f-H})^{[33]} = 10.5$$

$$k_2 = 3.27 \times 10^0 \text{ L mol}^{-1} \text{ s}^{-1}$$

Table 124: Kinetics of the reaction of **2f** with **1f** (20 °C, Conventional UV/Vis, at 635 nm).

$[\text{E}] / \text{mol L}^{-1}$	$[\text{2f}]_0 / \text{mol L}^{-1}$	$[\text{2f}]_{\text{eff}} / \text{mol L}^{-1}$	$[\text{KOH}]_{\text{eff}} / \text{mol L}^{-1}$	$[\text{Nu}]/[\text{E}]$	$k_{\text{obs}} / \text{s}^{-1}$	$k_{\text{OH}^-} / \text{s}^{-1}$	$k_{\text{eff}} / \text{s}^{-1}$
1.06×10^{-5}	7.83×10^{-4}	4.19×10^{-4}	3.64×10^{-4}	39.4	3.69×10^{-3}	1.25×10^{-3}	2.44×10^{-3}
1.06×10^{-5}	9.13×10^{-3}	5.11×10^{-4}	4.02×10^{-4}	48.0	4.24×10^{-3}	1.38×10^{-3}	2.86×10^{-3}
1.06×10^{-5}	1.04×10^{-3}	6.06×10^{-4}	4.38×10^{-4}	56.9	4.97×10^{-3}	1.51×10^{-3}	3.46×10^{-3}
1.06×10^{-5}	1.17×10^{-3}	7.02×10^{-4}	4.71×10^{-4}	66.0	5.65×10^{-3}	1.62×10^{-3}	4.03×10^{-3}
1.06×10^{-5}	1.32×10^{-3}	8.10×10^{-4}	5.06×10^{-4}	75.4	6.61×10^{-3}	1.74×10^{-3}	4.87×10^{-3}



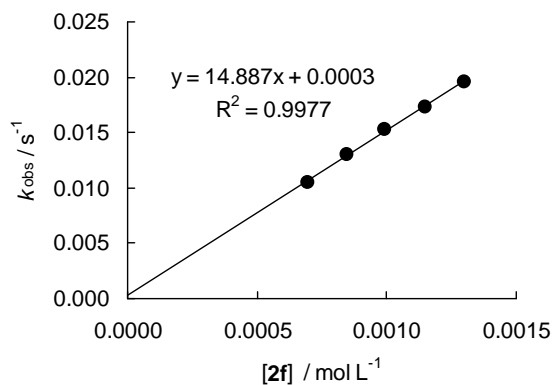
$$k_2(\text{OH}^-)^{[29]} = 3.44$$

$$\text{p}K_{\text{A}}(\text{2f-H})^{[33]} = 10.5$$

$$k_2 = 6.21 \times 10^0 \text{ L mol}^{-1} \text{ s}^{-1}$$

Table 125: Kinetics of the reaction of **2f** with **1e** (20 °C, Conventional UV/Vis, at 627 nm).

$[\text{E}] / \text{mol L}^{-1}$	$[\text{2f}]_0 / \text{mol L}^{-1}$	$[\text{2f}]_{\text{eff}} / \text{mol L}^{-1}$	$[\text{KOH}]_{\text{eff}} / \text{mol L}^{-1}$	$[\text{Nu}]/[\text{E}]$	$k_{\text{obs}} / \text{s}^{-1}$	$k_{\text{OH}^-} / \text{s}^{-1}$	$k_{\text{eff}} / \text{s}^{-1}$
1.43×10^{-5}	1.17×10^{-3}	6.97×10^{-4}	4.70×10^{-4}	48.7	1.55×10^{-2}	5.07×10^{-3}	1.04×10^{-2}
1.43×10^{-5}	1.36×10^{-3}	8.44×10^{-4}	5.17×10^{-4}	59.0	1.86×10^{-2}	5.58×10^{-3}	1.30×10^{-2}
1.43×10^{-5}	1.56×10^{-3}	9.95×10^{-4}	5.61×10^{-4}	69.5	2.13×10^{-2}	6.06×10^{-3}	1.52×10^{-2}
1.43×10^{-5}	1.75×10^{-3}	1.15×10^{-3}	6.02×10^{-4}	80.2	2.38×10^{-2}	6.51×10^{-3}	1.73×10^{-2}
1.43×10^{-5}	1.94×10^{-3}	1.30×10^{-3}	6.42×10^{-4}	91.1	2.65×10^{-2}	6.93×10^{-3}	1.96×10^{-2}



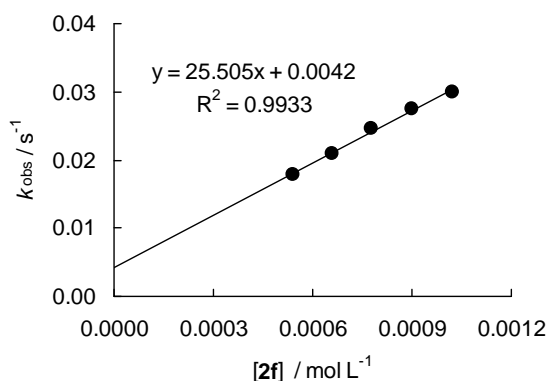
$$k_2(\text{OH}^-)^{[29]} = 10.8$$

$$\text{p}K_{\text{A}}(\mathbf{2f}\text{-H})^{[33]} = 10.5$$

$$k_2 = 1.49 \times 10^1 \text{ L mol}^{-1} \text{ s}^{-1}$$

Table 126: Kinetics of the reaction of **2f** with **1d** (20 °C, Conventional UV/Vis, at 618 nm).

$[\text{E}] / \text{mol L}^{-1}$	$[\mathbf{2f}\text{-H}]_0 / \text{mol L}^{-1}$	$[\mathbf{2f}]_{\text{eff}} / \text{mol L}^{-1}$	$[\text{KOH}]_{\text{eff}} / \text{mol L}^{-1}$	$[\text{Nu}]/[\text{E}]$	$k_{\text{obs}} / \text{s}^{-1}$	$k_{\text{OH}^-} / \text{s}^{-1}$	$k_{\text{eff}} / \text{s}^{-1}$
1.21×10^{-5}	9.56×10^{-4}	5.42×10^{-4}	4.14×10^{-4}	44.8	2.75×10^{-2}	9.73×10^{-3}	1.78×10^{-2}
1.21×10^{-5}	1.12×10^{-3}	6.59×10^{-4}	4.57×10^{-4}	54.4	3.17×10^{-2}	1.07×10^{-2}	2.10×10^{-2}
1.21×10^{-5}	1.28×10^{-3}	7.79×10^{-4}	4.96×10^{-4}	64.3	3.63×10^{-2}	1.17×10^{-2}	2.46×10^{-2}
1.21×10^{-5}	1.43×10^{-3}	9.01×10^{-4}	5.34×10^{-4}	74.4	4.00×10^{-2}	1.25×10^{-2}	2.75×10^{-2}
1.21×10^{-5}	1.59×10^{-3}	1.02×10^{-3}	5.69×10^{-4}	84.6	4.33×10^{-2}	1.34×10^{-2}	2.99×10^{-2}



$$k_2(\text{OH}^-)^{[29]} = 23.5$$

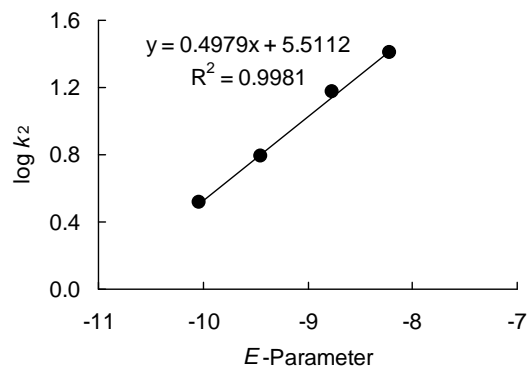
$$\text{p}K_{\text{A}}(\mathbf{2f}\text{-H})^{[33]} = 10.5$$

$$k_2 = 2.55 \times 10^1 \text{ L mol}^{-1} \text{ s}^{-1}$$

Determination of Reactivity Parameters N and s for the 2-Formylimidazole Anion (**2f**) in Water

Table 127: Rate Constants for the reactions of **2f** with different electrophiles (20 °C).

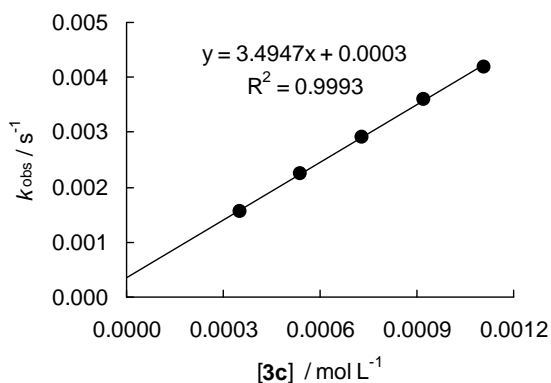
Electrophile	E	$k_2 / \text{L mol}^{-1} \text{ s}^{-1}$	$\log k_2$
1g	-10.04	3.27×10^0	0.51
1f	-9.45	6.21×10^0	0.79
1e	-8.76	1.49×10^1	1.17
1d	-8.22	2.55×10^1	1.41



$$N = 11.07, s = 0.50$$

Reactions of the Potassium Salt of Purine (3c)Table 128: Kinetics of the reaction of **3c** with **1g** (20 °C, Conventional UV/Vis, at 630 nm).

[E] / mol L ⁻¹	[3c-H] ₀ / mol L ⁻¹	[KOH] ₀ / mol L ⁻¹	[3c] _{eff} / mol L ⁻¹	[KOH] _{eff} / mol L ⁻¹	[Nu]/[E]	k _{obs} / s ⁻¹	k _{OH⁻} / s ⁻¹	k _{eff} / s ⁻¹
2.49 × 10 ⁻⁵	4.51 × 10 ⁻⁴	3.83 × 10 ⁻⁴	3.52 × 10 ⁻⁴	3.05 × 10 ⁻⁵	14.1	1.63 × 10 ⁻³	6.60 × 10 ⁻⁵	1.57 × 10 ⁻³
2.49 × 10 ⁻⁵	6.76 × 10 ⁻⁴	5.75 × 10 ⁻⁴	5.41 × 10 ⁻⁴	3.40 × 10 ⁻⁵	21.7	2.32 × 10 ⁻³	7.33 × 10 ⁻⁵	2.24 × 10 ⁻³
2.49 × 10 ⁻⁵	9.01 × 10 ⁻⁴	7.66 × 10 ⁻⁴	7.30 × 10 ⁻⁴	3.62 × 10 ⁻⁵	29.3	2.98 × 10 ⁻³	7.82 × 10 ⁻⁵	2.90 × 10 ⁻³
2.49 × 10 ⁻⁵	1.13 × 10 ⁻³	9.58 × 10 ⁻⁴	9.20 × 10 ⁻⁴	3.78 × 10 ⁻⁵	36.9	3.69 × 10 ⁻³	8.17 × 10 ⁻⁵	3.61 × 10 ⁻³
2.49 × 10 ⁻⁵	1.35 × 10 ⁻³	1.15 × 10 ⁻³	1.11 × 10 ⁻³	3.90 × 10 ⁻⁵	44.5	4.28 × 10 ⁻³	8.43 × 10 ⁻⁵	4.20 × 10 ⁻³



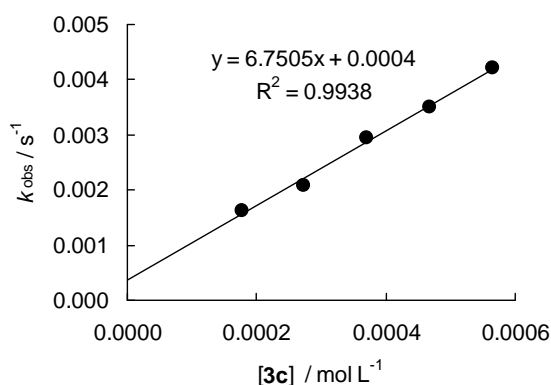
$$k_2(\text{OH}^-)^{[29]} = 2.16$$

$$\text{p}K_{\text{A}}(\mathbf{3c-H})^{[37]} = 8.93$$

$$k_2 = 3.49 \times 10^0 \text{ L mol}^{-1} \text{ s}^{-1}$$

Table 129: Kinetics of the reaction of **3c** with **1f** (20 °C, Conventional UV/Vis, at 635 nm).

[E] / mol L ⁻¹	[3c-H] ₀ / mol L ⁻¹	[KOH] ₀ / mol L ⁻¹	[3c] _{eff} / mol L ⁻¹	[KOH] _{eff} / mol L ⁻¹	[Nu]/[E]	k _{obs} / s ⁻¹	k _{OH⁻} / s ⁻¹	k _{eff} / s ⁻¹
1.81 × 10 ⁻⁵	2.49 × 10 ⁻⁴	1.97 × 10 ⁻⁴	1.77 × 10 ⁻⁴	2.07 × 10 ⁻⁵	9.8	1.70 × 10 ⁻³	7.12 × 10 ⁻⁵	1.63 × 10 ⁻³
1.81 × 10 ⁻⁵	3.73 × 10 ⁻⁴	2.96 × 10 ⁻⁴	2.73 × 10 ⁻⁴	2.30 × 10 ⁻⁵	15.1	2.17 × 10 ⁻³	7.91 × 10 ⁻⁵	2.09 × 10 ⁻³
1.81 × 10 ⁻⁵	4.98 × 10 ⁻⁴	3.94 × 10 ⁻⁴	3.70 × 10 ⁻⁴	2.45 × 10 ⁻⁵	20.4	3.04 × 10 ⁻³	8.43 × 10 ⁻⁵	2.95 × 10 ⁻³
1.81 × 10 ⁻⁵	6.22 × 10 ⁻⁴	4.93 × 10 ⁻⁴	4.67 × 10 ⁻⁴	2.56 × 10 ⁻⁵	25.8	3.58 × 10 ⁻³	8.80 × 10 ⁻⁵	3.49 × 10 ⁻³
1.81 × 10 ⁻⁵	7.47 × 10 ⁻⁴	5.91 × 10 ⁻⁴	5.65 × 10 ⁻⁴	2.64 × 10 ⁻⁵	31.2	4.30 × 10 ⁻³	9.08 × 10 ⁻⁵	4.21 × 10 ⁻³



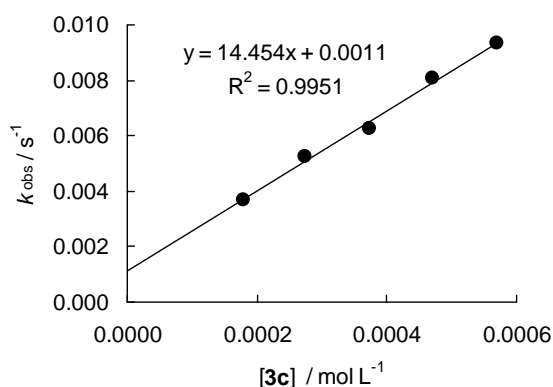
$$k_2(\text{OH}^-)^{[29]} = 3.44$$

$$\text{p}K_{\text{A}}(\mathbf{3c-H})^{[37]} = 8.93$$

$$k_2 = 6.75 \times 10^0 \text{ L mol}^{-1} \text{ s}^{-1}$$

Table 130: Kinetics of the reaction of **3c** with **1e** (20 °C, Conventional UV/Vis, at 627 nm).

[E] / mol L ⁻¹	[3c-H] ₀ / mol L ⁻¹	[KOH] ₀ / mol L ⁻¹	[3c] _{eff} / mol L ⁻¹	[KOH] _{eff} / mol L ⁻¹	[Nu]/[E]	<i>k</i> _{obs} / s ⁻¹	<i>k</i> _{OH⁻} / s ⁻¹	<i>k</i> _{eff} / s ⁻¹
2.21 × 10 ⁻⁵	2.51 × 10 ⁻⁴	1.99 × 10 ⁻⁴	1.78 × 10 ⁻⁴	2.07 × 10 ⁻⁵	8.1	3.93 × 10 ⁻³	2.24 × 10 ⁻⁴	3.71 × 10 ⁻³
2.21 × 10 ⁻⁵	3.76 × 10 ⁻⁴	2.98 × 10 ⁻⁴	2.75 × 10 ⁻⁴	2.30 × 10 ⁻⁵	12.4	5.49 × 10 ⁻³	2.49 × 10 ⁻⁴	5.24 × 10 ⁻³
2.21 × 10 ⁻⁵	5.02 × 10 ⁻⁴	3.97 × 10 ⁻⁴	3.73 × 10 ⁻⁴	2.46 × 10 ⁻⁵	16.9	6.54 × 10 ⁻³	2.65 × 10 ⁻⁴	6.27 × 10 ⁻³
2.21 × 10 ⁻⁵	6.27 × 10 ⁻⁴	4.96 × 10 ⁻⁴	4.71 × 10 ⁻⁴	2.56 × 10 ⁻⁵	21.3	8.36 × 10 ⁻³	2.77 × 10 ⁻⁴	8.08 × 10 ⁻³
2.21 × 10 ⁻⁵	7.53 × 10 ⁻⁴	5.96 × 10 ⁻⁴	5.69 × 10 ⁻⁴	2.64 × 10 ⁻⁵	25.8	9.64 × 10 ⁻³	2.85 × 10 ⁻⁴	9.35 × 10 ⁻³



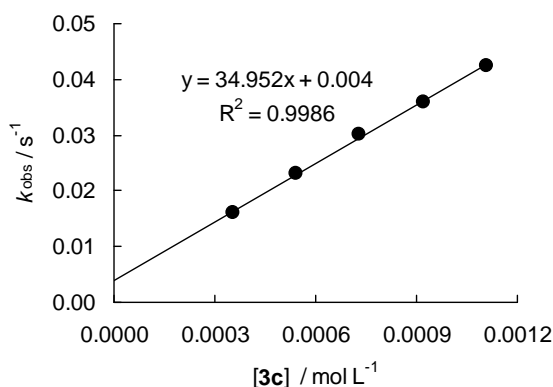
$$k_2(\text{OH}^-)^{[29]} = 10.8$$

$$\text{p}K_{\text{A}}(\mathbf{3c-H})^{[37]} = 8.93$$

$$k_2 = 1.45 \times 10^1 \text{ L mol}^{-1} \text{ s}^{-1}$$

Table 131: Kinetics of the reaction of **3c** with **1d** (20 °C, Conventional UV/Vis, at 618 nm).

[E] / mol L ⁻¹	[3c-H] ₀ / mol L ⁻¹	[KOH] ₀ / mol L ⁻¹	[3c] _{eff} / mol L ⁻¹	[KOH] _{eff} / mol L ⁻¹	[Nu]/[E]	<i>k</i> _{obs} / s ⁻¹	<i>k</i> _{OH⁻} / s ⁻¹	<i>k</i> _{eff} / s ⁻¹
2.42 × 10 ⁻⁵	4.51 × 10 ⁻⁴	3.83 × 10 ⁻⁴	3.52 × 10 ⁻⁴	3.05 × 10 ⁻⁵	14.6	1.67 × 10 ⁻²	7.18 × 10 ⁻⁴	1.60 × 10 ⁻²
2.42 × 10 ⁻⁵	6.76 × 10 ⁻⁴	5.75 × 10 ⁻⁴	5.41 × 10 ⁻⁴	3.40 × 10 ⁻⁵	22.3	2.38 × 10 ⁻²	7.98 × 10 ⁻⁴	2.30 × 10 ⁻²
2.42 × 10 ⁻⁵	9.01 × 10 ⁻⁴	7.66 × 10 ⁻⁴	7.30 × 10 ⁻⁴	3.62 × 10 ⁻⁵	30.2	3.10 × 10 ⁻²	8.51 × 10 ⁻⁴	3.01 × 10 ⁻²
2.42 × 10 ⁻⁵	1.13 × 10 ⁻³	9.58 × 10 ⁻⁴	9.20 × 10 ⁻⁴	3.78 × 10 ⁻⁵	38.0	3.69 × 10 ⁻²	8.88 × 10 ⁻⁴	3.60 × 10 ⁻²
2.42 × 10 ⁻⁵	1.35 × 10 ⁻³	1.15 × 10 ⁻³	1.11 × 10 ⁻³	3.90 × 10 ⁻⁵	45.9	4.35 × 10 ⁻²	9.17 × 10 ⁻⁴	4.26 × 10 ⁻²



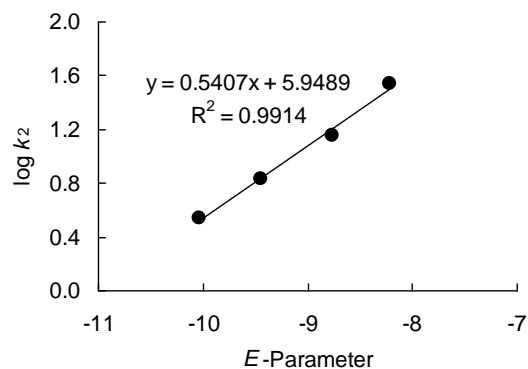
$$k_2(\text{OH}^-)^{[29]} = 23.5$$

$$\text{p}K_{\text{A}}(\mathbf{3c-H})^{[37]} = 8.93$$

$$k_2 = 3.50 \times 10^1 \text{ L mol}^{-1} \text{ s}^{-1}$$

Determination of Reactivity Parameters N and s for the Purine Anion (**3c**) in WaterTable 132: Rate Constants for the reactions of **3c** with different electrophiles (20 °C).

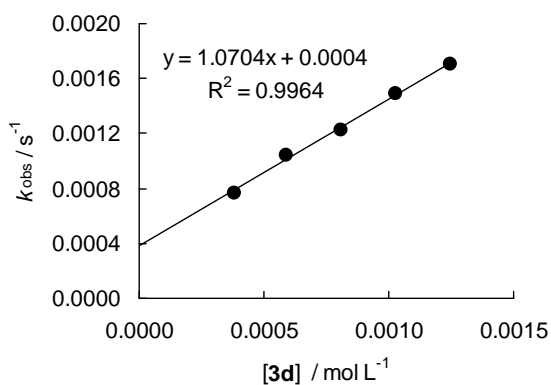
Electrophile	E	$k_2 / \text{L mol}^{-1} \text{s}^{-1}$	$\log k_2$
1g	-10.04	3.49×10^0	0.54
1f	-9.45	3.75×10^0	0.83
1e	-8.76	1.45×10^1	1.16
1d	-8.22	3.50×10^1	1.54



$$N = 11.00, s = 0.54$$

Reactions of the Potassium Salt of Theophylline (**3d**)Table 133: Kinetics of the reaction of **3d** with **1g** (20 °C, Conventional UV/Vis, at 630 nm) in 95 % water 5 % DMSO.

$[E] / \text{mol L}^{-1}$	$[3d]_0 / \text{mol L}^{-1}$	$[3d]_{\text{eff}} / \text{mol L}^{-1}$	$[\text{KOH}]_{\text{eff}} / \text{mol L}^{-1}$	$[\text{Nu}]/[E]$	$k_{\text{obs}} / \text{s}^{-1}$	$k_{\text{OH}^-} / \text{s}^{-1}$	$k_{\text{eff}} / \text{s}^{-1}$
3.68×10^{-5}	4.15×10^{-4}	3.80×10^{-4}	3.55×10^{-5}	10.3	8.45×10^{-4}	7.66×10^{-5}	7.68×10^{-4}
3.68×10^{-5}	6.37×10^{-4}	5.92×10^{-4}	4.43×10^{-5}	16.1	1.14×10^{-3}	9.57×10^{-5}	1.04×10^{-3}
3.68×10^{-5}	8.60×10^{-4}	8.08×10^{-4}	5.17×10^{-5}	22.0	1.34×10^{-3}	1.12×10^{-4}	1.23×10^{-3}
3.68×10^{-5}	1.08×10^{-3}	1.03×10^{-3}	5.83×10^{-5}	27.9	1.62×10^{-3}	1.26×10^{-4}	1.49×10^{-3}
3.68×10^{-5}	1.31×10^{-3}	1.24×10^{-3}	6.42×10^{-5}	33.8	1.84×10^{-3}	1.39×10^{-4}	1.70×10^{-3}



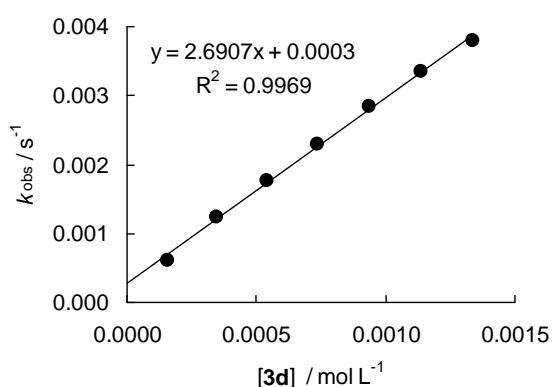
$$k_2(\text{OH}^-)^{[29]} = 2.16$$

$$\text{p}K_A(\text{3d-H})^{[38]} = 8.52$$

$$k_2 = 1.07 \times 10^0 \text{ L mol}^{-1} \text{ s}^{-1}$$

Table 134: Kinetics of the reaction of **3d** with **1f** (20 °C, Conventional UV/Vis, at 635 nm) in 95 % water 5 % DMSO.

[E] / mol L ⁻¹	[3d] ₀ / mol L ⁻¹	[3d] _{eff} / mol L ⁻¹	[KOH] _{eff} / mol L ⁻¹	[Nu]/[E]	<i>k</i> _{obs} / s ⁻¹	<i>k</i> _{OH⁻} / s ⁻¹	<i>k</i> _{eff} / s ⁻¹
2.29 × 10 ⁻⁵	1.80 × 10 ⁻⁴	1.57 × 10 ⁻⁴	2.28 × 10 ⁻⁵	6.9	6.87 × 10 ⁻⁴	7.85 × 10 ⁻⁵	6.08 × 10 ⁻⁴
2.29 × 10 ⁻⁵	3.79 × 10 ⁻⁴	3.45 × 10 ⁻⁴	3.38 × 10 ⁻⁵	15.1	1.36 × 10 ⁻³	1.16 × 10 ⁻⁴	1.24 × 10 ⁻³
2.29 × 10 ⁻⁵	5.81 × 10 ⁻⁴	5.39 × 10 ⁻⁴	4.23 × 10 ⁻⁵	23.5	1.92 × 10 ⁻³	1.45 × 10 ⁻⁴	1.77 × 10 ⁻³
2.29 × 10 ⁻⁵	7.86 × 10 ⁻⁴	7.36 × 10 ⁻⁴	4.94 × 10 ⁻⁵	32.1	2.47 × 10 ⁻³	1.70 × 10 ⁻⁴	2.30 × 10 ⁻³
2.29 × 10 ⁻⁵	9.91 × 10 ⁻⁴	9.35 × 10 ⁻⁴	5.57 × 10 ⁻⁵	40.8	3.04 × 10 ⁻³	1.91 × 10 ⁻⁴	2.85 × 10 ⁻³
2.29 × 10 ⁻⁵	1.20 × 10 ⁻³	1.14 × 10 ⁻³	6.13 × 10 ⁻⁵	49.6	3.57 × 10 ⁻³	2.11 × 10 ⁻⁴	3.36 × 10 ⁻³
2.29 × 10 ⁻⁵	1.40 × 10 ⁻³	1.34 × 10 ⁻³	6.65 × 10 ⁻⁵	58.4	4.02 × 10 ⁻³	2.29 × 10 ⁻⁴	3.79 × 10 ⁻³



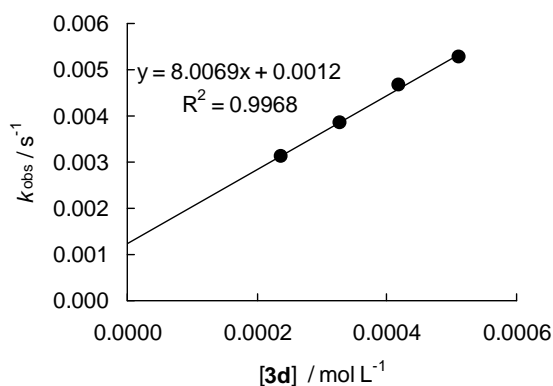
$$k_2(\text{OH}^-)^{[29]} = 3.44$$

$$\text{p}K_{\text{A}}(\mathbf{3d}\text{-H})^{[38]} = 8.52$$

$$k_2 = 2.69 \times 10^0 \text{ L mol}^{-1} \text{ s}^{-1}$$

Table 135: Kinetics of the reaction of **3d** with **1e** (20 °C, Conventional UV/Vis, at 627 nm) in 95 % water 5 % DMSO.

[E] / mol L ⁻¹	[3d] ₀ / mol L ⁻¹	[3d] _{eff} / mol L ⁻¹	[KOH] _{eff} / mol L ⁻¹	[Nu]/[E]	<i>k</i> _{obs} / s ⁻¹	<i>k</i> _{OH⁻} / s ⁻¹	<i>k</i> _{eff} / s ⁻¹
2.40 × 10 ⁻⁵	2.65 × 10 ⁻⁴	2.37 × 10 ⁻⁴	2.80 × 10 ⁻⁵	9.9	3.41 × 10 ⁻³	3.02 × 10 ⁻⁴	3.11 × 10 ⁻³
2.40 × 10 ⁻⁵	3.60 × 10 ⁻⁴	3.27 × 10 ⁻⁴	3.29 × 10 ⁻⁵	13.6	4.19 × 10 ⁻³	3.55 × 10 ⁻⁴	3.83 × 10 ⁻³
2.40 × 10 ⁻⁵	4.56 × 10 ⁻⁴	4.19 × 10 ⁻⁴	3.72 × 10 ⁻⁵	17.4	5.06 × 10 ⁻³	4.02 × 10 ⁻⁴	4.66 × 10 ⁻³
2.40 × 10 ⁻⁵	5.52 × 10 ⁻⁴	5.11 × 10 ⁻⁴	4.11 × 10 ⁻⁵	21.3	5.72 × 10 ⁻³	4.44 × 10 ⁻⁴	5.28 × 10 ⁻³



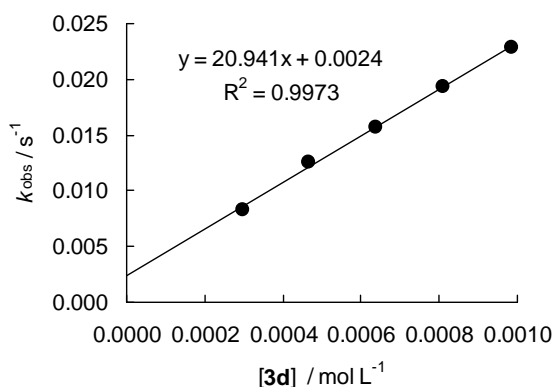
$$k_2(\text{OH}^-)^{[29]} = 10.8$$

$$\text{p}K_{\text{A}}(\mathbf{3d}\text{-H})^{[38]} = 8.52$$

$$k_2 = 8.01 \times 10^0 \text{ L mol}^{-1} \text{ s}^{-1}$$

Table 136: Kinetics of the reaction of **3d** with **1d** (20 °C, Conventional UV/Vis, at 618 nm) in 95 % water 5 % DMSO.

[E] / mol L ⁻¹	[3d] ₀ / mol L ⁻¹	[3d] _{eff} / mol L ⁻¹	[KOH] _{eff} / mol L ⁻¹	[Nu]/[E]	k _{obs} / s ⁻¹	k _{OH⁻} / s ⁻¹	k _{eff} / s ⁻¹
3.69 × 10 ⁻⁵	3.29 × 10 ⁻⁴	2.97 × 10 ⁻⁴	3.14 × 10 ⁻⁵	8.1	8.99 × 10 ⁻²	7.37 × 10 ⁻⁴	8.25 × 10 ⁻³
3.69 × 10 ⁻⁵	5.05 × 10 ⁻⁴	4.66 × 10 ⁻⁴	3.93 × 10 ⁻⁵	12.6	1.35 × 10 ⁻²	9.23 × 10 ⁻⁴	1.26 × 10 ⁻²
3.69 × 10 ⁻⁵	6.83 × 10 ⁻⁴	6.37 × 10 ⁻⁴	4.59 × 10 ⁻⁵	17.3	1.68 × 10 ⁻²	1.08 × 10 ⁻³	1.57 × 10 ⁻²
3.69 × 10 ⁻⁵	8.62 × 10 ⁻⁴	8.10 × 10 ⁻⁴	5.18 × 10 ⁻⁵	22.0	2.06 × 10 ⁻²	1.22 × 10 ⁻³	1.94 × 10 ⁻²
3.69 × 10 ⁻⁵	1.04 × 10 ⁻³	9.85 × 10 ⁻⁴	5.71 × 10 ⁻⁵	26.7	2.42 × 10 ⁻²	1.34 × 10 ⁻³	2.29 × 10 ⁻²



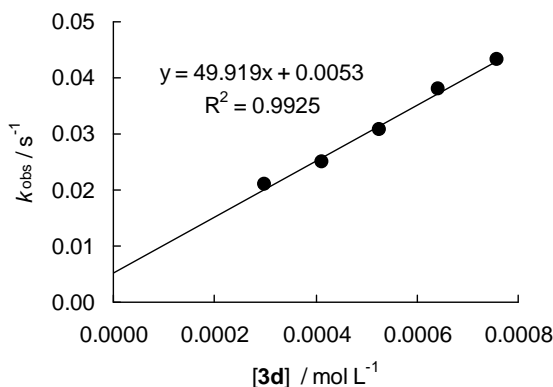
$$k_2(\text{OH}^-)^{[29]} = 23.5$$

$$\text{p}K_{\text{A}}(\text{3d-H})^{[38]} = 8.52$$

$$k_2 = 2.09 \times 10^1 \text{ L mol}^{-1} \text{ s}^{-1}$$

Table 137: Kinetics of the reaction of **3d** with **1c** (20 °C, Conventional UV/Vis, at 620 nm) in 95 % water 5 % DMSO.

[E] / mol L ⁻¹	[3d] ₀ / mol L ⁻¹	[3d] _{eff} / mol L ⁻¹	[KOH] _{eff} / mol L ⁻¹	[Nu]/[E]	k _{obs} / s ⁻¹	k _{OH⁻} / s ⁻¹	k _{eff} / s ⁻¹
2.63 × 10 ⁻⁵	3.31 × 10 ⁻⁴	3.00 × 10 ⁻⁴	3.15 × 10 ⁻⁵	11.4	2.26 × 10 ⁻²	1.53 × 10 ⁻³	2.11 × 10 ⁻²
2.63 × 10 ⁻⁵	4.49 × 10 ⁻⁴	4.12 × 10 ⁻⁴	3.69 × 10 ⁻⁵	15.7	2.68 × 10 ⁻²	1.79 × 10 ⁻³	2.50 × 10 ⁻²
2.63 × 10 ⁻⁵	5.68 × 10 ⁻⁴	5.26 × 10 ⁻⁴	4.17 × 10 ⁻⁵	20.0	3.28 × 10 ⁻²	2.02 × 10 ⁻³	3.08 × 10 ⁻²
2.63 × 10 ⁻⁵	6.88 × 10 ⁻⁴	6.41 × 10 ⁻⁴	4.61 × 10 ⁻⁵	24.4	4.02 × 10 ⁻²	2.24 × 10 ⁻³	3.80 × 10 ⁻²
2.63 × 10 ⁻⁵	8.08 × 10 ⁻⁴	7.57 × 10 ⁻⁴	5.01 × 10 ⁻⁵	28.8	4.56 × 10 ⁻²	2.43 × 10 ⁻³	4.32 × 10 ⁻²



$$k_2(\text{OH}^-)^{[29]} = 48.5$$

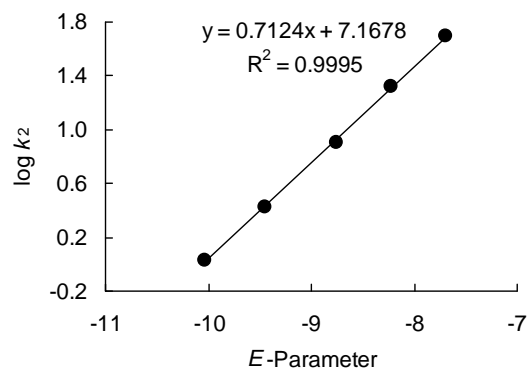
$$\text{p}K_{\text{A}}(\text{3d-H})^{[38]} = 8.52$$

$$k_2 = 4.99 \times 10^1 \text{ L mol}^{-1} \text{ s}^{-1}$$

Determination of Reactivity Parameters N and s for the Theophylline Anion (**3d**) in 95 % Water 5% DMSO

Table 138: Rate Constants for the reactions of **3d** with different electrophiles (20 °C).

Electrophile	E	$k_2 / \text{L mol}^{-1} \text{s}^{-1}$	$\log k_2$
1g	-10.04	1.07×10^0	0.03
1f	-9.45	2.69×10^0	0.43
1e	-8.76	8.01×10^0	0.90
1d	-8.22	2.09×10^1	1.32
1c	-7.69	4.99×10^1	1.70

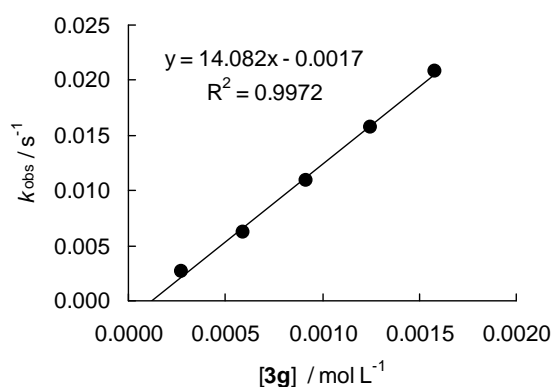


$$N = 10.06, s = 0.71$$

Reactions of the Potassium Salt of Guanosin (**3h**)

Table 139: Kinetics of the reaction of **3h** with **1g** (20 °C, Conventional UV/Vis, at 630 nm).

$[E] / \text{mol L}^{-1}$	$[\mathbf{3h-H}]_0 / \text{mol L}^{-1}$	$[\text{KOH}]_0 / \text{mol L}^{-1}$	$[\mathbf{3h}]_{\text{eff}} / \text{mol L}^{-1}$	$[\text{KOH}]_{\text{eff}} / \text{mol L}^{-1}$	$[\text{Nu}]/[E]$	$k_{\text{obs}} / \text{s}^{-1}$	$k_{\text{OH}^-} / \text{s}^{-1}$	$k_{\text{eff}} / \text{s}^{-1}$
1.98×10^{-5}	3.58×10^{-4}	3.48×10^{-4}	2.77×10^{-4}	7.05×10^{-5}	14.0	2.81×10^{-3}	1.52×10^{-4}	2.66×10^{-3}
1.98×10^{-5}	7.15×10^{-4}	6.96×10^{-4}	5.95×10^{-4}	1.01×10^{-4}	30.0	6.46×10^{-3}	2.18×10^{-4}	6.24×10^{-3}
1.98×10^{-5}	1.07×10^{-3}	1.04×10^{-3}	9.20×10^{-4}	1.23×10^{-4}	46.4	1.12×10^{-2}	2.66×10^{-4}	1.09×10^{-2}
1.98×10^{-5}	1.43×10^{-3}	1.39×10^{-3}	1.25×10^{-3}	1.41×10^{-4}	63.0	1.61×10^{-2}	3.05×10^{-4}	1.58×10^{-2}
1.98×10^{-5}	1.79×10^{-3}	1.74×10^{-3}	1.58×10^{-3}	1.57×10^{-4}	79.7	2.12×10^{-2}	3.39×10^{-4}	2.09×10^{-2}



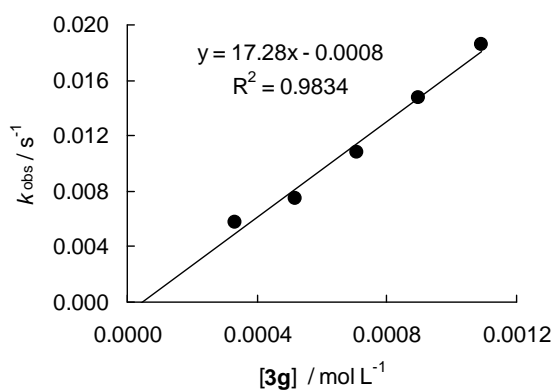
$$k_2(\text{OH}^-)^{[29]} = 2.16$$

$$\text{p}K_A(\mathbf{3h-H})^{[34]} = 9.31$$

$$k_2 = 1.41 \times 10^1 \text{ L mol}^{-1} \text{ s}^{-1}$$

Table 140: Kinetics of the reaction of **3h** with **1f** (20 °C, Conventional UV/Vis, at 635 nm).

[E] / mol L ⁻¹	[3h-H] ₀ / mol L ⁻¹	[KOH] ₀ / mol L ⁻¹	[3h] _{eff} / mol L ⁻¹	[KOH] _{eff} / mol L ⁻¹	[Nu]/[E]	k _{obs} / s ⁻¹	k _{OH⁻} / s ⁻¹	k _{eff} / s ⁻¹
2.55 × 10 ⁻⁵	4.10 × 10 ⁻⁴	4.17 × 10 ⁻⁴	3.31 × 10 ⁻⁴	8.56 × 10 ⁻⁵	13.0	6.06 × 10 ⁻³	2.94 × 10 ⁻⁴	5.77 × 10 ⁻³
2.55 × 10 ⁻⁵	6.15 × 10 ⁻⁴	6.25 × 10 ⁻⁴	5.17 × 10 ⁻⁴	1.08 × 10 ⁻⁴	20.3	7.85 × 10 ⁻³	3.71 × 10 ⁻⁴	7.48 × 10 ⁻³
2.55 × 10 ⁻⁵	8.20 × 10 ⁻⁴	8.33 × 10 ⁻³	7.07 × 10 ⁻⁴	1.27 × 10 ⁻⁴	27.7	1.12 × 10 ⁻²	4.36 × 10 ⁻⁴	1.08 × 10 ⁻²
2.55 × 10 ⁻⁵	1.03 × 10 ⁻³	1.04 × 10 ⁻³	8.98 × 10 ⁻⁴	1.44 × 10 ⁻⁴	35.2	1.52 × 10 ⁻²	4.95 × 10 ⁻⁴	1.47 × 10 ⁻²
2.55 × 10 ⁻⁵	1.23 × 10 ⁻³	1.25 × 10 ⁻³	1.09 × 10 ⁻³	1.59 × 10 ⁻⁴	42.8	1.91 × 10 ⁻²	5.48 × 10 ⁻⁴	1.86 × 10 ⁻²



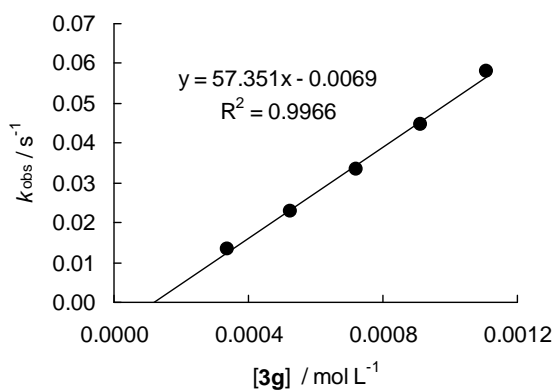
$$k_2(\text{OH}^-)^{[29]} = 3.44$$

$$\text{p}K_A(\mathbf{3h-H})^{[34]} = 9.31$$

$$k_2 = 1.73 \times 10^1 \text{ L mol}^{-1} \text{ s}^{-1}$$

 Table 141: Kinetics of the reaction of **3h** with **1e** (20 °C, Stopped-Flow, at 610 nm).

[E] / mol L ⁻¹	[3h-H] ₀ / mol L ⁻¹	[KOH] ₀ / mol L ⁻¹	[3h] _{eff} / mol L ⁻¹	[KOH] _{eff} / mol L ⁻¹	[Nu]/[E]	k _{obs} / s ⁻¹	k _{OH⁻} / s ⁻¹	k _{eff} / s ⁻¹
2.97 × 10 ⁻⁵	4.24 × 10 ⁻⁴	4.17 × 10 ⁻⁴	3.37 × 10 ⁻⁴	7.95 × 10 ⁻⁵	11.3	1.43 × 10 ⁻²	8.59 × 10 ⁻⁴	1.34 × 10 ⁻²
2.97 × 10 ⁻⁵	6.36 × 10 ⁻⁴	6.25 × 10 ⁻⁴	5.26 × 10 ⁻⁴	9.86 × 10 ⁻⁵	17.7	2.40 × 10 ⁻²	1.06 × 10 ⁻³	2.29 × 10 ⁻²
2.97 × 10 ⁻⁵	8.47 × 10 ⁻⁴	8.33 × 10 ⁻⁴	7.19 × 10 ⁻⁴	1.14 × 10 ⁻⁴	24.2	3.47 × 10 ⁻²	1.24 × 10 ⁻³	3.35 × 10 ⁻²
2.97 × 10 ⁻⁵	1.06 × 10 ⁻³	1.04 × 10 ⁻³	9.14 × 10 ⁻⁴	1.28 × 10 ⁻⁴	30.7	4.60 × 10 ⁻²	1.38 × 10 ⁻³	4.46 × 10 ⁻²
2.97 × 10 ⁻⁵	1.27 × 10 ⁻³	1.25 × 10 ⁻³	1.11 × 10 ⁻³	1.40 × 10 ⁻⁴	37.3	5.95 × 10 ⁻²	1.52 × 10 ⁻³	5.80 × 10 ⁻²



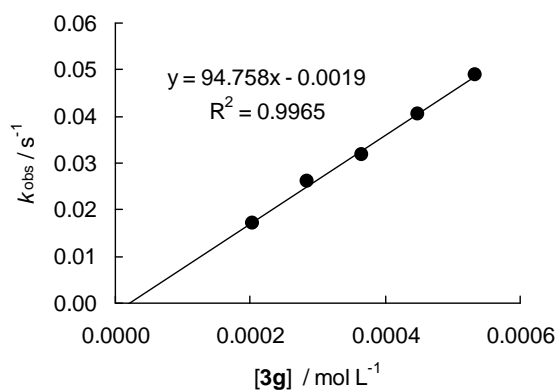
$$k_2(\text{OH}^-)^{[29]} = 10.8$$

$$\text{p}K_A(\mathbf{3h-H})^{[34]} = 9.31$$

$$k_2 = 5.74 \times 10^1 \text{ L mol}^{-1} \text{ s}^{-1}$$

Table 142: Kinetics of the reaction of **3h** with **1d** (20 °C, Stopped-Flow, at 618 nm).

[E] / mol L ⁻¹	[3h-H] ₀ / mol L ⁻¹	[KOH] ₀ / mol L ⁻¹	[3h] _{eff} / mol L ⁻¹	[KOH] _{eff} / mol L ⁻¹	[Nu]/[E]	k _{obs} / s ⁻¹	k _{OH⁻} / s ⁻¹	k _{eff} / s ⁻¹
1.80 × 10 ⁻⁵	2.77 × 10 ⁻⁴	2.62 × 10 ⁻⁴	2.04 × 10 ⁻⁴	5.75 × 10 ⁻⁵	11.3	1.85 × 10 ⁻²	1.35 × 10 ⁻⁴	1.71 × 10 ⁻²
1.80 × 10 ⁻⁵	3.71 × 10 ⁻⁴	3.51 × 10 ⁻⁴	2.84 × 10 ⁻⁴	6.68 × 10 ⁻⁵	15.8	2.76 × 10 ⁻²	1.57 × 10 ⁻³	2.60 × 10 ⁻²
1.80 × 10 ⁻⁵	4.66 × 10 ⁻⁴	4.41 × 10 ⁻⁴	3.66 × 10 ⁻⁴	7.47 × 10 ⁻⁵	20.3	3.36 × 10 ⁻²	1.76 × 10 ⁻³	3.18 × 10 ⁻²
1.80 × 10 ⁻⁵	5.61 × 10 ⁻⁴	5.31 × 10 ⁻⁴	4.49 × 10 ⁻⁴	8.17 × 10 ⁻⁵	24.9	4.23 × 10 ⁻²	1.92 × 10 ⁻³	4.04 × 10 ⁻²
1.80 × 10 ⁻⁵	6.58 × 10 ⁻⁴	6.22 × 10 ⁻⁴	5.34 × 10 ⁻⁴	8.81 × 10 ⁻⁵	29.6	5.11 × 10 ⁻²	2.07 × 10 ⁻³	4.90 × 10 ⁻²



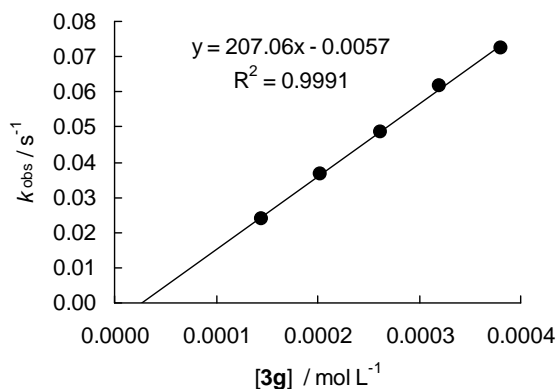
$$k_2(\text{OH}^-)^{[29]} = 23.5$$

$$\text{p}K_A(\mathbf{3h-H})^{[34]} = 9.31$$

$$k_2 = 9.48 \times 10^1 \text{ L mol}^{-1} \text{ s}^{-1}$$

 Table 143: Kinetics of the reaction of **3h** with **1c** (20 °C, Stopped-Flow, at 620 nm).

[E] / mol L ⁻¹	[3h-H] ₀ / mol L ⁻¹	[KOH] ₀ / mol L ⁻¹	[3h] _{eff} / mol L ⁻¹	[KOH] _{eff} / mol L ⁻¹	[Nu]/[E]	k _{obs} / s ⁻¹	k _{OH⁻} / s ⁻¹	k _{eff} / s ⁻¹
1.64 × 10 ⁻⁵	2.04 × 10 ⁻⁴	1.97 × 10 ⁻⁴	1.45 × 10 ⁻⁴	5.11 × 10 ⁻⁵	8.9	2.65 × 10 ⁻²	2.48 × 10 ⁻³	2.40 × 10 ⁻²
1.64 × 10 ⁻⁵	2.71 × 10 ⁻⁴	2.62 × 10 ⁻⁴	2.02 × 10 ⁻⁴	5.98 × 10 ⁻⁵	12.4	3.94 × 10 ⁻²	2.90 × 10 ⁻³	3.65 × 10 ⁻²
1.64 × 10 ⁻⁵	3.41 × 10 ⁻⁴	3.29 × 10 ⁻⁴	2.62 × 10 ⁻⁴	6.74 × 10 ⁻⁵	16.0	5.18 × 10 ⁻²	3.27 × 10 ⁻³	4.85 × 10 ⁻²
1.64 × 10 ⁻⁵	4.09 × 10 ⁻⁴	3.95 × 10 ⁻⁴	3.21 × 10 ⁻⁴	7.42 × 10 ⁻⁵	19.6	6.51 × 10 ⁻²	3.60 × 10 ⁻³	6.15 × 10 ⁻²
1.64 × 10 ⁻⁵	4.77 × 10 ⁻⁴	4.61 × 10 ⁻⁴	3.80 × 10 ⁻⁴	8.03 × 10 ⁻⁵	23.2	7.63 × 10 ⁻²	3.89 × 10 ⁻³	7.24 × 10 ⁻²



$$k_2(\text{OH}^-)^{[29]} = 48.5$$

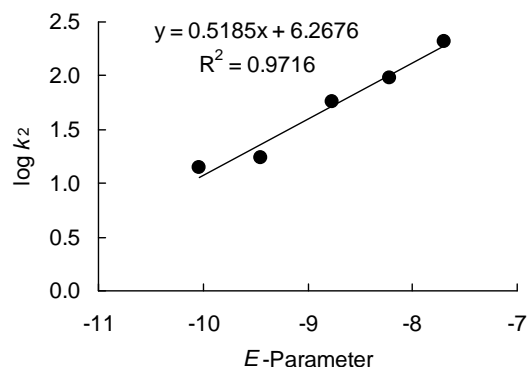
$$\text{p}K_A(\mathbf{3h-H})^{[34]} = 9.31$$

$$k_2 = 2.07 \times 10^2 \text{ L mol}^{-1} \text{ s}^{-1}$$

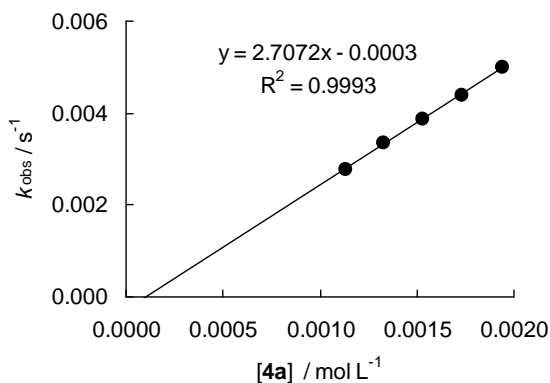
Determination of Reactivity Parameters N and s for the Anion of Guanosine (**3f**) in WaterTable 144: Rate Constants for the reactions of **3f** with different electrophiles (20 °C).

Electrophile	E	$k_2 / \text{L mol}^{-1} \text{s}^{-1}$	$\log k_2$
1g	-10.04	1.41×10^1	1.15
1f	-9.45	1.73×10^1	1.24
1e	-8.76	5.74×10^1	1.76
1d	-8.22	9.48×10^1	1.98
1c	-7.69	2.07×10^2	2.32

$$N = 12.09, s = 0.52$$

Reactions of the Potassium Salt of Uracil (**4a**)Table 145: Kinetics of the reaction of **4a** with **1g** (20 °C, Conventional UV/Vis, at 630 nm).

$[\text{E}] / \text{mol L}^{-1}$	$[\mathbf{4a}]_0 / \text{mol L}^{-1}$	$[\mathbf{4a}]_{\text{eff}} / \text{mol L}^{-1}$	$[\text{KOH}]_{\text{eff}} / \text{mol L}^{-1}$	$[\text{Nu}]/[\text{E}]$	$k_{\text{obs}} / \text{s}^{-1}$	$k_{\text{OH}^-} / \text{s}^{-1}$	$k_{\text{eff}} / \text{s}^{-1}$
2.40×10^{-5}	2.17×10^{-3}	1.94×10^{-3}	2.34×10^{-5}	80.8	5.51×10^{-3}	5.05×10^{-4}	5.00×10^{-3}
2.40×10^{-5}	1.96×10^{-3}	1.73×10^{-3}	2.21×10^{-5}	72.1	4.87×10^{-3}	4.77×10^{-4}	4.39×10^{-3}
2.40×10^{-5}	1.74×10^{-3}	1.53×10^{-3}	2.08×10^{-5}	63.8	4.31×10^{-3}	4.49×10^{-4}	3.86×10^{-3}
2.40×10^{-5}	1.52×10^{-3}	1.33×10^{-3}	1.93×10^{-5}	55.4	3.78×10^{-3}	4.17×10^{-4}	3.36×10^{-3}
2.40×10^{-5}	1.30×10^{-3}	1.13×10^{-3}	1.78×10^{-5}	47.1	3.17×10^{-3}	3.84×10^{-4}	2.79×10^{-3}



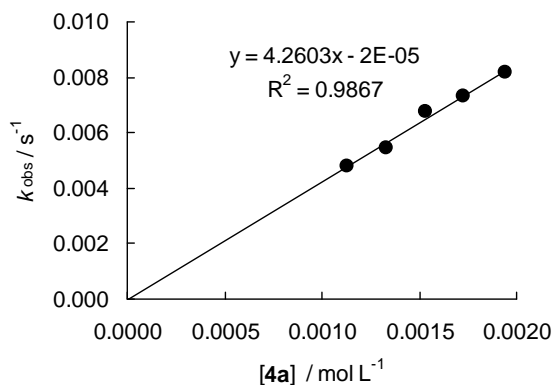
$$k_2(\text{OH}^-)^{[29]} = 2.16$$

$$\text{p}K_{\text{A}}(\mathbf{4a}\text{-H})^{[36]} = 9.45$$

$$k_2 = 2.71 \times 10^0 \text{ L mol}^{-1} \text{ s}^{-1}$$

Table 146: Kinetics of the reaction of **4a** with **1f** (20 °C, Conventional UV/Vis, at 635 nm).

$[\text{E}] / \text{mol L}^{-1}$	$[\mathbf{4a}]_0 / \text{mol L}^{-1}$	$[\mathbf{4a}]_{\text{eff}} / \text{mol L}^{-1}$	$[\text{KOH}]_{\text{eff}} / \text{mol L}^{-1}$	$[\text{Nu}]/[\text{E}]$	$k_{\text{obs}} / \text{s}^{-1}$	$k_{\text{OH}^-} / \text{s}^{-1}$	$k_{\text{eff}} / \text{s}^{-1}$
2.70×10^{-5}	2.17×10^{-3}	1.94×10^{-3}	2.34×10^{-5}	71.9	9.00×10^{-3}	8.05×10^{-4}	8.20×10^{-3}
2.70×10^{-5}	1.96×10^{-3}	1.73×10^{-3}	2.21×10^{-5}	64.1	8.07×10^{-3}	7.60×10^{-4}	7.31×10^{-3}
2.70×10^{-5}	1.74×10^{-3}	1.53×10^{-3}	2.08×10^{-5}	56.7	7.47×10^{-3}	7.16×10^{-4}	6.76×10^{-3}
2.70×10^{-5}	1.52×10^{-3}	1.33×10^{-3}	1.93×10^{-5}	49.3	6.14×10^{-3}	6.64×10^{-4}	5.48×10^{-3}
2.70×10^{-5}	1.30×10^{-3}	1.13×10^{-3}	1.78×10^{-5}	41.9	5.42×10^{-3}	6.12×10^{-4}	4.81×10^{-3}



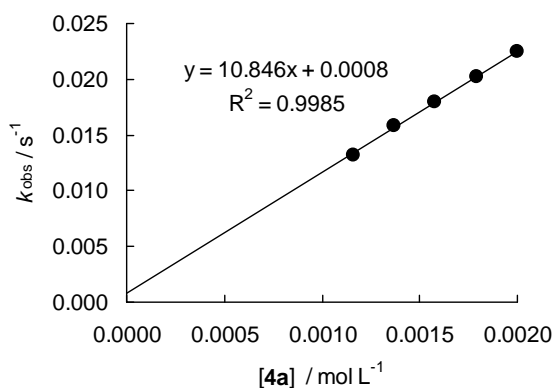
$$k_2(\text{OH}^-)^{[29]} = 3.44$$

$$\text{p}K_{\text{A}}(\mathbf{4a-H})^{[36]} = 9.45$$

$$k_2 = 4.26 \times 10^0 \text{ L mol}^{-1} \text{ s}^{-1}$$

Table 147: Kinetics of the reaction of **4a** with **1e** (20 °C, Conventional UV/Vis, at 627 nm).

[E] / mol L ⁻¹	[4a] ₀ / mol L ⁻¹	[4a] _{eff} / mol L ⁻¹	[KOH] _{eff} / mol L ⁻¹	[Nu]/[E]	$k_{\text{obs}} /$ s ⁻¹	$k_{\text{OH}^-} /$ s ⁻¹	$k_{\text{eff}} /$ s ⁻¹
2.55×10^{-5}	1.34×10^{-3}	1.16×10^{-3}	1.81×10^{-4}	45.5	1.52×10^{-2}	1.95×10^{-3}	1.32×10^{-2}
2.55×10^{-5}	1.57×10^{-3}	1.37×10^{-3}	1.96×10^{-4}	53.7	1.80×10^{-2}	2.12×10^{-3}	1.59×10^{-2}
2.55×10^{-5}	1.79×10^{-3}	1.58×10^{-3}	2.11×10^{-4}	62.0	2.03×10^{-2}	2.28×10^{-3}	1.80×10^{-2}
2.55×10^{-5}	2.01×10^{-3}	1.79×10^{-3}	2.25×10^{-4}	70.2	2.27×10^{-2}	2.43×10^{-3}	2.03×10^{-2}
2.55×10^{-5}	2.24×10^{-3}	2.00×10^{-3}	2.37×10^{-4}	78.4	2.50×10^{-2}	2.56×10^{-3}	2.24×10^{-2}



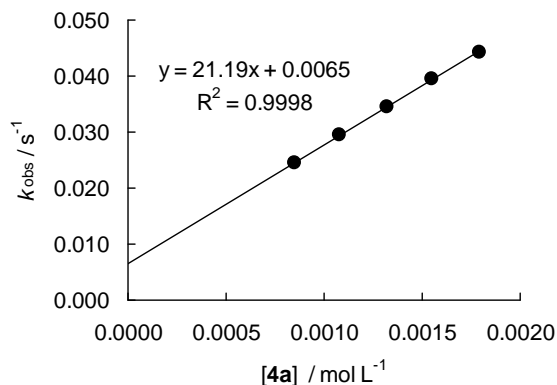
$$k_2(\text{OH}^-)^{[29]} = 10.8$$

$$\text{p}K_{\text{A}}(\mathbf{4a-H})^{[36]} = 9.45$$

$$k_2 = 1.08 \times 10^1 \text{ L mol}^{-1} \text{ s}^{-1}$$

Table 148: Kinetics of the reaction of **4a** with **1d** (20 °C, Conventional UV/Vis, at 618 nm).

[E] / mol L ⁻¹	[4a] ₀ / mol L ⁻¹	[4a] _{eff} / mol L ⁻¹	[KOH] _{eff} / mol L ⁻¹	[Nu]/[E]	$k_{\text{obs}} /$ s ⁻¹	$k_{\text{OH}^-} /$ s ⁻¹	$k_{\text{eff}} /$ s ⁻¹
2.37×10^{-5}	1.01×10^{-3}	8.51×10^{-4}	1.55×10^{-4}	35.9	2.81×10^{-2}	3.64×10^{-3}	2.45×10^{-2}
2.37×10^{-5}	1.26×10^{-3}	1.08×10^{-3}	1.75×10^{-4}	45.6	3.36×10^{-2}	4.11×10^{-3}	2.95×10^{-2}
2.37×10^{-5}	1.51×10^{-3}	1.32×10^{-3}	1.93×10^{-4}	55.7	3.90×10^{-2}	4.54×10^{-3}	3.45×10^{-2}
2.37×10^{-5}	1.76×10^{-3}	1.55×10^{-3}	2.09×10^{-4}	65.4	4.44×10^{-2}	4.91×10^{-3}	3.95×10^{-2}
2.37×10^{-5}	2.01×10^{-3}	1.79×10^{-3}	2.24×10^{-4}	75.5	4.96×10^{-2}	5.26×10^{-3}	4.43×10^{-2}



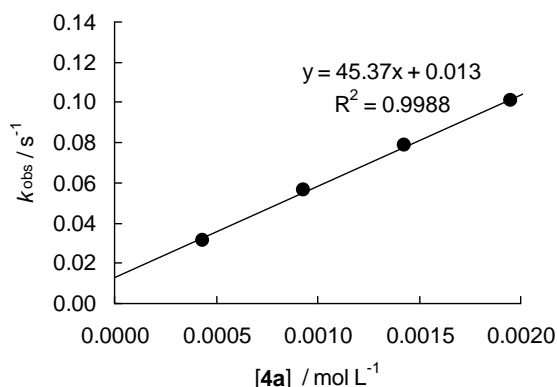
$$k_2(\text{OH}^-)^{[29]} = 23.5$$

$$\text{p}K_{\text{A}}(\mathbf{4a-H})^{[36]} = 9.45$$

$$k_2 = 2.12 \times 10^1 \text{ L mol}^{-1} \text{ s}^{-1}$$

Table 149: Kinetics of the reaction of **4a** with **1c** (20 °C, Conventional UV/Vis, at 620 nm).

[E] / mol L^{-1}	[4a] ₀ / mol L^{-1}	[4a] _{eff} / mol L^{-1}	[KOH] _{eff} / mol L^{-1}	[Nu]/[E]	$k_{\text{obs}} /$ s^{-1}	$k_{\text{OH}^-} /$ s^{-1}	$k_{\text{eff}} /$ s^{-1}
1.07×10^{-5}	5.44×10^{-3}	4.33×10^{-4}	1.11×10^{-4}	40.5	3.65×10^{-2}	5.38×10^{-3}	3.11×10^{-2}
1.07×10^{-5}	1.09×10^{-3}	9.28×10^{-4}	1.62×10^{-4}	86.7	6.44×10^{-2}	7.86×10^{-3}	5.65×10^{-2}
1.07×10^{-5}	1.63×10^{-3}	1.43×10^{-3}	2.01×10^{-4}	134	8.88×10^{-2}	9.75×10^{-3}	7.91×10^{-2}
1.07×10^{-5}	2.18×10^{-3}	1.95×10^{-3}	2.34×10^{-4}	182	1.12×10^{-1}	1.13×10^{-2}	1.01×10^{-1}
1.07×10^{-5}	2.72×10^{-3}	2.46×10^{-3}	2.63×10^{-4}	230	1.37×10^{-1}	1.28×10^{-2}	1.24×10^{-1}



$$k_2(\text{OH}^-)^{[29]} = 23.5$$

$$\text{p}K_{\text{A}}(\mathbf{4a-H})^{[36]} = 9.45$$

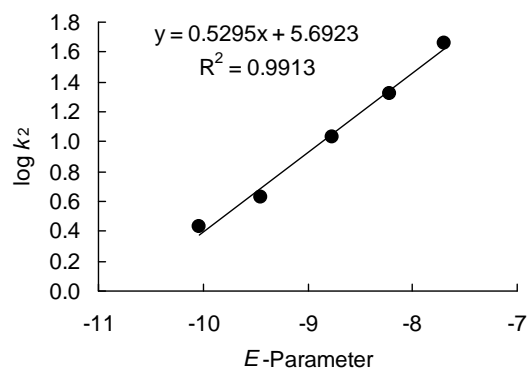
$$k_2 = 4.54 \times 10^1 \text{ L mol}^{-1} \text{ s}^{-1}$$

Determination of Reactivity Parameters N and s for the Anion of Uracil (**4a**) in Water

Table 150: Rate Constants for the Reactions of **4a** with Different Electrophiles (20 °C).

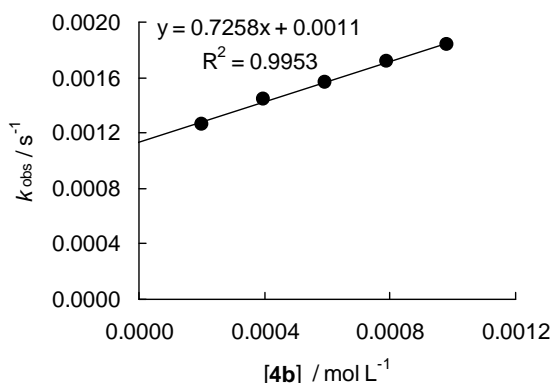
Electrophile	E	$k_2 / \text{L mol}^{-1} \text{ s}^{-1}$	$\log k_2$
1g	-10.04	2.71×10^0	0.43
1f	-9.45	4.26×10^0	0.63
1e	-8.76	1.08×10^1	1.03
1d	-8.22	2.12×10^1	1.33
1c	-7.69	4.54×10^1	1.66

$$N = 10.75, s = 0.53$$



Reactions of the Potassium Salt of 1-Methyluracile (4b)Table 151: Kinetics of the reaction of **4b** with **1e** (20 °C, Conventional UV/Vis, at 627 nm).

[E] / mol L ⁻¹	[4b-H] ₀ / mol L ⁻¹	[KOH] ₀ / mol L ⁻¹	[4b] _{eff} / mol L ⁻¹	[KOH] _{eff} / mol L ⁻¹	[Nu]/[E]	<i>k</i> _{obs} / s ⁻¹	<i>k</i> _{OH⁻} / s ⁻¹	<i>k</i> _{eff} / s ⁻¹
1.50 × 10 ⁻⁵	2.91 × 10 ⁻³	2.07 × 10 ⁻⁴	2.00 × 10 ⁻⁴	7.20 × 10 ⁻⁶	13.3	1.34 × 10 ⁻³	7.78 × 10 ⁻⁵	1.26 × 10 ⁻³
1.50 × 10 ⁻⁵	2.91 × 10 ⁻³	4.13 × 10 ⁻⁴	3.98 × 10 ⁻⁴	1.55 × 10 ⁻⁵	26.5	1.61 × 10 ⁻³	1.67 × 10 ⁻⁴	1.44 × 10 ⁻³
1.50 × 10 ⁻⁵	2.91 × 10 ⁻³	6.20 × 10 ⁻⁴	5.95 × 10 ⁻⁴	2.51 × 10 ⁻⁵	39.7	1.84 × 10 ⁻³	2.71 × 10 ⁻⁴	1.57 × 10 ⁻³
1.50 × 10 ⁻⁵	2.91 × 10 ⁻³	8.26 × 10 ⁻⁴	7.90 × 10 ⁻⁴	3.64 × 10 ⁻⁵	52.6	2.11 × 10 ⁻³	3.93 × 10 ⁻⁴	1.72 × 10 ⁻³
1.50 × 10 ⁻⁵	2.91 × 10 ⁻³	1.03 × 10 ⁻³	9.80 × 10 ⁻⁴	4.96 × 10 ⁻⁵	65.4	2.37 × 10 ⁻³	5.36 × 10 ⁻⁴	1.83 × 10 ⁻³



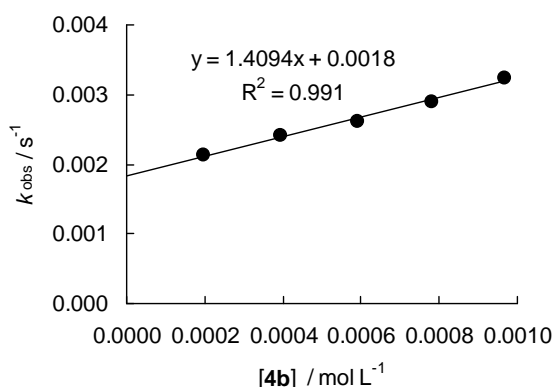
$$k_2(\text{OH}^-)^{[29]} = 10.8$$

$$\text{p}K_{\text{A}}(\mathbf{4b-H})^{[36]} = 9.99$$

$$k_2 = 7.26 \times 10^{-1} \text{ L mol}^{-1} \text{ s}^{-1}$$

Table 152: Kinetics of the reaction of **4b** with **1d** (20 °C, Conventional UV/Vis, at 618 nm).

[E] / mol L ⁻¹	[4b-H] ₀ / mol L ⁻¹	[KOH] ₀ / mol L ⁻¹	[4b] _{eff} / mol L ⁻¹	[KOH] _{eff} / mol L ⁻¹	[Nu]/[E]	<i>k</i> _{obs} / s ⁻¹	<i>k</i> _{OH⁻} / s ⁻¹	<i>k</i> _{eff} / s ⁻¹
1.47 × 10 ⁻⁵	2.51 × 10 ⁻³	2.07 × 10 ⁻⁴	1.99 × 10 ⁻⁴	8.40 × 10 ⁻⁶	13.5	2.32 × 10 ⁻³	1.97 × 10 ⁻⁴	2.12 × 10 ⁻³
1.47 × 10 ⁻⁵	2.51 × 10 ⁻³	4.13 × 10 ⁻⁴	3.95 × 10 ⁻⁴	1.82 × 10 ⁻⁵	26.9	2.84 × 10 ⁻³	4.29 × 10 ⁻⁴	2.41 × 10 ⁻³
1.47 × 10 ⁻⁵	2.51 × 10 ⁻³	6.20 × 10 ⁻⁴	5.90 × 10 ⁻⁴	3.00 × 10 ⁻⁵	40.1	3.31 × 10 ⁻³	7.06 × 10 ⁻⁴	2.60 × 10 ⁻³
1.47 × 10 ⁻⁵	2.51 × 10 ⁻³	8.26 × 10 ⁻⁴	7.82 × 10 ⁻⁴	4.42 × 10 ⁻⁵	53.2	3.94 × 10 ⁻³	1.04 × 10 ⁻³	2.90 × 10 ⁻³
1.47 × 10 ⁻⁵	2.51 × 10 ⁻³	1.03 × 10 ⁻³	9.69 × 10 ⁻⁴	6.14 × 10 ⁻⁵	65.9	4.68 × 10 ⁻³	1.44 × 10 ⁻³	3.24 × 10 ⁻³



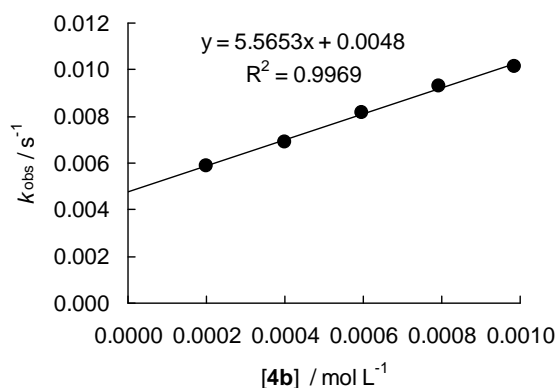
$$k_2(\text{OH}^-)^{[29]} = 23.5$$

$$\text{p}K_{\text{A}}(\mathbf{4b-H})^{[36]} = 9.99$$

$$k_2 = 1.41 \times 10^0 \text{ L mol}^{-1} \text{ s}^{-1}$$

Table 153: Kinetics of the reaction of **4b** with **1c** (20 °C, Conventional UV/Vis, at 620 nm).

[E] / mol L ⁻¹	[4b-H] ₀ / mol L ⁻¹	[KOH] ₀ / mol L ⁻¹	[4b] _{eff} / mol L ⁻¹	[KOH] _{eff} / mol L ⁻¹	[Nu]/[E]	<i>k</i> _{obs} / s ⁻¹	<i>k</i> _{OH⁻} / s ⁻¹	<i>k</i> _{eff} / s ⁻¹
1.49 × 10 ⁻⁵	3.15 × 10 ⁻³	2.07 × 10 ⁻⁴	2.00 × 10 ⁻⁴	6.64 × 10 ⁻⁶	13.4	6.19 × 10 ⁻³	3.22 × 10 ⁻⁴	5.87 × 10 ⁻³
1.49 × 10 ⁻⁵	3.15 × 10 ⁻³	4.13 × 10 ⁻⁴	3.99 × 10 ⁻⁴	1.42 × 10 ⁻⁵	26.8	7.61 × 10 ⁻³	6.87 × 10 ⁻⁴	6.92 × 10 ⁻³
1.49 × 10 ⁻⁵	3.15 × 10 ⁻³	6.20 × 10 ⁻⁴	5.97 × 10 ⁻⁴	2.29 × 10 ⁻⁵	40.1	9.27 × 10 ⁻³	1.11 × 10 ⁻³	8.16 × 10 ⁻³
1.49 × 10 ⁻⁵	3.15 × 10 ⁻³	8.26 × 10 ⁻⁴	7.93 × 10 ⁻⁴	3.29 × 10 ⁻⁵	53.2	1.09 × 10 ⁻²	1.59 × 10 ⁻³	9.31 × 10 ⁻³
1.49 × 10 ⁻⁵	3.15 × 10 ⁻³	1.03 × 10 ⁻³	9.86 × 10 ⁻⁴	4.45 × 10 ⁻⁵	66.1	1.23 × 10 ⁻²	2.16 × 10 ⁻³	1.01 × 10 ⁻²



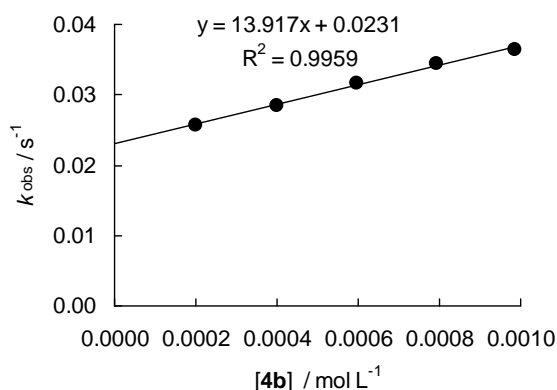
$$k_2(\text{OH}^-)^{[29]} = 48.5$$

$$\text{p}K_{\text{A}}(\mathbf{4b-H})^{[36]} = 9.99$$

$$k_2 = 5.57 \times 10^0 \text{ L mol}^{-1} \text{ s}^{-1}$$

Table 154: Kinetics of the reaction of **4b** with **1b** (20 °C, Conventional UV/Vis, at 613 nm).

[E] / mol L ⁻¹	[4b-H] ₀ / mol L ⁻¹	[KOH] ₀ / mol L ⁻¹	[4b] _{eff} / mol L ⁻¹	[KOH] _{eff} / mol L ⁻¹	[Nu]/[E]	<i>k</i> _{obs} / s ⁻¹	<i>k</i> _{OH⁻} / s ⁻¹	<i>k</i> _{eff} / s ⁻¹
1.60 × 10 ⁻⁵	3.15 × 10 ⁻³	2.07 × 10 ⁻⁴	2.00 × 10 ⁻⁴	6.64 × 10 ⁻⁶	12.5	2.66 × 10 ⁻²	8.70 × 10 ⁻⁴	2.57 × 10 ⁻²
1.60 × 10 ⁻⁵	3.15 × 10 ⁻³	4.13 × 10 ⁻⁴	3.99 × 10 ⁻⁴	1.42 × 10 ⁻⁵	24.9	3.04 × 10 ⁻²	1.86 × 10 ⁻³	2.85 × 10 ⁻²
1.60 × 10 ⁻⁵	3.15 × 10 ⁻³	6.20 × 10 ⁻⁴	5.97 × 10 ⁻⁴	2.29 × 10 ⁻⁵	37.3	3.47 × 10 ⁻²	2.99 × 10 ⁻³	3.17 × 10 ⁻²
1.60 × 10 ⁻⁵	3.15 × 10 ⁻³	8.26 × 10 ⁻⁴	7.93 × 10 ⁻⁴	3.29 × 10 ⁻⁵	49.6	3.87 × 10 ⁻²	4.31 × 10 ⁻³	3.44 × 10 ⁻²
1.60 × 10 ⁻⁵	3.15 × 10 ⁻³	1.03 × 10 ⁻³	9.86 × 10 ⁻⁴	4.45 × 10 ⁻⁵	61.6	4.23 × 10 ⁻²	5.83 × 10 ⁻³	3.65 × 10 ⁻²



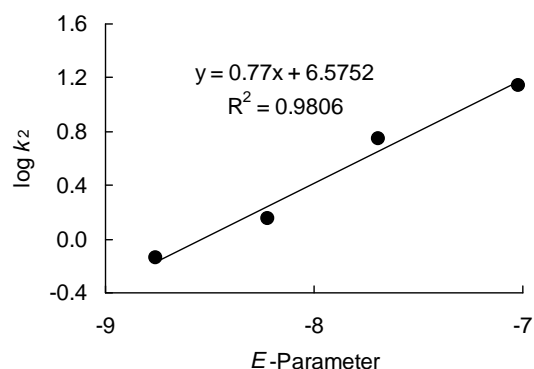
$$k_2(\text{OH}^-)^{[29]} = 131$$

$$\text{p}K_{\text{A}}(\mathbf{4b-H})^{[36]} = 9.99$$

$$k_2 = 1.39 \times 10^1 \text{ L mol}^{-1} \text{ s}^{-1}$$

Determination of Reactivity Parameters N and s for the 1-Methyluracile Anion (**4b**) in WaterTable 155: Rate Constants for the Reactions of **4b** with Different Electrophiles (20 °C).

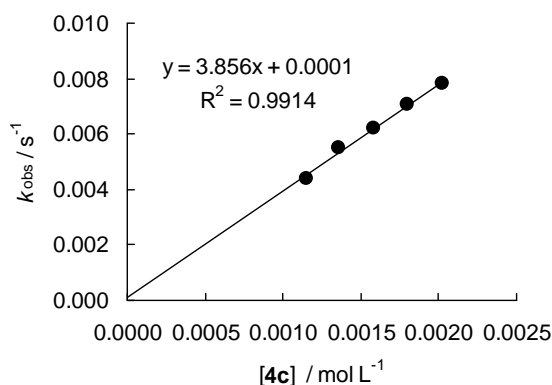
Electrophile	E	$k_2 / \text{L mol}^{-1} \text{s}^{-1}$	$\log k_2$
1e	-8.76	7.26×10^{-1}	-0.14
1d	-8.22	1.41×10^0	0.15
1c	-7.69	5.57×10^1	0.75
1b	-7.02	1.39×10^1	1.14



$$N = 8.54, s = 0.77$$

Reactions of the Potassium Salt of Thymine (**4c**)Table 156: Kinetics of the reaction of **4c** with **1g** (20 °C, Conventional UV/Vis, at 630 nm).

$[E] / \text{mol L}^{-1}$	$[4c]_0 / \text{mol L}^{-1}$	$[4c]_{\text{eff}} / \text{mol L}^{-1}$	$[\text{KOH}]_{\text{eff}} / \text{mol L}^{-1}$	$[\text{Nu}]/[E]$	$k_{\text{obs}} / \text{s}^{-1}$	$k_{\text{OH}^-} / \text{s}^{-1}$	$k_{\text{eff}} / \text{s}^{-1}$
2.54×10^{-5}	1.46×10^{-3}	1.15×10^{-3}	3.16×10^{-4}	45.3	5.07×10^{-3}	6.83×10^{-4}	4.39×10^{-3}
2.54×10^{-5}	1.71×10^{-3}	1.36×10^{-3}	3.44×10^{-4}	53.5	6.26×10^{-3}	7.43×10^{-4}	5.52×10^{-3}
2.54×10^{-5}	1.95×10^{-3}	1.58×10^{-3}	3.71×10^{-4}	62.2	7.00×10^{-3}	8.01×10^{-4}	6.20×10^{-3}
2.54×10^{-5}	2.20×10^{-3}	1.80×10^{-3}	3.96×10^{-4}	70.9	7.95×10^{-3}	8.55×10^{-4}	7.09×10^{-3}
2.54×10^{-5}	2.44×10^{-3}	2.02×10^{-3}	4.19×10^{-4}	79.5	8.71×10^{-3}	9.05×10^{-4}	7.80×10^{-3}



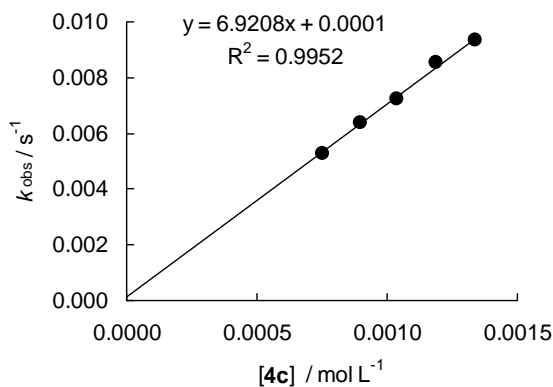
$$k_2(\text{OH}^-)^{[29]} = 2.16$$

$$\text{p}K_A(\mathbf{4c-H})^{[36]} = 9.94$$

$$k_2 = 3.86 \times 10^0 \text{ L mol}^{-1} \text{ s}^{-1}$$

Table 157: Kinetics of the reaction of **4c** with **1f** (20 °C, Conventional UV/Vis, at 635 nm).

$[E] / \text{mol L}^{-1}$	$[4c]_0 / \text{mol L}^{-1}$	$[4c]_{\text{eff}} / \text{mol L}^{-1}$	$[\text{KOH}]_{\text{eff}} / \text{mol L}^{-1}$	$[\text{Nu}]/[E]$	$k_{\text{obs}} / \text{s}^{-1}$	$k_{\text{OH}^-} / \text{s}^{-1}$	$k_{\text{eff}} / \text{s}^{-1}$
2.35×10^{-5}	1.01×10^{-3}	7.51×10^{-4}	2.56×10^{-4}	32.0	6.18×10^{-3}	8.81×10^{-4}	5.30×10^{-3}
2.35×10^{-5}	1.18×10^{-3}	8.96×10^{-4}	2.79×10^{-4}	38.1	7.36×10^{-3}	9.60×10^{-4}	6.40×10^{-3}
2.35×10^{-5}	1.34×10^{-3}	1.04×10^{-3}	3.01×10^{-4}	44.3	8.26×10^{-3}	1.04×10^{-3}	7.22×10^{-3}
2.35×10^{-5}	1.51×10^{-3}	1.19×10^{-3}	3.22×10^{-4}	50.6	9.64×10^{-3}	1.11×10^{-3}	8.53×10^{-3}
2.35×10^{-5}	1.68×10^{-3}	1.34×10^{-3}	3.41×10^{-4}	57.0	1.05×10^{-2}	1.17×10^{-3}	9.33×10^{-3}



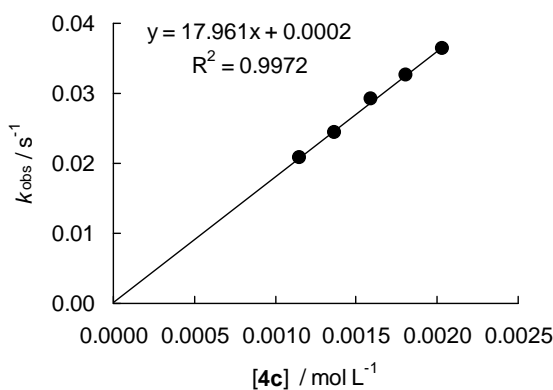
$$k_2(\text{OH}^-)^{[29]} = 3.44$$

$$\text{p}K_{\text{A}}(\mathbf{4c}\text{-H})^{[36]} = 9.94$$

$$k_2 = 6.92 \times 10^0 \text{ L mol}^{-1} \text{ s}^{-1}$$

Table 158: Kinetics of the reaction of **4c** with **1e** (20 °C, Conventional UV/Vis, at 627 nm).

$[\text{E}] / \text{mol L}^{-1}$	$[\mathbf{4c}]_0 / \text{mol L}^{-1}$	$[\mathbf{4c}]_{\text{eff}} / \text{mol L}^{-1}$	$[\text{KOH}]_{\text{eff}} / \text{mol L}^{-1}$	$[\text{Nu}]/[\text{E}]$	$k_{\text{obs}} / \text{s}^{-1}$	$k_{\text{OH}^-} / \text{s}^{-1}$	$k_{\text{eff}} / \text{s}^{-1}$
2.55×10^{-5}	1.47×10^{-3}	1.15×10^{-3}	3.17×10^{-4}	45.1	2.42×10^{-2}	3.42×10^{-3}	2.08×10^{-2}
2.55×10^{-5}	1.72×10^{-3}	1.37×10^{-3}	3.45×10^{-4}	53.7	2.82×10^{-2}	3.73×10^{-3}	2.45×10^{-2}
2.55×10^{-5}	1.96×10^{-3}	1.59×10^{-3}	3.72×10^{-4}	62.4	3.33×10^{-2}	4.02×10^{-3}	2.93×10^{-2}
2.55×10^{-5}	2.20×10^{-3}	1.81×10^{-3}	3.97×10^{-4}	71.0	3.69×10^{-2}	4.29×10^{-3}	3.26×10^{-2}
2.55×10^{-5}	2.45×10^{-3}	2.03×10^{-3}	4.20×10^{-4}	79.6	4.10×10^{-2}	4.54×10^{-3}	3.65×10^{-2}



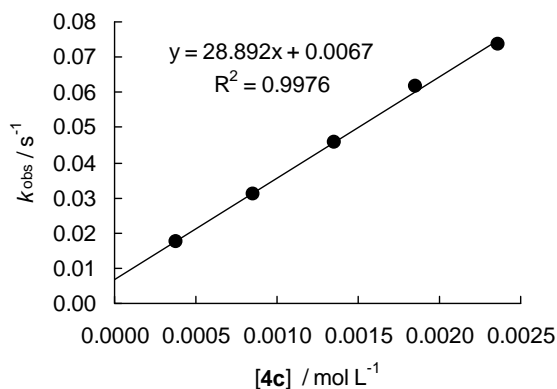
$$k_2(\text{OH}^-)^{[29]} = 10.8$$

$$\text{p}K_{\text{A}}(\mathbf{4c}\text{-H})^{[36]} = 9.94$$

$$k_2 = 1.80 \times 10^1 \text{ L mol}^{-1} \text{ s}^{-1}$$

Table 159: Kinetics of the reaction of **4c** with **1d** (20 °C, Conventional UV/Vis, at 618 nm).

$[\text{E}] / \text{mol L}^{-1}$	$[\mathbf{4c}]_0 / \text{mol L}^{-1}$	$[\mathbf{4c}]_{\text{eff}} / \text{mol L}^{-1}$	$[\text{KOH}]_{\text{eff}} / \text{mol L}^{-1}$	$[\text{Nu}]/[\text{E}]$	$k_{\text{obs}} / \text{s}^{-1}$	$k_{\text{OH}^-} / \text{s}^{-1}$	$k_{\text{eff}} / \text{s}^{-1}$
1.10×10^{-5}	5.62×10^{-4}	3.80×10^{-4}	1.82×10^{-4}	34.5	2.16×10^{-2}	4.28×10^{-3}	1.73×10^{-2}
1.10×10^{-5}	1.13×10^{-3}	8.57×10^{-4}	2.73×10^{-4}	77.9	3.76×10^{-2}	6.42×10^{-3}	3.12×10^{-2}
1.10×10^{-5}	1.69×10^{-3}	1.35×10^{-3}	3.43×10^{-4}	123	5.40×10^{-2}	8.06×10^{-3}	4.59×10^{-2}
1.10×10^{-5}	2.25×10^{-3}	1.85×10^{-3}	4.01×10^{-4}	168	7.13×10^{-2}	9.42×10^{-3}	6.19×10^{-2}
1.10×10^{-5}	2.81×10^{-3}	1.36×10^{-3}	4.53×10^{-4}	215	8.42×10^{-2}	1.06×10^{-2}	7.36×10^{-2}



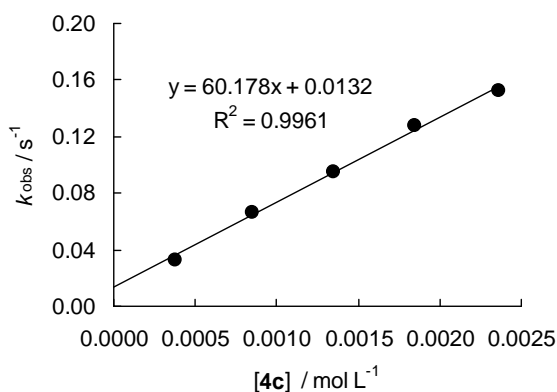
$$k_2(\text{OH}^-)^{[29]} = 23.5$$

$$\text{p}K_{\text{A}}(\mathbf{4c}\text{-H})^{[36]} = 9.94$$

$$k_2 = 2.89 \times 10^1 \text{ L mol}^{-1} \text{ s}^{-1}$$

Table 160: Kinetics of the reaction of **4c** with **1c** (20 °C, Conventional UV/Vis, at 620 nm).

[E] / mol L ⁻¹	[4c] ₀ / mol L ⁻¹	[4c] _{eff} / mol L ⁻¹	[KOH] _{eff} / mol L ⁻¹	[Nu]/[E]	<i>k</i> _{obs} / s ⁻¹	<i>k</i> _{OH⁻} / s ⁻¹	<i>k</i> _{eff} / s ⁻¹
1.07 × 10 ⁻⁵	5.62 × 10 ⁻⁴	3.80 × 10 ⁻⁴	1.82 × 10 ⁻⁴	35.5	4.19 × 10 ⁻²	8.83 × 10 ⁻³	3.31 × 10 ⁻²
1.07 × 10 ⁻⁵	1.13 × 10 ⁻³	8.48 × 10 ⁻⁴	2.72 × 10 ⁻⁴	79.3	7.98 × 10 ⁻²	1.32 × 10 ⁻²	6.66 × 10 ⁻²
1.07 × 10 ⁻⁵	1.69 × 10 ⁻³	1.35 × 10 ⁻³	3.43 × 10 ⁻⁴	126	1.12 × 10 ⁻¹	1.66 × 10 ⁻³	9.54 × 10 ⁻²
1.07 × 10 ⁻⁵	2.25 × 10 ⁻³	1.85 × 10 ⁻³	4.01 × 10 ⁻⁴	173	1.47 × 10 ⁻¹	1.94 × 10 ⁻²	1.28 × 10 ⁻¹
1.07 × 10 ⁻⁵	2.81 × 10 ⁻³	2.36 × 10 ⁻³	4.53 × 10 ⁻⁴	221	1.74 × 10 ⁻¹	2.20 × 10 ⁻²	1.52 × 10 ⁻¹



$$k_2(\text{OH}^-)^{[29]} = 48.5$$

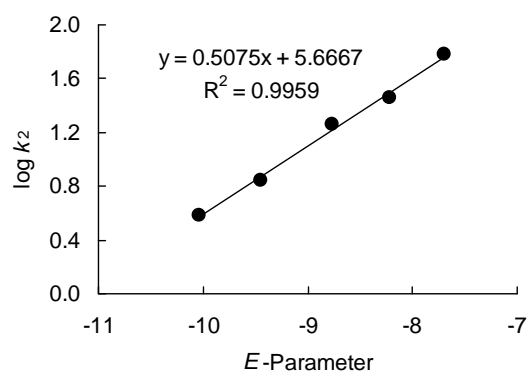
$$\text{p}K_{\text{A}}(\mathbf{4c}\text{-H})^{[36]} = 9.94$$

$$k_2 = 6.02 \times 10^1 \text{ L mol}^{-1} \text{ s}^{-1}$$

Determination of Reactivity Parameters *N* and *s* for Thymine Anion (**4c**) in Water

Table 161: Rate Constants for the Reactions of **4c** with Different Electrophiles (20 °C).

Electrophile	<i>E</i>	<i>k</i> ₂ / L mol ⁻¹ s ⁻¹	log <i>k</i> ₂
1g	-10.04	3.86 × 10 ⁰	0.59
1f	-9.45	6.92 × 10 ⁰	0.84
1e	-8.76	1.80 × 10 ¹	1.26
1d	-8.22	2.89 × 10 ¹	1.46
1c	-7.69	6.02 × 10 ¹	1.78



$$N = 11.17, s = 0.51$$

4.6 Solvent Effects in DMSO/Water Mixtures

General

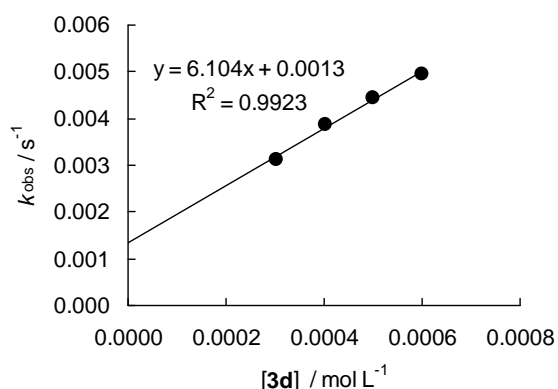
The influence of the solvent composition (DMSO/water mixtures) on the second-order rate constant k_2 of the reaction of the anion of theophylline **3d** with **1e** was additionally studied by UV/Vis-spectroscopy. As the pK_{aH} values for **3d** are not known in every solvent mixture, it was not possible to consider the contribution of hydroxide in this series. However, as shown above, the contribution of hydroxide to the observed rate constant is usually less than 10 % which justifies that approach.

Water/DMSO 97:3 (v/v)

Table 162: Kinetics of the reaction of **3d** with **1e** (20 °C, Conventional UV/Vis, at 627 nm).

[E] / mol L ⁻¹	[3d] / mol L ⁻¹	[3d]/[E]	k_{obs} / s ⁻¹
2.36×10^{-5}	3.02×10^{-4}	12.8	3.12×10^{-3}
2.36×10^{-5}	4.02×10^{-4}	17.0	3.87×10^{-3}
2.36×10^{-5}	5.01×10^{-4}	21.2	4.44×10^{-3}
2.36×10^{-5}	6.00×10^{-4}	25.4	4.95×10^{-3}

$$k_2 = 6.10 \times 10^0 \text{ L mol}^{-1} \text{ s}^{-1}$$

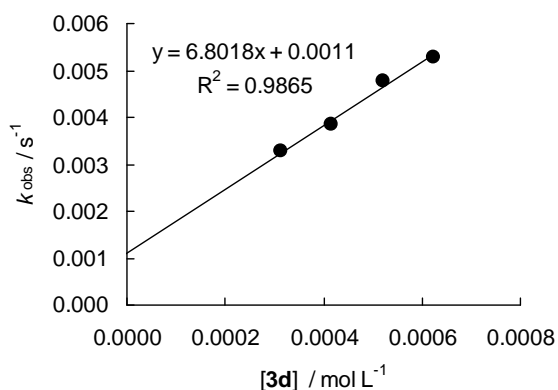


Water/DMSO 95:5 (v/v)

Table 163: Kinetics of the reaction of **3d** with **1e** (20 °C, Conventional UV/Vis, at 627 nm).

[E] / mol L ⁻¹	[3d] / mol L ⁻¹	[3d]/[E]	k_{obs} / s ⁻¹
2.40×10^{-5}	3.14×10^{-4}	13.1	3.27×10^{-3}
2.40×10^{-5}	4.17×10^{-4}	17.4	3.84×10^{-3}
2.40×10^{-5}	5.21×10^{-4}	21.7	4.79×10^{-3}
2.40×10^{-5}	6.23×10^{-4}	26.0	5.29×10^{-3}

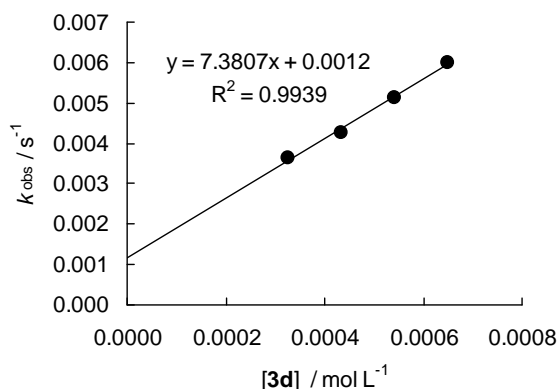
$$k_2 = 6.80 \times 10^0 \text{ L mol}^{-1} \text{ s}^{-1}$$



Water/DMSO 93:7 (v/v)Table 164: Kinetics of the reaction of **3d** with **1e** (20 °C, Conventional UV/Vis, at 627 nm).

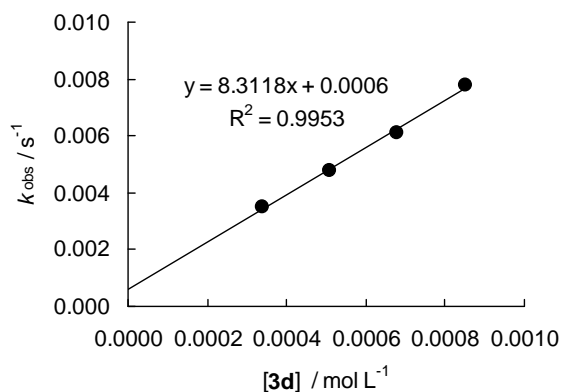
[E] / mol L ⁻¹	[3d] / mol L ⁻¹	[3d]/[E]	$k_{\text{obs}} / \text{s}^{-1}$
2.46×10^{-5}	3.26×10^{-4}	13.3	3.65×10^{-3}
2.46×10^{-5}	4.34×10^{-4}	17.6	4.27×10^{-3}
2.46×10^{-5}	5.42×10^{-4}	22.0	5.14×10^{-3}
2.46×10^{-5}	6.49×10^{-4}	26.4	6.01×10^{-3}

$$k_2 = 7.38 \times 10^0 \text{ L mol}^{-1} \text{ s}^{-1}$$

**Water/DMSO 90:10 (v/v)**Table 165: Kinetics of the reaction of **3d** with **1e** (20 °C, Conventional UV/Vis, at 627 nm).

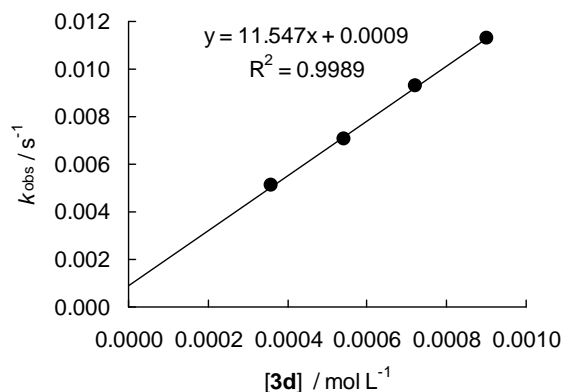
[E] / mol L ⁻¹	[3d] / mol L ⁻¹	[3d]/[E]	$k_{\text{obs}} / \text{s}^{-1}$
2.64×10^{-5}	3.40×10^{-4}	12.9	3.52×10^{-3}
2.64×10^{-5}	5.10×10^{-4}	19.3	4.79×10^{-3}
2.64×10^{-5}	6.80×10^{-4}	25.8	6.11×10^{-3}
2.64×10^{-5}	8.50×10^{-4}	32.2	7.79×10^{-3}

$$k_2 = 8.31 \times 10^0 \text{ L mol}^{-1} \text{ s}^{-1}$$

**Water/DMSO 80:20 (v/v)**Table 166: Kinetics of the reaction of **3d** with **1e** (20 °C, Conventional UV/Vis, at 627 nm).

[E] / mol L ⁻¹	[3d] / mol L ⁻¹	[3d]/[E]	$k_{\text{obs}} / \text{s}^{-1}$
2.80×10^{-5}	3.60×10^{-4}	12.9	5.12×10^{-3}
2.80×10^{-5}	5.41×10^{-4}	19.3	7.03×10^{-3}
2.80×10^{-5}	7.21×10^{-4}	25.8	9.31×10^{-3}
2.80×10^{-5}	9.01×10^{-4}	32.2	1.13×10^{-2}

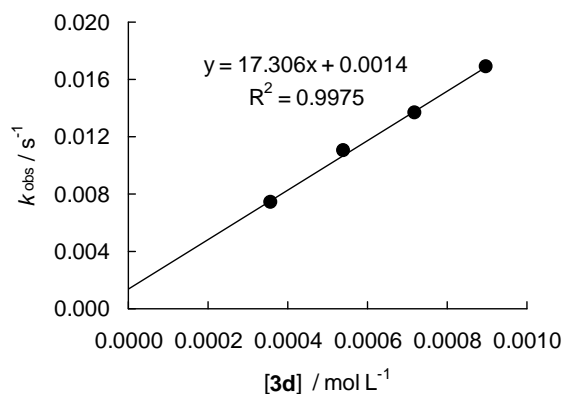
$$k_2 = 1.15 \times 10^1 \text{ L mol}^{-1} \text{ s}^{-1}$$



Water/DMSO 70:30 (v/v)Table 167: Kinetics of the reaction of **3d** with **1e** (20 °C, Conventional UV/Vis, at 627 nm).

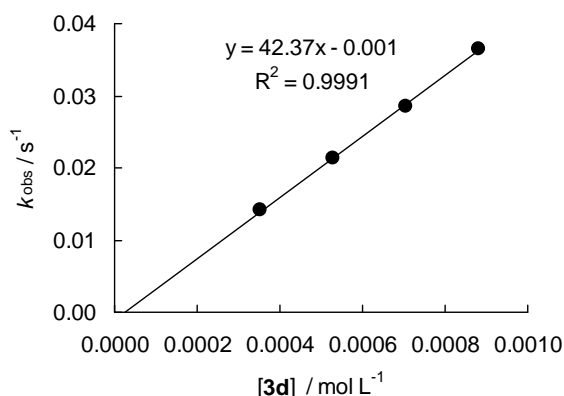
[E] / mol L ⁻¹	[3d] / mol L ⁻¹	[3d]/[E]	$k_{\text{obs}} / \text{s}^{-1}$
2.63×10^{-5}	3.59×10^{-4}	13.7	7.44×10^{-3}
2.63×10^{-5}	5.39×10^{-4}	20.5	1.10×10^{-2}
2.63×10^{-5}	7.18×10^{-4}	27.3	1.37×10^{-2}
2.63×10^{-5}	8.98×10^{-4}	34.1	1.69×10^{-2}

$$k_2 = 1.17 \times 10^1 \text{ L mol}^{-1} \text{ s}^{-1}$$

**Water/DMSO 60:40 (v/v)**Table 168: Kinetics of the reaction of **3d** with **1e** (20 °C, Conventional UV/Vis, at 627 nm).

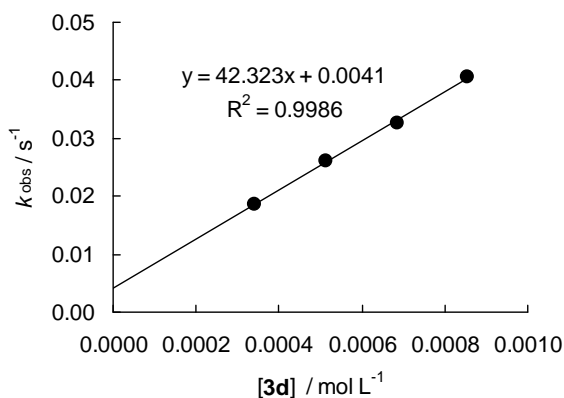
[E] / mol L ⁻¹	[3d] / mol L ⁻¹	[3d]/[E]	$k_{\text{obs}} / \text{s}^{-1}$
2.58×10^{-5}	3.52×10^{-4}	13.6	1.41×10^{-2}
2.58×10^{-5}	5.29×10^{-4}	20.5	2.13×10^{-2}
2.58×10^{-5}	7.05×10^{-4}	27.3	2.85×10^{-2}
2.58×10^{-5}	8.81×10^{-4}	34.1	3.66×10^{-2}

$$k_2 = 4.24 \times 10^1 \text{ L mol}^{-1} \text{ s}^{-1}$$

**Water/DMSO 50:50 (v/v)**Table 169: Kinetics of the reaction of **3d** with **1e** (20 °C, Conventional UV/Vis, at 627 nm).

[E] / mol L ⁻¹	[3d] / mol L ⁻¹	[3d]/[E]	$k_{\text{obs}} / \text{s}^{-1}$
2.51×10^{-5}	3.42×10^{-4}	13.6	1.86×10^{-2}
2.51×10^{-5}	5.14×10^{-4}	20.5	2.61×10^{-2}
2.51×10^{-5}	6.85×10^{-4}	27.3	3.26×10^{-2}
2.51×10^{-5}	8.56×10^{-4}	34.1	4.06×10^{-2}

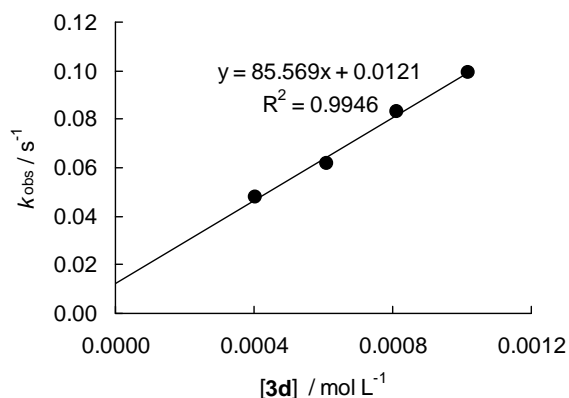
$$k_2 = 4.23 \times 10^1 \text{ L mol}^{-1} \text{ s}^{-1}$$



Water/DMSO 40:60 (v/v)Table 170: Kinetics of the reaction of **3d** with **1e** (20 °C, Conventional UV/Vis, at 627 nm).

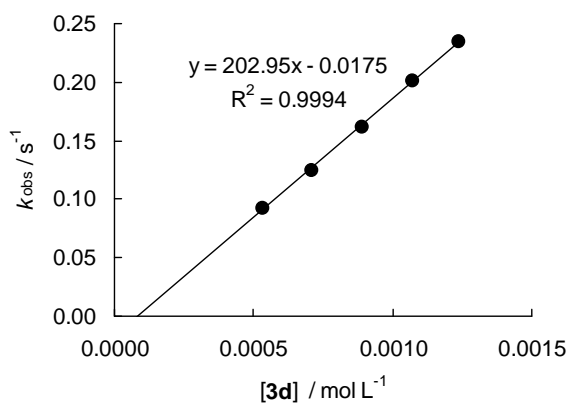
[E] / mol L ⁻¹	[3d] / mol L ⁻¹	[3d]/[E]	$k_{\text{obs}} / \text{s}^{-1}$
2.52×10^{-5}	4.06×10^{-4}	16.1	4.79×10^{-2}
2.52×10^{-5}	6.09×10^{-4}	24.2	6.20×10^{-2}
2.52×10^{-5}	8.12×10^{-4}	32.2	8.31×10^{-2}
2.52×10^{-5}	1.02×10^{-3}	40.5	9.92×10^{-2}

$$k_2 = 8.56 \times 10^1 \text{ L mol}^{-1} \text{ s}^{-1}$$

**Water/DMSO 30:70 (v/v)**Table 171: Kinetics of the reaction of **3d** with **1e** (20 °C, stopped-flow, at 627 nm).

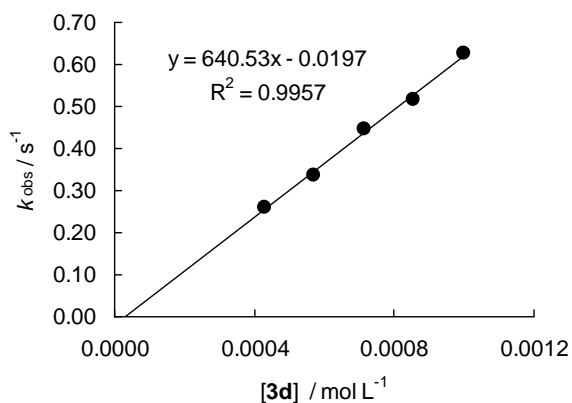
[E] / mol L ⁻¹	[3d] / mol L ⁻¹	[3d]/[E]	$k_{\text{obs}} / \text{s}^{-1}$
4.01×10^{-5}	5.33×10^{-4}	13.3	9.21×10^{-2}
4.01×10^{-5}	7.11×10^{-4}	17.7	1.25×10^{-1}
4.01×10^{-5}	8.89×10^{-4}	22.2	1.62×10^{-1}
4.01×10^{-5}	1.07×10^{-3}	26.7	2.01×10^{-1}
4.01×10^{-5}	1.24×10^{-3}	30.9	2.34×10^{-1}

$$k_2 = 2.03 \times 10^2 \text{ L mol}^{-1} \text{ s}^{-1}$$

**Water/DMSO 20:80 (v/v)**Table 172: Kinetics of the reaction of **3d** with **1e** (20 °C, stopped-flow, at 627 nm).

[E] / mol L ⁻¹	[3d] / mol L ⁻¹	[3d]/[E]	$k_{\text{obs}} / \text{s}^{-1}$
3.78×10^{-5}	4.28×10^{-4}	11.3	2.60×10^{-1}
3.78×10^{-5}	5.71×10^{-4}	15.1	3.37×10^{-1}
3.78×10^{-5}	7.14×10^{-4}	18.9	4.46×10^{-1}
3.78×10^{-5}	8.56×10^{-4}	22.6	5.17×10^{-1}
3.78×10^{-5}	9.99×10^{-4}	26.4	6.27×10^{-1}

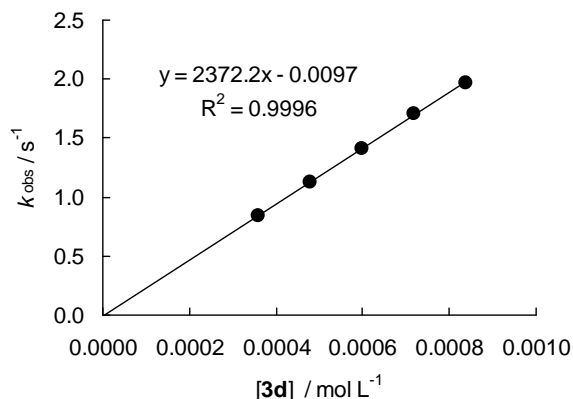
$$k_2 = 6.41 \times 10^2 \text{ L mol}^{-1} \text{ s}^{-1}$$



Water/DMSO 10:90 (v/v)Table 173: Kinetics of the reaction of **3d** with **1e** (20 °C, stopped-flow, at 627 nm).

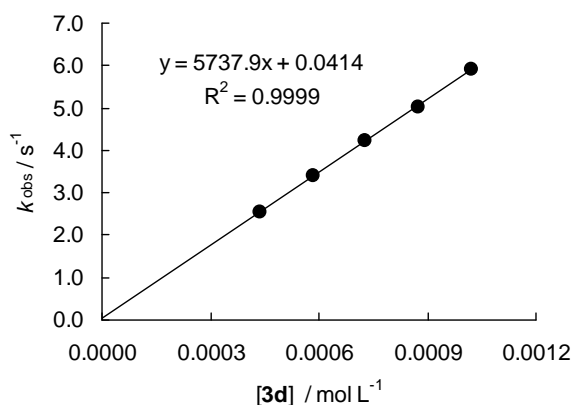
[E] / mol L ⁻¹	[3d] / mol L ⁻¹	[3d]/[E]	$k_{\text{obs}} / \text{s}^{-1}$
3.65×10^{-5}	3.60×10^{-4}	9.9	8.39×10^{-1}
3.65×10^{-5}	4.79×10^{-4}	13.1	1.13×10^0
3.65×10^{-5}	5.99×10^{-4}	16.4	1.41×10^0
3.65×10^{-5}	7.19×10^{-4}	19.7	1.71×10^0
3.65×10^{-5}	8.39×10^{-4}	23.0	1.97×10^0

$$k_2 = 2.37 \times 10^3 \text{ L mol}^{-1} \text{ s}^{-1}$$

**Water/DMSO 5:95 (v/v)**Table 174: Kinetics of the reaction of **3d** with **1e** (20 °C, stopped-flow, at 627 nm).

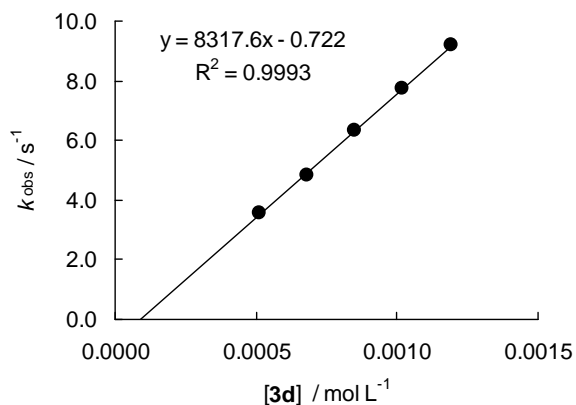
[E] / mol L ⁻¹	[3d] / mol L ⁻¹	[3d]/[E]	$k_{\text{obs}} / \text{s}^{-1}$
3.19×10^{-5}	4.37×10^{-4}	13.7	2.55×10^0
3.19×10^{-5}	5.83×10^{-4}	18.3	3.39×10^0
3.19×10^{-5}	7.29×10^{-4}	22.9	4.23×10^0
3.19×10^{-5}	8.74×10^{-4}	27.4	5.03×10^0
3.19×10^{-5}	1.02×10^{-3}	32.0	5.91×10^0

$$k_2 = 5.74 \times 10^3 \text{ L mol}^{-1} \text{ s}^{-1}$$

**Water/DMSO 3:97 (v/v)**Table 175: Kinetics of the reaction of **3d** with **1e** (20 °C, stopped-flow, at 627 nm).

[E] / mol L ⁻¹	[3d] / mol L ⁻¹	[3d]/[E]	$k_{\text{obs}} / \text{s}^{-1}$
3.95×10^{-5}	5.10×10^{-4}	12.9	3.59×10^0
3.95×10^{-5}	6.80×10^{-4}	17.2	4.84×10^0
3.95×10^{-5}	8.50×10^{-4}	21.5	6.35×10^0
3.95×10^{-5}	1.02×10^{-3}	25.8	7.76×10^0
3.95×10^{-5}	1.19×10^{-3}	30.1	9.20×10^0

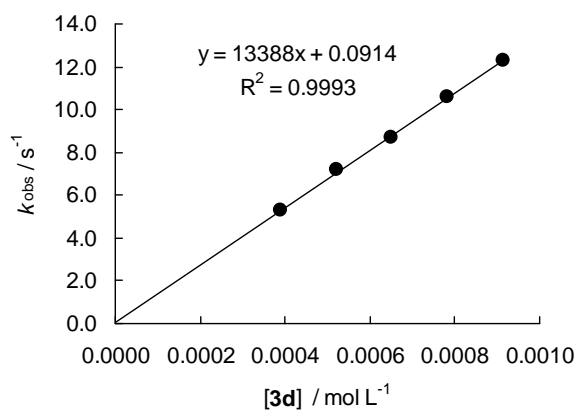
$$k_2 = 8.32 \times 10^3 \text{ L mol}^{-1} \text{ s}^{-1}$$



Water/DMSO 0:100 (v/v)Table 176: Kinetics of the reaction of **3d** with **1e** (20 °C, stopped-flow, at 627 nm).

[E] / mol L ⁻¹	[3d] / mol L ⁻¹	[3d]/[E]	$k_{\text{obs}} / \text{s}^{-1}$
3.30×10^{-5}	3.91×10^{-4}	11.8	5.28
3.30×10^{-5}	5.21×10^{-4}	15.8	7.17
3.30×10^{-5}	6.50×10^{-4}	19.7	8.71
3.30×10^{-5}	7.82×10^{-4}	23.7	10.6
3.30×10^{-5}	9.13×10^{-4}	27.7	12.3

$$k_2 = 1.34 \times 10^4 \text{ L mol}^{-1} \text{ s}^{-1}$$



5 References

- [1] a) M. R. Grimmett, *Compr. Org. Chem.* **1979**, *4*, 357–410; b) M. R. Grimmett, *Adv. Heterocycl. Chem.* **1980**, *27*, 241–326; c) A. F. Pozharskii, A. D. Garnovskii, A. M. Simonov, *Russ. Chem. Rev.* **1966**, *35*, 261–302; d) A. F. Požarskij, A. T. Soldatenkov, A. R. Katritzky, *Heterocycles in Life and Society*, Wiley, Chichester, **1997**; e) A. R. Katritzky, A. F. Pozharskii, *Handbook of Heterocyclic Chemistry*, Pergamon, Oxford, **2000**; f) A. R. Katritzky, X. Lan, J. Z. Yang, O. V. Denisko, *Chem. Rev.* **1998**, *98*, 409–548.
- [2] F. Schneider, *Angew. Chem.* **1978**, *90*, 616–625; *Angew. Chem. Int. Ed. Engl.* **1978**, *17*, 583–592.
- [3] H. A. Staab, *Angew. Chem.* **1962**, *74*, 407–423; H. A. Staab, *Angew. Chem. Int. Ed. Engl.* **1962**, *1*, 351–367.
- [4] a) A. Grimison, J. H. Ridd, B. V. Smith, *J. Chem. Soc.* **1960**, 1352–1356; b) A. Grimison, J. H. Ridd, B. V. Smith, *J. Chem. Soc.* **1960**, 1357–1362; c) J. H. Ridd, B. V. Smith, *J. Chem. Soc.* **1960**, 1363–1369.
- [5] M. W. Miller, H. L. Howes, R. V. Kasubick, A. R. English, *J. Med. Chem.* **1970**, *13*, 849–852.
- [6] a) F. Terrier, F. Debleds, J. C. Halle, M. P. Simonnin, *Tetrahedron Lett.* **1982**, *23*, 4079–4082; b) M. P. Simonnin, J. C. Halle, F. Terrier, M. J. Pouet, *Can. J. Chem.* **1985**, *63*, 866–870.
- [7] a) W. F. Veldhuyzen, Y.-F. Lam, S. E. Rokita, *Chem. Res. Toxicol.* **2001**, *14*, 1345–1351; b) W. F. Veldhuyzen, A. J. Shallop, R. A. Jones, S. E. Rokita, *J. Am. Chem. Soc.* **2001**, *123*, 11126–11132; c) E. E. Weinert, K. N. Frankenfield, S. E. Rokita, *Chem. Res. Toxicol.* **2005**, *18*, 1364–1370; d) E. E. Weinert, R. Dondi, S. Colloredo-Melz, K. N. Frankenfield, C. H. Mitchell, M. Freccero, S. E. Rokita, *J. Am. Chem. Soc.* **2006**, *128*, 11940–11947; e) M. Freccero, R. Gandolfi, M. Sarzi-Amade, *J. Org. Chem.* **2003**, *68*, 6411–6423.
- [8] J. C. Martin, D. F. Smee, J. P. H. Verheyden, *J. Org. Chem.* **1985**, *50*, 755–759.
- [9] R. V. Joshi, J. Zemlicka, *Tetrahedron* **1993**, *49*, 2353–2360.
- [10] S. Boncel, A. Gondela, K. Walczak, *Synthesis* **2010**, *2010*, 1573–1589.
- [11] A. Copik, J. Suwinski, K. Walczak, J. Bronikowska, Z. Czuba, W. Krol, *Nucleosides, Nucleotides Nucleic Acids* **2002**, *21*, 377–383.

- [12] O. D. Gupta, B. Twamley, R. L. Kirchmeier, J. n. M. Shreeve, *J. Flourine Chem.* **2000**, *106*, 199–204.
- [13] D. E. Jane, K. Hoo, R. Kamboj, M. Deverill, D. Bleakman, A. Mandelzys, *J. Med. Chem.* **1997**, *40*, 3645–3650.
- [14] H. J. Cleaves, II, *Astrobiology* **2002**, *2*, 403–415.
- [15] E. Wittenburg, *Chem. Ber.* **1966**, *99*, 2391–2398.
- [16] S. Ganguly, K. K. Kundu, *Can. J. Chem.* **1994**, *72*, 1120–1126.
- [17] a) A. Gambacorta, M. E. Farah, D. Tofani, *Tetrahedron* **1999**, *55*, 12615–12628; b) A. Gambacorta, D. Tofani, M. A. Loreto, T. Gasperi, R. Bernini, *Tetrahedron* **2006**, *62*, 6848–6854.
- [18] a) R. G. Pearson, *J. Am. Chem. Soc.* **1963**, *85*, 3533–3539; b) R. G. Pearson, *Science* **1966**, *151*, 172–177; c) R. G. Pearson, J. Songstad, *J. Am. Chem. Soc.* **1967**, *89*, 1827–1836.
- [19] a) G. Klopman, *J. Am. Chem. Soc.* **1968**, *90*, 223–234; b) L. Salem, *J. Am. Chem. Soc.* **1968**, *90*, 543–552.
- [20] M. Breugst, T. Tokuyasu, H. Mayr, *J. Org. Chem.* **2010**, *75*, 5250–5258.
- [21] a) H. Mayr, T. Bug, M. F. Gotta, N. Hering, B. Irrgang, B. Janker, B. Kempf, R. Loos, A. R. Ofial, G. Remennikov, H. Schimmel, *J. Am. Chem. Soc.* **2001**, *123*, 9500–9512; b) R. Lucius, R. Loos, H. Mayr, *Angew. Chem.* **2002**, *114*, 97–102; *Angew. Chem. Int. Ed.* **2002**, *41*, 91–95; c) H. Mayr, B. Kempf, A. R. Ofial, *Acc. Chem. Res.* **2003**, *36*, 66–77; d) H. Mayr, A. R. Ofial, *Pure Appl. Chem.* **2005**, *77*, 1807–1821; e) For a comprehensive listing of nucleophilicity parameters *N* and electrophilicity parameters *E*, see <http://www.cup.uni-muenchen.de/oc/mayr/DBintro.html>; f) D. Richter, N. Hampel, T. Singer, A. R. Ofial, H. Mayr, *Eur. J. Org. Chem.* **2009**, 3203–3211.
- [22] H. Mayr, M. Patz, *Angew. Chem.* **1994**, *106*, 990–1010; *Angew. Chem. Int. Ed. Engl.* **1994**, *33*, 938–957.
- [23] M. Baidya, F. Brotzel, H. Mayr, *Org. Biomol. Chem.* **2010**, *8*, 1929–1935.
- [24] S. Hoz, H. Basch, J. L. Wolk, T. Hoz, E. Rozental, *J. Am. Chem. Soc.* **1999**, *121*, 7724–7725.
- [25] B. C. Challis, J. Challis, in *The Chemistry of Amides* (Ed.: J. Zabicky), Interscience Publisher, London, **1970**, pp. 731–858.
- [26] D. Döpp, H. Döpp, in *Methoden der organischen Chemie (Houben-Weyl)*, Thieme, Stuttgart, **1985**.

- [27] a) T. H. Koch, R. J. Sluski, R. H. Moseley, *J. Am. Chem. Soc.* **1973**, *95*, 3957–3963;
b) D. R. Anderson, J. S. Keute, T. H. Koch, R. H. Moseley, *J. Am. Chem. Soc.* **1977**, *99*, 6332–6340.
- [28] W. N. Olmstead, Z. Margolin, F. G. Bordwell, *J. Org. Chem.* **1980**, *45*, 3295–3299.
- [29] S. Minegishi, H. Mayr, *J. Am. Chem. Soc.* **2003**, *125*, 286–295.
- [30] S. Minegishi, S. Kobayashi, H. Mayr, *J. Am. Chem. Soc.* **2004**, *126*, 5174–5181.
- [31] T. C. Bruice, G. L. Schmir, *J. Am. Chem. Soc.* **1958**, *80*, 148–156.
- [32] W. Pfeleiderer, *Liebigs Ann. Chem.* **1961**, *647*, 167–173.
- [33] M. G. Elliott, R. E. Shepherd, *Inorg. Chem.* **1987**, *26*, 2067–2073.
- [34] A. Albert, *Biochem. J.* **1953**, *54*, 646–654.
- [35] A. Albert, R. J. Goldacre, J. Phillips, *J. Chem. Soc.* **1948**, 2240–2249.
- [36] P. A. Levene, L. W. Bass, H. S. Simms, *J. Biol. Chem.* **1926**, *70*, 229–241.
- [37] A. Albert, D. J. Brown, *J. Chem. Soc.* **1954**, 2060–2071.
- [38] G. Volgyi, R. Ruiz, K. Box, J. Comer, E. Bosch, K. Takacs-Novak, *Anal. Chim. Acta* **2007**, *583*, 418–428.
- [39] H. F. W. Taylor, *J. Chem. Soc.* **1948**, 765–766.
- [40] H. A. Azab, Z. M. Anwar, M. Sokar, *J. Chem. Eng. Data* **2004**, *49*, 256–261.
- [41] F. G. Bordwell, *Acc. Chem. Res.* **1988**, *21*, 456–463.
- [42] M. I. Terekhova, E. S. Petrov, E. M. Rokhlina, D. N. Kravtsov, A. I. Shatenshtein, *Khim. Geterotsykl. Soedin.* **1979**, 1104–1108.
- [43] H. E. Gottlieb, V. Kotlyar, A. Nudelman, *J. Org. Chem.* **1997**, *62*, 7512–7515.
- [44] E. Anders, J. G. Tropsch, A. R. Katritzky, D. Rasala, J. J. Vanden Eynde, *J. Org. Chem.* **1989**, *54*, 4808–4812.
- [45] W. Micklitz, B. Lippert, H. Schoellhorn, U. Thewalt, *J. Heterocycl. Chem.* **1989**, *26*, 1499–1500.

Chapter 7: A Farewell to the HSAB Treatment of Ambident Reactivity

Herbert Mayr, Martin Breugst, and Armin R. Ofial

Angew. Chem. **2010**, accepted, DOI: 10.1002/anie.201007100.

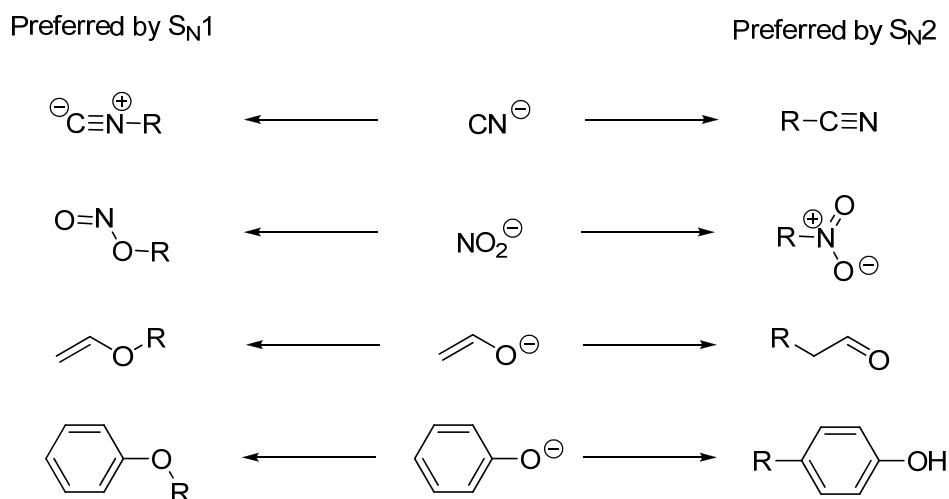
1 Introduction

Understanding and controlling ambident^{[1]*} reactivity is of eminent importance for a rational design of organic syntheses. Kornblum summarized his systematic investigations on the alkylations of ambident anions^[2] by the statement “*The greater the S_N1 character of the transition state the greater is the preference for covalency formation with the atom of higher electronegativity and, controversially, the greater the S_N2 contribution to the transition state the greater the preference for bond formation to the atom of lower electronegativity*”.^[2e]

These ideas were generalized within Pearson’s concept of hard and soft acids and bases (HSAB),^[3] which still represents the most popular rationalization of ambident reactivity, as illustrated by a quotation from the latest edition of March’s *Advanced Organic Chemistry* (Scheme 1).^[4]

„The principle of hard and soft acids and bases states that hard acids prefer hard bases and soft acids prefer soft bases. In an S_N1 mechanism, the nucleophile attacks a carbocation, which is a hard acid. In an S_N2 mechanism, the nucleophile attacks the carbon atom of a molecule, which is a softer acid. The more electronegative atom of an ambident nucleophile is a harder base than the less electronegative atom. We may thus make the statement: As the character of a given reaction changes from S_N1 - to S_N2 -like, an ambident nucleophile becomes more likely to attack with its less electronegative atom. Therefore, changing from S_N1 to S_N2 conditions should favor C attack by CN^- , N attack by NO_2^- , C attack by enolate or phenoxide ions, etc.“

* According to IUPAC^[1] an ambident system possesses two alternative and strongly interacting distinguishable reactive centers which both can undergo a certain reaction, but the reaction at either site stops or greatly retards subsequent attack at the second site.

Scheme 1: Preferred reaction pathways of ambident nucleophiles according to March (ref^[4]).

The Klopman-Salem concept of charge and orbital control of organic reactions uses similar ideas: Hard-hard interactions are charge-controlled and soft-soft interactions are orbital-controlled.^[5] Although these concepts have widely been accepted, they have also been criticized. Gompper and Wagner^[6] pointed out that the HSAB concept does not differentiate between kinetic and thermodynamic control though in many cases different conditions give rise to different products.^[7] Numerous reactions of ambident electrophiles which yield different products under conditions of kinetic and thermodynamic control have been reviewed by Hünig.^[8] Wagner and Gompper furthermore noted that the decision whether a certain reaction is dominated by charge or orbital control is often made a posteriori, i.e., after knowing the experimental facts, with the consequence that it has little predictive value. Drago summarized his criticism of the HSAB principle as follows: “*This can’t miss approach sweeps a lot of interesting chemistry under the rug and leads one to believe he has understanding when in reality he may not*”.^[9]

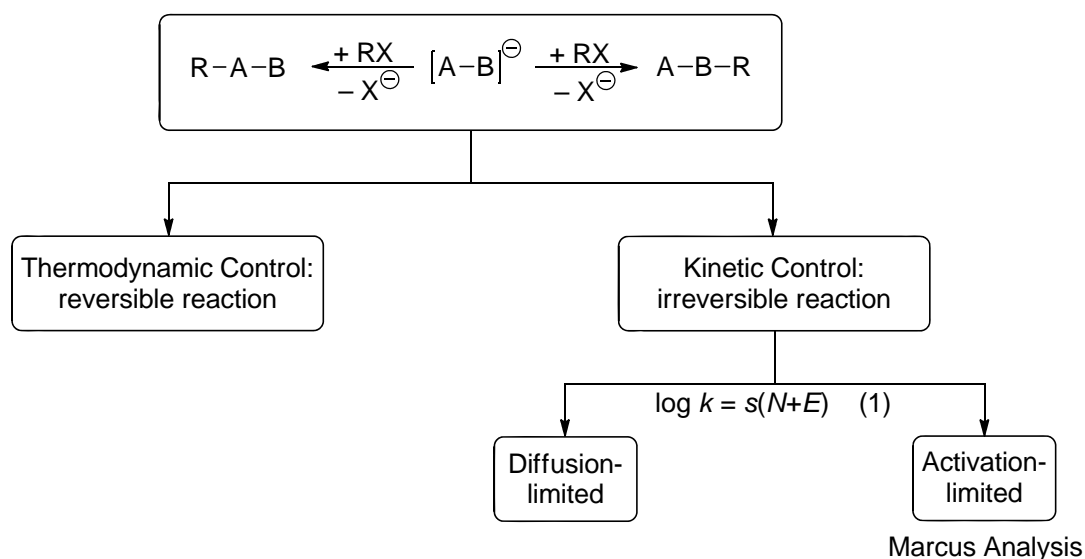
During recent years, we have extensively studied the kinetics of the reactions of benzhydrylium ions and structurally related quinone methides with a large variety of nucleophiles,^[10] including hard and soft ones. While the hardness of the electrophiles shown in Figure 1 increases significantly from left to right,^[11] one does not find that the correlation lines for hard nucleophiles are generally steeper than those for soft nucleophiles, which should be the case if hard nucleophiles had a particular preference to react with hard electrophiles.

Sensitized by these observations, we have analyzed literature reports on the regioselectivities of these and other ambident nucleophiles and electrophiles and we have realized that the number of cases where the HSAB principle and the concept of charge- and orbital-controlled reactions give correct predictions approximate the number of cases where they fail. For that reason, we suggest abandoning these concepts as guides for predicting ambident reactivity. In the following we will present an alternative approach to rationalize the behavior of ambident nucleophiles.

2 Systematic Analysis of Ambident Reactivity

2.1 General Procedure

As illustrated in Scheme 2, the first step of a systematic analysis is the clarification whether the isolated products are the results of thermodynamic or kinetic control. Methods to differentiate between kinetic and thermodynamic control are well-known and need not to be discussed in this context.^[4] An overview of relative product stabilities obtained for important ambident nucleophiles is given in Section 2.2. If the product ratio is kinetically controlled, one should analyze whether the product-determining step is diffusion-controlled ($k_2 = 10^9 - 10^{10} \text{ L mol}^{-1} \text{ s}^{-1}$) or activation-controlled ($k_2 < 10^9 \text{ L mol}^{-1} \text{ s}^{-1}$). This differentiation can be based on the correlation Equation (1) introduced in Section 2.3. If the product-determining step is activation-controlled, Marcus theory can be employed to predict relative activation energies as described in the Sections 2.4–2.6.



Scheme 2: A systematic approach to ambident reactivity.

2.2 Product Stabilities

Relative thermodynamic stabilities are usually determined by calorimetric measurements, equilibrium studies or by quantum chemical calculations. In order to use the same basis for comparing the thermodynamic stabilities of products which may be generated by alkylation of ambident nucleophiles, we have calculated the Gibbs energy of methyl migration at MP2/6-311+G(2d,p) level of theory (Table 1). A detailed discussion of the thermodynamic stabilities will be presented later in the individual sections for the different substrates.

2.3 Differentiation between Activation- and Diffusion-Controlled Reactions

The rates of bimolecular reactions in solution are limited by diffusion, i.e., the time needed by two reactant molecules to meet in an encounter complex. Sophisticated theories have been developed to calculate diffusion rate constants which consider the size of the molecules, the viscosity of the reaction medium, and the temperature.^[14] Since knowledge of the precise values of diffusion-controlled rate constants is not needed for our analysis, we derive rough estimates for the magnitude of diffusion-controlled rate constants from the upper limits of directly measured rate constants in various reaction series. Thus, the second-order rate constants for the reactions of laser-flash photolytically generated benzhydrylium and tritylium ions with neutral nucleophiles in common organic solvents (CH₂Cl₂, CH₃CN) or water never exceeded $4 \times 10^9 \text{ L mol}^{-1} \text{ s}^{-1}$. The upper limit for cation-anion combinations was $2 \times 10^{10} \text{ L mol}^{-1} \text{ s}^{-1}$ in acetonitrile and $\sim 5 \times 10^9 \text{ L mol}^{-1} \text{ s}^{-1}$ in water.^[15] Intermolecular selectivities are consistent with these numbers.^[16]

As reactions which proceed with such rates do not have activation energies, the corresponding regioselectivities (as well as stereoselectivities) cannot be derived from transition state models.

In numerous publications we have shown that the second-order rate constants for the reactions of carbocations and Michael acceptors with *n*-nucleophiles (alcohols, amines, etc.), π -nucleophiles (alkenes, arenes, etc.), and σ -nucleophiles (hydrides) can be calculated by Eq. (1), where nucleophiles are characterized by two parameters (nucleophilicity *N*, slope *s*) while electrophiles are characterized by one parameter (electrophilicity *E*).^[10] For the inclusion of S_N2 type reactions, an additional, electrophile-specific parameter *s_E* has to be added.^[12c]

$$\log k = s(N + E) \quad (1)$$

Table 1: Product Stabilities for Ambident Nucleophiles [MP2/6-311+G(2d,p)].

Entry	Isomerization	$\Delta G^0 / \text{kJ mol}^{-1}$
1	$\text{H}_3\text{C}-\text{N}^{\oplus}=\text{C}^{\ominus} \longrightarrow \text{H}_3\text{C}-\text{C}\equiv\text{N}$	-115 ^[a]
2		-19.7
3		-60.7
4	$\text{H}_3\text{C}-\text{S}-\text{C}\equiv\text{N} \longrightarrow \text{H}_3\text{C}-\text{N}=\text{C}=\text{S}$	-17.1 ^[a]
5	$\text{H}_3\text{C}-\text{O}-\text{C}\equiv\text{N} \longrightarrow \text{H}_3\text{C}-\text{N}=\text{C}=\text{O}$	-117 ^[a]
6	$\text{H}_3\text{C}-\text{O}-\text{N}^{\oplus}=\text{O}^{\ominus} \longrightarrow \text{H}_3\text{C}-\text{N}^{\oplus}(\text{O}^{\ominus})=\text{O}$	-28.3 ^[a]
7		-80.1
8		-20.1
9		-32.9 ^[b]
10		-13.7 ^[b]
11	$\text{H}_3\text{C}-\text{O}-\text{N}^{\oplus}(\text{O}^{\ominus})=\text{O} \longrightarrow \text{H}_3\text{C}-\text{N}^{\oplus}(\text{O}^{\ominus})=\text{O}$	-120
12	$\text{H}_3\text{C}-\text{O}-\text{C}=\text{O} \longrightarrow \text{H}_3\text{C}-\text{C}=\text{O}$	-93.9 ^[a]
13		-28.9
14		-50.4

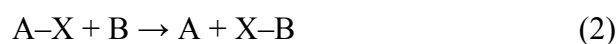
[a] From ref. ^[19]; [b] From ref. ^[13b].

As discussed elsewhere,^[10a] Eq. (1) is mathematically equivalent to a conventional linear free-energy relationship. However, unlike in conventional linear free-energy relationships, where the intercept on the ordinate is considered, Eq. (1) defines the nucleophilicity parameter N as the intercept with the abscissa; in this way it is possible to arrange nucleophiles of widely varying reactivity in a single scale without the need for long-ranging extrapolations. As Eq. (1) holds only for rate constants up to $10^8 \text{ L mol}^{-1} \text{ s}^{-1}$, calculated rate constants $\log k > 9$ are not real but indicate diffusion control. With published reactivity parameters for 579

nucleophiles and 145 electrophiles,^[17] one can already predict the border between activation and diffusion control for a considerable number of reactions. Reactions which proceed without a barrier at both sites of an ambident system are generally unselective, though exceptions have been observed.^[18] Selectivities of activation-controlled reactions can be rationalized by Marcus theory.

2.4 Marcus Theory

Marcus theory^[20] and related concepts consider reactant and product nestling in a parabolic bowl, and the transition state is approximated as the point of intersection of the two bowls. For electron-transfer reactions between metal ions, that is, the types of reactions first analyzed by the Marcus equation, the parabolic displacements refer to the movement of solvent molecules around the reactants and products. In the case of group-transfer reactions [Eq. (2)], which are depicted in Figure 2, a major contribution to the parabolic term comes from the A-X and B-X vibrations.^[20e]



The point of intersection of the two parabolas in Figure 2a can be expressed by the Marcus equation [Eq. (3)], where the working-term is neglected.

$$\Delta G^\ddagger = \Delta G_0^\ddagger + 0.5 \Delta G^0 + (\Delta G^0)^2/16 \Delta G_0^\ddagger \quad (3)$$

In Eq. (3), the Gibbs energy of activation, ΔG^\ddagger , is expressed by a combination of the Gibbs energy of reaction, ΔG^0 , and the intrinsic barrier, ΔG_0^\ddagger , which corresponds to ΔG^\ddagger of an identity reaction, where $\Delta G^0 = 0$ (Figure 2b). The intrinsic barrier ΔG_0^\ddagger can thus be considered as the fraction of ΔG^\ddagger which is left after eliminating the thermodynamic component.

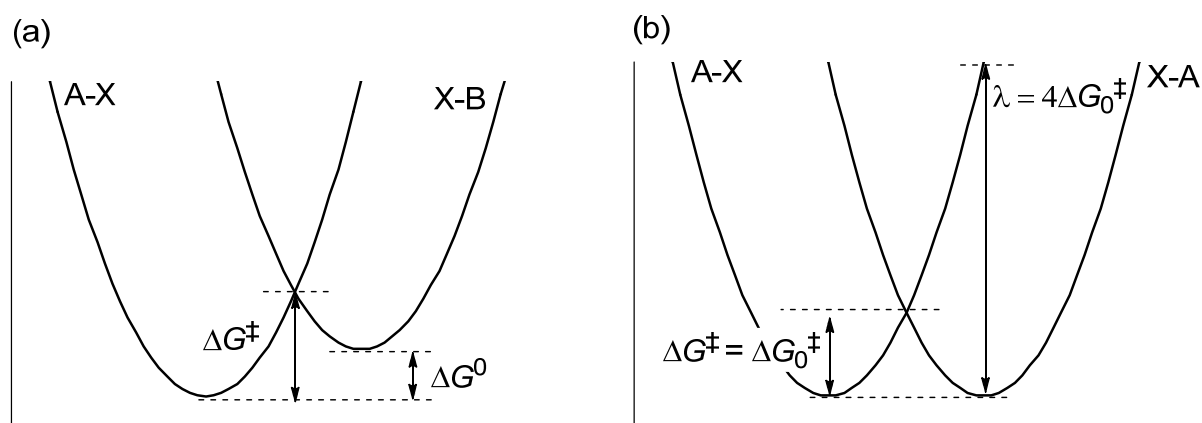


Figure 2: Intersecting parabolas in (a) non-identity reactions and (b) identity reactions.

Marcus suggested calculating the intrinsic barrier of a non-identity reaction as the average of the two corresponding identity reactions.^[20c, 20d, 21] Application of this so-called additivity principle to methyl transfer reactions yields Equation (7), wherein the intrinsic barrier ΔG_0^\ddagger for the S_N2 reaction in Equation (4) is calculated as the average of the activation energies of the identity reactions in Equations (5) and (6).



$$\Delta G_0^\ddagger [\text{Eq. (4)}] = 0.5(\Delta G^\ddagger [\text{Eq. (5)}] + \Delta G^\ddagger [\text{Eq. (6)}]) \quad (7)$$

The validity of this approach has been confirmed computationally and experimentally by several investigators.^[22] The excellent agreement of directly calculated activation energies with those obtained by the Marcus approach (Figure 3) already implies that there are no variable hard-hard or soft-soft interactions between the different groups in Equations (4)-(6). Thus, the intrinsic barrier for the reaction of $HS^- + H_3CF$ equals the average of the barriers for $F^- + CH_3F$ and $HS^- + H_3CSH$.

Application of the Marcus equation [Eq. (3)] on ambident reactivity thus requires knowledge of relative product stabilities ($\Delta\Delta G^0$) and relative magnitudes of the intrinsic barriers ($\Delta\Delta G_0^\ddagger$). As relative product stabilities ($\Delta\Delta G^0$) are usually known or can be derived experimentally or computationally by standard methods (Section 2.2), we will now focus on intrinsic barriers.

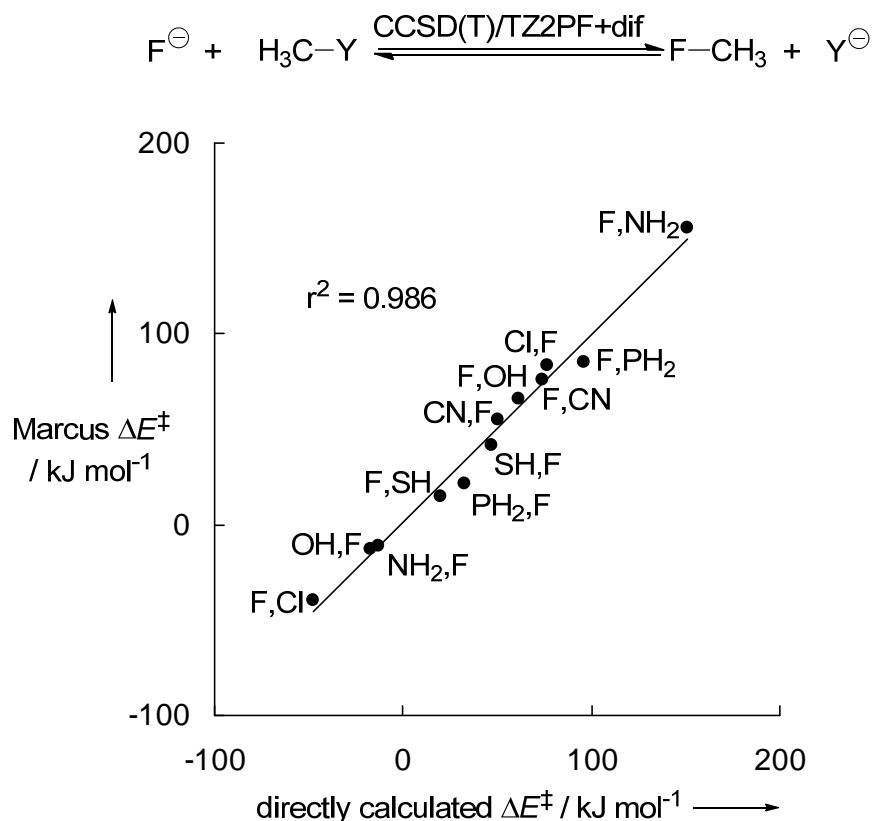


Figure 3: Correlation of the directly calculated activation energies with those derived from the Marcus equation; (F,X) values refer to forward reactions while (X,F) refer to the reverse reaction [CCSD(T)/TZ2PF+dif data from ref^[22e]].

2.5 How Can Relative Magnitudes of Intrinsic Barriers Be Predicted?

2.5.1 Hoz Approach

Using the G2(+) method, Hoz and co-workers were the first to recognize a continuous decrease of the intrinsic barriers, i.e., the Gibbs energies of activation for the identity reactions [Eq. (5)], as X changes from MeCH₂ to MeNH, MeO, and F (Table 2).^[23] Uggerud correlated this trend with the ionization energy of the nucleophile X⁻,^[24] and rationalized that those nucleophiles that form bonds to carbon atoms with stronger electrostatic character give rise to lower barriers because of decreased electron repulsion in the transition state. Furthermore, Hoz and co-workers noticed that the intrinsic barriers ΔG_0^\ddagger change only slightly as one moves from top to bottom within one group in the periodic table. The almost constant values of the intrinsic barriers within a group have been rationalized by Arnaut and Formosinho by two opposing effects:^[25] When moving from top to bottom within the periodic table, the C-X bond length increases, thereby leading to increasing separation of the parabolas and a rise of the energy of the transition state. At the same time, the force

constants decrease and cause a flattening of the parabola and a lowering of the transition-state energy. Both effects obviously compensate each other and result in almost constant values of ΔG_0^\ddagger within one group. While we usually employ SI units, the energies in Table 2 are given in kcal mol^{-1} , because the series $10 \rightarrow 20 \rightarrow 30 \rightarrow 40 \text{ kcal mol}^{-1}$ when moving from group 17 to group 14 can more easily be memorized.

Table 2: G2(+) Intrinsic Barriers for the Identity Reactions
(data from ref ^[23], all in **kcal mol⁻¹**).

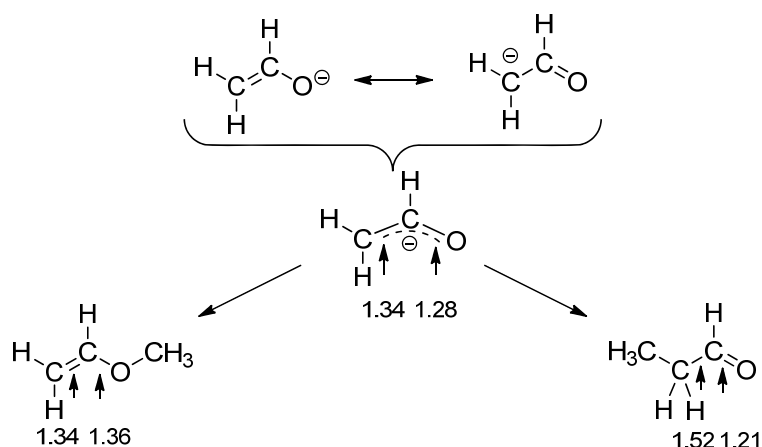
$X^- + \text{H}_3\text{C-X} \rightarrow \text{X-CH}_3 + X^-$			
MeCH ₂ ⁻	MeNH ⁻	MeO ⁻	F ⁻
44.7	29.3	19.5	11.6
MeSiH ₂ ⁻	MePH ⁻	MeS ⁻	Cl ⁻
45.8	29.8	21.9	13.2
MeGeH ₂ ⁻	MeAsH ⁻	MeSe ⁻	Br ⁻
38.1	24.5	17.8	10.8
MeSnH ₂ ⁻	MeSbH ⁻	MeTe ⁻	I ⁻
30.6	19.7	15.3	9.6

The organic chemist may associate the results of Table 2 with the well-known facts, that halide exchange reactions in S_N2 processes proceed smoothly (Finkelstein reaction), whereas transesterifications (alkoxide exchange reactions) or trans-aminations cannot be performed under basic conditions.

2.5.2 Principle of Least Nuclear Motion

A different access to relative intrinsic barriers can be derived from the reorganization energy λ that is required for the deformation of the reactants to the geometry of the products. According to Figure 2b, the intrinsic barrier ΔG_0^\ddagger equals $\frac{1}{4}$ of the reorganization energy λ . Thus, intrinsic barriers can be derived from the principle of least nuclear motion (PLNM),^[26] which claims that “*those elementary reactions will be favored that involve the least change in atomic position and electronic configuration*”.^[26d] Despite an excellent review by Hine^[26d] in 1977, the PLNM has become unfashionable in recent years. We think that this neglect is unjustified because the principle of least nuclear motion, as described by Hine, provides useful estimates of the relative magnitudes of intrinsic barriers. Let us consider the enolate

anion for example. From the bond lengths listed in Scheme 3, one can derive that the geometry of the enolate anion resembles that of the enol ether more closely than that of the aldehyde. In addition, *O*-alkylation avoids rehybridization of the $\text{H}_2\text{C}_{\text{sp}^2}$ -group and thus requires less reorganization energy λ ($= 4 \Delta G_0^\ddagger$) than *C*-alkylation. As a consequence, the PLNM predicts that the intrinsically favored site of attack is at oxygen, where the charge is located in the most important resonance structure of the enolate ion (Scheme 3, top left).

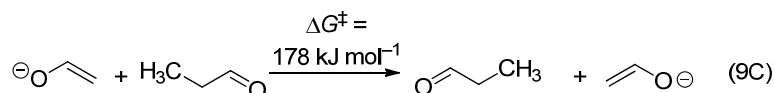
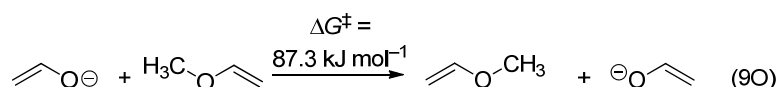
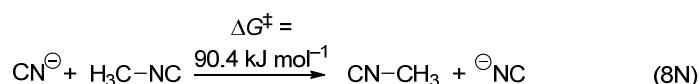
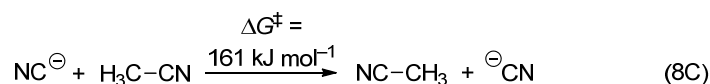


Scheme 3: Ambident reactivity of a π -delocalized system (Bond lengths in Å from ref^[27]).

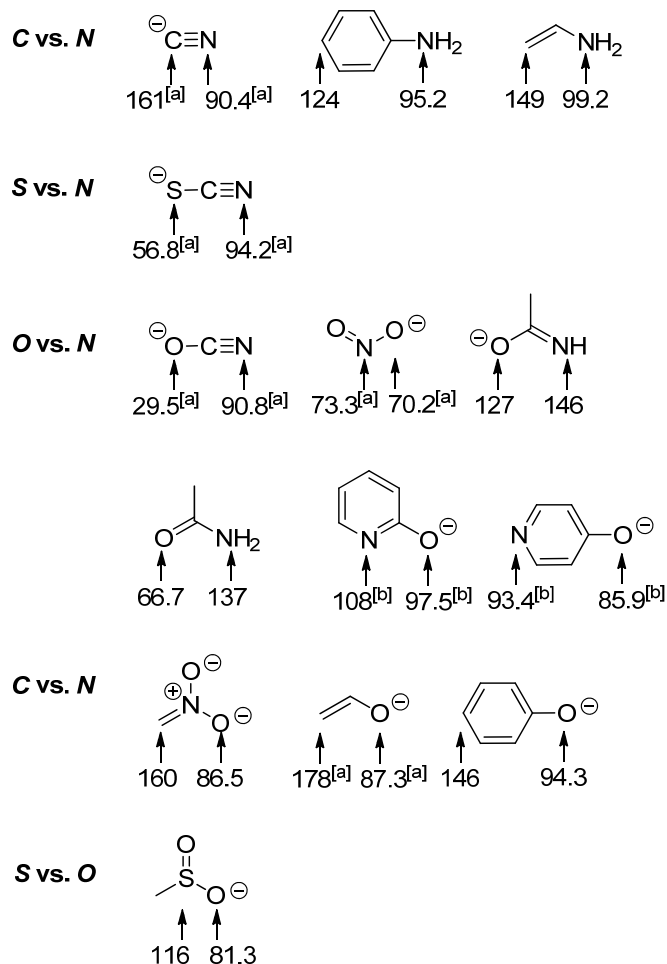
The situation discussed for the enolate anions is typical for π -delocalized systems: The intrinsically preferred process can usually be derived from the electron distribution in the most important resonance structure.

2.5.3 Calculated Barriers for Identity Reactions of Ambident Nucleophiles

As formulated in Equations (8C/8N) and (9O/9C), we have calculated the barriers for the identity methyl transfer reactions of ambident systems at the MP2/6-311+G(2d,p) level of theory; details of these calculations have previously been reported.^[19]



In analogy to the observations by Hoz, the intrinsic barrier for *N*-attack is lower for CN^- anions [Eqs (8C/8N)] and for *O*-attack at enolate anions [Eqs (9O/9C)]. The same trend, smaller intrinsic barriers for attack at the atom which is further right in the periodic table, has been observed for many other ambident nucleophiles as summarized in Scheme 4.



Scheme 4: Barriers [ΔG^\ddagger , kJ mol^{-1} , MP2/6-311+G(2d,p)] for identity methyl transfer reactions as exemplified in Eqs (8C/N) and (9O/C) ([a] from ref^[17], [b] from ref^[13h]; rest this work).

It should be noted that for π -delocalized systems the same ordering of intrinsic barriers can also be derived from the PLNM; less reorganization is needed for *O*-attack at enolates and phenolates and for *N*-attack at enamines and anilines.

2.6 A Qualitative Marcus Approach to Ambident Reactivity.

As recently reported, one can substitute the calculated values of intrinsic barriers ΔG_0^\ddagger and Gibbs energies ΔG^0 into the Marcus equation [Eq. (3)] to calculate ΔG^\ddagger and thus arrive at complete Gibbs energy diagrams for the reactions of cyanide, cyanate, thiocyanate, nitrite, and enolate anions with alkyl halides in the gas phase.^[19] Solvation models would be needed for a quantitative analysis in solution, particularly when reactions are considered, where ionic products are generated from neutral reactants.^[28] Though this approach appears feasible, a qualitative analysis of the thermodynamic data in Table 1 and of the intrinsic reactivities in Scheme 4 may be more practical.

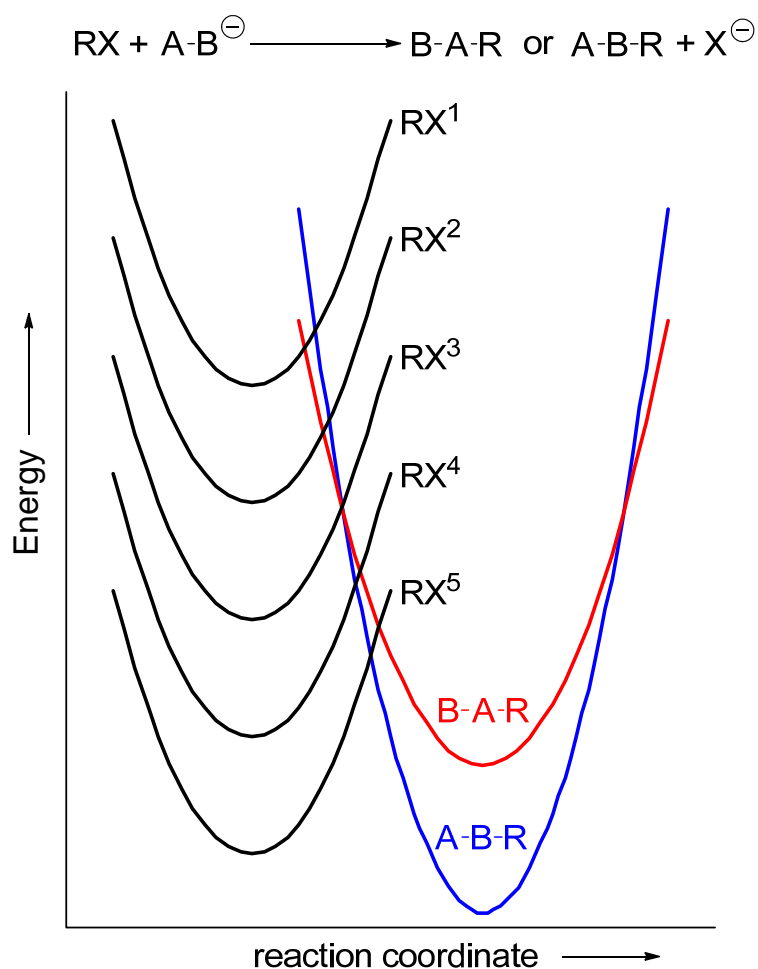


Figure 4: Influence of the Gibbs energy of reaction on the Gibbs energy of activation and thus on the regioselectivity of the attack at an ambident nucleophile with the reactive sites A and B.

Figure 4 represents a qualitative description of the reactions of an ambident nucleophile A-B^- with alkyl halides RX of different reactivity. For the sake of simplicity, all parabolas for RX^1

to RX^5 are assumed to have the same opening and just differ in their relative positions. The parabolas for the products on the right differ in position and opening. The product obtained by alkylation at atom B is thermodynamically favored (more negative ΔG^0) and intrinsically disfavored (steeper parabola) than the product obtained by alkylation at A.

Figure 4 now shows that the highly exergonic reactions with RX^1 and RX^2 follow the intrinsically favored pathway leading to *A*-alkylation. The reaction with RX^3 yields both products with equal rates, and the transition state for the reaction with RX^4 is already dominated by the $\Delta\Delta G^0$ term, which favors *B*-attack. A frequently encountered situation is shown for the reaction of RX^5 : As *A*-attack yields a product which is thermodynamically less stable than the reactants, only the products *AB*-R can be generated.

If the Marcus-inverse region^[29] is neglected (probably unproblematic for the reactions under consideration), the relative magnitudes of the Gibbs energy of activation ($\Delta\Delta G^\ddagger$) can be derived from the two first terms of Eq. (3). The following discussion of the individual ambident systems, which is based on the thermodynamic data in Table 1 and the intrinsic barriers in Scheme 4, assumes that the relative product stabilities are not inverted when the methyl group is replaced by another alkyl or aryl group; exceptions can be expected when two isomers differ only slightly in energy. According to the second term of Eq. (3) the ΔG^0 values given in Table 1 have to be divided by two for estimating the difference of the Gibbs energies of activation for attack at both sites of an ambident system. On the other hand, the calculation of the intrinsic barriers according to the additivity postulate in Eq. (7) also requires division of ΔG^\ddagger for the identity reactions given in Scheme 4 by a factor of two. As a result, one can directly compare the absolute values given in Table 1 and Scheme 4.

Neglecting the cross-term in the Marcus equation [Eq. (3)] effectively means that whenever the thermodynamically less stable product is formed preferentially under conditions of kinetic control, it must be generated via the lower intrinsic barrier. In contrast, the kinetically controlled reaction products are not necessarily formed via the lower intrinsic barrier.

3 Ambident Nucleophiles

3.1 Carbon vs. Nitrogen Attack

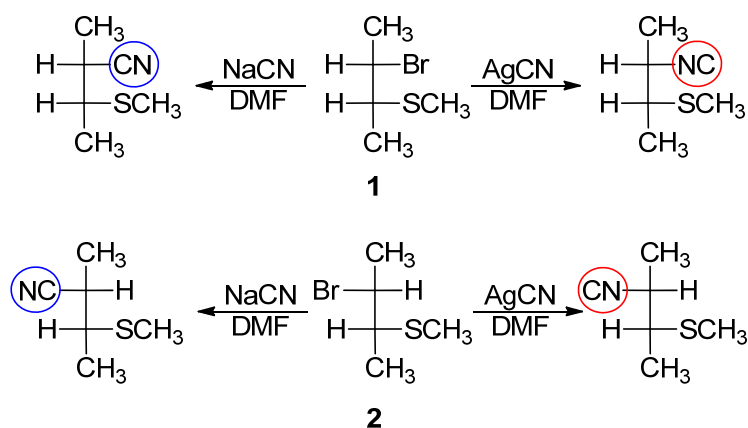
3.1.1 Cyanide Anion

The cyanide ion CN^- used to be one of the classical examples for illustrating the application of the Klopman-Salem equation and the HSAB principle. As described in Scheme 5, the formation of nitriles by the reactions of alkali cyanides with alkyl halides was explained by the preferred attack of the “soft” carbon terminus of the cyanide ion at the “soft” alkyl halides. A change from $\text{S}_{\text{N}}2$ to $\text{S}_{\text{N}}1$ mechanism was postulated to rationalize the formation of isocyanides in the reactions of alkyl halides with silver cyanide; in this case, the favorable hard-hard interaction between the carbocation and the nitrogen of cyanide was considered to be responsible for the change of regioselectivity.



Scheme 5: Common but incorrect description of the ambident reactivity of cyanide.

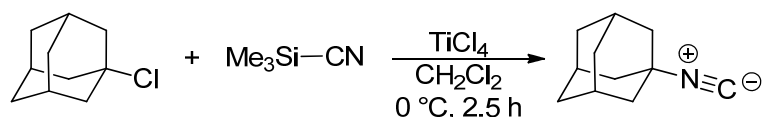
This rationalization is contradicted by several experimental findings. More than two decades ago, Carretero and Ruano reported that *erythro*(**1**)- and *threo*-2-bromo-3-(methylthio)butane (**2**) react with sodium cyanide and silver cyanide with retention of configuration and > 96 % regioselectivity to give cyanides and isocyanides, respectively, as illustrated in Scheme 6.^[30]



Scheme 6: Reactions of *erythro*- and *threo*-2-bromo-2-(methylthio)-butanes **1** and **2** with cyanides (from ref^[30]).

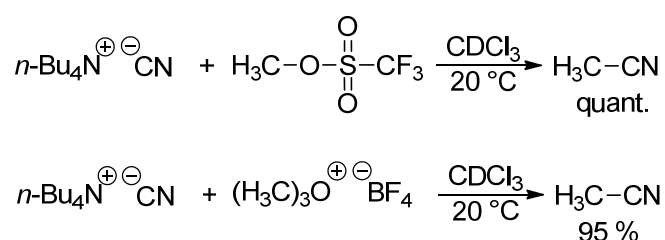
Their conclusion that the reactions with NaCN and AgCN follow the same mechanism and that "the observed regioselectivity with both metal cyanides (...) cannot be explained as variations in the hardness of the electrophilic carbon induced by the interactions between the metal cation and the halogen" found little attention.^[31] In agreement with "older hypotheses", the formation of isonitriles with AgCN (Scheme 6) was explained by the "participation of a species (non free CN^-) in which the Ag^+ is bonded to the carbon atom."^[30]

The formation of 1-isocyanoadamantane from 1-chloroadamantane and trimethylsilyl cyanide in the presence of $TiCl_4$ (Scheme 7) demonstrates that other ligands may replace Ag^+ in blocking the carbon atom of cyanide.^[32]



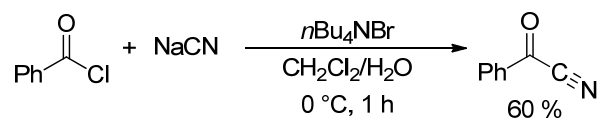
Scheme 7: Formation of 1-isocyanoadamantane (from ref^[32a]).

Exclusive nitrile formation, which is well known for reactions of primary alkyl bromides and alkyl iodides with NaCN and KCN, has also been observed for the methylation of $[Bu_4N]^+[CN]^-$ with methyl triflate and trimethyloxonium tetrafluoroborate, two of the hardest methylating agents available (Scheme 8). Attack at the hard nitrogen, as predicted by the HSAB principle, has not been observed.^[13b]



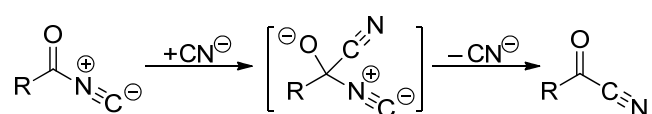
Scheme 8: Exclusive formation of acetonitrile in the reactions of $Bu_4N^+CN^-$ with the hard methylation agents methyl triflate and trimethyloxonium tetrafluoroborate (from ref^[13b]).

Only benzoyl cyanide has been formed when benzoyl chloride was combined with $[(Ph_3P)_2N]CN$,^[33] guanidinium cyanide,^[34] or NaCN under conditions of phase transfer catalysis^[35] (Scheme 9). This observation also contrasts the expectations based on the HSAB principle, which predicts the formation of isonitriles by attack of the "hard" nitrogen end of the cyanide at the "hard" acyl center of acid chlorides.



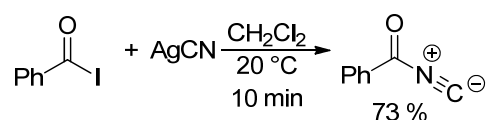
Scheme 9: Synthesis of benzoyl cyanide from NaCN and benzoyl chloride by phase transfer catalysis (from ref ^[35]).

As rearrangements of isocyanides into cyanides are well-known,^[36] one cannot a priori exclude that the acyl cyanides described in Scheme 9 are formed from intermediate acyl isocyanides, which may isomerize via acylium ions or the mechanism shown in Scheme 10.



Scheme 10: Rearrangement of acyl isocyanides to acyl cyanides.

However, this interpretation is not very likely because treatment of acyl iodides with silver cyanide gives rise to the formation of acyl isocyanides (Scheme 11), which are stable in dilute solution after removal of Ag^+ salts.^[37]



Scheme 11: Reaction of benzoyl iodide with silver cyanide yielding the isonitrile (from ref ^[37]).

From the cited experiments one can derive that free cyanide ions generally react at carbon with “hard” and “soft” electrophiles and that nitrogen attack only occurs when the attack at carbon is blocked by a ligand (e.g. by Ag^+ or Me_3Si^+).^[38]

For a systematic analysis of the behavior of cyanide ion we have studied the rates of its reactions with benzhydrylium ions (Figure 5), which have been used as reference electrophiles for the determination of nucleophilicity parameters. Exclusive formation of benzhydryl cyanides was observed in all reactions^[37] with stabilized benzhydrylium ions, and from the plot of $\log k$ vs. the electrophilicity parameter E of the benzhydrylium ions one can extrapolate that the diffusion limit is reached when the electrophilicity of the carbocations exceeds E values of approximately -2 to 0 (Figure 5).^[13b]

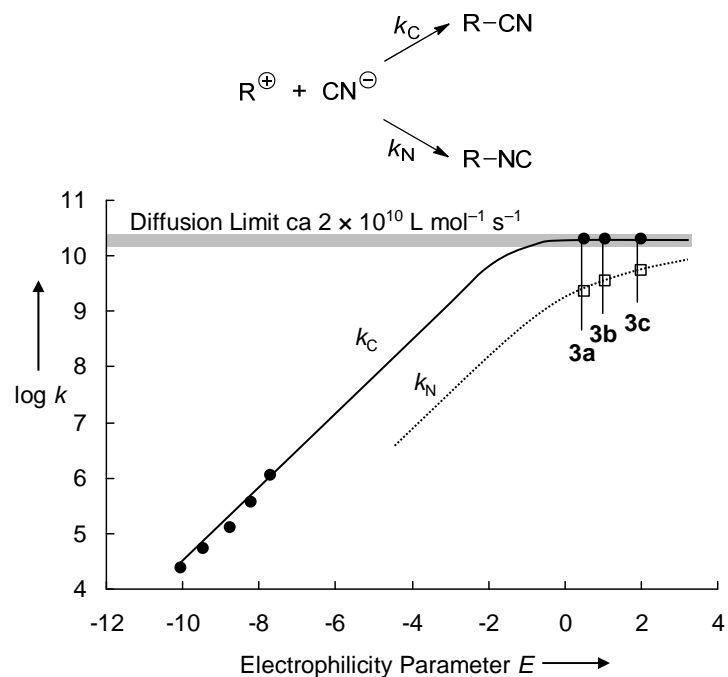
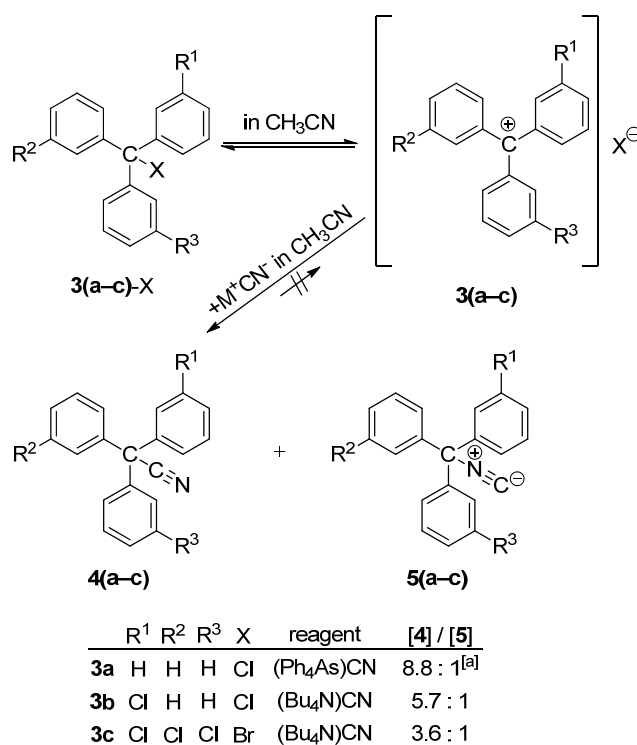


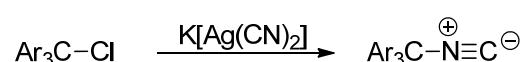
Figure 5: Plot of $\log k$ for the reactions of benzhydrylium Ar_2CH^+ and tritylium ions Ar_3C^+ with the cyanide ion vs. the electrophilicity parameters E (from ref^[13b], for structures of **3a–c** see Scheme 12).



Scheme 12: Product distribution in the reactions of trityl chlorides with cyanide ions ([a] from ref^[39], others from ref^[13b]).

As illustrated in Figure 5, Songstad's observation^[39] of 10 % of trityl isocyanide **5a** along with 88 % trityl cyanide **4a** from the reactions of trityl halides with free CN^- can be explained by barrier-less formation of trityl cyanide ($k_C \approx 2 \times 10^{10} \text{ L mol}^{-1} \text{ s}^{-1}$) and a ten-fold lower rate of *N*-attack. When the more electrophilic *m*-chloro-substituted tritylium ions were employed, the nitrile/isonitrile ratio decreased because the rate of *C*-attack remained constant while the rate of *N*-attack increased (Scheme 12).

All trityl chlorides gave trityl isocyanides exclusively when treated with $\text{K}[\text{Ag}(\text{CN})_2]$ (Scheme 13).^[13b]



Scheme 13: Selective formation of isonitriles in reactions of trityl chlorides with $\text{K}[\text{Ag}(\text{CN})_2]$ (from ref^[13b]).

From Figure 5 one can extrapolate that the unsubstituted benzhydrylium ion ($E = 5.9$), α -aryl alkyl cations (E ca. 3 to 9),^[40] and tertiary alkyl cations (E ca. 8)^[41] will undergo barrierless combination reactions with both termini of the free CN^- in acetonitrile. Therefore, attempts to explain *C/N* ratios by classical transition state models must be obsolete.

Furthermore, it has to be considered that $\text{S}_{\text{N}}1$ reactions with cyanide ions rarely occur in protic solvents. Because the nucleophilicity of CN^- decreases significantly from $N = 16.27$, $s = 0.70$ in CH_3CN ^[13b] to $N = 9.19$ and $s = 0.60$ in water,^[42] most electrophilic carbocations generated as $\text{S}_{\text{N}}1$ intermediates in alcoholic or aqueous solution react faster with the solvent (which is present in large excess) than with CN^- .^[43] Thus, the reaction of 1-chloro-1-(4-methoxyphenyl)ethane with KCN in ethanolic solution yields the corresponding ethyl ether in almost quantitative yield.^[44] Reactions of *tert*-haloalkanes with alkali-metal cyanides in alcohols give particularly low yields of substitution products owing to the high Brønsted basicity of CN^- . Depending on the reaction conditions, only small amounts of *tert*-alkyl cyanides are formed along with tertiary ethers and elimination products.^[45]

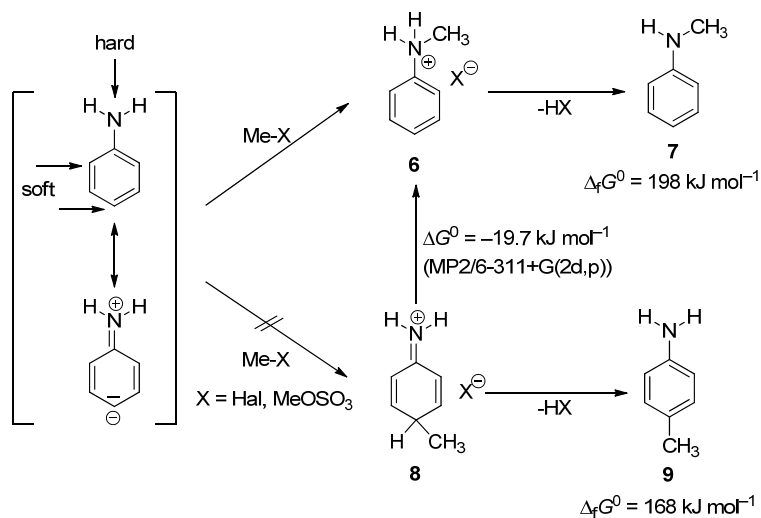
In summary, all experimental investigations indicate that free cyanide ions are attacked at the carbon atom by *C*-electrophiles. *C*-attack accompanied by *N*-attack is observed in diffusion-controlled reactions, and predominant attack at the nitrogen atom was only found when the carbon terminus was blocked by coordination with silver ions or other Lewis acids. The large

thermodynamic preference for *C*-alkylation (Table 1, entry 1) which is also reflected by Rüchardt's work on the isocyanide-cyanide rearrangement^[36b] overrules the intrinsically favored attack at nitrogen which is quantified in Scheme 4.

3.1.2 Anilines

Following the HSAB principle, one would expect hard electrophiles to attack at the nitrogen atom of aniline and soft electrophiles to attack at the carbon atom (Scheme 14). However, as shown in Scheme 14, soft alkyl halides as well as hard dialkyl sulfates react selectively with the nitrogen atom of aniline.^[46] From the known Gibbs energies of formation, we can derive that 4-methylaniline (**9**) is thermodynamically favored over *N*-methylaniline (**7**) by 30 kJ mol⁻¹.^[47] On the other hand, the anilinium ion **6**, the precursor of **7**, was calculated (MP2/6-311+G(2d,p)) to be 19.7 kJ mol⁻¹ more stable than the benzenium ion **8**.

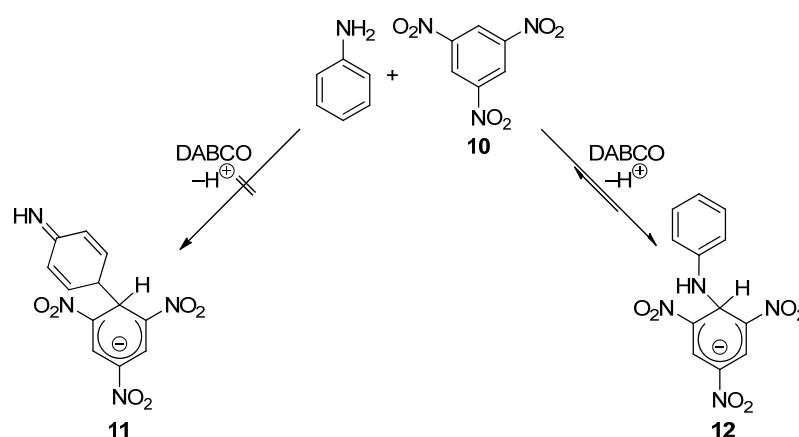
In line with the facts that N is further right in the periodic table than C and less reorganization is needed for *N*- than for *C*-attack, a lower intrinsic barrier was calculated for *N*-attack (Scheme 4). As both terms in Eq. (3), $\Delta\Delta G^0$ and $\Delta\Delta G_0^\ddagger$ indicate a preference for *N*-attack, one can rationalize that aniline is alkylated at nitrogen by hard and soft methylating agents.



Scheme 14: Methylation of aniline (attack in *ortho*-position is not shown; $\Delta_f G^0$ from ref^[47]).

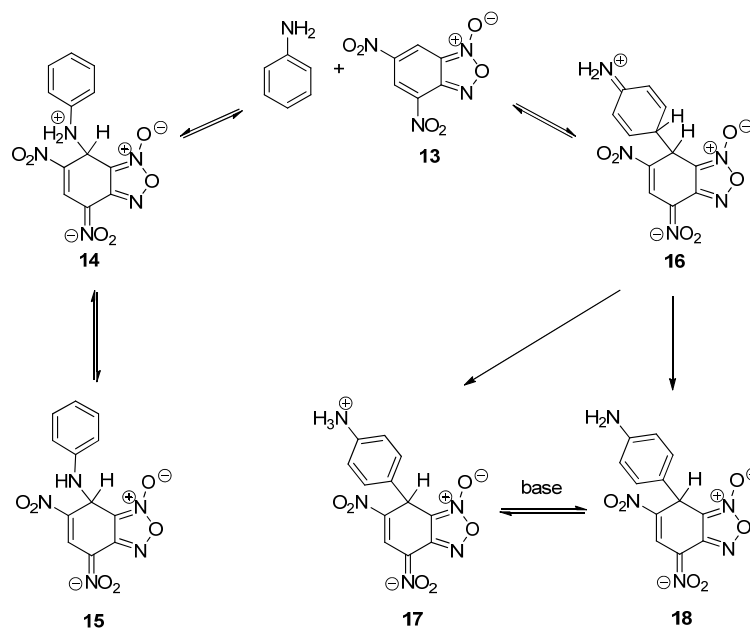
The kinetically preferred attack of carbon electrophiles at nitrogen can also be calculated by using the correlation equation (1). While $N = 12.62$ ($s = 0.73$)^[48] has been derived from the reactions of the amino group of aniline with electrophiles, $N \approx 4$ has been extrapolated for the *para*-position of aniline from the correlation of the *N*-values of monosubstituted benzenes with σ^+ of the corresponding substituents.^[49]

Nitrogen is also the site of attack of trinitrobenzene at aniline.^[50] From $E = -13.2$ ^[51] for trinitrobenzene (**10**) and $N \approx 4$, $s = 0.8$ to 1.0 for the p -position of aniline, one can estimate rate constants between 4×10^{-8} to 7×10^{-10} L mol⁻¹ s⁻¹ for the attack of trinitrobenzene at the aromatic ring of aniline. From these rate constants one can derive that the attack of trinitrobenzene at the p -position of aniline (electrophilic aromatic substitution) would have reaction times of 1 to 50 years in 1 M solutions of the reactants. As a consequence, rearrangement of the σ -adduct **12** to a biphenyl derivative **11** (Scheme 15) is not observable, even after extended reaction times.



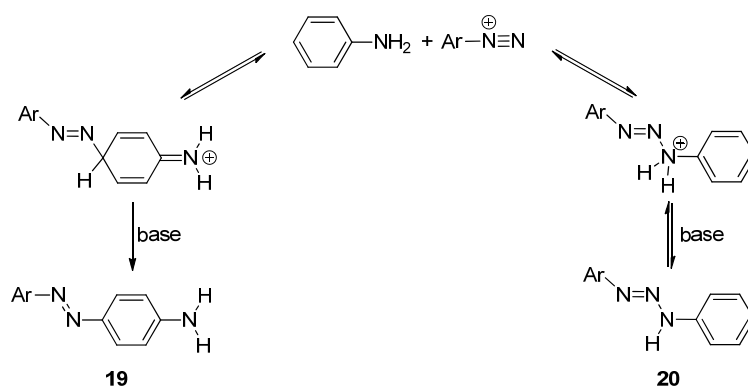
Scheme 15: Reaction of aniline and trinitrobenzene (**10**) yielding only the product of N -attack **12** (DABCO = 1,4-diazabicyclo[2.2.2]octane, from ref^[50]).

When 4,6-dinitrobenzofurazan (**13**) was treated with 1 equivalent of aniline, C -attack with rapid formation of **17** was observed (Scheme 17).^[52] A 1:1 mixture of **15** and **17** was found, however, when **13** was treated with 2 equivalents of aniline. These results are consistent with the assumption that, for the same reasons as discussed above, N -attack at aniline is kinetically preferred. When aniline is not used in excess, **14** cannot be deprotonated to give **15** and, therefore, undergoes dissociation with formation of the reactants, which eventually yield the thermodynamically preferred products **17/18**. Different from the situation described for trinitrobenzene (Scheme 15), the higher electrophilicity of **13** now enables the attack at the p -position of aniline (\rightarrow **16**), for which a rate constant of 0.1 L mol⁻¹ s⁻¹ (at 20 °C) can be calculated from $E(\mathbf{13}) = -5.1$ ^[53] and $N(p\text{-position of aniline}) \approx 4$.



Scheme 16: Ambident reactivity of aniline towards 4,6-dinitro-benzofurazan (**13**)
(from ref^[52b]).

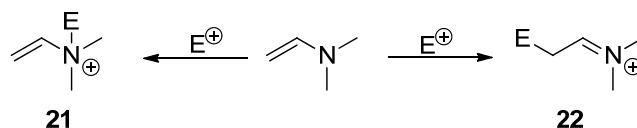
A similar regioselectivity is found in azo couplings. It has long been known that anilines as well as *N*-alkyl anilines initially form triazenes in coupling reactions with benzenediazonium salts (*N*-coupling), whereas *C*-coupling is observed for tertiary aromatic amines.^[54] Exceptions were only found when the nucleophilicity of the aromatic ring of the amine is raised by additional substituents; however, even in such cases an initial attack at nitrogen has to be considered.^[55] It was found that the reversible attack at the nitrogen atom is 20–25 times faster than the attack at the carbon atom. A mechanism that is consistent with the experimental findings is depicted in Scheme 17,^[55] which shows that even diazonium ions prefer *N*-attack under conditions of kinetic control. In the absence of base, the formation of the triazene **20** is reversible and one only obtains the azo compound **19** as the reaction product.



Scheme 17: Ambident reactivity of aniline in reactions with arene diazonium ions
(from ref^[55]).

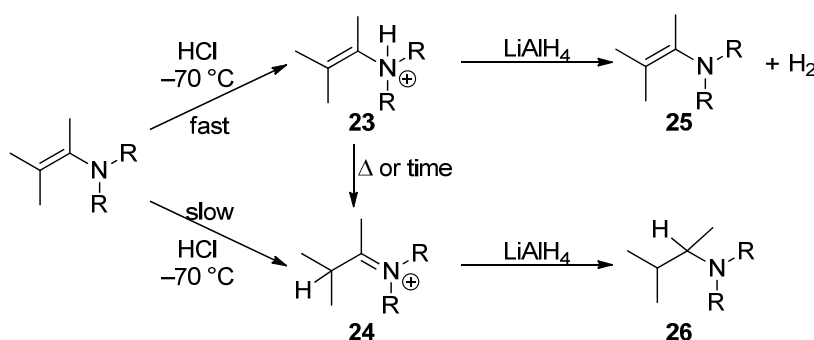
3.1.3 Enamines

Enamines can be attacked by electrophiles either at nitrogen yielding enammonium ions **21** or at carbon yielding iminium ions **22** (Scheme 18).^[56]



Scheme 18: Ambident reactivity of enamines.

A large variety of enamines derived from aldehydes and ketones have been reported to be exclusively protonated at nitrogen by gaseous HCl in hexane at $-70\text{ }^{\circ}\text{C}$.^[57] The resulting enammonium ions **23** rearranged to the thermodynamically more stable iminium ions **24** upon warming to room temperature. Spectroscopic methods as well as reactions of the protonated enamines have been employed to elucidate the site of protonation (Scheme 19).



Scheme 19: Protonation of enamines and subsequent reaction with LiAlH_4 (from ref^[57f]).

Freshly prepared hydrochlorides of 1-morpholino-2-ethyl-hexa-1,3-diene at $-70\text{ }^{\circ}\text{C}$ consist mainly of the *N*-protonated species; after several hours C2- and C4-protonated species were identified exclusively.^[57d, 57e]

The reactions with weaker acids like acetic or benzoic acid in ether yielded only iminium ions, while products of *N*-protonation were not detectable.^[57e] These and related^[58] observations led to the conclusion that protonation at nitrogen is fast and reversible while protonation at carbon is slow but yields the thermodynamically favored iminium ion (Figure 6). The enammonium ion is better deprotonated by the more basic counterion acetate than by the less basic chloride. Hence, only protonation at carbon can be observed in protonation experiments with carboxylic acids.

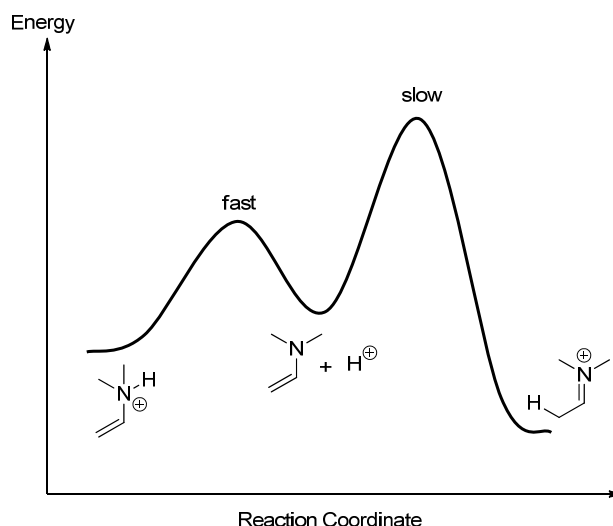
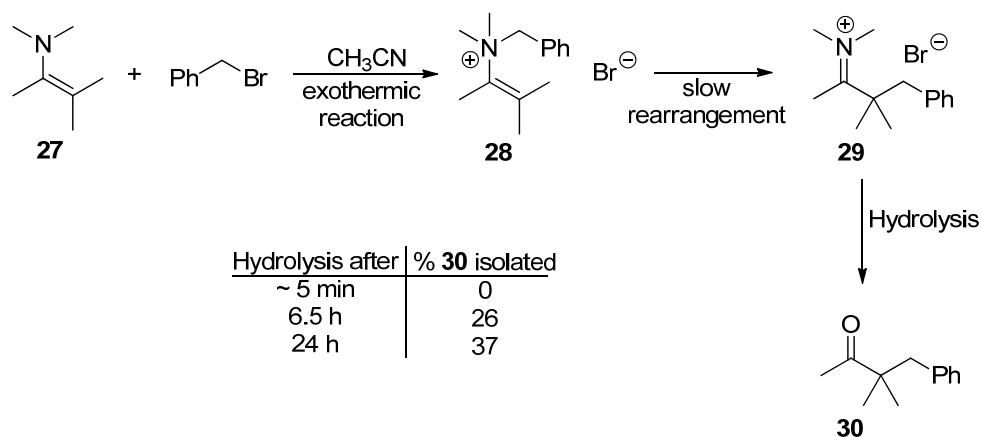


Figure 6: Energy profile for the protonation of enamines.

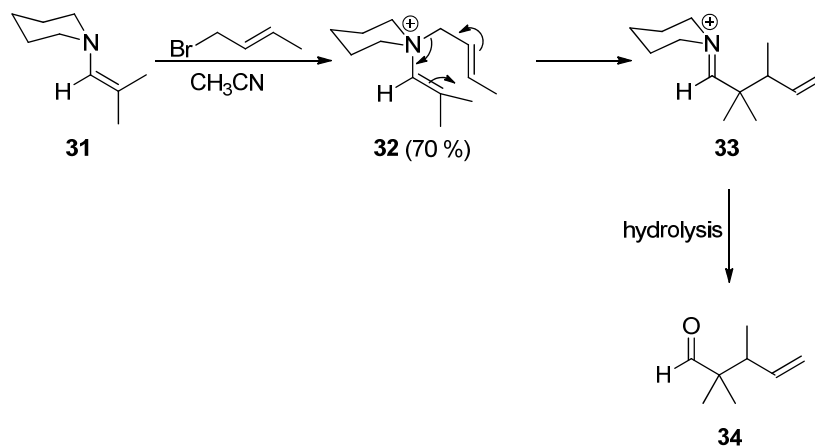
Although this behavior has been explained by hard/hard interactions between H^+ and the enamine, the following examples show that soft alkylating reagents show a similar pattern.

While Stork and co-workers reported that enamines of ketones generally give *C*-alkylated products when treated with alkylating agents under reflux,^[59] Elkik observed *N*-alkylation of some enamines derived from aliphatic aldehydes with methyl halides.^[60]

Scheme 20: Alkylation of an enamine with benzyl bromide in CH_3CN (from ref^[61]).

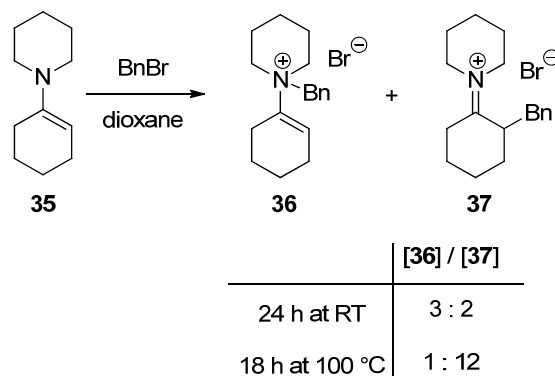
The selective *C*-alkylation of these enamines by allyl bromide prompted Elkik to suggest that enamines are also initially attacked by alkyl halides at nitrogen followed by a subsequent rearrangement yielding the product of *C*-attack. Further support for this hypothesis comes from results of Brannock and Burpitt^[61] who observed an exothermic reaction when benzyl bromide was added to the enamine **27** in acetonitrile (Scheme 20). The yield of ketone **30**

after hydrolysis of the reaction mixture at different time intervals also suggests that enamines are initially attacked at nitrogen (yielding the enammonium ion **28**). The thermodynamically more stable product of *C*-alkylation **29** is then formed in a subsequent slow rearrangement reaction.



Scheme 21: Reaction of enamine **31** with crotyl bromide in CH_3CN (from ref^[62]).

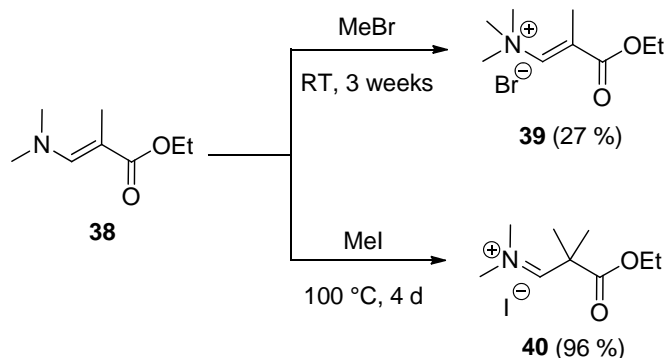
Consistent with these findings, Opitz isolated the *N*-allylated enamine **32** and showed that it isomerized via an aza-Claisen rearrangement to the corresponding iminium ion **33** (Scheme 21).^[62]



Scheme 22: Benzylation of 1-(piperidino)-cyclohexene (**35**) at different temperatures in dioxane (from ref^[63]).

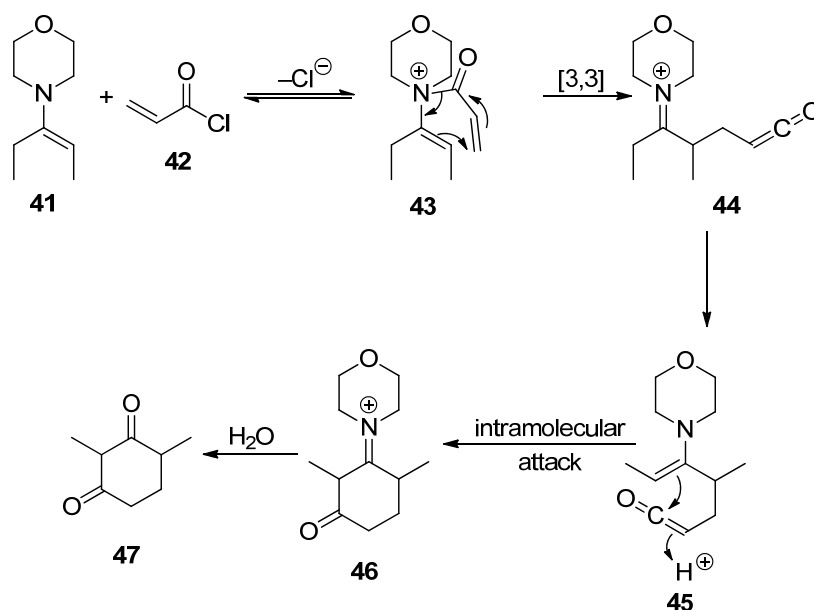
A systematic study by Kuehne and Grabacik revealed that a significant percentage of *N*-alkylated products is detectable, when ketone-derived enamines are treated with benzyl bromide or methyl iodide at room temperature (Scheme 22).^[62] In all cases the percentage of *C*-alkylated products increased when the reactions were performed at 100 °C, indicating that also in these cases, thermodynamic product control with formation of iminium ions is feasible. From the observation of *C*- and *N*-alkylated products at room temperature, one can derive that also in alkylations *N*-attack is intrinsically favored over *C*-attack.

In line with these observations, Böhme isolated exclusively the product of *N*-methylation **39** when **38** was treated with methyl bromide at room temperature (kinetic control), while *C*-methylation (\rightarrow **40**) was observed under conditions of thermodynamic control (Scheme 23).^[64]



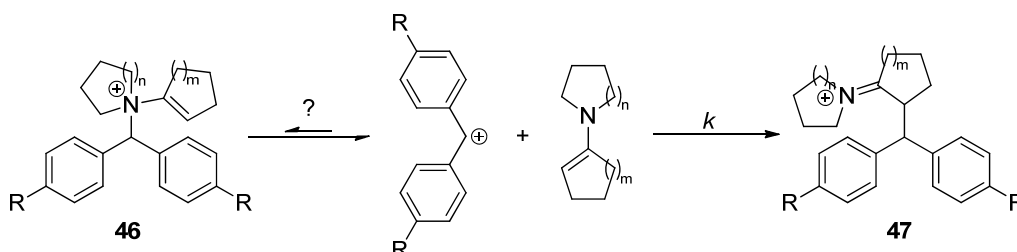
Scheme 23: Methylation of ethyl 3-(dimethylamino)-2-methylacrylate (**38**) by methyl halides (from ref^[64]).

Probably because of the high reversibility of the formation of *N*-acylated enamines, enamines generally react with acyl chlorides with formation of *C*-acylated enamines, which yield 1,3-dicarbonyl compounds by hydrolysis.^[65] Evidence for initial *N*-acylation comes from the isolation of cyclohexane-1,3-diones in reactions of enamines with α,β -unsaturated acyl chlorides, which was explained by *N*-acylation followed by a fast [3,3] sigmatropic rearrangement (Scheme 24).^[66]



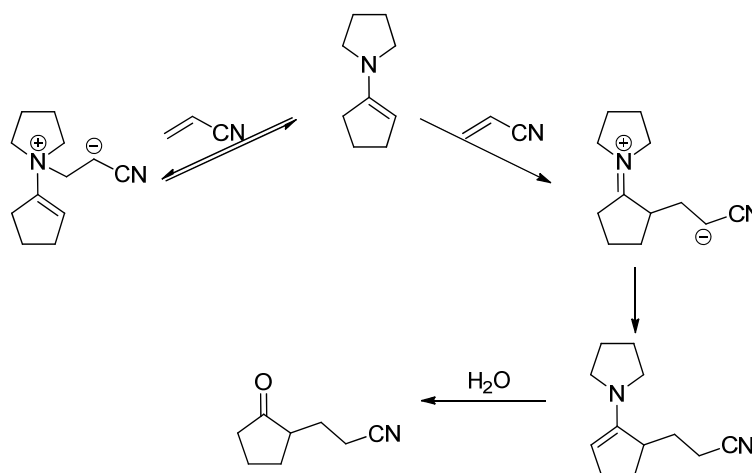
Scheme 24: *N*-acylation of enamines due to subsequent reactions (from ref^[66]).

Monoexponential decays of the absorbances of stabilized benzhydrylium ions were observed, when they were treated with an excess of various enamines. While this observation does not rigorously exclude initial *N*-attack, the concentration of *N*-alkylated enamines **46** must remain so low that their intermediacy is irrelevant for the observed kinetics (Scheme 25).^[67]



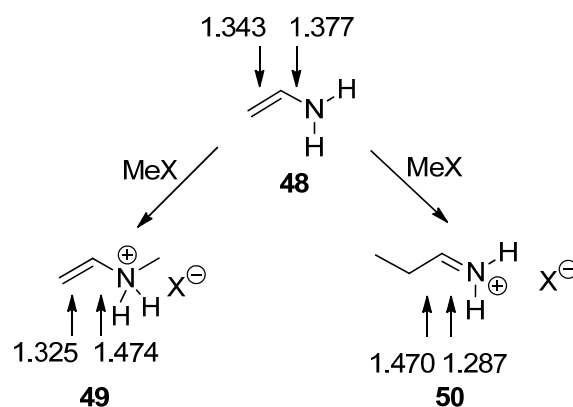
Scheme 25: Reactions of different enamines with benzhydrylium ions yielding iminium ions **47** (from ref^[67]).

The exclusive carbon-carbon bond formation in reactions of enamines with Michael acceptors had been rationalized by the more favorable frontier orbital interactions. In our view, it is better explained by thermodynamic product control, because *N*-attack of Michael acceptors can be assumed to be reversible, as previously suggested by Stork (Scheme 26).^[59c]



Scheme 26: Reactions of enamines with Michael acceptors (from ref^[59c]).

Calculated bond lengths of vinylamine and its *N*- and *C*-methylated derivatives show that less deformation is required for *N*-attack than for *C*-attack (Scheme 27). In combination with the “Hoz effect” which predicts lower intrinsic barriers for attack at the atom further right in the periodic table, one can qualitatively derive that *N*-attack is intrinsically preferred. A quantitative confirmation of this analysis has been obtained by MP2/6-311+G(2d,p) calculations of the identity reactions [Eq. (5)], which showed that the barriers are 50 kJ mol⁻¹ lower when methyl is transferred from *N* to *N* instead of *C* to *C* (Scheme 4).

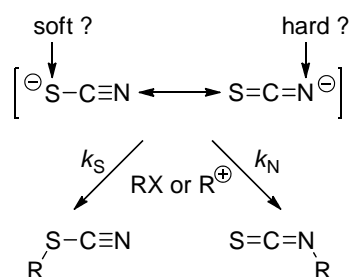


Scheme 27: Calculated bond lengths (in Å) for vinyl amine (**48**) and the products **49/50** obtained by *N*- and *C*-methylation [MP2/6-311+G(2d,p)].

3.2 Nitrogen vs. Sulfur Attack: Thiocyanate Anion

3.2.1 Alkylation Reactions

More than 100 years ago, Kaufler^[68] and Walden^[69] synthesized alkyl thiocyanates by treatment of potassium thiocyanate with dimethyl sulfate. A few decades later, extensive studies on alkylations of thiocyanate ions (Scheme 28) had shown that in S_N2 type reactions attack at sulfur is approximately 10^2 – 10^3 times faster than at nitrogen, while in S_N1 type reactions the S/N ratio decreased to 2–9 (Table 3).^[70]



Scheme 28: Ambident reactivity of thiocyanate anions.

Though preferential attack at nitrogen of SCN^- has never been observed with carbocations (hard electrophiles), the small S/N ratio in S_N1 reactions had been rationalized on the basis of the HSAB concept: "As the electrophilic character of the reaction center increases, the reactivity of the more basic nitrogen atom, which forms the stronger bond to carbon, increases with respect to that of the more polarizable sulfur atom".^[70e]

Table 3: Ambident Reactivity of Thiocyanate Anions Towards Different Electrophiles.

S _N 2 type reactions			S _N 1 type reactions		
Electrophile	k_S/k_N	ref.	Electrophile	k_S/k_N	ref.
(CH ₃) ₂ CHI	85	[70h]	(4-CH ₃ -C ₆ H ₄) ₂ CH ⁺	5	[70e]
C ₆ H ₅ CH ₂ Cl	430	[70h]	(4-CH ₃ -C ₆ H ₄) ₂ CH ⁺	8.3	[70i]
C ₆ H ₅ CH ₂ Br	850	[70h]	(C ₆ H ₅) ₂ CH ⁺	9.0	[70a]
C ₆ H ₅ CH ₂ I	1300	[70h]	(4-Cl-C ₆ H ₄)PhCH ⁺	3.3	[70g]
C ₆ H ₅ CH ₂ SCN	725	[70f]	C ₆ H ₅ CH ₂ ⁺	4.4	[70j]
4-MeO-C ₆ H ₄ CH ₂ Br	220	[70h]	(CH ₃) ₃ C ⁺	ca 2	[70a]
4-O ₂ N-C ₆ H ₄ CH ₂ Br	730	[70h]	CH ₃ CH ₂ CH ⁺ CH ₃	5	[70a]

This interpretation has recently been revised (Figure 7).^[13a] Laser flash photolytically generated benzhydrylium ions with electrophilicity parameters $-6 < E < -4$ showed bi-exponential decays in solutions of Bu₄N⁺ SCN⁻ in acetonitrile. Depending on the concentration of SCN⁻, up to 40 % of benzhydrylium ions were consumed by a fast reversible reaction ($10^7 < k_S < 3 \times 10^8$ L mol⁻¹ s⁻¹), and the remaining benzhydrylium ions reacted via a "slow" process ($5 \times 10^3 < k_N < 10^5$ L mol⁻¹ s⁻¹). While benzhydrylium ions with $E < -6$ did not react at all with SCN⁻ in acetonitrile, more electrophilic benzhydrylium ions ($E > -3.5$) were consumed quantitatively by a fast process ($k_S \approx 10^9 - 10^{10}$ L mol⁻¹ s⁻¹), and the rates of their reactions with the *N*-terminus of ⁻SCN could not be measured directly.

Figure 7 shows that *S*-attack is diffusion-controlled for all carbocations with $E > 0$. If one assumes that the log k_N vs. E correlation has a similar slope as the corresponding plots those for other anionic *n*-nucleophiles ($s \approx 0.6$), one can draw the dashed correlation line shown in Figure 6. Thus, the k_S/k_N ratio, which is approximately 2000 for carbocations of $-6 < E < -4$, can be expected to decrease as the electrophilicity E of the carbocations is increasing. Accordingly, small k_S/k_N ratios have been reported for (4-CH₃-C₆H₄)₂CH⁺ ($E = 3.63$), Ph₂CH⁺ ($E = 5.90$), and (4-Cl-C₆H₄)₂CH⁺ ($E = 6.02$) as quoted in Table 3. For the benzyl- and alkyl cations listed in Table 3, barrierless *N*-attack is expected, and the slightly higher k_S/k_N ratios for PhCH₂⁺ and *sec*-butyl cations may indicate nucleophilic assistance of ionization by sulfur (change to S_N2). Product ratios obtained from NCS⁻ and stabilized carbocations ($E < 3$) have not been reported because it was realized that thiocyanates R-SCN obtained from such carbocations would reionize and eventually give isothiocyanates R-NCS, the thermodynamically favored products.

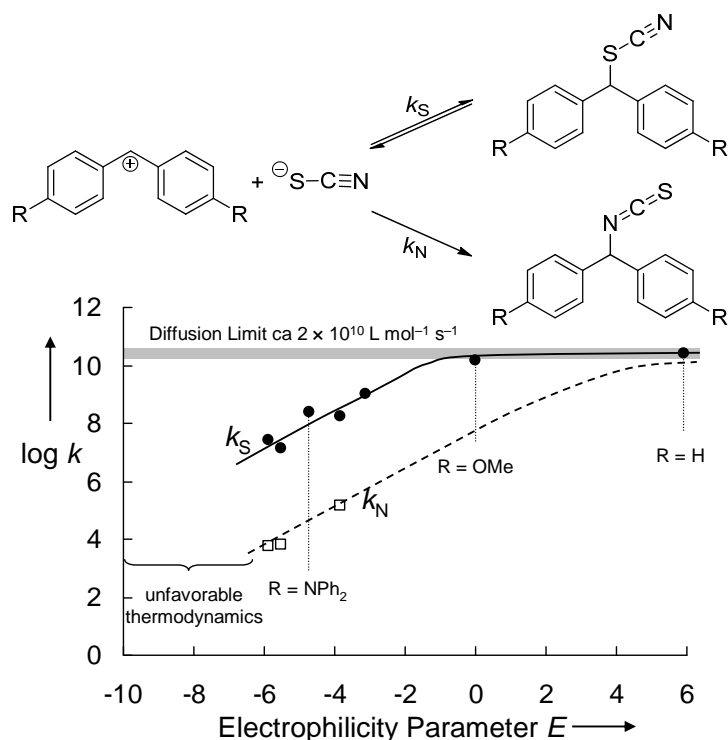
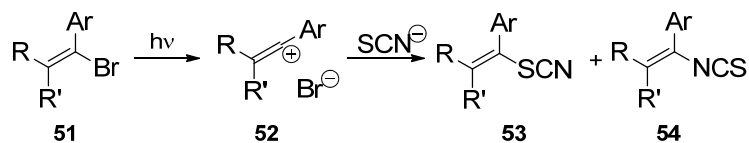


Figure 7: Rate constants ($\log k$) for the reactions of benzhydrylium ions with the thiocyanate ion at the *S* and *N* terminus (20 °C, CH₃CN, from ref^[13a]).

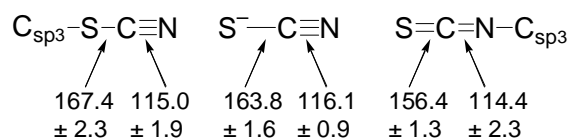
In agreement with this interpretation, photochemically generated vinyl cations **52** (E ca. 3.3 – 5.4)^[71] underwent diffusion-controlled reactions with thiocyanate anions at both termini of SCN⁻ with the *S*-attack slightly dominating (Scheme 29).^[72] Because the ionization of vinyl derivatives is generally very slow, isomerizations of the initially formed vinyl thiocyanates to vinyl isothiocyanates through ionization and subsequent ion recombination was not observed.



Scheme 29: Reaction of photochemically generated vinyl cations **52** with thiocyanate (from ref^[72]).

For some reactions of benzhydrylium ions with SCN⁻, rate and equilibrium constants could be measured.^[13a] Substitution of these data into the Marcus equation yielded intrinsic barriers of approximately 61 kJ mol⁻¹ for the attack of benzhydrylium ions at nitrogen and of 35–38 kJ mol⁻¹ for sulfur attack.

In line with these findings, lower intrinsic barriers for *S*-attack have been derived computationally [MP2/6-31+G(2d,p)] by comparing the Gibbs energies of activation of the identity reactions [Eq. (5), Scheme 4]. Qualitatively, the ordering of the intrinsic barriers follows Hoz' rule, since sulfur is further right in the periodic table than nitrogen. The smaller intrinsic barrier for sulfur attack can also be explained in terms of Hine's PLNM model, because less reorganization energy is required for the formation of thiocyanates than of isothiocyanates due to the closer structural resemblance of thiocyanate anions with alkyl thiocyanates than with alkylisothiocyanates (Scheme 30).



Scheme 30: Average bond lengths (in pm) of organic thiocyanates, “free” thiocyanate anions, and organic isothiocyanates derived from crystal structures (from ref ^[13a]).

As the thermodynamic preference of alkyl isothiocyanates over alkyl thiocyanates is relatively small ($\Delta\Delta G^0 = 17.1 \text{ kJ mol}^{-1}$ for H_3CNCS and H_3CSCN), kinetically controlled alkylations of NCS^- occur generally at the intrinsically preferred site (sulfur) to give alkyl thiocyanates that may rearrange to isothiocyanates under thermodynamically controlled conditions.

3.2.2 Acylation Reactions

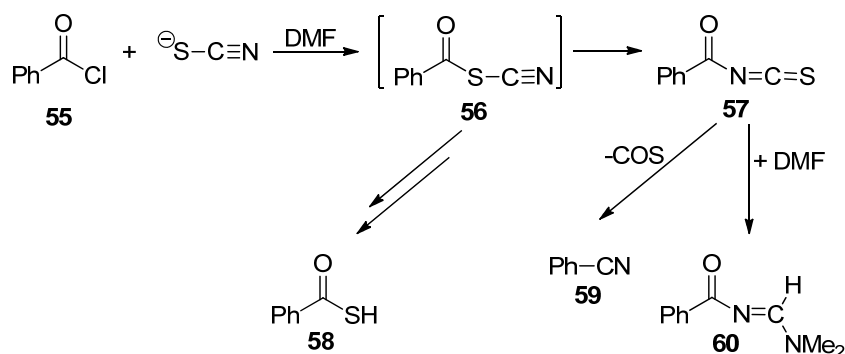
The reaction of acyl chlorides with thiocyanate ions (Scheme 31) first published by Miquel^[73] in 1877 is still the most common method for preparing acyl isothiocyanates.^[74] This regioselectivity was one of the experimental facts, Klopman set out to rationalize by the “Concept of Charge- and Frontier-Orbital-Controlled-Reactions”.^[5a]



Scheme 31: Synthesis of aryl isothiocyanates from an acyl chloride and thiocyanate.

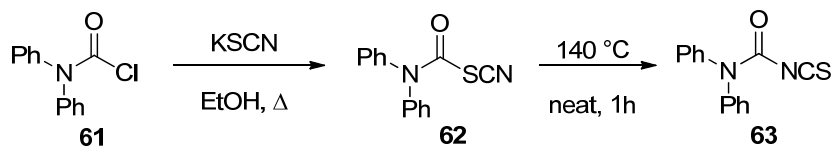
Trying to answer the question why acyl chlorides attack at the nitrogen terminus of SCN^- while methyl iodide attacks at sulfur, Kornblum overlooked that already in 1961 Ruske provided evidence for kinetically controlled *S*-attack of benzoyl chloride at SCN^- . Thiobenzoic acid (**58**), benzonitrile (**59**), and *N,N*-dimethyl-*N'*-benzoylformamide (**60**) were

isolated when benzoyl chloride (**55**) was combined with KSCN or Pb(SCN)₂ in DMF. As shown in Scheme 32, the formation of these products was interpreted by the initial formation of benzoyl thiocyanate (**56**), which was partially hydrolyzed before it rearranges to the thermodynamically more stable benzoyl isothiocyanate (**57**).^[75]



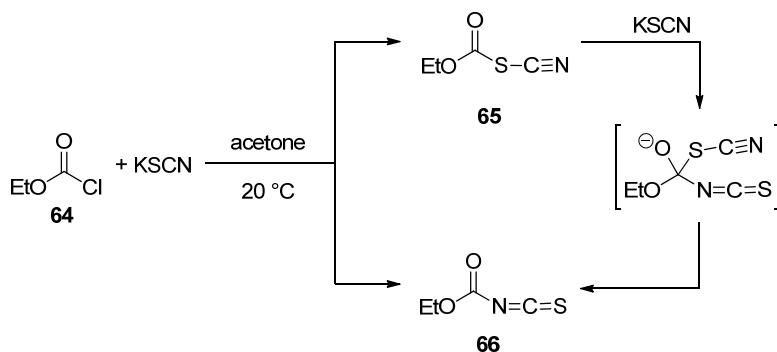
Scheme 32: Reaction of benzoyl chloride (**55**) with thiocyanate in DMF (from ref^[75]).

Analogously, SCN⁻ was exclusively attacked at sulfur when diphenylcarbamoyl chloride (**61**) was heated with KSCN in ethanol; the resulting carbamoyl thiocyanate **62** rearranged to the corresponding isothiocyanate **63** at 140 °C (Scheme 33).^[76]



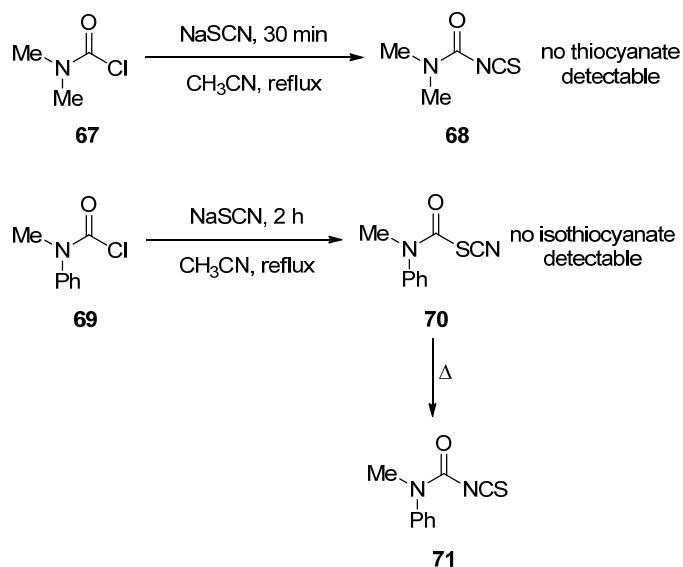
Scheme 33: Synthesis of diphenylcarbamoyl thiocyanate (**62**) and its rearrangement to the isothiocyanate (**63**) (from ref^[76]).

Takamizawa, Hirai, and Matsui^[77] isolated a 1:1 mixture of thiocyanate **65** and isothiocyanate **66** in the reaction of ethyl chloroformate (**64**) with potassium thiocyanate in acetone. The isolated ethoxycarbonyl thiocyanate **65** is thermally stable when refluxed in ethanol; however, an isomerization of the thiocyanate **65** to the isothiocyanate **66** occurs in the presence of KSCN in acetone at 20 °C (Scheme 34).



Scheme 34: Reaction of ethyl chloroformate (**64**) with potassium thiocyanate in acetone (from ref^[77]).

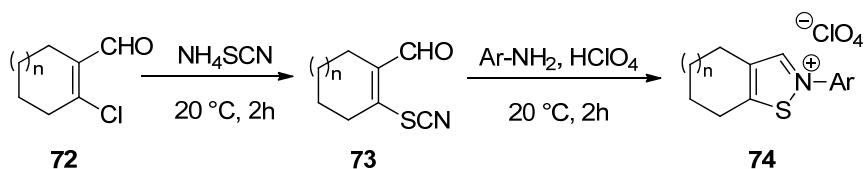
Goerdeler and Wobig studied the reactions of differently substituted carbamoyl chlorides with NaSCN in boiling acetonitrile and found a “dualism” in selectivity (Scheme 35); they stated that “*earlier investigators had sometimes failed to observe that these reactions are not unambiguous*”.^[78] According to Goerdeler and Wobig, aliphatic carbamoyl chlorides, like *N,N*-dimethylcarbamoyl chloride (**67**) reacted with NaSCN in refluxing acetonitrile to give the isothiocyanate **68** without the intermediate formation of thiocyanates. However, in liquid SO₂, mixtures of thiocyanates and isocyanates were formed as shown by IR spectroscopy. The analogous reaction of *N*-methyl-*N*-phenyl-carbamoyl chloride (**69**) with NaSCN in acetonitrile gave the thiocyanate **70** selectively which rearranged to the corresponding isothiocyanate **71** upon warming.



Scheme 35: Reactivity of thiocyanate anions with different carbamoyl chlorides in CH₃CN (from ref^[77]).

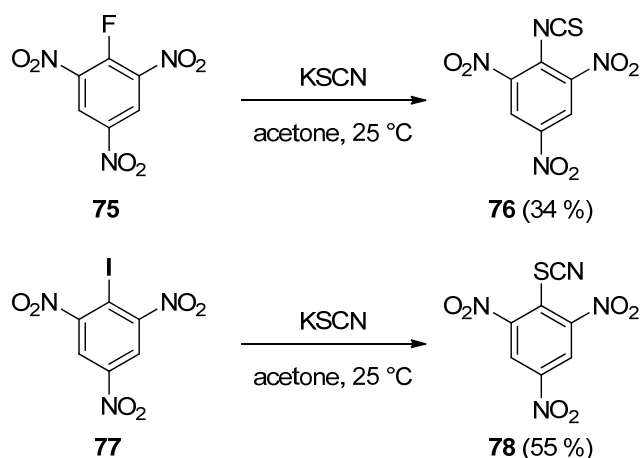
3.2.3 Nucleophilic Vinylic and Aromatic Substitution

Preferred *S*-attack was also reported in nucleophilic vinylic substitutions. Treatment of the chlorinated cyclohexene carbaldehyde **72** with NH_4SCN gave the vinyl thiocyanate **73** which was combined with aniline to yield the isothiazolium ion **74** (Scheme 36).^[79]



Scheme 36: Preferred *S*-attack of thiocyanates on vinyl chlorides (from ref.^[79b]).

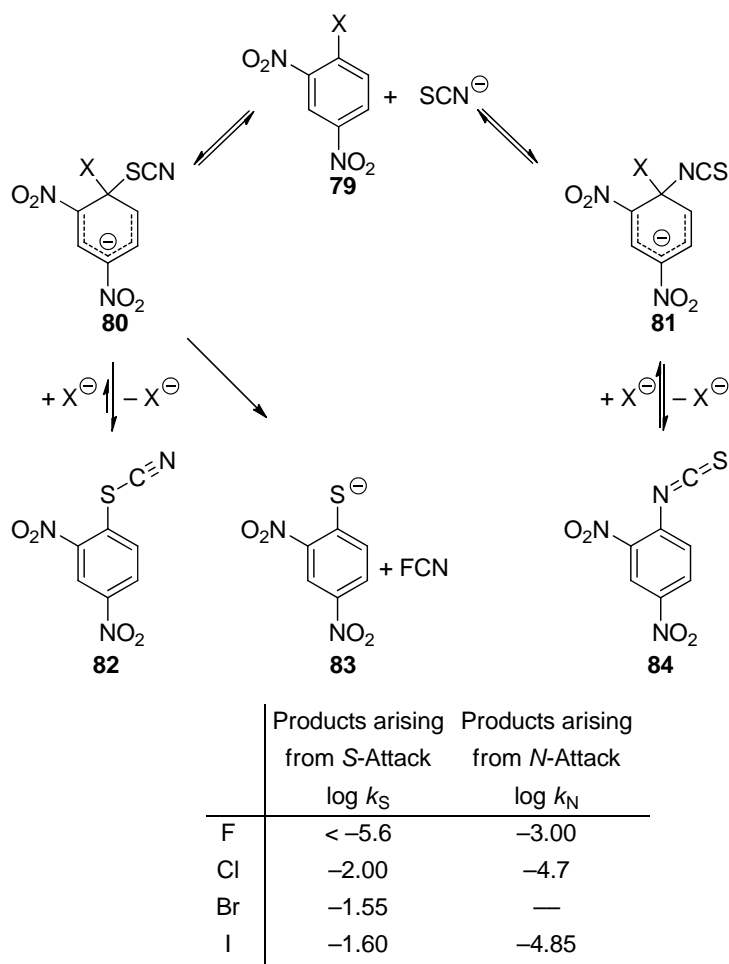
Giles and Parker^[80] studied the nucleophilic aromatic substitutions of dinitro- and trinitrohalobenzenes with the thiocyanate anion and concluded that the harder fluoro compounds react preferentially with the harder nitrogen of SCN^- whereas the softer iodo arene is attacked by the softer sulfur terminus (Scheme 37).



Scheme 37: Ambident reactivity of thiocyanate with aryl halides (from ref.^[80]).

However, the individual rate constants for the reactions of 2,4-dinitrohalobenzenes **79** with SCN^- reported in the same article (Scheme 38) suggest an alternative interpretation. We assume that also in this reaction *S*-attack with formation of the σ -adduct **80** is faster than the formation of **81**, independent of the nature of X. Since Cl^- , Br^- , and I^- are better leaving groups than NCS^- , the corresponding σ -adducts (**80**, X = Cl, Br, I) yield the aryl thiocyanates **82** which are thus formed in a fast reaction. As F^- is a poorer leaving group, the σ -adduct **80** (X = F) expels F^- only slowly and partially undergoes retroaddition with formation of **79** and SCN^- . In this way, the formation of σ -adduct **81**, which is thermodynamically more favorable

than **80**, becomes possible. Now elimination of F^- can occur, which leads to the formation of **84**. Although it is well established that attack of nucleophiles at 2,4-dinitrohalobenzenes initially occurs at C-3 or C-5, the corresponding intermediates are not relevant for the final products and are, therefore, neglected in Scheme 38.



Scheme 38: Nucleophilic aromatic substitution of 2,4-dinitrohalobenzenes **79** with thiocyanate in DMF at 75 °C (from ref^[80]).

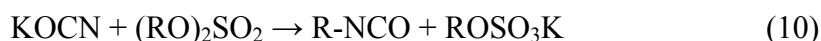
3.2.4 Summary: Ambident Behavior of SCN^-

In summary, thermodynamically controlled reactions with SCN^- generally yield isothiocyanates while kinetically controlled reactions yield thiocyanates. It is the lower intrinsic barrier for *S*-attack which controls the regioselectivity of kinetically controlled reactions because the thermodynamic preference for *N*-attack is too small to overrule the intrinsic preference for *S*-attack.

3.3 Nitrogen vs. Oxygen Attack

3.3.1 Cyanate Anion

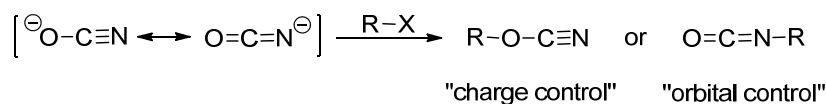
The most common method to synthesize alkyl isocyanates is the reaction of dialkyl sulfates with alkali metal cyanates [Eq. (10)], as reported by Wurtz^[81] and later modified by Slotta and Lorenz.^[82]



However, it cannot be excluded that the selective formation of alkyl isocyanates in these reactions is due to an (auto)catalyzed isomerization of an initially formed alkyl cyanate to the thermodynamically more stable isocyanate [Eq. (11)], since ethyl cyanate has been reported to rearrange to ethyl isocyanate in polar and nonpolar solvents.^[83]



According to semiempirical calculations, the charge density in cyanate ions is higher at oxygen, while the larger HOMO coefficient is at nitrogen.^[84] Employing the concept of charge and orbital control, Schädler and Köhler rationalized the preferred formation of isocyanates by the dominance of orbital control (Scheme 39).



Scheme 39: Common description of ambident reactivity of the cyanate anion.

Our studies on the reactions of OCN^- with benzhydrylium ions showed the exclusive formation of benzhydryl isocyanates (Figure 8).^[13d] As no break in the $\log k_2$ vs. E plot was observed when going from weakly electrophilic benzhydrylium ions to highly reactive ones, we concluded that the electrophilic attack at oxygen either does not occur or takes place with similar rates as the attack at nitrogen. However, because of the low thermodynamic stability of benzhydryl cyanates we cannot exclude that benzhydryl cyanates are formed in a fast, highly reversible initial step, which is irrelevant for the observed kinetics.

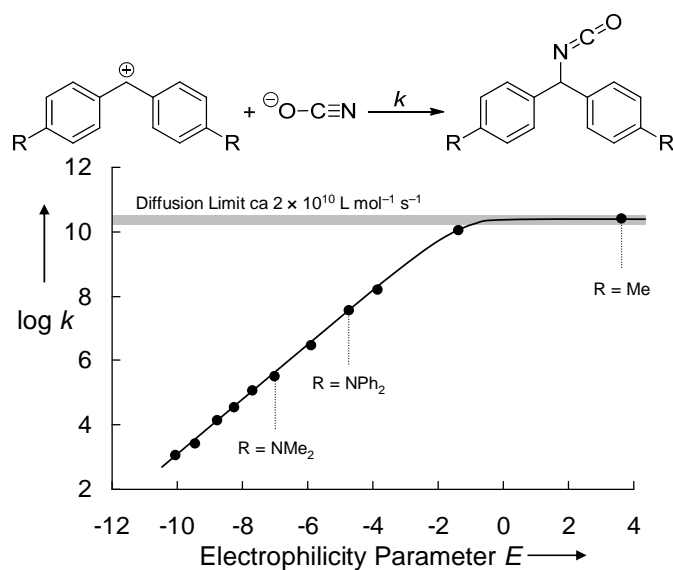


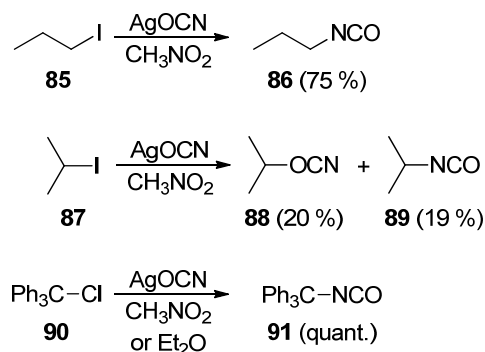
Figure 8: Plot of $\log k_2$ for the reactions of the cyanate ion with benzhydrylium ions vs. their electrophilicity parameters E (20 °C, CH_3CN) (from ref^[13d]).

Figure 8 shows that all carbocations with $E > -1$ (carbocations that are less stabilized than the dianisylcarbenium or the tritylium ion, i.e., typical $\text{S}_{\text{N}}1$ substrates) will undergo barrierless reactions with cyanate. These reactions proceed without passing through a transition state, and therefore, cannot be rationalized by transition state models.

According to Table 1, alkyl isocyanates are considerably more stable than alkyl cyanates. On the other hand, *O*-attack, i.e., attack at the atom further right in the periodic table, is preferred intrinsically as derived from the identity reactions summarized in Scheme 4. As the $\Delta\Delta G^0$ term (Table 1) is much larger than the $\Delta\Delta G_0^\ddagger$ term (Scheme 4), the experimentally observed *N*-alkylations are in line with the predictions of Marcus theory.

With the nucleophilicity parameters $N = 13.60$ and $s = 0.84$,^[13d] which can be derived from the linear part of Figure 8, one can now rationalize the change of regioselectivity in the reactions of alkyl halides with AgOCN described by Holm and Wentrup (Scheme 40).^[83d] As primary alkyl cations do not exist in the condensed phase, the exclusive formation of propyl isocyanate (**86**) from propyl iodide (**85**) can be explained by an $\text{S}_{\text{N}}2$ reaction, where the transition state is controlled by the product stability term and not by the intrinsic term for the reasons discussed above. The mixture of isopropyl cyanate (**88**) and isopropyl isocyanate (**89**) reflects the result of diffusion-controlled reactions of the cyanate anion with the isopropyl cation, which can be derived from Eq. (1) using N and s for NCO^- and an estimated

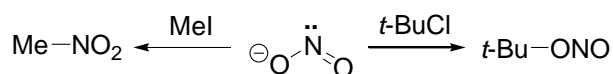
electrophilicity parameter of $E \gg 8$ for iPr^+ .^[40] From the low thermodynamic stability of alkyl cyanates (Table 1) and the low intrinsic barriers for *O*-attack, one can derive that a potentially generated trityl cyanate would rapidly reionize and generate the more stable trityl isocyanate (**91**) (thermodynamic product control).



Scheme 40: Experimentally observed regioselectivities for the reactions of silver cyanate with different alkyl halides (from ref^[83d]).

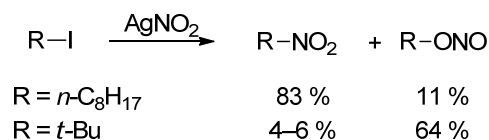
3.3.2 Nitrite Anion

Extensive investigations^[2b-g] on the reactions of the nitrite ion with alkylating agents led Kornblum to the conclusion "*The greater the carbonium contribution to the transition state, the greater is the yield of nitrite ester and the smaller is the yield of nitroparaffin*".^[2e] However, Pearson's specification of this rule, "**t*-C₄H₉Cl reacts with the hard oxygen atom of NO₂⁻, while the softer CH₃I reacts with the softer nitrogen atom,*"^[3c] which was expressed by Scheme 41 in later theoretical treatments of ambident reactivity,^[5a, 85] is not consistent with experimental findings; CH₃I and other primary haloalkanes actually yield mixtures of alkyl nitrites and nitroalkanes with either NaNO₂ or AgNO₂.^[2b-g, 86]



Scheme 41: Partially incorrect generalization of the ambident reactivity of the nitrite anion (from ref^[5a]).

Previous statements such as "*Although silver nitrite does react with alkyl halides to give nitrites, sodium nitrite gives more nitroalkane than alkyl nitrite*"^[5d] were contradicted by Streitwieser, Heathcock, and Kosower who refer to Kornblum's studies on the reactions of iodoalkanes with NaNO₂ and AgNO₂ and concluded "*Yields of nitroalkane are higher when silver nitrite is used, but this added economy is tempered by the cost of silver salt*" (Scheme 42).^[87]



Scheme 42: Reaction of silver nitrite with alkyl iodides yielding the nitroalkane and alkyl nitrite. (from ref^[2a, 2c]).

The HSAB model and the concept of charge and orbital control thus correctly predict that the reaction of *tert*-butyl chloride with silver nitrite yields *tert*-butyl nitrite preferentially (64 % *t*Bu-ONO and 4–6 % *t*Bu-NO₂)^[2c] but mislead the chemist intending to synthesize primary nitroalkanes. These concepts would advise not to combine alkyl halides with silver nitrite, the method which provides the highest yields of nitroalkanes (Scheme 42).

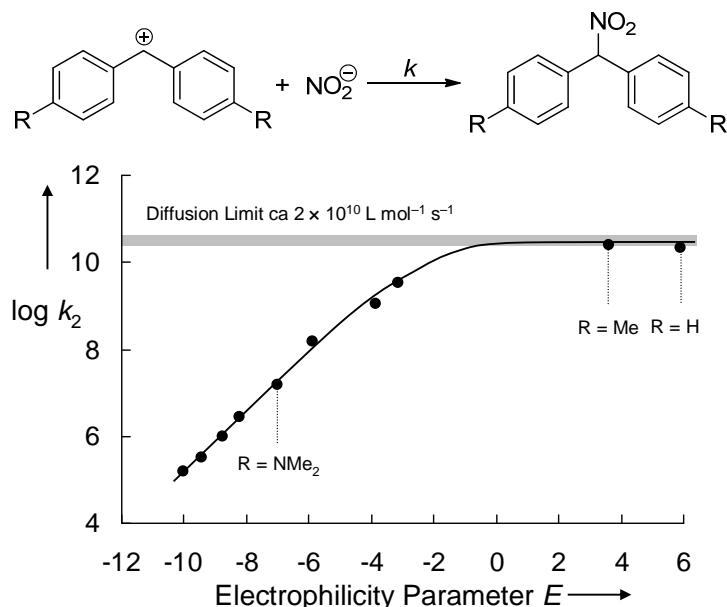
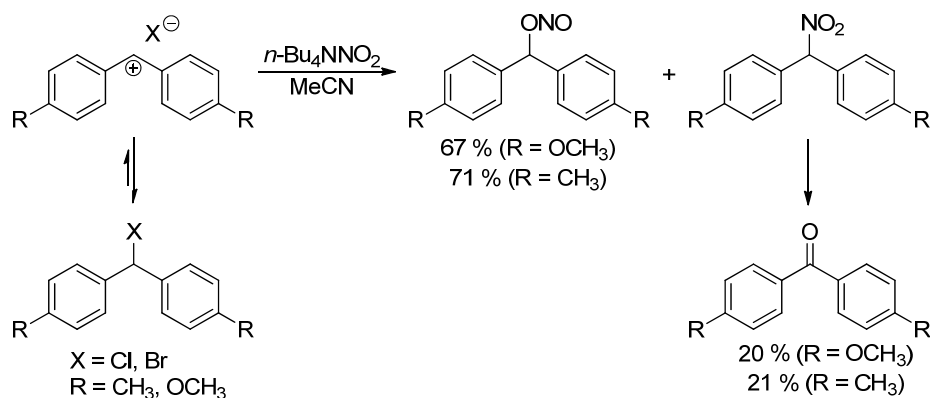


Figure 9: Plot of $\log k_2$ for the reactions of the nitrite ion with benzhydrylium ions vs. their electrophilicity parameters E (20 °C, CH₃CN, from ref^[13c]).

Our investigations on the rates of the reactions of benzhydrylium ions with nitrite ions in acetonitrile^[13c] showed (Figure 9) that carbocations with electrophilicity parameters $E > 0$, i.e., the bis(4-methoxyphenyl)carbenium ion and all less stabilized carbocations undergo diffusion-controlled reactions with the nitrite ion. For that reason, the reactions of *tert*-alkyl cations ($E \approx 7$ –8) with nitrite ions do not proceed through classical transition states, and attempts to predict relative activation energies for *O*- and *N*-attack by frontier orbital models are inappropriate.

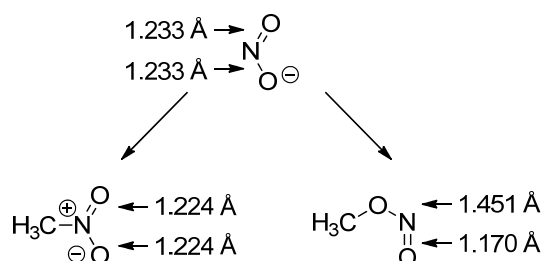
Carbocations with electrophilicities $E < -3$ have been found to react reversibly with NO_2^- , and the exclusive formation of nitro compounds was explained by thermodynamic control because the nitro compounds are thermodynamically more stable than the isomeric alkyl nitrites.^[88]

The bis(*p*-methoxy)- and the less stabilized bis(*p*-methyl)-substituted benzhydrylium ions **92** undergo diffusion controlled, irreversible reactions with nitrite anions to give ~70 % of benzhydryl nitrites **93** by *O*-attack and ~20 % of benzophenones **95** (Scheme 43) which are formed from the corresponding diarylnitromethanes as described by Wagner and Mioskowski.^[89]



Scheme 43: Reactions of less stabilized benzhydrylium ions with nitrite in acetonitrile (from ref^[13c]).

The exclusive formation of nitroalkanes under conditions of thermodynamic product control is in accordance with our calculations [MP2/6-311+G(2d,p)] which showed that nitromethane is 28.3 kJ mol^{-1} more stable than methyl nitrite (Table 1).



Scheme 44: Bond lengths in nitrite anion, nitromethane, and methyl nitrite (from ref^[90]).

Calculated activation energies for the identity reactions [Eq. (5)] showed similar intrinsic barriers for *O*- and *N*-attack (Scheme 4). In this case, the Hoz-effect, which favors attack at

oxygen because of its position in the periodic table, is obviously compensated by the high reorganization energy for *O*-attack, which can be derived from the greater change of bond lengths when generating methyl nitrite from nitrite anions (Scheme 44).^[90]

From almost identical intrinsic barriers for *O*- and *N*-attack and a thermodynamic term which favors *N*-attack, one would derive that nitroalkane formation is generally preferred over alkyl nitrite formation also in kinetically controlled reactions. As mixtures of methyl nitrite and nitromethane are observed when nitrite anions are treated with different methylating agents (Table 4) we have to conclude that in contrast to the results shown in Scheme 4 there must be a weak intrinsic preference for *O*-alkylation, which compensates the $\Delta\Delta G^0$ term in the Marcus equation. It should be noted, however, that the selectivities shown in Table 4 are also not related to the hardness of the electrophiles.

Table 4: *N/O* Selectivities for Methylation Reactions of Nitrite Salts.

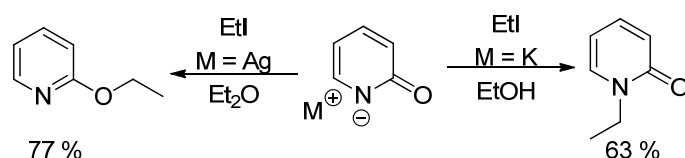
Nitrite	Electrophile	Solvent	MeNO ₂ / MeONO	ref.
AgNO ₂	MeI	DMSO	54 : 46	[86]
NaNO ₂	MeI	DMSO	46 : 54	[86]
AgNO ₂	MeI	DMF	46 : 54	[86]
NaNO ₂	MeI	DMF	46 : 54	[86]
(<i>n</i> Bu ₄ N)NO ₂	MeI	CDCl ₃	70 : 30	[13c]
(<i>n</i> Bu ₄ N)NO ₂	MeOSO ₂ Me	CDCl ₃	67 : 32	[13c]
(<i>n</i> Bu ₄ N)NO ₂	Me ₃ OBF ₄	CDCl ₃	50 : 50	[13c]
(<i>n</i> Bu ₄ N)NO ₂	MeOSO ₂ CF ₃	CDCl ₃	41 : 59	[13c]

3.3.3 Amides and Amide Anions

The observation that the potassium salt of 2-pyridone reacted with ethyl iodide at nitrogen^[91] while the corresponding silver salt was alkylated at oxygen^[92] (Scheme 45) was one of the examples which prompted Kornblum to formulate his rule, which later became integrated in the HSAB principle of ambident reactivity and the Klopman-Salem concept of charge and orbital controlled reactions.^[2e]

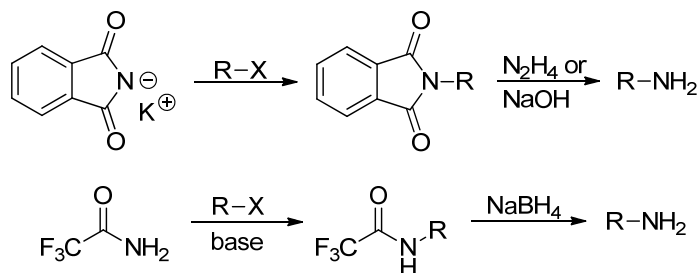
Systematic investigations of the alkylations of 2-pyridone salts by Tieckelmann^[92] showed “*that the results are completely consistent with Kornblum’s proposal that the silver ion enhances unimolecular character in the silver salt reactions, thereby favoring alkylation at*

the more electronegative oxygen atom”.^[92a] However, at the end of his thorough investigation, Tieckelmann stated: “The mechanism which leads to oxygen alkylation of the silver salts of 2-pyridones also needs further examination and may be more related to heterogeneous reaction than to the ability of the silver ion to promote unimolecular reaction as previously suggested”.^[92a]



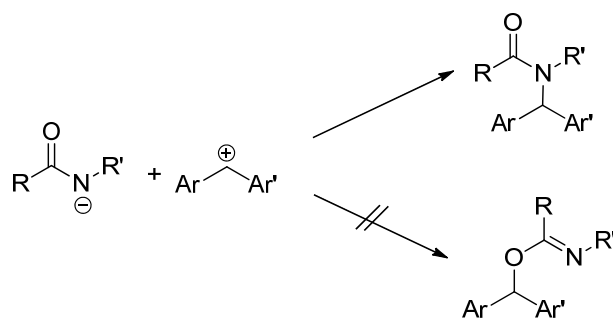
Scheme 45: Regioselective alkylation of potassium (from ref^[90]) and silver (from ref^[91]) salts of pyridones.

Selective *N*-attack has also been observed with alkali salts of other amide and imide anions.^[94] This selectivity is synthetically used in Gabriel syntheses and related reactions (Scheme 46).^[95]



Scheme 46: Gabriel synthesis and related methods for the preparation of amines (from ref^[95a, 96]).

Oxygen-alkylation of imide anions has only been observed when silver salts were employed.^[97] However, this effect cannot be explained by a change from S_N2 to S_N1 mechanism because systematic investigations of the reactions of amide and imide anions with benzydrylium ions showed, that nitrogen attack is also preferred with carbocations (Scheme 47).^[13h] X-ray investigations have shown that Ag^+ is coordinated to the nitrogen of imide anions^[98] and thus blocks the attack of electrophiles at *N*.



Scheme 47: Reactions of amide anions with benzhydrylium ions in DMSO (from ref ^[13g]).

According to entry 7 of Table 1, amides are 80 kJ mol^{-1} more stable than the isomeric imidates. The resulting larger $\Delta\Delta G^0$ term in the Marcus equation cannot be compensated by the small intrinsic preference for *O*-attack which is shown in Scheme 4. The selective *N*-alkylation of amide anions under conditions of kinetic and thermodynamic control can thus be explained.

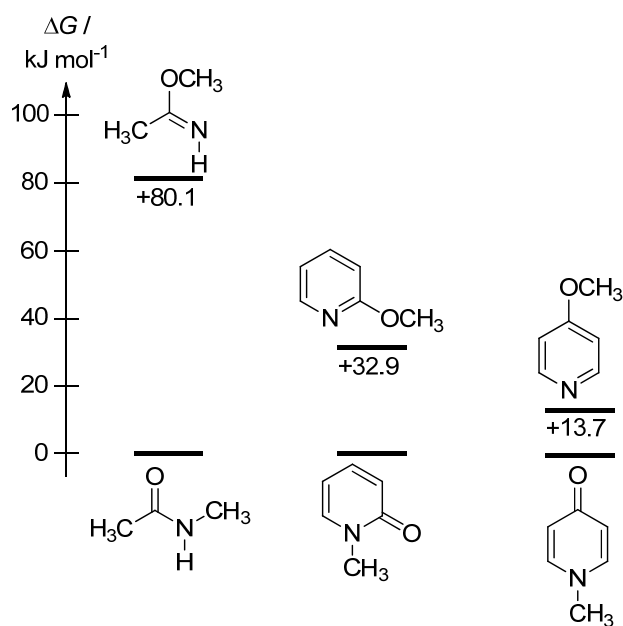


Figure 10: Comparison of the thermodynamic differences of *N*- and *O*-methylated ordinary amides, 2-pyridones, and 4-pyridones (data for pyridones from ref ^[13h]).

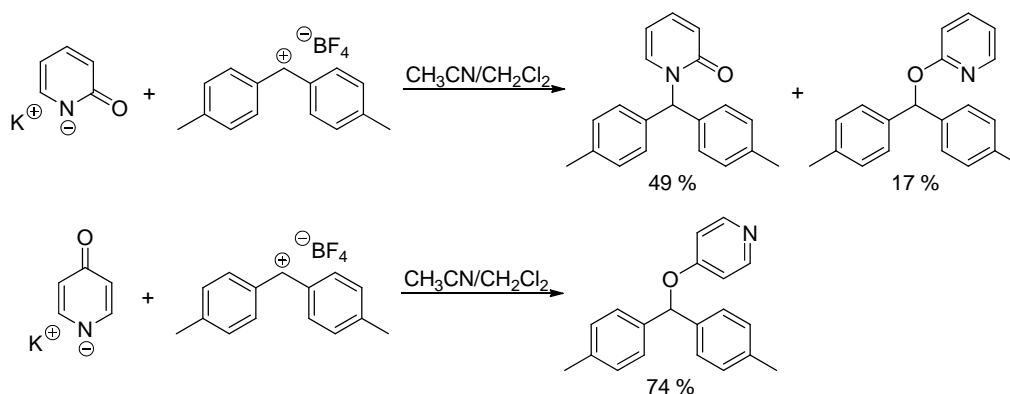
The large thermodynamic preference of the amide over the imidate structure (80 kJ mol^{-1}) is greatly reduced, when the $\text{C}=\text{N}$ bond becomes part of an aromatic ring in the two pyridones. As shown in entries 9 and 10 of Table 1 and Figure 10, *N*-methyl-2-pyridone and *N*-methyl-4-pyridone are only 33 and 14 kJ mol^{-1} more stable than the isomeric methoxypyridines. Because in both cases, *O*-attack is intrinsically slightly favored over *N*-attack (Scheme 4), *N*-attack remains preferred but *O*-attack can compete (Table 5). *O*-attack at the 2-pyridone anion becomes dominating with *i*Pr-I, which may be explained by a steric effect.

Table 5: Effect of Alkylating Agent and Counterion on the *N/O*-Alkylation Ratio for the Alkylation of 2-Pyridone Salts in DMF.^[92]

Entry	Electrophile	Counterion	<i>N/O</i> ratio
1	MeI	Na	95:5
2	MeI	K	92:8
3	PhCH ₂ Cl	Na	94:6
4	PhCH ₂ Br	Na	97:3
5	PhCH ₂ I	Na	98:2
6	EtI	Na	69:31
7	<i>i</i> PrI	Na	30:61 ^[a]

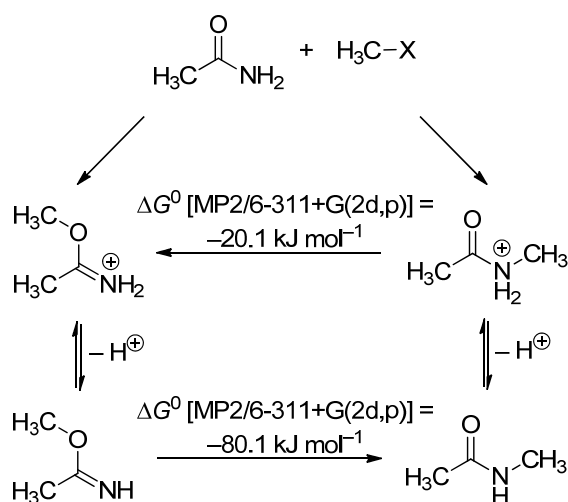
[a] 2-Pyridone was partially recovered.

In kinetically controlled reactions of pyridone anions, *N*-attack is mostly preferred as the thermodynamic contribution to the Gibbs energy of activation (favoring *N*-attack) outnumbers the contribution of the intrinsic barrier (favoring *O*-attack). Only for bulky alkylating agents, $\Delta\Delta G^0$ for *O*- and *N*-attack is strongly diminished, and then, *O*-attack becomes more favorable. While diffusion-controlled reactions of the 2-pyridone anion give mixtures of *O*- and *N*-attack, exclusive *O*-attack was observed in diffusion-controlled reactions with the 4-pyridone anion.^[13h]

Scheme 48: Reactions of the pyridone anions with highly reactive benzhydrylium ions (from ref ^{13h}).

As expected from the relative stabilities depicted in Figure 10, the thermodynamically controlled reactions of the 2- and 4-pyridone anions with amino-substituted benzhydrylium ions gave *N*-benzhydryl pyridones exclusively. *O*-attack was only found in the diffusion-controlled reactions of the pyridone anions with highly reactive carbocations which were quoted above (Scheme 48).

The situation changes dramatically, when neutral amides are alkylated instead of their anions. Whereas *N*-methylation of the acetamide anion is 80 kJ mol⁻¹ more favorable than *O*-methylation, *N*-methylation of the neutral amide is 20 kJ mol⁻¹ less favorable than *O*-methylation (Table 1). Since *O*-attack is also intrinsically highly favored over *N*-attack (Scheme 4), kinetically controlled alkylations of neutral amides should generally yield *O*-alkylation products. However, as the relative thermodynamic stabilities of *O*- and *N*-alkylation products are reversed, when the deprotonated products are considered (Scheme 49), *N*-alkylation takes place under conditions of thermodynamic control.^[99]



Scheme 49: Ambident reactivity of neutral amides.

Gompper and Christmann^[100] studied the alkylations of formamide and found that octyl bromide, a classical S_N2 substrate, yields *O*-alkylated formamide selectively, whereas the tritylium cation leads to selective *N*-alkylation (Table 6).

Table 6: Alkylation of Formamide with Different Alkyl Halides.^[101]

R-X	<i>N</i> -Alkylformamide	Alkyl formate
<i>n</i> -C ₈ H ₁₇ Br	-	92 %
PhCH ₂ Cl	5 %	74 %
Ph ₂ CHCl	95 %	-
Ph ₃ CCl	94 %	-

They concluded that S_N2 reactions as well as S_N1 reactions with “instable carbenium ions” occur preferentially at the oxygen atom, while S_N1 reactions with “stable carbenium ions” take place at the nitrogen terminus. In the reactions with stable carbenium ions, the initial O -attack at the neutral amide is reversible and subsequent rearrangement to the thermodynamically more stable amides takes place. As a consequence they concluded that Kornblum’s view “*The greater the S_N1 character of the transition state the greater is the preference for covalency formation with the atom of higher electronegativity*”^[2e] has to be modified for reactions of neutral carboxamides.^[100]

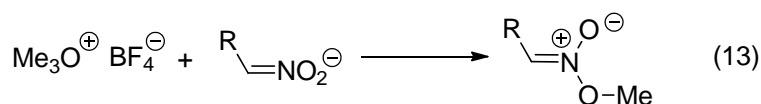
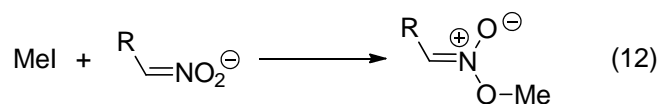
3.4 Oxygen vs. Carbon Attack

3.4.1 Nitronate Anions

Deprotonated nitroalkanes are an important class of ambident anions which are widely used in organic synthesis. According to the HSAB principle, nitronate anions are expected to react at carbon with soft electrophiles yielding nitroalkanes and at oxygen with hard electrophiles yielding nitronic esters.

In 1984 Katritzky and Musumarra^[102] clearly contradicted this interpretation. Referring to a 1945 paper by Weisler and Helmkamp,^[103] they stated: “*It is well known that the alkylation of nitronate anions by halides or tosylates, which are ionic reactions, give exclusively O -alkylations*”.

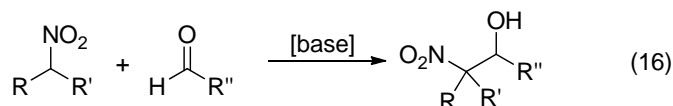
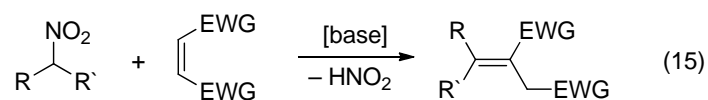
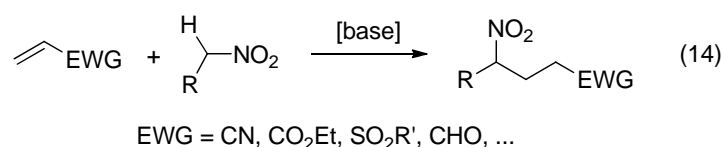
Preferred O -attack at nitronate anions by soft alkyl halides like methyl iodide [Eq. (12)] as well as with the hard methylating agent $\text{Me}_3\text{O}^+\text{BF}_4^-$ [Eq. (13)] has been confirmed by Severin^[104] and Kornblum.^[105] It depends on the reaction conditions, whether the nitronic esters can be isolated.^[103]



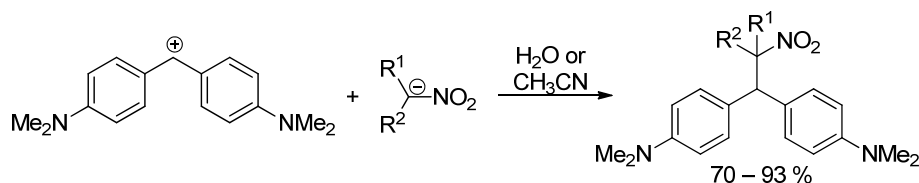
According to Table 1 (entry 11), nitroethane, the C -methylated product of the nitromethyl anion is much more stable (120 kJ mol^{-1}) than the methyl nitronate obtained by O -methylation of the nitromethyl anion. On the other hand, the intrinsic barrier for O -attack is much smaller than the barrier for C -attack (Scheme 4), in line with Hoz’ rule, because oxygen

is further right in the periodic table than carbon, and the Principle of Least Nuclear Motion, as *C*-alkylation requires a rehybridization from C_{sp^2} to C_{sp^3} .

We, therefore, explain the selective *C*-attack by Michael acceptors (acrylonitrile, alkyl acrylates, vinyl sulfones, etc., [Eqs (14), (15)]) and carbonyl groups [Eq. (16)] not by soft-soft interactions but by the fact that a potential *O*-attack would be reversible because of the low thermodynamic stability of the resulting products.



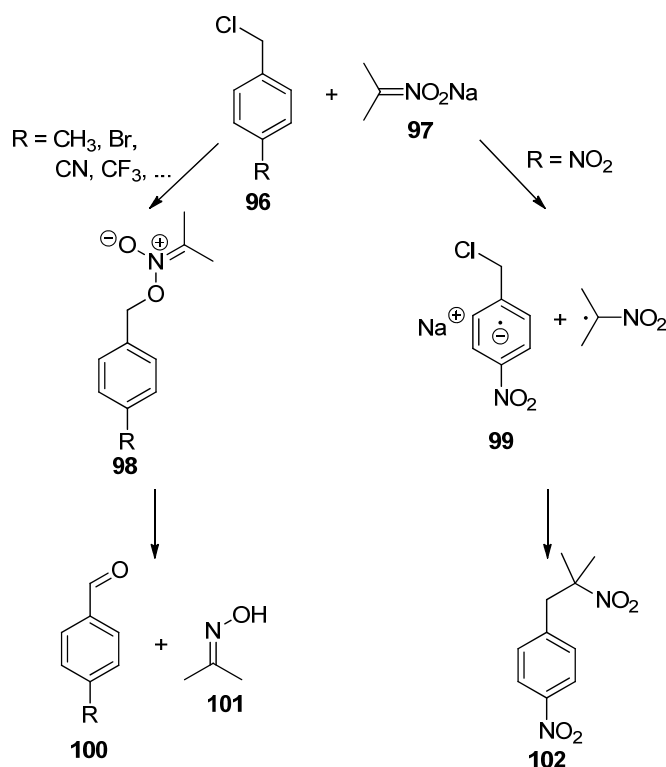
An analogous behavior was observed in the reactions with stabilized benzhydrylium ions. Though carbocations are generally regarded as hard electrophiles, amino-substituted benzhydrylium ions exclusively gave the products of *C*-attack with a large variety of nitronate ions (Scheme 50).^[13e]



Scheme 50: Reactions of nitronates with benzhydrylium ions yielding exclusively nitro compounds (from ref^[13e]).

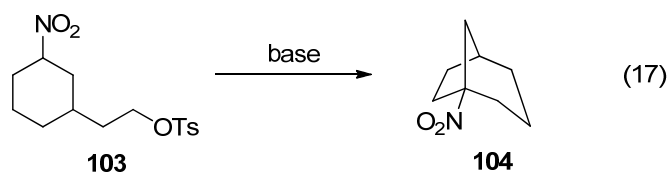
Possibly, these carbocations also react faster at oxygen than at carbon. However, *O*-nitronates are good leaving groups, and the initially generated nitronic esters may undergo retroaddition and finally yield the thermodynamically more stable nitro compounds.^[13e, 106] From the monoexponential decay of the concentrations of the benzhydrylium ions in the presence of excess nitronate anions, it has been derived that the concentration of nitronic esters – if they are formed at all – will always be very small when stabilized benzhydrylium ions are employed.

The intrinsic preference for *O*-attack at nitronate anions is so large that irreversible S_N2 reactions with a variety of alkylating agents generally proceed at oxygen. Thus, the sodium salt of 2-nitropropane (**97**) reacts with benzyl halides **96** at oxygen to give nitronic esters **98** which undergo subsequent cleavage with formation of the corresponding benzaldehydes **100** and the oxime of acetone **101**. Only *p*-nitrobenzyl chloride reacts differently and yields the *C*-alkylation product via a radical mechanism (Scheme 51).^[107] An earlier proposal^[108] that **99** is generated via rearrangement of an initially formed nitronic ester has been rejected by Boyd and Kelly.^[109]

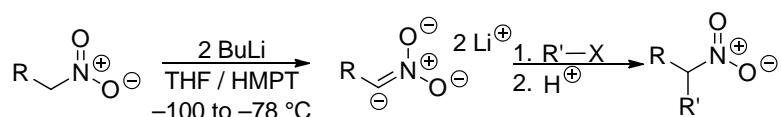


Scheme 51: Reactions of substituted benzyl chlorides **96** with the sodium salt of 2-nitropropane (**97**) (from ref^[107]).

The intramolecular cyclization [Eq. (17)] of **103** to give the bicyclic nitro compound **104**^[110] is another of the rare cases where S_N2 type reactions of nitronate anions proceed via *C*-alkylation.^[111]



Because of the failure to achieve *C*-alkylation of nitronate anions by simple substitution reactions, Seebach developed a method for the α -alkylation of nitroalkanes which proceeds via doubly deprotonated nitroalkanes (Scheme 52).^[112]

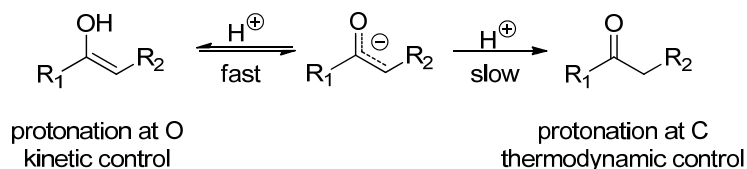


Scheme 52: C-alkylation of nitroalkanes via a dianionic intermediate according to Seebach (from ref^[111]).

3.4.2 Enolate Anions

Enolate anions are probably the most widely used ambident anions in organic synthesis. Their C-alkylation is an important method for the construction of carbon-carbon bonds, whereas O-silylation with formation of silyl vinyl ethers is often used for the protection of carbonyl groups.^[113] The site of attack at enolate anions depends on the structure of the enolate, and the nature of the electrophile, the solvent, and the counterion.^[114] Most alkylation reactions were again interpreted on the basis of the HSAB principle that predicts O-alkylation with hard and C-alkylation with soft electrophiles.

In line with this analysis, Zimmerman^[115] showed that protonation at the hard oxygen yielding the enols occurs in a fast and reversible reaction, whereas the protonation at the soft carbon leads to the thermodynamically more stable ketones in a slow reaction (Scheme 53).



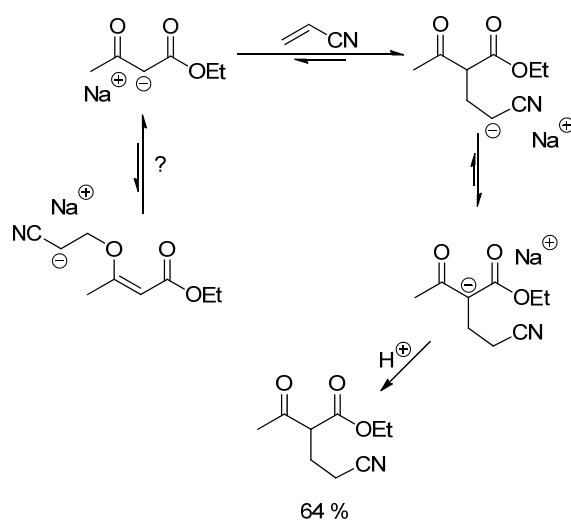
Scheme 53: Protonation of enolates.

However, already in 1986, there were numerous examples, particularly gas-phase studies, which indicated that alkylations of enolate anions may also occur at oxygen. For that reason, Houk and Paddon-Row^[116] investigated the ambident reactivity of the acetaldehyde-derived enolate ion computationally (HF/3-21G and HF/6-31G(d) level of theory) and came to the conclusion that under kinetic control “[...] O-alkylation of enolates is favored with all electrophiles. Changes in C/O alkylation ratios with the nature of the alkyl halide are probably not related to the ‘hardness’ or ‘softness’ of the alkyl halide but to the ability of the halide to influence the structures of metal enolate aggregates.” These conclusions were later confirmed by calculations using basis sets including diffuse functions.^[117]

Computations at the MP2/6-31+G(d)//MP2/6-31+G(d) and QCISD/6-31+G(d)//MP2/6-31+G(d) level of theory by Lee and co-workers^[118] showed that the transition state for the gas phase O-methylation of the enolate H_2CCHO^- by methyl fluoride is favored by 15 kJ mol^{-1}

over *C*-alkylation, which is thermodynamically preferred over *O*-methylation by 98.3 kJ mol⁻¹. A similar difference of product stabilities is given in Table 1.

The thermodynamic preference for *C*-alkylation is counteracted by the relative magnitudes of the intrinsic barriers. Scheme 4 shows that the intrinsic barrier for *C*-alkylation is significantly higher than that for *O*-alkylation, which was already rationalized by Lee with the imbalanced transition structures of *C*-alkylation, where rehybridization of the enolate carbon is required. Hoz' rule leads to the same ordering of intrinsic barriers as oxygen is further right in the periodic table than carbon. As product stabilities and intrinsic barrier favor different sites of attack, it depends on the position of the transition state whether *C*- or *O*-alkylation takes place (Figure 4).

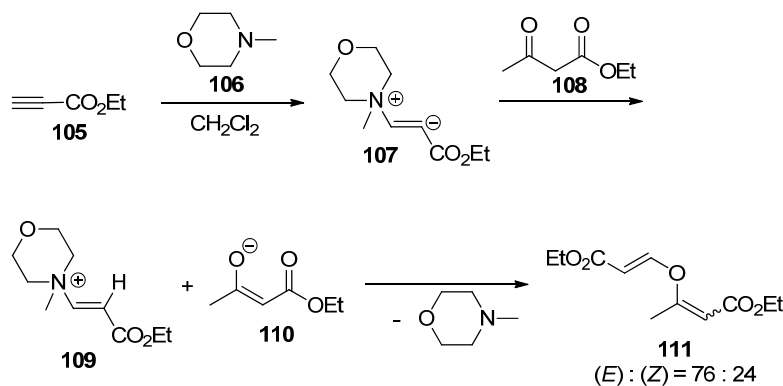


Scheme 54: Michael addition of the sodium salt of ethyl acetoacetate and acrylonitrile (from ref^[119]).

The synthetically important Michael additions of enolate anions to electron-deficient π -systems generally proceed via *C*-attack (Scheme 54). However, we do not interpret this regioselectivity by the favorable soft-soft interaction between the enolate carbon and the 4-position of the Michael acceptor in these reactions, but by the fact, that the corresponding *O*-attack is thermodynamically unfavorable and usually reversible.

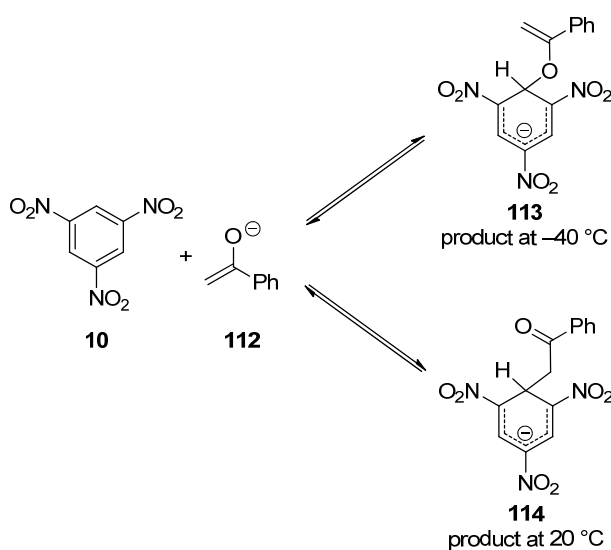
In line with this rationalization, products from *O*-attack can be isolated when the initial adduct formed from an enolate and a Michael system can be stabilized. Thus, Tae and Kim reported the exclusive formation of divinyl ethers **111** by *N*-methylmorpholine (**106**) catalyzed reactions of β -ketoesters or 1,3-diketones with ethyl propiolate (**105**).^[120] As illustrated in Scheme 55 this reaction was explained by initial attack of *N*-methylmorpholine at the alkyne, followed by proton transfer, addition of the enolate anion, and elimination of the tertiary

amine.^[120] The last step of this reaction sequence appears to be irreversible and locks the *O*-regioselectivity of the enolate anion. Exclusive *C*-attack was observed, when *N*-methylmorpholine was replaced by ethyldiisopropylamine.^[121]



Scheme 55: *O*-Attack of ethyl acetoacetate (**108**) at ethyl propiolate (**105**) according to Tae (from ref^[120]).

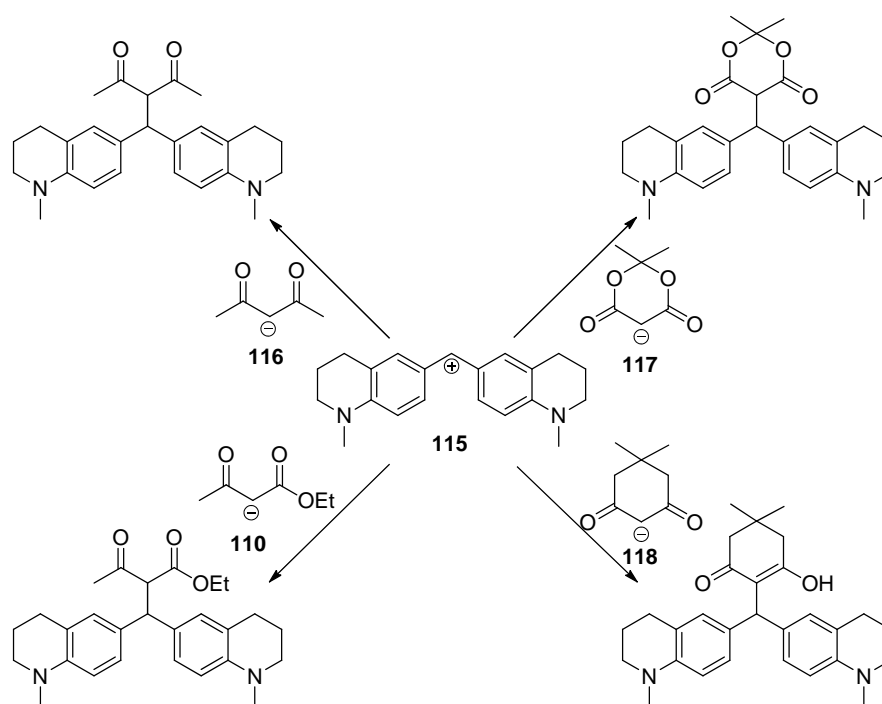
O-attack of an enolate anion at an electron-deficient π -system has also been observed in the reaction of the anion of acetophenone (**112**) at trinitrobenzene. Though 1,3,5-trinitrobenzene (**10**) is considered as a very soft electrophile, Buncler reported that it attacks exclusively the hard site of the enolate of acetophenone at $-40\text{ }^{\circ}\text{C}$.^[122] When the resulting solution of the oxygen-bonded enolate Meisenheimer complex **113** in acetonitrile/dimethoxyethane was warmed up to $20\text{ }^{\circ}\text{C}$, rearrangement to the product of carbon-attack **114** was detected by ^1H -NMR (Scheme 56).



Scheme 56: Kinetically controlled *O*-attack and thermodynamically controlled *C*-attack of the ambident enolate anion of acetophenone (**112**) at 1,3,5-trinitrobenzene (**10**) (from ref^[122]).

Obviously, in both cases the intrinsic preference for *O*-attack is responsible for the regioselectivity of the kinetically controlled reactions.

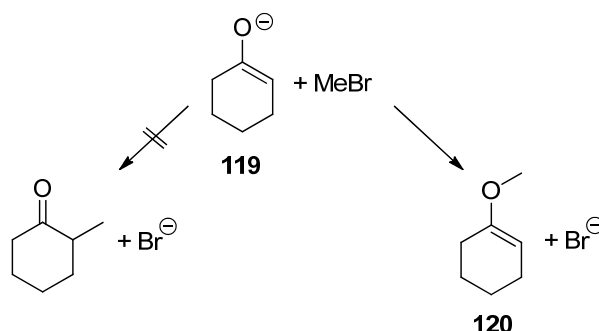
On the other hand, stabilized benzhydrylium ions, commonly regarded as hard electrophiles, attack exclusively at the carbon center of various enolates (Scheme 57), which we rationalize by thermodynamic product control, i.e., reionization of initially generated benzhydryl vinyl ethers.^[10c] From the observation of monoexponential decays of the benzhydrylium absorbance under conditions of pseudo-first-order kinetics (high excess of the enolate anions) one can conclude that the concentration of initially formed benzhydryl enol ethers remains so small that they are kinetically irrelevant.



Scheme 57: Selective C-alkylation of different enolate anions by benzhydrylium ions (from ref^[10c]).

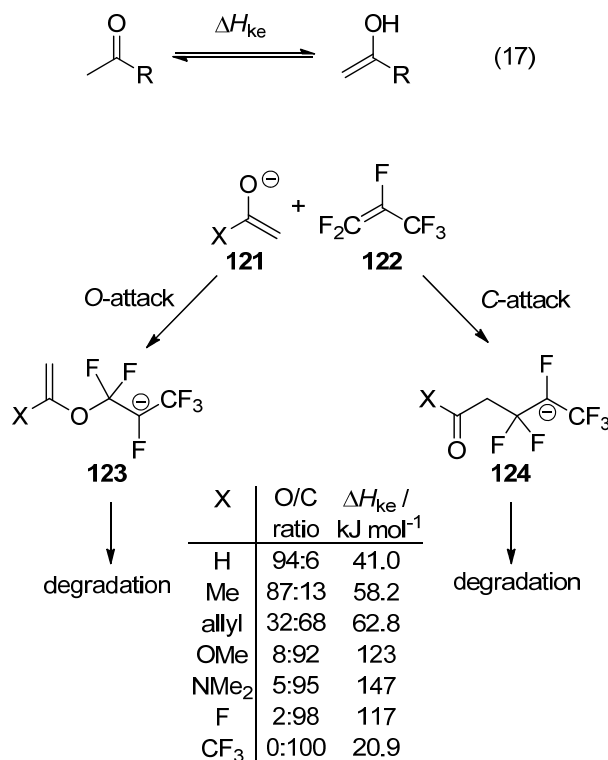
Let us now analyze changes of C/O ratios in gas phase reactions where counterion and solvent effects are eliminated.

Exclusive attack at oxygen was found in the reaction of the enolate derived from cyclohexanone (**119**) with methyl bromide in the gas phase (Scheme 58).^[123] As CH_3Br is commonly considered as a soft electrophile, this observation again contradicts the expectations derived from the HSAB principle.



Scheme 58: Exclusive *O*-alkylation of the cyclohexanone enolate anion with methyl bromide in the gas phase (from ref^[123]).

Brickhouse and Squires^[124] studied the reactions of a variety of enolate anions **121** with hexafluoropropene (**122**) in a flowing afterglow mass spectrometer. They observed that most aldehyde and ketone enolates reacted mainly at oxygen, while enolates with electronegative substituents (e.g., ester and amide enolates) reacted preferentially at carbon. It was reported that compounds with a low keto-enol energy difference ΔH_{ke} [Eq. (17)] tend to react through oxygen, while those with a high energy difference ΔH_{ke} prefer attack at carbon (Scheme 59). Only the enolate derived from trifluoroacetone **121** (X = CF₃) deviates from this rule of thumb.



Scheme 59: Ambident reactivity of enolate ions with hexafluoropropene in the gas phase (ΔH_{ke} from ref^[124-125]).

An analogous trend was reported by Zhong and Brauman who studied the acylation reaction of enolate anions with CF_3COCl in the gas phase by FT-ICR spectroscopy.^[125] While *O*-attack is generally preferred, the *O/C* ratio decreases with increasing keto-enol energy difference ΔH_{ke} (Figure 11).

The first example of Scheme 59, which shows highly preferred *O*-attack, can be rationalized by the dominance of the intrinsic term over the $\Delta\Delta G^0$ term of Eq. (3). The increasing keto-enol energy difference ΔH_{ke} from top to bottom of Scheme 59 implies that the $\Delta\Delta G^0$ term in Eq. (3), which favors *C*-alkylation, increases from top to bottom, and thus explains the observed changes of selectivity.

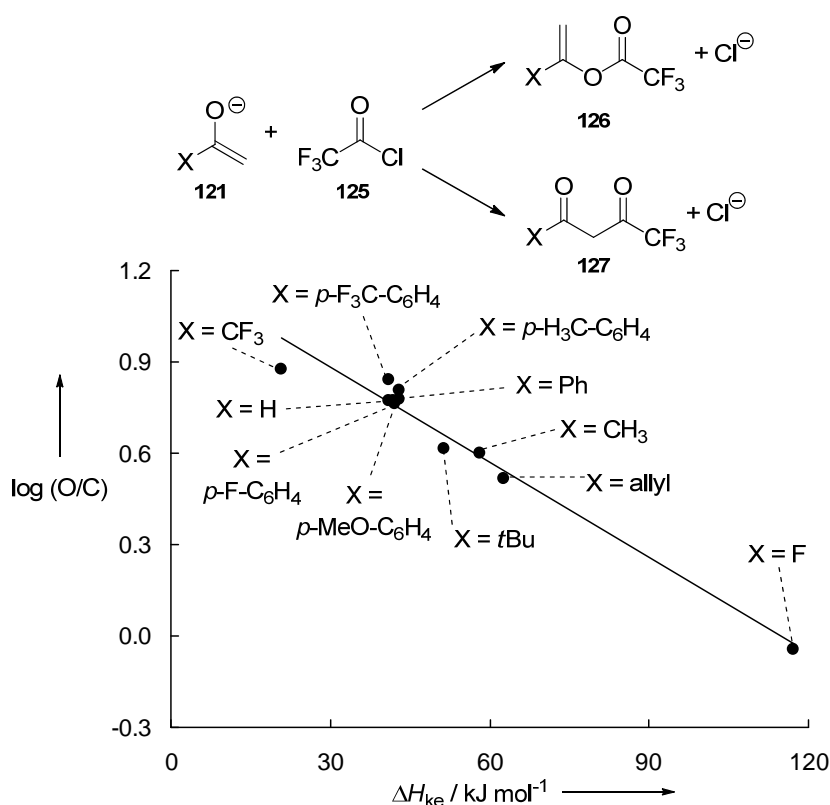
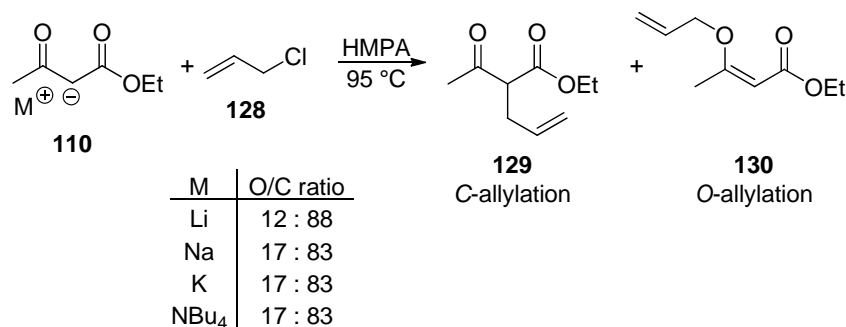


Figure 11: Correlation of *O/C* ratio [$\log(O/C)$] versus the keto-enol-energy difference ΔH_{ke} for several enolate anions (from ref^[125]).

Reactions of enolates in solution are well-known to depend on the nature of the counterion and the solvent.^[114] Le Noble and Morris studied the reaction of ethyl acetoacetate salts **110** with different alkylation agents (Scheme 60) and found that the *O/C* ratio did not change from Na^+ to NBu_4^+ indicating the reactivity of free carbanions.^[126] Only for lithium salts a smaller *O/C* ratio was reported.



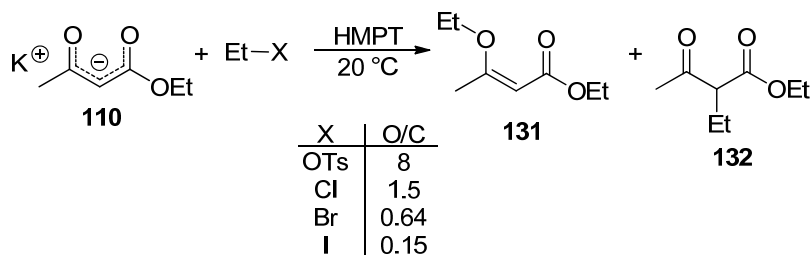
Scheme 60: Dependence of the O/C ratios on different counterions in allylations of ethyl acetoacetate salts (**110**) by allyl chloride (**128**) in HMPA at 95 °C (from ref^[126b]).

In line with these findings, Reutov and co-workers reported that the C/O ratios in the reactions of different alkali salts of ethyl acetoacetate with ethyl tosylate in HMPT are independent of the counterions, and concluded that under these conditions only the free enolate ions were alkylated.^[127]

A much larger effect of the counterions was found in the reaction of the anion of isobutyrophenone with methyl iodide in dimethoxyethane. While almost exclusive C-attack (C/O-ratio > 200) was observed for the lithium salt, the free anion obtained from the lithium salt and a [2.1.1]-cryptand resulted in a C/O ratio of 8.^[128]

Le Noble and co-workers showed that the O/C ratio increases with increasing solvent basicity in the series from acetone, acetonitrile, DMSO, DMF to HMPA.^[126] In less basic solvents the counterion will be less solvated and will coordinate with the oxygen terminus of the enolate. The authors summarized their observations for ethyl acetoacetate concisely: "*The freer the anion, the larger the O/C ratio.*" They concluded that dissociated ions yield high O/C ratios, ion pairs yield intermediate O/C ratios and higher aggregates lead to low O/C ratios.^[126]

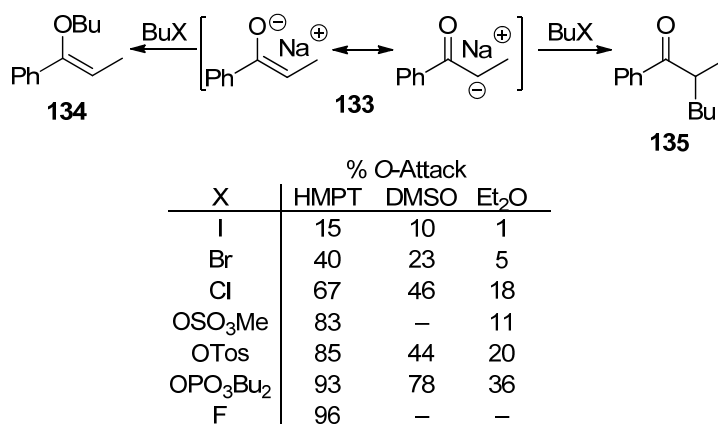
In line with this rule of thumb, the selective formation of O-acylated enols was achieved by the reaction of "naked" enolates (obtained from silyl enol ethers and *n*Bu₄NF) with acyl chlorides.^[121]



Scheme 61: Alkylation of the potassium enolate of ethyl acetoacetate by different alkylating agents in HMPT (from^[127c]).

The change of the O/C ratio in ethylations of the ethyl acetoacetate anion (**110**) with different ethylating agents (Scheme 61) has been rationalized by the decreasing hardness of the electrophile from top to bottom.^[127] This trend cannot be explained by the qualitative Marcus analysis depicted in Figure 5, which neglects the different force constants in the reagents R–X and only considers the different exergonicities of the reactions.

Heiszwolf and Kloosterziel^[129] employed the Principle of Least Nuclear Motion to rationalize the increasing O/C ratio in alkylations of enolate ions with increasing reactivity of the alkylating agent. This suggestion, which is in agreement with the qualitative Marcus analysis in Figure 5, has been rejected by Gompper and Wagner,^[6b] who reported that 1-fluorobutane, the least reactive 1-halobutane gives the highest percentage of *O*-alkylation (Scheme 62). While the increase of the O/C ratio in Scheme 62 with increasing solvent polarity can again be rationalized by the nakedness of the anions, we cannot presently rationalize the dependence of the O/C ratio on the nature of the electrophile. For a detailed discussion, knowledge of the experimental details of Scheme 62 would be needed, which are not accessible for us.

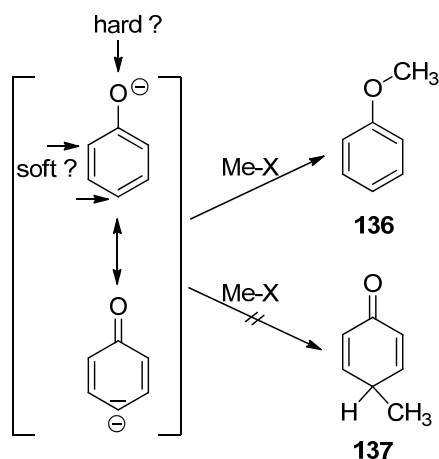


Scheme 62: Proportion of *O*-butylation of the reaction of an enolate with different *n*-butyl derivatives in several solvents (from ref^[6b]).

Due to the high O–H bond energy, the energy differences between carbonyl groups and their enol tautomers^[130] are much smaller than those between carbonyl groups and the isomeric enol ethers (Table 1, entry 12). As a consequence, the ΔG^0 term favors *C*-protonation over *O*-protonation to a much smaller extent than *C*-alkylation over *O*-alkylation. For that reason, kinetically controlled protonations of enolates occur generally at oxygen, the intrinsically favored site of attack.^[115]

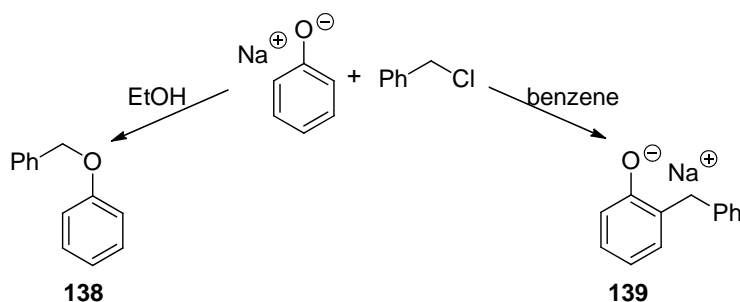
3.4.3 Phenoxides and Phenols

Phenolates comprise the enolate substructure, and one can expect analogous control mechanisms for ambident reactivity. The synthesis of phenol ethers by treatment of phenolate with soft haloalkanes as well as with hard dialkyl sulfates is a well-known synthetic procedure.^[131] In order to explain why also soft electrophiles prefer attacking at oxygen, one has to correct for the unfavorable loss of aromaticity in the case of *C*-attack (**137**) (Scheme 63).



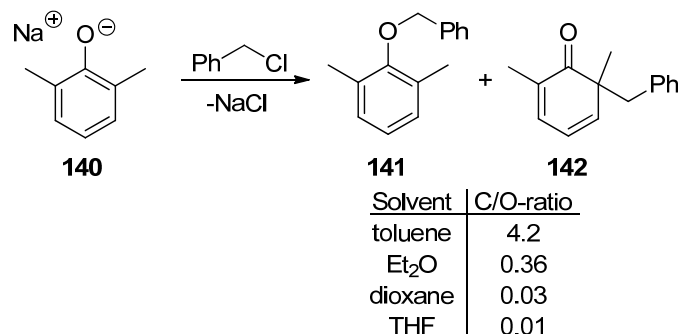
Scheme 63: Methylation of the ambident phenolate anion.

The Marcus analysis of phenolate anions reveals, that the attack at the oxygen atom is preferred intrinsically ($\Delta\Delta G_0^\ddagger = 51.6 \text{ kJ mol}^{-1}$, Scheme 4), again in line with Hoz' rule, and thermodynamically ($\Delta\Delta G^0 = 28.9 \text{ kJ mol}^{-1}$, Table 1 entry 13). Therefore, kinetically controlled alkylations generally occur at oxygen. However, in nonpolar solvents, oxygen attack may be blocked by the counterion, and *C*-alkylation may occur.^[132] Thus, Claisen reported that phenolates are typically attacked at oxygen unless coordination effects in the solvent or steric hindrance plays a crucial role.^[133] Thus treatment of sodium phenoxide with benzyl chloride in benzene solution led to the carbon-attack **139** as the main product (Scheme 64).



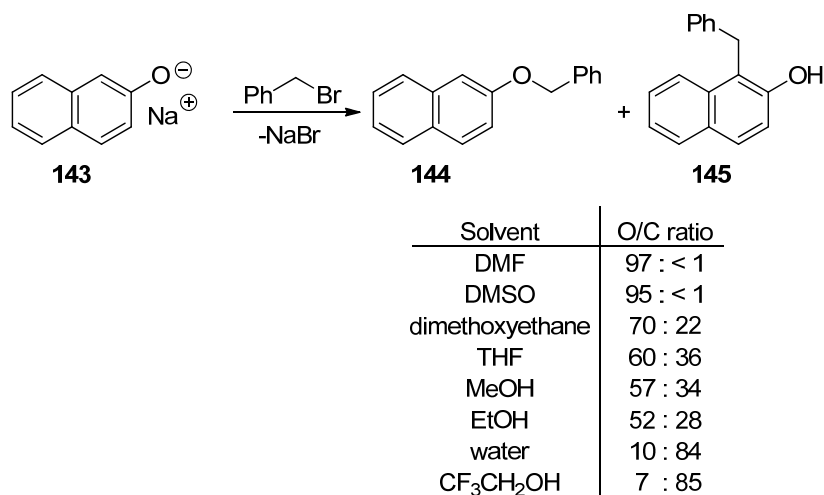
Scheme 64: Benzylation of the ambident phenolate anion (from ref^[133]).

Analogously, in the benzylation and alkylation reactions of sodium 2,6-dimethylphenolate (**140**) the highest percentage of *C*-attack was obtained in toluene, whereas in THF *O*-attack was almost exclusive (Scheme 65).^[134]



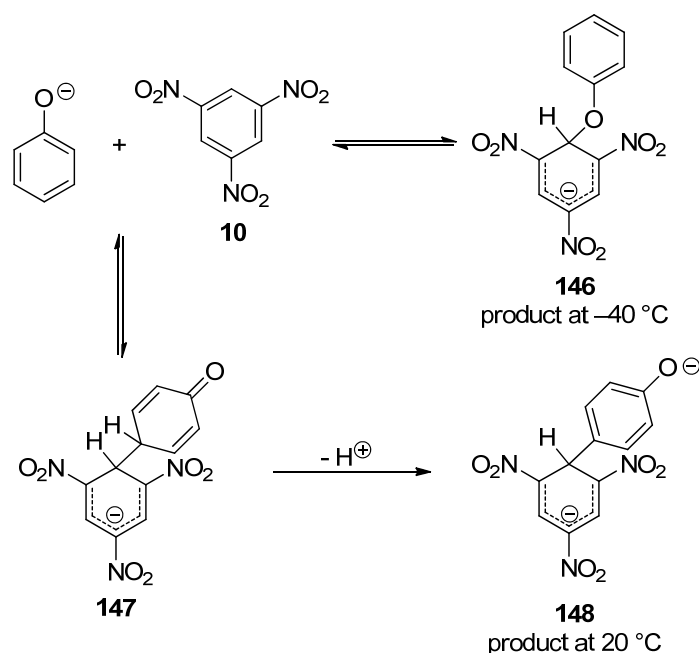
Scheme 65: Reactions of sodium 2,6-dimethylphenolate (**140**) with benzyl chloride in different solvents (from ref^[134a]).

Due to the smaller loss of aromaticity in the initial step of *C*-alkylation of naphthoxide (**143**), *C*-attack becomes more likely than in phenoxides. Thus, Scheme 66 shows that *C*-attack occurs in nonpolar solvents (dimethoxyethane, THF) where oxygen is coordinated to Na⁺ and in protic solvents (ROH, H₂O) which block *O*-attack by hydrogen bonding.^[134e-h] Kornblum summarized that in solvents like water, phenol, and fluorinated alcohols “*the oxygen of the phenoxide ion is so intensively solvated that the availability of the oxygen for nucleophilic displacement is greatly decreased; as a consequence, displacements employing the otherwise unfavored ortho and para carbon atoms can compete successfully.*”^[134g] Accordingly, the site of benzylation can be completely inverted by variation of the solvent (Scheme 66).



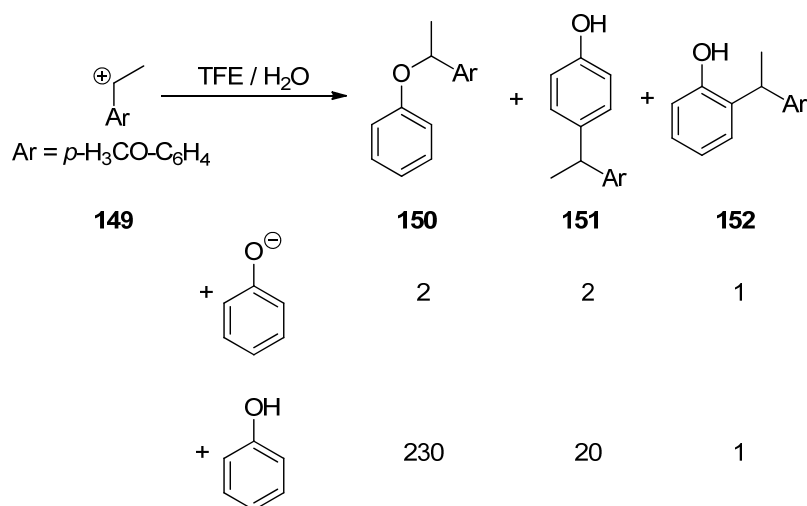
Scheme 66: Dependence of the site of benzylation of sodium 2-naphthoxide in various solvents (from ref^[134h]).

Even the “very soft” electrophiles trinitrobenzene (**10**) or trinitroanisole attack the hard phenolate oxygen under kinetically controlled conditions to give **146** in CD₃CN-glyme-*d*¹⁰ at -40 °C.^[135] At ambient temperature rearrangement to the product of electrophilic aromatic substitution takes place, accompanied by decomposition (Scheme 67).^[135b, 136] Analogous behavior, i.e., kinetically controlled attack at the phenolate oxygen and subsequent rearrangement to the product of electrophilic aromatic substitution has been reported for the reactions of phenolates with the highly electrophilic nitrobenzofuroxans and nitrobenzotriazole-1-oxides.^[52b, 137]



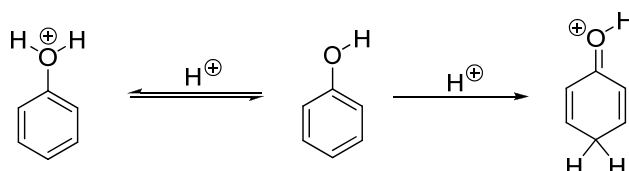
Scheme 67: Ambident reactivity of the phenolate anion towards 1,3,5-trinitrobenzene (from ref^[135]).

Richard and co-workers studied the reactions of phenol and phenolate with the 1-(4-methoxyphenyl)ethyl cation (**149**) in trifluoroethanol/water-mixtures.^[138] The low selectivity (2 : 2 : 1) for the reaction of **149** with the phenolate anion was explained by diffusion-controlled reactions. As depicted in Scheme 68, a much higher selectivity was found for the reaction of **149** with phenol, indicating that also in the reaction with the neutral phenol, *O*-attack is kinetically preferred.^[138]



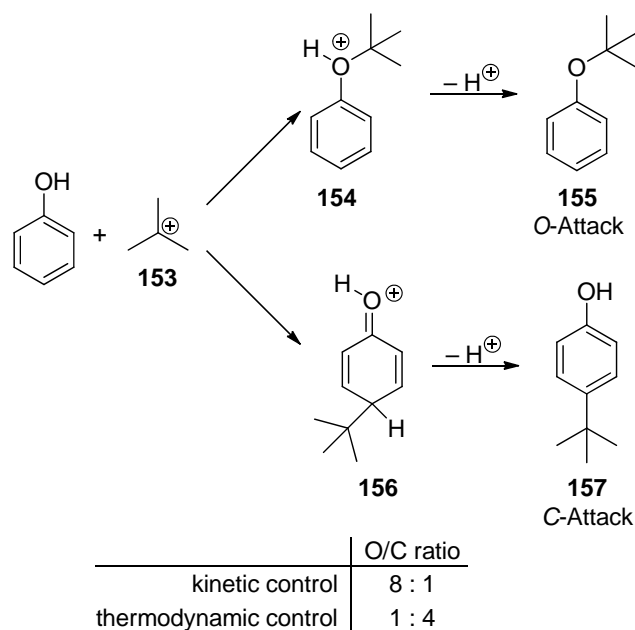
Scheme 68: Alkylation of phenolate and phenol in TFE/H₂O (1:1) by the 1-(4-methoxyphenyl)ethyl cation (from ref^[138]).

Analogously, Olah and Mo^[139] showed that the protonation of phenol initially occurs on oxygen. However, *O*-protonation is reversible, and the rearrangement to the thermodynamically more stable hydroxybenzenium ion is so fast that exclusive *C*-protonation was observed in 70 % perchloric acid and fluorosulphuric acid at low temperatures (Scheme 69).^[140]

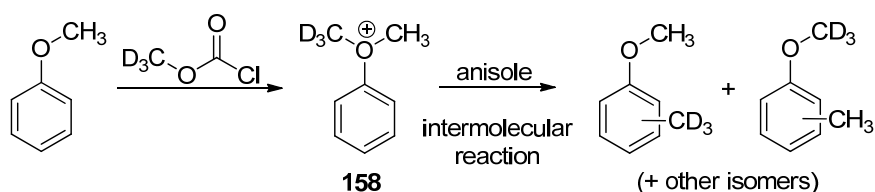


Scheme 69: Protonation of phenol according to Olah and Mo (from ref^[139]).

In the gas phase, where solvent effects are absent, phenol is also preferentially attacked at oxygen under conditions of kinetic control (i.e., higher pressure for an effective collisional deactivation and presence of gaseous NH₃) by the *tert*-butyl cation (**153**) to form *tert*-butyl phenyl ether (**155**) whereas under thermodynamic control (i.e., lower pressure) *tert*-butylphenol (**157**) dominated among the reaction products (Scheme 70).^[141]

Scheme 70: Gas phase reaction of phenol and the *tert*-butyl cation (from ref^[141c]).

Beak and co-workers^[142] reported that also in chlorobenzene the methylation of anisole proceeds via an initial formation of the dimethylphenyloxonium ion (**158**). Subsequent intermolecular reactions with anisole give a mixture of unlabeled, *d*₃-, and *d*₆-labeled methyl anisoles (Scheme 71).

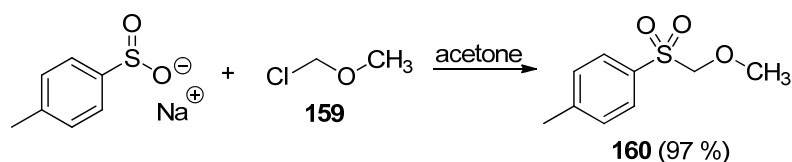
Scheme 71: Methylation of anisole by methyl-*d*₃ chloroformate (from ref^[142]).

In summary, the ambident reactivity of phenolates is analogous to that of enolates: *O*-alkylation of phenolates is intrinsically favored over *C*-alkylation unless the oxygen attack is blocked by coordination to metal ions or by hydrogen bonding in protic solvents. Reactions with strong electrophiles, which proceed under diffusion control, are unselective and occur at oxygen as well as on *ortho*- and *para*-carbon. Similarly, we have to conclude that also in alkylations of phenols and phenol ethers *O*-attack is intrinsically favored over *C*-attack, but *C*-alkylation leads to the thermodynamically preferred products.

3.5 Oxygen vs. Sulfur Attack

3.5.1 Sulfinate Anions

Although sulfinate anions are ambident anions with nucleophilic sites at oxygen and sulfur, for a long time, these anions were believed to react exclusively at sulfur with formation of sulfones.^[143] Already in 1880, Otto reported the formation of sulfones by the reactions of alkali salts of aromatic and aliphatic sulfinic acids with a variety of alkyl halides in ethanol at 80 °C.^[144] Tertiary alkyl halides did not alkylate sulfinate salts and underwent elimination reactions with formation of olefins.^[145] In an extensive study, Schank showed that primary and secondary alkyl halides, α -halocarbonyl compounds as well as α -haloethers exclusively attack at the sulfur atom of *p*-toluenesulfinate salts (Scheme 72).^[146]



Scheme 72: Reaction of sulfinate salts with chloromethyl methyl ether (**159**) yielding the corresponding sulfone **160** (from ref^[146]).

Lindberg derived exclusive *S*-attack from the kinetics of the reactions of *m*- and *p*-substituted aromatic sodium sulfonates with bromoacetate and bromoacetamide in water.^[147]

Other displacement reactions at saturated carbon atoms, e.g., epoxides^[148] or β -propiolactones,^[149] and nucleophilic aromatic substitutions of *p*-nitrochlorobenzene also proceeded at sulfur to give sulfones exclusively.^[150] Sulfones are also the only reaction products in Michael-type additions of sulfinate anions to acceptor substituted alkenes like chalcones,^[151] haloacrylonitriles,^[152] or nitroolefins,^[153] which are often reversible.^[143]

On the other hand, Meek and Fowler observed concomitant *S*- and *O*-attack in methylations of *p*-toluenesulfinate salts (Table 7).^[154] As an interconversion between the resulting methyl sulfinic esters and the isomeric methyl sulfones was shown not to occur under the reaction conditions, the product ratios given in Table 7 are the result of kinetic control.

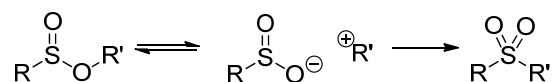
Table 7: Methylation of *p*-toluenesulfinate salts (TolSO₂⁻) with different methylating agents.^[154]

Entry	Substrate	Methylating Agent	Solvent	% O	% S
1	TolSO ₂ H	CH ₂ N ₂	Et ₂ O:MeOH (9:1)	100	0
2	TolSO ₂ ⁻	TsCHCHP(OMe) ₃ ⁺	none	95	5
3	TolSO ₂ Na	(MeO) ₂ SO ₂	DMF	84 ^[a]	16 ^[a]
			DMF	88 ^[b]	12 ^[b]
4	TolSO ₂ Na	MeOTs	DMF	77	23
5	TolSO ₂ Na	(MeO) ₂ SO ₂	MeOH	69	31
6	TolSO ₂ Na	MeOTs	MeOH	54	46
7	TolSO ₂ Ag	MeI	DMF	9	91
8	TolSO ₂ Na	MeI	none	7	93
9	TolSO ₂ Na	MeI	MeOH	2	98

[a] after 30 minutes, [b] after 17 hours

Though the preferred or exclusive *O*-attack by the in-situ generated methyldiazonium ion (entry 1 in Table 7) and the methyl sulfates (entries 3 and 5) and sulfonates (entries 4 and 6) on one side and the preferred *S*-attack by CH₃I (entries 7, 8) on the other might be explained by the HSAB principle, it should be noted that the silver salt of *p*-toluenesulfinate also gives *S*-attack with high selectivity (entry 9 in Table 7). Attack at the oxygen atom of the sulfinate anions has also been observed in the reactions of sulfinate salts with triethyloxonium tetrafluoroborate,^[155] acetyl chloride,^[146] or ethyl chloroformate.^[144c]

In order to rationalize these findings on the basis of Scheme 2, we have calculated $\Delta\Delta G^0$ and $\Delta\Delta G_0^\ddagger$ for the two sites of attack, i.e., the quantities needed for the Marcus treatment, and experimentally determined the nucleophilicity of the phenylsulfinate ion in order to differentiate between activation and diffusion-limited reactions. According to MP2/6-311+G(2d,p) calculations, dimethyl sulfone is 50.4 kJ mol⁻¹ ($\Delta\Delta G^0$) more stable than the isomeric methyl methanesulfinate. In line with this calculated energy difference, alkyl,^[156] alkenyl,^[157] and acetylenic^[158] sulfinic esters rearrange to the thermodynamically more stable sulfones. For allylic sulfinic esters this rearrangement is believed to proceed by a [2,3] sigmatropic shift^[157, 159] whereas the rearrangement proceeds via ionization and ion pair recombination if R⁺ is a stabilized carbocation (Scheme 73).^[156] Independent of the mechanism of the rearrangement, these observations demonstrate the higher thermodynamic stabilities of the sulfones.



Scheme 73: Rearrangement of sulfinate esters to the corresponding sulfones.

On the other hand, smaller intrinsic barriers for oxygen attack can be derived from the identity reactions summarized in Scheme 4 ($\Delta\Delta G_0^{\ddagger} = 34.7 \text{ kJ mol}^{-1}$). As sulfur and oxygen are in the same group of the periodic table, and crystal structures indicate that *O*-alkylation requires larger geometric changes than *S*-alkylation, we assume that steric interactions are responsible for the higher intrinsic barriers of the *S*-alkylations.^[160]

The observed exclusive *S*-attack in the reaction of sodium phenyl sulfinate with highly stabilized benzhydrylium ions (Figure 12) can, therefore, be explained by thermodynamic product control. From the plot of $\log k$ vs. the electrophilicity parameters E of the benzhydrylium ions one can extrapolate that the diffusion limit is reached when the electrophilicity of the carbocations exceeds E values of approximately -2 .^[13f] The observed mixtures resulting from *O*- and *S*-attack of more reactive benzhydrylium ions, i.e., $E > -2$ (Figure 12), can therefore not be explained by classical transition state models, and the same situation should hold for reactions with other carbocations.

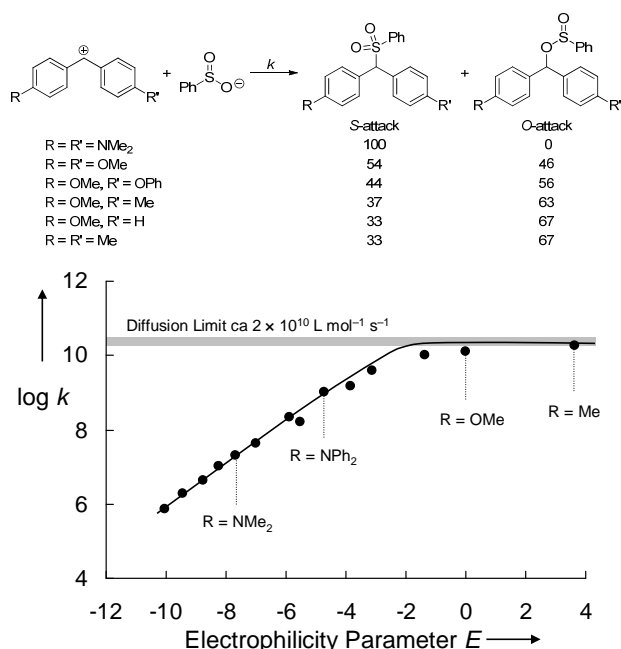


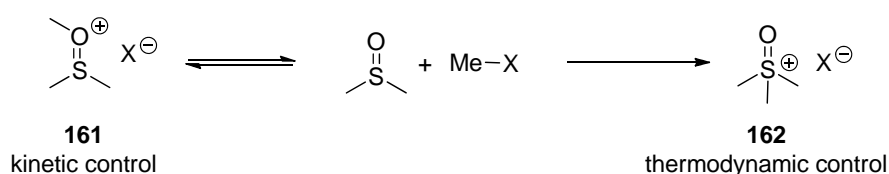
Figure 12: Plot of $\log k$ for the reactions of the benzhydrylium ions with the phenyl sulfinate ion vs. the electrophilicity parameters E (from ref^[13f]).

From the rate constants of the reactions of $(p\text{-MeOC}_6\text{H}_4)_2\text{CH}^+$ with the oxygen of phenylsulfinate and the rate constant for the back reaction, an intrinsic barrier of $\Delta G_0^\ddagger = 48 \text{ kJ mol}^{-1}$ was derived from Eq. (3). Rate and equilibrium constants for the reactions of amino-substituted benzhydrylium ions with the sulfur of PhSO_2^- allowed us to calculate intrinsic barriers of $\Delta G_0^\ddagger = 60\text{--}64 \text{ kJ mol}^{-1}$. Though a small amount of this difference can be assigned to the different nature of the carbocations, it is remarkable that the difference between these two intrinsic barriers is close to 50 % of the calculated difference of the corresponding identity reactions summarized in Scheme 4,^[13f] as expected from the combination of Eqs (3) and (7).

In summary, sulfinate anions are attacked at sulfur under conditions of thermodynamic control. In diffusion-limited reactions, mixtures of sulfones and sulfinate are typically obtained and it depends on the reaction conditions, whether *S*- or *O*-attack dominates under activation-controlled conditions (Figure 4).

3.5.2 Sulfoxides

A similar situation as previously described for sulfinate can be expected for sulfoxides. When DMSO was methylated by methyl brosylate, methyl tosylate, or methyl nitrate, exclusive *O*-attack (**161**) was observed.^[161] On the other hand, only products of *S*-attack (**162**) were isolated when methyl iodide was used as methylating agent.^[162] Smith and Winstein concluded from the fact that a rapid conversion from *O*- to *S*-methylated DMSO takes place at 50 °C, that the regioselectivity of the alkylation of DMSO can be rationalized by kinetically and thermodynamically controlled reactions.^[161] The methylation of the DMSO-oxygen occurs under kinetically controlled conditions whereas under conditions of thermodynamic control an attack at sulfur can be observed (Scheme 74). Probably, the reaction yielding *O*-attack is more reversible in the case of iodide as counterion and therefore, the thermodynamically more stable sulfonium ion **162** can be isolated as the sole reaction product.

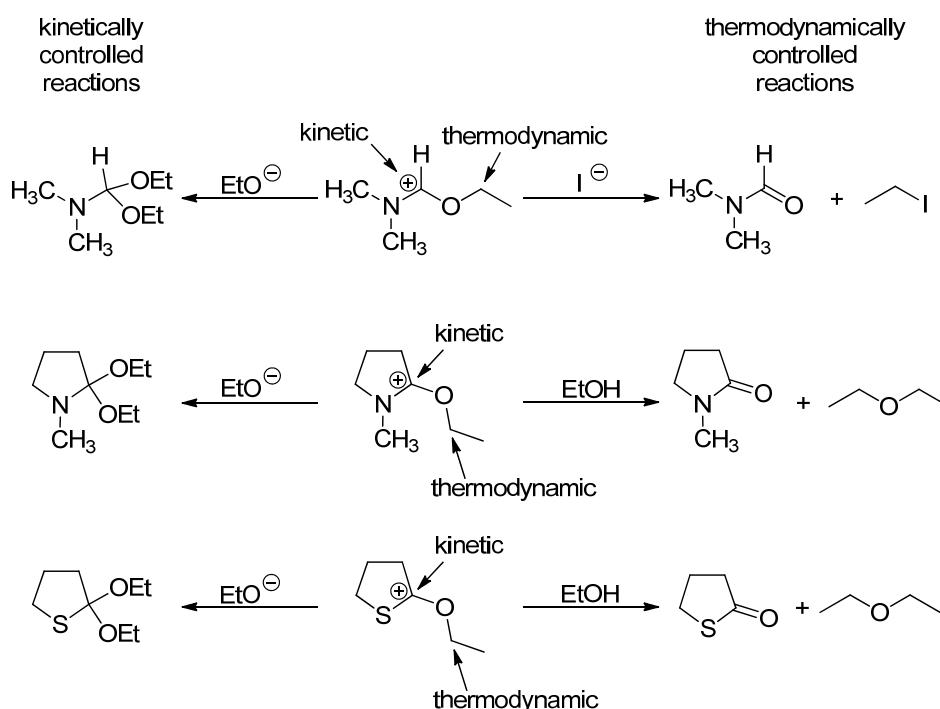


Scheme 74: Methylation of DMSO under kinetic and thermodynamic control.

4 Ambident Electrophiles

Because of the limitation of space, ambident electrophiles shall not be treated explicitly. We just want to emphasize that the same procedure which has been applied for rationalizing the regioselectivities of ambident nucleophiles should also be applicable to ambident electrophiles.

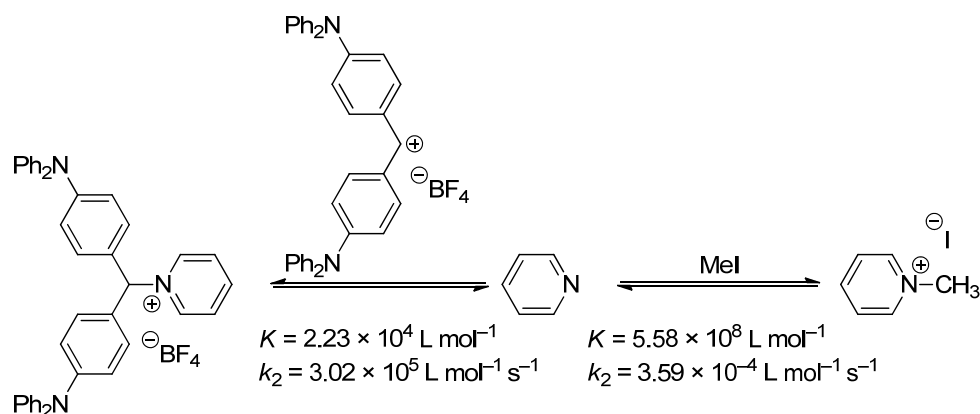
In an excellent review published in 1964, Hünig had carefully analyzed the modes of reactions of ambident cations derived from amides or esters (Scheme 75). The results of numerous reactions, which gave different products under different reaction conditions, were summarized as follows: “*The structures of the products isolated are determined by competition between a kinetically controlled but reversible reaction and a thermodynamically controlled reaction*”.^[8]



Scheme 75: Kinetic and thermodynamic product control in the reactions of ambident electrophiles (from ref^[8]).

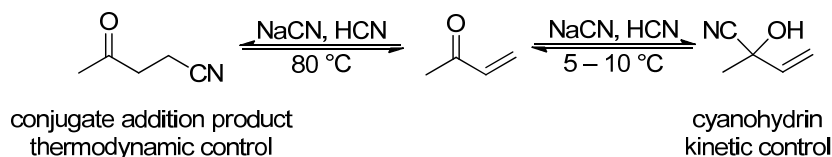
As outlined in Section 2.6, the isolation of different products under conditions of kinetic and thermodynamic control implies that the “kinetic” products are intrinsically preferred. In numerous experimental studies, it has been shown that additions of nucleophiles to C_{sp^2} centers (carbocations or Michael acceptors) generally have low intrinsic barriers.^[163] In contrast, $\text{S}_{\text{N}}2$ reactions, where a σ -bond must be broken in the rate-determining step require more reorganization and are characterized by higher intrinsic barriers. This relationship is

nicely illustrated in Scheme 76, which compares rate constants of the reactions of pyridine with different electrophiles. While the reaction with methyl iodide has a 4 orders of magnitude larger equilibrium constant than the reaction with the benzhydrylium ion, the reaction with MeI is 9 orders of magnitude slower than the reaction with the benzhydrylium ion.^[163a, 164] This clearly illustrates that the intrinsic barrier for the S_N2 reaction is much larger than the intrinsic barrier for reactions with carbocations.



Scheme 76: Reactions of pyridine with a benzhydrylium ion and methyl iodide (from ref. ^[163a, 164]).

If 1,4-additions of organocuprates, which follow a special mechanism,^[165] are disregarded, most 1,4- vs. 1,2-selectivities at α,β -unsaturated carbonyl compounds can also be rationalized by the competition of kinetic vs. thermodynamic product control, as illustrated for cyanide additions to methyl vinyl ketone in Scheme 77.^[113b, 166] Additions to a C=C-double bond are generally more exothermic than additions to a C=O-double bond. For that reason, Michael additions are thermodynamically favored over additions to the carbonyl group. On the other hand, conjugate addition requires much more structural reorganization, and is therefore intrinsically disfavored.

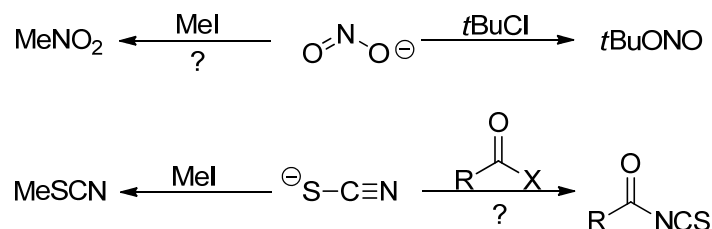


Scheme 77: Ambident reaction of cyanide anions with methyl vinyl ketones (from ref ^[113b]).

As a consequence, nucleophiles with high Lewis basicity, which react irreversibly, usually give 1,2-additions, whereas nucleophiles with low Lewis basicity will react reversibly with the carbonyl group and eventually yield the thermodynamically more stable Michael adducts.

5 Conclusions

The HSAB treatment of ambident reactivity may be considered as a generalization of Kornblum's rule which states that the site of attack at ambident nucleophiles is related to the S_N1/S_N2 character of the reaction. A main argument for Kornblum's rule was the observation that silver cyanide as well as the silver salts of 2-pyridone and of other carboxamides give different products than the corresponding alkali salts. There is convincing evidence, however, that the change of selectivity triggered by the silver salts is not due to a switch from S_N2 to S_N1 mechanism but due to blocking of carbon in CN^- and of nitrogen in amide and α -pyridone anions by Ag^+ . We, furthermore, presented examples showing that silver ions do not have any or only marginal effects on the regioselectivities of nitrite, sulfinate, and 4-pyridone anions.



Scheme 78: The questionable experimental basis which triggered the development of the concept of charge- and frontier-orbital-controlled reactions (from ref^[5a]).

Ironically, the two examples which Klopman selected as a motivation for developing the concept of charge- and frontier-orbital-controlled reactions^[5a] do not proceed as postulated in Scheme 78. Methyl iodide gives a mixture of nitromethane and methyl nitrite,^[86] and seven years before Klopman's work, Ruske provided evidence that SCN^- is attacked by acyl chlorides at sulfur to give acyl thiocyanates which may rearrange to the corresponding isothiocyanates under certain conditions.^[75] As not even the prototypes of ambident nucleophiles can properly be described in this way, the rationalization of ambident reactivity by the HSAB or the Klopman-Salem concept has to be abandoned.

A consistent approach to ambident reactivity is suggested in Scheme 2. In the first step, it should always be examined whether the isolated products are the result of kinetic or thermodynamic control. In the case of kinetic product control, one has to find out whether the reactions proceed with or without activation energy. This differentiation can be made on the basis of the reactivity parameters N , s , and E [Eq. (1)]. As most ambident anions analyzed in

this review undergo diffusion controlled reactions with those carbocations, which are less stabilized than the tritylium ion, transition state models are inappropriate to rationalize the resulting regioselectivities.

Eventually, Marcus theory which derives the Gibbs energy of activation ΔG^\ddagger from the Gibbs energy of reaction ΔG^0 and the intrinsic barrier ΔG_0^\ddagger has been shown to be suitable for rationalizing the regioselectivities of kinetically controlled reactions. A rule of thumb for deriving the intrinsically preferred site of attack at ambident nucleophiles is provided by Hoz' rule: The further right the nucleophilic reaction center in the periodic table, the lower the intrinsic barrier. Application of the Principle of Least Nuclear Motion, which compares geometrical parameters in reactants and products, leads to the same ordering of intrinsic barriers.

The success of Marcus theory to rationalize ambident reactivity (ΔG^\ddagger) by a combination of intrinsic (ΔG_0^\ddagger) and product stability effects (ΔG^0) suggests to employ Marcus theory more generally for analyzing structure reactivity relationships. Whereas the influence of ΔG^0 on ΔG^\ddagger is well known and is quantitatively described by Brønsted correlations,^[167] the Bell-Evans-Polanyi principle,^[168] or the Leffler-Hammond relationship,^[169] much less is presently known about intrinsic barriers, the second term which controls the rates of chemical reactions [Eq. (3)]. Promising approaches to elucidate the origin of intrinsic barriers as described by C. F. Bernasconi,^[170] F. G. Bordwell,^[171] S. Hoz,^[23] M. M. Kreevoy,^[20d] E. S. Lewis,^[172] J. R. Murdoch,^[173] J. P. Richard,^[16a] and F. Terrier^[174] should, therefore, be further developed.

6 Computational Details

6.1 General

Free energies G_{298} were calculated at MP2/6-311+G(2d,p) level of theory for both geometry optimizations and frequency calculations. Thermal corrections to 298.15 K have been calculated using unscaled harmonic vibrational frequencies in this case. All calculations were performed with Gaussian 03.^[165] Details of the quantum chemical calculations for cyanide, thiocyanate, cyanate, nitrite, and enolate can be found elsewhere.^[17]

6.2 Archive Entries for Geometry Optimization

6.2.1 Aniline

Aniline

```
1|1|UNPC-RUTHENIUM|FOpt|RMP2-FC|6-311+G(2d,p)|C6H7N1|MARTIN|04-Aug-2010|0|#p MP2/6-311+G(2d,p) opt freq||Anilin||0,1|C,-0.9356813827,0.000000094,-0.0073765257|C,-0.2225160677,-1.2051377252,-0.006482226|C,1.1712157151,-1.2033735039,0.0030939858|C,1.8782208214,0.000001168,0.0078546647|C,1.1712148156,1.2033752607,0.0030928238|H,-0.7648747297,-2.147454295,-0.0161857574|H,1.7045858277,-2.1490376512,0.0070505172|H,2.9629482638,0.00001497,0.0155849548|H,1.7045840924,2.1490398787,0.0070487574|C,-0.2225171,1.2051383535,-0.0064831625|H,-0.7648763048,2.1474546334,-0.0161864038|N,-2.339041794,-0.0000009943,-0.0869697216|H,-2.7670048721,-0.8314494026,0.3010616622|H,-2.7670052851,0.831452455,0.3010504312||Version=I A32W-G09RevA.02|State=1-A|HF=-285.8128167|MP2=-286.8712738|RMSD=7.333e-009|RMSF=2.381e-005|Dipole=-0.3957875,0.0000024,0.4265085|PG=C01 [X(C6H7N1)]||@
```

N-Methyl-anilinium Cation (N-attack)

```
1\1\GINC-NODE25\FOpt\RMP2-FC\6-311+G(2d,p)\C7H10N1(1+)\MAY04\04-Aug-2010\0\#p MP2/6-311+G(2d,p) opt freq\N-Methyl anilinium Cation\1,1\C,0.385350725,-0.0022927016,-0.3087998825\C,-0.2647858725,-1.2221965956,-0.1733198302\C,-1.6323290664,-1.2099836781,0.102428279\C,-2.3090810691,0.0036116585,0.2381695553\C,-1.6283269523,1.2142428043,0.0957776648\H,0.2691931789,-2.1629673847,-0.283870415\H,-2.1650675544,-2.1487459538,0.2061399571\H,-3.372602559,0.0059446429,0.4501772692\H,-2.1580127517,2.1552904263,0.1942969501\C,-0.2607705712,1.2204964371,-0.1799426458\H,0.2762573567,2.1588919202,-0.2957294528\N,1.8423836924,-0.0053004981,-0.5569306915\H,2.0867288526,-0.8287328432,-1.1176263501\H,2.0883437542,0.8090596191,-1.1300465568\C,2.6642423148,0.0032941649,0.7044694807\H,3.7202223613,0.0002748138,0.4392592899\H,2.4040307493,0.8995625477,1.2622984117\H,2.4021654112,-0.8841013798,1.2754839671\Version=AM64L-G03RevD.01|State=1-A|HF=-325.2149317|MP2=-326.4219963|RMSD=8.397e-09|RMSF=3.315e-05|Thermal=0.|Dipole=2.2573106,-0.0050782,-0.4389335|PG=C01 [X(C7H10N1)]\@
```

4-Methylcyclohexa-2,5-dieniminium Cation (C-attack)

```
1\1\GINC-NODE10\FOpt\RMP2-FC\6-311+G(2d,p)\C7H10N1(1+)\MAY04\05-Aug-2010\0\#p MP2/6-311+G(2d,p) opt freq\4-methylcyclohexa-2,5-dieniminium Cation\1,1\C,-0.1940695887,1.3858767,0.\C,-0.2000951372,0.6718040683,1.2465816853\C,-0.1989131841,-0.679948345,1.2409534289\C,-0.168131089,-1.4864158194,0.\C,-0.1989131841,-0.679948345,-1.2409534289\H,-0.2057048827,1.2311719873,2.1773007967\H,-0.2015888128,-1.2150575031,2.1873256445\H,-0.2015888128,-1.2150575031,-2.1873256445\C,-0.2000951372,0.6718040683,-1.2465816853\H,-0.2057048827,1.2311719873,-2.1773007967\N,-0
```

. 1843683961, 2. 702879828, 0. \H, -0. 181565836, 3. 2294963044, 0. 8659567311\H, -0. 181565836, 3. 2294963044, -0. 8659567311\H, -1. 0589520908, -2. 1357766828, 0. \C, 1. 0617568959, -2. 4350163538, 0. \H, 1. 042005464, -3. 0710197866, 0. 8854989407\H, 1. 042005464, -3. 0710197866, -0. 8854989407\H, 1. 9857100465, -1. 8546151229, 0. \Versi on=AM64L-G03RevD. 01\State=1-A' \HF=-325. 2204475\MP2=-326. 4129131\RMSD=8. 742e-09\RMSF=5. 232e-06\Thermal =0. \Di pol e=-0. 1812996, 1. 3618066, 0. \PG=CS [SG(C3H2N1), X(C4H8)]\ \@

Transition State for N-Attack

1\1\GINC-NODE27\FTS\RMP2-FC\6-311+G(2d, p)\C13H17N2(1+)\MAY04\10-Aug-2010\0\#p MP2/6-311+G(2d, p) opt=(ts, noigentest, readfc) freq geom=check\ \PhNH2---Me---H2NPh (Anilin N-Angri ff)\ \1, 1\C, 4. 4382821526, -0. 1786237329, 0. 7488335982\C, 3. 5046637518, -0. 9947500355, 0. 1104506814\C, 2. 5341760527, -0. 4145193251, -0. 7058590642\C, 2. 4769378796, 0. 9685703111, -0. 8786398553\C, 3. 4147827403, 1. 7772673084, -0. 2367721735\H, 5. 2036545999, -0. 6275981988, 1. 3728326786\H, 3. 5478329355, -2. 0748273036, 0. 2311814339\H, 1. 7230922797, 1. 4108541471, -1. 5262559233\H, 3. 3832419769, 2. 851940335, -0. 381384654\C, -0. 0000057295, -1. 3069177573, -0. 0000515635\H, -0. 6333059556, -1. 842048068, -0. 691907163\H, 0. 6332984898, -1. 842059424, 0. 6917896078\H, -0. 0000137028, -0. 227231273, -0. 0000407455\C, -2. 534174887, -0. 4145317191, 0. 7058409375\C, -2. 476940712, 0. 9685474935, 0. 8786996839\C, -3. 5046663745, -0. 9947194228, -0. 1104956475\C, -3. 4147947692, 1. 7772774522, 0. 2368860673\H, -1. 7230911515, 1. 4107975276, 1. 5263342002\C, -4. 4382937977, -0. 1785611544, -0. 7488240365\H, -3. 5478318111, -2. 0747899795, -0. 2312879249\H, -3. 3832570573, 2. 8519422351, 0. 3815604981\H, -5. 2036688117, -0. 627502847, -1. 372843509\C, -4. 3931152614, 1. 2061987553, -0. 5786577671\H, -5. 1238418079, 1. 83733983, -1. 0724087411\C, 4. 3930991857, 1. 2061453565, 0. 5787469453\H, 5. 1238190586, 1. 8372606719, 1. 0725406372\N, 1. 5102765364, -1. 2391663313, -1. 2862068507\H, 1. 1646431109, -0. 8474160852, -2. 1627818171\N, -1. 5102692347, -1. 2392103742, 1. 286130483\H, -1. 1646131485, -0. 8475062025, 2. 1627174075\H, 1. 8480272864, -2. 1831075783, -1. 4757514813\H, -1. 8480198245, -2. 1831596113, 1. 4756360576\ \Versi on=AM64L-G03RevD. 01\State=1-A\HF=-610. 987484\MP2=-613. 2736486\RMSD=9. 525e-09\RMSF=1. 189e-06\Thermal =0. \Di pol e=0. 0000183, -1. 5304014, -0. 0000535\PG=C01 [X(C13H17N2)]\ \@

Transition State for C-Attack

1\1\GINC-NODE9\FTS\RMP2-FC\6-311+G(2d, p)\C13H17N2(1+)\MAY04\11-Aug-2010\0\#p MP2/6-311+G(2d, p) opt=(ts, noigentest, readfc) freq geom=check\ \H2NPh---Me---PhNH2 (Anilin C-Angri ff)\ \1, 1\C, -1. 7915239241, -0. 5756692837, -1. 473386762\C, -2. 6670893808, -1. 2483531756, -0. 6460471936\C, -3. 5175927936, -0. 535217595, 0. 2297638552\C, -3. 4632276237, 0. 8777384272, 0. 2344163303\C, -2. 5880757097, 1. 5475200738, -0. 5954912053\H, -1. 1591141508, -1. 1384565057, -2. 1544852118\H, -2. 7226001832, -2. 3329876922, -0. 6776121359\H, -4. 1340174392, 1. 4349620882, 0. 8824629926\H, -2. 5773510154, 2. 6339333585, -0. 5968309276\C, -0. 0000117855, 0. 860856246, -0. 0000764134\H, -0. 619784896, 0. 3278317517, 0. 7054976122\H, 0. 6197546651, 0. 3277719181, -0. 7056119455\H, 0. 0000018459, 1. 9401096059, -0. 0001124046\C, 2. 5880651499, 1. 5475248496, 0. 5953700889\C, 1. 7914615347, -0. 575597246, 1. 4733717693\C, 3. 4632630307, 0. 8776829965, -0. 2344396833\H, 2. 5773439002, 2. 633938365, 0. 5966309851\C, 2. 6670714488, -1. 2483415558, 0. 6461284199\H, 1. 1590141954, -1. 1383363568, 2. 1544752218\C, 3. 5176249922, -0. 535272621, -0. 2296864051\H, 4. 1340875758, 1. 4348603072, -0. 8824903197\H, 2. 7225750064, -2. 3329742007, 0. 6777724902\C, -1. 6790681632, 0. 8355354842, -1. 4161344344\H, -1. 1320838682, 1. 3618255294, -2. 1925460277\C, 1. 6790162607, 0. 8356027188, 1. 41602065\H, 1. 1320010302, 1. 3619489846, 2. 1923722189\N, -4. 3489521534, -1. 1984697821, 1. 0802049867\H, -4. 5291512526, -2. 1797993394, 0. 9259552818\H, -5. 0830027204, -0. 6870815546, 1. 5482183217\N, 4. 3490300218, -1. 1985872495, -1. 0800341073\H, 5. 0831076864, -0. 6872342142, -1. 5480433091\H, 4. 5292177157, -2. 1799063321, -0. 9257047384\ \Versi on=AM64L-G03RevD. 01\State=1-A\HF=-610. 9610537\MP2=-613. 2528056\RMSD=9. 047e-09\RMSF=8. 690e-07\Thermal =0. \Di pol e=-0. 0000031, -0. 337458, 0. 000021\PG=C01 [X(C13H17N2)]\ \@

6.2.2 Enamine

Vinylamine

```
1|1|UNPC-RUTHENIUM|FOpt|RMP2-FC|6-311+G(2d,p)|C2H5N1|MARTIN|02-Aug-2010|0|0|#p opt MP2/6-311+G(2d,p) freq||Vinyl Amine||0,1|C,-1.2559758226,-0.2021859267,0.0000762982|H,-2.1677489255,0.3768460434,0.0004814013|H,-1.3312411667,-1.2837665674,-0.0000196645|C,-0.0701320347,0.4272341358,-0.0003513009|H,-0.0347951484,1.5126281398,-0.0002896|N,1.1721939739,-0.1674128589,-0.0013192336|H,1.2647461504,-1.1683216855,0.0009845173|H,2.0088349736,0.3846727194,0.0012305821||Version=IA32W-G09RevA.02|State=1-A|HF=-133.1084684|MP2=-133.6027816|RMSD=6.727e-009|RMSF=3.047e-005|Dipole=0.6651466,0.0010542,0.0029989|PG=C01 [X(C2H5N1)]||@
```

Methyl-vinylammonium Cation (N-Attack)

```
1|1|UNPC-OLE|FOpt|RMP2-FC|6-311+G(2d,p)|C3H8N1(1+)|TINO|02-Aug-2010|0|0|#p opt freq MP2/6-311+G(2d,p) freq||N-Methyl vinyl ammonium Ion||1,1|N,-0.5058478535,0.4493871423,-0.3490055344|H,-0.3125349397,1.3512249455,0.0996419671|C,0.7224062552,-0.3652452081,-0.3364410705|H,0.622479914,-1.2997451488,-0.8741014|C,1.8071640482,0.0471710934,0.303026802|H,1.8523662763,0.9951123354,0.8294522474|H,2.6912297946,-0.5772170665,0.3057572245|C,-1.6673345657,-0.2177885701,0.3388482532|H,-1.3860358499,-0.3875064834,1.3750639415|H,-2.5359239911,0.4337678785,0.2701693257|H,-1.8581408173,-1.1636845591,-0.1626046283|H,-0.7665232712,0.663809641,-1.3183401281||Version=IA32W-G09RevA.02|State=1-A|HF=-172.5070808|MP2=-173.1475567|RMSD=4.568e-009|RMSF=3.494e-005|Dipole=-0.6484032,0.5260194,-0.2976216|PG=C01 [X(C3H8N1)]||@
```

Propyliminium Cation (C-Attack)

```
1|1|UNPC-RUTHENIUM|FOpt|RMP2-FC|6-311+G(2d,p)|C3H8N1(1+)|MARTIN|02-Aug-2010|0|0|#p opt freq MP2/6-311+G(2d,p)||Propyl Iminium Cation||1,1|C,0.559575795,0.5646075529,0.3357179666|H,0.359127263,1.4874287988,-0.2127594483|C,-0.6323367862,-0.2952115429,0.3665076609|H,-0.6180675065,-1.2220758909,0.9377151175|N,-1.7166113712,-0.0442981947,-0.279382694|H,-1.8103977353,0.802864008,-0.8370059564|H,-2.5134371027,-0.6765963155,-0.2502900725|H,0.7949151568,0.8235441928,1.3741595738|C,1.7458344712,-0.2139224365,-0.2735730652|H,2.6300245398,0.4209598325,-0.2426086376|H,1.957151372,-1.1208735863,0.2941057252|H,1.5485749041,-0.4818804183,-1.31174817||Version=IA32W-G09RevA.02|State=1-A|HF=-172.5346771|MP2=-173.1701137|RMSD=5.483e-009|RMSF=1.760e-005|Dipole=-1.5610888,-0.1151966,-0.0564018|PG=C01 [X(C3H8N1)]||@
```

Transition State for N-Attack

```
1\1\GINC-NODE28\FTS\RMP2-FC\6-311+G(2d,p)\C5H13N2(1+)\MAY04\03-Aug-2010\0\0\#p opt=(ts,noeigentest,calcfrc) MP2/6-311+G(2d,p) freq\H2CCHNH2--Me--H2NCHCH2\1,1|C,-0.0000010883,-0.0000060743,-0.1158066843|H,-0.4904832238,0.8040128564,-0.6429546994|H,0.0000166537,-0.0000287541,0.9625420513|H,0.4904672036,-0.8040056517,-0.6429989942|N,-1.7394218937,-0.977889699,-0.1264912002|H,-1.9653521283,-1.1796238035,-1.1008807105|H,-1.6213277707,-1.8669570199,0.3586245162|N,1.7394171596,0.9778842303,-0.1264972291|H,1.9653450262,1.1796121425,-1.1008892943|H,1.6213179376,1.8669568691,0.3586121749|C,-2.7510522565,-0.1658236527,0.4831880275|H,-2.7475943919,-0.1882065462,1.5673349832|C,-3.5715775005,0.6182545177,-0.2141695668|H,-3.5761859267,0.6260441149,-1.2993879391|H,-4.2765645186,1.2558714595,0.3016658025|C,2.7510547837,0.1658312877,0.4831870479|H,2.7476003951,0.1882248719,1.56733377|C,3.5715831699,-0.6182485096,-0.2141651356|H,3.5761886594,-0.626048753,-1.2993834642|H,4.27657571,-1.2558558861,0.3016745441||Version=AM64L-G03RevD.01|State=1-A|HF=-305.5778472|MP2=-306.7296359|RMSD=5.221e-09|RMSF=1.008e-06|Thermal=0.0|Dipole=-0.0000081,-0.0000045,-0.2501576|PG=C01 [X(C5H13N2)]||@
```

Transition State for C-Attack

```

1\1\GI NC-NODE20\FTS\RMP2-FC\6-311+G(2d,p)\C5H13N2(1+)\MAY04\02-Aug-201
0\0\#P MP2/6-311+G(2d,p) opt=(ts,calcfc,noigentest) freq\HNCNHCH---
Me---CHCHCNH\1,1\C,0.0078580529,0.1037475502,0.3689667875\H,0.4506627
403,1.0667911957,0.1679878979\H,-0.18987273,-0.5883099097,-0.434155694
8\H,-0.2421131113,-0.1725073469,1.3804795241\C,-1.8649254779,1.0781710
826,0.0340557652\H,-1.6912177965,1.4181127407,-0.9821937189\H,-1.79987
10003,1.8244128637,0.8151299867\C,1.9364101504,-0.7145722964,0.7858797
19\H,2.1645479774,-0.1423315944,1.6796352368\H,1.6417367098,-1.7458588
739,0.9304322859\C,-2.7159343698,0.0149283751,0.2516918562\H,-3.027644
4822,-0.2248658068,1.2654487826\C,2.5823936857,-0.4041317207,-0.392225
1488\H,2.4940462645,-1.0707377239,-1.246784257\N,-3.121859178,-0.85665
31638,-0.6790315614\H,-3.7334294053,-1.6210823637,-0.435312836\N,3.239
5258456,0.7357063535,-0.6377271003\H,3.4891606778,1.3631468873,0.11452
88074\H,3.6758221482,0.8954330501,-1.5331153912\H,-3.0006202314,-0.659
6637089,-1.6629464108\Version=AM64L-G03RevD.01\State=1-A\HF=-305.5701
883\MP2=-306.7323895\RMSD=4.113e-09\RMSF=1.096e-05\Thermal=0.\Di pol e=0
.008279,-0.1033947,-0.4892773\PG=C01 [X(C5H13N2)]\@

```

6.2.3 Acetamide-AnionAcetamide-Anion

```

1\1\GI NC-NODE16\F0pt\RMP2-FC\6-311+G(2d,p)\C2H4N101(1-)\MAY04\20-Sep-2
010\0\#p MP2/6-311+G(2d,p) opt freq\Acetami de-Ani on\1,1\C,-0.16326
01649,0.0143019743,0.0003000403\O,-0.5856290009,1.2161590536,0.0005368
721\N,-0.8525305392,-1.1199308745,-0.0003808148\C,1.3607367171,-0.1630
150103,0.0000675551\H,1.7813162436,0.3311677943,0.8810799313\H,1.64518
95844,-1.2168321547,-0.0005408655\H,1.7811909212,0.3321591951,-0.88044
78005\H,-1.8392847612,-0.8340549777,-0.0004149179\Version=AM64L-G03Re
vD.01\State=1-A\HF=-207.4449036\MP2=-208.1674744\RMSD=5.622e-09\RMSF=8
.059e-05\Thermal=0.\Di pol e=0.9628008,-0.0193154,-0.000038\PG=C01 [X(C2
H4N101)]\@

```

N-Methyl-acetamide (N-attack)

```

1\1\GI NC-NODE22\F0pt\RMP2-FC\6-311+G(2d,p)\C3H7N101\MAY04\20-Sep-2010\
0\#p MP2/6-311+G(2d,p) opt freq\N-Methyl acetami de\0,1\C,-0.46588241
27,0.0912231154,0.2226557917\O,-0.3524718392,1.2139811608,0.7053438769
\N,0.6183441619,-0.6246677333,-0.1829615236\C,-1.8108536013,-0.5785499
164,0.0433780698\H,-1.7441272188,-1.5738437228,-0.3986874095\H,-2.2949
627364,-0.6508334683,1.0177307846\H,-2.4319773024,0.0545630992,-0.5909
021926\C,1.9558002815,-0.0738327247,-0.0561600977\H,2.1828201465,0.147
2557617,0.9876694534\H,2.6724260525,-0.8014034692,-0.4346318984\H,2.04
59430223,0.8519751951,-0.6260888523\H,0.4864344461,-1.5418952974,-0.57
59030023\Version=AM64L-G03RevD.01\State=1-A\HF=-247.0834485\MP2=-247.
9465281\RMSD=4.751e-09\RMSF=9.669e-06\Thermal=0.\Di pol e=0.2919716,-1.3
64129,-0.6243308\PG=C01 [X(C3H7N101)]\@

```

O-Methyl-acetamide (O-attack)

```

1\1\GI NC-NODE10\F0pt\RMP2-FC\6-311+G(2d,p)\C3H7N101\MAY04\20-Sep-2010\
0\#p MP2/6-311+G(2d,p) opt freq\O-Methyl acetami de\0,1\C,0.445417892
8,0.1357520669,-0.0000268572\O,-0.5873300063,-0.7370286033,0.000007634
6\N,0.236326544,1.3958640321,-0.0000513975\C,1.7507388423,-0.605292090
1,0.0000116512\H,1.8113970311,-1.2460671464,-0.8812240902\H,2.59014667
87,0.088598045,-0.0002492982\H,1.8115865453,-1.2456146007,0.8815657525
\H,1.1289237058,1.8872761404,-0.0000719702\C,-1.8899725083,-0.13519466
02,0.0000293102\H,-2.5902426236,-0.9667290691,0.0000611768\H,-2.022556
3643,0.4851178203,0.8863650673\H,-2.0225997375,0.4850860652,-0.8863220
794\Version=AM64L-G03RevD.01\State=1-A\HF=-247.0563214\MP2=-247.91939
85\RMSD=4.212e-09\RMSF=6.640e-05\Thermal=0.\Di pol e=0.3972366,-0.274926
,0.0000283\PG=C01 [X(C3H7N101)]\@

```

Transition State for N-Attack

1\1\G\I NC-NODE16\FTS\RMP2-FC\6-311+G(2d, p)\C5H11N2O2(1-)\MAY04\13-Sep-2010\0\#\p MP2/6-311+G(2d, p) opt=(ts, noigentest, cal cfc) freq\Amide N-Attack Identity\ -1, 1\N, -1.86621421, -0.6184890462, -0.5557350227\C, 0.000460695, 0.0003306297, -0.5298441485\H, -0.2753402457, 0.8866259687, -1.0699745559\H, -0.000151123, -0.0000663389, 0.5422502216\H, 0.2756387422, -0.885573509, -1.0705169032\N, 1.8663219893, 0.6191460192, -0.554593309\C, -2.9839367423, -0.0710211764, -0.0694956818\O, -4.1490238323, -0.524900758, -0.1755634555\C, 2.9839264228, 0.0711022622, -0.0687303399\O, 4.1490911181, 0.5248909271, -0.1743377372\C, 2.796756127, -1.2400661992, 0.6906670647\H, 1.7589614737, -1.5737440082, 0.7326009794\H, 3.4048422737, -2.0110479509, 0.2119791655\H, 3.1746523153, -1.1118528778, 1.7075440193\C, -2.797039738, 1.2395353472, 0.6910237891\H, -1.7593373186, 1.5734873996, 0.7330904781\H, -3.4054384476, 2.0107522827, 0.2131143713\H, -3.1747346536, 1.1103167383, 1.7078492314\H, -2.0954315338, -1.4831808741, -1.0492322447\H, 2.0957043133, 1.4841971641, -1.0473829218\Version=AM64L-G03RevD.01\State=1-A\HF=-454.4684654\MP2=-456.0738411\RMSD=7.950e-09\RMSF=1.669e-06\Thermal=0.\Dipole=-0.0000694, 0.0000137, 0.2341106\PG=C01 [X(C5H11N2O2)]\@

Transition State for O-Attack

1\1\G\I NC-NODE24\FTS\RMP2-FC\6-311+G(2d, p)\C5H11N2O2(1-)\MAY04\12-Sep-2010\0\#\p MP2/6-311+G(2d, p) opt=(cal cfc, ts, noigentest) freq\Amide Anion O-Attack Identity\ -1, 1\C, -0.0006699972, 0.0366424422, 0.672718839\H, -0.2890885292, -0.8119060122, 1.2639648967\H, 0.0134133167, -0.0311709474, -0.3973399619\H, 0.2790977637, 0.9501225119, 1.1629453555\C, -2.7470515746, 0.099583606, 0.080683835\C, 2.7684464342, -0.0801767242, 0.2041844246\C, 2.4202369723, 1.0008515505, -0.8218320432\H, 1.8187771805, 0.5759658796, -1.6302044906\H, 1.8307438664, 1.7991022862, -0.3648419035\H, 3.3205828039, 1.4392925936, -1.2561740504\C, -2.4077855035, -1.1307289102, -0.7410271056\H, -1.7508243605, -0.8658117597, -1.5741759272\H, -1.8820556373, -1.8741290425, -0.1370684238\H, -3.3246386185, -1.566081362, -1.1354447545\O, -1.7653334167, 0.7310094464, 0.6734569864\O, 1.7683118404, -0.646433376, 0.8123545489\N, -4.003603588, 0.4451649499, 0.1241172495\N, 4.0046126239, -0.4273378861, 0.442907109\H, 4.6073612352, 0.1370034447, -0.1571967911\H, -4.0524078117, 1.2856593095, 0.710598207\Version=AM64L-G03RevD.01\State=1-A\HF=-454.4481555\MP2=-456.054315\RMSD=3.529e-09\RMSF=1.312e-06\Thermal=0.\Dipole=0.2434459, 0.6886488, -1.1466784\PG=C01 [X(C5H11N2O2)]\@

6.2.4 AcetamideAcetamide

1\1\G\I NC-NODE13\FOpt\RMP2-FC\6-311+G(2d, p)\C2H5N1O1\MAY04\20-Sep-2010\0\#\p MP2/6-311+G(2d, p) opt freq\Acetamide\O, 1\C, 0.078514934, 0.1355929517, 0.0221608928\O, 0.4086229803, 1.3094540383, 0.1062910305\N, 0.9979766433, -0.8792595874, -0.0066967065\C, -1.370279586, -0.3023068031, 0.0104564989\H, -1.5145600468, -1.2872332576, -0.4357031083\H, -1.7319818837, -0.3309530752, 1.0401988272\H, -1.9534101257, 0.4376873617, -0.5344185147\H, 0.7306654232, -1.8213027854, -0.2367999657\H, 1.9725026614, -0.6240268431, -0.0646279541\Version=AM64L-G03RevD.01\State=1-A\HF=-208.0461709\MP2=-208.7520016\RMSD=3.593e-09\RMSF=6.770e-06\Thermal=0.\Dipole=-0.1284719, -1.4778965, -0.2300171\PG=C01 [X(C2H5N1O1)]\@

N-Methyl-acetamide Cation (N-attack)

1\1\G\I NC-NODE18\FOpt\RMP2-FC\6-311+G(2d, p)\C3H8N1O1(1+)\MAY04\20-Sep-2010\0\#\p MP2/6-311+G(2d, p) opt freq\N-Methyl-acetamide-Cation\1, 1\C, 0.5968120722, 0.2507515175, -0.0000441465\O, 0.3343582281, 1.4036183304, -0.0001220351\N, -0.6442979386, -0.7464891358, -0.0001034166\C, 1.896937385, -0.4724570301, 0.0000704893\H, 1.975408384, -1.1080058868, 0.8860470331\H, 1.9753362222, -1.1085136169, -0.8855436312\H, 2.7026912425, 0.2585833405, -0.0001559074\C, -1.9614776176, -0.0358440677, 0.0000432684\H, -2.0158874154, 0.586663798, -0.8885730209\H, -2.7540821285, -0.7806469046, -0.0000205087\H, -2.0158137225, 0.586434931, 0.8888246901\H, -0.5642583163, -1.3586832

333, -0.8198904454\H, -0.5641843951, -1.358909042, 0.8195066797\\Version=AM64L-G03RevD.01\State=1-A\HF=-247.4124159\MP2=-248.2717214\RMSD=9.373e-09\RMSF=9.000e-05\Thermal=0.\Dipole=-0.4496975, -1.7698249, 0.0000013\PG=C01 [X(C3H8N101)]\@

O-Methyl-acetamide Cation (O-attack)

1\1\GINC-NODE17\F0pt\RMP2-FC\6-311+G(2d,p)\C3H8N101(1+)\MAY04\20-Sep-2010\0\#p MP2/6-311+G(2d,p) opt freq\0-Methylacetamide-Cation\1,1\C, 0.48751317, -0.0838960492, -0.0000484069\O, -0.6243890426, -0.7434316689, -0.0000617694\N, 1.5731077525, -0.8141899559, -0.000096579\C, 0.5551576103, 1.398975723, 0.0000859006\H, 0.0459949247, 1.7887612993, 0.8841545127\H, 1.5865250521, 1.7449871528, -0.0001674189\H, 0.0454700217, 1.7889840681, -0.835741751\H, 2.4880240557, -0.3835635686, -0.0000830147\C, -1.9061846529, -0.0353276246, -0.000043672\H, -2.6461187868, -0.827722127, 0.0002089752\H, -1.9886521586, 0.5671954889, 0.9012587691\H, -1.9888649421, 0.5669070494, -0.9014415534\H, 1.5052719958, -1.8275837874, -0.0001428975\\Version=AM64L-G03RevD.01\State=1-A\HF=-247.4352633\MP2=-248.2821685\RMSD=8.147e-09\RMSF=3.245e-05\Thermal=0.\Dipole=0.7143709, 0.1991007, 0.0000299\PG=C01 [X(C3H8N101)]\@

Transition State for N-Attack

1\1\GINC-NODE14\FTS\RMP2-FC\6-311+G(2d,p)\C5H13N202(1+)\MAY04\12-Sep-2010\0\#p MP2/6-311+G(2d,p) opt=(calcfc,ts,noigentest) freq\Amide N-Attack Identity\1,1\N, 1.8150327513, -0.5827748, -0.892017507\C, -0.000035957, -0.5269043785, 0.0000378177\H, 0.4458354849, -1.0540109316, 0.8295104196\H, -0.0000217711, 0.5516901371, -0.0000156865\H, -0.4458247907, -1.0541083038, -0.829382505\N, -1.8150379662, -0.5827476573, 0.8920986014\C, 2.7292308674, -0.0039951945, 0.0735079791\O, 2.9699057114, -0.6360771689, 1.0726486228\C, -2.7292558316, -0.004096879, -0.0734852941\O, -2.9699095568, -0.636288421, -1.072561735\C, -3.2254219874, 1.3704013448, 0.2572372772\H, -3.9449772, 1.3071005898, 1.0782904939\H, -2.4061884416, 2.0163995073, 0.5828072712\H, -3.7142331968, 1.7969206865, -0.6153859684\C, 3.2253510855, 1.3704858861, -0.2573544241\H, 3.9449080872, 1.3071250416, -1.0784014966\H, 2.406096091, 2.0164235532, -0.5829903679\H, 3.714148469, 1.7971105383, 0.6152250776\H, 1.9820281465, -1.5856943584, -0.9793642405\H, -1.9819991071, -1.5856640756, 0.9795467295\H, 1.8252195441, -0.1366688465, -1.808686977\H, -1.8252397931, -0.1365492694, 1.8087229121\\Version=AM64L-G03RevD.01\State=1-A\HF=-455.4163508\MP2=-456.9922191\RMSD=3.271e-09\RMSF=3.083e-06\Thermal=0.\Dipole=-0.0000072, 0.4455449, -0.0000227\PG=C01 [X(C5H13N202)]\@

Transition State for O-Attack

1\1\GINC-NODE25\FTS\RMP2-FC\6-311+G(2d,p)\C5H13N202(1+)\MAY04\12-Sep-2010\0\#p opt=(calcfc,ts,noigentest) freq MP2/6-311+G(2d,p)\Amide O-Attack Identity\1,1\C, -0.000024032, 0.0000124518, -0.2304711609\H, -0.2857847693, 0.8827086422, -0.7725878376\H, 0.0000319602, -0.0001769161, 0.8450904172\H, 0.2856791877, -0.8824897246, -0.772934522\C, -2.8120342449, -0.0609979647, -0.0162291519\C, 2.8119887006, 0.0610111451, -0.0163067381\C, 2.7827416144, -1.4053466254, 0.3063727478\H, 2.0723434204, -1.5907652441, 1.124082719\H, 2.4543354341, -1.9599151678, -0.5750026635\H, 3.7604070727, -1.7791050535, 0.6056406635\C, -2.7827793368, 1.4053249068, 0.3066086847\H, -2.0723047576, 1.5906682749, 1.1125941738\H, -2.4544693126, 1.9599924905, -0.5747410837\H, -3.7604217117, 1.7790356412, 0.6060108481\O, -1.7755953603, -0.7262173801, -0.2575687854\O, 1.7755424003, 0.7262592554, -0.2575359469\N, -3.9991421772, -0.6663573779, -0.0546135692\N, 3.9990962297, 0.6663731886, -0.0546617471\H, 4.8539805154, 0.1647689344, 0.1299162439\H, -4.0444358696, -1.6496229579, -0.2882228144\H, -4.8540211866, -0.1647750277, 0.1300484373\H, 4.0443832232, 1.649666509, -0.2881554676\\Version=AM64L-G03RevD.01\State=1-A\HF=-455.4632845\MP2=-457.0264628\RMSD=4.378e-09\RMSF=1.617e-06\Thermal=0.\Dipole=0.0000031, -0.0000206, 0.2798135\PG=C01 [X(C5H13N202)]\@

6.2.5 Nitromethane Anion

Nitromethane Anion

```
1|1|UNPC-OLE|FOpt|RMP2-FC|6-311+G(2d,p)|C1H2N1O2(1-)|TINO|30-Jul-2010|0|
0|#p MP2/6-311+G(2d,p) opt freq||Nitromethane Anion||-1,1|C,0.,0.,-1.
2950652058|H,0.,0.95665331,-1.7909145695|H,0.,-0.95665331,-1.790914569
5|N,0.,0.,0.051892115|O,0.,-1.1111335427,0.6933211149|O,0.,1.111133542
7,0.6933211149||Version=IA32W-G09RevA.02|State=1-A1|HF=-243.1512015|MP
2=-243.9507547|RMSD=3.909e-009|RMSF=8.533e-005|Dipole=0.,0.,-0.9533002
|PG=C02V [C2(C1N1),SGV(H2O2)]||@
```

Nitroethane (O-attack)

```
1|1|UNPC-OLE|FOpt|RMP2-FC|6-311+G(2d,p)|C2H5N1O2|TINO|30-Jul-2010|0|
p MP2/6-311+G(2d,p) opt freq||Nitroethane||0,1|C,0.6929624753,-0.46814
5587,0.5535938701|H,0.8004621447,-0.0905537005,1.5694550896|H,0.632545
9794,-1.5541076381,0.5501421676|N,-0.6265272428,0.0265294087,0.0651715
591|O,-1.3459733541,-0.766614752,-0.5503384832|O,-0.8895418864,1.21309
92905,0.2805894804|C,1.7900365643,0.0543972717,-0.3577804863|H,2.75654
5041,-0.3058885013,-0.0030142313|H,1.6432930863,-0.3007202628,-1.37887
0118|H,1.8009701923,1.1441914708,-0.3548178481||Version=IA32W-G09RevA.
02|State=1-A|HF=-282.7872104|MP2=-283.7385347|RMSD=7.259e-009|RMSF=8.4
19e-006|Dipole=1.3537989,-0.4275778,0.4002223|PG=C01 [X(C2H5N1O2)]||@
```

Methyl Methyleneazinic Acid (C-attack)

```
1|1|UNPC-OLE|FOpt|RMP2-FC|6-311+G(2d,p)|C2H5N1O2|TINO|31-Jul-2010|0|
p opt freq MP2/6-311+G(2d,p)||s-trans Methyl Methyleneazinic Acid (Ni
tronate)||0,1|C,-1.707790212,-0.556524354,0.0000216596|H,-1.6599103346,
-1.6310553978,-0.0002247657|H,-2.6030696006,0.0419655409,0.000380412|N
,-0.5718049043,0.1029866058,-0.0000479616|O,-0.3483064535,1.3081084776
,0.0003539681|O,0.5593699646,-0.7978916953,-0.0002870685|C,1.787425319
3,-0.0629017563,0.000095289|H,2.542243763,-0.8468572043,-0.0001761282
|H,1.8833377223,0.5553377935,-0.8918206664|H,1.8832307358,0.5548089898
,0.8922180217||Version=IA32W-G09RevA.02|State=1-A|HF=-282.7399387|MP2=
-283.6904697|RMSD=8.047e-009|RMSF=1.206e-004|Dipole=0.1532662,-0.50972
31,0.0000218|PG=C01 [X(C2H5N1O2)]||@
```

Transition State for O-Attack

```
1\1\GINC-NODE26\FTS\RMP2-FC\6-311+G(2d,p)\C3H7N2O4(1-)\MAY04\09-Aug-20
10\0\#p MP2/6-311+G(2d,p) opt=(calcf,ts,noigentest) freq\TS-Nitronat
e-O-Attack\|-1,1|C,-0.0002043299,0.0004292648,1.047132451|H,-0.031055
4849,0.9369498466,0.5149090918|H,0.0308774649,-0.9367555694,0.51610618
1|H,-0.0004224302,0.0011181919,2.1228749252|O,1.9006995456,0.062490877
1,1.1094234381|N,2.3561666302,-0.3497065117,-0.0721175165|O,2.18331361
94,-1.5567628606,-0.4008910118|O,-1.9011249125,-0.0615541299,1.1086967
221|N,-2.3561212218,0.3496661249,-0.073364261|O,-2.1830727519,1.556446
551,-0.4030964175|C,-2.9631667179,-0.5487895739,-0.8408881998|H,-3.348
4742809,-0.2028815705,-1.7862694287|C,2.963447251,0.5481386765,-0.8401
70209|H,3.3491210587,0.2014603138,-1.7851199256|H,3.0322406297,1.55497
64682,-0.4665406972|H,-3.0321570695,-1.5553090988,-0.4664381422||Versi
on=AM64L-G03RevD.01|State=1-A|HF=-525.8667523|MP2=-527.6242701|RMSD=4.
793e-09|RMSF=2.890e-06|Thermal=0.|Dipole=-0.0000244,-0.0001849,-0.3867
76|PG=C01 [X(C3H7N2O4)]||@
```

Transition State for C-Attack

```
1\1\GINC-NODE14\FTS\RMP2-FC\6-311+G(2d,p)\C3H7N2O4(1-)\MAY04\10-Aug-20
10\0\#p MP2/6-311+G(2d,p) opt=(ts,calcf,calcf,noigentest) freq\Ni tronat
e-C-Angri ff\|-1,1|C,-0.0000003748,0.4015198511,0.0000003572|H,0.51623890
02,0.9388645068,0.7875835957|H,-0.0000004484,-0.6826707635,-0.00000029
11|H,-0.5162395941,0.9388655097,-0.7875822443|C,-1.7167467651,0.414733
6295,1.0395464491|H,-1.5524008141,-0.2627587963,1.8679910895|H,-1.8848
92594,1.4627469543,1.2528863267|C,1.7167460069,0.4147346731,-1.0395457
```

```
249\H, 1. 5524000224, -0. 262756834, -1. 8679911101\H, 1. 8848918867, 1. 4627482
24, -1. 2528844518\N, -2. 6002177996, -0. 0871278455, 0. 093928614\O, -2. 756647
8071, -1. 3365866265, 0. 006570077\O, -3. 0875641184, 0. 7134455783, -0. 7556354
599\N, 2. 6002170232, -0. 0871278823, -0. 0939284455\O, 2. 7566469798, -1. 33658
67651, -0. 006571285\O, 3. 0875633808, 0. 7134445864, 0. 7556365056\\Versi on=A
M64L-G03RevD. 01\State=1-A\HF=-525. 8558157\MP2=-527. 6464114\RMSD=4. 630e
-09\RMSF=2. 622e-06\Thermal =0. \Di pol e=0. , 0. 9961237, 0. 0000006\PG=C01 [X(
C3H7N204)]\@
```

6.2.6 Phenolate Anion

Phenolate Anion

```
1|1|UNPC-OLE|FOpt|RMP2-FC|6-311+G(2d,p)|C6H5O1(1-)|TI NO|03-Aug-2010|O|
|#p opt freq MP2/6-311+G(2d,p)||Phenolate Ani on||-1,1|C,1. 8265251111, -
0. 0000004754, 0. 0000776346|C,1. 1013279335, -1. 2002710193, -0. 000001345|C, -
0. 291566123, -1. 2063971145, 0. 000079057|C, -1. 0816147143, 0. 0000004867, 0.
0004359626|C, -0. 2915654028, 1. 2063975284, 0. 0000790567|C, 1. 1013286916, 1.
2002705121, -0. 0000013452|H, 2. 913366252, -0. 0000007965, 0. 0000273606|H, 1.
6356325747, -2. 1509338136, -0. 0001190212|H, -0. 8339821175, -2. 1508809492, -
0. 0000743656|H, -0. 8339807671, 2. 1508817259, -0. 0000743662|H, 1. 6356338384
, 2. 1509330166, -0. 0001190204|O, -2. 3585572766, 0. 0000008037, -0. 0002296078
||Versi on=I A32W-G09RevA. 02|State=1-A|HF=-305. 0674414|MP2=-306. 1640545|
RMSD=2. 868e-009|RMSF=4. 208e-005|Di pol e=1. 8281673, -0. 0000006, 0. 0000584|
PG=C01 [X(C6H5O1)]||@
```

Anisole (O-Attack)

```
1\1\GI NC-NODE23\FOpt\RMP2-FC\6-311+G(2d,p)\C7H8O1\MAY04\04-Aug-2010\O\
|#p opt freq MP2/6-311+G(2d,p)\Ani sol e\0,1\C,2. 26514419, 0. 33108879, 0.
00000525\C,1. 31204015, 1. 34570624, 0. 00000993\C, -0. 05485344, 1. 04648435,
0. 00000536\C, -0. 4648548, -0. 29000644, -0. 00000309\C, 0. 48954911, -1. 313890
8, -0. 00000873\C, 1. 84452632, -1. 00268853, -0. 00000456\H, 3. 32277593, 0. 5724
9478, 0. 00000936\H, 1. 62380847, 2. 38566478, 0. 00001751\H, -0. 77599599, 1. 854
47124, 0. 00000622\H, 0. 14482026, -2. 34300449, -0. 00001714\H, 2. 57594211, -1.
80494795, -0. 00000935\O, -1. 76991145, -0. 69970349, -0. 00000616\C, -2. 758062
42, 0. 32275835, 0. 00000577\H, -3. 71671221, -0. 19096711, -0. 0000005\H, -2. 679
25439, 0. 94919922, 0. 89339537\H, -2. 67925383, 0. 94922005, -0. 89336925\\Vers
i on=AM64L-G03RevD. 01\State=1-A\HF=-344. 6771543\MP2=-345. 9137273\RMSD=9
. 233e-09\RMSF=5. 475e-05\Thermal =0. \Di pol e=-0. 2907125, 0. 4410243, 0. 00000
43\PG=C01 [X(C7H8O1)]\@
```

4-Methylcyclohexa-2,5-dienone (C-Attack)

```
1\1\GI NC-NODE25\FOpt\RMP2-FC\6-311+G(2d,p)\C7H8O1\MAY04\04-Aug-2010\O\
|#p opt freq MP2/6-311+G(2d,p)\4-methyl cycl ohexa-2,5-di enone\0,1\C,1
. 378292236, -0. 0000004367, -0. 435860055\C, 0. 5662800494, 1. 2473501931, -0. 3
093203505\C, -0. 7548136893, 1. 2521649807, -0. 0572128282\C, -1. 5169679753, 0
. 0000001995, 0. 0949296279\C, -0. 7548143872, -1. 2521649413, -0. 0572125922\C
, 0. 5662794602, -1. 2473505864, -0. 309319196\H, 1. 8431167173, -0. 000000691, -
1. 4335105414\H, 1. 0988221204, 2. 1912848584, -0. 4127049348\H, -1. 3142293868
, 2. 1772203603, 0. 0445296461\H, -1. 3142304236, -2. 1772202119, 0. 0445293187\
H, 1. 0988211812, -2. 1912853857, -0. 4127040558\C, 2. 5241192245, 0. 0000001864
, 0. 594637483\H, 3. 1517843191, -0. 8856267957, 0. 4733199401\H, 3. 151780175, 0
. 8856306271, 0. 4733234019\H, 2. 1140854958, -0. 0000026824, 1. 6070236346\O, -
2. 7252371168, 0. 0000002803, 0. 3353835017\\Versi on=AM64L-G03RevD. 01\State
=1-A\HF=-344. 6712386\MP2=-345. 9012347\RMSD=4. 161e-09\RMSF=4. 541e-06\Th
ermal =0. \Di pol e=1. 7743166, -0. 0000003, -0. 2966565\PG=C01 [X(C7H8O1)]\@
```

Transition State for O-Attack

```
1\1\GI NC-NODE13\FTS\RMP2-FC\6-311+G(2d,p)\C13H13O2(1-)\MAY04\08-Aug-20
10\O\|#p MP2/6-311+G(2d,p) opt=(ts,noigentest,readfc) freq GEOM=ALLCH
ECK GUESS=READ SCRF=CHECK\\Ph0---Me---OPh (Phenolat O-Angriff)\-1,1\C
, -5. 0706806421, -0. 6912267624, 0. 1614729758\C, -3. 9040159396, -1. 188353545
```

8, -0.4107862147\C, -2.6762838389, -0.4718556426, -0.3680631695\C, -2.7107259113, 0.7867254517, 0.2942468689\C, -3.8878631144, 1.2757567277, 0.8647133694\H, -5.9845759878, -1.2792284076, 0.1020477635\H, -3.8996064276, -2.1527979401, -0.912709012\H, -1.8081154783, 1.3841289024, 0.3618105523\H, -3.8672790388, 2.2433504092, 1.3622544141\O, -1.6065021067, -0.9894162968, -0.9253078861\C, 0.0000262909, 0.0009612182, -0.8712448298\H, 0.4398069844, -0.8176792019, -1.4123739186\H, -0.4398446532, 0.8206002287, -1.4107873163\H, 0.0001186935, -0.0000284208, 0.2048464895\O, 1.6065449125, 0.9914696319, -0.9237636641\C, 2.6763250184, 0.4729146938, -0.36744374\C, 3.9040513987, 1.1894955963, -0.4088243695\C, 2.710768808, -0.7868838586, 0.2925564779\C, 5.0707060685, 0.6913254817, 0.162546264\H, 3.8996506454, 2.1548591355, -0.9089776966\C, 3.8878944078, -1.2769520544, 0.8621504555\H, 1.8081671648, -1.3844280616, 0.3589849184\H, 5.9845975047, 1.2794431729, 0.1042166812\H, 3.8673068236, -2.2454593505, 1.3579104923\C, 5.079647515, -0.5516107087, 0.807136273\H, 5.9895465293, -0.9416569314, 1.2536289795\C, -5.0796211975, 0.5505293712, 0.8083393623\H, -5.9895254294, 0.939765162, 1.2555284798\\Version=AM64L-G03RevD.01\State=1-A\HF=-649.7026324\MP2=-652.0575437\RMSD=6.556e-09\RMSF=9.537e-07\Thermal=0.\Di pol e=-0.0000341, -0.0005251, 0.5591945\PG=C01 [X(C13H1302)]\@

Transition State for C-Attack

1\1\GINC-NODE28\FTS\RMP2-FC\6-311+G(2d,p)\C13H1302(1-)\MAY04\06-Aug-2010\#\#p MP2/6-311+G(2d,p) opt=(ts,noigentest,readfc) freq GEOM=ALLCHECK GUESS=READ SCRF=CHECK\O\Ph---Me---PhO (Phenol at-C-Attack)\-1,1\C, -1.9134435416, -0.7600356683, -1.3258613443\C, -2.8295212912, -1.3242148235, -0.4723778421\C, -3.683070826, -0.5258112224, 0.3932435251\C, -3.5047986172, 0.911693924, 0.259403738\C, -2.5867661443, 1.4607457799, -0.6019643682\H, -1.2922498069, -1.4033525531, -1.947794498\H, -2.9531313794, -2.4034924535, -0.4243298133\H, -4.1500558087, 1.5448264226, 0.8641079524\H, -2.4977590945, 2.5449165656, -0.670082437\O, -4.5140597622, -1.0346740873, 1.1871330491\C, 0.000003916, 0.7054171019, 0.000008946\H, -0.6279658193, 0.1758905913, 0.7025716654\H, 0.6279708537, 0.1758851202, -0.702552068\H, 0.0000026377, 1.7844054705, 0.0000039994\C, 2.5867711366, 1.4607491099, 0.601961733\C, 1.9134527495, -0.7600282602, 1.3258715001\C, 3.5047881636, 0.9116931439, -0.2594199508\H, 2.497767978, 2.5449203025, 0.6700781073\C, 2.8295164589, -1.3242112711, 0.4723762449\H, 1.2922664392, -1.4033423177, 1.9478149417\C, 3.6830568372, -0.5258125866, -0.3932591533\H, 4.1500385728, 1.5448231561, -0.8641340935\H, 2.9531235472, -2.4034893912, 0.4243304179\O, 4.5140335829, -1.034679406, -1.1871583803\C, -1.6805457541, 0.6472986317, -1.3433990617\H, -1.1353291688, 1.0835662506, -2.1757515557\C, 1.6805571928, 0.6473062513, 1.3434080531\H, 1.1353509973, 1.0835772188, 2.1757656927\\Version=AM64L-G03RevD.01\State=1-A\HF=-649.6554417\MP2=-652.0270932\RMSD=3.087e-09\RMSF=1.543e-05\Thermal=0.\Di pol e=0.000032, 1.7118014, 0.0000193\PG=C01 [X(C13H1302)]\@

6.2.7 Methyl Sulfinat Anion

Methyl Sulfinat Anion

1|1|UNPC-OLE|FOpt|RMP2-FC|6-311+G(2d,p)|C1H3O2S1(1-)|TINO|02-Aug-2010|0|1|#p MP2/6-311+G(2d,p) opt freq|Methyl sulfinate||-1,1|C, 1.5487364626, -0.0000814544, 0.154395025|H, 2.0403657951, 0.9007985871, -0.2203160888|H, 2.0402532795, -0.9010579742, -0.220232363|H, 1.5187905515, -0.0000295099, 1.2470073923|S, -0.2253738835, 0.0000053998, -0.3822968983|O, -0.7077419969, -1.2692623715, 0.294291014|O, -0.7076042082, 1.2693533231, 0.2942389189|Version=I A32W-G09RevA.02|State=1-A|HF=-586.9123077|MP2=-587.6847201|RMSD=6.151e-009|RMSF=1.587e-004|Di pol e=1.3038272, -0.000081, -0.4666424|PG=C01 [X(C1H3O2S1)]||@

O-Methyl Methylsulfinate (O-Attack)

1|1|UNPC-OLE|FOpt|RMP2-FC|6-311+G(2d,p)|C2H6O2S1|TINO|02-Aug-2010|0|1|#p MP2/6-311+G(2d,p) opt freq|Methyl methanesulfinate||0,1|C, -1.2400509542, -0.8878974478, 0.6081927553|H, -1.100331951, -1.9216940488, 0.2921411713|H, -2.3014740076, -0.6529842537, 0.6901903739|H, -0.7462877236, -0.6828

768123, 1. 5574649003|S, -0. 5625450357, 0. 2228156235, -0. 65140948|O, -0. 5050471091, 1. 5424042753, 0. 0186621529|O, 0. 9650136963, -0. 4392301732, -0. 7392019477|C, 1. 7849095422, -0. 2823231632, 0. 4373624628|H, 2. 8123890324, -0. 3734362102, 0. 0934231158|H, 1. 6294878932, 0. 70156009, 0. 8832985823|H, 1. 5688866171, -1. 0687418795, 1. 1626289131||Version=I A32W-G09RevA. 02|State=1-A|HF=-626. 4963436|MP2=-627. 4129255|RMSD=4. 136e-009|RMSF=2. 398e-005|Dipole=0. 021399, -1. 1067121, 0. 5826128|PG=C01 [X(C2H6O2S1)]||@

Dimethyl Sulfone (*S*-Attack)

1|1|UNPC-RUTHENIUM|FOpt|RMP2-FC|6-311+G(2d, p)|C2H6O2S1|MARTIN|02-Aug-2010|0|#p MP2/6-311+G(2d, p) opt freq|(Methyl sulfonyl)methane||0, 1|C, -1. 3983068316, -0. 0000014011, 0. 9226325701|H, -1. 3748280381, -0. 9018148963, 1. 5322165129|H, -2. 2804536527, -0. 0000005882, 0. 2823994783|H, -1. 3748281319, 0. 9018103242, 1. 5322191332|S, -0. 0000000007, 0. 0000002788, -0. 1823418289|O, 0. 0000000158, -1. 2641619949, -0. 8982956742|O, -0. 0000000181, 1. 264164684, -0. 8982918821|C, 1. 3983068339, -0. 0000013269, 0. 9226325656|H, 2. 2804536573, -0. 0000001872, 0. 2823994792|H, 1. 3748279558, 0. 9018102971, 1. 5322192792|H, 1. 374828207, -0. 901814921, 1. 5322163668||Version=I A32W-G09RevA. 02|State=1-A|HF=-626. 5152772|MP2=-627. 4338647|RMSD=6. 418e-009|RMSF=1. 828e-005|Dipole=0. , -0. 0000027, 1. 8058501|PG=C01 [X(C2H6O2S1)]||@

Transition State for *O*-Attack

1\1\GINC-NODE20\FTS\RMP2-FC\6-311+G(2d, p)\C3H9O4S2(1-)\MAY04\09-Aug-2010\0\#p opt=(ts, noigentest, calcfc) MP2/6-311+G(2d, p) freq\H3CS00---Me---00SCH3\1, 1\C, 0. 0001998661, -0. 2739675791, 0. 0006856135\H, -0. 4847585901, -0. 8129633579, 0. 7946511846\H, 0. 4848424667, -0. 8150146677, -0. 7920770237\H, 0. 0005122508, 0. 7983371824, -0. 0005094039\O, -1. 5989772844, -0. 2666111828, -1. 0966357115\O, 1. 599380965, -0. 2651003867, 1. 097989142\S, -2. 9785537472, -0. 1560069156, -0. 3797475537\S, 2. 9790205882, -0. 1568881376, 0. 3808575113\O, 3. 0673254645, -1. 0606601576, -0. 8174732732\O, -3. 0673850505, -1. 0570697824, 0. 8205828148\C, 2. 802313558, 1. 4905628029, -0. 4132179037\H, 2. 5649389295, 2. 2363275432, 0. 3473287977\H, 3. 7478893128, 1. 7262685729, -0. 9041151287\H, 2. 0077831542, 1. 4155562886, -1. 1570534359\C, -2. 8008878562, 1. 4930966259, 0. 4106757369\H, -3. 7463268595, 1. 7304404617, 0. 9010467901\H, -2. 0064023497, 1. 4192757788, 1. 1546778066\H, -2. 5630778183, 2. 2370359108, -0. 3515209597\Version=AM64L-G03RevD. 01|State=1-A|HF=-1213. 3826929\MP2=-1215. 0834317\RMSD=4. 303e-09\RMSF=2. 006e-07\Thermal=0. \Dipole=0. 0006618, 2. 2619224, -0. 0025061\PG=C01 [X(C3H9O4S2)]\@

Transition State for *S*-Attack

1\1\GINC-NODE28\FTS\RMP2-FC\6-311+G(2d, p)\C3H9O4S2(1-)\MAY04\05-Aug-2010\0\#p opt=(ts, noigentest, calcfc) MP2/6-311+G(2d, p) freq\H3C02S---Me---S02CH3\1, 1\C, -0. 0014678307, -0. 0217420717, -0. 0038714442\H, 0. 09700628, -0. 5838171978, -0. 9224948223\H, -0. 0936903718, -0. 5592022155, 0. 930050742\H, -0. 0076866114, 1. 058991066, -0. 018941711\S, 2. 2570584468, -0. 0245742989, 0. 327579298\O, 2. 8256724643, 1. 3355556349, 0. 5496066008\O, 2. 6339330152, -1. 0812087245, 1. 3113762507\S, -2. 2597655159, -0. 0597486782, -0. 3345471998\O, -2. 8435948551, 1. 2867637239, -0. 5965946493\O, -2. 6246467228, -1. 1492819246, -1. 2865397429\C, 3. 0510922047, -0. 5762486302, -1. 2202526005\H, 4. 1232792691, -0. 5884803162, -1. 0159448985\H, 2. 6943661389, -1. 5764395588, -1. 4677956464\H, 2. 8174639075, 0. 1350329663, -2. 0129795186\C, -3. 0476402031, -0. 5742223552, 1. 2291748601\H, -4. 1196202383, -0. 6044393168, 1. 0256509366\H, -2. 6797893948, -1. 5626145878, 1. 5060860436\H, -2. 8219718456, 0. 1627554851, 2. 000445381\Version=AM64L-G03RevD. 01|State=1-A|HF=-1213. 3746323\MP2=-1215. 0868997\RMSD=5. 279e-09\RMSF=9. 662e-06\Thermal=0. \Dipole=0. 0041348, -0. 7186841, 0. 010659\PG=C01 [X(C3H9O4S2)]\@

7 References

- [1] P. Müller, *Pure Appl. Chem.* **1994**, *66*, 1077–1184.
- [2] a) N. Kornblum, B. Taub, H. E. Ungnade, *J. Am. Chem. Soc.* **1954**, *76*, 3209–3211; b) N. Kornblum, H. O. Larsen, D. D. Mooberry, R. K. Blackwood, E. P. Oliveto, G. E. Graham, *Chem. Ind.* **1955**, 443; c) N. Kornblum, R. A. Smiley, H. E. Ungnade, A. M. White, B. Taub, S. A. Herbert, Jr., *J. Am. Chem. Soc.* **1955**, *77*, 5528–5533; d) N. Kornblum, L. Fishbein, R. A. Smiley, *J. Am. Chem. Soc.* **1955**, *77*, 6261–6266; e) N. Kornblum, R. A. Smiley, R. K. Blackwood, D. C. Iffland, *J. Am. Chem. Soc.* **1955**, *77*, 6269–6280; f) N. Kornblum, H. O. Larson, R. K. Blackwood, D. D. Mooberry, E. P. Oliveto, G. E. Graham, *J. Am. Chem. Soc.* **1956**, *78*, 1497–1501; g) N. Kornblum, *Organic Reactions* **1962**, *12*, 101–156.
- [3] a) R. G. Pearson, *J. Am. Chem. Soc.* **1963**, *85*, 3533–3539; b) R. G. Pearson, *Science* **1966**, *151*, 172–177; c) R. G. Pearson, J. Songstad, *J. Am. Chem. Soc.* **1967**, *89*, 1827–1836; d) R. G. Pearson, *J. Chem. Educ.* **1968**, *45*, 581–587; e) R. G. Pearson, *J. Chem. Educ.* **1968**, *45*, 643–648; f) R. G. Pearson, *Chemical Hardness*, Wiley-VCH, Weinheim, **1997**.
- [4] M. B. Smith, J. March, *March's Advanced Organic Chemistry Reactions, Mechanisms, and Structure*, 6th ed., Wiley, Hoboken (NJ), **2007**.
- [5] a) G. Klopman, *J. Am. Chem. Soc.* **1968**, *90*, 223–234; b) L. Salem, *J. Am. Chem. Soc.* **1968**, *90*, 543–552; c) G. Klopman, *Chemical Reactivity and Reaction Paths*, Wiley, **1974**; d) I. Fleming, *Frontier Orbitals and Organic Chemical Reactions*, Wiley-VCH, London, **1976**; e) I. Fleming, *Molecular Orbitals and Organic Chemical Reactions; Student Edition*, John Wiley & Sons, Chichester, **2009**.
- [6] a) R. Gompper, *Angew. Chem.* **1964**, *76*, 412–423; *Angew. Chem. Int. Ed. Engl.* **1964**, *3*, 560–570; b) R. Gompper, H. U. Wagner, *Angew. Chem.* **1976**, *88*, 389–401; *Angew. Chem. Int. Ed. Engl.* **1976**, *15*, 321–333.
- [7] J. A. Berson, *Angew. Chem.* **2006**, *118*, 4842–4847; *Angew. Chem. Int. Ed.* **2006**, *45*, 4724–4729.
- [8] S. Hünig, *Angew. Chem.* **1964**, *76*, 400–412; *Angew. Chem. Int. Ed. Engl.* **1964**, *3*, 548–560.
- [9] R. S. Drago, *J. Chem. Educ.* **1974**, *51*, 300–307.
- [10] a) H. Mayr, M. Patz, *Angew. Chem.* **1994**, *106*, 990–1010; *Angew. Chem. Int. Ed. Engl.* **1994**, *33*, 938–957; b) H. Mayr, T. Bug, M. F. Gotta, N. Hering, B. Irrgang, B.

- Janker, B. Kempf, R. Loos, A. R. Ofial, G. Remennikov, H. Schimmel, *J. Am. Chem. Soc.* **2001**, *123*, 9500–9512; c) R. Lucius, R. Loos, H. Mayr, *Angew. Chem.* **2002**, *114*, 97–102; *Angew. Chem. Int. Ed.* **2002**, *41*, 91–95; d) H. Mayr, B. Kempf, A. R. Ofial, *Acc. Chem. Res.* **2003**, *36*, 66–77; e) H. Mayr, A. R. Ofial, *Pure Appl. Chem.* **2005**, *77*, 1807–1821.
- [11] P. Perez, A. Toro-Labbe, A. Aizman, R. Contreras, *J. Org. Chem.* **2002**, *67*, 4747–4752.
- [12] a) J. W. Bunting, J. M. Mason, C. K. M. Heo, *J. Chem. Soc., Perkin Trans. 2* **1994**, 2291–2300; b) J. P. Richard, M. M. Toteva, J. Crugeiras, *J. Am. Chem. Soc.* **2000**, *122*, 1664–1674; c) T. B. Phan, M. Breugst, H. Mayr, *Angew. Chem.* **2006**, *118*, 3954–3959; *Angew. Chem. Int. Ed.* **2006**, *45*, 3869–3874.
- [13] a) R. Loos, S. Kobayashi, H. Mayr, *J. Am. Chem. Soc.* **2003**, *125*, 14126–14132; b) A. A. Tishkov, H. Mayr, *Angew. Chem.* **2005**, *117*, 145–148; *Angew. Chem. Int. Ed.* **2005**, *44*, 142–145; c) A. A. Tishkov, U. Schmidhammer, S. Roth, E. Riedle, H. Mayr, *Angew. Chem.* **2005**, *117*, 4699–4703; *Angew. Chem. Int. Ed.* **2005**, *44*, 4623–4626; d) H. F. Schaller, U. Schmidhammer, E. Riedle, H. Mayr, *Chem. Eur. J.* **2008**, *14*, 3866–3868; e) T. Bug, T. Lemek, H. Mayr, *J. Org. Chem.* **2004**, *69*, 7565–7576; f) M. Baidya, S. Kobayashi, H. Mayr, *J. Am. Chem. Soc.* **2010**, *132*, 4796–4805; g) M. Breugst, T. Tokuyasu, H. Mayr, *J. Org. Chem.* **2010**, *75*, 5250–5258; h) M. Breugst, H. Mayr, *J. Am. Chem. Soc.* **2010**, *132*, 15380–15389.
- [14] P. W. Atkins, J. de Paula, *Physical Chemistry*, 9th ed., Oxford University Press, Oxford, **2009**.
- [15] R. A. McClelland, V. M. Kanagasabapathy, N. S. Banait, S. Steenken, *J. Am. Chem. Soc.* **1991**, *113*, 1009–1014.
- [16] a) J. P. Richard, T. L. Amyes, M. M. Toteva, *Acc. Chem. Res.* **2001**, *34*, 981–988; b) J. P. Richard, T. L. Amyes, M. M. Toteva, Y. Tsuji, *Adv. Phys. Org. Chem.* **2004**, *39*, 1–26; c) H. Mayr, A. R. Ofial, *Angew. Chem.* **2006**, *118*, 1876–1886; *Angew. Chem. Int. Ed.* **2006**, *45*, 1844–1854.
- [17] For a comprehensive listing of nucleophilicity parameters N and electrophilicity parameters E , see <http://www.cup.uni-muenchen.de/oc/mayr/DBintro.html>.
- [18] For selective, diffusion-controlled reactions discussed in this manuscript: see refs 2c, 13h, 38.
- [19] M. Breugst, H. Zipse, J. P. Guthrie, H. Mayr, *Angew. Chem.* **2010**, *122*, 5291–5295; *Angew. Chem. Int. Ed.* **2010**, *49*, 5165–5169.

- [20] a) R. A. Marcus, *Annu. Rev. Phys. Chem.* **1964**, *15*, 155–196; b) R. A. Marcus, *J. Phys. Chem.* **1968**, *72*, 891–899; c) R. A. Marcus, *J. Am. Chem. Soc.* **1969**, *91*, 7224–7225; d) W. J. Albery, M. M. Kreevoy, *Adv. Phys. Org. Chem.* **1978**, *16*, 87–157; e) W. J. Albery, *Annu. Rev. Phys. Chem.* **1980**, *31*, 227–263; f) R. A. Marcus, *Angew. Chem.* **1993**, *105*, 1161–1172; *Angew. Chem. Int. Ed. Engl.* **1993**, *32*, 1111–1121; g) R. A. Marcus, *Pure Appl. Chem.* **1997**, *69*, 13–29.
- [21] S. S. Shaik, H. B. Schlegel, P. Wolfe, *Theoretical Aspects of Physical Organic Chemistry: The S_N2 Mechanism*, Wiley, New York, **1992**.
- [22] a) S. Wolfe, D. J. Mitchell, H. B. Schlegel, *J. Am. Chem. Soc.* **1981**, *103*, 7692–7694; b) S. Wolfe, D. J. Mitchell, H. B. Schlegel, *J. Am. Chem. Soc.* **1981**, *103*, 7694–7696; c) J. M. Gonzales, R. S. Cox III, S. T. Brown, W. D. Allen, H. F. Schaefer III, *J. Phys. Chem. A* **2001**, *105*, 11327–11346; d) J. M. Gonzales, C. Pak, R. S. Cox, W. D. Allen, H. F. Schaefer III, A. G. Csaszar, G. Tarczay, *Chem. Eur. J.* **2003**, *9*, 2173–2192; e) J. M. Gonzales, W. D. Allen, H. F. Schaefer III, *J. Phys. Chem. A* **2005**, *109*, 10613–10628.
- [23] S. Hoz, H. Basch, J. L. Wolk, T. Hoz, E. Rozental, *J. Am. Chem. Soc.* **1999**, *121*, 7724–7725.
- [24] E. Uggerud, *J. Phys. Org. Chem.* **2006**, *19*, 461–466.
- [25] a) L. G. Arnaut, A. A. C. C. Pais, S. J. Formosinho, *J. Mol. Struct.* **2001**, *563–564*, 1–17; b) L. G. Arnaut, S. J. Formosinho, *Chem. Eur. J.* **2007**, *13*, 8018–8028.
- [26] a) F. O. Rice, E. Teller, *J. Chem. Phys.* **1938**, *6*, 489–496; b) J. Hine, *J. Org. Chem.* **1966**, *31*, 1236–1244; c) J. Hine, *J. Am. Chem. Soc.* **1966**, *88*, 5525–5528; d) J. Hine, *Adv. Phys. Org. Chem.* **1977**, *15*, 1–61.
- [27] a) S. Samdal, H. M. Seip, *J. Mol. Struct.* **1975**, *28*, 193–203; b) C. Lambert, Y. D. Wu, P. v. R. Schleyer, *J. Chem. Soc., Chem. Commun.* **1993**, 255–256; c) G. Da Silva, J. W. Bozzelli, *J. Phys. Chem. A* **2006**, *110*, 13058–13067.
- [28] When ions are formed from neutral reactants, ΔG^0 (gas phase) becomes highly positive with the consequence that $\Delta\Delta G^\ddagger$ is now dominated by the cross-term of the Marcus equation. Consideration of the highly exergonic reverse reaction reveals the relationship to the Marcus-inverse region.
- [29] G. L. Closs, L. T. Calcaterra, N. J. Green, K. W. Penfield, J. R. Miller, *J. Phys. Chem.* **1986**, *90*, 3673–3683.
- [30] J. C. Carretero, J. L. Garcia Ruano, *Tetrahedron Lett.* **1985**, *26*, 3381–3384.

- [31] Before publication in 2005 (ref. 13b), these results were only quoted twice: a) E. D. Soli, A. S. Manoso, M. C. Patterson, P. DeShong, D. A. Favor, R. Hirschmann, A. B. Smith III, *J. Org. Chem.* **1999**, *64*, 3171–3177; b) L. R. Subramanian, *Science of Synthesis* **2004**, *19*, 173–195.
- [32] a) T. Sasaki, A. Nakanishi, M. Ohno, *J. Org. Chem.* **1981**, *46*, 5445–5447; b) M. T. Reetz, I. Chatziiosifidis, H. Kuenzer, H. Müller-Starke, *Tetrahedron* **1983**, *39*, 961–965.
- [33] K. B. Dillon, M. Hodgson, D. Parker, *Synth. Commun.* **1985**, *15*, 849–854.
- [34] W. Kantlehner, J. J. Kapassakalidis, P. Speh, H. J. Braeuner, *Liebigs Ann. Chem.* **1980**, 389–393.
- [35] K. E. Koenig, W. P. Weber, *Tetrahedron Lett.* **1974**, *15*, 2275–2278.
- [36] a) M. Meier, C. Rüchardt, *Chem. Ber.* **1987**, *120*, 1–4; b) C. Rüchardt, M. Meier, K. Haaf, J. Pakusch, E. K. A. Wolber, B. Müller, *Angew. Chem.* **1991**, *103*, 907–915; *Angew. Chem. Int. Ed. Engl.* **1991**, *30*, 893–901; c) E. K. A. Wolber, M. Schmittel, C. Rüchardt, *Chem. Ber.* **1992**, *125*, 525–531.
- [37] G. Höfle, B. Lange, *Angew. Chem.* **1977**, *89*, 272–273 *Angew. Chem. Int. Ed. Engl.* **1977**, *16*, 262–263.
- [38] a) L. B. Engemyr, A. Martinsen, J. Songstad, *Acta Chem. Scand., Ser. A* **1974**, *28*, 255–266; b) P. G. Gassman, R. S. Gremban, *Tetrahedron Lett.* **1984**, *25*, 3259–3262.
- [39] T. Austad, J. Songstad, L. J. Stangeland, *Acta Chem. Scand.* **1971**, *25*, 2327–2336.
- [40] a) H. Mayr, in *Rate Constants and Reactivity Ratios in Carbocationic Polymerizations* (Eds.: J. E. Puskas, A. Michel, S. Barghi, C. Paulo), Kluwer Academic Publishers, Dordrecht, **1999**, pp. 99–115; b) J. Ammer, H. Mayr, *Macromolecules* **2010**, *43*, 1719–1723.
- [41] M. Roth, H. Mayr, *Angew. Chem.* **1995**, *107*, 2428–2430; *Angew. Chem. Int. Ed. Engl.* **1995**, *34*, 2250–2252.
- [42] S. Minegishi, H. Mayr, *J. Am. Chem. Soc.* **2003**, *125*, 286–295.
- [43] S. Minegishi, S. Kobayashi, H. Mayr, *J. Am. Chem. Soc.* **2004**, *126*, 5174–5181.
- [44] R. Quelet, *Bull. Soc. Chim. Fr.* **1940**, *7*, 205–215.
- [45] R. N. Lewis, P. V. Susi, *J. Am. Chem. Soc.* **1952**, *74*, 840–841.
- [46] J. Goerdeler, *Methoden Org. Chem. (Houben-Weyl) 4th ed. 1952–, Vol E 16a*, **1990**, pp 977–1002.

- [47] a) M. Censky, J. Sedlbauer, V. Majer, V. Ruzicka, *Geochim. Cosmochim. Acta* **2007**, *71*, 580–603; b) J. P. Guthrie, J. Barker, P. A. Cullimore, J. Lu, D. C. Pike, *Can. J. Chem.* **1993**, *71*, 2109–2122.
- [48] F. Brotzel, Y. C. Chu, H. Mayr, *J. Org. Chem.* **2007**, *72*, 3679–3688.
- [49] M. F. Gotta, H. Mayr, *J. Org. Chem.* **1998**, *63*, 9769–9775.
- [50] a) E. Buncl, H. W. Leung, *J. Chem. Soc., Chem. Commun.* **1975**, 19–20; b) E. Buncl, W. Eggimann, H. W. Leung, *J. Chem. Soc., Chem. Commun.* **1977**, 55–56; c) E. Buncl, W. Eggimann, *J. Am. Chem. Soc.* **1977**, *99*, 5958–5964; d) E. Buncl, W. Eggimann, *J. Chem. Soc., Perkin Trans. 2* **1978**, 673–677; e) E. Buncl, C. Innis, I. Onyido, *J. Org. Chem.* **1986**, *51*, 3680–3686.
- [51] F. Terrier, S. Lakhdar, T. Boubaker, R. Goumont, *J. Org. Chem.* **2005**, *70*, 6242–6253.
- [52] a) M. J. Strauss, R. A. Renfrow, E. Buncl, *J. Am. Chem. Soc.* **1983**, *105*, 2473–2474; b) E. Buncl, R. A. Renfrow, M. J. Strauss, *J. Org. Chem.* **1987**, *52*, 488–495; c) M. R. Crampton, L. C. Rabbitt, *J. Chem. Soc., Perkin Trans. 2* **1999**, 1669–1674; d) M. R. Crampton, L. C. Rabbitt, F. Terrier, *Can. J. Chem.* **1999**, *77*, 639–646.
- [53] S. Lakhdar, M. Westermaier, F. Terrier, R. Goumont, T. Boubaker, A. R. Ofial, H. Mayr, *J. Org. Chem.* **2006**, *71*, 9088–9095.
- [54] H. Zollinger, *Diazo Chemistry I: Aromatic and Heteroaromatic Compounds*, VCH, Weinheim, **1994**.
- [55] a) V. Beranek, M. Vecera, *Collect. Czech. Chem. Commun.* **1969**, *34*, 2753–2762; b) V. Beranek, M. Vecera, *Collect. Czech. Chem. Commun.* **1970**, *35*, 3402–3409; c) V. Beranek, H. Korinkova, P. Vetesnik, M. Vecera, *Collect. Czech. Chem. Commun.* **1972**, *37*, 282–288; d) J. R. Penton, H. Zollinger, *J. Chem. Soc., Chem. Commun.* **1979**, 819–821; e) J. R. Penton, H. Zollinger, *Helv. Chim. Acta* **1981**, *64*, 1717–1727; f) J. R. Penton, H. Zollinger, *Helv. Chim. Acta* **1981**, *64*, 1728–1738.
- [56] a) P. Perez, A. Toro-Labbe, *Theor. Chem. Acc.* **2001**, *105*, 422–430; b) Y. Cheng, Z.-T. Huang, M.-X. Wang, *Curr. Org. Chem.* **2004**, *8*, 325–351.
- [57] a) G. Opitz, H. Hellmann, H. W. Schubert, *Liebigs Ann. Chem.* **1959**, *623*, 112–117; b) G. Opitz, H. Hellmann, H. W. Schubert, *Liebigs Ann. Chem.* **1959**, *623*, 117–124; c) G. Opitz, W. Merz, *Liebigs Ann. Chem.* **1962**, *652*, 139–158; d) G. Opitz, W. Merz, *Liebigs Ann. Chem.* **1962**, *652*, 158–162; e) G. Opitz, W. Merz, *Liebigs Ann. Chem.* **1962**, *652*, 163–175; f) G. Opitz, A. Griesinger, *Liebigs Ann. Chem.* **1963**, *665*, 101–113.
- [58] L. Alais, R. Michelot, B. Tchoubar, *C. R. Acad. Sci., Ser. C* **1971**, *273*, 261–264.

- [59] a) G. Stork, R. Terrell, J. Szmuszkovicz, *J. Am. Chem. Soc.* **1954**, 76, 2029–2030; b) G. Stork, H. K. Landesman, *J. Am. Chem. Soc.* **1956**, 78, 5128–5129; c) G. Stork, A. Brizzolara, H. Landesman, J. Szmuszkovicz, R. Terrell, *J. Am. Chem. Soc.* **1963**, 85, 207–222.
- [60] E. Elkik, *Bull. Soc. Chim. Fr.* **1960**, 972–975.
- [61] K. Brannock, R. Burpitt, *J. Org. Chem.* **1961**, 26, 3576–3577.
- [62] G. Opitz, *Liebigs Ann. Chem.* **1961**, 650, 122–132.
- [63] M. E. Kuehne, T. Garbacik, *J. Org. Chem.* **1970**, 35, 1555–1558.
- [64] H. Böhme, J. G. Von Grätz, *Tetrahedron* **1977**, 33, 841–845.
- [65] a) P. W. Hickmott, in *The Chemistry of Enamines* (Ed.: Z. Rappoport), Wiley, Chichester, **1994**, pp. 727–871; b) S. Hünig, E. Benzing, E. Lücke, *Chem. Ber.* **1957**, 90, 2833–2840; c) S. Hünig, W. Lendle, *Chem. Ber.* **1960**, 93, 909–913.
- [66] J. R. Hargreaves, P. W. Hickmott, B. J. Hopkins, *J. Chem. Soc. C* **1968**, 2599–2603.
- [67] B. Kempf, N. Hampel, A. R. Ofial, H. Mayr, *Chem. Eur. J.* **2003**, 9, 2209–2218.
- [68] F. Kaufler, C. Pomeranz, *Monatsh. Chem.* **1901**, 22, 492–496.
- [69] P. Walden, *Ber. Dtsch. Chem. Ges.* **1907**, 40, 3214–3217.
- [70] a) L. G. Cannell, R. W. Taft, *Abstr. Pap. Am. Chem. Soc. (ISSN: 0065-7727)* **1956**, 129, p 46N; b) A. Iliceto, A. Fava, U. Mazzucato, *Tetrahedron Lett.* **1960**, 1, 27–35; c) A. Iliceto, A. Fava, U. Mazzucato, O. Rossetto, *J. Am. Chem. Soc.* **1961**, 83, 2729–2734; d) E. S. Lewis, J. E. Cooper, *J. Am. Chem. Soc.* **1962**, 84, 3847–3852; e) A. Fava, A. Iliceto, A. Ceccon, P. Koch, *J. Am. Chem. Soc.* **1965**, 87, 1045–1049; f) A. Fava, A. Iliceto, S. Bresadola, *J. Am. Chem. Soc.* **1965**, 87, 4791–4794; g) U. Tonellato, *Boll. Sci. Fac. Chim. Ind. Bologna* **1969**, 27, 249–259; h) U. Tonellato, G. Levorato, *Boll. Sci. Fac. Chim. Ind. Bologna* **1969**, 27, 261–268; i) A. Ceccon, A. Fava, I. Papa, *J. Am. Chem. Soc.* **1969**, 91, 5547–5550; j) E. H. White, M. Li, S. Lu, *J. Org. Chem.* **1992**, 57, 1252–1258.
- [71] S. Minegishi, Dissertation, LMU München, **2004**.
- [72] T. Kitamura, S. Kobayashi, H. Taniguchi, *J. Org. Chem.* **1990**, 55, 1801–1805.
- [73] P. Miquel, *Ann. Chim.* **1877**, 11, 289–356.
- [74] J. Goerdeler, *Quart. Rep. Sulfur Chem.* **1970**, 5, 169–175.
- [75] W. Ruske, M. Keilert, *Chem. Ber.* **1961**, 94, 2695–2701.
- [76] T. B. Johnson, L. H. Levy, *Am. Chem. J.* **1908**, 38, 456–461.
- [77] A. Takamizawa, K. Hirai, K. Matsui, *Bull. Chem. Soc. Jpn* **1963**, 36, 1214–1220.
- [78] J. Goerdeler, D. Wobig, *Liebigs Ann. Chem.* **1970**, 731, 120–141.

- [79] a) M. S. Korobov, L. E. Nivorozhkin, V. I. Minkin, *Zh. Org. Khim.* **1973**, *9*, 1717–1724; b) F. G. Gelalcha, B. Schulze, *J. Org. Chem.* **2002**, *67*, 8400–8406.
- [80] D. E. Giles, A. J. Parker, *Aust. J. Chem.* **1973**, *26*, 273–299.
- [81] A. Wurtz, *Liebigs Ann. Chem.* **1849**, *71*, 326–342.
- [82] K. H. Slotta, L. Lorenz, *Ber. Dtsch. Chem. Ges.* **1925**, *58*, 1320–1323.
- [83] a) K. A. Jensen, A. Holm, *Acta Chem. Scand.* **1964**, *18*, 826–828; b) K. A. Jensen, A. Holm, *Acta Chem. Scand.* **1964**, *18*, 2417–2418; c) K. A. Jensen, M. Due, A. Holm, *Acta Chem. Scand.* **1965**, *19*, 438–442; d) A. Holm, C. Wentrup, *Acta Chem. Scand.* **1966**, *20*, 2123–2127; e) D. Martin, *Tetrahedron Lett.* **1964**, *5*, 2829–2832; f) D. Martin, W. Mucke, *Chem. Ber.* **1965**, *98*, 2059–2062; g) D. Martin, H.-J. Niclas, D. Habisch, *Liebigs Ann. Chem.* **1969**, *727*, 10–21.
- [84] H. D. Schädler, H. Köhler, *Z. Chem.* **1990**, *30*, 67.
- [85] a) R. F. Hudson, *Angew. Chem.* **1973**, *85*, 63–84; *Angew. Chem. Int. Ed. Engl.* **1973**, *12*, 36–56; b) S. J. Formosinho, L. G. Arnaut, *J. Chem. Soc., Perkin Trans. 2* **1989**, 1947–1952.
- [86] K. O. Schoeps, C. Halldin, S. Stone-Elander, B. Laangstroem, T. Greitz, *J. Labelled Compd. Radiopharm.* **1988**, *25*, 749–758.
- [87] A. Streitwieser, C. H. Heathcock, E. M. Kosower, *Introduction to organic chemistry*, Macmillan, New York, **1992**.
- [88] B. M. Rice, S. V. Pai, J. Hare, *Combust. Flame* **1999**, *118*, 445–458.
- [89] A. Gissot, S. N'Gouela, C. Matt, A. Wagner, C. Mioskowski, *J. Org. Chem.* **2004**, *69*, 8997–9001.
- [90] a) A. P. Cox, S. Waring, *J. Chem. Soc., Faraday Trans. 2* **1972**, *68*, 1060–1071; b) B. J. van der Veken, R. Maas, G. A. Guirgis, H. D. Stidham, T. G. Sheehan, J. R. Durig, *J. Phys. Chem.* **1990**, *94*, 4029–4039; c) G. B. Carpenter, *Acta Crystallogr.* **1952**, *5*, 132–135.
- [91] C. Räth, *Liebigs Ann. Chem.* **1931**, *489*, 107–118.
- [92] H. v. Pechmann, O. Baltzer, *Ber. Dtsch. Chem. Ges.* **1891**, *24*, 3144–3153.
- [93] a) G. C. Hopkins, J. P. Jonak, H. J. Minnemeyer, H. Tieckelmann, *J. Org. Chem.* **1967**, *32*, 4040–4044; b) N. M. Chung, H. Tieckelmann, *J. Org. Chem.* **1970**, *35*, 2517–2520.
- [94] D. Döpp, H. Döpp, *Methoden Org. Chem. (Houben-Weyl) 4th ed. 1952–, Vol E 5a*, **1985**, pp 934–1135.

- [95] a) S. Gabriel, *Ber. Dtsch. Chem. Ges.* **1887**, *20*, 2224–2236; b) M. S. Gibson, R. W. Bradshaw, *Angew. Chem.* **1968**, *80*, 986–996; *Angew. Chem. Int. Ed. Engl.* **1968**, *7*, 919–930; c) U. Ragnarsson, L. Grehn, *Acc. Chem. Res.* **1991**, *24*, 285–289.
- [96] F. Weygand, E. Frauendorfer, *Chem. Ber.* **1970**, *103*, 2437–2449.
- [97] a) T. H. Koch, R. J. Sluski, R. H. Moseley, *J. Am. Chem. Soc.* **1973**, *95*, 3957–3963; b) D. R. Anderson, J. S. Keute, T. H. Koch, R. H. Moseley, *J. Am. Chem. Soc.* **1977**, *99*, 6332–6340.
- [98] a) W. Khayata, D. Baylocq, F. Pellerin, N. Rodier, *Acta Crystallogr., Sect. C: Cryst. Struct. Commun.* **1984**, *C40*, 765–767; b) J. Perron, A. L. Beauchamp, *Inorg. Chem.* **1984**, *23*, 2853–2859; c) D. R. Whitcomb, M. Rajeswaran, *J. Chem. Crystallogr.* **2006**, *36*, 587–598; d) D. R. Whitcomb, M. Rajeswaran, *Acta Crystallogr., Sect. E: Struct. Rep. Online* **2007**, *E63*, m2753; e) X. Tao, Y.-Q. Li, H.-H. Xu, N. Wang, F.-L. Du, Y.-Z. Shen, *Polyhedron* **2009**, *28*, 1191–1195.
- [99] a) B. C. Challis, J. Challis, in *The Chemistry of Amides* (Ed.: J. Zabicky), Interscience Publisher, London, **1970**, pp. 731–858; b) C. J. M. Stirling, *J. Chem. Soc.* **1960**, 255–262.
- [100] R. Gompper, O. Christmann, *Chem. Ber.* **1959**, *92*, 1935–1943.
- [101] H. Brederick, R. Gompper, G. Theilig, *Chem. Ber.* **1954**, *87*, 537–546.
- [102] A. R. Katritzky, G. Musumarra, *Chem. Soc. Rev.* **1984**, *13*, 47–68.
- [103] L. Weisler, R. W. Helmkamp, *J. Am. Chem. Soc.* **1945**, *67*, 1167–1171.
- [104] T. Severin, B. Brück, P. Adhikary, *Chem. Ber.* **1966**, *99*, 3097–3102.
- [105] a) N. Kornblum, R. A. Brown, *J. Am. Chem. Soc.* **1963**, *85*, 1359–1360; b) N. Kornblum, R. A. Brown, *J. Am. Chem. Soc.* **1964**, *86*, 2681–2687.
- [106] M. Bersohn, *J. Am. Chem. Soc.* **1961**, *83*, 2136–2138.
- [107] a) R. C. Kerber, G. W. Urry, N. Kornblum, *J. Am. Chem. Soc.* **1965**, *87*, 4520–4528; b) N. Kornblum, *Angew. Chem.* **1975**, *87*, 797–808; *Angew. Chem. Int. Ed. Engl.* **1975**, *14*, 734–745.
- [108] a) H. B. Hass, M. L. Bender, *J. Am. Chem. Soc.* **1949**, *71*, 1767–1769; b) H. B. Hass, E. J. Berry, M. L. Bender, *J. Am. Chem. Soc.* **1949**, *71*, 2290–2291; c) H. B. Hass, M. L. Bender, *J. Am. Chem. Soc.* **1949**, *71*, 3482–3485.
- [109] R. N. Boyd, R. J. Kelly, *J. Am. Chem. Soc.* **1952**, *74*, 4600–4602.
- [110] S. J. Etheredge, *Tetrahedron Lett.* **1965**, *6*, 4527–4530.
- [111] D. Seebach, E. W. Colvin, F. Lehr, T. Weller, *Chimia* **1979**, *33*, 1–18.

- [112] a) D. Seebach, F. Lehr, *Angew. Chem.* **1976**, *88*, 540–541; *Angew. Chem. Int. Ed. Engl.* **1976**, *15*, 505–506; b) D. Seebach, R. Henning, F. Lehr, J. Gonnermann, *Tetrahedron Lett.* **1977**, *16*, 1161–1164; c) D. Seebach, F. Lehr, *Helv. Chim. Acta* **1979**, *62*, 2239–2257.
- [113] a) T. H. Black, *Org. Prep. Proced. Int.* **1989**, *21*, 179–217; b) J. Clayden, N. Greeves, S. Warren, P. Wothers, *Organic Chemistry*, Oxford University Press, Oxford, **2001**.
- [114] O. A. Reutov, I. P. Beletskaya, A. L. Kurts, *Ambident Anions*, Consultants Bureau, New York, **1983**.
- [115] H. E. Zimmerman, *Acc. Chem. Res.* **1987**, *20*, 263–268.
- [116] K. N. Houk, M. N. Paddon-Row, *J. Am. Chem. Soc.* **1986**, *108*, 2659–2662.
- [117] E. Sanchez Marcos, J. Bertran, *J. Chem. Soc., Faraday Trans. 2* **1989**, *85*, 1531–1538.
- [118] I. Lee, H. Y. Park, I.-S. Han, C. K. Kim, C. K. Kim, B.-S. Lee, *Bull. Korean Chem. Soc.* **1999**, *20*, 559–566.
- [119] N. F. Albertson, J. L. Fillman, *J. Am. Chem. Soc.* **1949**, *71*, 2818–2820.
- [120] J. Tae, K.-O. Kim, *Tetrahedron Lett.* **2003**, *44*, 2125–2128.
- [121] a) C. Wiles, P. Watts, S. J. Haswell, E. Pombo-Villar, *Lab Chip* **2002**, *2*, 62–64; b) C. Wiles, P. Watts, S. J. Haswell, E. Pombo-Villar, *Tetrahedron* **2005**, *61*, 10757–10773.
- [122] E. Buncl, J. M. Dust, R. A. Manderville, *J. Am. Chem. Soc.* **1996**, *118*, 6072–6073.
- [123] M. E. Jones, S. R. Kass, J. Filley, R. M. Barkley, G. B. Ellison, *J. Am. Chem. Soc.* **1985**, *107*, 109–115.
- [124] M. D. Brickhouse, R. R. Squires, *J. Phys. Org. Chem.* **1989**, *2*, 389–409.
- [125] M. Zhong, J. I. Brauman, *J. Am. Chem. Soc.* **1996**, *118*, 636–641.
- [126] a) W. J. Le Noble, J. E. Puerta, *Tetrahedron Lett.* **1966**, *7*, 1087–1090; b) W. J. Le Noble, H. F. Morris, *J. Org. Chem.* **1969**, *34*, 1969–1973.
- [127] a) A. L. Kurts, A. Macias, I. P. Beletskaya, O. A. Reutov, *Tetrahedron* **1971**, *27*, 4759–4767; b) A. L. Kurts, P. I. Dem'yanov, A. Macias, I. P. Beletskaya, O. A. Reutov, *Tetrahedron* **1971**, *27*, 4769–4776; c) A. L. Kurts, N. K. Genkina, A. Macias, L. P. Beletskaya, O. A. Reutov, *Tetrahedron* **1971**, *27*, 4777–4785.
- [128] L. M. Jackman, B. C. Lange, *J. Am. Chem. Soc.* **1981**, *103*, 4494–4499.
- [129] G. J. Heiszwolf, H. Kloosterziel, *Recl. Trav. Chim. Pays-Bas* **1970**, *89*, 1153–1169.
- [130] a) *The Chemistry of Enols* (Ed.: Z. Rappoport), John Wiley & Sons, Chichester, **1990**; b) A. J. Kresge, *Chem. Soc. Rev.* **1996**, *25*, 275–280.
- [131] E. S. Lewis, S. Vanderpool, *J. Am. Chem. Soc.* **1977**, *99*, 1946–1949.
- [132] W. Wislicenus, *Angew. Chem.* **1921**, *34*, 257–261.

- [133] F. Kremers, F. Roth, E. Tietze, L. Claisen, *Liebigs Ann. Chem.* **1925**, 442, 210–245.
- [134] a) D. Y. Curtin, R. J. Crawford, M. Wilhelm, *J. Am. Chem. Soc.* **1958**, 80, 1391–1397; b) J. Ugelstad, A. Berge, H. Listou, *Acta Chem. Scand.* **1965**, 19, 208–216; c) A. Berge, J. Ugelstad, *Acta Chem. Scand.* **1965**, 19, 742–750; d) J. Ugelstad, T. Ellingsen, A. Berge, *Acta Chem. Scand.* **1966**, 20, 1593–1598; e) N. Kornblum, A. P. Lurie, *J. Am. Chem. Soc.* **1959**, 81, 2705–2715; f) N. Kornblum, P. J. Berrigan, W. J. Le Noble, *J. Am. Chem. Soc.* **1960**, 82, 1257–1258; g) N. Kornblum, P. J. Berrigan, W. J. Le Noble, *J. Am. Chem. Soc.* **1963**, 85, 1141–1147; h) N. Kornblum, R. Seltzer, P. Haberfield, *J. Am. Chem. Soc.* **1963**, 85, 1148–1154.
- [135] a) E. Buncl, J. M. Dust, A. Jonczyk, R. A. Manderville, I. Onyido, *J. Am. Chem. Soc.* **1992**, 114, 5610–5619; b) E. Buncl, R. A. Manderville, *J. Phys. Org. Chem.* **1993**, 6, 71–82.
- [136] R. A. Manderville, J. M. Dust, E. Buncl, *J. Phys. Org. Chem.* **1996**, 9, 515–528.
- [137] E. Buncl, J. M. Dust, *Can. J. Chem.* **1988**, 66, 1712–1719.
- [138] Y. Tsuji, M. M. Toteva, H. A. Garth, J. P. Richard, *J. Am. Chem. Soc.* **2003**, 125, 15455–15465.
- [139] G. A. Olah, Y. K. Mo, *J. Org. Chem.* **1973**, 38, 353–366.
- [140] a) T. Birchall, A. N. Bourns, R. J. Gillespie, P. J. Smith, *Can. J. Chem.* **1964**, 42, 1433–1439; b) R. F. Childs, B. D. Parrington, *Can. J. Chem.* **1974**, 52, 3303–3312.
- [141] a) M. Attina, F. Cacace, G. Ciranna, P. Giacomello, *J. Chem. Soc., Chem. Comm.* **1976**, 466–467; b) M. Attina, F. Cacace, G. Ciranni, P. Giacomello, *J. Am. Chem. Soc.* **1977**, 99, 4101–4105; c) M. Attina, F. Cacace, G. Ciranni, P. Giacomello, *J. Am. Chem. Soc.* **1977**, 99, 5022–5026.
- [142] P. Beak, J. T. Adams, P. D. Klein, P. A. Szczepanik, D. A. Simpson, S. G. Smith, *J. Am. Chem. Soc.* **1973**, 95, 6027–6033.
- [143] C. J. M. Stirling, *Int. J. Sulfur Chem. B* **1971**, 6, 277–320.
- [144] a) R. Otto, *Ber. Dt. Chem. Ges.* **1880**, 13, 1272–1282; b) R. Otto, *Ber. Dt. Chem. Ges.* **1885**, 18, 154–162; c) R. Otto, A. Rössing, *Ber. Dt. Chem. Ges.* **1885**, 18, 2493–2509; d) R. Otto, W. Otto, *Ber. Dt. Chem. Ges.* **1888**, 21, 992–998; e) R. Otto, *Liebigs Ann. Chem.* **1894**, 283, 181–208; f) R. Otto, *Liebigs Ann. Chem.* **1895**, 284, 300–306.
- [145] W. E. Truce, J. P. Millionis, *J. Org. Chem.* **1952**, 17, 1529–1533.
- [146] K. Schank, *Liebigs Ann. Chem.* **1967**, 702, 75–85.
- [147] B. Lindberg, *Acta Chem. Scand.* **1963**, 17, 393–410.
- [148] C. C. J. Culvenor, W. Davies, N. S. Heath, *J. Chem. Soc.* **1949**, 278–282.

- [149] T. L. Gresham, J. E. Jansen, F. W. Shaver, M. R. Frederick, F. T. Fiedorek, R. A. Bankert, J. T. Gregory, W. L. Beears, *J. Am. Chem. Soc.* **1952**, *74*, 1323–1325.
- [150] C. W. Ferry, J. S. Buck, R. Baltzly, *Org. Synth.* **1942**, *22*, 31–33.
- [151] H. Gilman, L. F. Cason, *J. Am. Chem. Soc.* **1950**, *72*, 3469–3472.
- [152] M. V. Kalnins, B. Miller, *Chem. Ind.* **1966**, 555–556.
- [153] L. F. Cason, C. C. Wanser, *J. Am. Chem. Soc.* **1951**, *73*, 142–145.
- [154] J. S. Meek, J. S. Fowler, *J. Org. Chem.* **1968**, *33*, 3422–3424.
- [155] M. Kobayashi, *Bull. Chem. Soc. Jpn* **1966**, *39*, 1296–1297.
- [156] D. Darwish, R. McLaren, *Tetrahedron Lett.* **1962**, *3*, 1231–1237.
- [157] A. C. Cope, D. E. Morrison, L. Field, *J. Am. Chem. Soc.* **1950**, *72*, 59–67.
- [158] C. J. M. Stirling, *Chem. Commun.* **1967**, 131.
- [159] a) G. Büchi, R. M. Freidinger, *J. Am. Chem. Soc.* **1974**, *96*, 3332–3323; b) J. E. Baldwin, O. W. Lever, Jr., N. R. Tzodikov, *J. Org. Chem.* **1976**, *41*, 2312–2314.
- [160] For selected bond lengths for free sulfinates, sulfones, and sulfonates see: a) R. Allmann, W. Hanefeld, M. Krestel, B. Spangenberg, *Angew. Chem.* **1987**, *99*, 1175–1176; *Angew. Chem. Int. Ed. Engl.* **1987**, *26*, 1133–1134; b) I. Brito, M. Lopez-Rodriguez, A. Cardenas, A. Reyes, *Acta Crystallogr., Sect. E Struct. Rep. Online* **2006**, *E62*, o4017–o4019; c) E. Horn, E. R. T. Tiekink, *J. Chem. Crystallogr.* **1995**, *25*, 459–462; d) R. Anulewicz, R. Luboradzki, K. Suwinska, A. Zakrzewski, *Acta Crystallogr., Sect. C: Cryst. Struct. Commun.* **1990**, *C46*, 907–909; e) I. Tickle, J. Hess, A. Vos, J. B. F. N. Engberts, *J. Chem. Soc. Perkin Trans. 2* **1978**, 460–465; f) F. W. Heinemann, I. Weber, U. Zenneck, *J. Chem. Crystallogr.* **2007**, *37*, 165–170.
- [161] S. G. Smith, S. Winstein, *Tetrahedron* **1958**, *3*, 317–319.
- [162] R. Kuhn, H. Trischmann, *Liebigs Ann. Chem.* **1958**, *611*, 117–121.
- [163] a) F. Brotzel, B. Kempf, T. Singer, H. Zipse, H. Mayr, *Chem. Eur. J.* **2007**, *13*, 336–345; b) C. F. Bernasconi, *Pure Appl. Chem.* **1982**, *54*, 2335–2348.
- [164] E. M. Arnett, R. Reich, *J. Am. Chem. Soc.* **1980**, *102*, 5892–5902.
- [165] a) N. Krause, A. Gerold, *Angew. Chem.* **1997**, *109*, 194–213; *Angew. Chem. Int. Ed. Engl.* **1997**, *36*, 186–204; b) E. Nakamura, S. Mori, *Angew. Chem.* **2000**, *112*, 3902–3924; *Angew. Chem. Int. Ed.* **2000**, *39*, 3750–3771.
- [166] W. Nagata, M. Yoshioka, *Org. React.* **1977**, *25*, 255–476.
- [167] A. Williams, *Free Energy Relationships in Organic and Bio-Organic Chemistry*, The Royal Society of Chemistry, Cambridge, **2003**.

- [168] M. J. S. Dewar, R. C. Dougherty, *The PMO Theory of Organic Chemistry*, Plenum Press, New York, **1975**.
- [169] J. E. Leffler, E. Grunwald, *Rates and Equilibria of Organic Reactions*, John Wiley and Sons, New York, **1963**.
- [170] a) C. F. Bernasconi, *Acc. Chem. Res.* **1987**, *20*, 301-308; b) C. F. Bernasconi, *Acc. Chem. Res.* **1992**, *25*, 9-16.
- [171] F. G. Bordwell, *Acc. Chem. Res.* **1970**, *3*, 281-290.
- [172] a) E. S. Lewis, *J. Phys. Org. Chem.* **1990**, *3*, 1-8; b) E. S. Lewis, T. A. Douglas, M. L. McLaughlin, in *Nucleophilicity* (Eds.: J. M. Harris, S. P. McManus), American Chemical Society, Chicago, 1987, pp. 35-49.
- [173] J. R. Murdoch, *J. Am. Chem. Soc.* **1983**, *105*, 2159-2164.
- [174] F. Terrier, E. Magnier, E. Kizilian, C. Wakselman, E. Buncl, *J. Am. Chem. Soc.* **2005**, *127*, 5563-5571.

Lebenslauf

Persönliche Daten:

Name: Robert Martin Breugst
Geburtsdatum: 14.10.1980
Geburtsort: München
Nationalität: Deutsch

Schulausbildung:

06/2001 Abitur, Feodor-Lynen-Gymnasium, Planegg

Zivildienst:

08/2000 – 06/2001 Klinikum Großhadern der Ludwig-Maximilians-Universität, München

Studium:

10/2001 – 09/2005 Chemiestudium an der Ludwig-Maximilians-Universität, München
Abschluss: Bachelor of Science
Bachelor-Arbeit: *Quantitative Analyse der Elektrophilie des S-Methyldibenzothiophenium-Ions*

10/2005 – 09/2006 Chemiestudium an der Ludwig-Maximilians-Universität, München
Abschluss: Master of Science
Master-Arbeit: *Nucleophile Reaktivität von Amid-Anionen*

seit 10/2006 Promotionsstudium am Department Chemie der Ludwig-Maximilians-Universität, München

05/2008 – 09/2008 Gastwissenschaftler an der University of Western Ontario, London, ON, Kanada. (Gastgeber: Prof. Dr. J. Peter Guthrie)

Universitäre Tätigkeiten:

10/2003 – 09/2006 Tutor für Organische Chemie und Mathematik; Ludwig-Maximilians-Universität, Department Chemie und Biochemie

seit 10/2006 Wissenschaftlicher Mitarbeiter, Department Chemie, Ludwig-Maximilians-Universität, München